

Université de Montréal

Development of a Phase Separation Strategy in Macrocyclization Reactions

par

Anne-Catherine Bédard

Département de Chimie
Faculté des Arts et des Sciences

Thèse présentée à la Faculté des Études Supérieures et Postdoctorale
en vue de l'obtention du grade de
Philosophiæ Doctor (Ph.D.) en chimie

Avril 2015

© Anne-Catherine Bédard, 2015

Résumé

La réaction de macrocyclisation est une transformation fondamentale en chimie organique de synthèse. Le principal défi associé à la formation de macrocycles est la compétition inhérente avec la réaction d'oligomérisation qui mène à la formation de sous-produits indésirables. De plus, l'utilisation de conditions de dilutions élevées qui sont nécessaires afin d'obtenir une cyclisation "sélective", sont souvent décourageantes pour les applications à l'échelle industrielle. Malgré cet intérêt pour les macrocycles, la recherche visant à développer des stratégies environnementalement bénignes, qui permettent d'utiliser des concentrations normales pour leur synthèse, sont encore rares. Cette thèse décrit le développement d'une nouvelle approche générale visant à améliorer l'efficacité des réactions de macrocyclisation en utilisant le contrôle des effets de dilution. Une stratégie de "séparation de phase" qui permet de réaliser des réactions à des concentrations plus élevées a été développée. Elle se base sur un mélange de solvant agrégé contrôlé par les propriétés du poly(éthylène glycol) (PEG). Des études de tension de surface, spectroscopie UV et tagging chimique ont été réalisées afin d'élucider le mécanisme de "séparation de phase". Il est proposé que celui-ci fonctionne par diffusion lente du substrat organique vers la phase où le catalyseur est actif. La nature du polymère co-solvant joue donc un rôle crucial dans le contrôle de l'aggrégation et de la catalyse. La stratégie de "séparation de phase" a initialement été étudiée en utilisant le couplage oxydatif d'alcynes de type Glaser-Hay co-catalysé par un complexe de cuivre et de nickel puis a été transposée à la chimie en flux continu. Elle fut ensuite appliquée à la cycloaddition d'alcynes et d'azotures catalysée par un complexe de cuivre en "batch" ainsi qu'en flux continu.

Mots-clés : Macrocyclisation, séparation de phase, poly(éthylène glycol), couplage d'alcynes de type Glaser-Hay, diynes, catalyseur de cuivre, cycloaddition d'azotures et d'alcynes, triazole, chimie en flux continu

Abstract

Macrocyclization is a fundamentally important transformation in organic synthetic chemistry. The main challenge associated with the synthesis of large ring compounds is the competing oligomerization processes that lead to unwanted side-products. Moreover, the high dilution conditions needed to achieved “selective” cyclization are often daunting for industrial applications. Despite the level of interest in macrocycles, research aimed at developing sustainable strategies that focus on catalysis at high concentrations in macrocyclization are still rare. The following thesis describes the development of a novel approach aimed at improving the efficiency of macrocyclization reactions through the control of dilution effects. A “phase separation” strategy that allows for macrocyclization to be conducted at higher concentrations was developed. It relies on an aggregated solvent mixture controlled by a poly(ethylene glycol) (PEG) co-solvent. Insight into the mechanism of “phase separation” was probed using surface tension measurements, UV spectroscopy and chemical tagging. It was proposed to function by allowing slow diffusion of an organic substrate to the phase where the catalyst is active. Consequently, the nature of the polymer co-solvent plays a role in controlling both aggregation and catalysis. The “phase separation” strategy was initially developed using the copper and nickel co-catalyzed Glaser-Hay oxidative coupling of terminal alkynes in batch and was also transposed to continuous flow conditions. The “phase separation” strategy was then applied to the copper-catalyzed alkyne-azide cycloaddition in both batch and continuous flow.

Keywords : Macrocyclization, phase separation, poly(ethylene glycol), Glaser-Hay alkyne coupling, diynes, copper catalysis, azide-alkyne cycloaddition, triazole, continuous flow chemistry

Table of Content

Résumé.....	i
Abstract.....	iii
Table of Content	iv
List of Tables	ix
List of Figures.....	xi
List of Schemes.....	xiv
List of Abbreviations	xviii
Acknowledgements.....	xxv
Chapitre 1 : Introduction.....	1
1.1 – The Importance and Applications of Macrocycles	2
1.1.1 – Medicinal Chemistry.....	2
1.1.2 – Macrocycles in Conjugated Materials	4
1.1.3 – Macrocycles in Perfumery	5
1.1.4. – Macrocycles in Supramolecular Chemistry.....	6
1.2 – Synthetic Challenges Associated with Macrocyclization	7
1.2.1 – Reactive Conformation	9
1.3 – Traditional Solutions for Macrocyclization Reactions	12
1.3.1 – High Dilution and Slow Addition.....	12
1.3.2 – Conformational Control	17
1.4 – Alternative Solutions for Macrocyclization Reactions.....	21
1.4.1 – Cycloaddition.....	21
1.4.2 – Ring Expansion and Fragmentation.....	22
1.5 – Conclusion	24
1.6 – Bibliography	25
PART 1	28

Chapter 2 : The Glaser-Hay Oxidative Coupling and an Introduction to Poly(ethylene glycol) Properties	29
2.1 – Glaser-Hay Reaction.....	29
2.1.1 – Seminal Discovery	29
2.1.2 – Reaction Mechanism.....	30
2.1.3 – Modern Reaction Conditions	33
2.1.4 – Synthesis of Unsymmetrical 1,3-Diynes.....	34
2.1.5 – Naturally Occuring Diynes	39
2.1.6 – Applications of the Glaser-Hay Reaction in Synthesis.....	40
2.1.7 – Conclusion	43
2.2 – Introduction to Poly(ethylene glycol) Properties and Concepts of Phase Transfer and Micellar Catalysis	44
2.2.1 – Definition and Physical Properties of Poly(ethylene glycol).....	44
2.2.2 – Industrial Applications of PEGs	47
2.2.3 – Chemical Applications of PEGs	47
2.2.4 – Micellar Catalysis	51
2.2.5 – Conclusion	53
2.3 – Bibliography	54
Chapter 3 : Phase Separation as a Strategy Towards Controlling Dilution Effects in Macrocylic Glaser-Hay Couplings.....	57
3.1 – Abstract.....	58
3.2 – Introduction.....	59
3.3 – Results and Discussion	64
3.3.1 – Developing Hydrophilic Ligands for Transition Metal Complexes for Use in “Green” Macrocyclizations.....	64
3.3.2 – Poly(ethylene glycol) (PEG) as a Solvent for “Green” Macrocyclization.	68
3.4 – Conclusions.....	75
3.5 – Bibliography	77
Chapter 4 : Microwave Accelerated Glaser-Hay Macrocyclizations at High Concentrations .	79
4.1 – Abstract.....	80

4.2 – Introduction.....	80
4.3 – Results and Discussion	81
4.4 – Conclusion	88
4.5 – Bibliography	89
Chapter 5 : Exploiting Aggregation to Achieve Phase Separation in Macrocyclization.....	91
5.1 – Abstract.....	92
5.2 – Introduction.....	93
5.3 – Results and Discussion	96
5.3.1 – Aggregate Formation in Poly(ethylene glycol) Homogenous Mixtures.....	96
5.3.2 – Determination of the Phase Preference of Substrate and Catalyst.....	100
5.3.3 – Chemical “Tagging” of Substrate and Catalyst	102
5.4 – Conclusion	105
5.5 – Bibliography	107
Chapter 6 : Influence of Poly(ethylene glycol) Structure in Catalytic Macrocyclization Reactions.....	109
6.1 – Abstract.....	110
6.2 – Introduction.....	111
6.3 – Results and Discussion	115
6.3.1 – “Capping” of the Terminal Hydroxyl Groups of PEG.....	117
6.3.2 – Different Chain Lengths of PEG.....	120
6.3.3 – Branched Polymers of PEG: PPG and Pluronic.	124
6.4 – Conclusion	130
6.5 – Bibliography	133
PART 2	137
Chapter 7 : Introduction to Continuous Flow Chemistry.....	138
7.1 – Description of Flow Equipment and Important Parameters	138
7.1.1 – Flow Equipment.....	138
7.1.2 – Important Parameters	141
7.2 – Advantages of Continuous Flow Synthesis vs Microwave and Batch Chemistry.....	142
7.2.1 – Glaser-Hay Reactions in Continuous Flow.....	144

7.3 – Challenges Associated with Macrocyclization in Continuous Flow	146
7.4 – Examples of Macrocyclization in Continuous Flow	147
7.5 – Conclusion	149
7.6 – Bibliography	150
Chapter 8 : Continuous Flow Macrocyclization at High Concentrations: Synthesis of Macrocyclic Lipids	151
8.1 – Abstract	152
8.2 – Introduction	152
8.3 – Results and Discussion	154
8.4 – Conclusion	165
8.5 – Bibliography	167
PART 3	168
Chapter 9 : Introduction to the Copper-Catalyzed Azide-Alkyne Cycloaddition.....	169
9.1 – Discovery and Improvement of the Azide-Alkyne Cycloaddition Reaction	169
9.2 – Applications of the Copper-Catalyzed Azide-Alkyne Cycloaddition Reaction	171
9.3 – Mechanistic Aspects of the Copper-Catalyzed Azide-Alkyne Cycloaddition Reaction	175
9.3.1 – Importance of the Copper Source	175
9.3.2 – Importance of Ligands	176
9.3.3 – Proposed Catalytic Cycle	179
9.4 – Copper-Catalyzed Iodoalkyne-Azide Cycloaddition	181
9.4.1 – Proposed Catalytic Cycle	184
9.4.2 – Application of Copper-Catalyzed Iodo-Alkyne-Azide Cycloaddition	185
9.5 – Conclusion	186
9.6 – Bibliography	187
Chapter 10. Advanced Strategies for Efficient Macrocyclic Cu(I)-Catalyzed Cycloaddition of Azides	189
10.1 – Abstract	190
10.2 – Introduction	191
10.3 – Results and Discussion	192

10.4 – Conclusion	200
10.5 – Bibliography	202
Chapter 11: Efficient Continuous Flow Synthesis of Macrocyclic Triazoles.....	204
11.1 – Abstract.....	205
11.2 – Introduction.....	205
11.3 – Results and Discussion	207
11.4 – Conclusion	213
11.5 – Bibliography	214
Chapter 12 : Conclusion and Perspectives.....	215
12.1 – Bibliography	224
Supporting Information.....	a
Chapter 13 : Supporting Information of Chapter 2: Phase Separation as a Strategy Towards Controlling Dilution Effects in Macrocyclic Glaser-Hay Couplings	b
Chapter 14 : Supporting Information of Chapter 3: Microwave Accelerated Glaser-Hay Macrocyclizations at High Concentrations.....	xx
Chapter 15 : Supporting Information of Chapter 4: Exploiting Aggregation to Achieve Phase Separation in Macrocyclization	nnn
Chapter 16 : Supporting Information of Chapter 5: Influence of Poly(ethylene glycol) Structure in Catalytic Macrocyclization Reactions.....	iiii
Chapter 17 : Supporting Information of Chapter 7: Continuous Flow Macrocyclization at High Concentrations: Synthesis of Macrocyclic Lipids	uuuu
Chapter 18 : Supporting Information of Chapter 9: Advanced Strategies for Efficient Macrocyclic Cu(I)-Catalyzed Cycloaddition of Azides	wwwww
Chapter 19 : Supporting Information of Chapter 10: Efficient Continuous Flow Synthesis of Macrocyclic Triazoles.....	oooooooo

List of Tables

Table 1.1 – Optimization of the macrocyclic ring closing metathesis reaction of 1.31	16
Table 2.1 Cu/Ni co-catalyzed synthesis of unsymmetrical diynes.	38
Table 3.1 – Model studies on the macrocyclization of 3 using a copper/T-PEG ₁₉₀₀ system and phase separation as a strategy to control reactivity.....	67
Table 3.2 – Model studies on the macrocyclization of 2 using a copper/nickel catalyst system and phase separation as a strategy to control reactivity.....	70
Table 3.3 – Model studies on the macrocyclization of 3 using a copper/T-PEG ₁₉₀₀ system and phase separation as a strategy to control reactivity.....	71
Table 4.1 – Optimization of macrocyclization of diyne 1 under microwave irradiation.....	83
Table 4.2 – Comparison of macrocyclic Glaser-Hay couplings of diynes under traditional heating versus microwave irradiation. ^a	85
Table 5.1 – Yields of macrocycle 4 at various ratios of PEG ₄₀₀ or ethylene glycol in MeOH. ¹⁷	99
Table 6.1 – Yields of macrocycle 4 at various ratios of PEG in MeOH.....	116
Table 6.2 – Effect of PEG structure on the catalyst loading in the macrocyclization to form 4	130
Table 8.1 – Optimization of Reaction Conditions For Macrocyclic Glaser-Hay Coupling of 3	156
Table 8.2 – Macrocyclic Lactones and Ethers Synthesized via Continuous Flow-Macrocyclization Using “Phase Separation”.....	158
Table 8.3 – Optimization of Reactions Conditions for the Synthesis of a Protected Macrocyclic Lipid 8	160
Table 8.4 – Macrocyclic Lipids Synthesized via Continuous Flow-Macrocyclization Using “Phase Separation”.....	162
Table 8.5 – Reduction of Catalyst Loadings when Using PPG ₄₂₅ for the Synthesis of a Protected Macrocyclic Lipid 8	164
Table 9.1 – Comparison of ligand effects in CuAAC.....	178
Table 10.1 – Optimization of Macrocyclic CuAiAC using a Phase Separation Strategy.....	193

Table 10.2 – Concentration Effects of Macrocyclic CuAiAC Using Both Traditional High Dilution and Phase Separation Strategies.	195
Table 10.3 – Substrate Scope of Macrocyclic CuAiAC Using a Phase Separation Strategy. ^a	199
Table 11.1 – Optimization of Macrocyclic CuAiAC using a Phase Separation Strategy in Batch.	208
Table 11.2 – Optimization of Macrocyclic CuAiAC under Continuous Flow Conditions. ...	209
Table 11.3 – Substrate Scope of Macrocyclic CuAiAC Using a Phase Separation Strategy in Continuous Flow. ^a	210
Table 11.4 – Substrate Scope of Macrocyclic CuAAC Using a Phase Separation Strategy in Continuous Flow. ^a	212

List of Figures

Figure 1.1 – Structures of biologically active macrocycles. a) erythromycin 1.1 , b) rapamycin 1.2 , c) Sonic hedgehog modulator 1.3 , d) neutral endopeptidase inhibitor 1.4	3
Figure 1.2 – Structures of conjugated macrocycles. a) heme B 1.5 , b) [14]annulene 1.6 , c) diethynylcarbazole macrocycle 1.7	4
Figure 1.3 – Structures of macrocyclic musks. a) muscone 1.8 , b) exaltolide 1.9 , c) isoambrettolide 1.10	6
Figure 1.4 – Structures of macrocyclic supramolecules. a) α -cyclodextrin 1.11 , b) [18]-crown-6 1.12 , c) AFP-Cide 1.13	7
Figure 1.4 – Attempts to synthesize the Pro-Ala-Ala-Phe-Leu macrocycle 1.20 using a Pfp ester activation strategy in dilute media.	11
Figure 1.5 – Impact of concentration on ratio of macrocyclization vs dimerization rate and solvent volume.	14
Figure 2.1 – Relative reactivity of alkynes in oxidative couplings.	34
Figure 2.2 – Naturally occurring diynes.	40
Figure 2.2 – Structure of PEG ₄₀₀	44
Figure 3.1 – a) Traditional macrocyclization in homogeneous hydrophobic media. b) Macrocyclization employing phase separation.	60
Figure 3.2 – Simplified experimental set-up for the “green” macrocyclization using phase separation.	65
Figure 4.1 – Macrocyclization employing phase separation.	81
Figure 4.2 – (<i>top</i>) Comparison of the rate of formation of macrocycle 3 using different heating techniques. (<i>bottom</i>) Comparing homogenous solutions vs. phase separation in macrocyclizations at high concentrations	87
Figure 5.1 – Surface tension measurements for homogenous mixtures of PEG ₄₀₀ (<i>top</i>) or ethylene glycol (<i>bottom</i>) in MeOH (in red) at 60 °C and influence on macrocyclization (3 → 4) (in green, see Table 5.1).	97
Figure 5.2 – Absorbance measurements of diyne 3 in various solvent mixtures.	101

Figure 6.1 – The proposed origin of selectivity in Glaser-Hay macrocyclization reactions employing PEG ₄₀₀ /MeOH mixtures.....	113
Figure 6.2 – Short chain PEG polymers having different "capping" groups.....	117
Figure 6.4 – PEG polymers having different chain lengths.....	120
Figure 6.5b – The effect of using different polymer lengths of PEG polymer (PEG ₁₉₀ (<i>top</i>), PEG ₄₀₀ (<i>middle</i>), PEG ₁₄₅₀ (<i>bottom</i>)) when promoting macrocyclic Glaser-Hay coupling (3 → 4) at high concentration (0.03 M). Surface tension measurements (red) and isolated yields (green) are plotted on the same figure. The region highlighted in grey indicated PEG/MeOH ratios in which catalyst inhibition is observed and the remaining mass balance in re-isolated diyne 3	123
Figure 5.6 – Comparison of different PEG polymers having different chain lengths and branching substituents.....	124
Figure 6.7 – The effect of using branched polymers of short-chained PEGs (PEG ₄₀₀ (<i>top</i>) and PPG ₄₂₅ (<i>bottom</i>)) when promoting macrocyclic Glaser-Hay coupling (3 → 4) at high concentration (0.03M). Surface tension measurements (red) and isolated yields (green) are plotted on the same figure. The region highlighted in grey indicated PEG/MeOH ratios in which catalyst inhibition is observed and the remaining mass balance in re-isolated diyne 3	126
Figure 6.8 – The effect of using branched polymers of long chained PEGs (PEG ₁₄₅₀ (<i>top</i>) and Pluornic ₁₁₀₀ (<i>bottom</i>)) when promoting macrocyclic Glaser-Hay coupling (3 → 4) at high concentration (0.03 M). Surface tension measurements (red) and isolated yields (green) are plotted on the same figure. The region highlighted in grey indicated PEG/MeOH ratios in which catalyst inhibition is observed and the remaining mass balance in re-isolated diyne 3	127
Figure 7.2 – General schematic diagram of a high-temperature/high-pressure continuous flow conditions.....	140
Figure 7.3 – Flow reactors : a) High-temperature/high-pressure stainless steel reactor, b) PFA reactor, c) Cooled reactor (PFA), d) UV reactor	141
Figure 9.1 – a) Tripeptide 9.8 structure (blue) overlay with balhimycin (red), b) Tripeptide 9.9 structure (blue) overlay with balhimycin (red). (Reproduced with permission from ref 10. Copyright 2011 American Chemical Society.).....	172

Figure 9.2 – Structure of ligands for CuAAC.....	177
Figure 9.3 – Proposed di-copper species 9.39 that could be favored in the presence of polytriazole or benzimidazole ligands.	181
Figure 9.4 – Effect of the addition of an iodine on the triazole moiety of a <i>Escherichia coli</i> PDHc-E1 inhibitor and antifungal.	186
Figure 10.1 – Macrocyclic azide-alkyne cycloaddition processes.....	191
Figure 11.1 – Macrocyclic azide-alkyne cycloaddition processes in continuous flow.....	206

List of Schemes

Scheme 1.1 – (<i>top</i>) Lactone 1.15 formation reaction for the corresponding bifunctional precursor 1.14 and (<i>bottom</i>) reactivity profile in function of the ring size formed. (Reproduced with permission from ref 22. Copyright 1981 American Chemical Society.).....	8
Scheme 1.2 – The importance of conformation in macrocyclization by RCM.	10
Scheme 1.3. – Macrolactonization of seco-acids derived from octalactins.	12
Scheme 1.4 – (<i>top</i>) Rate of macrocyclization vs dimerization and (<i>bottom</i>) effective molarity equation.....	13
Scheme 1.5 – Initial macrocyclic ring closing metathesis in the synthesis of BILN 2061 1.30	15
Scheme 1.6 – Effect of solid supported catalyst on macrocyclic isomerization reaction.	17
Scheme 1.7 – Lithium salt’s template effect in the synthesis of 1.40	18
Scheme 1.8 – Synthesis of dioxoporphyrin-derived macrocycles using a template strategy. ...	19
Scheme 1.9 – Synthesis of small cyclic peptide 1.49 <i>via</i> Heck reaction assisted by an intramolecular H-bond interaction.	20
Another supramolecular approach used to favor productive conformations for macrocyclization is through supramolecular π -stacking interactions. An example is in the synthesis of rigid cyclophane structures which is challenging even under high dilution conditions. ⁴⁶ When diene precursor 1.50 is submitted to a ruthenium-based catalyst to perform a macrocyclic ring-closing metathesis, no desired product 1.51 is formed and only oligomerization products are obtained (Scheme 1.10, <i>top</i>). Collins reported the use of an electron-poor aryl group as a conformational control element (CCE) to promote macrocyclization. ⁴⁷ The π -stacking interaction allows precursor 1.52 to adopt a productive conformation 1.53 which is productive for macrocyclization, affording 41 % yield of the cyclophane 1.54 (Scheme 1.10, <i>bottom</i>).	20
Scheme 1.10 – Synthesis of cyclophane macrocycle 1.54 using a CCE.	21
Scheme 1.11 – Wilke’s trimerization and synthesis of cyclododecanone.	22
Scheme 1.12 – Story synthesis of exaltolide <i>via</i> ring expansion.	22
Scheme 1.13 – Cyclopropane ring expansion.	23
Scheme 1.14 – Translactonization strategy for the synthesis of large ring compounds.	23

Scheme 1.15 – Acid-catalyzed ring expansion.	24
Scheme 2.1 – General reaction conditions for : a) Glaser, b) Glaser-Eglinton and c) Glaser-Hay acetylene coupling reactions.	30
Scheme 2.2 – Bohlmann’s proposed mechanism for Glaser coupling.	31
Scheme 2.3. – Glaser-Hay catalytic cycle based on DFT calculations.....	32
Scheme 2.4. – Proposed synergistic cooperative effect of Cu(I) and Cu(II) salts in the cupration of alkyne.	32
Scheme 2.5 – Unsymmetrical diyne coupling protocols. a) Cadiot-Chodkiewicz, b) Lei’s Cu/Pd protocol and c) CuNPs protocol.....	35
Scheme 2.6 – Unsymmetrical diyne coupling protocols. a) Decarboxylative cross-coupling from dihaloalkenes, b) Negishi’s protocol, c) Cu/Pd/Ag decarboxylative cross-coupling.....	36
Scheme 2.7 – Shi’s heterocoupling of terminal alkynes protocol.	37
Scheme 2.8 – Mechanistic investigation of the Cu/Ni co-catalyzed oxidative coupling of alkynes.	39
Another technique that can be used to access unsymmetrical 1,3-diynes is the use of solid-supported synthesis. Immobilizing one of the coupling partners allows for selective coupling with the solubilized partner in high yield. ²⁵	39
Scheme 2.9 – Synthesis of falcarindiol <i>via</i> Cadiot-Chodkiewicz coupling.....	40
Scheme 2.10 – Synthesis of an optically active cyclophane capable of carbohydrate recognition.	41
Scheme 2.11 – Synthesis of molecular rods incorporating cyclopentadienyl- π complexes.	42
Scheme 2.12 – Synthesis a spirocyclopropanated macrocyclic polydiacetylene.	42
Scheme 2.13 – Synthesis of low polydispersity monofunctional PEG polymer.	44
Figure 2.3 – Calculated structure of PEG ₆₅₀ in water (2 ns). (Reproduced with permission from ref 39. Copyright 1996 American Chemical Society.)	46
Scheme 2.14 – PEG ₁₀₀₀ as a recyclable medium for Glaser-Hay couplings.....	48
Scheme 2.15 – Ring opening metathesis polymerization using water soluble ruthenium based catalysts.....	49
Scheme 2.16 – Hydroformylation of 1-decene under thermoregulated phase-transfer catalysis (TRPTC).	51

For example, the rhodium catalyzed intramolecular [4+2] annulation of 1,3-dien-8-yne was conducted under micellar catalysis using sodium dodecylsulfate (SDS) in water. It was proposed that the rhodium catalyst exchanged its chlorine ligand for a SDS anion in aqueous media. The formation of a highly active cationic rhodium species **2.81** was proposed to be stabilized by the negative charges on the polar heads of the micelle (Scheme 1.17). The use of SDS was shown to be highly efficient, yielding 93 % of the desired bicyclic product **2.51** in only 20 min. 51

Scheme 1.17 – Proposed formation of a micellar catalyst..... 52

Scheme 2.18 – Rhodium catalyzed intramolecular [4+2] annulation of 1,3-dien-8-yne in water. 53

Scheme 3.1 – Synthesis of **3** based upon traditional conditions..... 64

Scheme 3.2 – Synthesis of PEGylated TMEDA derivative, T-PEG₁₉₀₀. 65

Scheme 4.1 – Comparing macrocyclization routes to diyne **2**..... 82

Scheme 5.1 – Comparing macrocyclization routes to diyne **2**..... 94

Scheme 5.2 – Macrocyclization to form **2** using biphasic conditions (PhMe/H₂O) and using homogenous mixtures of PEG₄₀₀/MeOH..... 95

Scheme 5.3 – Macrocyclization behavior of tagged ester **7**. 103

Scheme 5.4 – Macrocyclization of diyne **5** with a tagged TMEDA derivative **9**..... 103

Scheme 6.1 – Comparing macrocyclization routes to diyne **2**..... 112

Figure 7.4 – Control of the reaction time in continuous flow. (Reproduced with permission from ref 6. Copyright 2013 Royal Society of Chemistry.) 143

Scheme 7.1 – Glaser-Hay coupling in flow using a gas-liquid reactor. 145

Scheme 7.2 – Macrocyclization of alkyne-azide **6.3** precursor in batch vs. continuous flow 148

Scheme 7.3 – Iodo-“Click” macrocyclization in continuous flow. 149

Fogg and co-workers reported the transposition of the ruthenium-catalysed ring closing metathesis reaction in continuous flow. The authors found that high yield could be obtained when a continuous stirred tank reactor (CSTR) was used in series with the flow to help remove the ethylene **7.11** from the reaction media (Scheme 7.4). Noteworthy, a 16-membered macrolactone **7.10** was synthesized in 99 % yield.¹⁷ 149

Scheme 7.4 – Ring closing metathesis in continuous flow..... 149

Scheme 8.1 – Advantages of the “phase separation” strategy in macrocyclization 154

Scheme 8.2 – Synthesis of a dimeric macrocyclic lipid 13 as a mixture of head-to-tail and head-to-head isomers.	164
Scheme 8.3 – Conversion of Bn-protected macrocycle 8 into novel macrocyclic phosphonate containing lipid 14	165
Scheme 9.1 – (<i>top</i>) Triazole numbering (<i>bottom</i>) Synthesis of triazoles under a) thermal conditions, b) copper catalysis, c) ruthenium catalysis.....	170
Scheme 9.2 – CuAAC and RuAAC macrocyclization of vancomycin-inspired tripeptides. .	172
Scheme 9.3 – CuAAC macrocyclization using a template strategy.	174
Scheme 9.4 – CuAAC promoted by <i>in situ</i> reduction of a Cu(II) salt.....	175
Scheme 9.5 – CuAAC promoted by a Cu(I) salt and amine ligand.....	176
Scheme 9.6 – Mechanistic investigations of the CuAAC reaction.....	180
Scheme 9.7 –Proposed catalytic cycle for the CuAAC	180
Scheme 9.8 – Rare example of CuAAC with an internal alkyne.....	181
Scheme 9.9 – Copper-catalyzed cycloaddition of azides and 1-bromoalkynes.....	182
Scheme 9.10 – Copper-catalyzed cycloaddition of azide and 1-iodoalkynes.....	182
Scheme 9.11 – Copper-NHC and copper-phosphine complex catalyzed cycloaddition of azide and 1-iodoalkynes.	183
Scheme 9.12 – Synthesis and derivatization of the iodotriazole moiety	184
Scheme 9.13 – Mechanistic postulation for CuAiAC.....	185
Scheme 9.14 – Proposed catalytic cycle for CuAiAC	185
Scheme 10.1 – Macrocyclic CuAiAC under continuous flow conditions.....	197

List of Abbreviations

α	Alpha
Abs	Absorbance
Ac	Acetate
acac	Acetylacetonate
Ala	Alanine
atm	Atmosphere (pressure)
B	Base
bipy	2,2'-bipyridine
Bn	Benzyl
BPR	Back-pressure regulator
br	Broad
Bu	Butyl
C	Celsius
calcd	Calculated
COD	1,5-Cyclooctadiene
Cp	Cyclopentadienyl
Cy	Cyclohexyl
Δ	Heat
δ	Chemical Shift
d	Day
D	Dimension
DCC	N,N'-Dicyclohexylcarbodiimide
DCM	Dichloromethane

DFT	Density-Functional Theory
DIAD	Diisopropyl azodicarboxylate
DIPEA	N,N-Diisopropylethylamine
DMAP	4-Dimethylaminopyridine
DMF	N,N-dimethylformamide
DMSO	Dimethylsulfoxide
dppe	Diphenylphosphinoethane
dppm	Diphenylphosphinomethane
E	Energie
e ⁻	electron
EDCI	1-Ethyl-3-(3-dimethylaminopropyl)carbodiimide
Et	Ethyl
equiv	Equivalents
ESI	Electrospray ionisation mass spectrometry
FDA	Food and Drug Administration
FVP	Flash vacuum pyrolysis
g	gram
h	Hours
H	Hydrogen
HCV	Hepatitis C virus
HPLC	High pressure liquid chromatography
HR-ESIMS	High-Resolution Electro Spray Ionization Mass Spectrometry
HRMS	High-Resolution Mass Spectrometry
hv	Light irradiation
intra	Intramolecular

inter	Intermolecular
IR	Infrarouge
IUPAC	International Union of Pure and Applied Chemistry
k	Rate
kcal	Kilocalorie
kg	Kilogram
λ_{ab}	Absorption wavelength
λ_{max}	Maximal absorption wavelength
L	Ligand
Leu	Leucine
m/z	Mass on charge
m	meta
Me	Methyl
MHz	Mega Hertz
min	Minute
mL	Milliliter
mm	Millimeter
mM	Millimolar
mol	Mole
mg	Milligram
Mn	Average molecular weight
mN/m	Millinewton per meter
MPa	Mega Pascal (pressure)
MS	Mass spectrometry

Ms	Methanesulfonyl
MW	Microwave (irradiation)
NA	Non-available
Naph	Naphthyl
nbd	Norbornadiene
NBS	N-Bromosuccinimide
NHC	N-Heterocyclic carbene
NIS	N-Iodosuccinimide
NMR	Nuclear magnetic resonance
ns	Nanosecond
o	ortho
oct	Octyl
p	para
PDI	Polydispersion index
Ph	Phenyl
PFA	Perfluoroalkoxy alcane polymer
Phe	Phenylalanine
phen	1,10-phenanthroline
poly	Polymers
ppm	Parts per million
pKa	Acid dissociation constant at logarithmic scale
Pro	Proline
pTsOH	p-Toluenesulfonic acid
rac	Racemic

r.t.	Room temperature
s	Second
S _N 2	Nucleophilic substitution
t	Triplet
tBu	tert-Butyl
THF	Tetrahydrofuran
TFA	Trifluoroacetic acid
TMEDA	Tetramethylethylene diamine
TMS	Trimethylsilyl
Tol	Tolyl
UV	Ultraviolet
vis	Visible
°	Degree
%	Percent

À André,

À ma famille.

*« Most people say that it is the intellect which makes a great scientist.
They are wrong: it is character. »*
- Albert Einstein

Acknowledgements

“Isn’t it funny how day by day nothing changes, but when you look back everything is different?” – C.S. Lewis

The past five years in grad school have been the absolute best and worst of my life all wrapped into one but looking back at it now, I would do it all over exactly the same way. Every success made me want to push ever harder, so did every hurdle. I was blessed to meet many amazing people without whom I couldn't have done any of this.

First, I would like to thank my supervisor, now turned friend, Shawn. They say “you live and you learn” but you never actually know *who* is going to teach you. I sincerely appreciate all the time you took to teach me. You are the chemist with the biggest heart that I know and I hope you keep doing science with the same passion for a long time! Thank you for believing in me every step of the way and for pushing me to be the best I could. I’m proud to be part of the great Collins family!

All the years wouldn't have been the same without all the Collins group members. We shared everything, from laughter to tears. I couldn't have done it without all of you! First, the “old gang”: Phil, Marie-Eve, Tatiana, Mike, Tito. Thank you for being so welcoming and wonderful! Phil, even if you often took over all of our bench, I’m gonna miss our afternoon of discussion and karaoke. Tito, I admire how dedicated to your work and your family you have been over the years. No one could have done a better “senior of the lab” job than you. I’m sure that “the *best* is yet to come” for you! Mike, the lab wouldn't have been the same without the joy (and hot sauce!) that you brought. I’m lucky to consider you my friend; you were always there to lend an helping hand and I truly appreciate it. Anna, the two years you were here were simply the best! Your presence always light up the room and it was an honour for me to be

part of your pyrene project. Thanks for teaching me how to be fabulous! I hope all of your dreams come true.

Second, the “new gang” : Mylène, Maddawg, Jeff, Antoine, Junior, Émilie and Éric. Mylène, thank you for being the designated grammar nazi of the lab and taking care of all of our social outings! Maddawg, it was nice sharing the vaniprevir project with you, I hope you keep dancing! Jeff, I can’t thank you enough for all the good times we have had together (in and out of the lab!). I really loved working with you on projects; Zearalane will forever be our baby! It was great being part of “team macro” with all of you. Antoine, I couldn't have asked for a better “son”, you had a way of putting everybody in a good mood. I hope you don't starve once I’m gone and cannot feed you anymore! Junior, you are the sassiest chemist I’ve ever met, keep on being fabulous! Emiric, you guys are the cutest chemistry couple ever. I hope you guys have a great life together in the apartment. A very special thanks to Mike and Jeff who took the time to read over my thesis.

I also had the chance of working with three wonderful stagiaires: Sophie, Florence and Émilie. I was really lucky to be able to supervise you, these summer passed by so fast. Sophie, thanks for being so entertaining and so positive with the steep learning curve of flow! Florence, you were a joy to work with and I hope to visit you in Belgium sometime. Émilie, you are the sweetest person I’ve ever had the chance to meet. I’m so proud of all of you; you girls rock!

I would also like to acknowledge all the other chemist from the UdeM that made my Ph.D. years so memorable! First, our next door neighbour, the Schmitzer group: Vincent, your music will keep on inspiring me. Vanessa, I love you my fabulous babi, you're the best and I

hope we can flow together sometime! Julie, Julien, Solène and Audrey you guys were the greatest neighbour of all time, I'll miss you deeply. Second, the Charette and Lebel group, our organic partners: Louis-Philippe, Soula, Léa, Daniella, Carolyn, Éric, Guillaume, William, Patrick, Dominic, Sylvain, Guillaume and Carl, Nicolas, Johan, Henri, Laura, Maroua. And finally the Hanessian boys: Stephane, Rob and Etienne. I consider you guys like brothers. It was a real pleasure discussing chemistry with all of you! A special thanks to Éric Levesque for the continuous flow schemes; you have a undeniable talent.

I would also like to acknowledge the UdeM support team. The NMR people, Sylvie, Antoine and Cédric who were always available to help me. Also, the MS people, Marie-Christine, Karine and Alexandra who were very patient with all the work I kept sending! A special thanks to all the support people, the secretaries and in particular Barbara, you are an angel.

I would also like to thank Isabelle, Joe, Pam and Marie-Eve from the Beauchemin lab. You showed me everything I know about chemistry and I'll forever be grateful! Isabelle, everytime I do something, I always think : WWID and make sure I do it right!

I wouldn't have survived the past few years without any of these people and some good music to dance to in the lab! Beyoncé, Drake and The Fray also deserve a big thank you for their constant support while I worked!

None of thing could have happenned without the financial support that I received from NSERC and FQRNT. I was trully blessed during my Ph. D. and I'll be forever grateful for the confidence that was placed in me. I've done my very best everyday and will keep doing so.

On a personal note, I would like to thank my family. Mom and Dad, your faith in me is unbreakable. Not many people can say that their parent are also their best friends, but I was blessed with the smartest, most wonderful and craziest parents ever! You made me the woman I am today. Frank, you're probably the most brilliant and most genuine person I know. You are the most wonderful brother in the world! I love you guys more than everything.

André, mon amour, I'm not sure how I found you, but you definitively changed my life for the better. You are the strongest, kindest and most passionate person I know. You inspire me to become a better person everyday. Thank you infinitely for everything that you've done for me. I cannot wait for the next chapter of our lives! You are simply my everything.

Chapitre 1 : Introduction

Macrocyclization is a fundamentally important and challenging transformation in organic synthetic chemistry. Despite the level of interest in macrocycles, research aimed at developing sustainable strategies in macrocyclization are still rare.¹ The lack of sustainable approaches to prepare macrocycles is surprising, given how the principles of green chemistry have influenced synthetic organic chemists to promote a more responsible and environmentally benign approach in science.² The following thesis describes the development of a novel approach aimed at improving the efficiency of macrocyclization reactions through the control of dilution effects. A “phase separation” strategy that allows for macrocyclization to be conducted at higher concentrations was developed relying on an aggregated solvent mixture controlled by a poly(ethylene glycol) (PEG) co-solvent. The subsequent introduction to the thesis will first discuss the importance and applications of macrocycles, including a brief description of the challenges and general solutions associated with their synthesis. Following the general section on macrocycles, an introduction to the properties and uses of poly(ethylene glycol) in synthetic organic chemistry will be presented (Chapter 2.2). An overview of concepts such as aggregation, phase transfer catalysis and micellar catalysis will also be presented, as they provide a background for the understanding of the mechanism of the “phase separation” strategy. The novel strategy was initially developed with the Glaser-Hay oxidative coupling of alkynes (Chapter 2.1) and later applied to continuous flow condition. An overview of the reaction as well as a brief introduction to continuous flow chemistry (Chapter 7) will be presented. Finally, copper-catalyzed alkyne-azide cycloadditions will be introduced (Chapter 9) as the “phase separation” strategy was later

applied to the synthesis of triazole containing medicinally relevant macrocycles (Chapter 10 and 11).

1.1 – The Importance and Applications of Macrocycles

Formally, macrocycles are defined by IUPAC as a ring architecture comprising of 12 or more atoms in the ring.³ Noteworthy, it is common in the literature that >8-membered ring sizes are considered macrocycles. As they occupy a unique chemical space, their distinctive properties have impacted many areas of chemistry including medicinal chemistry, the development of conjugated materials, perfumery and supramolecular chemistry.

1.1.1 – Medicinal Chemistry

In medicinal chemistry, macrocyclic structures provide a compromise between optimal structural preorganization, that moderates the entropic factors upon binding onto a biological target, and flexibility to adjust to the active site.⁴ Although the structural properties of macrocycles makes them potential drug candidates, macrocycles are only scarcely explored in medicinal chemistry.⁵ The lack of interest may be due to the acceptance of Lipinski's rule of five^{6,7} as the predominant guidelines for identifying desirable drug candidates in the pharmaceutical industry. Due to their prohibitively large molecular weight, the integration of macrocyclic structures in medicine has been limited despite their known therapeutic potential.^{4-5,8} Some exceptions include naturally occurring macrocycles such as erythromycin **1.1** (Figure 1.1a) or vancomycin, two potent antibiotics that can be isolated and produced from a bacterial source in significant quantities. Rapamycin **1.2** (Figure 1.1b) is another naturally occurring macrocycle that is

used as an immunomodulator for cancer therapy.⁹ Macrocyclic peptides are also prominent drug candidates due to their efficiency at modulating protein-protein interactions (PPIs), a challenge not easily solved by small molecule therapeutics.⁴⁻⁵ For example, macrolactone **1.3** (Figure 1.1c) can modulate PPIs of the Sonic hedgehog (Shh) pathway, a key factor in embryonic development.¹⁰ Furthermore, large ring compounds with low molecular weights (<500 g/mol) can also possess interesting biological activity as MacPherson reported macrocycle **1.4**, a small molecule neutral endopeptidase (NEP) inhibitor (Figure 1.1d), implicated in cardiovascular diseases.¹¹

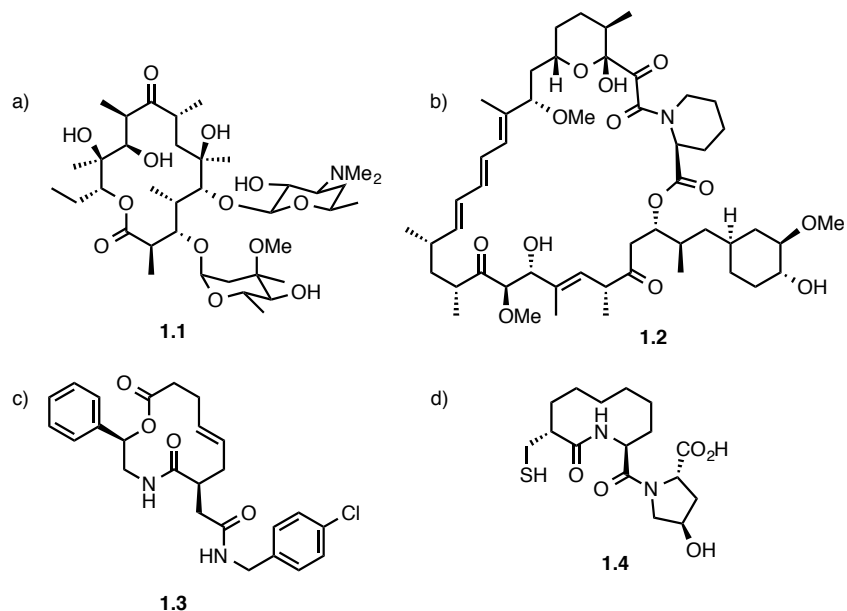


Figure 1.1 – Structures of biologically active macrocycles. a) erythromycin **1.1**, b) rapamycin **1.2**, c) Sonic hedgehog modulator **1.3**, d) neutral endopeptidase inhibitor **1.4**.

1.1.2 – Macrocycles in Conjugated Materials

Porphyrin is one of the most widely known macrocycles. Its planar cyclic structure makes it Nature's ligand of choice for metal ion integration. For example, the cofactor of hemoglobin, heme B **1.5** (Figure 1.2a), integrates a Fe^{2+} cation, allowing for oxygen transport in the human body.¹² Light-harvesting in plants also relies on conjugated macrocycle chlorophyll *c* bearing a Mg^{2+} cation at its center.¹³

In material sciences, the study of shape persistent conjugated macrocyclic structures attracts significant research interest since they can be used as building blocks for nanotubes or 2D porous materials.¹⁴ A recognized family of conjugated macrocycles are annulenes, such as [14]annulene **1.6** (Figure 1.2b). Interestingly, the alkyne moiety is often used in the synthesis of conjugated, shape persistent macrocycles due to its well-defined geometry (typically 180°) and ability to rigidify the parent structures. For example, diethynylcarbazole macrocycle **1.7** (Figure 1.2c) has been reported to display interesting optical, electronic and magnetic properties.¹⁵

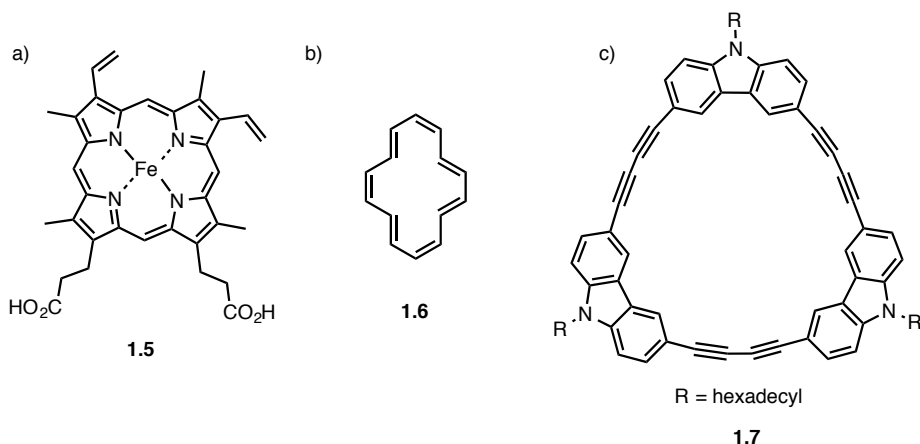


Figure 1.2 – Structures of conjugated macrocycles. a) heme B **1.5**, b) [14]annulene **1.6**, c) diethynylcarbazole macrocycle **1.7**.

1.1.3 – Macrocycles in Perfumery

The quest for new flavors and fragrances continues to be an active field of both academic and industrial importance.¹⁶ In the 1920's, muscone **1.8** (Figure 1.3a), a macrocyclic musk, was extracted from the musk deer apocrine glands. The death of the animal was a prerequisite for the extraction of the scent. Historically, the word “musk” is derived from the Sanskrit *muská*, which means testicle, and refers to the fragrant secretions of the apocrine glands of the male musk deer (*Moschus moschiferus*), a small asian deer.¹⁷ Other animals have also been scavenged and a large family of odorant macrocyclic ketones have been isolated. Moreover plants have also been investigated in the quest for new perfumes.¹⁸ Intriguingly, animal sources yielded macrocyclic ketone containing musks such as muscone **1.8**, while vegetable sources provided macrocyclic ester containing scents such as exaltolide **1.9** and isoambrettolide **1.10** (Figure 1.3 b and c, respectively).^{16,19}

Macrocyclic musks are of interest to the perfume industry as they have unique odor properties and possess superior biodegradability over polycyclic or nitro-containing musks.¹⁶ While the synthesis of macrocyclic musks was initially prohibitively challenging,¹⁹ their synthesis was rigorously optimized and they can now be manufactured on industrial scale; macrocyclic musks are commonly found in fine fragrances, shampoos, shower gels, soaps and detergents.^{16,18}

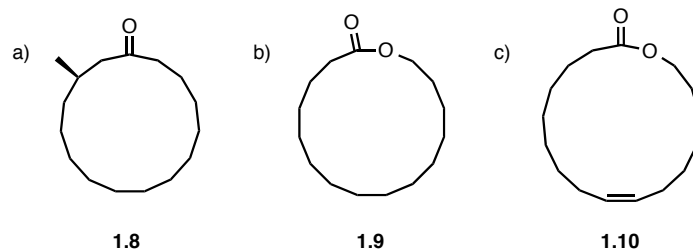


Figure 1.3 – Structures of macrocyclic musks. a) muscone **1.8**, b) exaltolide **1.9**, c) isoambrettolide **1.10**.

1.1.4. – Macrocycles in Supramolecular Chemistry

Heteroatom rich macrocycles are often used in supramolecular chemistry to take advantage of their available lone pairs in a cooperative manner.²⁰ One example of such macrocycles are cyclodextrins (CD), cyclic oligomers of α -D-glucopyranose. The smallest cyclodextrin known is α -CD **1.11** (Figure I.4a) incorporating six glucose units. α -CD **1.11** is used in the food industry as soluble dietary fiber.²¹ CDs have also found applications in drug delivery since their hydrophobic interior cavity can accommodate organic molecules while their hydrophilic exterior ensures solubility in aqueous media.²² Crown ethers such as [18]-crown-6 **1.12** (Figure 1.4b) are also widely exploited in supramolecular chemistry for their ability to coordinate cations.²³ The 1987 Nobel Prize in Chemistry rewarded, in part, Charles Petersen for his synthesis and studies on cyclic polyethers.²⁴ An additional example of a heteroatom rich macrocycle is the anti-cancer agent AFP-Cide **1.13** (Figure I.4c), whose core is derived from DOTA (1,4,7,10-tetraazacyclododecane-1,4,7,10-tetraacetic acid), a 12-membered macrocycle that can chelate and deliver a radioactive ytterbium isotope ($^{90}\text{Y}^{3+}$) while being linked with the Tacatuzumab antibody.²⁵

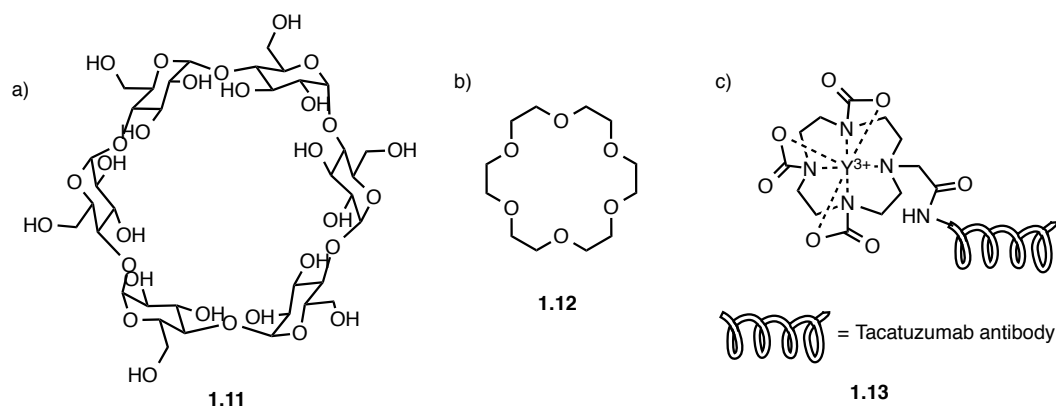
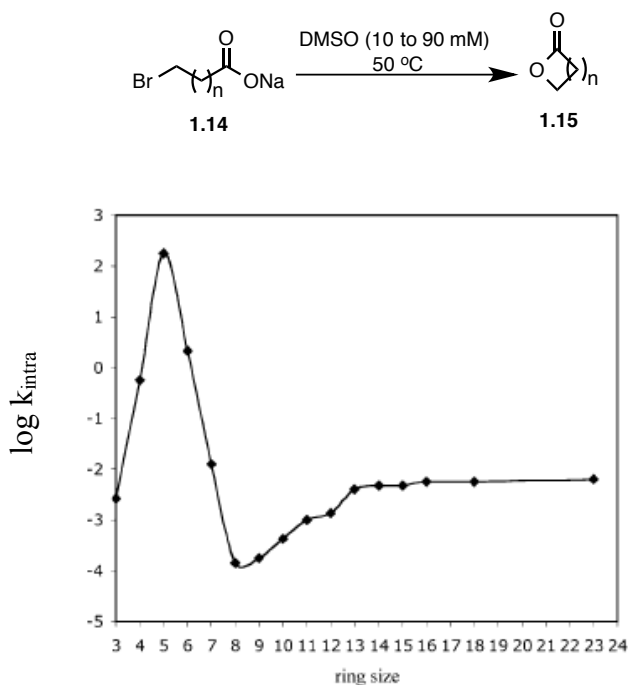


Figure 1.4 – Structures of macrocyclic supramolecules. a) α -cyclodextrin **1.11**, b) [18]-crown-6 **1.12**, c) AFP-Cide **1.13**.

1.2 – Synthetic Challenges Associated with Macrocyclization

The synthetic challenges associated with macrocyclization reactions have been widely recognized by the scientific community.²⁶ There are both entropic and enthalpic obstacles associated with the synthesis of large ring compounds. The first to overcome is related to entropy. It has been demonstrated by Illuminati and Mandolini that the probability of an encounter between two reactive functionalities decreases as the number of atoms between them increases.²⁷ Enthalpy is the second obstacle to surmount. The enthalpy of activation associated with a macrocyclization reaction arises from three components: 1) bond opposition forces due to imperfect staggering or torsional strain (Pitzer strain); 2) deformation of bond angles (Baeyer strain) and 3) transannular strain due to repulsive steric interactions from atoms across the ring (Prelog strain).²⁸ In medium-sized rings, the entropic factor is outweighed by the enthalpic factor due to substantial ring strain. In larger rings, the entropic factor increases, but as the ring strain decreases, so does the enthalpic factor. Chemists tend to summarize the aforementioned

data with the reactivity profile graph for lactone **1.15** formation *via* S_N2 from the corresponding bifunctional precursor **1.14** (Scheme 1.1, *top*) and the graph is often used as a guideline for macrocyclization (Scheme 1.1, *bottom*). As depicted in the graphic, 4 to 6-membered rings have the highest rate of cyclization, while medium-sized rings (8 to 12-membered rings) are the most challenging size to prepare as they have the lowest rate of intramolecular ring closure (k_{intra}).²⁹ Macrocycles ranging from 13 to 24-membered rings tend to have the similar rate of ring closure which are comparable to those for 3 or 7-membered rings.

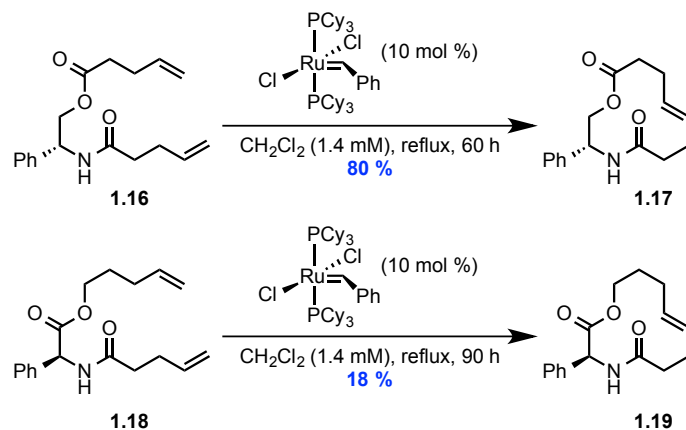


Scheme 1.1 – (*top*) Lactone **1.15** formation reaction for the corresponding bifunctional precursor **1.14** and (*bottom*) reactivity profile in function of the ring size formed. (Reproduced with permission from ref 22. Copyright 1981 American Chemical Society.)

In order to compare the relative efficiency of a wide range of macrocyclization reactions, an index (Emac) was developed by James and co-workers in 2012 based on a literature review.³⁰ They surveyed 896 macrocyclization reactions from 327 publications. The “Emac” is a comparative index that takes into account the yield of the reaction as well as its concentration and is defined as : $Emac = \log_{10}(Y^3 \times C)$, where Y is the yield in % and C the concentration in mM. In the index, the yield of the reaction is worth three times the importance of the concentration. Arguably, the most common solution to the challenges associated with large ring synthesis is to perform the reaction under high dilution conditions (refer to section 1.3.1), hence the presence of the concentration factor in the “Emac” index. Unfortunately, no parameter for catalytic efficiency, stoichiometric use of reagents, or conformational bias of the precursor are included in the index.

1.2.1 – Reactive Conformation

Neither previous analysis (Scheme 1.1 and “Emac”) take into account any substitution of the linear precursor that could lead to spatial preorganization that would affect the rate of cyclization. Importantly, it has been demonstrated that ring size is not the dictating factor in many macrocyclization reactions, but rather the ease with which the linear precursor can adopt the reactive conformation.^{27,31} A striking example is the macrocyclization by ring-closing metathesis (RCM) of diene precursor **1.16** (Scheme 1.2, *top*). As the precursor can easily adopt the reactive conformation, the cyclization yields 80 % of desired macrocycle **1.17**. On the other hand, the productive conformation is less abundant when the structure of the ester is inverted (the carbonyl has been transposed to the opposite side of the ester oxygen atom). Consequently, diene precursor **1.18** only affords 18 % of the desired macrocycle **1.19**.³²



Scheme 1.2 – The importance of conformation in macrocyclization by RCM.

Unfortunately, successful macrocyclization reactions can not always be predicted *a priori* based on the structure of the linear precursor or desired product. For example, the cyclization of a macropeptide typically involves a retrosynthetic disconnection at the amide bond. When more than one amide is present, multiple disconnections are possible. In Figure 1.4, five disconnections of the five different amide bonds were investigated in an attempt to synthesize the Pro-Ala-Ala-Phe-Leu macrocycle **1.20** using a pentafluorophenyl (Pfp) ester activation strategy in dilute *media*. Each attempt either failed to give the desired product or resulted in low yield.³³ The macrocyclization to form cyclic peptide **1.20** is an example where the stereochemical centers and dense heteroatom functionalities force the compound to adopt conformations that are not conducive to ring closure.

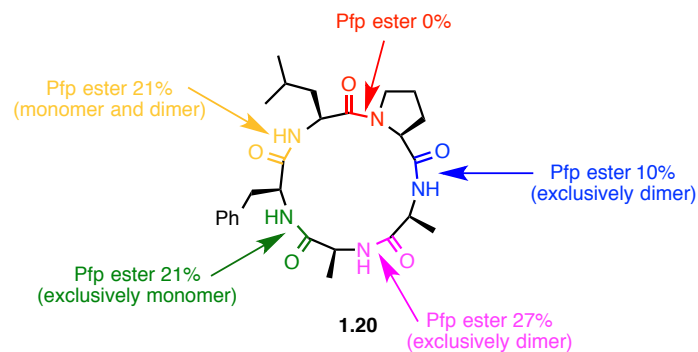
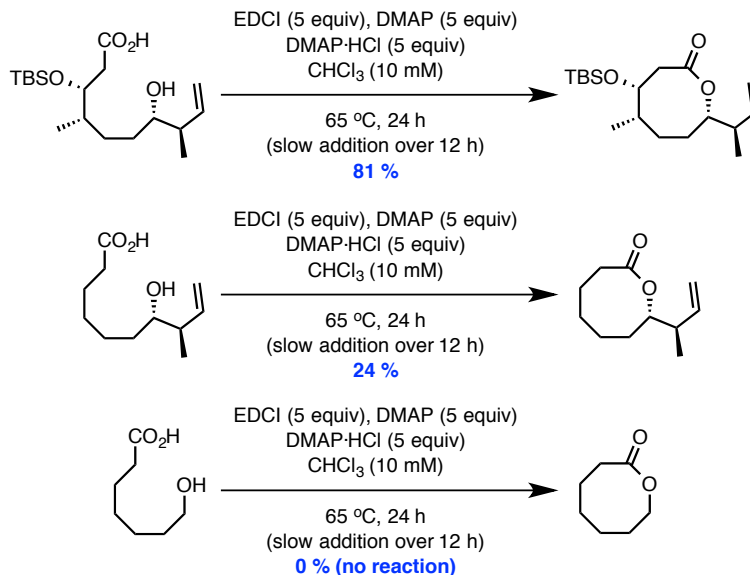


Figure 1.4 – Attempts to synthesize the Pro-Ala-Ala-Phe-Leu macrocycle **1.20** using a Pfp ester activation strategy in dilute media.

Another example where the substituents play an essential role in the cyclization is in the synthesis of 8-membered macrolactones from the corresponding seco-acid derived-octalactins (Scheme 1.3). As discussed previously (Scheme 1.1), 8-membered rings are one of the most challenging ring size to obtain; in the comparative study, the authors had to use an excess of reagents, high dilution and slow addition techniques to favor the intramolecular selectivity (*vide infra*). It was postulated that the precursor adopts a chair-boat conformation with the substituents in pseudoequatorial positions.^{34,35} It is yet the case in the preceding example, the substituents have a positive effect on the rate of the macrocyclization as they decrease the entropic barrier by promoting a favorable conformation. Fully substituted precursor **1.21** yields 81 % of the desired macrocycle **1.22**. Removal of two substituents on precursor **1.23** decreased the cyclization yield to 24 % of macrocycle **1.24**. Unsubstituted seco-acid **1.25** is unreactive in the same reaction conditions and no macrolactone **1.26** is formed.



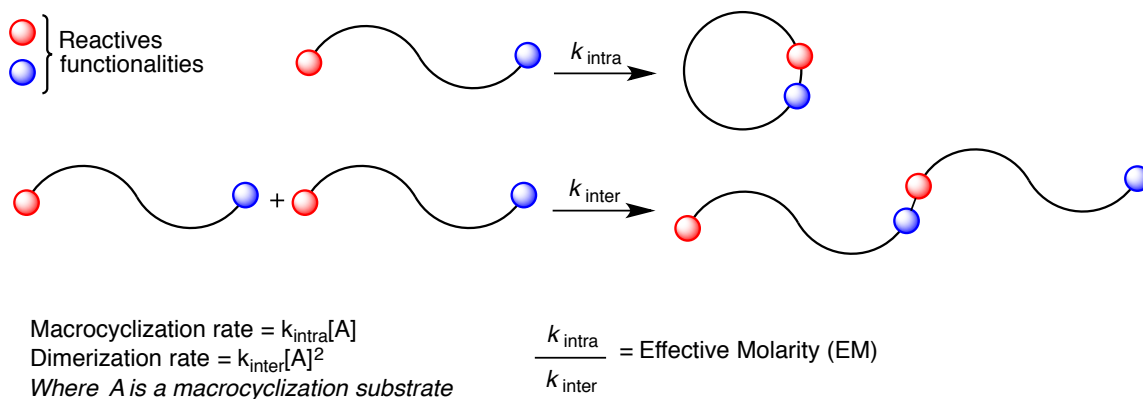
Scheme 1.3. – Macrolactonization of seco-acids derived from octalactins.

1.3 – Traditional Solutions for Macrocyclization Reactions

1.3.1 – High Dilution and Slow Addition

Ruzicka's application of physical chemistry principles to the synthesis of macrocycles³⁶ established that the reaction between two reactive functionalities intramolecularly to yield a macrocycle was a first order reaction. The process is in competition with an intermolecular oligomerization, a second order reaction (Scheme 1.4, *top*). In order to favor the desired intramolecular pathway, Ziegler proposed that the high dilution of a reaction would favor the unimolecular reaction to afford the macrocycle.³⁷ The ratio of the rate constant for the two reactions is referred to as the effective molarity (EM) (Scheme 1.4, *bottom*).³⁸ For an unstrained macrocyclization, the ratio is expected to

be one to one. Unfortunately, ring strain is often present and reduction of the intramolecular rate is observed.



Scheme 1.4 – (top) Rate of macrocyclization vs dimerization and (bottom) effective molarity equation.

The concept of effective molarity can be useful when choosing a concentration at which to run a macrocyclization reaction. As depicted in Figure 1.5, high dilution significantly decreases the rate of intermolecular processes, favouring the desired cyclization. Pfizer Pharmaceutical Sciences reported that the benchmark concentration for a process macrocyclization is 200 mM.³⁰ Similar comments on preferred concentrations were also made in a publication on the synthesis of macrocyclic HCV protease inhibitor BILN 2061 **1.27** (Figure 1.6) from Boehringer Ingelheim Pharmaceuticals (refer to Table 1.1).³⁹ Unfortunately, few macrocyclization reactions can be performed at such high concentration. Typically, a starting point for a tentative cyclization is approximately 2 mM and oftentimes more dilute.³⁰ James and co-workers describe the hypothetical cyclization of a 500 Daltons molecular weight substrate on a kilogram scale (Figure 1.5).³⁰ With the 1000 L of solvent needed at 2 mM to perform a

“selective” macrocyclization, it is obvious that high dilution is not an optimal solution at industrial scales.

Concentration (M)	Macrocyclization rate	Macrocyclization rate	Solvent Volume (L) 1 kg Substrate MW 500
	Dimerization rate	Dimerization rate	
0.2	When $\frac{k_{intra}}{k_{inter}} = 1$ 5	When $\frac{k_{intra}}{k_{inter}} = 0.2$ 1	10
0.02	50	10	100
0.002	500	100	1000

Figure 1.5 – Impact of concentration on ratio of macrocyclization vs dimerization rate and solvent volume.

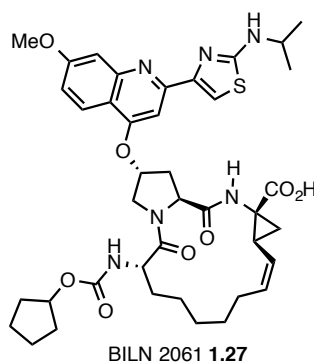
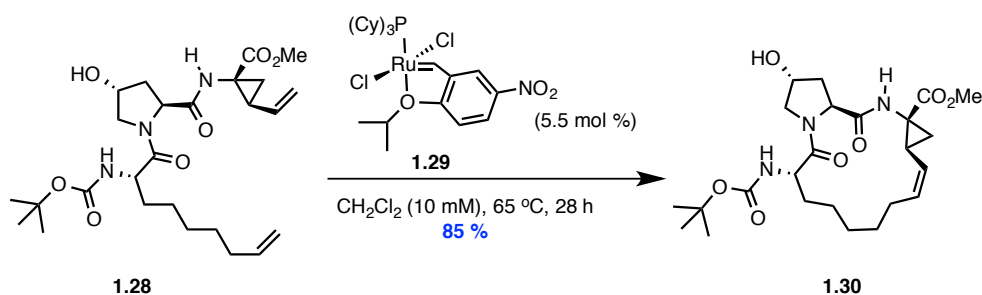


Figure 1.6 – Structure of macrocyclic HCV protease inhibitor BILN 2061 1.27.

A striking example of the industrial challenges associated with macrocyclization is the synthesis of HCV protease inhibitor **1.27** (Figure 1.6). When initially reported, the macrocyclic ring closing metathesis step of linear precursor **1.28** was performed under high dilution conditions (10 mM) with a high catalyst loading (Scheme 1.5) and afforded

the desired macrocycle **1.30** in 85 % yield.⁴⁰ Although the transformation seemed somewhat efficient, it was still far from suitable for industrial production.



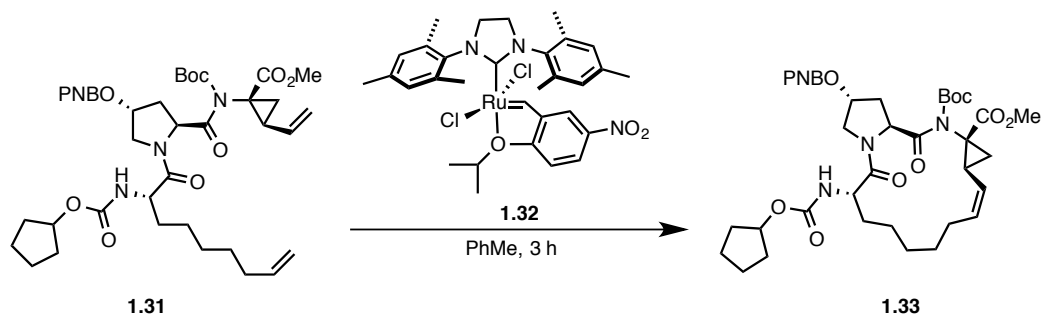
Scheme 1.5 – Initial macrocyclic ring closing metathesis in the synthesis of BILN 2061 **1.30**.

An optimization was performed to render the macrocyclization viable on an industrial level.³⁹⁻⁴¹ Fortunately, the “benchmark” of 200 mM was achieved for the cyclization of diene precursor **1.31** to yield macrocycle **1.33**. As seen in Table 1.1, lower concentrations afforded higher yields (Entry 1 vs 2 and 3). A careful optimization of the structure of the precursor allowed for significant improvement in efficiency and selectivity of the macrocyclization. Moreover, lowering the catalyst loading, while increasing the concentration helped to maintain an intramolecular selectivity (Entry 4 to 7).

An “artificial” way to achieve high dilution conditions is to use a slow addition process where the macrocyclization substrate is slowly added to the reaction mixture, typically *via* a syringe pump. The technique allows the chemist to perform a reaction with less solvent while maintaining a low concentration of the linear precursor in solution.

Although the strategy is efficient at controlling the effective molarity, the setup is tedious and not optimal for industrial scale up.

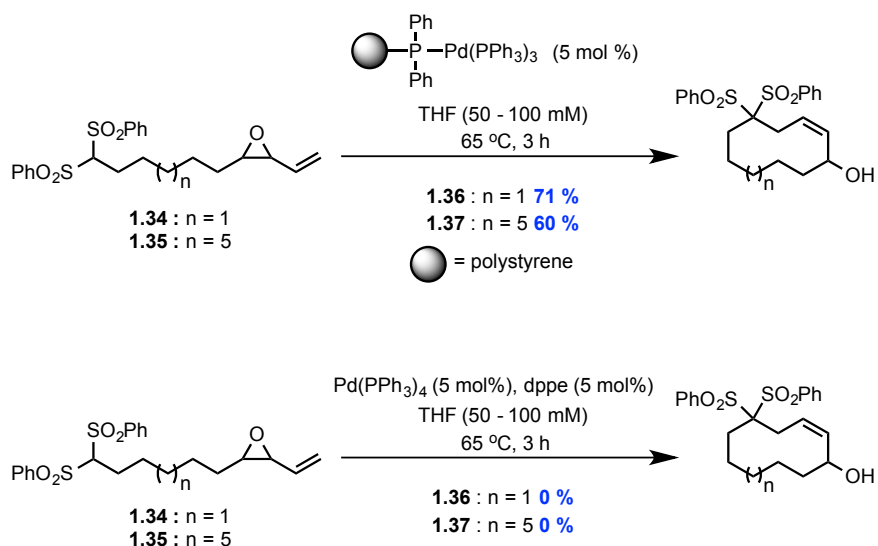
Table 1.1 – Optimization of the macrocyclic ring closing metathesis reaction of **1.31**.



Entry	Concentration (mM)	1.32 (mol %)	Temperature (°C)	Yield (%)
1	10	1	60	98
2	50	1	60	87
3	100	1	60	80
4	50	0.1	110	97
5	100	0.1	110	95
6	200	0.1	110	93
7	400	0.1	110	80

Another means to artificially achieve high dilution is *via* synthesis on solid support. Traditionally used to prepare peptides or oligonucleotides, the technique has demonstrated that having a linear precursor attached on a solid support can create a “pseudo-dilution” effect and increase the yield of the macrocyclization. An example was reported by Trost where the use of a solid-supported palladium catalyst allowed for facile macrocyclization of 10- and 15-membered rings **1.36** and **1.37** in good yields (Scheme

1.6, *top*).⁴² The corresponding reaction in solution (using a soluble catalyst) only formed unwanted oligomerization products (Scheme 1.6, *bottom*).



Scheme 1.6 – Effect of solid supported catalyst on macrocyclic isomerization reaction.

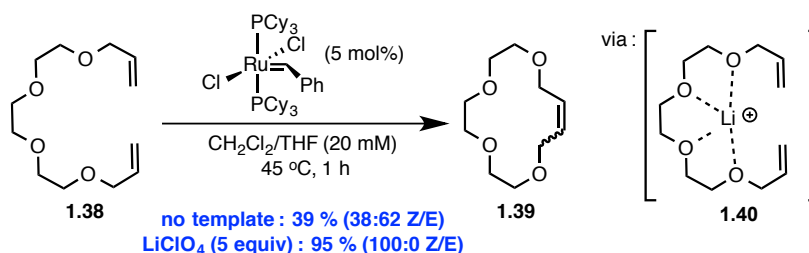
1.3.2 – Conformational Control

An alternative strategy to high dilution/slow addition toward promoting a productive macrocyclization is to favor the end-to-end interactions of the linear substrate, thus facilitating ring closure. Conformational control is a valuable tool that can be used to lower the entropic barrier associated with preorganization of the linear precursor prior to cyclization. Favoring end-to-end interactions and augmenting the rate of macrocyclization (k_{intra}) is often achieved through supramolecular interactions.

1.3.2.1 – Templating and Metal Ion Chelates

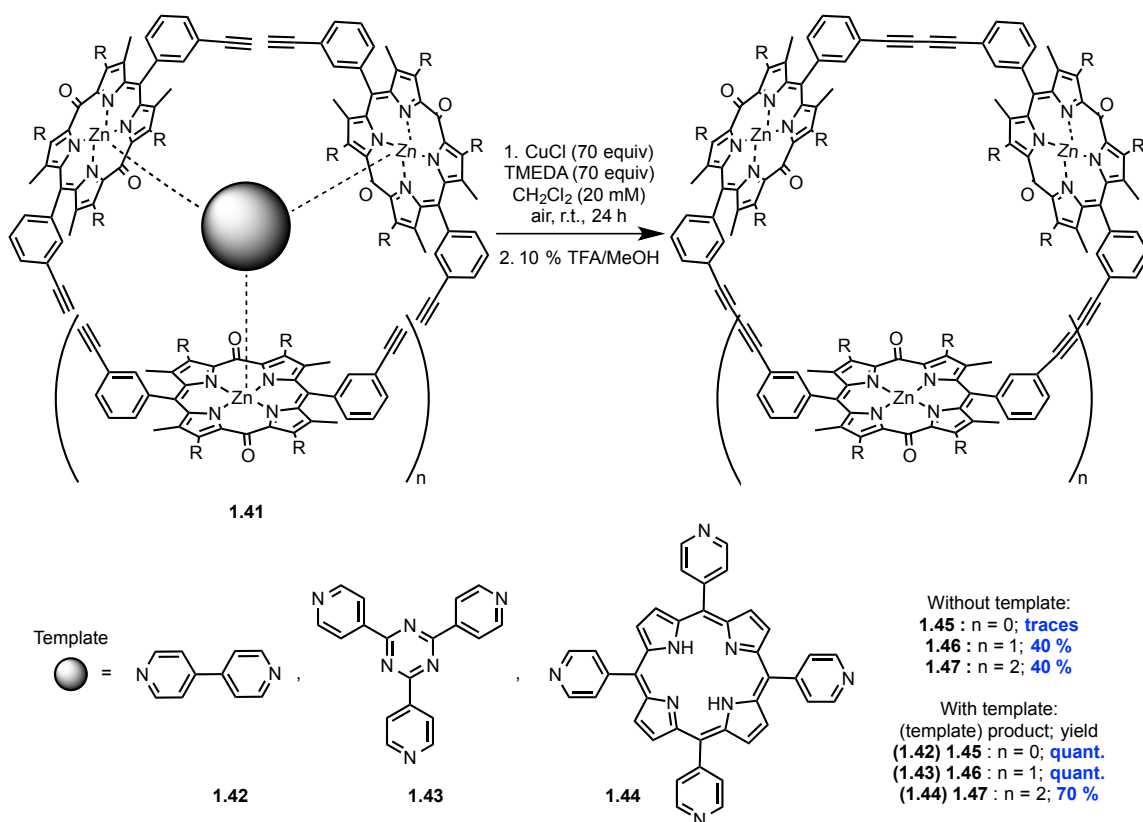
Templating a system to fix its conformation is a well known strategy to promote a macrocyclization. A well known example is the synthesis of crown ethers.^{23a} For example, the efficiency of the macrocyclization to form crown ether-type structure **1.39** is

increased in the presence of a lithium salt, as the complexation of the ether functionalities to the cation prior to ring formation decreases the entropy associated with macrocyclization by bringing the reactive functionalities in close proximity of one another. (Scheme 1.7).



Scheme 1.7 – Lithium salt’s template effect in the synthesis of **1.40**.

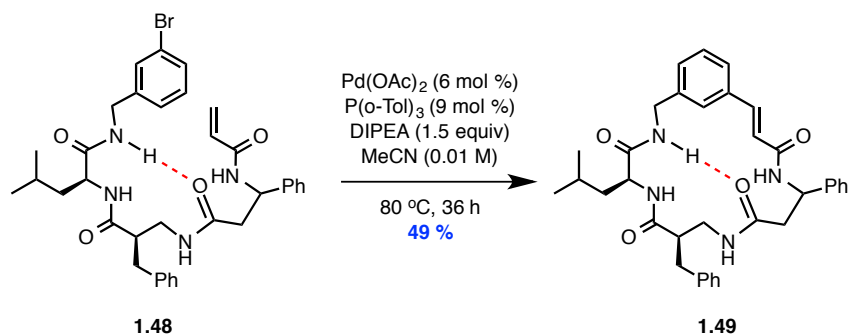
Sanders reported the synthesis of dioxoporphyrin-derived macrocycles by templating with multidentate pyridine based ligands before performing a Glaser-Hay cyclization (Scheme 1.8). It was observed that the shape of the ligand could efficiently direct the formation of the product. Without a template, a mixture of trimer **1.46** and tetramer **1.47** was obtained. Remarkably, cyclic dimer **1.45** was obtained quantitatively when template **1.42** was used, while the use of template **1.43** or **1.44** yielded selectively the trimer **1.46** and tetramer **1.47**, respectively (Scheme 1.8).⁴³



Scheme 1.8 – Synthesis of dioxoporphyrin-derived macrocycles using a template strategy.

1.3.2.2 – H-Bonding Interactions

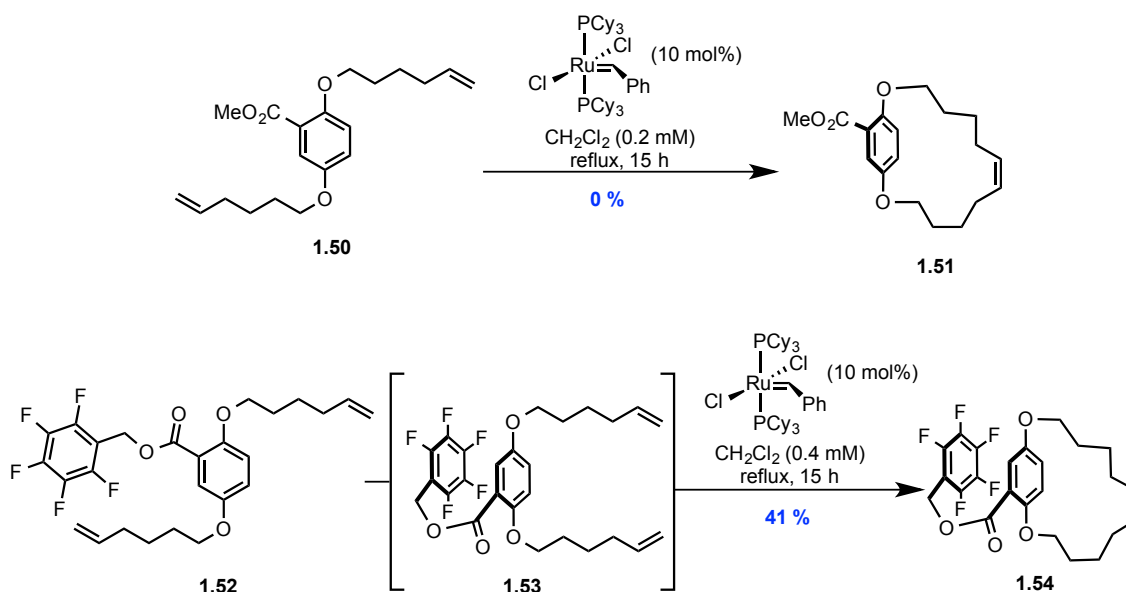
Intramolecular hydrogen (H)-bonding interactions can also assist in the preorganization of a linear precursor to favor productive macrocyclization.^{33,44} The synthesis of cyclic tripeptides *via* Heck reaction exploits transannular H-bonds. The authors noted that the presence of an intramolecular H-bond interaction locks the linear precursor **1.48** into a conformation resembling a peptidic β -turn (Scheme 1.9). The presence of the intramolecular H-bond in both the precursor **1.48** and the cyclized product **1.49** was confirmed by variable temperature NMR experiments.⁴⁵ The strategy has been extensively used in the synthesis of peptide-containing macrocycles.^{33,44}



Scheme 1.9 – Synthesis of small cyclic peptide **1.49** via Heck reaction assisted by an intramolecular H-bond interaction.

1.3.2.3 – Auxiliary Based Methods

Another supramolecular approach used to favor productive conformations for macrocyclization is through supramolecular π -stacking interactions. An example is in the synthesis of rigid cyclophane structures which is challenging even under high dilution conditions.⁴⁶ When diene precursor **1.50** is submitted to a ruthenium-based catalyst to perform a macrocyclic ring-closing metathesis, no desired product **1.51** is formed and only oligomerization products are obtained (Scheme 1.10, *top*). Collins reported the use of an electron-poor aryl group as a conformational control element (CCE) to promote macrocyclization.⁴⁷ The π -stacking interaction allows precursor **1.52** to adopt a productive conformation **1.53** which is productive for macrocyclization, affording 41 % yield of the cyclophane **1.54** (Scheme 1.10, *bottom*).



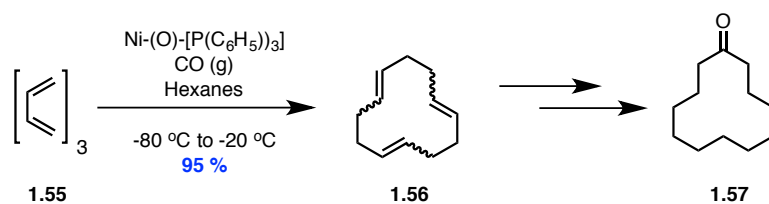
Scheme 1.10 – Synthesis of cyclophane macrocycle **1.54** using a CCE.

1.4 – Alternative Solutions for Macrocyclization Reactions

Alternatives to the high dilution and conformational control strategies for macrocyclization have been developed. In order to avoid the tedious macrocyclization step, cycloadditions, ring expansions or fragmentations have been employed for the formation of macrocyclic compounds.

1.4.1 – Cycloaddition

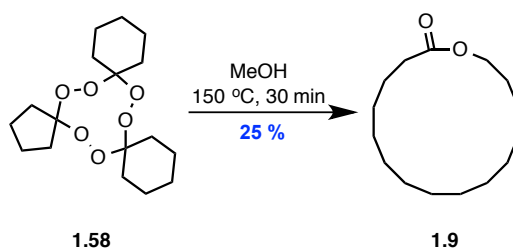
The Wilke trimerization reaction of diene **1.55** is a nickel catalyzed [4+4+4] cycloaddition that affords 12-membered macrocycle **1.56** in 95 % yield (Scheme 1.11).⁴⁸ The trienic **1.56** macrocycle can then easily be converted in two steps to the corresponding cyclododecanone **1.57**. Cyclododecanone **1.57** is noteworthy as it is produced on industrial scale at more than 100,000 tons per year.¹⁹



Scheme 1.11 – Wilke’s trimerization and synthesis of cyclododecanone.

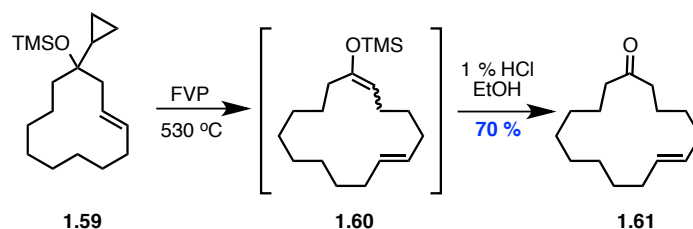
1.4.2 – Ring Expansion and Fragmentation

The Story synthesis of exaltolide **1.9** was discovered in 1968 and involves a thermal or photochemical decomposition of trisepoxide **1.58** (Scheme 1.12).⁴⁹ It should be noted that the strategy can be used to form various ring sizes depending on the number of carbons in the peroxide precursor.



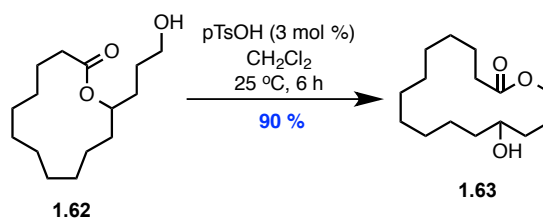
Scheme 1.12 – Story synthesis of exaltolide *via* ring expansion.

Starting from commercially available medium-sized rings and proceeding *via* ring expansion is an alternative strategy to obtain macrocycles. Rüedi reported a thermal three-carbon ring expansion from cyclopropane-bearing precursor **1.59** to obtain the corresponding enone **1.60** (Scheme 1.13).⁵⁰ The strategy allows for the formation of macrocyclic musk **1.61** with a well-defined olefin geometry. A ring expansion was also used to obtain the 10-membered macrolactam **1.4** (Figure 1.1d) in the synthesis of a NEP inhibitor by MacPherson.¹¹



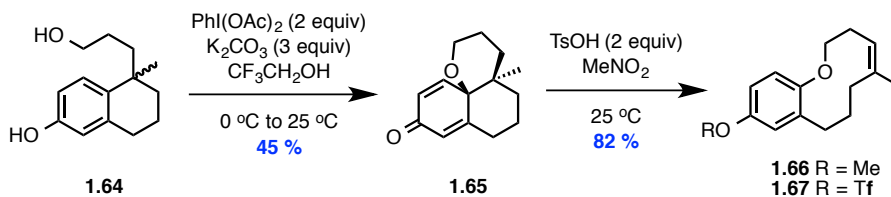
Scheme 1.13 – Cyclopropane ring expansion.

Translactonization is a commonly employed ring-expansion strategy. When 12-membered ring lactone **1.62** is submitted to acidic conditions, translactonization to the thermodynamically more stable 15-membered macrolactone **1.63** is observed (Scheme 1.14).⁵¹



Scheme 1.14 – Translactonization strategy for the synthesis of large ring compounds.

Tan and co-workers reported that macrocyclic ketones could also be obtained by Grob fragmentation of a tricyclic system under acidic conditions.⁵² The authors were able to synthesize a library of medium-sized macrocycles using a biomimetic ring expansion strategy (Scheme 1.15). The tricyclic precursor **1.65** can be obtained from the corresponding phenol **1.64** using an hypervalent iodide reagent. It has been proposed that the ring-expansion and subsequent rearomatization reaction of polycyclic structures such as **1.65** could be the biosynthetic route for protostephanine and erythrina alkaloids.⁵³



Scheme 1.15 – Acid-catalyzed ring expansion.

1.5 – Conclusion

The preceding discussion underlines the inherent importance of macrocyclic structures as well as their existing and potential applications. Although several strategies have been developed for the synthesis of these types of structures, the high dilution of the reaction media is the only strategy that is applicable for a wide scope of structures and macrocyclization reactions. With the idea of broadening the use of the dilution control strategy, it is appealing to develop a novel way to control the efficient concentration of the reaction in order to render it more environmentally benign. The phase separation strategy discussed herein allows to perform macrocyclization reactions up to 500 times the “traditional” high-dilution concentration while relying on the key control of dilution effects. The strategy has already been applied to three key bond forming macrocyclic reactions : Glaser-Hay oxidative coupling of alkynes, azide-alkyne cycloaddition and metathesis (not reviewed herein).

1.6 – Bibliography

- (1) Roxburgh, C. J. *Tetrahedron* **1995**, *51*, 9767-9822.
- (2) Beach, E. S.; Cui, Z.; Anastas, P. T. *Energy Environ. Sci.* **2009**, *2*, 1038-1049.
- (3) IUPAC. Compendium of Chemical Terminology, 2nd ed. (the "Gold Book"). Compiled by A. D. McNaught and A. Wilkinson. Blackwell Scientific Publications, Oxford (1997).
- (4) Driggers, E. M.; Hale, S. P.; Lee, J.; Terrett, N. K. *Nat Rev Drug Discov* **2008**, *7*, 608-624.
- (5) Marsault, E.; Peterson, M. L. *J. Med. Chem.* **2011**, *54*, 1961-2004.
- (6) Lipinsky's rule of 5 : 1) No more than 5 hydrogen-bond donor 2) No more than 10 hydrogen-bond acceptor 3) Molecular weight less than 500 4) LogP not greater than 5
- (7) Lipinski, C. A.; Lombardo, F.; Dominy, B. W.; Feeney, P. J. *Adv. Drug Del. Rev.* **1997**, *23*, 3-25.
- (8) Collins, J. C.; Farley, K. A.; Limberakis, C.; Liras, S.; Price, D.; James, K. *J. Org. Chem.* **2012**, *77*, 11079-11090.
- (9) Dumont, F. J.; Su, Q. *Life Sciences* **1995**, *58*, 373-395.
- (10) a) Stanton, B. Z.; Peng, L. F. *Molecular BioSystems* **2009**, *6*, 44-54; b) Stanton, B. Z.; Peng, L. F.; Maloof, N.; Nakai, K.; Wang, X.; Duffner, J. L.; Taveras, K. M.; Hyman, J. M.; Lee, S. W.; Koehler, A. N.; Chen, J. K.; Fox, J. L.; Mandinova, A.; Schreiber, S. L. *Nat Chem Biol* **2009**, *5*, 154-156.
- (11) MacPherson, L. J.; Bayburt, E. K.; Capparelli, M. P.; Bohacek, R. S.; Clarke, F. H.; Ghai, R. D.; Sakane, Y.; Berry, C. J.; Peppard, J. V.; Trapani, A. J. *J. Med. Chem.* **1993**, *36*, 3821-3828.
- (12) Heme, B. F. *Adv. Prot. Chem.* **1964**, *19*, 73.
- (13) Rothmund, P. *J. Am. Chem. Soc.* **1936**, *58*, 625-627.
- (14) Iyoda, M.; Yamakawa, J.; Rahman, M. J. *Angew. Chem. Int. Ed.* **2011**, *50*, 10522-10553.
- (15) Zhao, T.; Liu, Z.; Song, Y.; Xu, W.; Zhang, D.; Zhu, D. *J. Org. Chem.* **2006**, *71*, 7422-7432.
- (16) Kraft, P. In *Chemistry and Technology of Flavors and Fragrances*; Blackwell Publishing Ltd.: 2009, p 143-168.
- (17) Sokolov, V. E.; Kagan, M. Z.; Vasilieva, V. S.; Prihodko, V. I.; Zinkevich, E. P. *J Chem Ecol* **1987**, *13*, 71-83.
- (18) Sell, C. In *The Chemistry of Fragrances: From Perfumer to Consumer (2)*; Sell, C. S., Ed.; The Royal Society of Chemistry: 2006, p 24-51.
- (19) Williams, A. S. *Synthesis* **1999**, *1999*, 1707-1723.
- (20) a) Steed, J. W.; Atwood, J. L. In *Supramol. Chem.*; John Wiley & Sons, Ltd: 2009, p 223-284; b) Steed, J. W.; Atwood, J. L. In *Supramol. Chem.*; John Wiley & Sons, Ltd: 2009, p 105-222.
- (21) Artiss, J. D.; Brogan, K.; Brucal, M.; Moghaddam, M.; Jen, K. L. C. *Metabol. Clin. Exp.*, *55*, 195-202.
- (22) Crini, G. *Chem. Rev.* **2014**, *114*, 10940-10975.
- (23) a) Pedersen, C. J. *J. Am. Chem. Soc.* **1967**, *89*, 7017-7036; b) Pedersen, C. J. *J. Am. Chem. Soc.* **1967**, *89*, 2495-2496.

- (24) http://www.nobelprize.org/nobel_prizes/chemistry/laureates/1987/ (consulted April 14th, 2015)
- (25) Stasiuk, G. J.; Long, N. J. *Chem. Commun.* **2013**, *49*, 2732-2746.
- (26) Galli, C.; Mandolini, L. *J. Chem. Soc., Chem. Commun.* **1982**, 251-253.
- (27) Illuminati, G.; Mandolini, L. *Acc. Chem. Res.* **1981**, *14*, 95-102.
- (28) Allinger, N. L.; Tribble, M. T.; Miller, M. A.; Wertz, D. H. *J. Am. Chem. Soc.* **1971**, *93*, 1637-1648.
- (29) a) Parenty, A.; Moreau, X.; Campagne, J. M. *Chem. Rev.* **2006**, *106*, 911-939; b) Galli, C.; Illuminati, G.; Mandolini, L. *J. Am. Chem. Soc.* **1973**, *95*, 8374-8379.
- (30) Collins, J. C.; James, K. *MedChemComm* **2012**, *3*, 1489-1495.
- (31) Blankenstein, J.; Zhu, J. *Eur. J. Org. Chem.* **2005**, *2005*, 1949-1964.
- (32) Lee, D.; Sello, J. K.; Schreiber, S. L. *J. Am. Chem. Soc.* **1999**, *121*, 10648-10649.
- (33) Yudin, A. K. *Chem. Sci.* **2015**, *6*, 30-49.
- (34) Andrus, M. B.; Argade, A. B. *Tetrahedron Lett.* **1996**, *37*, 5049-5052.
- (35) Buszek, K. R.; Jeong, Y.; Sato, N.; Still, P. C.; Muiño, P. L.; Ghosh, I. *Synth. Commun.* **2001**, *31*, 1781-1791.
- (36) Ruzicka, L.; Stoll, M.; Schinz, H. *Helv. Chim. Acta* **1926**, *9*, 249-264.
- (37) Ziegler, K.; Eberle, H.; Ohlinger, H. *Justus Liebigs Annalen der Chemie* **1933**, *504*, 94-130.
- (38) Illuminati, G.; Mandolini, L.; Masci, B. *J. Am. Chem. Soc.* **1977**, *99*, 6308-6312.
- (39) Shu, C.; Zeng, X.; Hao, M.-H.; Wei, X.; Yee, N. K.; Busacca, C. A.; Han, Z.; Farina, V.; Senanayake, C. H. *Org. Lett.* **2008**, *10*, 1303-1306.
- (40) Faucher, A.-M.; Bailey, M. D.; Beaulieu, P. L.; Brochu, C.; Duceppe, J.-S.; Ferland, J.-M.; Ghiro, E.; Gorys, V.; Halmos, T.; Kawai, S. H.; Poirier, M.; Simoneau, B.; Tsantrizos, Y. S.; Llinàs-Brunet, M. *Org. Lett.* **2004**, *6*, 2901-2904.
- (41) a) Nicola, T.; Brenner, M.; Donsbach, K.; Kreye, P. *Org. Process Res. Dev.* **2005**, *9*, 513-515; b) Yee, N. K.; Farina, V.; Houpis, I. N.; Haddad, N.; Frutos, R. P.; Gallou, F.; Wang, X.-j.; Wei, X.; Simpson, R. D.; Feng, X.; Fuchs, V.; Xu, Y.; Tan, J.; Zhang, L.; Xu, J.; Smith-Keenan, L. L.; Vitous, J.; Ridges, M. D.; Spinelli, E. M.; Johnson, M.; Donsbach, K.; Nicola, T.; Brenner, M.; Winter, E.; Kreye, P.; Samstag, W. *J. Org. Chem.* **2006**, *71*, 7133-7145; c) Farina, V.; Shu, C.; Zeng, X.; Wei, X.; Han, Z.; Yee, N. K.; Senanayake, C. H. *Org. Process Res. Dev.* **2009**, *13*, 250-254.
- (42) Trost, B. M.; Warner, R. W. *J. Am. Chem. Soc.* **1982**, *104*, 6112-6114.
- (43) a) McCallien, D. W. J.; Sanders, J. K. M. *J. Am. Chem. Soc.* **1995**, *117*, 6611-6612; b) Anderson, H. L.; Sanders, J. K. M. *Angew. Chem. Int. Ed.* **1990**, *29*, 1400-1403.
- (44) a) White, C. J.; Yudin, A. K. *Nat. Chem.* **2011**, *3*, 509-524; b) Marsden, J. A.; Miller, J. J.; Haley, M. M. *Angew. Chem. Int. Ed.* **2004**, *43*, 1694-1697; c) Miller, S. J.; Blackwell, H. E.; Grubbs, R. H. *J. Am. Chem. Soc.* **1996**, *118*, 9606-9614.
- (45) Rajamohan Reddy, P.; Balraju, V.; Madhavan, G. R.; Banerji, B.; Iqbal, J. *Tetrahedron Lett.* **2003**, *44*, 353-356.
- (46) Bolduc, P.; Jacques, A.; Collins, S. K. *J. Am. Chem. Soc.* **2010**, *132*, 12790-12791.
- (47) El-Azizi, Y.; Zakarian, J. E.; Boullierand, L.; Schmitzer, A. R.; Collins, S. K. *Adv. Synth. Catal.* **2008**, *350*, 2219-2225.

- (48) Gunther, W.; Borislav, B.; Paul, H.; Michael, K.; Ernst Willi, M. In *Polymerization and Polycondensation Processes*; American Chemical Society: 1962; Vol. 34, p 137-144.
- (49) a) Story, P. R.; Denson, D. D.; Bishop, C. E.; Clark, B. C.; Farine, J. C. *J. Am. Chem. Soc.* **1968**, *90*, 817-818; b) Story, P. R.; Lee, B.; Bishop, C. E.; Denson, D. D.; Busch, P. *J. Org. Chem.* **1970**, *35*, 3059-3062.
- (50) Rüedi, G.; Nagel, M.; Hansen, H.-J. *Org. Lett.* **2004**, *6*, 2989-2991.
- (51) Corey, E. J.; Brunelle, D. J.; Nicolaou, K. C. *J. Am. Chem. Soc.* **1977**, *99*, 7359-7360.
- (52) Fehr, C.; Galindo, J.; Etter, O.; Thommen, W. *Angew. Chem. Int. Ed.* **2002**, *41*, 4523-4526.
- (53) Bauer, R. A.; Wenderski, T. A.; Tan, D. S. *Nat Chem Biol* **2013**, *9*, 21-29.

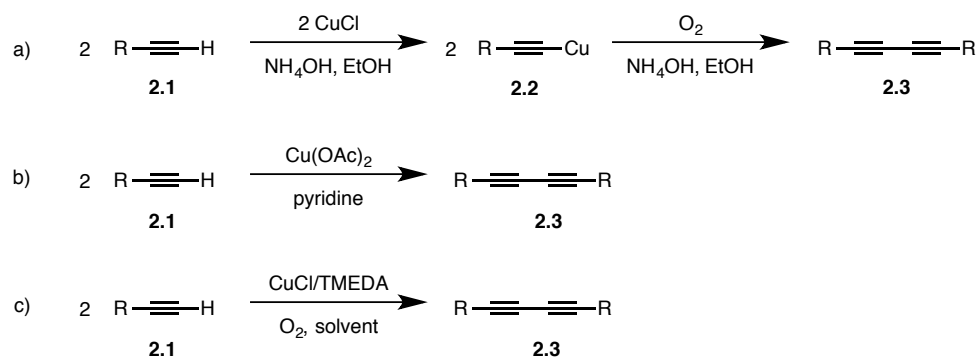
PART 1

Chapter 2 : The Glaser-Hay Oxidative Coupling and an Introduction to Poly(ethylene glycol) Properties

2.1 – Glaser-Hay Reaction

2.1.1 – Seminal Discovery

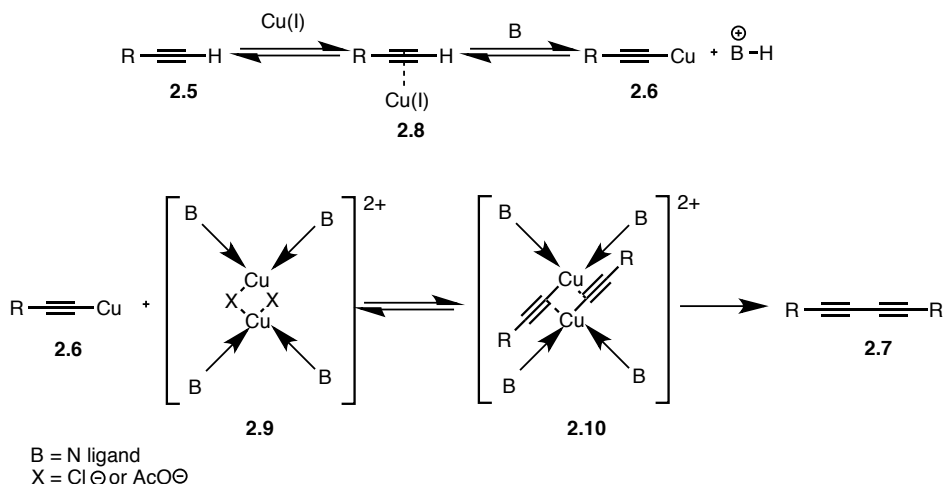
In 1869, Glaser discovered that copper acetylide **2.2** could be dimerized under an oxidative atmosphere to yield the corresponding diyne **2.3** (Scheme 2.1a).¹ Since the isolation of copper acetylide **2.2** is tedious, the reaction did not attract much attention until 1959, when Eglinton discovered that diynes **2.3** could be formed in one pot from terminal alkynes using a stoichiometric amount of a Cu(II) salt in pyridine (Scheme 2.1b).² Subsequently, it was reported that a catalytic amount of Cu(I)/pyridine could also be used in combination with O₂ as a terminal oxidant.^{2,3} Hay reported that the use of a bidentate ligand, such as TMEDA, could form a catalytically active and soluble complex (Scheme 2.1c).³ The Hay modification solved the issues associated with the unreliable solubility of the Cu(I)/pyridine complex in organic solvents. To date, the Glaser-Hay reaction has become a valuable synthetic tool in organic chemistry.⁴



Scheme 2.1 – General reaction conditions for : a) Glaser, b) Glaser-Eglinton and c) Glaser-Hay acetylene coupling reactions.

2.1.2 – Reaction Mechanism

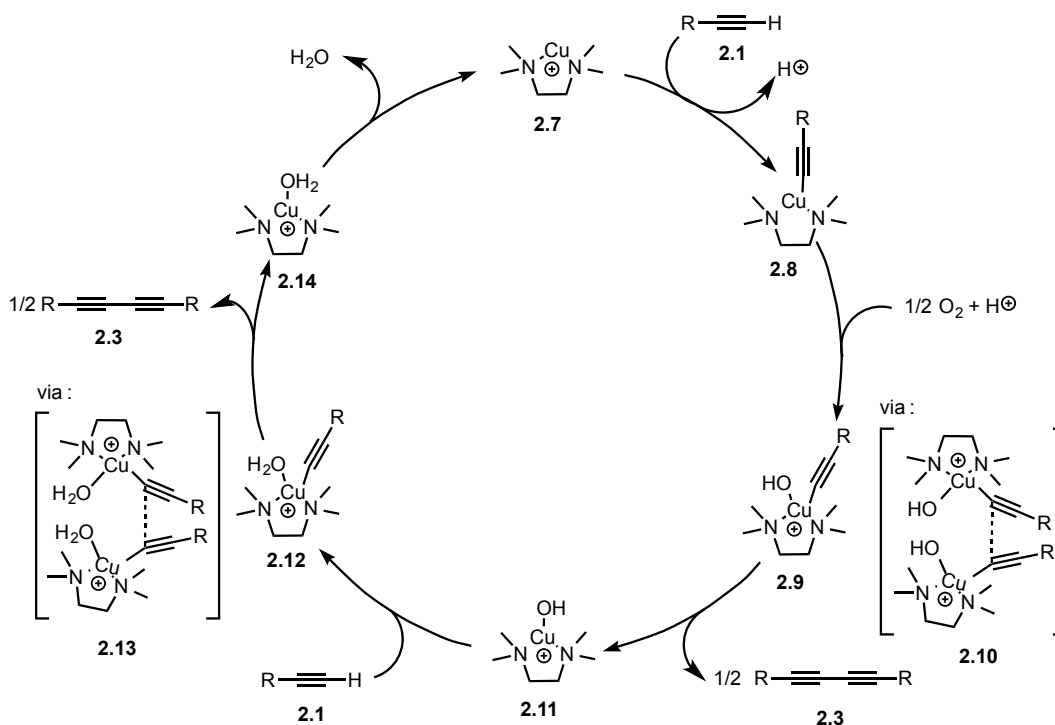
The reaction mechanism for the Glaser-Hay reaction is highly dependant on the reaction conditions. Bohlmann was the first to propose a mechanism in 1964.⁵ He suggested the cupration of the alkyne **2.1** using a base (Scheme 2.2, *top*). The first cupration step is widely accepted by the scientific community and is implied in various organometallic reactions.⁶ Based on the fact that the reaction is second order in alkyne, the following step was proposed to be the formation of the bisacetylide complex **2.6**, a subsequent reductive elimination would afford the desired diyne **2.3** (Scheme 2.2, *bottom*). However, Bohlmann's mechanism neglected the crucial oxidation step as he implied a bimetallic Cu(II) complex **2.6** that gets reduced to Cu(I) upon formation of the product.



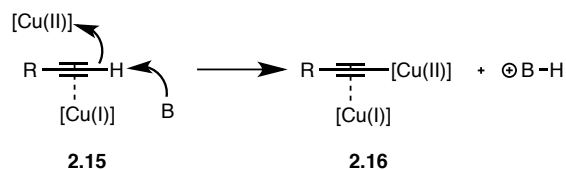
Scheme 2.2 – Bohlmann's proposed mechanism for Glaser coupling.

As the Glaser-Hay coupling became more prevalent in synthesis, interest into the reaction mechanism grew. Extensive DFT studies of the Glaser mechanism have been completed independently by Fomina⁷ and Masera.⁸ Empirically, electron-poor alkynes react faster. Basic conditions also improve the reaction rate. The proposed catalytic cycle from the DFT studies begins with a Cu(I)-TMEDA complex **2.7** that coordinates with an acetylene (Scheme 1.3). The resulting Cu(I)-acetylide complex **2.8** gets oxidized by O₂ to generate a Cu(III)-oxoacetylide complex **2.9**. It was calculated that the complex **2.9** undergoes bimolecular reductive elimination to generate a Cu(II) complex and the diyne product **2.3**. The Cu(II) intermediate **2.11** would then complex another molecule of acetylene to give complex **2.12** followed by bimolecular reductive elimination to regenerate the Cu(I) catalyst **2.7** and yield the diyne product **2.3**. The last step intercepts Bohlmann's proposed mechanism. Another study reporting the direct observation of reduction from Cu(II) to Cu(I) by a terminal alkyne further supports the computationally proposed mechanism.⁹ From the proposed catalytic cycle, both Cu(I) and Cu(II) salts could be used as the catalyst for the reaction. Even more interesting, it has been shown

that a positive effect can be obtained by using both oxidation states at the same time.⁶ Lan and Lei reported that the formation of complex **2.12** is the rate determining step (RDS) and that the addition of a copper(I) salt helped lower the activation barrier of the step (Scheme 2.4)



Scheme 2.3. – Glaser-Hay catalytic cycle based on DFT calculations.



Scheme 2.4. – Proposed synergistic cooperative effect of Cu(I) and Cu(II) salts in the cupration of alkyne.

2.1.3 – Modern Reaction Conditions

The synthesis of 1,3-diynes remains an active field of research (*vide infra*). Many variants of the Glaser-Hay oxidative coupling have been developed with new reaction conditions to access conjugated 1,3-diynes that are mild, efficient, functional group tolerant and selective.

Shi and co-workers reported a mild, copper-catalyzed base-free oxidative coupling of terminal alkynes using diaziridinone.¹⁰ Noteworthy, the authors proposed a reductive elimination from a dialkynyl Cu(III) species. Sommer has shown that Cu(I)-modified zeolites could be used as efficient and mild catalysts for Glaser couplings.¹¹ A large zeolite pore size was important to achieve good yields. The method was tolerant of sensitive carbohydrate derivatives. A CuBr/NBS/DIPEA catalytic system was also shown to be highly active at room temperature and tolerant of sensitive functional groups such as acetals, silyl ethers, esters and sugars.¹² The improvements in Glaser couplings has opened the door for applications in the design and synthesis of biomolecules such as complex sugars and peptides.⁴

Heterogeneous catalysis has also emerged as an efficient tool for Glaser-Hay coupling. Silica-supported copper catalysts have been shown to be active for the coupling of terminal alkynes.¹³ Radivoy also reported the use of Cu-nanoparticles on silica coated maghemite nanoparticles (CuNPs/MagSilica) as a heterogeneous recoverable catalyst to perform the Glaser transformation. Importantly CuNPs/MagSilica is also a competent catalyst for the azide-alkyne cycloaddition reaction.¹⁴

1,3-Diynes can also be formed using a cobalt catalyst with nitrobenzene as the stoichiometric oxidant. The reaction manifold is formally reductive due to the presence of

a stoichiometric amount of zinc powder. The mild conditions may allow the scope to be expanded to include more oxidant sensitive functional groups.¹⁵

2.1.4 – Synthesis of Unsymmetrical 1,3-Diynes

The synthesis of unsymmetrical 1,3-diynes is challenging because the reactivity profile of the alkyne in the Glaser coupling is highly dependant on its pKa. Hay found in his seminal discovery that aryl alkyne **2.17** underwent homocoupling faster than propargyl alcohol **2.18**, while the alkyl alkyne **2.19** was the slowest to react (Figure 2.1).^{3b} Consequently, any attempts at forming a mixed 1,3-diyne *via* Glaser coupling usually resulted in a mixture of the three possible products favouring the homocoupling of the most reactive alkyne. Consequently, for the synthesis of unsymmetrical 1,3-diynes, a five-fold excess of the most reactive alkyne is typically used (refer to Table 2.1).

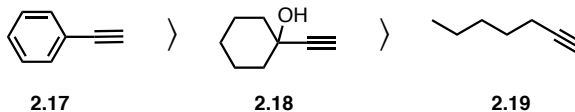
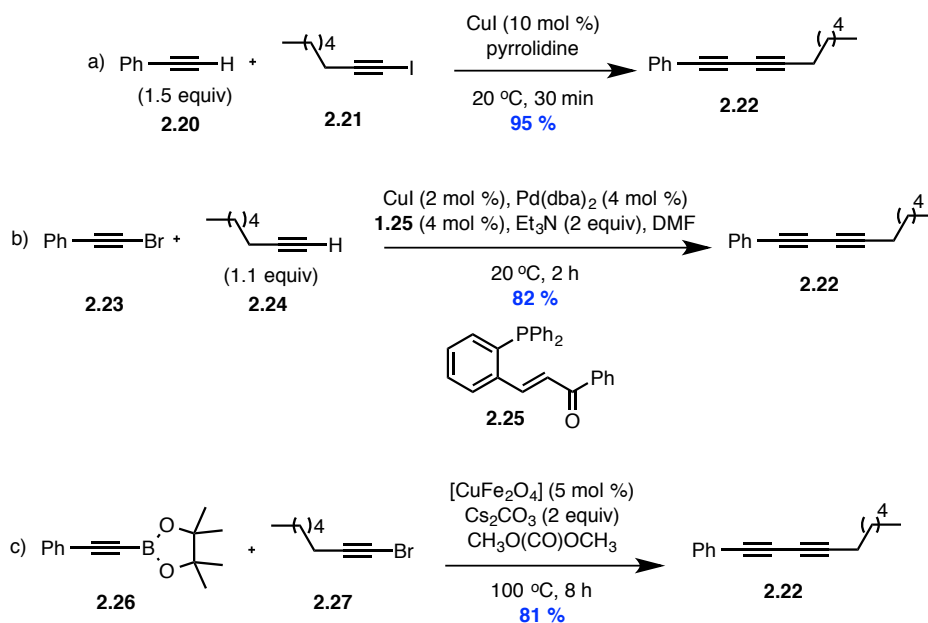


Figure 2.1 – Relative reactivity of alkynes in oxidative couplings.

Although many strategies have been reported for the synthesis of unsymmetrical diynes,¹⁶ the Cadiot-Chodkiewicz coupling remains the preferred method. The reaction was reported in 1957 as the first protocol for alkyne heterocoupling and has since been used in numerous syntheses.¹⁷ The reaction takes place between a terminal alkyne **2.20** and a 1-haloalkyne **2.21** under copper catalysis to yield the mixed diyne **2.22** (Scheme 2.5a). Although the method can be a powerful tool, some limitations exist. When the electronic properties of the alkynes are similar a substantial amount of dimerization of the halo-alkyne can be observed. To solve the selectivity issue, Lei recently reported a Pd/Cu

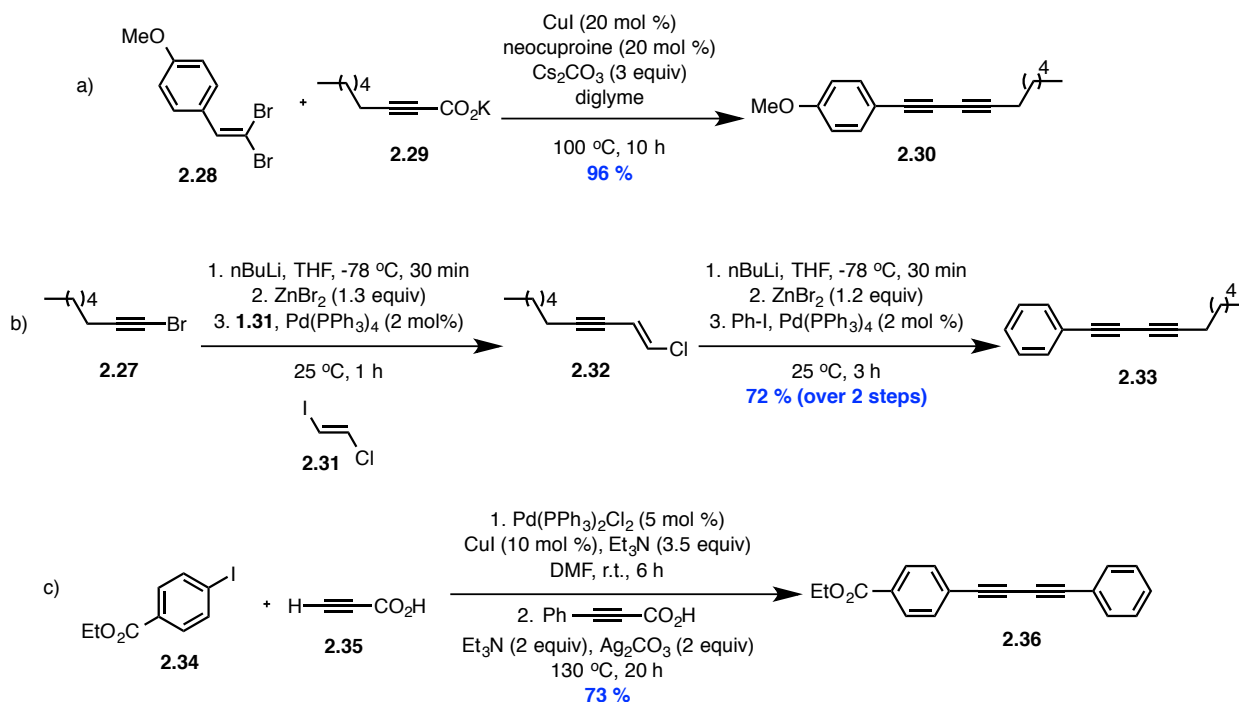
co-catalyzed coupling of a terminal alkyne **2.24** with an haloalkyne **2.23**. The reaction proceeds smoothly at room temperature and can also be used to synthesize triynes in one pot (Scheme 2.5b).¹⁸ Unsymmetrical 1,3-diyne **2.22** can also be accessed using magnetic copper nanoparticles (CuFe_2O_4) to couple alkynyl bromide **2.27** with alkynyl boronate **2.26** (Scheme 2.5c).¹⁶



Scheme 2.5 – Unsymmetrical diyne coupling protocols. a) Cadiot-Chodkiewicz, b) Lei's Cu/Pd protocol and c) CuNPs protocol.

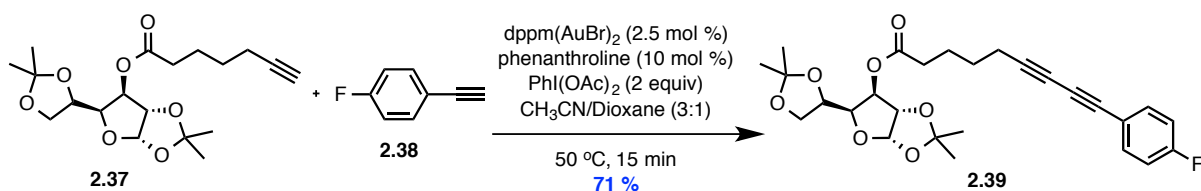
Heterocoupling of different alkynes is also possible when one of the reactive partners is functionalized as an alkynylcarboxylic acid. As such, copper-catalyzed decarboxylative cross-coupling have been reported, affording unsymmetrical diyne from functionalized alkyne **2.29** and 1,1-dibromoalkenes **2.28** (Scheme 2.6a).¹⁹ The reaction takes place *via in situ* elimination of **2.28** to form an alkyne coupling partner. The elimination strategy is somewhat inspired by an analogous Negishi protocol in palladium-catalyzed cross-coupling of a halo-alkyne **2.27** with $\text{ICH}=\text{CHCl}$ **2.31** (Scheme 2.6b).²⁰

Alternatively, a palladium catalyzed decarboxylative homocoupling of haloarene **2.34** with propiolic acid **2.35** using a silver salt was reported by Kim (Scheme 2.6c).^{18b,21} The method could also be applied to the synthesis of unsymmetrical 1,3-diyne **2.36** and does not require prefunctionalization of the aryl group with an alkyne.



Scheme 2.6 – Unsymmetrical diyne coupling protocols. a) Decarboxylative cross-coupling from dihaloalkenes, b) Negishi's protocol, c) Cu/Pd/Ag decarboxylative cross-coupling.

In 2014, Shi reported a gold-catalyzed heterocoupling of terminal alkynes using a hypervalent iodide reagent as the oxidant.²² The reaction shows impressive functional group tolerance (Scheme 2.7). The authors propose that the gold cation might provide a discrimination effect toward different alkynes, thus leading to selective heterocoupling.

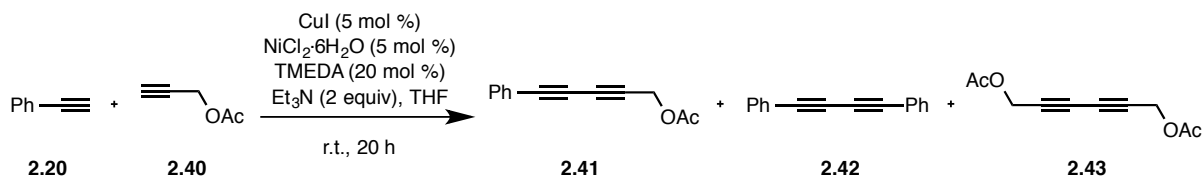


Scheme 2.7 – Shi's heterocoupling of terminal alkynes protocol.

The development of a simple Glaser-like protocol for heterocoupling using unfunctionalized alkynes remains a challenge. Recently, Lei and co-workers reported the use of a nickel(II) co-catalyst to promote the formation of mixed 1,3-diynes **2.41** from terminal alkynes **2.20** and **2.40**.²³ As expected, using a five-fold excess of the less reactive alkyne **2.40** didn't significantly improve the yield of the desired product **2.41** (Table 2.1 entry 2). An excess of the most reactive alkyne **2.20** had to be used to obtain 86 % yield of the mixed diyne **2.41** (Table 2.1, entry 3). Interestingly, the Cu and Ni co-catalysts seemed to work synergistically to promote efficient coupling at room temperature as a lower yield of 30 % was obtained in the absence of the nickel co-catalyst (Table 2.1, entry 4). Similar to a palladium-catalyzed cross coupling, the authors proposed that a Ni(II) complex **2.44** could undergo transmetallation from a Cu(I)-acetylide intermediate **2.45** to form a Ni(II)-bisacetylide complex **2.46**. Reductive elimination would give the expected diyne **2.42** and a Ni(0) complex **2.47** that could be reoxidized by O₂ (Scheme 2.8a). Reductive elimination from a Ni(II)-bisacetylide complex **2.46** is well documented in the literature.²⁴ The authors briefly investigated the proposed mechanism by monitoring the O₂ consumption of the reaction. In a traditional copper-catalyzed oxidative coupling of terminal alkynes, each mole of O₂ consumed leads to 2 moles of diyne (Scheme 2.8a). The authors observed a 1:1 ratio of O₂ to diyne formed, supporting their proposed mechanism involving reductive elimination from a

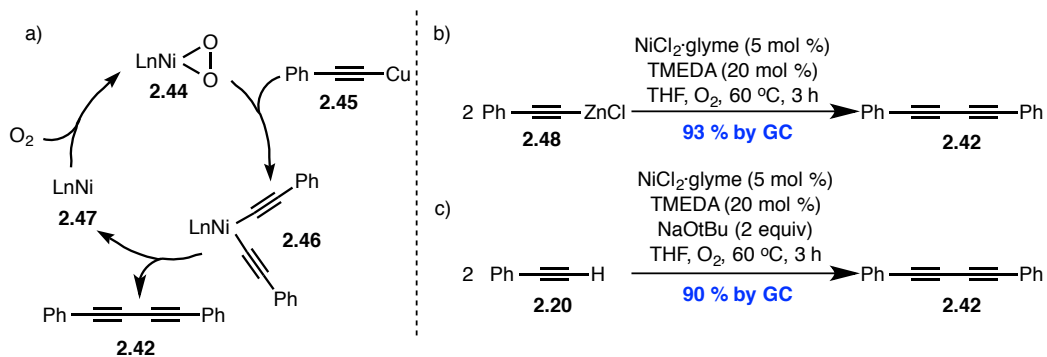
Ni(II)-intermediate. To further support a transmetalation pathway, the authors performed the reaction in absence of the copper salt but used a preformed Zn(II)-acetylide **2.48**. As expected, the reaction proceeded smoothly (Scheme 2.8b). Similarly, the reaction in absence of Cu but with added base (NaOtBu) also yielded the desired diyne **2.42** (Scheme 2.8c). It should be noted that Lei's Cu/Ni strategy also accelerates the homocoupling of terminal alkynes.

Table 2.1 Cu/Ni co-catalyzed synthesis of unsymmetrical diynes.



Entry	2.20 (mmol)	2.40 (mmol)	2.41 yield (%)	2.42 yield (%)	2.43 yield (%)
1	1	1	46	42	54
2	1	5	50	8	64
3	5	1	86	64	6
4*	5	1	30	20	8

* Nickel catalyst was omitted.



Scheme 2.8 – Mechanistic investigation of the Cu/Ni co-catalyzed oxidative coupling of alkynes.

Another technique that can be used to access unsymmetrical 1,3-diynes is the use of solid-supported synthesis. Immobilizing one of the coupling partners allows for selective coupling with the solubilized partner in high yield.²⁵

2.1.5 – Naturally Occurring Diynes

Interestingly, many natural products possess a diyne moiety (*vide infra*). For example, faltarindiol **2.49** is a polyene isolated from carrots which was found to exhibit antimicrobial activity (Figure 2.2a).²⁶ EV-086 **2.50** is a potent antiplasmodial which also makes it a potential anti-malarial candidate (Figure 2.2b). The furan-containing lipid **2.50** is part of a larger family of diyne-containing fatty acids that exhibit activity against tuberculosis, malaria, type 1 Herpes and lung cancer.²⁷ Thiarubrine A **2.51** is a pseudo-antiaromatic compound extracted from short ragweed roots that possesses antibacterial activity (Figure 2.2c).²⁸ The naturally occurring 18-membered macrolactone ivorenolide A **2.52** (Figure 2.2d) exhibits immunosuppressive activity that could be exploited for the management of organ grafts or rheumatoid arthritis.²⁹

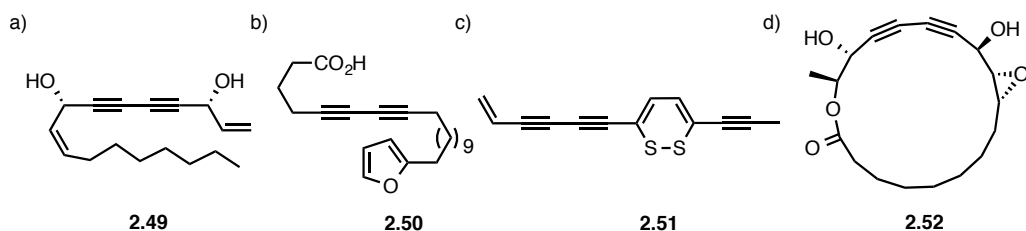
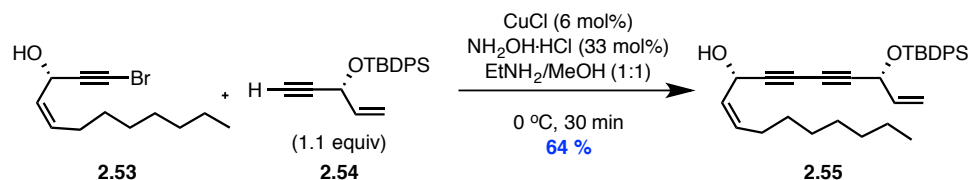


Figure 2.2 – Naturally occurring diyynes.

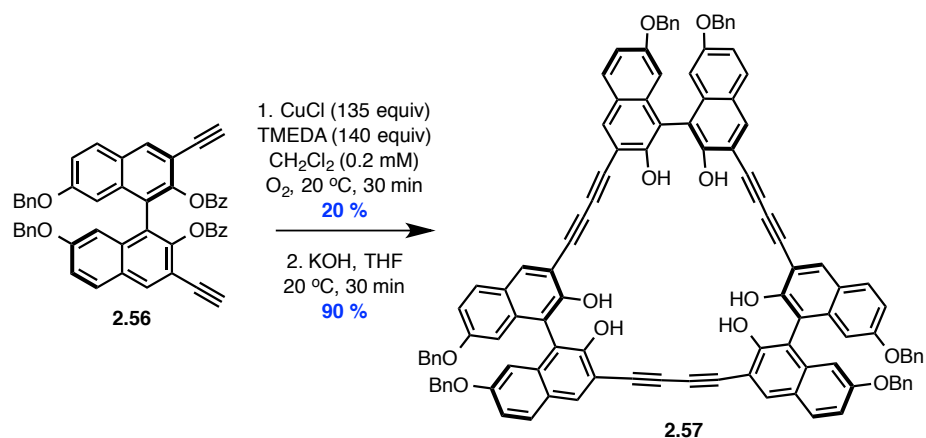
2.1.6 – Applications of the Glaser-Hay Reaction in Synthesis

With all the synthetic methods available for the synthesis of 1,3-diyynes, it is not surprising that many diyne containing molecules have been successfully prepared. An enantioselective synthesis of faltarindiol has been reported where the key bond-forming step was a Cadiot-Chodkiewicz coupling. The natural product was obtained after subsequent deprotection of the silyl group from diyne **2.55** (Scheme 2.9).³⁰ A similar strategy was used by Li and Yue in the total synthesis of macrolide iveronolide A **2.52**.²⁹



Scheme 2.9 – Synthesis of faltarindiol *via* Cadiot-Chodkiewicz coupling.

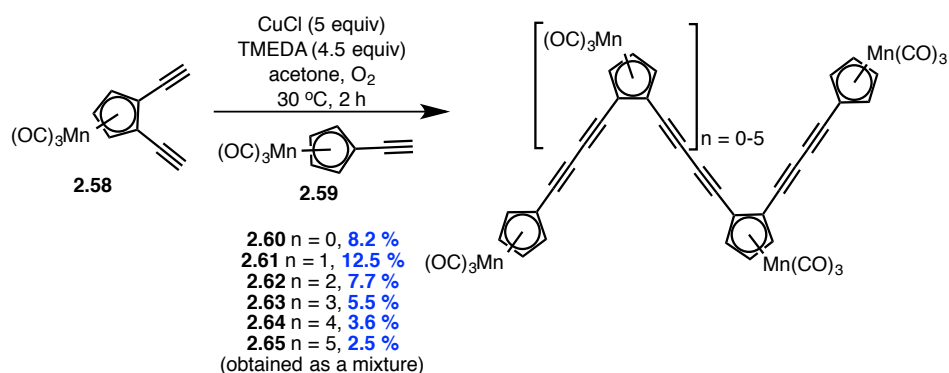
Perhaps the greatest impact of the Glaser-Hay reaction has been in materials and supramolecular chemistry, where the reaction is used in the construction of macrosystems with interesting and unique properties. Oxidative coupling of alkynes has been used to synthesize a family of optically active cyclophanes capable of carbohydrate-recognition. The trimer **2.57** is obtained in low yield and after deprotection, the internal cavity is aligned with other hydroxyl groups to coordinate with monosaccharides (Scheme 2.10).³¹



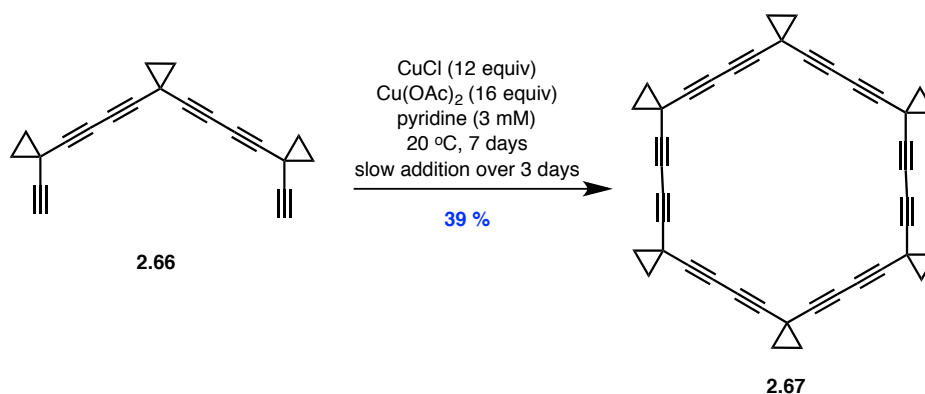
Scheme 2.10 – Synthesis of an optically active cyclophane capable of carbohydrate recognition.

The mildness of the Glaser-Hay coupling was demonstrated in the synthesis of molecular rods incorporating cyclopentadienyl- π complexes that have interesting material properties.³² The sensitive MnCp(CO)₃ units were stable under the oxidative conditions and the Glaser-Hay reaction yielded a mixture of separable oligomers **2.60** to **2.65** with an overall yield of 40 %. (Scheme 2.11)

Another example of the use of alkyne coupling reactions in synthesis is the preparation of spirocyclopropanated macrocyclic polydiacetylenes by a combination of Glaser-Hay couplings and the Cadiot-Chodkiewicz reaction. The formation of the terminal diyne **2.66** by Cadiot-Chodkiewicz reaction followed by Glaser-Hay coupling afforded cyclic hexamer **2.67** in 39 % yield (Scheme 2.12).³³



Scheme 2.11 – Synthesis of molecular rods incorporating cyclopentadienyl- π complexes.



Scheme 2.12 – Synthesis a spirocyclopropanated macrocyclic polydiacetylene.

Additionally, 1,3-diynes have also found applications in biochemistry due to their pronounced intensity in Raman spectroscopy and consequent ability to visualize mobile small molecules in living cells.³⁴ The molecules used in the study possessed both bioactive functionalities and a diyne moiety that was synthesized using Lei's Cu/Ni protocol.²³

2.1.7 – Conclusion

The Glaser-Hay coupling of terminal alkyne is an important transformation in organic synthesis. Since its discovery in 1869, it has impacted many fields of research such as synthesis, materials and biological chemistry. The reaction allows the formation of a challenging carbon-carbon bond under selective and mild catalytic conditions. Examples of catalytic macrocyclization reactions that allows for the formation of carbon-carbon bonds are scarce and the Glaser-Hay reaction would be an ideal starting point for the proof of concept of the “phase separation strategy”.

2.2 – Introduction to Poly(ethylene glycol) Properties and Concepts of Phase Transfer and Micellar Catalysis

2.2.1 – Definition and Physical Properties of Poly(ethylene glycol)

Poly(ethylene glycol) (PEG) is a polyether polymer with the repeating unit H-[O-CH₂-CH₂]_n-OH. PEGs are synthesized by aqueous anionic polymerization of ethylene oxide and are generally sold as polydispersed mixtures. For example, PEG₄₀₀ **2.68** refers to a polydisperse mixture of PEGs with an average molecular weight of 400 g/mol, meaning that there are approximately nine repeating units ($n \approx 9$) of ethylene oxide present (Figure 2.2). Davies demonstrated that a well-controlled polymerization of ethylene oxide **2.69** can produce monofunctional PEG **2.70** with polydispersity indices approaching 1 (Scheme 1.13).³⁵

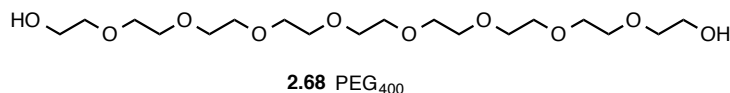
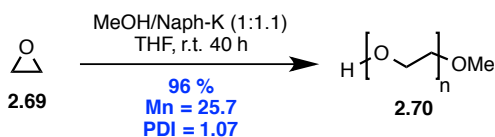


Figure 2.2 –Structure of PEG₄₀₀.



Scheme 2.13 – Synthesis of low polydispersity monofunctional PEG polymer.

Although PEGs have a large solubility preference for water (LogP = -4.8 for PEG₄₀₀),³⁶ they are regarded as a class of amphiphilic molecules as they can also dissolve in organic media. Low molecular weight PEGs (250 to 1000 g/mol) are typically viscous liquids and high molecular weight (≥ 1000 g/mol) PEGs are usually solids. Importantly,

they are also non-toxic and the FDA has approved PEGs for intravenous, oral and dermal applications.³⁷ PEGs are also known for their ability to help solubilize organic molecules in aqueous media. Other characteristics of PEG-derived solvents include, thermal stability, low cost and high boiling points.³⁸

2.2.1.1 – Structure of PEG in Aqueous Media

PEGs are completely soluble in water, but closely related polymers such as poly(propylene glycol)s $\text{H}[\text{O}-\text{CH}(\text{CH}_3)-\text{CH}_2]_n\text{-OH}$ or poly(butylene glycol)s $\text{H}[\text{O}-\text{CH}_2-\text{CH}_2-\text{CH}_2]_n\text{-OH}$ have variable solubility depending on the length of the polymer. Their water solubility typically decreases with increasing molecular weight. Interestingly, poly(methylene oxide)s $\text{H}[\text{O}-\text{CH}_2]_n\text{-OH}$ are also completely insoluble in water. Tasaki performed molecular dynamic calculations to investigate the conformation of PEG₆₅₀ in water.³⁹ Contrary to the gas phase where PEG is proposed to have an all-*trans* conformation, it was found that the polymer adopts a helical conformation in water with the backbone stabilized by a hydrogen bonding network (Figure 2.3). Unfortunately, the number of water molecules interacting with each unit of the polymer is still a debate in the literature, ranging from 1 to 6.^{39,40} PEGs are well known to aggregate in aqueous media.⁴⁰ Privat recently demonstrated that PEG aggregates present themselves in the form of hydrated helices covered with CH_2 groups, yielding hydrophobic regions.

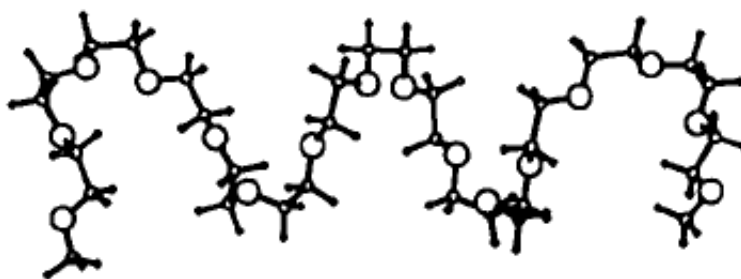


Figure 2.3 – Calculated structure of PEG₆₅₀ in water (2 ns). (Reproduced with permission from ref 39. Copyright 1996 American Chemical Society.)

Recently, the structure of a discrete polymer of PEG **2.71** ($n = 16$) has been studied by X-ray crystallography. Analysis of the structure of the discrete PEG polymer revealed that it also adopts a helical conformation in the solid state with the oxygens pointing towards the interior of the helix when crystallization occurred in organic media (Figure 2.4).³⁵

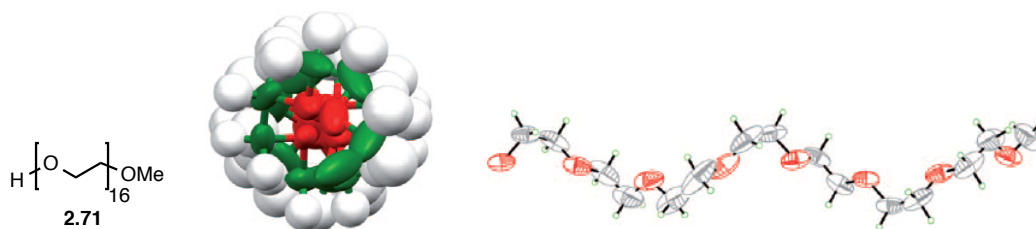


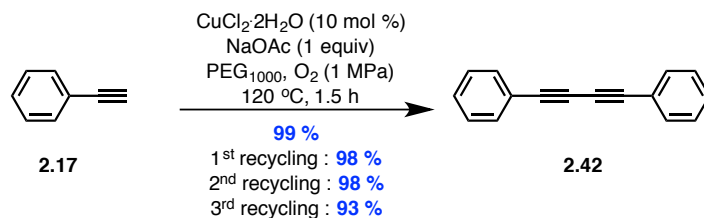
Figure 2.4 – X-ray structure of discrete PEG polymer **2.71**. (*top view*) Red = oxygen, green = carbon, white = hydrogen. (*side view*) Red = oxygen, grey = carbon, green = hydrogen. (Reproduced with permission from ref 35. Copyright 2009 WILEY-VCH Verlag GmbH & Co. KGaA, Weinheim.)

2.2.2 – Industrial Applications of PEGs

PEGs have found myriad commercial uses.^{41,42} In medicine, they are often used to treat irritable bowel syndrome and constipation by osmotically attracting water in the intestine.⁴¹ PEGs are also often used as an excipient (*i.e.* substance formulated with the active ingredient) for various drugs. Other examples of pharmaceutical uses for low molecular weight PEGs involve its use as a solvent in soft capsules, while high molecular weight PEGs can be used as a binder for the ingredients in a tablet.⁴² In addition PEGs have also been used to improve the solubility of small molecule therapeutics and PEGylation of biologically active molecules has been shown to positively influence their stability, pharmacokinetics and mode of action.^{37a}

2.2.3 – Chemical Applications of PEGs

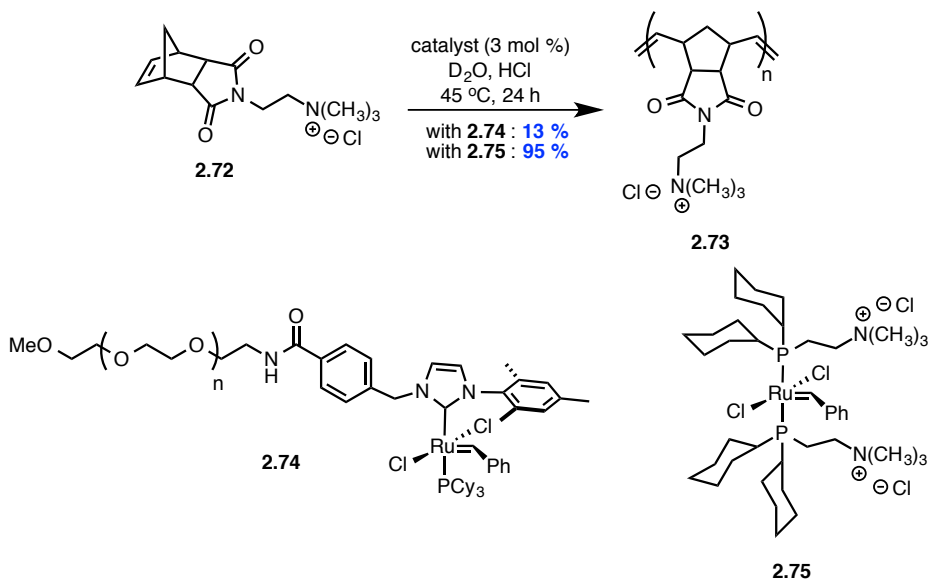
The unique physical properties of PEGs open up opportunities in organic synthesis. In contrast to polyethylene or polypropylene, PEGs are soluble polymers that have been used as a recyclable solvent in various organic reactions such as Ullmann⁴³, Suzuki⁴⁴ and Glaser-Hay⁴⁵ couplings. Wang and He reported the use of PEG₁₀₀₀ as a recyclable reaction medium (*i.e.* catalyst containing solvent) for Glaser-Hay coupling. Interestingly, PEG₁₀₀₀ is a solid at ambient temperature and becomes a liquid upon heating. The authors demonstrated that extractions with diethyl ether could separate the desired product **2.42** from the reaction mixture which could then be reused (Scheme 2.14).



Scheme 2.14 – PEG₁₀₀₀ as a recyclable medium for Glaser-Hay couplings.

2.2.3.1 – Homogeneous Catalysis

In contrast to less soluble polymers such as polystyrene, derivatization of PEGs can be done in a straightforward manner using synthetic procedures that mimic those used for the functionalization of small molecules; derivatized PEGs can be characterized using standard methods such as NMR and MS. The derivatization strategy is used when catalysis in water is desirable. PEGylation of a catalyst is often used to render it hydrophilic. For example, Grubbs reported a PEGylated ruthenium-based metathesis catalyst **2.74** that is highly active and stable in water (Scheme 2.15).⁴⁶ When compared to cationic ruthenium catalyst **2.75**, the PEGylation strategy produced a more active catalyst for ring opening metathesis polymerization (ROMP) of cationic norbornene substrate **2.72**. Moreover, the PEGylated catalyst **2.74** is also active in solvents such as methanol and dichloromethane and can be recycled by precipitation using diethyl ether. The precipitation strategy is a commonly employed procedure to recycle poly(ethylene glycol)-bound catalysts.⁴⁷



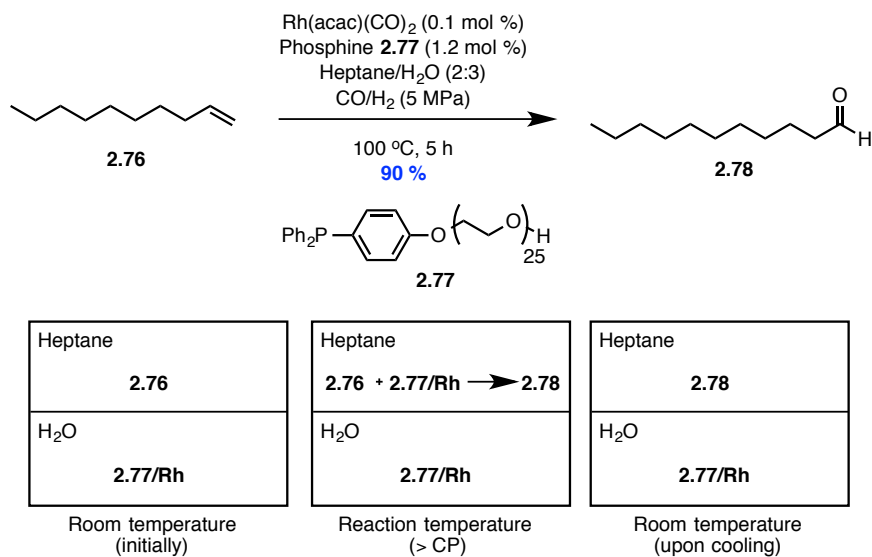
Scheme 2.15 – Ring opening metathesis polymerization using water soluble ruthenium based catalysts.

2.2.3.2 – Phase Transfer Catalysis

Traditional phase transfer catalysis typically consists of a biphasic reaction mixture involving an aqueous phase and an organic phase.⁴⁸⁻⁵¹ In many instances, researchers design polymer-supported catalysts that render the catalyst water soluble. As such, the organic phase typically contains the organic substrate and the reaction could then occur at the interface of the aqueous and organic phases. After the reaction is completed, a facile extraction can be performed to obtain the organic product and recycle the hydrophilic catalyst. The strategy has been employed in numerous instances.⁴⁹⁻⁵¹ For example, a hydrophilic phosphine ligand was designed to form a recyclable and water soluble rhodium complex that has shown catalytic activity in the hydroformylation of propene to yield butanal.⁴⁹ Although the use of water soluble catalysts is a promising area of research, the use of water as a reaction medium can limit the choice of organic

substrates due to solubility issues. In the previous reaction, higher olefins were unreactive because of their lipophilicity. As an alternative, researchers have used co-solvents, surfactants and even biphasic fluoruous systems in order to resolve the solubility issue.⁵⁰

An alternative strategy for phase transfer catalysis involves exploiting the intrinsic properties of PEGs. Zheng has developed a rhodium-catalyzed hydroformylation of higher olefins using PEG solvents (Scheme 2.16, *top*). The general principle involves thermoregulated phase-transfer catalysis (TRPTC) which exploits the temperature dependant solubility of PEGs. The cloud point (CP) for PEGs is defined as the temperature at which the polymer's solubility in water decreases to the point where it forms an emulsion.⁵¹ Upon heating a biphasic mixture, the PEGylated catalyst (in the case of Zheng, PEGylation of the phosphine ligand of the rhodium catalyst) becomes preferentially solubilized in the organic phase. When the mixture is cooled below its cloud point, the PEGylated catalyst returns to the aqueous phase and the desired product can be obtained by liquid-liquid phase separation (Scheme 2.16, *bottom*).⁵⁰



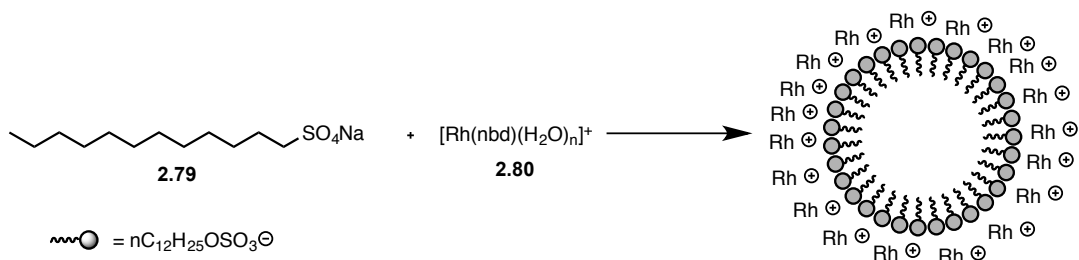
Scheme 2.16 – Hydroformylation of 1-decene under thermoregulated phase-transfer catalysis (TRPTC).

2.2.4 – Micellar Catalysis

Micellar catalysis involves the acceleration of a chemical reaction in solution by the addition of a surfactant at a concentration higher than its critical micellar concentration (CMC) so that the reaction can proceed in the environment of surfactant aggregates or micelles. Rate enhancements may be due to higher concentrations of the reactants in that environment, more favourable orientations and solvation of the reactive species, or enhanced rate constants in the micellar pseudophase of the surfactant aggregate.⁵²

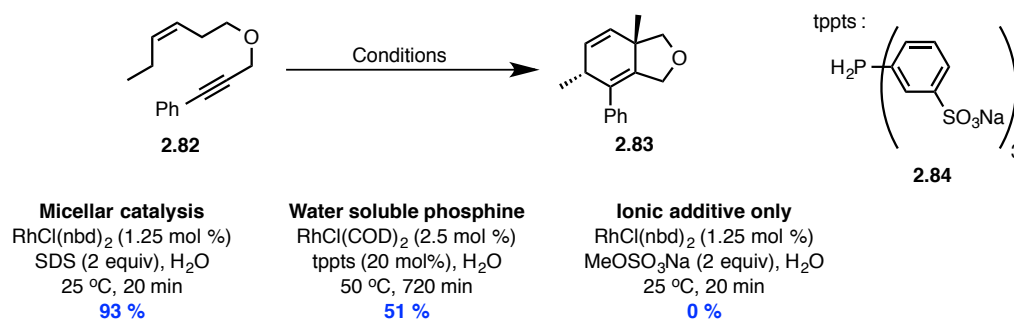
For example, the rhodium catalyzed intramolecular [4+2] annulation of 1,3-dien-8-yne was conducted under micellar catalysis using sodium dodecylsulfate (SDS) in water. It was proposed that the rhodium catalyst exchanged its chlorine ligand for a SDS anion in aqueous media. The formation of a highly active cationic rhodium species **2.81**

was proposed to be stabilized by the negative charges on the polar heads of the micelle (Scheme 1.17). The use of SDS was shown to be highly efficient, yielding 93 % of the desired bicyclic product **2.51** in only 20 min.



Scheme 1.17 – Proposed formation of a micellar catalyst.

To demonstrate the advantages of using micellar catalysis versus water solubilization of the catalyst, the same reaction was performed using a water soluble phosphine **2.84** and the catalytic activity in water was studied. Although the reaction afforded a 51 % yield of the desired bicyclic product **2.83**, the reaction required a higher catalyst loading as well as elevated temperature and increased reaction time. The result demonstrates the advantages of micellar catalysis. Finally, the advantages of micellar catalysis were also demonstrated by replacing SDS by sodium methyl sulfate, which is unable to form micelles. The subsequent [4+2] annulation of 1,3-dien-8-yne **2.82** showed a complete loss of reactivity and no desired bicycle product **2.83** was observed.⁵³



Scheme 2.18 – Rhodium catalyzed intramolecular [4+2] annulation of 1,3-dien-8-yne in water.

2.2.5 – Conclusion

The use of hydrophilic polymers in organic synthesis is emerging. Poly(ethylene glycol) has several desirable features such as thermal stability, low cost and biological compatibility. Interestingly, although the aggregation properties of PEG have found many application in the biological field, they have yet to be explored in organic chemistry. Moreover, it has been demonstrated on several occasions that micellar catalysis is an efficient way to perform reactions in aqueous/polar media. Combining the aggregation properties of PEG with the micellar catalysis concept could be an efficient way to control the dilution effect in macrocyclization reactions.

2.3 – Bibliography

- (1) Glaser, C. *Ber. Deuts. Chem. Ges.* **1869**, *2*, 422-424.
- (2) Eglinton, G.; Galbraith, A. R. *J. Chem. Soc.* **1959**, 889-896.
- (3) a) Hay, A. S. *J. Org. Chem.* **1960**, *25*, 1275; b) Hay, A. S. *J. Org. Chem.* **1962**, *27*, 3320-3321.
- (4) Sindhu, K. S.; Anilkumar, G. *RSC Advances* **2014**, *4*, 27867-27887.
- (5) Bohlmann, F.; Schönowsky, H.; Inhoffen, E.; Grau, G. *Chem. Ber.* **1964**, *97*, 794-800.
- (6) Bai, R.; Zhang, G.; Yi, H.; Huang, Z.; Qi, X.; Liu, C.; Miller, J. T.; Kropf, A. J.; Bunel, E. E.; Lan, Y.; Lei, A. *J. Am. Chem. Soc.* **2014**, *136*, 16760-16763.
- (7) Fomina, L.; Vazquez, B.; Tkatchouk, E.; Fomine, S. *Tetrahedron* **2002**, *58*, 6741-6747.
- (8) Jover, J.; Spuhler, P.; Zhao, L.; McArdle, C.; Maseras, F. *Catal. Sci. Tech.* **2014**, *4*, 4200-4209.
- (9) Zhang, G.; Yi, H.; Zhang, G.; Deng, Y.; Bai, R.; Zhang, H.; Miller, J. T.; Kropf, A. J.; Bunel, E. E.; Lei, A. *J. Am. Chem. Soc.* **2014**, *136*, 924-926.
- (10) Zhu, Y.; Shi, Y. *Org. Biomol. Chem.* **2013**, *11*, 7451-7454.
- (11) Kuhn, P.; Alix, A.; Kumarraja, M.; Louis, B.; Pale, P.; Sommer, J. *Eur. J. Org. Chem.* **2009**, *2009*, 423-429.
- (12) Li, L.; Wang, J.; Zhang, G.; Liu, Q. *Tetrahedron Lett.* **2009**, *50*, 4033-4036.
- (13) van Gelderen, L.; Rothenberg, G.; Roberto Calderone, V.; Wilson, K.; Raveendran Shiju, N. *Appl. Organomet. Chem.* **2013**, *27*, 23-27.
- (14) Nador, F.; Volpe, M. A.; Alonso, F.; Feldhoff, A.; Kirschning, A.; Radivoy, G. *Appl. Catal., A* **2013**, *455*, 39-45.
- (15) Hilt, G. H.; Christoph; Arndt, Marion *Synthesis* **2009**, 395-398.
- (16) Ahammed, S.; Kundu, D.; Ranu, B. C. *J. Org. Chem.* **2014**, *79*, 7391-7398.
- (17) Siemsen, P.; Livingston, R. C.; Diederich, F. *Angew. Chem. Int. Ed.* **2000**, *39*, 2632-2657.
- (18) a) Shi, W.; Luo, Y.; Luo, X.; Chao, L.; Zhang, H.; Wang, J.; Lei, A. *J. Am. Chem. Soc.* **2008**, *130*, 14713-14720; b) Weng, Y.; Cheng, B.; He, C.; Lei, A. *Angew. Chem. Int. Ed.* **2012**, *51*, 9547-9551.
- (19) Huang, Z.; Shang, R.; Zhang, Z.-R.; Tan, X.-D.; Xiao, X.; Fu, Y. *J. Org. Chem.* **2013**, *78*, 4551-4557.
- (20) Negishi, E.-i.; Hata, M.; Xu, C. *Org. Lett.* **2000**, *2*, 3687-3689.
- (21) Park, J.; Park, E.; Kim, A.; Park, S.-A.; Lee, Y.; Chi, K.-W.; Jung, Y. H.; Kim, I. S. *J. Org. Chem.* **2011**, *76*, 2214-2219.
- (22) Peng, H.; Xi, Y.; Ronaghi, N.; Dong, B.; Akhmedov, N. G.; Shi, X. *J. Am. Chem. Soc.* **2014**, *136*, 13174-13177.
- (23) Yin, W.; He, C.; Chen, M.; Zhang, H.; Lei, A. *Org. Lett.* **2008**, *11*, 709-712.
- (24) a) Rhee, I.; Ryang, M.; Tsutsumi, S. *Tetrahedron Lett.* **1969**, *10*, 4593-4596; b) Crowley, J. D.; Goldup, S. M.; Gowans, N. D.; Leigh, D. A.; Ronaldson, V. E.; Slawin, A. M. Z. *J. Am. Chem. Soc.* **2010**, *132*, 6243-6248.
- (25) Tripp, V. T.; Lampkowski, J. S.; Tyler, R.; Young, D. D. *ACS Comb. Sci.* **2014**, *16*, 164-167.
- (26) Kemp, M. S. *Phytochem.* **1978**, *17*, 1002.

- (27) a) Knechtle, P.; Diefenbacher, M.; Greve, K. B. V.; Brianza, F.; Folly, C.; Heider, H.; Lone, M. A.; Long, L.; Meyer, J.-P.; Roussel, P.; Ghannoum, M. A.; Schneiter, R.; Sorensen, A. S. *Antimicrob. Agents Chemother.* **2014**, *58*, 455-466; b) Kanokmedhakul, S.; Kanokmedhakul, K.; Kantikeaw, I.; Phonkerd, N. *J. Nat. Prod.* **2006**, *69*, 68-72.
- (28) Reyes, J.; Morton, M.; Hoffman, G. G.; O'Shea, K. E.; Downum, K. *J. Chem. Educ.* **2001**, *78*, 781.
- (29) Zhang, B.; Wang, Y.; Yang, S.-P.; Zhou, Y.; Wu, W.-B.; Tang, W.; Zuo, J.-P.; Li, Y.; Yue, J.-M. *J. Am. Chem. Soc.* **2012**, *134*, 20605-20608.
- (30) Zheng, G.; Lu, W.; Cai, J. *J. Nat. Prod.* **1999**, *62*, 626-628.
- (31) Bähr, A.; Droz, A. S.; Püntener, M.; Neidlein, U.; Anderson, S.; Seiler, P.; Diederich, F. *Helv. Chim. Acta* **1998**, *81*, 1931-1963.
- (32) Bunz, U. H. F.; Enkelmann, V.; Beer, F. *Organomet.* **1995**, *14*, 2490-2495.
- (33) de Meijere, A.; Kozhushkov, S.; Haumann, T.; Boese, R.; Puls, C.; Cooney, M. J.; Scott, L. T. *Chem. Eur. J.* **1995**, *1*, 124-131.
- (34) Yamakoshi, H.; Dodo, K.; Palonpon, A.; Ando, J.; Fujita, K.; Kawata, S.; Sodeoka, M. *J. Am. Chem. Soc.* **2012**, *134*, 20681-20689.
- (35) French, A. C.; Thompson, A. L.; Davis, B. G. *Angew. Chem. Int. Ed.* **2009**, *48*, 1248-1252.
- (36) Ma, T. Y. H., D.; Krugliak, P.; Katz, K. *Gastroenterology* **1990**, *98*, 39-46.
- (37) a) Zalipsky, S. *Adv. Drug Del. Rev.* **1995**, *16*, 157-182; b) Greenwald, R. B.; Choe, Y. H.; McGuire, J.; Conover, C. D. *Adv. Drug Del. Rev.* **2003**, *55*, 217-250.
- (38) a) Nagarapu, L.; Mallepalli, R.; Arava, G.; Yeramanchi, L. *Eur. J. Chem.* **2010**, *1*, 228; b) Candeias, N. R.; Branco, L. C.; Gois, P. M. P.; Afonso, C. A. M.; Trindade, A. F. *Chem. Rev.* **2009**, *109*, 2703; c) Zhang, Z. H. *Res. J. Chem. Environ.* **2006**, *10*, 97.
- (39) a) Tasaki, K. *J. Am. Chem. Soc.* **1996**, *118*, 8459-8469; b) Derkaoui, N.; Said, S.; Grohens, Y.; Olier, R.; Privat, M. *J. Colloid Interface Sci.* **2007**, *305*, 330-338.
- (40) Azri, A.; Giamarchi, P.; Grohens, Y.; Olier, R.; Privat, M. *J. Colloid Interface Sci.* **2012**, *379*, 14-19.
- (41) Di Palma, J. A.; Cleveland, M. v.; McGowan, J.; Herrera, J. L. *Am J Gastroenterol* **2007**, *102*, 1964-1971.
- (42) Katdare, A.; Chaubal, M. V.; Informa Healthcare: New York, 2006.
- (43) Colacino, E.; Villebrun, L.; Martinez, J.; Lamaty, F. *Tetrahedron* **2010**, *66*, 3730-3735.
- (44) Namboodiri, V. V.; Varma, R. S. *Green. Chem.* **2001**, *3*, 146-148.
- (45) Li, Y.-N.; Wang, J.-L.; He, L.-N. *Tetrahedron Lett.* **2011**, *52*, 3485-3488.
- (46) Gallivan, J. P.; Jordan, J. P.; Grubbs, R. H. *Tetrahedron Lett.* **2005**, *46*, 2577-2580.
- (47) Bergbreiter, D. E. *Chem. Rev.* **2002**, *102*, 3345-3384.
- (48) a) Rogers, R. D.; Willauer, H. D.; Griffin, S. T.; Huddleston, J. G. *J. Chromatogr. B* **1998**, *711*, 255-263; b) Totten, G. E.; Clinton, N. A. *J. Macromol. Sci., C* **1988**, *28*, 293-337.
- (49) Arhancet, J. P.; Davis, M. E.; Merola, J. S.; Hanson, B. E. *Nature* **1989**, *339*, 454-455.
- (50) Zheng, X.; Jiang, J.; Liu, X.; Jin, Z. *Catal. Today* **1998**, *44*, 175-182.

- (51) Jimenez, Y. P.; Taboada, M. E.; Galleguillos, H. R. *J. Chem. Thermodyn.* **2011**, *43*, 1204-1210.
- (52) Haber, J. In *Pure Appl. Chem.* 1991; Vol. 63, p 1227.
- (53) Motoda, D.; Kinoshita, H.; Shinokubo, H.; Oshima, K. *Angew. Chem. Int. Ed.* **2004**, *43*, 1860-1862.

Chapter 3 : Phase Separation as a Strategy Towards Controlling Dilution Effects in Macrocyclic Glaser-Hay Couplings

Anne-Catherine Bédard and Shawn K. Collins*

Département de Chimie, Center for Green Chemistry and Catalysis, Université de Montréal, CP 6128 Station Downtown, Montréal, Québec H3C 3J7 Canada

Journal of the American Chemical Society **2011**, *133*, 19976-19981.

Contributions:

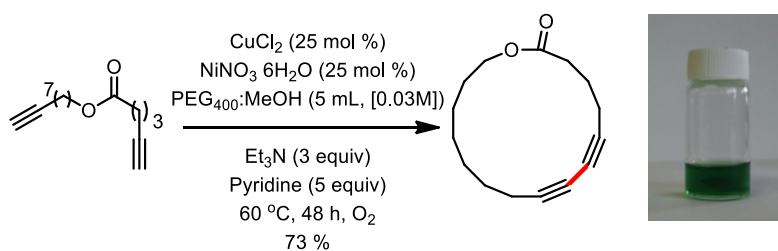
- Anne-Catherine Bédard participated in the design of the experiments, did all the experimental work and contributed to the writing of the manuscript.
- Shawn K. Collins participated in the design of the experiments and writing of the manuscript.

Reproduced by permission from the American Chemical Society

Permanent link to the article (DOI) : [10.1021/ja208902t](https://doi.org/10.1021/ja208902t)

3.1 – Abstract

Macrocycles are abundant in numerous chemical applications, however the traditional strategy for the preparation of these compounds remains cumbersome and environmentally damaging; involving tedious reaction set-ups and extremely dilute reaction media. The development of a macrocyclization strategy conducted at high concentrations is described which exploits phase separation of the catalyst and substrate, as a strategy to control dilution effects. Sequestering a copper catalyst in a highly polar and/or hydrophilic phase can be achieved using a hydrophilic ligand, T-PEG₁₉₀₀, a PEGylated TMEDA derivative. Similarly, phase separation is possible when suitable copper complexes are soluble in PEG₄₀₀, a green and efficient solvent which can be utilized in biphasic mixtures for promoting macrocyclization at high concentrations. The latter phase separation technique can be exploited for the synthesis of a wide range of industrially relevant macrocycles with varying ring sizes and functional groups.



3.2 – Introduction

Macrocycles are one of the most common cyclic motifs found in Nature.¹ Their unique chemical structures and properties have important applications in numerous scientific fields. Perhaps the greatest impact of macrocycles has been felt in the pharmaceutical and cosmetic industries.² In terms of drug discovery, synthetic macrocycles with structures inspired from natural products have been used successfully against many biological targets, often as rigidified peptide ligand mimics.³ The cosmetic industry has been exploiting naturally occurring macrocyclic musks for use as perfumes,^{4,6} however these compounds are not obtained from their respective plant sources and are prepared by synthesis on a multi-ton scale annually. Strangely, as the application of macrocycles continues to grow, the general strategy for the preparation of these compounds remains a challenge.

The efficiency of a macrocyclization is often controlled by the nature of the three-dimensional conformation of the macrocyclization precursor. Although some exceptions are known where a precursor adopts a conformation that allows for selective and efficient macrocyclization,⁷⁻⁸ in most instances the preparation of large rings is plagued by slow rates of intramolecular cyclization (Figure 3.1a). Consequently, the rates of the intermolecular reactions between precursors become competitive and oligomerization or extensive polymerization becomes problematic. Accordingly, synthetic chemists have devised two techniques to improve macrocyclization processes. The first involves conformational control, whereby through some chemical method, the macrocyclization precursor is made to adopt a conformation highly conducive to ring closure, thereby increasing the rate of intramolecular cyclization.

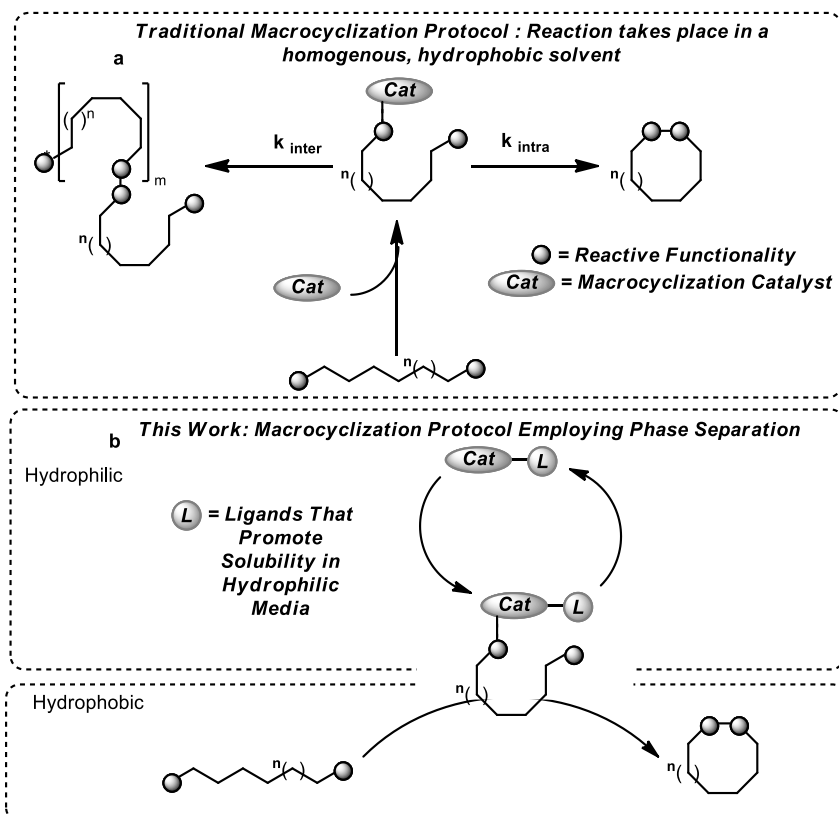


Figure 3.1 – a) Traditional macrocyclization in homogeneous hydrophobic media. b) Macrocyclization employing phase separation.

In contrast, the second and most popular strategy to improve macrocyclization reactions involves slowing the rate of intermolecular reactions. Most often, macrocyclization reactions are run at very low concentration and it is common that the precursor will be added to the reaction mixture *via* slow addition over an extended period of time. The extremely dilute reaction media requires that large volumes of solvent are used. In an era where most chemical processes are scrutinized for their environmental impact, the traditional macrocycle synthesis is perhaps one of the greatest offenders of the principles of green chemistry.⁹ Indeed, in both academic and industrial laboratories, macrocycle synthesis involving common

methods such as standard peptide coupling techniques, the Yamaguchi lactonization¹⁰ and ring closing olefin metathesis^{11,12} are all normally conducted under high dilution conditions. In addition to the obvious environmental concerns, both the issues of cost and scale-up to industrially relevant quantities of material combine to make macrocyclization reactions prohibitive in many industrial applications. In some rare instances, a significant effort can result in a substantial increase in yields and concentrations for a macrocyclization process,¹³⁻¹⁵ but the scarcity of examples underscores the need for new synthetic strategies. Considering both the importance of synthetic macrocycles and the widespread appeal of green chemical processes, the development of a general and green macrocyclization protocol that could be conducted *via* catalysis at high concentration, eliminating the need for high dilution, is an important synthetic goal that has yet to be achieved.¹⁶ Herein we describe a phase separation strategy that can be applied to catalytic macrocyclic Glaser-Hay couplings and demonstrate its application in the synthesis of macrocyclic musks.

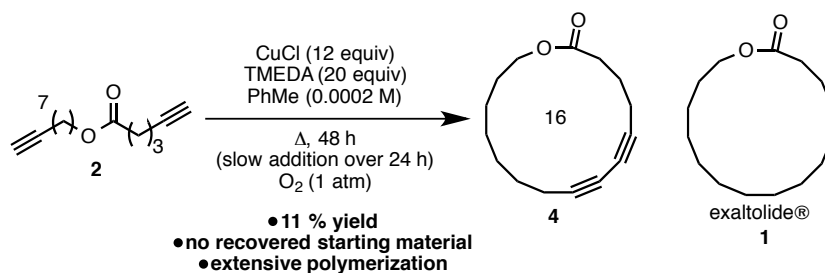
In traditional methods, the macrocyclization precursor is normally placed in a dilute homogeneous solution with a reagent or catalyst which mediates the cyclization at low concentrations (Figure 3.1a). In order to achieve macrocyclization at high concentrations, we chose to investigate techniques whereby the macrocyclization event between the catalyst and precursor would take place in an environment where the relative concentration of the precursor is low. It was believed that replacing traditional homogeneous reaction media with biphasic media could achieve this goal. While chemistry at the solid/liquid interface has become common in organic synthesis, organic synthesis at a liquid/liquid interface is surprisingly rare¹⁷ and often instead exploited in separation techniques.¹⁸

In order to force a macrocyclization event to occur at the interface of the two phases, the catalyst or reagent that catalyzes or mediates the macrocyclization would be sequestered in a single phase while the substrate would preferentially solubilize in a different phase (Figure 3.1b).¹⁹ In doing so, the effective concentration of the substrate at the interface would be small and mirror the low concentration typically employed in traditional macrocyclization reactions. Through phase separation of the catalyst and precursors, the need for high dilution becomes unnecessary and intramolecular cyclization should become the favoured reaction pathway. One method to achieve such a process would be to use two solvents that are sparingly miscible in conjunction with a catalyst whose ligands allow for it to be soluble and active in only one of the phases. Given that most organic substrates are soluble in hydrophobic media, the catalysts developed for such a process must maintain their activity in highly polar and/or hydrophilic media.²⁰

In order to evaluate whether such a process is feasible, we turned our attention towards developing a macrocyclization reaction that would not only demonstrate the proof-of-principle for phase separation as technique for achieving macrocyclization at high concentration, but also highlight its applicability towards macrocyclization in industrially relevant processes. We were attracted by the chemical challenges associated with the synthesis of macrocyclic musks, particularly the macrolactone exaltolide® **1**, which is currently the most industrially produced macrocyclic musk (Scheme 3.1).²¹ In examining a retrosynthesis of **1**, we choose to develop a route to **3** based upon a Glaser-Hay oxidative coupling of terminal alkynes. The Glaser-Hay coupling²²⁻²⁴ of **2** provides an appropriate starting point for the investigations for a number of reasons including: 1) the copper catalysts for these reactions are inexpensive, non-toxic and can easily be modified with ligands that permit solubility in hydrophilic media, 2) the reaction

results in the formation of a carbon-carbon bond, classically referred to as one of the most difficult bonds to prepare in organic synthesis and 3) the diyne precursor **2** exists as a linear aliphatic chain devoid of any conformational bias, hence efficient macrocyclization would only be achieved through control of the reaction concentration.

The investigations began by conducting traditional Glaser-Hay coupling on diyne **2** using standard conditions from the chemical literature.²⁵ The cyclization of alkyl alkynes is notoriously slower than aryl alkynes and super-stoichiometric amounts of copper reagent are normally necessary to achieve acceptable rates of cyclization. As such, **2** was added by syringe pump to a solution of CuCl, tetramethylethylene diamine (TMEDA) in refluxing CH₂Cl₂ under an oxygen atmosphere over 24 h and the solution was allowed to stir for an additional 24 h (Scheme 3.1). Following purification by chromatography, a complete conversion of **2** was observed but only an 11 % yield of the desired macrocycle **3** was obtained. In addition, when the macrocyclization of **2** is carried out using the same reaction conditions but at 150X the concentration shown in Figure 3.2, only extensive polymerization of **2** is observed. With the result of the traditional macrocyclization at various concentrations in hand, we sought to explore the phase separation strategy to improve the synthesis of **3**.

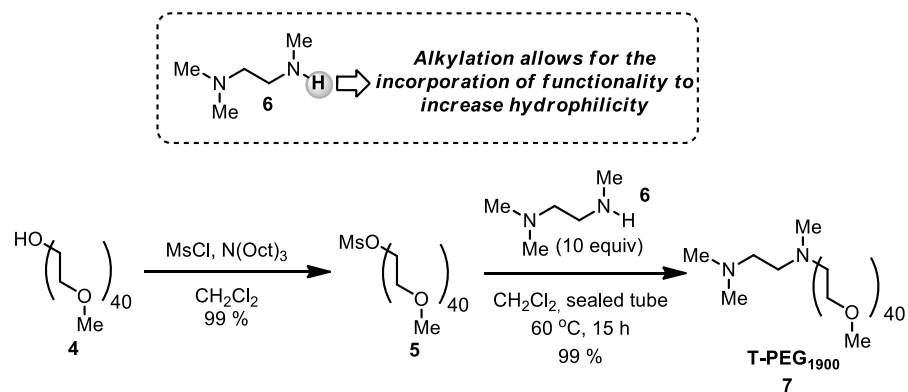


Scheme 3.1 – Synthesis of **3** based upon traditional conditions.

3.3 – Results and Discussion

3.3.1 – Developing Hydrophilic Ligands for Transition Metal Complexes for Use in “Green” Macrocyclizations

In order to develop a catalyst for macrocyclization via a Glaser-Hay coupling that could impart a preference for the catalyst complex to solubilize in hydrophilic media, it was necessary to modify the traditional TMEDA ligand to increase its water solubility. Our approach involved replacing one of the methyl groups of the ligand with a poly(ethylene glycol) (PEG) polymer (Scheme 3.2). The PEG alcohol monomethyl ether **4** can be easily transformed into its corresponding mesylate and used to alkylate trimethyldiamine **6**, affording the ligand **7** (T-PEG₁₉₀₀). After both the mesylation of alcohol **4** and the alkylation of amine **6**, the products are easily recovered via precipitation from the reaction mixture with Et₂O. T-PEG₁₉₀₀ **7** can also be further purified by filtration on a short column of neutral alumina.



Scheme 3.2 – Synthesis of PEGylated TMEDA derivative, T-PEG₁₉₀₀.

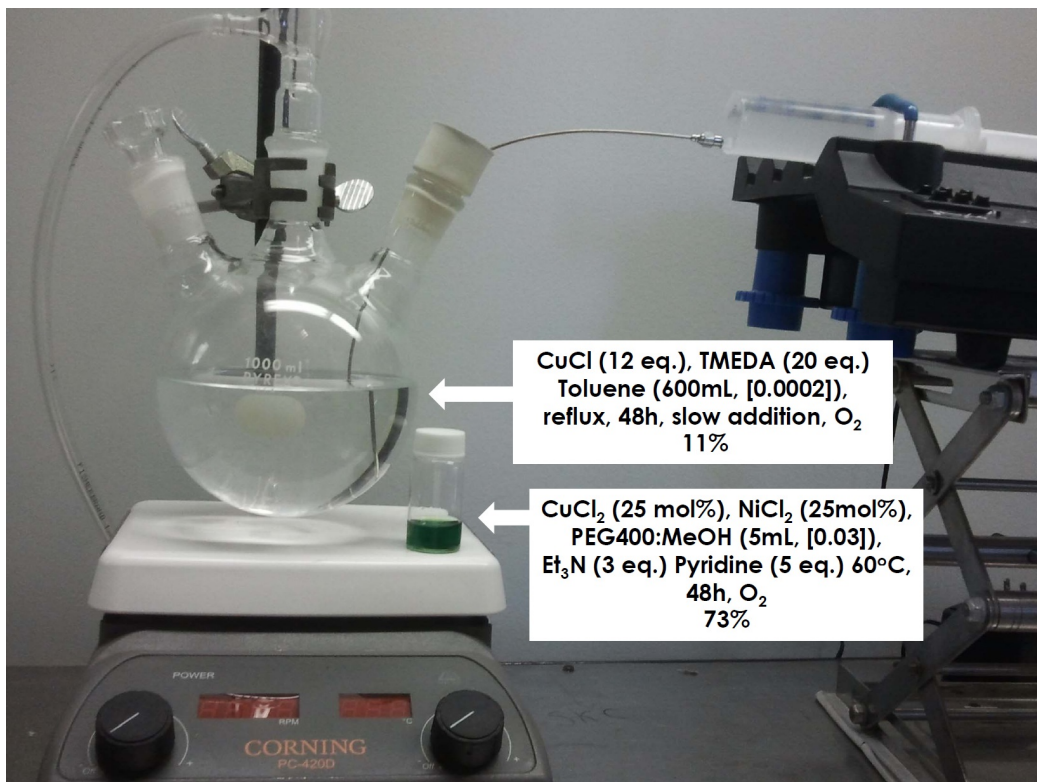
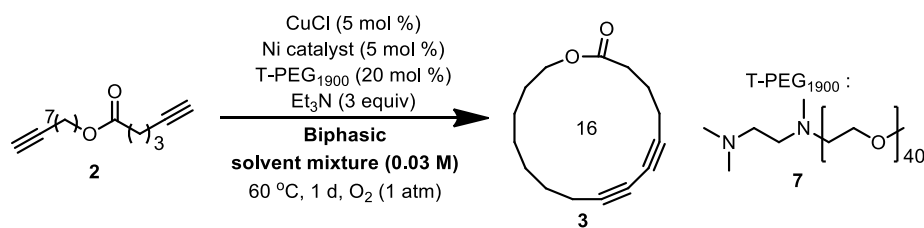


Figure 3.2 – Simplified experimental set-up for the “green” macrocyclization using phase separation.

As only extensive polymerization of **2** is observed under classical catalysis (CuCl, TMEDA) at 150X greater concentrations than the traditional synthesis depicted in Scheme 3.1, we next moved to investigating the macrocyclization of **2** in solvent mixtures. Initially, it was sought to study complexes of copper with the T-PEG₁₉₀₀ ligand in a mixture of non-miscible solvents such as H₂O/PhMe (1:1), again at 150X the traditional concentration (Table 3.1). Under the aqueous solvent conditions however, the T-PEG₁₉₀₀ Cu complexes were not active in the Glaser-Hay coupling, however gratifyingly the starting material **2** was recovered quantitatively. As such, we chose to further improve the reactivity of the Glaser-Hay coupling through the inclusion of a Ni-based co-catalyst. Lei and co-workers²⁶ have previously shown that a Ni co-catalyst can improve the reaction rates of Glaser-Hay couplings. Despite the addition of NiCl₂ to the reaction mixture, no macrocyclization was observed. Substitution of H₂O with MeOH in the solvent mixture produced a reaction that was initially biphasic but slowly became homogeneous at elevated temperatures. Gratifyingly, an isolated yield of 15 % for **3** was obtained, although the remaining starting material was oligomerized. Even though we had achieved identical yields to the traditional macrocycle synthesis (Figure 3.2), we sought to further improve the reaction through optimization of both the nature of the solvent and the ratio of hydrophilic to hydrophobic media. It was found that Et₂O/MeOH (1:1) was an optimal solvent combination which resulted in a 34-42 % isolated yield of the 1,3-diyne product **3**. Under these conditions, the NiCl₂ co-catalyst was finely suspended in the reaction mixture and it was believed that the heterogeneity was responsible for the varying yields. A variety of Ni salts were investigated as alternatives to NiCl₂ and Ni(NO₃)₂•6H₂O was found to be highly soluble and provided similar yields of **3** (35 %). Finally, when the catalyst loading was increased to 25 mol %, the isolated yield of macrocycle **3** was also increased to 65 %.

Table 3.1 – Model studies on the macrocyclization of **3** using a copper/T-PEG₁₉₀₀ system and phase separation as a strategy to control reactivity.



entry	Ni catalyst	Solvent (ratio)	yield (%)
1	none	PhMe/H ₂ O (1:1)	0
2	NiCl ₂	PhMe/H ₂ O (1:1)	0
3	NiCl ₂	PhMe/MeOH (1:1)	15
4	NiCl ₂	Et ₂ O/MeOH (1:1)	34-42 ^a
5 ^b	Ni(NO ₃) ₂ ·6H ₂ O	Et ₂ O/MeOH (1:1)	35
6 ^c	Ni(NO ₃) ₂ ·6H ₂ O	Et ₂ O/MeOH (1:1)	65

- a) In some cases complete consumption of the starting material was observed while in other instances 10-20 % could be recovered and up to 38 % of a linear dimer could be isolated. b) 5 days reaction time. c) 25 mol % of CuCl and Ni(NO₃)₂·6H₂O were used. 50 mol % of **7** was used.

The above results demonstrate that phase separation can be an effective technique to promote efficient macrocyclization at high concentrations. A novel Cu and Ni-based catalyst system was developed using a PEGylated diamine ligand T-PEG₁₉₀₀ which allowed the diyne macrocycle **3** to be prepared at significantly higher concentration (0.0002 M (600 mL) → 0.03 M (5 mL)) and yields (11 % → 65 %) than that utilized in traditional methods.

3.3.2 – Poly(ethylene glycol) (PEG) as a Solvent for “Green” Macrocyclization.

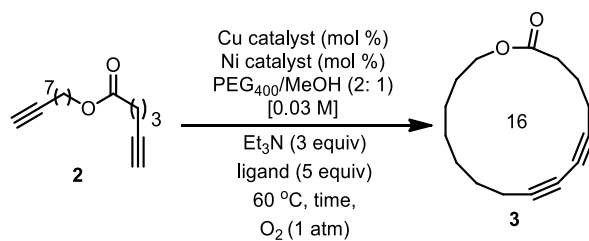
The success of the T-PEG₁₉₀₀ ligand in the previous macrocyclization reactions encouraged us to investigate the use of PEG itself as a solvent in the phase separation strategy. Poly(ethylene glycol) (PEG) has already been extensively studied as a reaction media for transition metal catalyzed reactions, particularly cross coupling transformations.^{27,28} PEG (low molecular weight) is well suited as a “green” solvent as it is a water soluble hydrophilic polymer that is relatively non-toxic, non-volatile, inexpensive and thermally stable.²⁹⁻³¹

The aforementioned properties of PEG are normally highly sought after when searching for alternatives to traditional organic solvents and consequently, PEG₄₀₀ was chosen as an ideal solvent for the development of a “green” macrocyclization protocol. In order to investigate the macrocyclization of **2** at high concentrations using PEG₄₀₀ as a hydrophilic solvent, we initially performed a control experiment to demonstrate that complexes of Cu salts with TMEDA or pyridine were soluble and homogeneous in PEG₄₀₀ solution under rapid stirring. Control experiments also demonstrated that in either homogeneous MeOH or PEG₄₀₀ solution, only polymerization of **2** is observed under classical catalysis (CuCl, TMEDA) at 150X the concentration used in the traditional conditions.

As with the macrocyclization reactions employing the T-PEG₁₉₀₀ ligand, we sought to improve the macrocyclization reaction using PEG₄₀₀ as a solvent through the use of Ni-based co-catalysts. Upon repeating the macrocyclization reaction of **2** in the presence of a stoichiometric amount of NiCl₂ a similar yield of 24 % yield was observed (Table 3.2).³² The reaction yields and rates could be increased (24→57 %, 3→1 day) by adjusting the ratio of PEG₄₀₀/MeOH from 1:1 to 2:1. We investigated other ligands for the Cu catalyzed process and

pyridine was shown to be superior (66 % yield of **3**) to TMEDA, phenanthroline or 2,6-bipyridine (Table 3.2, entries 3-6). Gratifyingly, the catalyst loading could be decreased to 25 mol % for both CuCl₂ and NiCl₂ without significant decreases in yield, although the reaction time was longer (Table 3.2, entries 6-9). The macrocyclization of **2** under these reaction conditions was slightly irreproducible, perhaps due to the fact that the NiCl₂ co-catalyst was not completely soluble in the reaction media. Analogous to previous studies, a series of more soluble Ni co-catalysts was surveyed (Table 3.2, entries 10-14) and Ni(NO₃)₂·6H₂O was again found to be highly soluble in PEG₄₀₀, and afforded good yields of the product **3** (73 %) at 25 mol % catalyst loading (Table 3.2, entry 16).

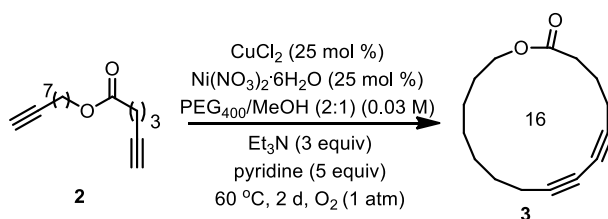
Table 3.2 – Model studies on the macrocyclization of **2** using a copper/nickel catalyst system and phase separation as a strategy to control reactivity.



entry	Cu/Ni (mol %); ligand	time (d)	yield (%)
1 ^a	CuCl (100); TMEDA	1	22
2 ^a	CuCl/NiCl ₂ (100); TMEDA	3	24
3	CuCl/NiCl ₂ (100); TMEDA	1	57
4	CuCl/NiCl ₂ (100); bipy	2	48
5	CuCl/NiCl ₂ (100); phen	4	26
6	CuCl/NiCl ₂ (100); pyridine	1	80
7	CuCl ₂ /NiCl ₂ (100); pyridine	1	78
8	CuCl ₂ / NiCl ₂ (50); pyridine	4	79
9	CuCl ₂ / NiCl ₂ (25); pyridine	4	68
10	CuCl ₂ /Ni(acac) ₂ (50); pyridine	5	22
11	CuCl ₂ /NiBr ₂ (100); pyridine	1	67
12	CuCl ₂ /NiF ₂ ·4H ₂ O (100); pyridine	1	68
13	CuCl ₂ /Ni (100); pyridine	2	76
14	CuCl ₂ /Ni(NO ₃) ₂ ·6H ₂ O (100); pyridine	1	83
15	CuCl ₂ /Ni(NO ₃) ₂ ·6H ₂ O (50); pyridine	1	68
16	CuCl ₂ /Ni(NO ₃) ₂ ·6H ₂ O (25); pyridine	2	73

a) Solvent ratio PEG₄₀₀/MeOH (1:1).

Table 3.3 – Model studies on the macrocyclization of **2** using a copper/T-PEG₁₉₀₀ system and phase separation as a strategy to control reactivity.



entry	scale (mmol 2)	yield (%)	solvent volume, ^a biphasic (mL)	solvent volume, ^b monophasic (mL)
1	0.12	73	5	600
2	0.36	65	15	1800
3	1.00	60	45	5400

a) Total volume of solvent required for the reaction using PEG₄₀₀/MeOH solvent mixture. b) Total solvent required if an analogous reaction were performed using the traditional conditions reported in Scheme 2.1.

Upon optimization of the catalytic system and the reaction conditions, we performed some preliminary investigations on the feasibility of scale-up using the phase separation strategy for macrocyclization (Table 3.3). When the macrocyclization of diyne **2** was performed on three times the previous scale (0.36 mmol), we were pleased to observe very little change in the overall isolated yield of the reaction (Table 3.3, entry 2). When the reaction was scaled up to 1 mmol scale, an isolated yield of 60 % was obtained for the desired macrocycle **3**. Importantly, the macrocyclization on 1 mmol scale needed only 45 mL of a mixture of PEG₄₀₀/MeOH while the analogous macrocyclization would have required 5400 mL of PhMe or CH₂Cl₂ to perform (Table 3.3).

While further optimization of the catalyst and/or ligand structure may afford higher yields, the increase in concentration, reduction of solvent and high yields demonstrate a significant step towards achieving a general and green macrocyclization protocol. In addition,

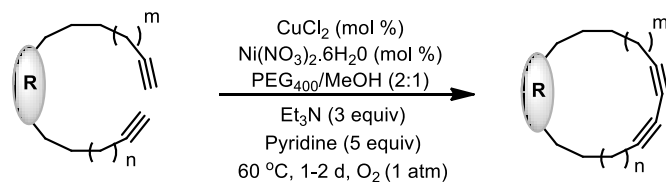
it should be noted that the phase separation strategy allows for a simpler experimental set-up when conducting the macrocyclization (Figure 3.2), whereby the use of cumbersome syringe pumps and expensive glassware is avoided and replaced by a simple screw-cap vial.

To demonstrate some generality of the optimized catalytic system and reaction conditions, we explored the substrate scope of the macrocyclization. We first explored the scope of the ring size for the synthesis of macrolactones using the phase separation strategy (Table 3.4, entries 1-6). Each macrocyclization was performed using both stoichiometric and catalytic amounts of Cu and Ni complexes. In general, yields are good to excellent using catalytic amounts of Cu and Ni and only small increases were observed when using stoichiometric quantities. First, a smaller rigidified 14-membered macrolactone **8** was isolated in 62 % yield (Table 3.4, entry 1). Second, the macrocyclization of larger macrolactones was investigated and it was found that lactones having ring sizes of 18, 21 and 23 atoms at high concentrations were all possible using the phase separation strategy. The 18-membered macrolactone **9** was isolated in 74 % yield using 25 mol % of catalysts (stoichiometric Cu/Ni = 87 %). The synthesis of 21- and 23-membered macrolactones was equally efficient. The diyne macrocycles **10** and **11** were isolated in 81 % and 78 % yield respectively under catalytic conditions. Finally, a 28-membered macrolactone **12** was prepared in 91 % isolated yield using stoichiometric reagents and in 98 % when using the catalytic Cu/Ni combination. A variety of functional groups were also tolerant of the reactions conditions (Table 3.4, entries 7-10). An 18-membered diyne macrocycle embedded within a suitably-protected glucose core **13** was isolated in 65 % yield under catalytic conditions. Similarly, esters and phenolic ethers all afforded high yields of the corresponding macrocyclization products. Under catalytic conditions, the ester-containing macrocycle **14** was isolated in 70 % yield under the catalytic

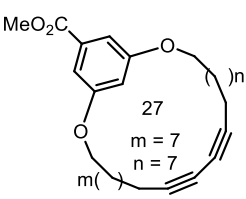
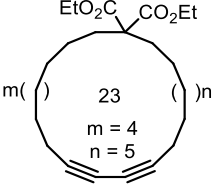
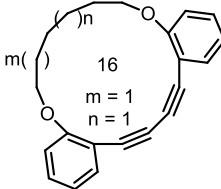
conditions. In addition, the malonate derived macrocycle **15** was isolated in 63 % yield under catalytic conditions. Macrocyclization of aryl substituted alkynes was similarly efficient, as the the 16-membered diether **16** was isolated in nearly quantitative yields (98 %) under the optimized catalytic conditions.³³

Importantly, in all of the above examples, control reactions whereby the substrates were placed in homogeneous MeOH solution at the identical high concentrations only resulted in complete consumption of the diyne precursors and the formation of polymer products demonstrating that phase separation using transitional metal complexes solubilized in PEG₄₀₀ can be exploited to promote efficient macrocyclization of a wide range of diyne macrocycles (**8-16**) in good to excellent yields (65-98 %) at high concentrations.

Table 3.4 – Macrocyclization via Glaser-Hay coupling of various diynes using a copper/nickel co-catalyst system and phase separation.



entry	product		catalyst (mol %)	yield (%)
1	 16 m = 1 n = 1	3	100 25	83 73
2	 14 m = 1 n = 1	8	100 25	68 62
3	 18 m = 1 n = 3	9	100 25	87 74
4	 21 m = 1 n = 5	10	100 25	93 81
5	 23 m = 2 n = 5	11	100 25	85 78
6	 28 m = 7 n = 7	12	100 25	91 98
7	 18 m = 1 n = 3	13	100 25	67 65

8		14	100 25	69 70
9		15	100 25	65 63
10		16	100 25	77 98

3.4 – Conclusions

Macrocyclic Glaser-Hay coupling at high concentrations can be achieved using phase separation as a strategy to control dilution effects. Two different strategies for performing macrocyclizations in biphasic media have been developed using the diyne macrocycle **3** as a target to demonstrate that the developed macrocyclizations could be performed on industrially relevant compounds. First, we demonstrated that when necessary, phase separation between catalyst and substrates can be achieved by developing hydrophilic ligands for transition metal complexes that allow for the catalysts to be sequestered in a highly polar and/or hydrophilic phase. To demonstrate this strategy, a PEGylated TMEDA derivative T-PEG₁₉₀₀ was prepared and promoted the cyclization of **2** at a significantly higher concentration (0.0002 M (600 mL) → 0.03 M (5 mL)) and better yields (11 % → 65 %) than that utilized in traditional methods (Figure 2.3). Secondly, solubilization of Cu/pyridine complexes in PEG₄₀₀ demonstrates it

applicability as a green and efficient solvent for use in biphasic mixtures for macrocyclization at high concentrations. Copper/nickel co-catalysts systems can be used to promote the macrocyclization of a wide range of macrocycles with varying ring sizes and functional groups. The concept that phase separation can be used to control dilution effects in macrocyclization reactions should allow for the practical synthesis of this class of compounds to provide highly valuable chemical products using practices that are significantly more environmentally benign. In addition, the phase separation strategies discussed herein are currently being applied to develop other macrocyclization protocols for macrocyclic olefin metathesis and macrolactonization, using environmentally benign solvents and concentrations.

Acknowledgements

The authors acknowledge the Natural Sciences and Engineering Research Council of Canada (NSERC), Université de Montreal and the Centre for Green Chemistry and Catalysis for generous funding. A.-C.B. thanks NSERC for an Alexander-Graham Bell Graduate Scholarship and an FQRNT Graduate Scholarship.

Associated content

Experimental procedures, spectroscopic data for all new compounds and complete reference 3. This material is available free of charge via the Internet at <http://pubs.acs.org>.

3.5 – Bibliography

- (1) Roxburgh, J. C. *Tetrahedron* **1995**, *51*, 9767-9822.
- (2) Driggers, E. M.; Hale, S. P.; Lee, J.; Terrett, N. K. *Nat. Rev. Drug Discovery* **2008**, *7*, 608–624.
- (3) Lamarre, D. et al. *Nature* **2003**, *426*, 186-189.
- (4) Matsuda, H.; Watanabe, S.; Yamamoto, K. *Chem. Biodiversity* **2004**, *1*, 1985-1991.
- (5) Rueedi, G.; Nagel, M.; Hansen, H.-J. *Org. Lett.* **2004**, *6*, 2989-2991.
- (6) Fehr, C.; Galindo, J.; Etter, O.; Thommen, W. *Angew. Chem., Int. Ed.* **2002**, *41*, 4523-4526.
- (7) Bolduc, P.; Jacques, A.; Collins, S. K. *J. Am. Chem. Soc.* **2010**, *132*, 12790-12791.
- (8) White, C. J.; Yudin, A. K. *Nature Chem.* **2011**, *3*, 509-524.
- (9) Beach, E. S.; Cui, Z; Anastas, P. T. *Energy & Environmental Science* **2009**, *2*, 1038-1049.
- (10) Parenty, A.; Moreau, X.; Campagne, J. M. *Chem. Rev.* **2006**, *106*, 911–939.
- (11) Gradillas, A.; Pérez-Castellsm J. *Angew. Chem., Int. Ed.* **2006**, *45*, 6086-6101.
- (12) Fürstner, A.; Langemann, K. *Synthesis* **1997**, *7*, 792-803.
- (13) Shu, C.; Zeng, X.; Hao, M.-H.; Wei, X.; Yee, N. K.; Busacca, C. A.; Han, Z.; Farina, V.; Senanayake, C. H. *Org. Lett.* **2008**, *10*, 1303-1306.
- (14) Nicola, T.; Brenner, M.; Donsbach, K.; Kreye, P. *Org. Proc. Res. Dev.* **2005**, *9*, 513-515.
- (15) Farina, V.; Shu, C.; Zeng, X.; Wei, X.; Han, Z.; Yee, N. K.; Senanayake, C. H. *Org. Proc. Res. Dev.* **2009**, *13*, 250-254.
- (16) Gupta, M.; Paul, S.; Gupta, R. *Curr. Sci.* **2010**, *99*, 1341-1360.
- (17) For an example of a liquid/liquid phase separation strategies in an industrial process see: Herrmann, W. A.; Kohlpaintner, C. W. *Angew. Chem., Int. Ed. Engl.* **1993**, *32*, 1524-1544.
- (18) Phase separation strategies in organic synthesis typically involve synthesis on solid phase supports. Some examples of liquid/liquid phase separation techniques in synthesis include fluoruous biphasic systems: Horvath, I. T.; Rabai, J. *Science* **1994**, *266*, 72-75.
- (19) The term phase separation is used in a general sense, as it could be achieved by various mechanisms, including hydrophilic/hydrophobic solvent mixtures with no miscibility, to the formation of aggregates or micelles. Micellar catalysis could achieve a similar phase separation, but has been mostly exploited as a route towards achieving catalysis in hydrophilic media, see: (a) Stavber, G. *Aust. J. Chem.* **2010**, *63*, 849-849. For examples of micelles formed from PEG400 see: (b) Hasegawa, U.; van der Vlies, A. J.; Simeoni, E.; Wandrey, C.; Hubbell, J. A. *J. Am. Chem. Soc.* **2010**, *132*, 18273-18280. (c) Dong, W.-F.; Kishimura, A.; Anraku, Y.; Chuanoi, S.; Kataoka, K. *J. Am. Chem. Soc.* **2009**, *131*, 3804-3805.
- (20) Hong, S. H.; Grubbs, R. H. *J. Am. Chem. Soc.* **2006**, *128*, 3508-3509.
- (21) William, A. S. *Synthesis* **1999**, *10*, 1707-1723.
- (22) *Acetylene Chemistry: Chemistry, Biology, and Material Science*; Diederich, F., Stang, P. J., Tykwinski, R. R., Eds.; Wiley-VCH: Weinheim, Germany, 2005.
- (23) Hay, A. S. *J. Org. Chem.* **1960**, *25*, 1275-1276.

- (24) Hay, A. S. *J. Org. Chem.* **1962**, *27*, 3320-3321.
- (25) Haley, M. M.; Pak, J. J.; Brand, S. C. *Top. Curr. Chem.* **1999**, *201*, 81-130.
- (26) Yin, W.; He, C.; Chen, M.; Zhang, H.; Lei, A. *Org. Lett.* **2009**, *11*, 709-712.
- (27) Namboodir, V. V.; Varma, S. R. *Green Chem.* **2001**, *3*, 146-148.
- (28) Bai, L.; Wang, J.-X. *Curr. Org. Chem.* **2005**, *9*, 535-553.
- (29) Nagarapu, L.; Mallepalli, R.; Arava, G.; Yeramanchi, L. *Eur. J. Chem.* **2010**, *1*, 228-231.
- (30) Candeias, N. R.; Branco, L. C.; Gois, P. M. P.; Afonso, C. A. M.; Trindade, A. F. *Chem. Rev.* **2009**, *109*, 2703-2802.
- (31) Zhang, Z.-H. *Research Journal of Chemistry and Environment* 2006, *10*, 97-98.
- (32) Although the reactions appear homogeneous upon extended stirring or after the reaction have begun to warm to 60 °C, it should be noted that there is ample precedent to suggest that indeed PEG₄₀₀ is forming micellar structures in solution that may be responsible for the phase separation effect (see ref 19). To date, we have performed preliminary experiments using salt effects (using LiClO₄ and (NH₄)₂SO₄) to determine whether micelles may be present, however the experiments were inconclusive. For a discussion of salt effects in macromolecular structures that were used in our preliminary studies see: Zhang, Y.; Cremer, P. S. *Curr Opin Chem. Biology* **2006**, *10*, 658-663.
- (33) Jones, C. S.; O'Connor, M. J.; Haley, M. M. *Acetylene Chemistry* **2005**, 303-385.

Chapter 4 : Microwave Accelerated Glaser-Hay Macrocyclizations at High Concentrations

Anne-Catherine Bédard and Shawn K. Collins*

Département de Chimie, Center for Green Chemistry and Catalysis, Université de
Montréal, CP 6128 Station Downtown, Montréal, Québec H3C 3J7 Canada

Chemical Communications **2012**, 48, 6420-6422.

Contributions:

- Anne-Catherine Bédard participated in the design of the experiments, did all the experimental work and contributed to the writing of the manuscript.
- Shawn K. Collins participated in the design of the experiments and writing of the manuscript.

Reproduced by permission from the Royal Society of Chemistry

Permanent link to the article (DOI) : [10.1039/C2CC32464D](https://doi.org/10.1039/C2CC32464D)

4.1 – Abstract

Efficient macrocyclization can be conducted at high concentrations employing microwave irradiation and a phase separation strategy. The rate of the Glaser-Hay macrocyclization is accelerated using microwave irradiation and reaction times decreased from 48 h to 1-6 h, depending on the nature of the substrate. Macrocyclization concentrations could be increased up to 0.1 M compared to traditional concentrations (0.2 mM).

4.2 – Introduction

The application of macrocycles in drug discovery, pharmaceuticals, agrochemicals and cosmetics continues to increase due to their unique chemical structures and properties.¹⁻³ The preparation of macrocycles is often hampered by competing oligomerization reactions, hence the requirement that they be conducted under relatively low concentration.⁴ The large volumes of solvent required to attain the necessary dilution renders macrocyclization processes problematic on larger scales.⁵ It is also customary to heat macrocyclization reactions to high temperatures to help promote the slow rate of ring closure. Consequently, the rapid heating and high temperatures possible *via* microwave irradiation would seem an ideal tool to exploit in the synthesis of macrocycles.⁶ Microwave promoted macrocyclizations have been used to prepare macrocyclic peptides, most commonly during syntheses employing solid supports.⁷ However, a drawback to the strategy is that most microwave reactors are restricted in size and it may be impossible to scale up or to use slow addition techniques to improve yields.⁸ Hence, it is difficult to envision performing macrocyclizations in a microwave reactor when low concentrations are required. Herein we report a microwave accelerated synthesis of

macrocycles via Glaser-Hay coupling at high concentrations made possible through the use of a phase separation strategy.

4.3 – Results and Discussion

We have recently reported an improved protocol for macrocyclic Glaser-Hay coupling that employs phase separation as a strategy to control the effective molarity.⁹ The procedure employed mixtures of PEG₄₀₀/MeOH as a solvent combination. It is assumed that the formation of aggregates by the PEG₄₀₀ allows for separation of the substrate¹⁰ and catalyst and promotes reactions at the interphase of the two solvents,¹¹ effectively controlling the molarity during the key bond forming process (Figure 4.1).¹²

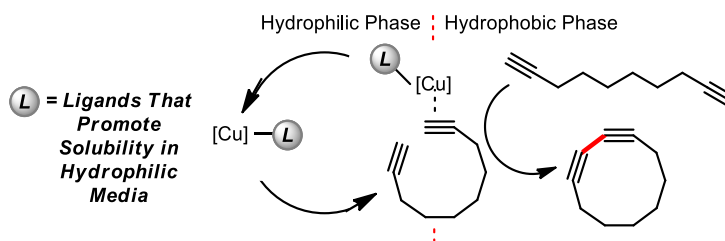
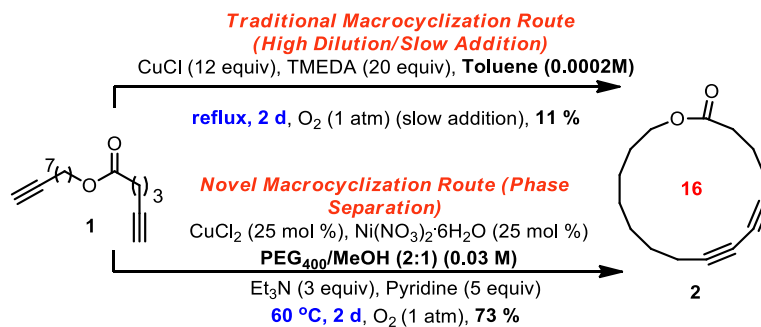


Figure 4.1 – Macrocyclization employing phase separation.

As a result of the phase separation strategy, macrocycles containing 1,3-diyne moieties were prepared in increased yield compared to a traditional synthesis using high dilution and slow addition techniques. For example, the 16-membered macrolactone **2**,¹³ was prepared in only 11 % yield when performed using high dilution conditions. Alternatively, when using the phase separation conditions employing a PEG₄₀₀/MeOH solvent mixture, the product **2** was obtained in 73 % yield using catalytic amounts of catalysts and at 150X greater concentration.

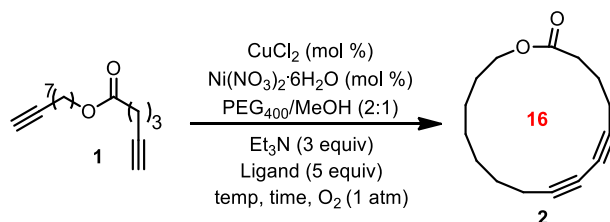


Scheme 4.1 – Comparing macrocyclization routes to diyne **2**.

A drawback of the phase separation strategy was the long reaction times (1-2 d) due to slow reaction at the solvent interface (Scheme 4.1). In an effort to accelerate the reactions, we decided to investigate performing the cyclizations under microwave heating. The phase separation strategy described herein is ideally suited for batch reactor microwaves as it allows for the reactions to be conducted at relatively high concentrations, eliminating the need for a continuous flow microwave set-up.^{14,15}

Our initial investigations began with performing the previously reported macrocyclization with diyne **1** at 100 °C in a microwave vessel (Table 4.1). No desired product was isolated and precipitation of the catalyst (and/or precipitation of catalyst decomposition products) was observed. As such, we surveyed other bidentate ligands which may prevent the precipitation of the catalyst and/or co-catalyst and identified tetramethylethylene diamine (TMEDA) as the optimal ligand. The macrocycle **2** was then isolated in a yield (75 %) that was identical to what was observed under traditional heating (73 %) and in just 6 h (traditional heating = 48 h)

Table 4.1 – Optimization of macrocyclization of diyne **1** under microwave irradiation.



entry	Cu/Ni (mol%)	ligand	temp (°C); time (h)	yield (%) ^a
1	50	pyridine	100; 6	0
2	50	bipy	100; 6	18
3	50	phen	100; 6	14
4	50	TMEDA	100; 6	75
5	25	TMEDA	100; 6	57 ¹
6	25	TMEDA	100; 12	81

a) Isolated yields following flash chromatography. b) Precipitation and/or decomposition of the Cu complex is observed at the elevated temperatures. bipy = 2,2'-bipyridine, phen = 1,10-phenanthroline

Having identified efficient reaction conditions (120 °C, TMEDA, 6 h), we decided to investigate the substrate scope (Table 4.2). Macrolactones having sizes of 21, 23 and 28-membered rings were prepared using the microwave protocol and the results compared to the yields and rates obtained with traditional heating (Table 4.2, entries 2-4). In all cases, the reaction rate was improved from 48 h to just 6 h. In the case of the 21- and 23-membered macrolactones **3** and **4**, the yields of the final products were within 10 % of those obtained with traditional heating. For the diester **5**, the isolated yield of 61 % was lower than what was

¹ There is an error in the reported table. The yield at 100 °C for 6 h is 54 % (entry 5) and the yield at 120 °C for 6

obtained with traditional heating, however the reaction was stopped at 6 h and 25 % of the starting diyne was re-isolated.¹⁶ It is assumed that by extending the reaction further would result in complete conversion and an increase in the final yield of the product **5**.

The macrocyclic ether **6** was also obtained in yields that resemble those obtained with traditional heating (65 % vs. 70 % respectively) in just 6 h. Finally the diaryl macrocycle **7** was also prepared in good yield (71 %) using the microwave heating in only 1 h.¹⁷ Having demonstrated that microwave assisted macrocyclizations were possible at higher concentrations using phase separation techniques, we also sought to illustrate the usefulness of the microwave protocol in the synthesis of some new macrocyclic structures (Table 4.2, entries 7 and 8). Consequently, we first sought to investigate the cyclization of some substrates having one aryl alkyne and one alkyl alkyne (Table 4.2, entries 7 and 8). The macrolactones **8** and **9** were synthesized using the established conditions in just 3 h at 120 °C in yields of 67 and 64 % respectively. The decrease in reaction time from the typical 6 h to 3 h is expected with substrates having more reactive aryl alkynes.

Table 4.2 – Comparison of macrocyclic Glaser-Hay couplings of diynes under traditional heating versus microwave irradiation.^a

entry	product	entry	product
1		2	
	(Δ): 60 °C; 48 h, 73 % (μw): 100 °C; 6 h, 57 %		(Δ): 60 °C; 48 h, 81 % (μw): 100 °C; 6 h, 81 %
3		4	
	(Δ): 60 °C; 48 h, 78 % (μw): 100 °C; 6 h, 69 %		(Δ): 60 °C; 24 h, 98 % (μw): 120 °C; 6 h, 61 % ^b
5		6	
	(Δ): 60 °C; 24 h, 70 % (μw): 120 °C; 6 h, 65 %		(Δ): 60 °C; 24 h, 98 % (μw): 120 °C; 1 h, 71 %
7		8	
	(μw): 120 °C; 3 h, 67 %		(μw): 120 °C; 3 h, 64 %

a) Isolated yields following flash chromatography. b) 25% of the starting diyne was recovered.

To further confirm the increase in the rate when using microwave irradiation, the cyclization of diyne **10** was conducted using both microwave irradiation and traditional heating. The isolated yield of macrocycle **3** was determined for various reaction times (Figure 4.2). While a rapid formation of **3** under microwave irradiation was observed in the first two hours (with a 81 % yield observed after 6 h), the formation of **3** was much slower under traditional heating in an oil bath, where only 28 % of **3** was observed after 2 h and 36 % after 6 h.¹⁸

To demonstrate that the developed chemistry using microwave irradiation could potentially be used for performing reactions on larger scales, we performed the reactions using even higher concentrations (Figure 4.2). The macrocyclizations were run in either homogenous MeOH solution or in PEG₄₀₀/MeOH (2:1) solvent mixture. When the reactions were conducted under traditional heating at 0.1 M in PEG₄₀₀/MeOH (2:1), a 53 % isolated yield of macrocycle **3** was obtained. When the corresponding reaction was run in homogeneous MeOH, the yield of the desired product dropped significantly to only ~5 %. Similar trends were observed when the macrocyclizations were performed at high concentrations using microwave irradiation. The diyne **3** was formed in 75 % yield under the microwave irradiation protocol in PEG₄₀₀/MeOH (2:1) at 0.03 M, but only 24 % was formed in MeOH solution. When the concentration was increased to 0.05 M, the use of phase separation conditions allowed for a 57 % isolated yield while MeOH alone as solvent gave 16 %. Finally, at 0.1 M, 42 % of macrocyclic diyne **3** was obtained and only ~8 % was isolated when using MeOH as a solvent. The above results demonstrate the ability of phase separation to promote efficient cyclization at high concentrations (traditional 0.2 mM vs. phase separation 0.1 M).

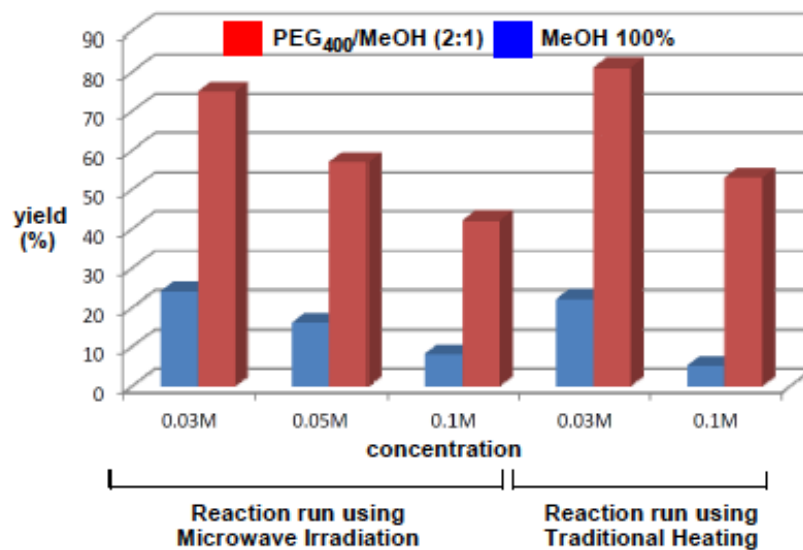
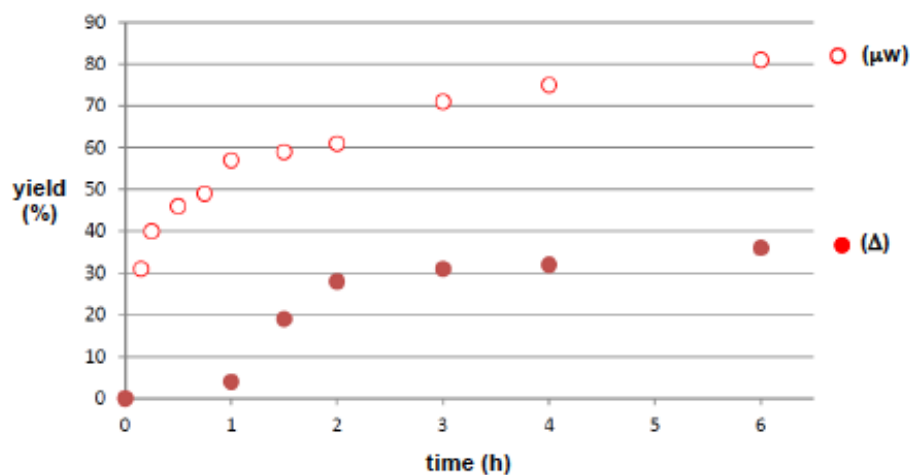
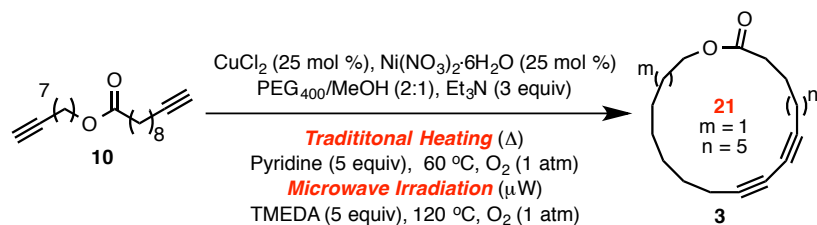


Figure 4.2 – (top) Comparison of the rate of formation of macrocycle **3** using different heating techniques. (bottom) Comparing homogenous solutions vs. phase separation in macrocyclizations at high concentrations

4.4 – Conclusion

A protocol that allows for Glaser-Hay macrocyclizations to be performed at high concentrations using microwave reactors commonly used in academic/industrial laboratories without the need for a continuous flow apparatus. The microwave irradiation strategy utilizing a Cu/TMEDA catalyst and PEG₄₀₀/MeOH solvent mixture promotes rate acceleration (*versus* thermal heating). Reactions could be effectively performed at concentrations up to 0.1 M.¹⁹ Further study is aimed at studying the origin of the phase separation and understanding the role that aggregates may play in controlling the effective molarity.

Acknowledgement. This work was financially supported by the Natural Sciences and Engineering Research Council of Canada (NSERC), Université de Montreal and the Centre for Green Chemistry and Catalysis for generous funding.

Supporting Information Available: Electronic Supplementary Information (ESI) available: Experimental procedures and characterisation data for all new compounds. See DOI: 10.1039/b000000x/

4.5 – Bibliography

- (1) J. C. Roxburgh, *Tetrahedron* 1995, **51**, 9767.
- (2) E. M. Driggers, S. P. Hale, J. Lee and N. K. Terrett, *Nat. Rev. Drug Discovery*, 2008, **7**, 608.
- (3) (a) E. Marsault, M. L. Peterson, *J. Med. Chem.*, 2011, **54**, 1961. (b) H. Matsuda, S. Watanabe and K. Yamamoto, *Chem. Biodiversity*, 2004, **1**, 1985 (c) G. Rueedi, M. Nagel and H.-J. Hansen, *Org. Lett.*, 2004, **6**, 2989. (d) C. Fehr, J. Galindo, O. Etter and W. Thommen, *Angew. Chem., Int. Ed.*, 2002, **41**, 4523.
- (4) For examples of macrocyclizations aided by conformational preorganization: (a) P. Bolduc, A. Jacques and S. K. Collins, *J. Am. Chem. Soc.*, 2010, **132**, 12790. (b) C. J. White and A. K. Yudin, *Nature Chem.*, 2011, **3**, 509.
- (5) V. Farina, C. Shu, X. Zeng, X. Wei, Z. Han, N. K. Yee and C. H. Senanayake, *Org. Proc. Res. Dev.*, 2009, **13**, 250.
- (6) (a) L. R. Odell and M. Larhed, in *Handbook of Green Chemistry*, Eds. P. T. Anastas and R. H. Crabtree, 2009, **1**, 79. (b) C. O. Kappe and D. Dallinger, *Nat. Rev. Drug Discovery*, 2006, **5**, 51.
- (7) (a) A. Lampa, A. E. Ehrenberg, A. Vema, E. Aakerblom, G. Lindeberg, U. H. Danielson, A. Karlen and A. Sandstroem, *Bioorg. Med. Chem.*, 2011, **19**, 4917. (b) S. N. Khan, A. Kim, R. H. Grubbs and Y.-U. Kwon, *Org. Lett.*, 2011, **13**, 1582.
- (8) (a) D. Obermayer, T. N. Glasnov, C. O. Kappe, *J. Org. Chem.*, **2011**, **76**, 6657. (b) M. Damm, T. N. Glasnov and C. O. Kappe, *Org. Process Res. Dev.*, **2010**, **14**, 215.
- (9) A.-C. Bédard and S. K. Collins, *J. Am. Chem. Soc.*, 2011, **133**, 19976.
- (10) The term phase separation is used in a general sense, as it could be achieved by various mechanisms, including hydrophilic/hydrophobic solvent mixtures with no miscibility, to the formation of aggregates or micelles. Micellar catalysis could achieve a similar phase separation, but has been mostly exploited as a route towards achieving catalysis in hydrophilic media, see: (a) G. Stavber, *Aust. J. Chem.*, 2010, **63**, 849. For examples of micelles formed from PEG₄₀₀ see: (b) U. Hasegawa, A. J. van der Vlies, E. Simeoni, C. Wandrey and J. A. Hubbell, *J. Am. Chem. Soc.*, 2010, **132**, 18273. (c) W.-F. Dong, A. Kishimura, Y. Anraku, S. Chuanoi and K. Kataoka, *J. Am. Chem. Soc.*, 2009, **131**, 3805.
- (11) For examples of a liquid/liquid phase separation strategy see: (a) W. A. Herrmann and C. W. Kohlpaintner, *Angew. Chem., Int. Ed. Engl.*, 1993, **32**, 1524. (b) I. T. Horvath and J. Rabai, *Science*, 1994, **266**, 72.
- (12) For other examples of controlling dilution effects in fluorous phase media see: (a) R. Correa da Costa and J. A. Gladysz, *Adv. Synth. Cat.*, 2007, **349**, 243. (b) D. P. Curran, S. Hadida, S.-Y. Kim and Z. Luo, *J. Am. Chem. Soc.*, 1999, **121**, 6607.
- (13) Macrocyclic **2** is a precursor of Exaltolide®: A. S. William, *Synthesis*, 1999, **10**, 1707.
- (14) (a) S. E. Wolkenberg, W. D. Shipe, C. W. Lindsley, J. P. Guare and J. M. Pawluczyk, *Curr. Opin. Drug Discovery & Development*, 2005, **8**, 701. (b) M. G. Organ, P. R. Hanson, A. Rolfe, T. B. Samarakoon and F. Ullah, *J. Flow Chem.*, 2011, **1**, 32. (c) G. Shore, W.-J. Yoo, C.-J. Li, M. G. Organ, *Chem.-Eur. J.*, 2010, **16**, 126.
- (15) C. Conner and G. A. Tompsett, *J. Phys. Chem. B*, 2008, **112**, 2110.

- (16) Reactions heated under microwave irradiation typically occur with complete conversion of the starting material to macrocycle or what are believed to be oligomers.
- (17) (a) *Acetylene Chemistry: Chemistry, Biology, and Material Science*; F. Diederich, P. J. Stang, R. R. Tykwinski, Eds.; Wiley-VCH: Weinheim, Germany, 2005. (b) A. S. Hay, *J. Org. Chem.*, 1960, **25**, 1275. (c) A. S. Hay, *J. Org. Chem.*, 1962, **27**, 3320.
- (18) The cyclization of **10** performed in an oil bath (sealed tube) at 120 °C after 6 h gave 60 % of **3**.
- (19) Cyclization of **10** at 1 mmol scale at 0.1 M under the developed conditions afforded a 40 % yield of the product **3**, demonstrating that the reaction is easily scaled up to larger scales.

Chapter 5 : Exploiting Aggregation to Achieve Phase Separation in Macrocyclization

Anne-Catherine Bédard and Shawn K. Collins*

Département de Chimie, Center for Green Chemistry and Catalysis, Université de Montréal, CP 6128 Station Downtown, Montréal, Québec H3C 3J7 Canada

Chemistry, a European Journal **2013**, *19*, 2108-2113.

Contributions:

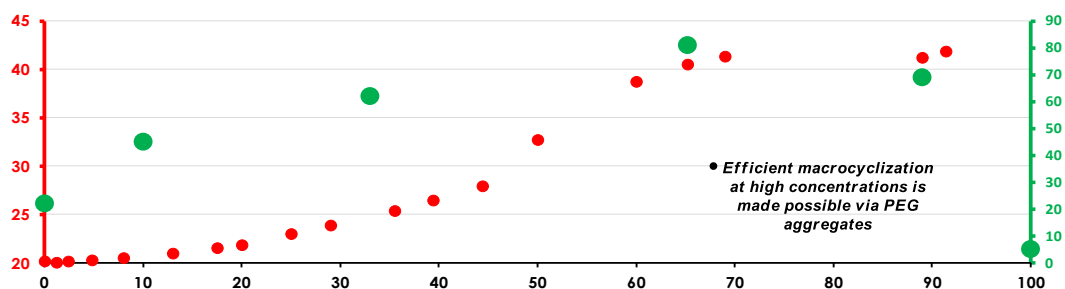
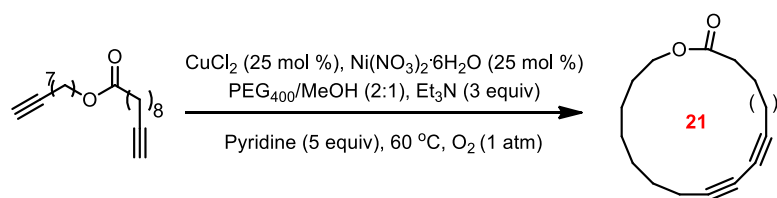
- Anne-Catherine Bédard participated in the design of the experiments, did all the experimental work and contributed to the writing of the manuscript.
- Shawn K. Collins participated in the design of the experiments and writing of the manuscript.

Reproduced by permission from Wiley-VCH

Permanent link to the article (DOI) : [10.1002/chem.201203433](https://doi.org/10.1002/chem.201203433)

5.1 – Abstract

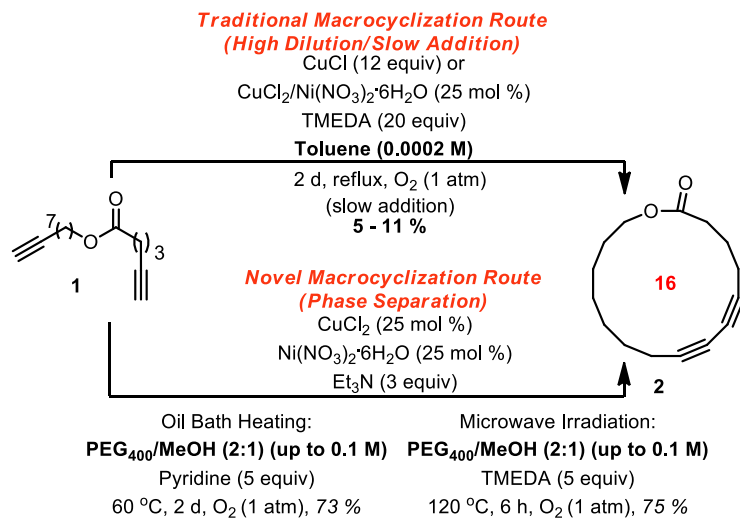
The aggregation properties of PEG can be exploited in organic synthesis to control dilution effects. Through the use of solvent mixtures containing PEG₄₀₀/MeOH, macrocyclization via Glaser-Hay coupling can be conducted at high concentrations. The origin of the selectivity has been studied using surface tension measurements, UV spectroscopy and chemical “tagging” and demonstrate the dependence of the yield and selectivity on the aggregation of PEG₄₀₀ and its ability to preferentially solubilize organic substrates, resulting in a phase separation from the catalyst system.



5.2 – Introduction

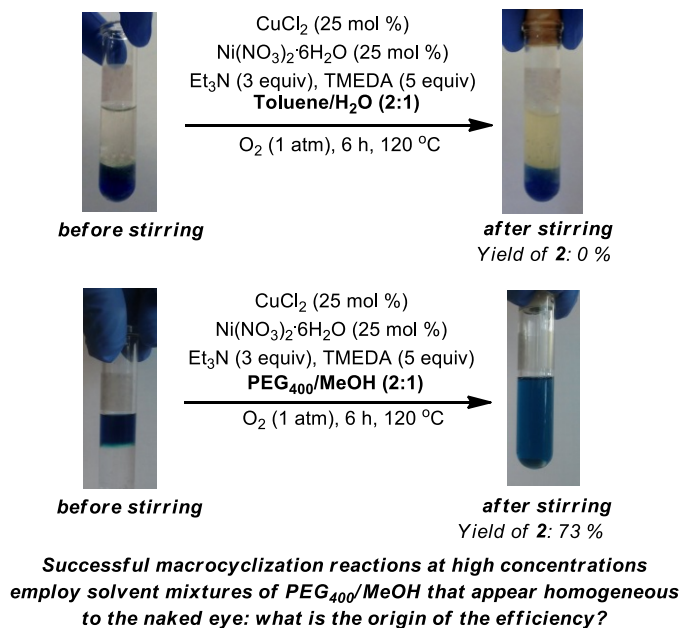
The study of macrocycles and their unique properties,¹ in both industrial and academic settings, are plagued by the difficulties associated with their synthesis. In the absence of any conformational restraint, the key ring closing reaction to synthesize a macrocycle is typically slow resulting in competing oligomerization. High dilution is the most common solution² to inhibit intermolecular reactions between substrates, but the large volumes of solvent required can be problematic.³ In addition, the associated environmental impact of solvent disposal renders most macrocyclization reactions unacceptable under the principles of green chemistry.⁴

In a program aimed at developing new macrocyclization strategies, our group has recently devised an alternative strategy for Glaser-Hay macrocyclization reactions, allowing them to be conducted at high concentrations (Scheme 5.1).⁵ The macrocyclization procedure employed mixtures of poly(ethylene glycol) (PEG)₄₀₀/MeOH as a solvent combination and could be performed even at high temperatures using microwave heating.^{5b} Employing the PEG₄₀₀/MeOH solvent combination, the cyclization of diynes could be conducted at concentrations up to 0.1 M, which is an increase in the concentration of the reaction by a factor of 500 when compared to traditional conditions. The discovery of the PEG₄₀₀/MeOH solvent system was spurred by the desire to develop a biphasic macrocyclization protocol.



Scheme 5.1 – Comparing macrocyclization routes to diyne **2**.

It was hoped that by sequestering the catalyst system and macrocyclization substrate into different phases,⁶ the key bond forming process would take place at the interface of the two solvents, where the relative concentration of substrate is low. Unfortunately, our initial investigations using organic/aqueous systems (PhMe/H₂O) that remained biphasic throughout the reaction were unsuccessful at promoting the cyclization (Scheme 5.2). Remarkably, when homogeneous mixtures of PEG₄₀₀/MeOH were employed, the macrocyclizations were promoted with high efficiency and selectivity.^{7,8} Although anxious to investigate whether PEG₄₀₀/MeOH mixtures could be used in other macrocyclization reactions, we believed that the scope of the macrocyclization protocol could not be extended before more insight into the origin of the selectivity could be obtained. Given the well documented tendency for PEG to form aggregates in solution and consequently the numerous applications in medicinal chemistry and materials science,^{9,10} it is surprising that exploitation of its aggregation effects in organic synthesis had not previously been explored.



Scheme 5.2 – Macrocyclization to form **2** using biphasic conditions (PhMe/H₂O) and using homogenous mixtures of PEG₄₀₀/MeOH.

Herein, we provide insight into a possible mechanism for the high selectivity observed during macrocyclization utilizing PEG₄₀₀/MeOH mixtures that invokes the formation of aggregates by the PEG₄₀₀. The importance of PEG aggregates has been studied using three different techniques including surface tension measurements, UV spectroscopy and chemical modification of the substrate and catalyst.

5.3 – Results and Discussion

5.3.1 – Aggregate Formation in Poly(ethylene glycol) Homogenous Mixtures

Poly(ethylene glycol) (PEG) is well known to form aggregate structures in solution; their properties can often be controlled through judicious choice of the length of the PEG polymer chain.⁹⁻¹⁰ The biocompatibility of PEG derived polymers has led to applications as possible drug delivery agents in biological systems.¹¹ PEG is considered a green solvent since in addition to its relative non-toxicity, it has a low volatility and its solubility properties are often tunable.¹² In the Glaser-Hay macrocyclization systems previously reported (Scheme 5.1), the formation of aggregates by PEG₄₀₀ was proposed to account for the phase separation between the catalyst systems and the organic substrates, thus effectively controlling the molarity of the macrocyclization reaction. To confirm the existence of aggregates and their impact on macrocyclization, surface tension measurements¹³ with PEG₄₀₀ in MeOH mixtures at 60 °C were performed to mimic the previously optimized reaction conditions (Figure 5.1, *top*).

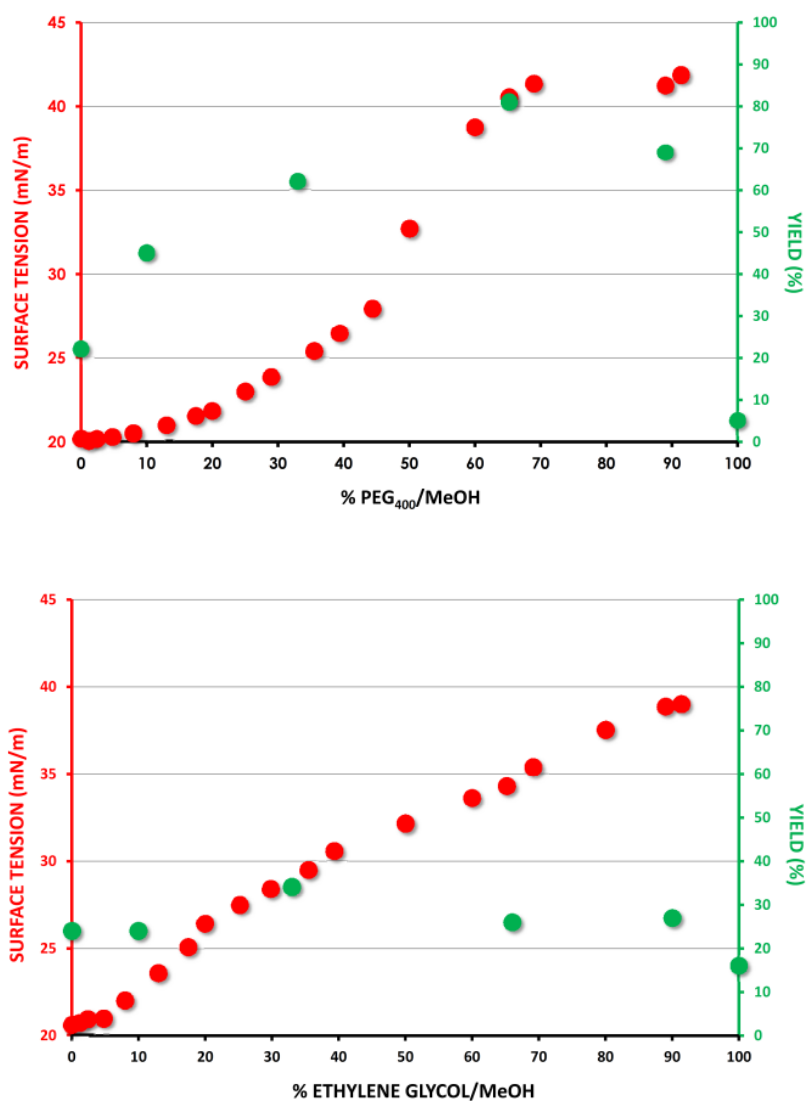


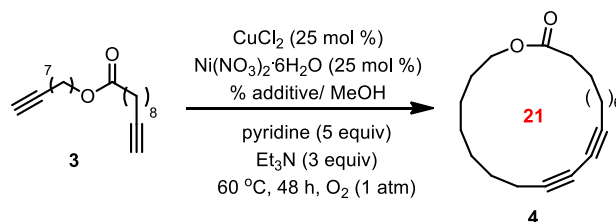
Figure 5.1 – Surface tension measurements for homogenous mixtures of PEG₄₀₀ (*top*) or ethylene glycol (*bottom*) in MeOH (in red) at 60 °C and influence on macrocyclization (**3** → **4**) (in green, see Table 5.1).

The surface tensions of homogenous mixtures of PEG₄₀₀ in various ratios with MeOH were first studied (Figure 5.1, *top*). Gratifyingly, the resulting S-shaped curve confirmed the formation of aggregates with increasing ratios of PEG₄₀₀/MeOH.¹⁴ The surface tension was

found to slowly increase at low ratios of PEG₄₀₀/MeOH, then rapidly increase between 40-70 % PEG₄₀₀/MeOH ending in a plateau at approximately 70 % PEG₄₀₀/MeOH, from which a critical aggregate concentration be calculated.¹⁴ As a control, surface tensions were measured in homogenous mixtures where the PEG solvent was replaced by ethylene glycol, as it represents the smallest building block or monomer of PEG, but is sufficiently short in length that it should not form aggregates in solution (Figure 5.1, *bottom*). As expected, the surface tension measurements showed a linear trend ($R^2 = 0.9922$) over a range of different mixtures of ethylene glycol/MeOH which is indicative of a non-aggregated solution.

Having confirmed the presence of aggregates in homogenous mixtures of PEG₄₀₀/MeOH, we sought to study their influence on the yield of the cyclization of diyne **3** at various ratios of PEG₄₀₀/MeOH (Table 5.1, entries 1-6). When the cyclization was performed in pure MeOH solution, a small quantity of product **4** was observed (22 %) and the remaining starting material **3** was oligomerized.¹⁵ However, even when only a small amount of PEG₄₀₀ was added (10 % PEG₄₀₀/MeOH), the isolated yield of the desired macrocyclic diyne **4** was increased to 45 % yield. As the ratio of PEG₄₀₀/MeOH increased, so did the isolated yield of diyne **4** (62 % at 33 % PEG₄₀₀/MeOH and 81 % at 66 % PEG₄₀₀/MeOH). However, when the solvent ratio was further increased to 90 % PEG₄₀₀/MeOH, the yield of the desired product **4** dropped to 69 %. At the high ratio of 90 % PEG₄₀₀/MeOH, the remaining mass balance was unreacted **3**, suggesting that the reactivity of the catalyst system was decreased at high PEG₄₀₀/MeOH ratios. Reactions performed in pure PEG₄₀₀ exhibited extremely slow reaction rates and very little desired product was observed even after 7 days.¹⁶

Table 5.1 – Yields of macrocycle **4** at various ratios of PEG₄₀₀ or ethylene glycol in MeOH.¹⁷



entry	additive	% additive/ MeOH	yield 4 (%) ^a
1		0	24
2		10	45
3	PEG ₄₀₀	33	62
4		66	81
5		90	69 ^{b,c}
6		100	<5 ^{b,c}
7		0	24
8		10	24
9	ethylene	33	34
10	glycol	66	26 ^b
11		90	27 ^b
12		100	16 ^b

a) All compounds were isolated by silica gel flash chromatography. Unless otherwise stated, all remaining starting material **3** was oligomerized, see ref 15. b) Some precipitation of the catalyst mixture was observed after 2 d. c) Remaining mass balance was recovered **3**.

Once again as a control, the macrocyclization of **3** was investigated in solvent mixtures of ethylene glycol in MeOH which were confirmed to not form aggregates in solution (Figure 5.1, *bottom* and Table 4.1, entries 7-12). When the cyclization of **3** to form **4** was conducted with low ratios of ethylene glycol/MeOH (10 % or 33 %), the yields were low and mirrored

the yields that were obtained when the cyclization was conducted in pure MeOH (Table 5.1, entry 7: 24 %). At higher ratios of ethylene glycol (66 % or 90 %), again the yields remained low (26 % and 27 % respectively) and identical to what was previously observed at other ratios of ethylene glycol/MeOH. In addition, when 90 % ethylene glycol or pure ethylene glycol was used, the starting diyne **3** was not recovered at the end of the reaction and extensive oligomerization was observed. The fact that the yield of **4** does not vary significantly in ethylene glycol/MeOH solutions that do not form aggregates further implies the importance of aggregation in achieving efficient macrocyclization at high concentrations. These results as a whole verify that aggregation has a direct influence on the yield of the macrocyclization reaction and proves its importance in achieving efficient macrocyclization at high concentrations.

5.3.2 – Determination of the Phase Preference of Substrate and Catalyst

Poly(ethylene glycol) has good solubility in a variety of organic solvents and can effectively dissolve organic molecules.¹² The preferential conformation of PEG in polar media has been determined to be helical; this minimizes interactions of the aliphatic chains with the solvent.^{18,19} The folding creates a lipophilic environment that is responsible for PEG's ability to solubilise organic molecules within its aggregates. Consequently, it was believed that the organic macrocyclization substrates were residing preferentially in the PEG aggregate as opposed to the MeOH solvent. To probe the solvent environment about a typical organic substrate, UV spectroscopy measurements were performed with the acyclic diyne **3** in homogenous mixtures of PEG₄₀₀ and MeOH (Figure 5.2).²⁰

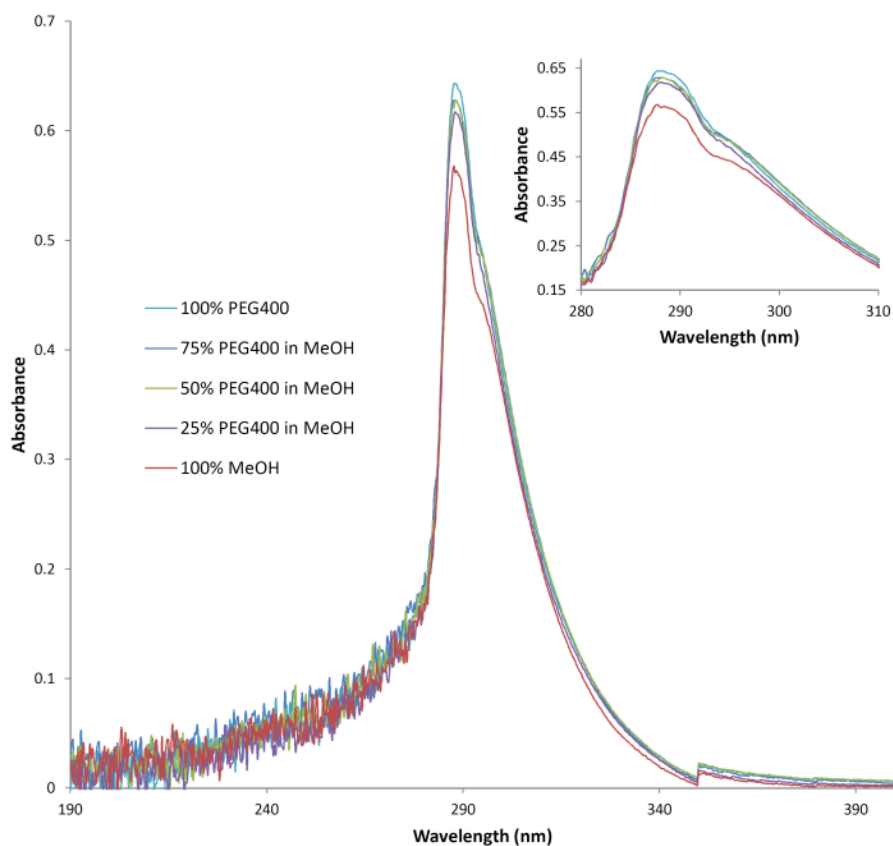


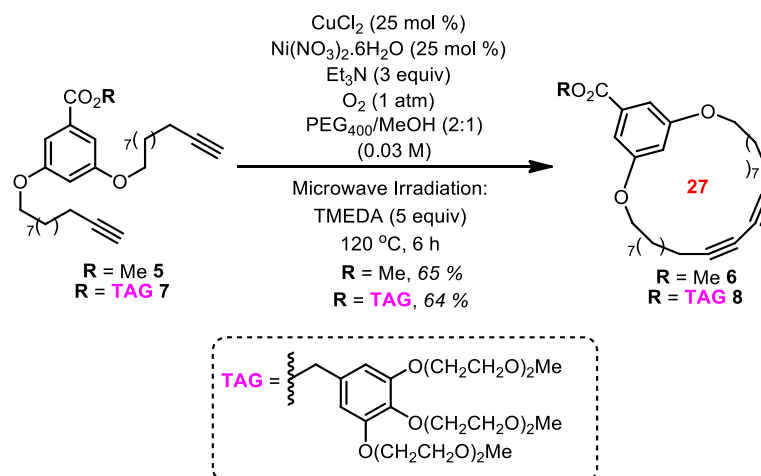
Figure 5.2 – Absorbance measurements of diyne **3** in various solvent mixtures.

Evidence for the preferential solubilization of the organic substrate **3** in PEG₄₀₀ comes from the spectral changes observed under mixing **3** with various percentages of PEG₄₀₀ in MeOH. The absorption maxima of the diyne **3** in 100 % PEG₄₀₀ was 288 nm and was essentially identical to the absorption maxima in 100 % MeOH. However the absorbance intensities were different, with the absorbance maxima smaller in 100 % MeOH (0.64 in PEG₄₀₀ vs. 0.57 in MeOH). When the spectrum was recorded for the diyne **3** in 75 % PEG₄₀₀/MeOH (very close to the ratio of 66 % PEG₄₀₀/MeOH which gave the highest yields of **3** in previous studies, see Table 4.1), the absorbance measured was very similar (0.63) and the

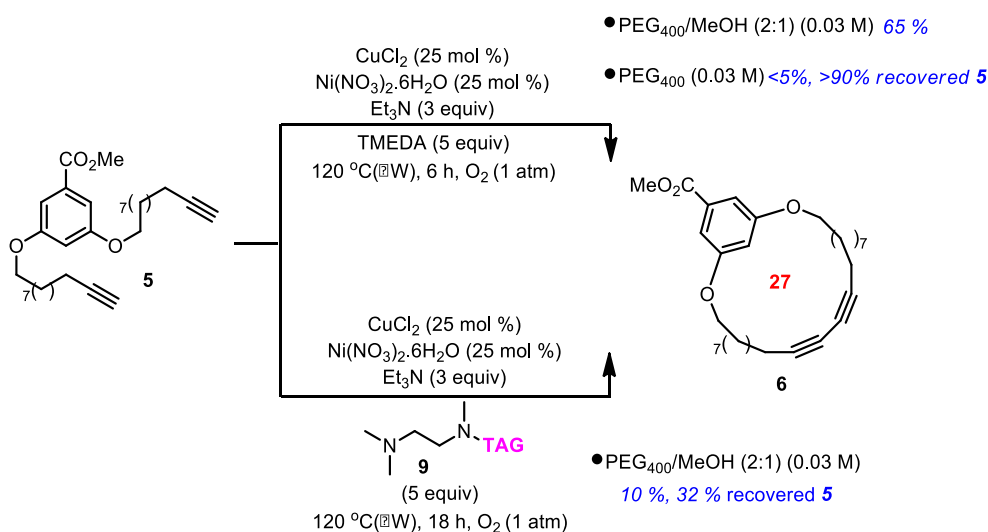
spectrum closely resembled that of **3** in 100 % PEG₄₀₀. As the amount of MeOH was increased to 50 %, the absorbance intensity (0.62) and curve shape continued to almost overlap with the spectrum obtained for **3** in PEG₄₀₀. Even the spectra obtained for **3** in 25 % PEG₄₀₀/MeOH shows only a slightly smaller absorbance intensity and is still similar to the curve observed for the diyne **3** in 100 % MeOH. The similarity of all the curves to the spectrum of **3** in 100 % PEG₄₀₀ point to a preference for diyne **3** to reside within the PEG₄₀₀ aggregate. To provide further insight into where the substrate and catalyst were preferentially solubilized, chemical tagging of both catalyst and substrate was performed.

5.3.3 – Chemical “Tagging” of Substrate and Catalyst

To elucidate the phase preference of the substrate and catalyst in the macrocyclization process, the ester diyne **7**, in which the appended benzyl ester was substituted with three poly(ethylene ether) sidechains was prepared.²¹ The benzyl ester tag was included at a remote ester position to be sufficiently far away from the diynes as to not directly affect the macrocyclization. Most importantly, the appended tag can be used as a means to assure the ester **7** prefers inclusion into a PEG aggregate.²² The macrocyclization studies could then be compared to the isolated yields obtained for the ester substrate **5** that was previously investigated under the optimized macrocyclization conditions (Scheme 5.3).



Scheme 5.3 – Macrocyclization behavior of tagged ester **7**.



Scheme 5.4 – Macrocyclization of diyne **5** with a tagged TMEDA derivative **9**.

Macrocyclization of diyne methyl ester **5** under the $\text{PEG}_{400}/\text{MeOH}$ optimized conditions afforded a 65 % yield of the desired product **6** when using microwave irradiation. As expected, when the tagged acyclic diyne **7** was submitted to identical reactions conditions, little change in yield was observed (64 % yield of **8** using microwave

irradiation). Because the cyclization behavior of the two esters **5** and **7** were identical, it suggests that the organic substrate **5** preferentially resides within the PEG aggregate. Next, the solubility preference of the copper catalyst was probed. Towards this goal, a derivative of TMEDA **9** was prepared and tagged with the same benzyl group as ester **7** (see **9**), and was studied in the macrocyclization of **5** (Scheme 5.4). Once again, the macrocyclization using ligand **9** would be compared to the cyclization using TMEDA (**5** → **6**, 65 % yield). It was assumed that the PEGylated **9** would force the resulting Cu complex into the PEG phase. The macrocyclization of **5** in homogenous PEG₄₀₀ using TMEDA/Cu complexes displayed very slow reaction rates (>90 % **5** recovered) and low yields of desired products (<5 % yield of **6** in 100 % PEG₄₀₀, Scheme 4.4). As such, we expected the results of the macrocyclization of **5** using tagged ligand **9** to display a similar reactivity profile to reactions that were performed in pure PEG₄₀₀. When the cyclization (**5** → **6**) using ligand **9** was performed the yield of the macrocyclization dropped dramatically (65→10 %). In addition, the reaction rate had slowed considerably and even after 18 h of microwave irradiation, 32 % of the starting material **5** was recovered. The rest of **5** was assumed to be converted to oligomers.¹⁵ The results of the above experiment point to the Cu/TMEDA catalyst system preferentially residing in a MeOH phase, while the organic substrate resides within a PEG₄₀₀ aggregate or phase.

The surface tension measurements, UV spectroscopy and chemical tagging experiments clearly invoke the formation of aggregates by the PEG₄₀₀. The preferential solubility of the organic substrates within the PEG aggregate suggest that slow diffusion of the organic diyne towards the MeOH phase, in which the relative concentration of the diyne would be low, would be necessary for reaction with the catalyst system. The slow diffusion of

the organic diyne towards another phase effectively mimics the low concentration achieved using high dilution conditions.

5.4 – Conclusion

In summary, surface tension measurements, UV spectroscopy and chemical tagging have been used to elucidate the origin of the efficiency in macrocyclic Glaser-Hay couplings that can be performed at high concentrations. The present study confirms that the aggregation abilities of PEG₄₀₀ can be harnessed for use in organic synthesis. In the Glaser-Hay macrocyclization protocol previously developed, the cyclization of diynes could be conducted in high yields at concentrations up to 0.1 M, which is an increase in the concentration of the reaction by a factor of 500.

These selective and high yielding macrocyclizations are due to aggregates of PEG₄₀₀ that can act to mimic phase separation normally achieved using organic/aqueous mixtures. Chemical tagging displayed the solubility preferences of the catalyst system for MeOH and substrate for inclusion within a PEG aggregate. Furthermore, the degree of aggregation was shown to greatly influence the yields of macrocyclization. Despite the variety of applications for PEG-derived aggregates in medicinal chemistry and materials science, the application of its aggregation effects in organic synthesis have not been explored. The insight gained by the present can now be exploited to expand the scope to other important transformations such as macrocyclic olefin metathesis and macrolactonization. In addition, the present study suggests that the aggregation properties of PEG could be used to control concentration effects in other chemical reactions²³ or as an alternative to traditional aqueous/organic biphasic reaction conditions.

Acknowledgement. The authors acknowledge the Natural Sciences and Engineering Research Council of Canada (NSERC), Université de Montreal and the Centre for Green Chemistry and Catalysis (CGCC) for generous funding. A.-C. B. thanks NSERC (Vanier Graduate Scholarship), the FQRNT and CGCC for graduate scholarships. The authors thank Mr. Pierre Ménard-Tremblay for help with the surface tension measurements, Mr. Claude-Rosny Elie for help with the UV spectroscopy measurements and Prof. Andreea Schmitzer and Ms. Vanessa Kairouz for helpful discussions.

Supporting Information Available: Supporting information for this article is available on the WWW under <http://dx.doi.org/10.1002/chem.201203433>

5.5 – Bibliography

- (1) a) J. C. Roxburgh, *Tetrahedron* **1995**, *51*, 9767-9822; b) E. M. Driggers, S. P. Hale, J. Lee, N. K. Terrett, *Nat. Rev. Drug Discovery* **2008**, *7*, 608–624; c) E. Marsault, M. L. Peterson, *J. Med. Chem.* **2011**, *54*, 1961-2004; d) H. Matsuda, S. Watanabe, K. Yamamoto, *Chem. Biodiversity* **2004**, *1*, 1985-1991.
- (2) For some recent examples of macrocyclizations conducted at higher concentrations due to conformational preorganization see: a) P. Bolduc, A. Jacques, S. K. Collins, *J. Am. Chem. Soc.* **2010**, *132*, 12790-12791; b) C. J. White, A. K. Yudin, *Nature Chem.* **2011**, *3*, 509-524.
- (3) Dilution can render macrocyclization problematic on larger scales, for an impressive example of industrial macrocyclization see: V. Farina, C. Shu, X. Zeng, X. Wei, Z. Han, N. K. Yee, C. H. Senanayake, *Org. Proc. Res. Dev.* **2009**, *13*, 250-254.
- (4) a) P. T. Anastas, *ChemSusChem* **2009**, *2*, 391-392; b) I. T. Horvath, P. T. Anastas, *Chem. Rev.* **2007**, *107*, 2169-2173.
- (5) a) A.-C. Bédard, S. K. Collins, *J. Am. Chem. Soc.* **2011**, *133*, 19976-19981; b) A.-C.; Bédard, S. K. Collins, *Chem. Commun.* **2012**, *48*, 6420-6422.
- (6) Micellar catalysis could achieve a similar phase separation, but has been mostly exploited as a route towards achieving catalysis in hydrophilic media, see: a) G. Stavber, *Aust. J. Chem.* **2010**, *63*, 849-849; For examples of micelles formed from PEG₄₀₀ see: b) U. Hasegawa, A. J. van der Vlies, E. Simeoni, C. Wandrey, J. A. Hubbell, *J. Am. Chem. Soc.* **2010**, *132*, 18273-18280; c) W.-F. Dong, A. Kishimura, Y. Anraku, S. Chuanoi, K. Kataoka, *J. Am. Chem. Soc.* **2009**, *131*, 3804-3805.
- (7) For an example of a liquid/liquid phase separation strategies in an industrial process see: a) W. A. Herrmann, C. W. Kohlpaintner, *Angew. Chem.* **1993**, *41*, 544-550; *Angew. Chem., Int. Ed. Engl.* **1993**, *32*, 1524-1544; Phase separation strategies in organic synthesis typically involve synthesis on solid phase supports. Some examples of liquid/liquid phase separation techniques in synthesis include fluorous biphasic systems: b) I. T. Horvath, J. Rabai, *Science* **1994**, *266*, 72-75.
- (8) PEG₄₀₀/MeOH (2:1) solvent mixtures remained homogeneous at room temperature for over a year.
- (9) a) N. Fairley, B. Hoang, Allen, C. *Biomacromolecules* **2008**, *9*, 2283-2291; b) L. Vuković, F. A. Khatib, S. P. Drake, A. Madriaga, K. S. Brandenburg, P. Král, H. Onyuksel, *J. Am. Chem. Soc.* **2011**, *133*, 13481–13488; c) J. A. Johnson, Y. Y. Lu, A. O. Burts, Y.-H. Lim, M. G. Finn, J. T. Koberstein, N. J. Turro, D. A. Tirrell, R. H. Grubbs, *J. Am. Chem. Soc.* **2011**, *133*, 559–566.
- (10) a) D. E. Bergbreiter, *Chem. Rev.* **2002**, *102*, 3345-3384; b) *Polyethylene Glycol Chemistry: Biotechnological and Biomedical Applications*, (Ed: J. M. Harris), Plenum: New York, **1992**
- (11) For examples of the use of PEG in biosystems see: (a) K. Fuhrmann, J. D. Schulz, M. A. Gauthier, J.-C. Leroux, *ACS Nano* **2012**, *6*, 1667-1676; b) M. Zheng, Z. Zhong, L. Zhou, F. Meng, R. Peng, Z. Zhong, *Biomacromolecules* **2012**, *13*, 881-888; c) U. P. Shinde, M. K. Joo, H. J. Moon, B. Jeong, *J. Mater. Chem.* **2012**, *22*, 6072-6079.
- (12) For examples of the use of PEG in green synthesis see: (a) Z.-Z. Yang, Y.-N. Zhao, L.-N. He, J. Gao, Z.-S. Yin, *Green Chem.* **2012**, *14*, 519-527; b) S. G. Konda, V. T.

- Humne, P. D. Lokhande, *Green Chem.* **2011**, *13*, 2354-2358; c) G. Chen, J. Xie, J. Weng, X. Zhu, Z. Zheng, J. Cai, Y. Wan, *Synth. Commun.* **2011**, *41*, 3123-3133; d) D. E. Bergbreiter, S. Furyk, *Green Chem.* **2004**, *6*, 280-285.
- (13) For examples of the use of surface tension measurements for the analysis of PEG aggregates see: a) J. Dey, S. Shrivastava, *Soft Matter* **2012**, *8*, 1305-1308; b) S.-C. Yang, R. Faller, *Langmuir* **2012**, *28*, 2275-2280; c) M. S. Alam, A. B. Mandal, *J. Mol. Liq.* **2012**, *168*, 75-79.
- (14) Critical aggregation concentration (CAC) = 28 % PEG₄₀₀/MeOH.
- (15) The formation of cyclic dimers and acyclic dimers or trimers can be observed by TLC analysis. Mass spectrometric analysis of crude reaction mixtures can be used to identify these oligomers.
- (16) The addition of PEG₄₀₀ to the reaction does increase the viscosity of the reaction medium. Reactions performed at different stirring speeds or in the absence of stirring all afforded similar yields.
- (17) For clarity, the effect of solvent mixture composition on the yield of **4** is shown in Table 1 for reactions using traditional (oil bath) heating. The same trends in yield were observed using microwave heating. This data can be found in the Supporting Information.
- (18) a) N. Derkaoui, S. Said, Y. Grohen, R. Olier, M. Privat, *J. Colloid Interface Sci.* **2007**, *305*, 330–338; b) K. Tasaki, *J. Am. Chem. Soc.* **1996**, *118*, 8459-8469.
- (19) In an effort to probe the average size of the aggregates, light scattering studies were performed but indicated a non-uniform size distribution to the aggregates. Stirring reaction mixtures extended periods of time or treatment under ultrasonication did not promote the formation of uniform aggregates.
- (20) For examples of the use of UV and IR spectroscopy for the analysis of PEG aggregates see: a) E. Froehlich, J. S. Mandeville, D. Arnold, L. Kreplak, H. A. Tajmir-Riahi, *Biomacromolecules* **2012**, *13*, 282-287; b) C. Ouyang, S. Chen, B. Che, G. Xue, *Colloids Surf., A* **2007**, *301*, 346-351.
- (21) For a full description of the synthesis of the “tagged” compounds **7** and **9** see Supporting Information and W. Yang, P. F. Xia, M. S. Wong, *Org. Lett.* **2010**, *12*, 4018-4021.
- (22) For an example of inclusion of organic substrates into PEG see: H. Siu, J. Duhamel, *J. Phys. Chem. B* **2012**, *116*, 1226-1233.
- (23) For an elegant example of phase separation used to minimize the concentration of hazardous intermediates see: B. Morandi, E. M. Carreira, *Science* **2012**, *335*, 1471-1474

Chapter 6 : Influence of Poly(ethylene glycol) Structure in Catalytic Macrocyclization Reactions

Anne-Catherine Bédard and Shawn K. Collins*

Département de Chimie, Center for Green Chemistry and Catalysis, Université de
Montréal, CP 6128 Station Downtown, Montréal, Québec H3C 3J7 Canada

ACS Catalysis **2013**, 3, 773-782.

Contributions:

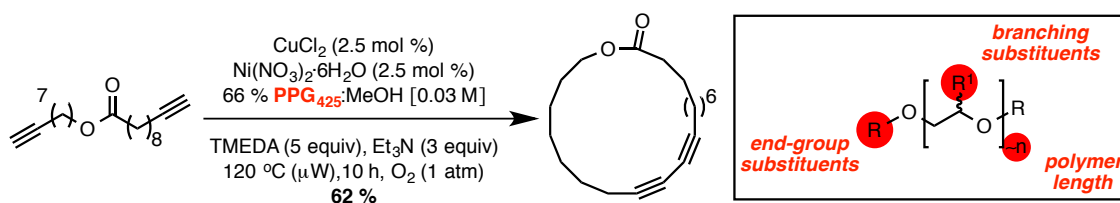
- Anne-Catherine Bédard participated in the design of the experiments, did all the experimental work and contributed to the writing of the manuscript.
- Shawn K. Collins participated in the design of the experiments and writing of the manuscript.

Reproduced by permission from the American Chemical Society

Permanent link to the article (DOI) : [10.1021/cs400050g](https://doi.org/10.1021/cs400050g)

6.1 – Abstract

The first evaluation of the structural effects of six different poly(ethylene glycol) (PEG)-derived polymers in MeOH mixtures on their aggregation abilities, ability to control dilution effects, and catalysis has been performed through examining surface tension measurements and the isolated yields of a model Glaser-Hay macrocyclization reaction of diyne **3**. Three different structural effects were studied involving: 1) the presence of capping groups on the terminal hydroxyl functionalities of the polymers, 2) the length of the polymer chain, and 3) the effects of branching alkyl groups in the polymer backbone. The data obtained provides important guidelines for conducting macrocyclizations using PEG/MeOH, suggesting that macrocyclizations are most efficient at high ratios of PEG/MeOH and when employing medium-length lipophilic branched poly(propylene glycol) (PPG) polymers. In particular, the use of PPG bearing terminal uncapped hydroxyl groups allows for a significant reduction in the catalyst loading. The macrocyclization studies reinforce that the aggregation characteristics of PEG-derived solvents can be harnessed in catalysis, particularly in reactions where control of concentration effects is important.

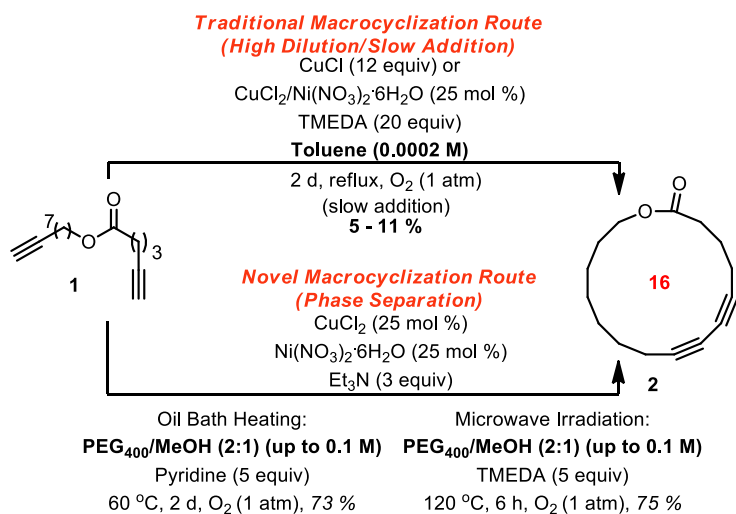


Optimization of PEG structure (length of chain, substituents and capping end-groups) results in an increase in catalytic activity !!!

6.2 – Introduction

Concentration effects play an important role in the development of synthetic methodologies. For example, the rate of bimolecular reactions can be significantly accelerated or decelerated through changes in the reaction concentration. The specific concentration of reactive intermediates in chemical transformations can be controlled by using biphasic mixtures,¹⁻³ through phase transfer catalysis, or both. The nature of a given reaction's solvent and its concentration have become increasingly scrutinized in organic synthesis as chemists weigh the efficiency of a chemical transformation against the environmental impact and costs associated with the use of that solvent under the principles of green chemistry.⁴ Maintaining this balance becomes increasingly difficult when considering the preparation of highly valuable compounds. Macrocycles are a class of molecules whose unique structural features⁵ have allowed them to find application in diverse fields of the chemical industry, including agrochemical, pharmaceutical, petrochemical, cosmetics, and materials science. Despite the abundance of possible applications, macrocycles are not as broadly investigated as other cyclic compounds because of the difficulties associated with their synthesis.⁶ The control of concentration effects is intrinsically key to conducting efficient macrocyclization reactions that avoid problematic oligomerization. Maintaining a relatively low concentration of a given substrate *via* high dilution, often using toxic, volatile organic solvents, is commonly employed⁷ to inhibit intermolecular reactions among substrates. The large volumes of solvent required can be problematic when conducting reactions on larger scales, and the disposal or recycling of the solvents is either environmentally damaging or energy-inefficient.⁸

In a program aimed at developing new catalytic macrocyclization strategies, our group recently reported a strategy for conducting Glaser–Hay macrocyclization reactions at high concentrations (Scheme 6.1).⁹ The macrocyclization procedure employed Cu catalysis and mixtures of poly(ethylene glycol) (PEG)₄₀₀/MeOH as a solvent combination, which was postulated to form aggregates and control the dilution effects. The methodology afforded the diyne **2** and a series of related industrially relevant macrolactones in good to high yields in 48 h, at concentrations ranging from 150 to 500 times greater than traditional protocols. The slow rate of the macrocyclization was subsequently improved upon through the development of a microwave heating strategy.^{9b}



Scheme 6.1 – Comparing macrocyclization routes to diyne **2**.

Although the aggregation properties of poly(propylene glycol) (PEG) solvents have been well documented in the literature, no report of their use in organic synthesis had been previously reported. Consequently, a mechanistic investigation was undertaken to understand the origin of efficient macrocyclization. Surface tension measurements confirmed the presence

of aggregates in PEG₄₀₀/MeOH mixtures (Figure 6.1). As such, the acyclic diyne, the catalysts, and the resulting macrocycle all theoretically exist in equilibrium between the two phases. Subsequent investigations revealed that the acyclic diyne preferentially solubilized within the PEG aggregate¹⁰ and that the rate of reaction was significantly higher in MeOH than in PEG₄₀₀. We concluded that high selectivity for macrocyclization vs. oligomerization could be achieved when there is a significant preference for the substrate to exist in a certain “phase” in which the rate of cyclization is very slow. Diffusion of the substrate into a separate “phase” in small concentration where the rate of cyclization is significantly greater would result in selective formation of macrocycles such as **2**.¹¹

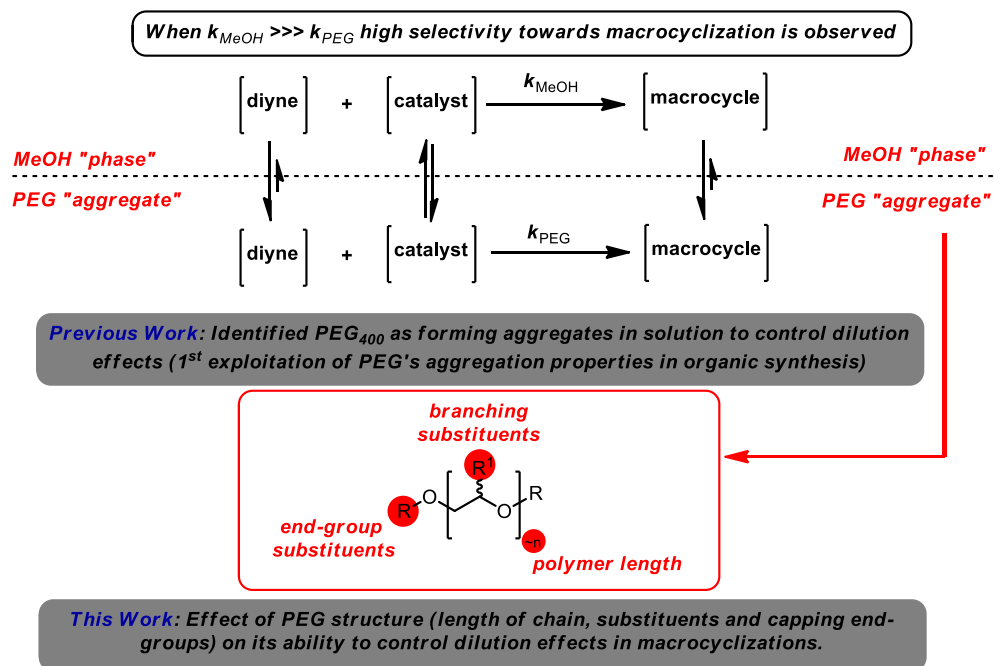


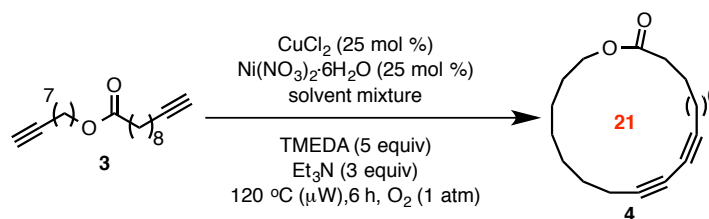
Figure 6.1 – The proposed origin of selectivity in Glaser-Hay macrocyclization reactions employing PEG₄₀₀/MeOH mixtures.

The development of a macrocyclization protocol in which PEG was used to control concentration effects was the first report of exploiting PEG's aggregation properties¹² in organic synthesis. This was surprising, given the advantages to using PEG as a solvent in organic synthesis.¹³ PEG₄₀₀ has already been used as a “green” solvent, particularly in cross-coupling transformations,¹⁴ because it is a water-soluble hydrophilic polymer that is relatively nontoxic, nonvolatile, inexpensive, and thermally stable.¹⁵⁻¹⁷ The use of PEG in macrocyclization to partially replace existing toxic and volatile organic solvents was viewed as a step toward the development of a “green” macrocyclization protocol. An additional advantage to using PEG-derived solvents is the wide variety of structurally distinct PEG-derived polymers that are commercially available. Indeed, PEG polymers can be obtained in varying chain lengths and with different functionalities attached to or replacing the terminal hydroxyl groups. Various poly(propylene glycols) (PPGs) can also be obtained and could be viewed as derivatives of PEG in which a branching Me group is located upon the polymer backbone. At first glance, it was unknown what effects these structural modifications to PEG₄₀₀ would have upon the efficiency and selectivity of the macrocyclization reaction previously developed. However, we were motivated by the potential for further improvements in catalytic efficiency and a more detailed understanding of PEGs ability to control concentration effects. Consequently, herein, we report the first investigation of the effect of PEG structure on catalysis and its ability to control concentration effects in Glaser–Hay macrocyclization reactions.

6.3 – Results and Discussion

The cyclization of the acyclic diyne **3** to macrocyclic diyne **4** under previously developed catalytic conditions at high concentration was investigated using different PEG or PPG polymers. The isolated yield of macrocycle **4** was determined at eight different ratios of PEG/MeOH (Table 6.1).¹⁸ In general, the yield of **4** tends to increase with an increase in the PEG/MeOH ratio. At a specific high ratio of PEG/MeOH that is characteristic of each PEG polymer studied, catalyst inhibition is observed, the yields of **4** drop, and the remaining mass balance is reisolated acyclic diyne **3**.¹⁹ To investigate the effect of aggregation on the yield of the macrocyclization, surface tension measurements for each PEG/MeOH combination were also obtained.²⁰ The plot of the surface tension experiments were conducted at 60 °C,²¹ and the resulting measurements (in red, Figures 6.3, 6.5, 6.7 and 6.8) were then overlaid with the isolated yields of macrocycle **4** (in green, Figures 6.3, 6.5, 6.7 and 6.8) that were obtained at the various ratios of PEG/MeOH. Depicted on each of the plots (Figures 6.3, 6.5, 6.7 and 6.8) is a region highlighted in gray, which indicates the PEG/MeOH ratios in which catalyst inhibition is observed and the remaining mass balance in reisolated diyne **3**.

Table 6.1 – Yields of macrocycle **4** at various ratios of PEG in MeOH.



entry	% solvent/ MeOH	solvent	yield 4 (%) ^a	entry	solvent	yield 4 (%) ^a	entry	solvent	yield 4 (%) ^a
1	0		24	17		24	33		24
2	10		40	18		46	34		43
3	33		56	19		53	35		45
4	50	PEG ₁₉₀	59	20	PEG ₁₄₅₀	61	36	PPG ₄₂₅	49
5	66		69	21		68	37		62
6	80		71	22		55 ^b	38		56
7	90		42 ^b	23		45 ^b	39		58
8	100		5 ^b	23		5 ^b	40		9 ^b
9	0		24	25		24	41		24
10	10		30	26		36	42		44
11	33		36	27		43	43		54
12	50	PEG ₂₅₀ (OMe)	36	28	Pluronic	49	44	PEG ₄₀₀	62
13	66		38 ^b	29		59	45		75
14	80		44 ^b	30		62	46		77
15	90		46 ^b	31		42 ^b	47		56 ^b
16	100		15 ^b	32		24 ^b	48		5 ^b

a) All compounds were isolated by silica gel flash chromatography. Unless otherwise stated, all remaining starting material **3** was oligomerized, see ref 17. b) Remaining mass balance was recovered **3**.

With six different PEG/PPG polymers in hand, the effect of structural modifications of PEG polymers on their ability to promote Glaser–Hay macrocyclization at high concentration could be investigated. Three key structural features of the PEG solvents were to be explored: (1) the effect of “capping” the terminal hydroxyl groups of the PEG polymer, (2) the effects of the polymer length, and (3) the effect of branching in the PEG polymer (*i.e.*, increased hydrophobicity).

6.3.1 – “Capping” of the Terminal Hydroxyl Groups of PEG.

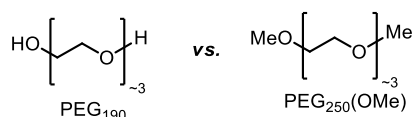


Figure 6.2 – Short chain PEG polymers having different "capping" groups.

The terminal hydroxyl groups of PEG polymers can participate in a number of chemical transformations to allow for the further functionalization of PEG polymers for various applications.²² Consequently, a number of PEGs bearing differently substituted hydroxyl groups are commercially available. In an effort to study the effect of the terminal hydroxyl groups on both the aggregation characteristics of the PEG and its ability to promote macrocyclization of acyclic diyne **3**, PEG₂₅₀(OMe) was identified as an ideal PEG for study (Figure 6.2).²³ The two “capping” groups of the hydroxyl functionalities in PEG₂₅₀(OMe) are simple methyl groups, which minimizes the contribution of the capping groups themselves on the macrocyclization reaction. In addition, PEG₁₉₀, another commercially available PEG polymer, has a similar average molecular weight, allowing for a more accurate comparison of the similarities and differences between the two PEG solvents.

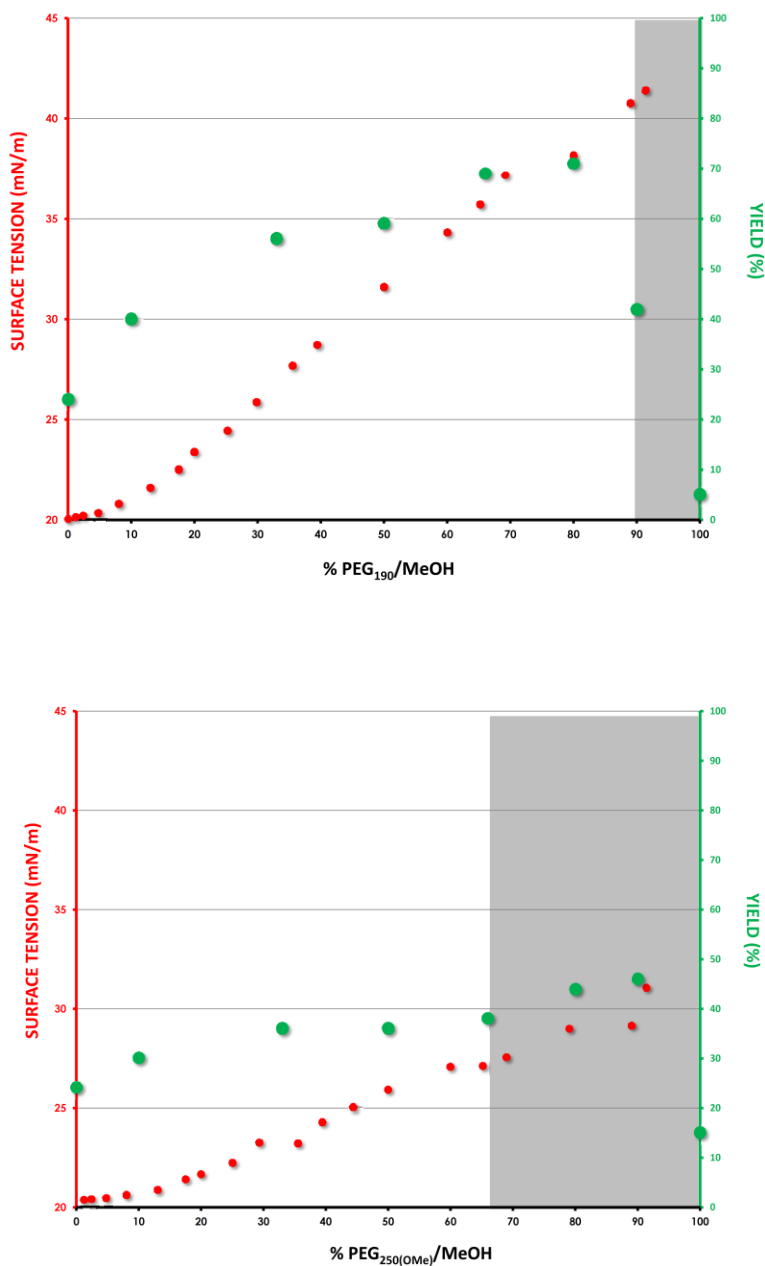


Figure 6.3 — The effect of using a "capped" PEG polymer PEG₂₅₀(OMe) (*bottom*) versus PEG₁₉₀ (*top*) when promoting macrocyclic Glaser-Hay coupling (**3** → **4**) at high concentration (0.03M). Surface tension measurements (red) and isolated yields (green) are plotted on the same figure. The region highlighted in grey indicated PEG/MeOH ratios in which catalyst inhibition is observed and the remaining mass balance in re-isolated diyne **3**.

When comparing the surface tension measurements obtained for ratios of PEG₁₉₀/MeOH (Figure 6.3, *top*) and PEG₂₅₀(OMe)/MeOH (Figure 6.3, *bottom*), both solvents exhibit a nonlinear increase in the surface tension. The S-shaped increase in surface tension is characteristic of aggregate formation in solution; however, the surface tension measurements between the two PEG polymers changes as the ratio of PEG/MeOH increases. As the ratio of PEG/MeOH increases, the surface tension of mixtures of PEG₁₉₀/MeOH increases much more dramatically than for the “capped” PEG₂₅₀(OMe)/MeOH. More importantly, the ability of each PEG solvent to promote macrocyclization of diyne **3** was also very different. In solvent mixtures of PEG₁₉₀/MeOH, the isolated yield of macrocycle **4** increases from 24 % at 100 % MeOH to a maximum of ~71 % yield at 80 % PEG₁₉₀/MeOH. At all the different ratios of PEG₁₉₀/MeOH, no starting acyclic diyne **3** was recovered, and the formation of oligomers was observed.¹⁷ When the ratio of solvents was further increased to 90 % PEG₁₉₀/MeOH, a significant drop in the isolated yield of **4** was observed (42 %). Macrocyclization of **3** in 100 % PEG₁₉₀ provided only traces of **4**. Interestingly, at 90 % and 100% PEG₁₉₀/MeOH, the remaining starting material **3** could be recovered, suggesting that the high ratios of PEG₁₉₀/MeOH caused some degree of catalyst deactivation.²⁴ The ability of PEG₂₅₀(OMe)/MeOH solvent mixtures to promote macrocyclization of diyne **3** was markedly different. The isolated yield of macrocycle **4** also increased with the ratio of PEG₂₅₀(OMe)/MeOH; however, the yields of **4** were almost always much lower than what was obtained in the PEG₁₉₀/MeOH solvent mixtures.

The yields of **4** using PEG₂₅₀(OMe)/MeOH do not vary as dramatically as they do in PEG₁₉₀/MeOH, just as the surface tension does not rapidly increase to same degree in PEG₂₅₀(OMe)/MeOH as it does in PEG₁₉₀/MeOH mixtures. The maximum yield of **4** when

using the “capped” PEG was observed at 90 % PEG₂₅₀(OMe)/MeOH, although the yield of **4** again dropped to 15 % at 100 % PEG₂₅₀(OMe). Again, in contrast to what was observed with PEG₁₉₀/MeOH, the PEG₂₅₀(OMe)/MeOH solvent mixture displayed catalyst inhibition at much lower ratios of PEG₂₅₀(OMe)/MeOH (~66 % PEG₂₅₀(OMe)/MeOH), perhaps accounting for the lower yields of **4** observed. Taken as a whole, these results suggest that the terminal hydroxyl groups of PEG polymers play an important role in aggregation, and PEGs having terminal hydroxyl groups are much more efficient at promoting the Glaser–Hay macrocyclization at high concentrations.

6.3.2 – Different Chain Lengths of PEG.

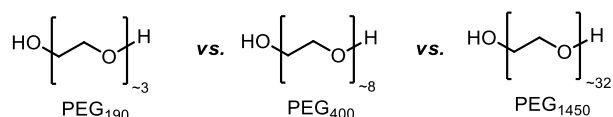


Figure 6.4 – PEG polymers having different chain lengths.

The chain length of PEG polymers can be exploited to alter their solubility properties, where the interior of a PEG polymer normally becomes increasingly hydrophobic as the number of ethylene glycol units multiply. Small-chain PEGs, such as PEG₁₉₀, are normally free-flowing liquids, whereas larger-chain PEGs, such as PEG₁₄₅₀, are available as solids that can be melted to act as a solvent at elevated temperatures (Figure 6.4). Because the hydroxyl groups of the PEG polymer were identified to be important for aggregation and obtaining high yields of macrocycle product **4**, three different PEG polymers (PEG₁₉₀, PEG₄₀₀, and PEG₁₄₅₀), all having terminal hydroxyl groups, were chosen to evaluate the benefit of increased chain length.

In general, the surface tension plots for all three solvent mixtures studied utilizing different chain-length polymers of PEG displayed a nonlinear increase in the surface tension between 100 % MeOH and ~15–30 % PEG/MeOH, resulting in an S-shaped curve signaling the presence of aggregates in solution (Figure 6.5, PEG₁₉₀ (*top*), PEG₄₀₀ (*middle*), PEG₁₄₅₀ (*bottom*)). Regardless of the chain length of the PEG used, all the solvent mixtures had rapid increases in surface tension as the ratio of PEG/MeOH increased. Notably, the shorter PEG₁₉₀/MeOH never reaches a plateau, but the longer PEG₄₀₀/MeOH mixture does have its surface tension plateau at ~70 % PEG₄₀₀/MeOH. It was not possible to obtain surface tension data for the PEG₁₄₅₀/MeOH mixtures at ratios above 70 % PEG₁₄₅₀/MeOH because PEG₁₄₅₀ is a solid and forms saturated suspension at high ratios at 60 °C. The macrocyclization of acyclic diyne **3** was also investigated in each PEG/MeOH mixture; the isolated yields of macrocycle **4** are plotted in Figure 5.5 (PEG₁₉₀ (*top*), PEG₄₀₀ (*middle*), PEG₁₄₅₀ (*bottom*)). All three different chain lengths gave high yields of the macrocycle **4** at their optimal PEG/MeOH ratio. For PEG₁₉₀/MeOH and PEG₄₀₀/MeOH, the maximum yields of 71 % and 77 % occurred at a ratio of 80 % PEG/MeOH, whereas the longer PEG₁₄₅₀ had a lower maximum yield (69 %) at a lower ratio of 66 % PEG₁₄₅₀/MeOH. Note that isolated yields for macrocycle **4** were obtained at high ratios of PEG₁₄₅₀/MeOH, since PEG₁₄₅₀ is a liquid at the elevated temperatures in the microwave. The biggest difference when comparing the behavior of all three PEG chain lengths in that the longer PEG₁₄₅₀ tended to show lower yields and caused catalyst inhibition at lower ratios of PEG/MeOH (catalyst inhibition was observed at 90 % PEG₁₉₀ or PEG₄₀₀/MeOH and at 66 % PEG₁₄₅₀/MeOH). In summary, short- and medium-chain-length PEG polymers can be used as solvents to efficiently promote Glaser–Hay macrocyclization at high concentration when high ratios of PEG/MeOH are employed. Large-

chain polymers can be problematic as a result of greater levels of catalyst inhibition at the high ratios of PEG/MeOH normally needed to promote efficient cyclization.

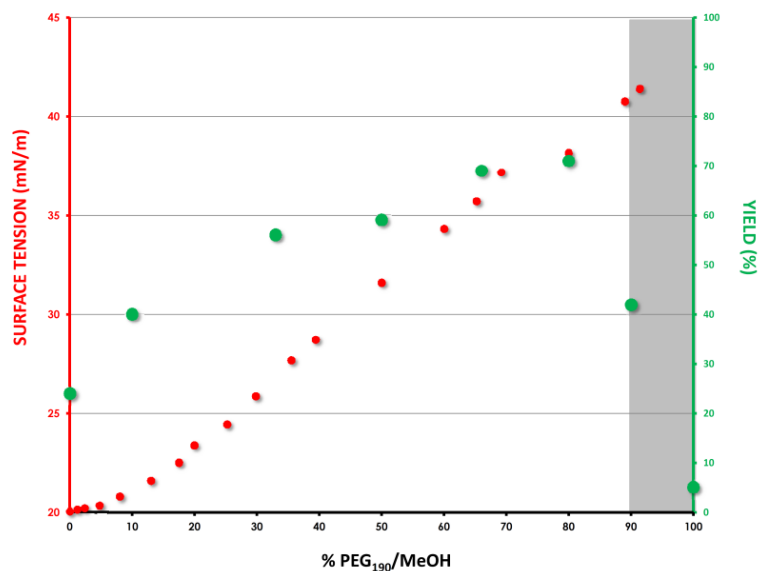


Figure 6.5a – The effect of using different polymer lengths of PEG polymer (PEG₁₉₀ (*top*), PEG₄₀₀ (*middle*), PEG₁₄₅₀ (*bottom*)) when promoting macrocyclic Glaser-Hay coupling (**3**→**4**) at high concentration (0.03 M). Surface tension measurements (red) and isolated yields (green)

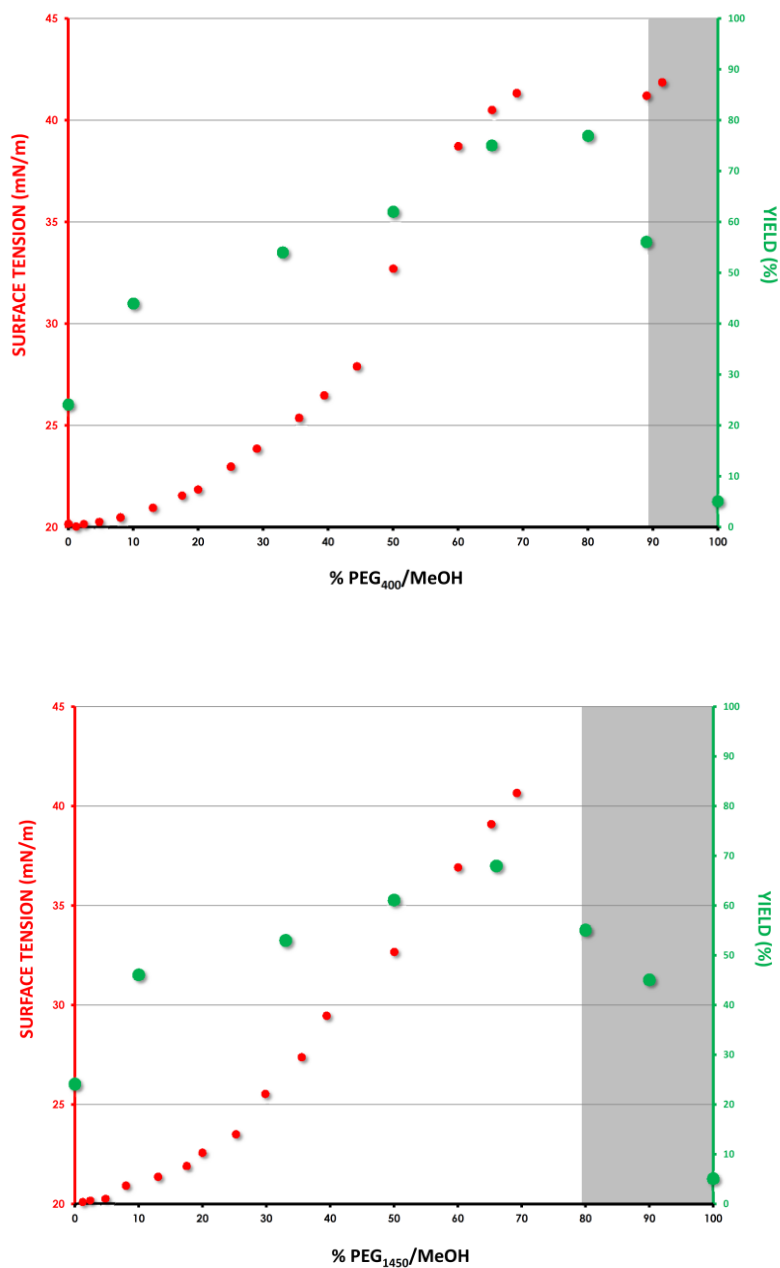


Figure 6.5b – The effect of using different polymer lengths of PEG polymer (PEG₁₉₀ (*top*), PEG₄₀₀ (*middle*), PEG₁₄₅₀ (*bottom*)) when promoting macrocyclic Glaser-Hay coupling (**3**→**4**) at high concentration (0.03 M). Surface tension measurements (red) and isolated yields (green) are plotted on the same figure. The region highlighted in grey indicated PEG/MeOH ratios in which catalyst inhibition is observed and the remaining mass balance in re-isolated diyne **3**.

6.3.3 – Branched Polymers of PEG: PPG and Pluronic.

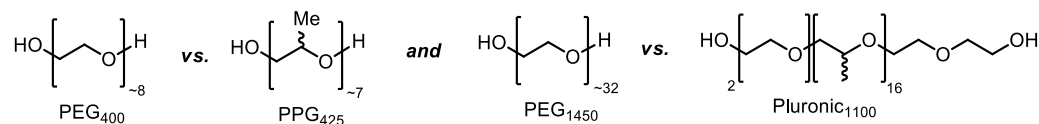


Figure 5.6 – Comparison of different PEG polymers having different chain lengths and branching substituents.

PPG polymers have a Me group along the ethylene subunit of the polymer and have been found to be slightly more toxic than PEG.²⁵ PPG formed from polymerization of *rac*-propylene oxide affords an atactic polymer, and polymerization from the optically pure epoxide monomer or polymerization with chiral catalysts affords the isotactic polymer.²⁶ For the evaluation of branched PEG-derived polymers in controlling the effective molarity in macrocyclization reactions, the cheaper, commercially available atactic polymers were chosen for investigation. The addition of the Me group along the backbone makes PPG much more lipophilic than PEG, but PPG still prefers a tightly wound helix conformation in aqueous solution.²⁷⁻²⁹ To study the effects of branching in the macrocyclization reactions, two separate branched polymers having different chain lengths were identified for study (Figure 6.6).

First, because PEG₄₀₀ was identified as the optimal PEG solvent to date, PPG₄₂₅ was evaluated, since it has a similar chain length and molecular weight and surface tension measurements of mixtures of PPG₄₂₅/MeOH were obtained (Figure 6.7). The surface tension measurements of PPG₄₂₅/MeOH closely mirror those obtained for mixtures of PEG₄₀₀/MeOH, in that an S-shaped curve was observed with a plateau occurring at approximately 70 % PPG₄₂₅/MeOH. The surface tension measurements for PPG₄₂₅/MeOH, however, do not exhibit the steep increase in surface tension between 40 % and 60 % PPG₄₂₅/MeOH that is observed in

the same region for mixtures of PEG₄₀₀/MeOH. When the macrocyclization of diyne **3** was investigated at different ratios of Pluronic₁₁₀₀/MeOH, the yields of macrocycle **4** reached a maximum 62 % isolated yield at 80 % Pluronic₁₁₀₀/MeOH. Overall yields were similar or only slightly lower than those obtained in PEG₁₄₅₀/MeOH mixtures (see Table 6.1 to compare isolated yields). One distinct difference observed with PPG₄₂₅/MeOH mixtures was that there was much less catalyst inhibition, and polymerization of the starting acyclic diyne **3** was observed, even when the macrocyclization was conducted in 100 % PPG₄₂₅/MeOH. The lack of catalyst inhibition could be due to an increased solubility preference for the catalyst in MeOH, as opposed to the PPG₄₂₅ aggregates, although further work is necessary to elucidate the origin of the reactivity in PPG₄₂₅ mixtures.

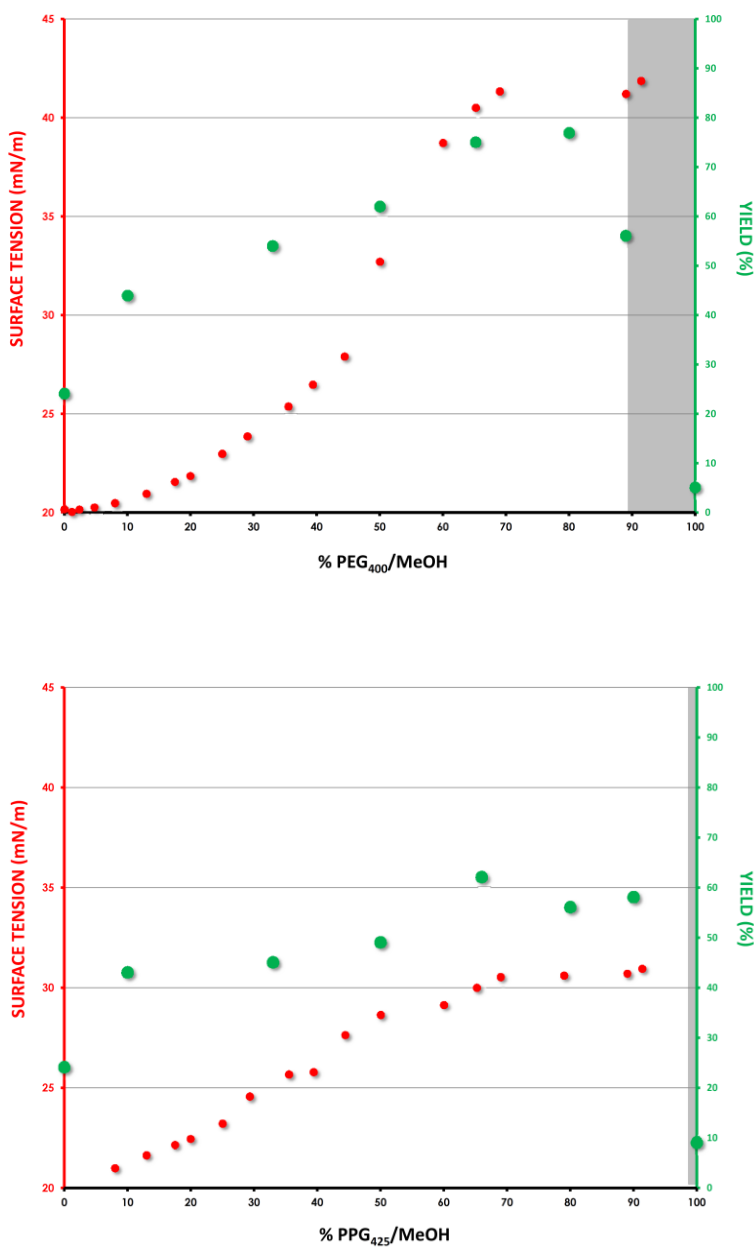


Figure 6.7 – The effect of using branched polymers of short-chained PEGs (PEG₄₀₀ (*top*) and PPG₄₂₅ (*bottom*)) when promoting macrocyclic Glaser-Hay coupling (**3**→**4**) at high concentration (0.03M). Surface tension measurements (red) and isolated yields (green) are plotted on the same figure. The region highlighted in grey indicated PEG/MeOH ratios in which catalyst inhibition is observed and the remaining mass balance in re-isolated diyne **3**.

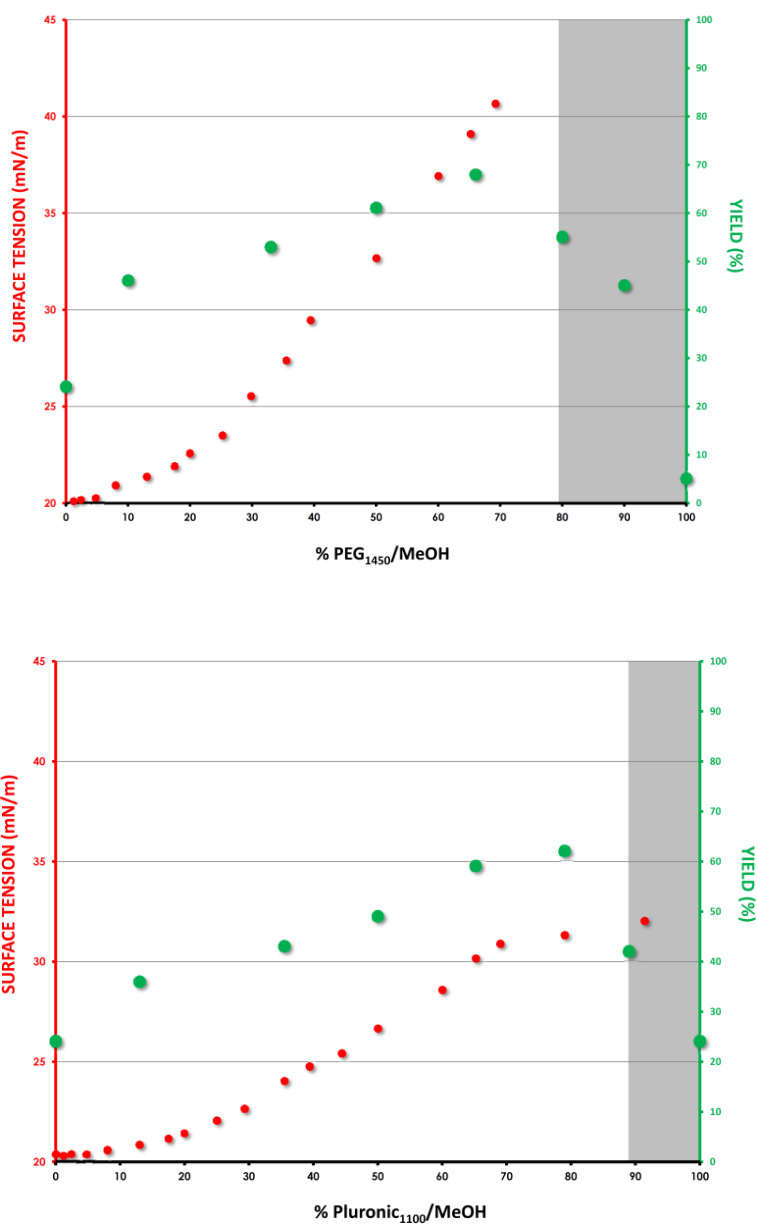


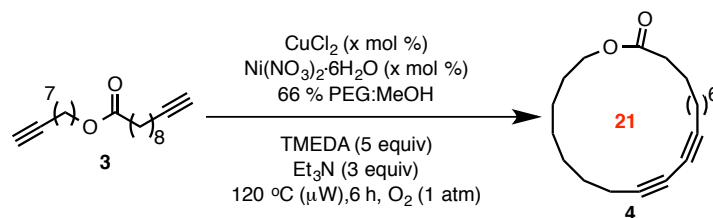
Figure 6.8 – The effect of using branched polymers of long chained PEGs (PEG₁₄₅₀ (*top*) and Pluronic₁₁₀₀ (*bottom*)) when promoting macrocyclic Glaser-Hay coupling (**3**→**4**) at high concentration (0.03 M). Surface tension measurements (red) and isolated yields (green) are plotted on the same figure. The region highlighted in grey indicated PEG/MeOH ratios in which catalyst inhibition is observed and the remaining mass balance in re-isolated diyne **3**.

The effects of branching in PEGs on the macrocyclization reaction of **3** were also investigated with longer polymer lengths. To make comparisons with the previously studied PEG₁₄₅₀, Pluronic₁₁₀₀ was chosen for study. Pluronic₁₁₀₀ is a well-defined block polymer having two ethylene oxide units at each terminus and 16 *rac*-propylene units (Figure 6.6). The resulting polymer has surfactant properties that are useful in cosmetic and pharmaceutical applications, most often for increasing the solubility of lipophilic substances in aqueous environments.³⁰ Pluronics have also been evaluated for various drug delivery applications and were shown to have their own inherent biological activity due to their propensity to incorporate into cellular membranes.³¹ In contrast with the surface tension measurement observed for PEG₁₄₅₀/MeOH, the surface tension measurements of Pluronic₁₁₀₀/MeOH could be obtained even up to 100 % Pluronic₁₁₀₀/MeOH, since Pluronic₁₁₀₀ is a liquid at room temperature. (Figure 6.8). The surface tension measurements for Pluronic₁₁₀₀/MeOH do not exhibit a steep increase in surface tension between 40 % and 60 % Pluronic₁₁₀₀/MeOH that is observed in the same region for mixtures of PEG₁₄₅₀/MeOH, but a distinct plateau and S-shaped curve were observed, confirming the aggregation of Pluronic₁₁₀₀/MeOH mixtures at high ratios. When the macrocyclization of diyne **3** was investigated at different ratios of Pluronic₁₁₀₀/MeOH and the yields of macrocycle **4** reached a maximum 62 % isolated yield at 80 % Pluronic₁₁₀₀/MeOH, overall yields were similar or only slightly lower than those obtained in PEG₁₄₅₀/MeOH mixtures (see Table 6.1 to compare isolated yields). As was observed with PPG₄₂₅/MeOH mixtures, the branching in Pluronic₁₁₀₀/MeOH mixtures allows for much less catalyst inhibition at high ratios of Pluronic₁₁₀₀/MeOH when compared with PEG₁₄₅₀/MeOH. The reduction in catalyst inhibition can easily be observed when comparing the yields of macrocycle **4** at 100 % Pluronic₁₁₀₀ (24 %) and 100 % PEG₁₄₅₀ (< 5%).

Because catalyst inhibition was observed to a much lesser degree when reactions were performed in branched polymer solvents, such as PPG₄₂₅ and Pluronic₁₁₀₀, it was believed that these solvents could allow for a reduction in the catalyst loading used to promote macrocyclization. Consequently, the catalyst loading in the cyclization of diyne **3** to macrocycle **4** was investigated in mixtures of 66 % PEG₄₀₀/MeOH and 66 % PPG₄₂₅/MeOH (Table 6.2). When the catalyst loading of the Cu and Ni catalysts was decreased in the macrocyclization of diyne **3** using a 66 % PEG₄₀₀/MeOH solvent mixture, the yields of the desired macrocycle **4** also decreased (entries 1–4). Although the yield of macrocycle **4** was 75 % when using a 25 mol % catalyst loading, macrocycle **4** was isolated in 67 % yield when decreasing the catalyst loading to 10 mol %. The use of even lower catalyst loadings of 5 or 2.5 mol % resulted in even lower overall yields (54 % and 35 %, respectively) of the desired macrocycle **4** and large quantities of reisolated **3**. In contrast, when the catalyst loading of the Cu and Ni catalysts was decreased in the macrocyclization of diyne **3** using the branched polymer solvent (66 % PPG₄₂₅/MeOH), the yields of the desired macrocycle **4** were either maintained or increased (Table 6.2, entries 5–8). When the mol % of the Cu/Ni catalyst system was dropped from 25 % to 10 %, the yield of macrocycle **4** increased from 62 % to 81 %. Because reducing the catalyst loading is expected to slow the rate of reaction, it could consequently increase the selectivity for cyclization vs oligomerization and explain the increase in the isolated yield of **4**. When the catalyst loading in the macrocyclization of diyne **3** using 66 % PPG₄₂₅/MeOH was dropped to 5 mol %, the yield of macrocycle **4** remained high (74 %), and the remaining mass balance was recovered unreacted diyne **3**. Finally, the catalyst loading was dropped to 2.5 mol %, which resulted in a very slow macrocyclization. However, if the reaction time was slightly increased (from 6 to 10 h), the

macrocycle **4** could be isolated in exactly the same yield as was obtained with a catalyst loading 10 times higher (entry 8 versus 5, Table 6.2).

Table 6.2 – Effect of PEG structure on the catalyst loading in the macrocyclization to form **4**.



entry	solvent	catalyst loading (x mol%)	yield 4 (%) ^a
1	PEG ₄₀₀	25	75
2		10	67 ^b
3		5	54 ^b
4		2.5	35 ^b
5	PPG ₄₂₅	25	62
6		10	81
7		5	74 ^b
8		2.5	62 ^{b,c}

^a All compounds were isolated by silica gel flash chromatography. Unless otherwise stated, all remaining starting material **3** was oligomerized¹⁷. ^b Remaining mass balance was recovered **3**. ^c Reaction time was 10 h (O₂ was bubbled through the solution a second time after 5 h).

6.4 – Conclusion

In summary, the first evaluation of the structural effects of PEG-derived polymers and their aggregation abilities for exploitation in organic synthesis has been described. The evaluation of six different PEG polymers in MeOH mixtures for their ability to control

dilution effects has been performed through examining surface tension measurements and the isolated yields of a model Glaser–Hay macrocyclization reaction of diyne **3**. Three different structural effects were studied involving (1) the presence of capping groups on the terminal hydroxyl functionalities of the polymers, (2) the length of the polymer chain, and (3) the effects of branching alkyl groups in the polymer backbone. The data obtained for isolated yields of macrocycle **4** provide important guidelines for conducting macrocyclizations using PEG/solvent mixtures: (1) regardless of the nature of the PEG solvent, the macrocyclizations exhibit greater efficiency at high ratios of PEG/MeOH, normally affording high yields and often recovered unreacted starting material, and (2) very high ratios (>90 % PEG/MeOH) often result in catalyst inhibition and lower yields. Importantly, when comparing the structural features of the various PEGs, other valuable insights come to light: (1) the terminal hydroxyl groups are important for inducing aggregation and provide surface tension graphs with a well-defined S-shaped curve and overall higher yields of macrocycle **4** than when using “capped” PEGs; (2) long chained PEGs can provide a more lipophilic environment, but result in much greater degrees of catalyst inhibition at the high ratios of PEG/MeOH normally needed for efficient macrocyclization, which resulted in lower yields of macrocycle **4**; and (3) polypropylene-containing PEGs (PPG₄₂₅ and Pluronic₁₁₀₀) provided good yields of macrocycle **4** and are much more lipophilic than PEG, making them interesting alternatives for substrates that have problematic solubility. It should be noted that PPG₄₂₅ and Pluronic₁₁₀₀ mixtures exhibited very high catalyst reactivities, even at very high ratios (>90 % PEG/MeOH), which resulted in greater levels of oligomerization observed and less efficient macrocyclization selectivity (*i.e.*, macrocyclization vs oligomerization); however, the increase in catalyst reactivity when compared with other PEG solvents could be exploited to develop

macrocyclization reactions with reduced catalyst loadings. When macrocyclization was conducted in 66 % PPG₄₂₅/MeOH, the catalyst loading could be reduced 10-fold (from 25 to 2.5 mol %) and afford high yields of the desired macrocycle product.³²

The macrocyclization studies outlined herein reinforce that the aggregation characteristics of PEG-derived solvents can be harnessed in organic synthesis and are not limited to exploitation in medicinal chemistry and materials science. It is expected that as the properties of these solvents continue to be explored, they will become increasingly employed in catalysis. In particular, the high catalyst activities observed in branched PEG solvents could be especially useful in other fields of catalysis in which the “green” characteristics of PEG solvents are desired in concert with high catalyst activities. Considering the wealth of other synthetic processes that suffer from concentration effects,³³ it is reasonable to assume that PEG or PEG/solvent mixtures could be used to improve such processes or provide alternatives to traditional aqueous/organic biphasic reaction conditions.

Acknowledgement. The authors acknowledge the Natural Sciences and Engineering Research Council of Canada (NSERC), Université de Montreal and the Centre for Green Chemistry and Catalysis (CGCC) for generous funding. A.-C. B. thanks NSERC (Vanier Graduate Scholarship), the FQRNT and CGCC for graduate scholarships.

Supporting Information Available: Representative experimental procedures and all surface tension data. This information is available free of charge via the Internet at <http://pubs.acs.org/>

6.5 – Bibliography

- (1) Phase separation could be achieved by various other mechanisms, including hydrophilic/hydrophobic solvent mixtures with no miscibility and the formation of micelles. Micellar catalysis could achieve a similar phase separation, but has been mostly exploited as a route toward achieving catalysis in hydrophilic media. See: (a) Stavber, G. *Aust. J. Chem.* **2010**, *63*, 849–849. For examples of micelles formed from PEG₄₀₀, see: (b) Hasegawa, U.; van der Vlies, A. J.; Simeoni, E.; Wandrey, C.; Hubbell, J. A. *J. Am. Chem. Soc.* **2010**, *132*, 18273–18280. (c) Dong, W.-F.; Kishimura, A.; Anraku, Y.; Chuanoi, S.; Kataoka, K. *J. Am. Chem. Soc.* **2009**, *131*, 3804–3805.
- (2) For an example of a liquid/liquid phase separation strategy in an industrial process, see: (a) Herrmann, W. A.; Kohlpaintner, C. W. *Angew. Chem., Int. Ed. Engl.* **1993**, *32*, 1524–1544. Phase separation strategies in organic synthesis typically involve synthesis on solid phase supports. Some examples of liquid/liquid phase separation techniques in synthesis include fluoruous biphasic systems: (b) Horvath, I. T.; Rabai, J. *Science* **1994**, *266*, 72–75.
- (3) PEG₄₀₀/MeOH (2:1) solvent mixtures remained homogeneous at room temperature for over a year.
- (4) (a) Anastas, P. T. *ChemSusChem* **2009**, *2*, 391–392. (b) Horvath, I. T.; Anastas, P. T. *Chem. Rev.* **2007**, *107*, 2169–2173. (c) Constable, D. J. C.; Curzons, A. D.; Cunningham, V. L. *Green Chem.* **2002**, *4*, 521–527. (d) Curzons, A. D.; Constable, D. J. C.; Mortimer, D. N.; Cunningham, V. L. *Green Chem.* **2001**, *3*, 1–6.
- (5) (a) Roxburgh, J. C. *Tetrahedron* **1995**, *51*, 9767–9822. (b) Driggers, E. M.; Hale, S. P.; Lee, J.; Terrett, N. K. *Nat. Rev. Drug Discovery* **2008**, *7*, 608–624. (c) Marsault, E.; Peterson, M. L. *J. Med. Chem.* **2011**, *54*, 1961–2004. (d) Matsuda, H.; Watanabe, S.; Yamamoto, K. *Chem. Biodiversity* **2004**, *1*, 1985–1991. (e) Rueedi, G.; Nagel, M.; Hansen, H.-J. *Org. Lett.* **2004**, *6*, 2989–2991. (f) Fehr, C.; Galindo, J.; Etter, O.; Thommen, W. *Angew. Chem., Int. Ed.* **2002**, *41*, 4523–4526.
- (6) For examples of recent macrocyclizations that could be conducted at relatively high concentration, see: (a) Bogdan, A. R.; James, K. *Chem.–Eur. J.* **2010**, *16*, 14506–14512. (b) Chouhan, G.; James, K. *Org. Lett.* **2011**, *13*, 2754–2757.
- (7) For some recent examples of macrocyclizations conducted at higher concentrations because of conformational preorganization, see: (a) Bolduc, P.; Jacques, A.; Collins, S. K. *J. Am. Chem. Soc.* **2010**, *132*, 12790–12791. (b) White, C. J.; Yudin, A. K. *Nat. Chem.* **2011**, *3*, 509–524.
- (8) Dilution can render macrocyclization problematic on larger scales. See: (a) Farina, V.; Shu, C.; Zeng, X.; Wei, X.; Han, Z.; Yee, N. K.; Senanayake, C. H. *Org. Process Res. Dev.* **2009**, *13*, 250–254.
- (9) (a) Bedard, A.-C.; Collins, S. K. *J. Am. Chem. Soc.* **2011**, *133*, 19976–19981. (b) Bedard, A.-C.; Collins, S. K. *Chem. Commun.* **2012**, *48*, 6420–6422. (c) Bedard, A.-C.; Collins, S. K. *Chem. Eur. J.* **2013**, *19*, 2108–2113.
- (10) For an example of inclusion of organic substrates into PEG, see: Siu, H.; Duhamel, J. J. *Phys. Chem. B* **2012**, *116*, 1226–1233.

- (11) For other examples of phase separation used in synthesis, see: (a) Ge, Z.; Zhou, Y.; Xu, J.; Liu, H.; Chen, D.; Liu, S. *J. Am. Chem. Soc.* **2009**, *131*, 1628–1629. (b) Kinoshita, H.; Shinokubo, H.; Oshima, K. *Angew. Chem., Int. Ed.* **2005**, *44*, 2397–2400. (c) Wang, X.-S.; Dykstra, T. E.; Salvador, M. R.; Manners, I.; Scholes, G. D.; Winnik, M. A. *J. Am. Chem. Soc.* **2004**, *126*, 7784–7785.
- (12) For examples of aggregation using PEG₄₀₀, see: (a) Hasegawa, U.; van der Vlies, A. J.; Simeoni, E.; Wandrey, C.; Hubbell, J. A. *J. Am. Chem. Soc.* **2010**, *132*, 18273–18280. (b) Dong, W.-F.; Kishimura, A.; Anraku, Y.; Chuanoi, S.; Kataoka, K. *J. Am. Chem. Soc.* **2009**, *131*, 3804–3805. For examples of the use of PEG in biosystems, see: (c) Fuhrmann, K.; Schulz, J. D.; Gauthier, M. A.; Leroux, J.-C. *ACS Nano* **2012**, *6*, 1667–1676. (d) Zheng, M.; Zhong, Z.; Zhou, L.; Meng, F.; Peng, R.; Zhong, Z. *Biomacromolecules* **2012**, *13*, 881–888. (e) Shinde, U. P.; Joo, M. K.; Moon, H. J.; Jeong, B. *J. Mater. Chem.* **2012**, *22*, 6072–6079.
- (13) (a) Bergbreiter, D. E. *Chem. Rev.* **2002**, *102*, 3345–3384. (b) Polyethylene Glycol Chemistry: Biotechnological and Biomedical Applications; Harris, J. M., Ed.; Plenum: New York, 1992.
- (14) For examples of the use of PEG in green synthesis, see: (a) Yang, Z.-Z.; Zhao, Y.-N.; He, L.-N.; Gao, J.; Yin, Z.-S. *Green Chem.* **2012**, *14*, 519–527. (b) Konda, S. G.; Humne, V. T.; Lokhande, P. D. *Green Chem.* **2011**, *13*, 2354–2358. (c) Chen, G.; Xie, J.; Weng, J.; Zhu, X.; Zheng, Z.; Cai, J.; Wan, Y. *Synth. Commun.* **2011**, *41*, 3123–3133. (d) Bergbreiter, D. E.; Furyk, S. *Green Chem.* **2004**, *6*, 280–285. (e) Namboodir, V. V.; Varma, S. R. *Green Chem.* **2001**, *3*, 146–148. (f) Bai, L.; Wang, J.-X. *Curr. Org. Chem.* **2005**, *9*, 535–553.
- (15) Nagarapu, L.; Mallepalli, R.; Arava, G.; Yeramanchi, L. *Eur. J. Chem.* **2010**, *1*, 228–231.
- (16) Candeias, N. R.; Branco, L. C.; Gois, P. M. P.; Afonso, C. A. M.; Trindade, A. F. *Chem. Rev.* **2009**, *109*, 2703–2802.
- (17) Zhang, Z.-H. *Res. J. Chem. Environ.* **2006**, *10*, 97–98.
- (18) No attempt to measure the respective water content of the individual PEGs was made, although trace water was not found to impact the Glaser–Hay coupling reactions. No effort to determine the effect of polymer dispersity on the reaction was made. All PEGs were used as received from Aldrich.
- (19) The formation of cyclic dimers and acyclic dimers or trimers can be observed by TLC analysis. Mass spectrometric analysis of crude reaction mixtures can be used to identify these oligomers.
- (20) Surface tension measurements are well-precedented for the analysis of PEG aggregates. For examples, see: (a) Dey, J.; Shrivastava, S. *Soft Matter* **2012**, *8*, 1305–1308. (b) Yang, S.-C.; Faller, R. *Langmuir* **2012**, *28*, 2275–2280. (c) Alam, M. S.; Mandal, A. B. *J. Mol. Liq.* **2012**, *168*, 75–79. PEG aggregates can also be analyzed by the use of UV and IR spectroscopy. See: (d) Froehlich, E.; Mandeville, J. S.; Arnold, D.; Kreplak, L.; Tajmir-Riahi, H. A. *Biomacromolecules* **2012**, *13*, 282–287. (e) Ouyang, C.; Chen, S.; Che, B.; Xue, G. *Colloids Surf. A.*, **2007**, *301*, 346–351.
- (21) The data shown in Table 1 are reactions using microwave heating. Surface tension measurements were, however, recorded at 60 °C. Macrocyclization reactions performed with microwave heating provided yields similar to those conducted using traditional (oil bath) heating. See ref 9c.

- (22) PEGylation can occur through “click” chemistry with alkyne functionalized PEGs: (a) Das, M.; Bandyopadhyay, D.; Singh, R. P.; Harde, H.; Kumar, S.; Jain, S. *J. Mater. Chem.* **2012**, *22*, 24652–24667. Also via azide-functionalized PEGs: (b) Freichels, H.; Alaimo, D.; Auzely-Velty, R.; Jerome, C. *Bioconjugate Chem.* **2012**, *23*, 1740–1752.
- (23) Different PEGs can have vastly different viscosities and impact the overall viscosity of the reaction medium during macrocyclization. Reactions run in PEG₄₀₀ were performed at different stirring speeds or in the absence of stirring and afforded similar yields. See ref 8.
- (24) Catalyst deactivation is presumed to occur through coordination of the PEG or PPG solvent (PEG and PPG are structurally similar to crown ethers) to the metal catalysts. Longer-chained PEGs and PPGs exhibit increased catalyst inhibition at high PEG or PPG ratios. A possible explanation for this inhibition could be the PEG/metal coordination.
- (25) Shideman, F. E.; Procita, L. *J. Pharmacol. Exp. Ther.* **1951**, *103*, 293–305.
- (26) Peretti, K. L.; Ajiro, H.; Cohen, C. T.; Lobkovsky, E. B.; Coates, G. W. *J. Am. Chem. Soc.* **2005**, *127*, 11566–11567.
- (27) For a discussion of the different conformations of PEG and PPG at different interfaces, see: Chen, C.-y.; Even, M. A.; Wang, J.; Chen, Z. *Macromolecules* **2002**, *35*, 9130–9135.
- (28) PEG or PPG molecules can have different conformations in different physical states or in different chemical environments (e.g., polar or nonpolar solvents). See: (a) Linse, P.; Bjorling, M. *Macromolecules* **1991**, *24*, 6700–6711. (b) Bailey, F. E., Jr.; Koleske, J. V. *Poly(ethylene oxide)*; Academic Press: New York, 1976. (c) Smith, G. D.; Yoon, D. Y.; Jaffe, R. L.; Colby, R. H.; Krishnamoorti, R.; Fetters, L. *J. Macromolecules* **1996**, *29*, 3462–3469. (d) Tasaki, K. *J. Am. Chem. Soc.* **1996**, *118*, 8459–8469.
- (29) The addition of PEG₄₀₀ or PPG₄₂₅ to the reaction does increase the viscosity of the reaction medium. All reactions performed at different stirring speeds or in the absence of stirring afforded similar yields.
- (30) (a) Discher, D. E.; Ahmed, F. *Annu. Rev. Biomed. Eng.* **2006**, *8*, 323–341. (b) Adams, M. L.; Lavasanifar, A.; Kwon, G. S. *J. Pharm. Sci.* **2003**, *92*, 1343–1355. (c) Batrakova, E. V.; Li, S.; Brynskikh, A. M.; Sharma, A. K.; Li, Y. L.; Boska, M.; Gong, N.; Mosley, R. L.; Alakhov, V. Y.; Gendelman, H. E.; Kabanov, A. V. *J. Controlled Release* **2010**, *143*, 290–301. (d) Sriadibhatla, S.; Yang, Z.; Gebhart, C.; Alakhov, V. Y.; Kabanov, A. *Mol. Ther.* **2006**, *13*, 804–813.
- (31) (a) Nawaz, S.; Redhead, M.; Mantovani, G.; Alexander, C.; Bosquillon, C.; Carbone, P. *Soft Matter* **2012**, *8*, 6744–6754. (b) Wu, G.; Majewski, J.; Ege, C.; Kjaer, K.; Weygand, M. J.; Lee, K. Y. C. *Phys. Rev. Lett.* **2004**, *93*, 028101. (c) Wu, G.; Majewski, J.; Ege, C.; Kjaer, K.; Weygand, M. J.; Lee, K. Y. C. *Biophys. J.* **2005**, *89*, 3159–3173. (d) Wu, G.; Lee, K. Y. C. *Langmuir* **2009**, *25*, 2133–2139.
- (32) Although the macrocyclization of **3** to **4** can be conducted at low catalyst loadings (2.5 mol %), the highest Emac factor for the cyclization of **3** to **4** would be obtained when using a catalyst loading of 10 mol % (81 % isolated yield, 0.03 M, Emac = 7.2). For a discussion on grading the efficiency of macrocyclization reactions through the use of the Emac factor, see: Collins, J. C.; James, K. *Med. Chem. Commun.* **2012**, *3*, 1489–1495.

- (33) For an elegant example of phase separation used to minimize the concentration of hazardous intermediates, see: (a) Morandi, B.; Carreira, E. M. *Science* **2012**, *335*, 1471–1474. (b) Morandi, B.; Carreira, E. M. *Angew. Chem., Int. Ed.* **2010**, *49*, 938–941.

PART 2

Chapter 7 : Introduction to Continuous Flow Chemistry

With rare exceptions, the improvement of chemical synthesis has focused more on the reactions themselves, rather than the reaction vessel. Modern organic synthesis generally uses the same glass or Pyrex round bottom flasks that were used in 19th century laboratories. In recent years, flow chemistry has become a fast growing area of synthetic organic chemistry research.^{1,2} In contrast with traditionally used batch chemistry, flow chemistry is described as a reaction performed in a continuous fashion as a stream in tubes. Continuous flow strategies have found numerous applications in large scale manufacturing³ and more recently in the preparative laboratory scale.^{1,2} The following chapter will address the description of flow chemistry equipment, the advantages of flow vs. batch chemistry and comparisons to microwave chemistry. The challenges associated with the synthesis of macrocycles in continuous flow will also be discussed. It should be noted, in the following chapter, continuous flow refers solely to mesofluidic flow (≥ 0.5 mm tubing) and not microfluidic flow (< 0.5 mm tubing).^{1b,2}

7.1 – Description of Flow Equipment and Important

Parameters

7.1.1 – Flow Equipment

An example of an integrated continuous flow apparatus is depicted in Figure 7.1. There are six key features: 1) the reservoir, such as the reagents bottles or the injection loops, 2) the pumping module, 3) the mixer, 4) the reactors, 5) the in-line analysis

instrumentation and 6) the fraction collector. A supplementary pumping module can be added if more than one reaction is performed in sequence.⁴

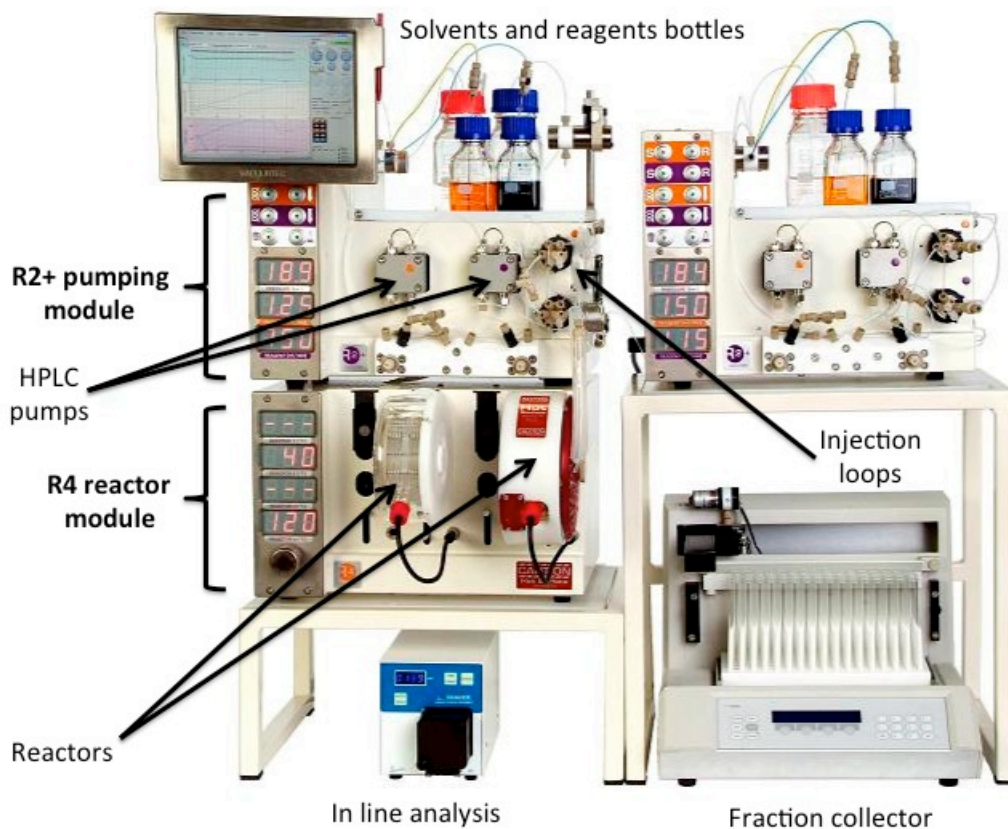


Figure 7.1 – Example of an integrated flow system.

A schematic of an integrated continuous flow reaction is shown in Figure 7.2. First, the reaction mixture is placed in the reservoir either in a bottle if the scale is large or in the injection loop if the scale is small (< 10 mL). The mixture is then moved toward the reacting module using a pump, usually an HPLC or high pressure pump that allows for high back pressures in the reaction (70-180 bar). If needed, a mixer can be installed to mix the reagents before entering the reactor, or at any point in the reaction set-up that would require addition of a reagent. The chemical transformation occurs in the reactor,

usually a PFA or stainless steel coil. The reaction can either be cooled down, heated or irradiated with light. The reactor (Figure 7.3) can typically accommodate reaction temperatures in the range of approximately -80 to +350 °C. When the reaction exits the reactor, the reaction mixture passes through a back-pressure regulator. The regulator is crucial to guarantee the homogeneity of the reaction especially when superheating solvents. After the reaction is completed, the product can be analyzed and collected either in another reservoir or using a fraction collector.

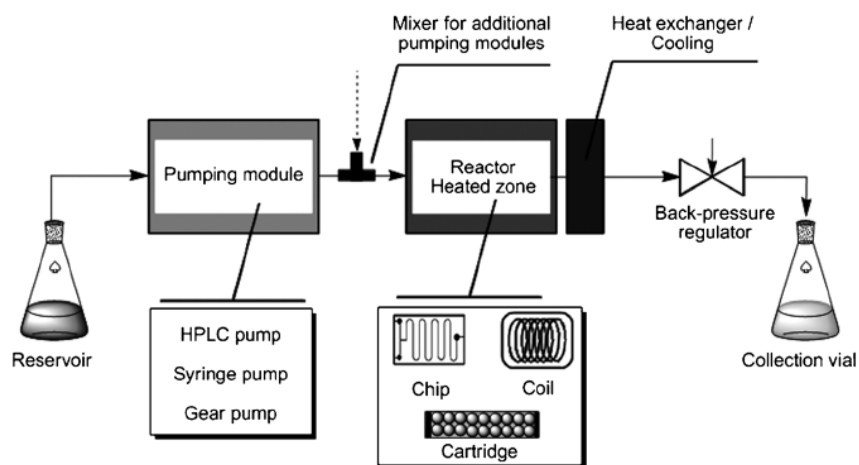


Figure 7.2 – General schematic diagram of a high-temperature/high-pressure continuous flow conditions.

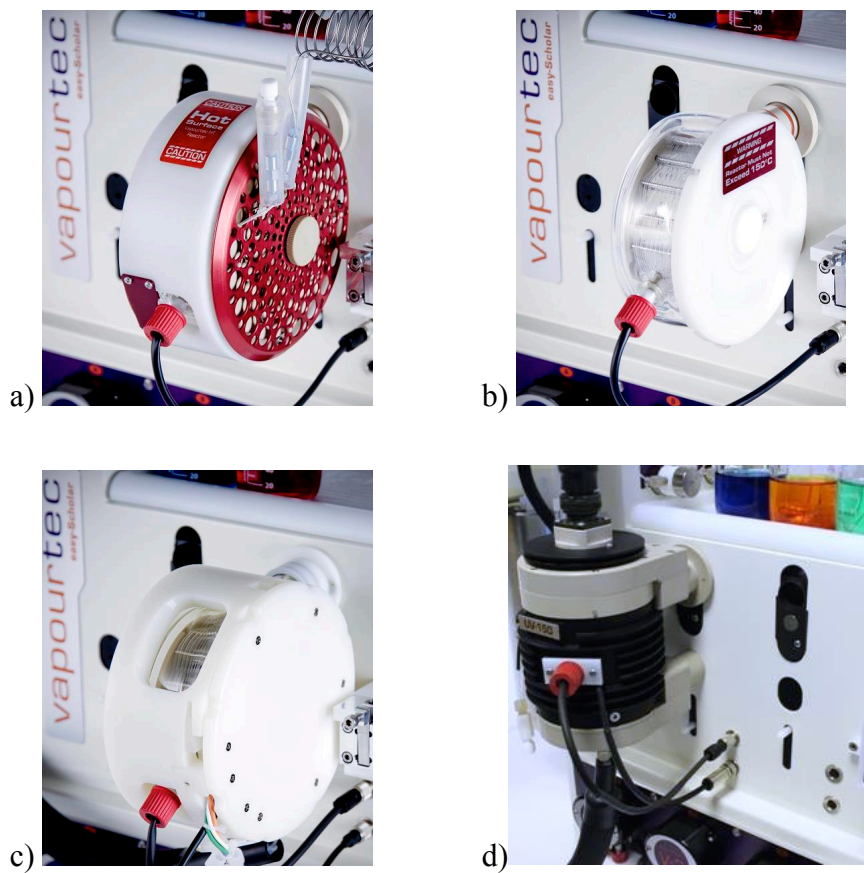


Figure 7.3 – Flow reactors : a) High-temperature/high-pressure stainless steel reactor, b) PFA reactor, c) Cooled reactor (PFA), d) UV reactor

7.1.2 – Important Parameters

In flow chemistry, the flow rate (mL/min) dictates the residence time (min) of the reaction mixture in the reactor. Hence, the residence time is the same as the reaction time in batch chemistry. To optimize a reaction, one can either modify the flow rate or the reactor volume to adjust the reaction time. For example, for a 10 mL reactor volume and a 2.5 mL/min flow rate, the reaction time is 4 minutes. A 4 minutes reaction time can alternatively be maintained with a 1 mL/min flow rate using a 4 mL reactor. The

temperature and pressure of the system are also crucial parameters and will be discussed in detail in Section 7.2.

7.2 – Advantages of Continuous Flow Synthesis vs Microwave and Batch Chemistry

In academic laboratories, chemical reactions are typically performed on relatively small scale (< 1 mol). Hence, the inconveniences associated with scaling up a reaction are minimal. On an industrial level where the scales are much larger, continuous flow synthesis has been readily integrated.^{3a,5} In recent years, academics have found that flow chemistry was more than a scale up tool, but also exhibited several advantages over batch processes.

The main advantages of flow over batch chemistry are summarized in Table 7.1. The precise control of the reaction temperature is perhaps the most important feature of flow chemistry. Since the tubing has a small diameter, the heat transfer is more efficient than in batch. As depicted in Figure 7.4⁶, performing a reaction in small diameter tubing allows for precise control of the time and temperature reaction parameters.^{1b,7} In other words, the reaction starts and ends at very precise points (Figure 7.4, *bottom*) in the reactor and the chemist can precisely control the formation of the product or consumption of the substrate with the length of the reactor used (Figure 7.4, *top*).

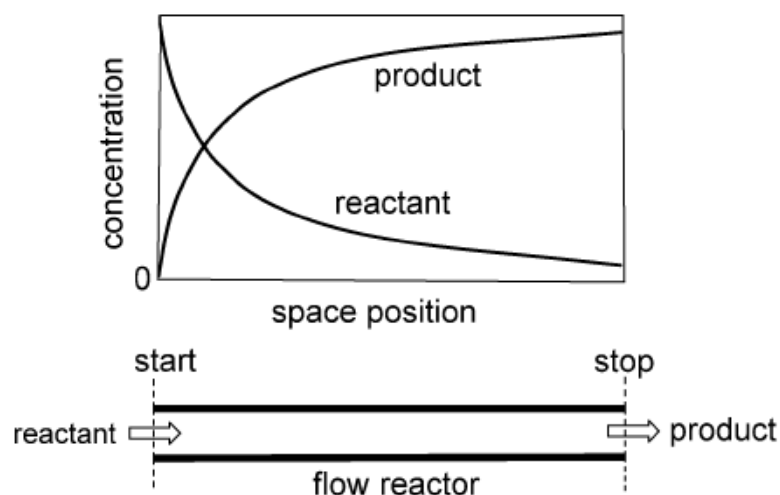


Figure 7.4 – Control of the reaction time in continuous flow. (Reproduced with permission from ref 6. Copyright 2013 Royal Society of Chemistry.)

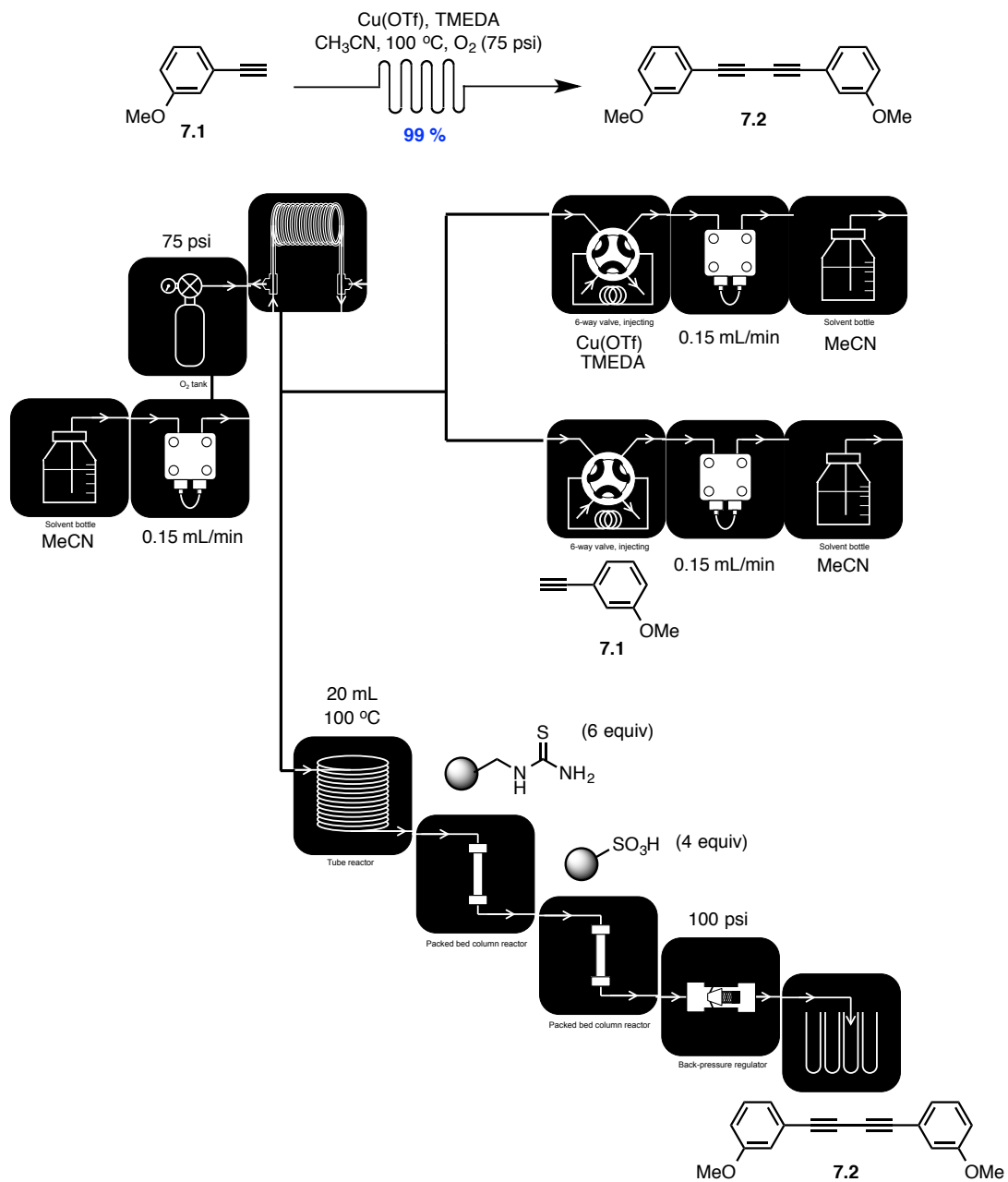
The direct scalability is also a valuable feature of continuous flow. In continuous flow, it is straightforward to reproducibly synthesize either 2 mg or 2 kg of product since the reaction occurs on very small scale in a continuous fashion. Mixing efficiency in a continuous flow process is also superior to a batch process since the mixing occurs through mixers with small interior diameters which accelerates diffusion.⁶ Finally, very high temperatures and pressures can be used in continuous flow. While superheating of solvent and high pressure can also be achieved using microwave irradiation, the head space present in the microwave reactor vessel makes the technology susceptible to explosions.^{1a,8} Although continuous flow chemistry is not appropriate for heterogeneous reaction mixtures because of the possible blockage of reactors, insoluble reagents can be used on solid-supports in packed-bed cartridges.⁹

Table 7.1 – Different properties and advantages of the various techniques currently available.

	Batch	Flow (mesofluidics)
Advantages	Accessible Suitable for heterogeneous mixtures	Superheating solvent High pressure (>200 bar) High temperature (>350 °C) Directly scalable No headspace
Disadvantages	Explosions Scalability	No heterogeneous mixture

7.2.1 – Glaser-Hay Reactions in Continuous Flow

The growing interest in continuous flow chemistry has opened opportunities to explore well established reactions in a novel way. For example, Ley and co-workers reported the continuous flow synthesis of 1,3-diynes using the Glaser-Hay coupling.¹⁰ The Ley group reported the use of a gas-liquid reactor (Scheme 7.1) with a permeable membrane that allows for facile inclusion of O₂ in the reaction mixture, thus enhancing the rate of the Glaser-Hay coupling. The authors also reported the use of solid-supported reagents to perform an in-line work-up of the reaction. A first column was packed with a solid-supported thiourea to remove the copper catalyst while the second column contained an acid to scavenge the amine ligand.



Scheme 7.1 – Glaser-Hay coupling in flow using a gas-liquid reactor.

7.3 – Challenges Associated with Macrocyclization in

Continuous Flow.

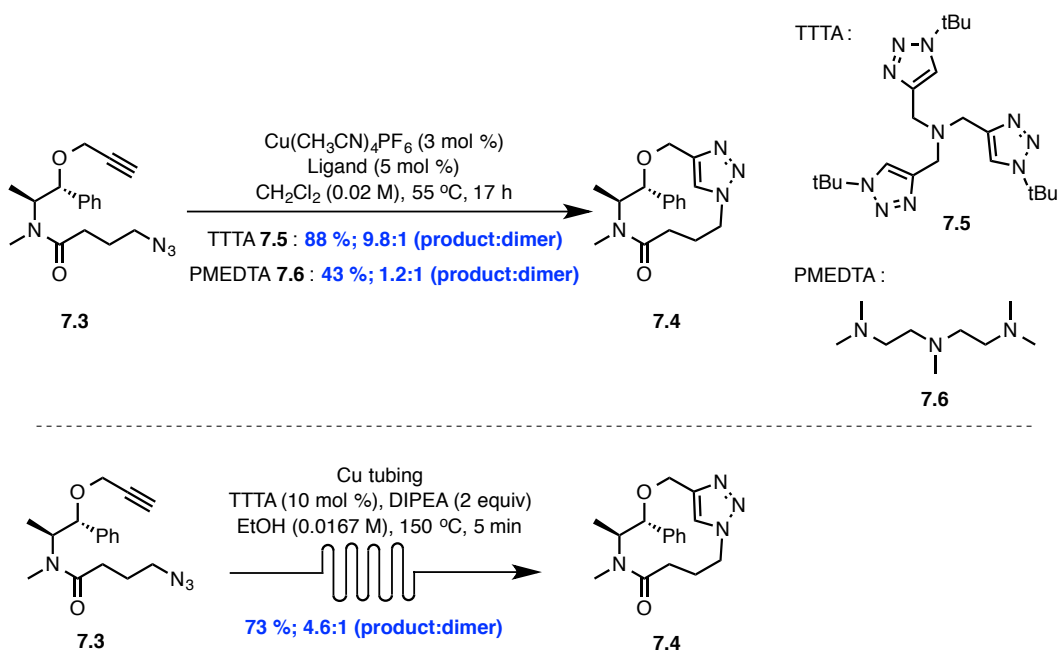
The synthesis of macrocyclic structures is challenging due to the slow rate of ring closure. The use of high dilution or slow addition strategies also complicates the reaction set-up and scalability. Macrocyclization reactions are often plagued by the competing formation of oligomers which can precipitate from the reaction mixture. Therefore, it is not surprising that until 2010, macrocyclization had not been achieved in continuous flow.

Macrocyclization often exhibits a slow rate of reaction, with many examples of macrocyclizations that require several days even with the use of slow addition techniques.¹¹ The long reaction times can be problematic for a continuous flow process in which a minimal flow rate has to be maintained. Even if one managed to steadily pump at a very low flow rate for days, the procedure would be inefficient. In the synthesis of small ring molecules (5-8 membered rings), increasing the temperature could improve the reactivity and lower the reaction time, but in macrocyclization the increase in temperature can also lead to polymerization of the substrate. In order to transpose a macrocyclization from batch to continuous flow, one must render the macrocyclization more efficient while maintaining the intramolecular selectivity.¹²

An additional challenge to overcome for performing macrocyclization in continuous flow is the potential formation of insoluble oligomers. The formation of unwanted oligomeric side-products with problematic solubility can clog the reactor upon precipitation.

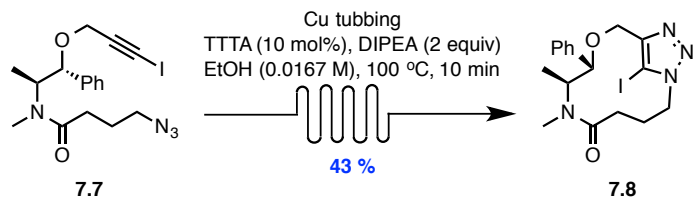
7.4 – Examples of Macrocyclization in Continuous Flow

James and co-workers were the first to report a macrocyclization reaction in continuous flow.¹³ With the goal to prepare a library of drug-like short peptide macrocycles, they developed a copper-catalyzed macrocyclization reaction using a tris-(triazolyl) ligand in batch. James had shown that the family of ligands could improve the macrocycle to dimer ratio (Scheme 7.2).¹⁴ When compared to other amine-based ligands such as PMEDTA **7.6**, tris-(triazolyl) tert-butylamine (TTTA) **7.5** was found to afford the highest yield along with the best product to dimer ratio. Using the same model substrate **7.3**, James transposed the copper-catalyzed azide-alkyne cycloaddition (CuAAC) macrocyclization to continuous flow. As discussed previously (Section 7.3), in order to achieve a suitable reactivity profile for flow, the reaction's temperature had to be increased. James obtained the desired product **7.4**, *albeit* in lower yield and with lower product/dimer selectivity. Although the authors cannot determine with certainty the identity of the active copper species involved in the reaction, they suggest that the use of a copper reactor might contribute to a 'pseudo-dilution' effect while increasing the reactivity profile of the cyclization. In the reported substrate scope, the yields are variable (28-87 %) depending on the inherent preorganization in the linear precursor. The methodology was also used to synthesize various strained cyclophane macrocycles.¹⁵



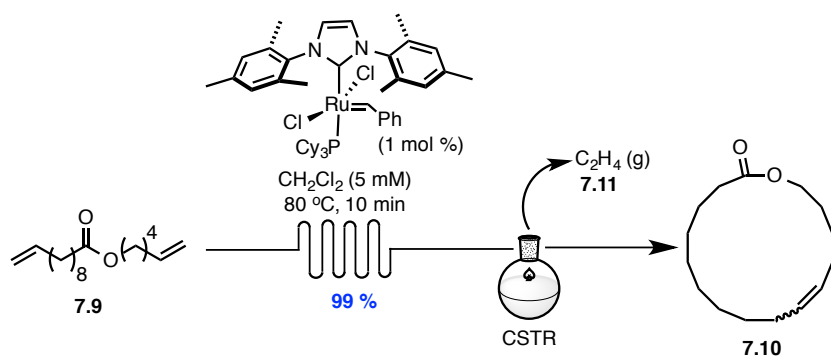
Scheme 7.2 – Macrocyclization of alkyne-azide **6.3** precursor in batch vs. continuous flow

In 2011, James and co-workers used copper coil reactors to also perform an iodoalkyne-azide reaction in continuous flow. Similarly to the alkyne-azide macrocyclizations in continuous flow, the yield of the iodo-version of the reaction is strongly affected by the structure of the precursor, and affords yields ranging from 20 to 80 %. When compared to the azide-alkyne cycloaddition reaction in continuous flow previously reported by James, the iodoalkyne-azide continuous flow variant is not as efficient (Scheme 7.3).¹⁶ The cycloaddition of iodinated precursor **7.7** that is analogous to precursor **7.3** only gave 43 % yield of the desired macrocycle **7.8**, while the analogous macrocycle **7.4** was obtained in 73 % yield.



Scheme 7.3 – Iodo-“Click” macrocyclization in continuous flow.

Fogg and co-workers reported the transposition of the ruthenium-catalysed ring closing metathesis reaction in continuous flow. The authors found that high yield could be obtained when a continuous stirred tank reactor (CSTR) was used in series with the flow to help remove the ethylene **7.11** from the reaction media (Scheme 7.4). Noteworthy, a 16-membered macrolactone **7.10** was synthesized in 99 % yield.¹⁷



Scheme 7.4 – Ring closing metathesis in continuous flow.

7.5 – Conclusion

Continuous flow methodology has revolutionised the chemical sector, not only from an environmental standpoint but also from a quality, safety and economic perspective. In the optic of the development of a green macrocyclization protocol, the use of such technology is imperative.

7.6 – Bibliography

- (1) a) Glasnov, T. N.; Kappe, C. O. *Chem. Eur. J.* **2011**, *17*, 11956-11968; b) Hartman, R. L.; McMullen, J. P.; Jensen, K. F. *Angew. Chem. Int. Ed.* **2011**, *50*, 7502-7519.
- (2) Wiles, C.; Watts, P. *Green. Chem.* **2012**, *14*, 38-54.
- (3) a) Dudukovic, M. P.; Larachi, F.; Mills, P. L. *Chem. Eng. Sci.* **1999**, *54*, 1975-1995; b) Weissermel, K.; Arpe, H.-J. In *Industrial Organic Chemistry*; Wiley-VCH Verlag GmbH: 2008, p I-XIX.
- (4) Webb, D.; Jamison, T. F. *Chem. Sci.* **2010**, *1*, 675-680.
- (5) Weissermel, K.; Arpe, H.-J. In *Industrial Organic Chemistry*; Wiley-VCH Verlag GmbH: 2008, p 467-491.
- (6) Yoshida, J.-i.; Takahashi, Y.; Nagaki, A. *Chem. Commun.* **2013**, *49*, 9896-9904.
- (7) Zaborenko, N.; Bedore, M. W.; Jamison, T. F.; Jensen, K. F. *Org. Process Res. Dev.* **2010**, *15*, 131-139.
- (8) Razzaq, T.; Kappe, C. O. *Chem. Asian J.* **2010**, *5*, 1274-1289.
- (9) a) Hartman, R. L.; Naber, J. R.; Zaborenko, N.; Buchwald, S. L.; Jensen, K. F. *Org. Process Res. Dev.* **2010**, *14*, 1347-1357; b) Li, W.; Pham, H. H.; Nie, Z.; MacDonald, B.; Güenther, A.; Kumacheva, E. *J. Am. Chem. Soc.* **2008**, *130*, 9935-9941; c) Baxendale, I. R.; Deeley, J.; Griffiths-Jones, C. M.; Ley, S. V.; Saaby, S.; Tranmer, G. K. *Chem. Commun.* **2006**, 2566-2568.
- (10) Petersen, T. P.; Polyzos, A.; O'Brien, M.; Ulven, T.; Baxendale, I. R.; Ley, S. V. *ChemSusChem* **2012**, *5*, 274-277.
- (11) a) Illuminati, G.; Mandolini, L.; Masci, B. *J. Am. Chem. Soc.* **1977**, *99*, 6308-6312; b) Illuminati, G.; Mandolini, L. *Acc. Chem. Res.* **1981**, *14*, 95-102; c) Allinger, N. L.; Tribble, M. T.; Miller, M. A.; Wertz, D. H. *J. Am. Chem. Soc.* **1971**, *93*, 1637-1648; d) Parenty, A.; Moreau, X.; Campagne, J. M. *Chem. Rev.* **2006**, *106*, 911-939; e) Collins, J. C.; James, K. *MedChemComm* **2012**, *3*, 1489-1495.
- (12) Bedard, A.-C.; Collins, S. K. *Chem. Commun.* **2012**, *48*, 6420-6422.
- (13) Bogdan, A. R.; James, K. *Chem. Eur. J.* **2010**, *16*, 14506-14512.
- (14) Chouhan, G.; James, K. *Org. Lett.* **2011**, *13*, 2754-2757.
- (15) Bogdan, A. R.; Jerome, S. V.; Houk, K. N.; James, K. *J. Am. Chem. Soc.* **2011**, *134*, 2127-2138.
- (16) Bogdan, A. R.; James, K. *Org. Lett.* **2011**, *13*, 4060-4063.
- (17) Monfette, S.; Eyholzer, M.; Roberge, D. M.; Fogg, D. E. *Chem. Eur. J.* **2010**, *16*, 11720-11725.

Chapter 8 : Continuous Flow Macrocyclization at High Concentrations: Synthesis of Macrocyclic Lipids

Anne-Catherine Bédard, Sophie Régnier and Shawn K. Collins*

Département de Chimie, Center for Green Chemistry and Catalysis, Université de Montréal, CP 6128 Station Downtown, Montréal, Québec H3C 3J7 Canada

Green Chemistry **2013**, *15*, 1962-1966.

Contributions:

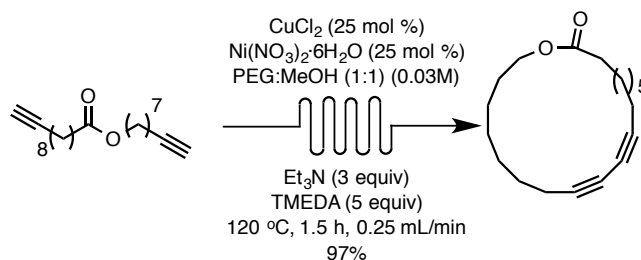
- Anne-Catherine Bédard participated in the design of the experiments, experimental work and contributed to the writing of the manuscript.
- Sophie Régnier contributed to the optimization of the reaction in continuous flow.
- Shawn K. Collins participated in the design of the experiments and writing of the manuscript.

Reproduced by permission from the Royal Society of Chemistry

Permanent link to the article (DOI) : [10.1039/C3GC40872H](https://doi.org/10.1039/C3GC40872H)

8.1 – Abstract

A phase separation/continuous flow macrocyclization protocol eliminates the need for high-dilution conditions and can be used to prepare gram quantities of biologically relevant macrocyclic lipid structures. The method presents several green advantages towards macrocycle synthesis: 1) the prevention of unwanted oligomers and waste, 2) a reduction in the large quantities of toxic, volatile organic solvents and 3) the use of PEG as an environmentally benign reaction media. Macrocycles could be synthesized in high yields (up to 99 %) in short reaction times (1.5 h) and on gram scales without the need to alter the reaction conditions.



8.2 – Introduction

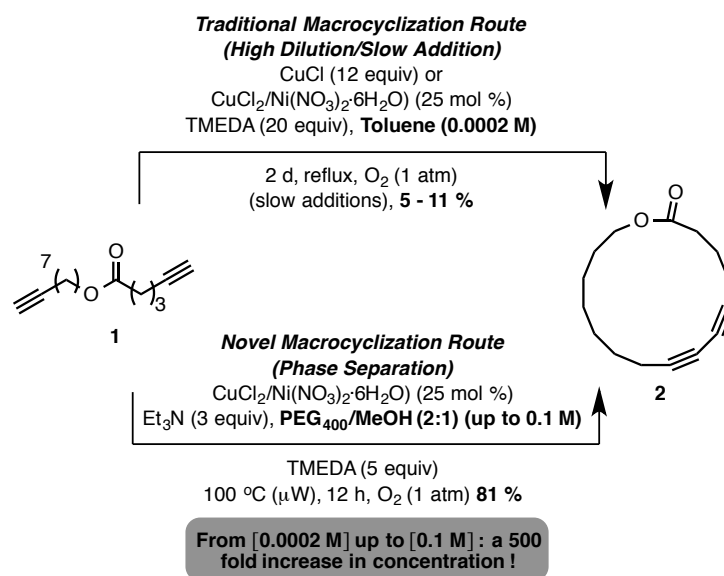
Continuous flow strategies for green chemical synthesis have impacted every area of organic synthesis, from academic to industrial research.¹ Flow chemistry represents a powerful technology whose advantages include precise control of reaction time, temperature, concentration and stoichiometry. Consequently, many of the principles of green chemistry are fulfilled such as reduced energy requirements, minimized exposure to hazardous chemicals or intermediates and reduced amounts of unwanted by-products and waste. Given these advantages, flow chemistry is an ideal technique to use in tackling the challenges associated with macrocycle synthesis. Macrocycles are important structural motifs found in compounds

with applications in pharmaceutical, agrochemical, cosmetic and material sciences.² Their synthesis is challenging, often requiring significant amounts of solvent to control concentration effects and prevent the formation of undesirable oligomers. When the dilution requirements and inconvenient set-up are considered, macrocyclization reactions in general would benefit from improved protocols employing flow techniques.

Macrocyclization *via* continuous flow presents several challenges, including: 1) the need to accelerate the normally slow cyclization reactions to improve their efficiency and most importantly, 2) the need to prevent oligomerization, as these by-products have low solubilities and could block the flow reactor. Recently, James and co-workers have reported the first flow-macrocyclization reaction that involved the synthesis of constrained macrocycles *via* alkyne-azide cycloaddition chemistry.³ The reaction rates of the macrocyclizations reported were accelerated through judicious choice of ligands and the exploitation of copper tubing as the flow reactor. The efficient heat transfer that can be achieved in flow would seem to provide a solution to the challenge of macrocyclization efficiency, however the challenge of reaction dilution is often more daunting.⁴

Consequently, our group has recently reported a general, efficient and green macrocyclization protocol *via* oxidative Glaser-Hay coupling at high concentrations through the use of a “phase separation” strategy (Scheme 8.1).⁵ The concentration effects of the macrocyclization reaction were controlled through the aggregation properties of poly(ethylene glycol)₄₀₀ (PEG₄₀₀). The “phase separation” technique allowed for significantly higher concentrations (150-500x), a reduction of the amounts of toxic organic solvents that are eventually converted to waste, and replacement of the majority of the volatile organic solvents by the environmentally benign PEG. Given the advantages presented by the “phase

separation” strategy, we sought to apply it to the development of a continuous flow process to synthesize important medically relevant classes of macrocycles. Consequently, herein we report on the development of efficient continuous flow macrocyclization for the preparation of macrocyclic lipids that mimic those found in Archaeal membranes.⁶



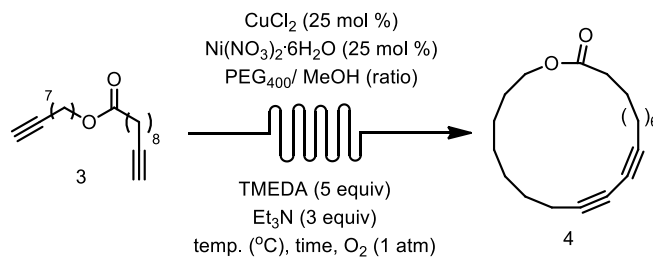
Scheme 8.1 – Advantages of the “phase separation” strategy in macrocyclization

8.3 – Results and Discussion

The investigations into a continuous flow/macrocyzclization protocol began by transposing the previously optimized reaction conditions for the Glaser-Hay coupling utilizing microwave heating.⁷ The preliminary studies utilized the formation of macrolactone **4**, as it provides a valid comparison for the continuous flow protocol versus other existing macrocyclization strategies (Table 8.1). TMEDA was chosen as the ligand as its bidentate nature provides increased solubility and stability of the resulting transition metal complexes at high temperatures.⁵ Intermolecular Glaser-Hay couplings have been previously studied in

continuous flow settings, where semi-permeable Teflon AF-2400 membranes⁸ were used to increase contact with oxygen gas. In the present study, the solutions for macrocyclization were only sparged with O₂ for 5 min before injection into the flow apparatus. First, we investigated the effect of the temperature on the yields of the desired 21-membered macrolactone **4** (Table 8.1, entries 1→4). When the reaction was performed at the same temperature as in the microwave heated reaction (120 °C), **4** was formed in higher yield using a flow strategy (85 % vs. 81 %, entry 3). Lower temperatures resulted in lower conversions and isolated yields. Increasing the temperature (140 °C) resulted in a decrease of selectivity (macrocyclization vs. oligomerization) as the yield of **4** decreased (72 %) and oligomers could be observed. Changing the ratio of PEG₄₀₀/MeOH (Table 8.1, entries 4→6) did not result in significant changes in isolated yield, although larger ratios of PEG result in better solubility of the organic substrates. Higher ratios of PEG₄₀₀/MeOH were not explored as previous work has indicated that catalyst inhibition becomes problematic at higher ratios.⁵

Table 8.1 – Optimization of Reaction Conditions For Macrocylic Glaser-Hay Coupling of **3**.



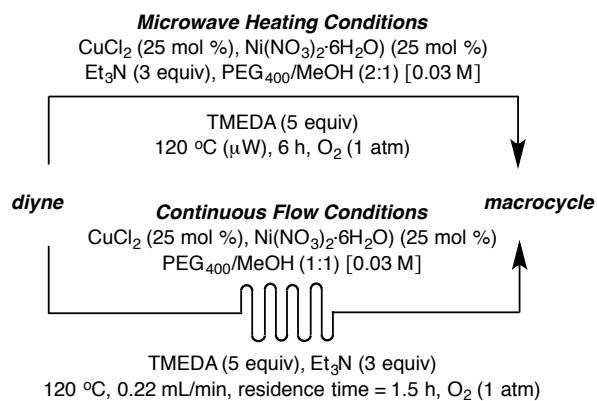
Entry	Temp. (°C)	PEG ₄₀₀ /MeOH (ratio)	Flow Rate (mL/min); Residence Time (h)	Yield (%)
1	80	2 : 1	5; 3	74
2	100	2 : 1	5; 3	73
3	120	2 : 1	5; 3	85
4	140	2 : 1	5; 3	72
5	120	1 : 1	5; 3	86
6	120	1 : 2	5; 3	82
7	120	1 : 1	5; 1.5	96
8	120	1 : 1	1; 1.5	91
9	120	1 : 1	0.22; 1.5	97

The influence of reaction time and flow/rate were also investigated (Table 8.1, entries 7→9). Due to the viscosity of PEG₄₀₀, high flow rates were found to cause irregularities in pressure control. It was found that by using lower flow rates, pressure control was easily maintained and helped to provide more reproducible results. Gratifyingly, it was found that flow rates of 0.22 mL/min and a residence time of 1.5 h afforded a nearly quantitative yield (97 %) of the macrocyclic product **4**. The high yield of macrocycle **4** achieved at relatively high concentration ([0.03 M]) denotes the high efficiencies that are possible when combining the two green chemistry techniques of phase separation and continuous flow synthesis. The calculated E_{mac} (a recently proposed meter for grading the efficiency of macrocyclizations)⁹ of ~7.4 for the macrocyclization (**3**→**4**) is high and similar to those obtained in James' previously

reported continuous flow synthesis of constrained macrocycles via alkyne-azide cycloadditions.

In an effort to evaluate the generality of the optimized continuous flow conditions, the macrocyclization of three other diynes was performed (Table 8.2, entries 2→4). In each case, the results of the cyclization using the continuous flow conditions were compared with the isolated yields obtained utilizing the previously developed microwave heating protocol. First, the isolated yield of the 21-membered macrolactone **4** obtained *via* continuous flow (97 %) was found to be much better than that obtained *via* microwave heating (81 %). Given the excellent yield obtained for **4**, the macrocyclization to afford **4** was scaled to 1 mmol and a 93 % yield was obtained.

Table 8.2 – Macrocyclic Lactones and Ethers Synthesized via Continuous Flow-Macrocyclization Using “Phase Separation”.



Entry	Product	Yield: Flow (%)	Yield: Microwave (%)
1		97 ^a	81
2		58	75
3		72	47
4		71 ^b	65

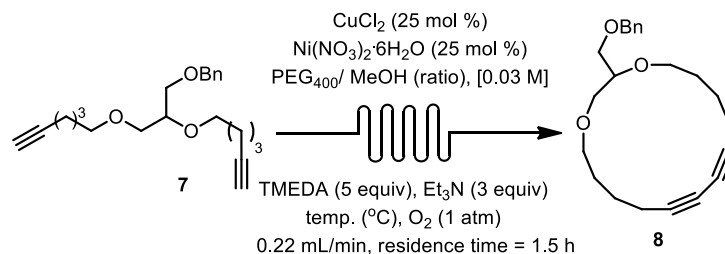
^a On a 1 mmol scale, **4** was isolated in 93 % yield. ^b The corresponding diyne precursor of **7** was insoluble in PEG₄₀₀/MeOH mixtures. As such, a PEG₄₀₀/MeOH (2:1) ratio was used.

The macrocyclization of other diynes was then investigated. When the cyclization to form the 20-membered macrocyclic diester **5** was investigated, a 72 % yield of the product was obtained utilizing continuous flow. A much lower yield (47 %) of **5** was obtained using the microwave heating protocol. The preparation of macrocyclic ether **6** was initially problematic, as its corresponding diyne precursor was partially insoluble in the PEG₄₀₀/MeOH (1:1) mixture. However, as previous experiments demonstrated very little difference in yield between PEG₄₀₀/MeOH (2:1) and (1:1) mixtures, the cyclization to form **6** was conducted using the higher ratio of PEG₄₀₀/MeOH (2:1). The macrocycle **6** was once again obtained in higher yields (71 %) when using the continuous flow strategy. However, it was noted that when the synthesis of a smaller and significantly more strained macrocycle **2** was investigated, the trend reversed. The 16-membered macrocycle **2** was obtained in higher yield using microwave heating (75 %) versus the continuous flow (58 %).

Encouraged by the preliminary optimization of a continuous flow-macrocyclization protocol employing a “phase separation” strategy, the optimal conditions were also explored with a macrocyclic lipid precursor **7** which bears a protected glycerol motif (Table 8.3). The macrocyclic Archaeal lipids are typically composed of polyprenyl chains with glycerol or polyol head groups.⁶ Within the structure of the lipids, macrocyclization can occur through the alkyl chains of the same head group or between two lipids, producing dimers. As such, 36- or 72-membered rings can be formed.¹⁰ Recently, much attention has been given to macrocyclic lipids for potential anti-cancer activities or in the design of novel vehicles for liposomal drug delivery.¹¹ When the benzyl-protected glycerol derivative **7** was subjected to the optimized conditions from Table 8.2, it was found that **7** was poorly soluble in the 1:1 PEG₄₀₀/MeOH solvent mixture (Table 8.3, entry 1). However, when the ratio of PEG₄₀₀/MeOH was increased

(2:1), the 16-membered macrocyclic lipid **9** was isolated in 71 % yield. Variations in the reaction temperature followed the same trends that were observed for the synthesis of macrolactone **4** (Table 8.3). Lower temperatures resulted in lower conversions and isolated yields, although excellent selectivity was observed and the remaining mass balance was recovered starting diyne **7** (Table 8.3, entry 3). Increasing the reaction temperature once again lowered selectivity, resulting in the formation of oligomers and decreased isolated yields (63 %).

Table 8.3 – Optimization of Reactions Conditions for the Synthesis of a Protected Macrocyclic Lipid **8**.



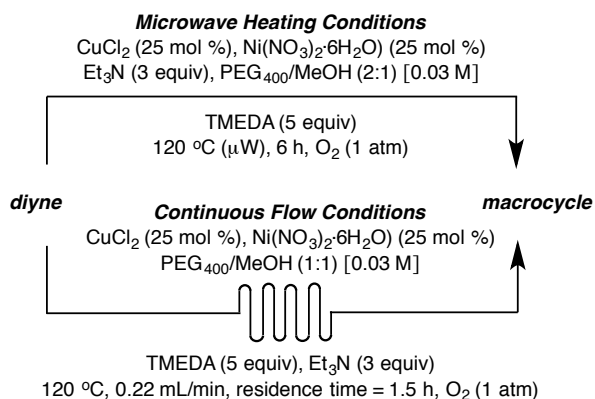
Entry	Temp. (°C)	PEG ₄₀₀ /MeOH (ratio)	Yield (%)
1	120	1 : 1	- ^a
2	120	2 : 1	71
3	100	2 : 1	66
4	140	2 : 1	63

^a Diyne **7** precipitates from the solution when a PEG₄₀₀/MeOH (1:1) ratio is used.

With optimized continuous flow conditions in hand for the synthesis of macrocyclic lipids, the macrocyclization of 3 other substrates were performed (Table 8.4). The isolated yield of the 16-membered macrolipid **8** was found to be slightly higher under continuous flow conditions (71 %) compared to cyclization under microwave heating (65 %) (Table 8.4, entry 1). As one of the advantages of continuous flow methods is the facile scale-up, the synthesis of

8 was repeated on ~4 mmol scale. The yield of the 16-membered macrolipid **8** did not change significantly (66 % isolated yield on ~4 mmol scale). Similar macrolipids based upon a glycerol head group were then prepared having different ring sizes. When the 26-membered macrocycle **9** was prepared *via* continuous flow, the isolated yield of 78 % was again higher than what was obtained *via* microwave heating (62 %). Similarly, the 30-membered macrocycle **10** was isolated in 99 % yield after synthesis *via* continuous flow (92 % isolated yield was obtained using microwave heating). As many macrocyclic lipids can be prepared with ester linkages, the macrocycle **11** was prepared by continuous flow synthesis and was isolated in 45 % yield. In all of the macrocyclizations, the products were obtained in higher yield when using continuous flow versus microwave heating. In general, the yields of the larger 21-, 26- and 30-membered macrocyclic lipids were higher than smaller macrocycles, perhaps due to the ring strain caused by the incorporation of a linear 1,3-diyne within the cyclic motif.

Table 8.4 — Macrocyclic Lipids Synthesized via Continuous Flow-Macrocyclization Using “Phase Separation”.

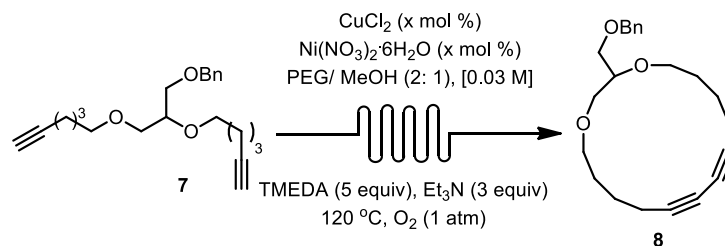


Entry	Product	Yield: Flow (%)	Yield: Microwave (%)
1	 8	71 ^a	65
2	 9	78	62
3	 10	99	92
4	 11	45	42

^a When cyclization was performed on 3.8 mmol scale, the macrocycle was obtained in 66 % yield.

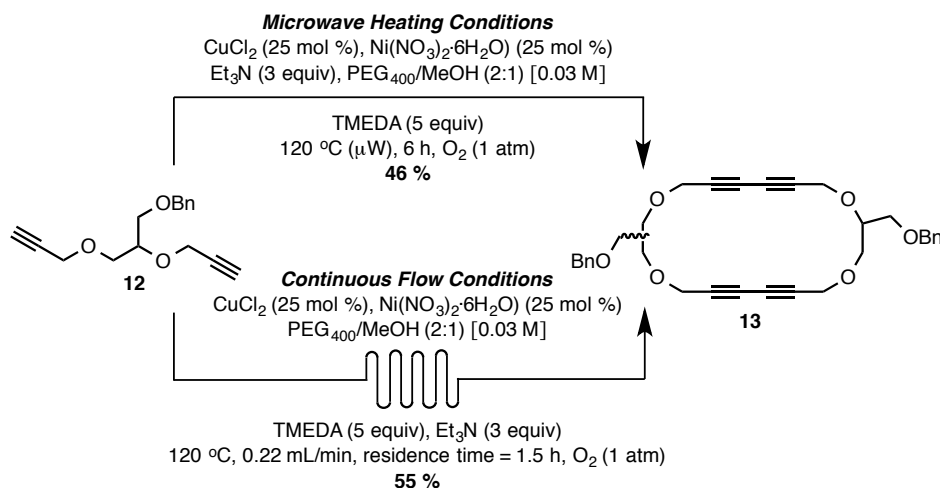
In an effort to further improve the continuous flow process, the use of other PEG solvents were investigated with the goal of reducing the catalyst loadings (Table 8.4).⁵ When the diyne **7** had been previously cyclised under optimum conditions using 25 mol % of catalysts and PEG₄₀₀ as a co-solvent, the yield of the corresponding lipid macrocycle **8** was 71 %. When the solvent PPG₄₂₅ was used as a substitute for PEG₄₀₀ at identical catalyst loadings a similar yield was observed (Table 8.4, entry 2). However, when the catalyst loading was dropped to 10 mol %, continuous flow conditions could be developed so that the desired macrocycle **8** could be isolated in 92 % yield. These preliminary results demonstrate that the catalyst loadings could be lowered and the yields increased through judicious choice of the PEG co-solvent in the continuous flow conditions. Further reductions in the catalyst loading to 5 mol % also provided good yields of macrocycle **8** (78 %) and excellent selectivity for macrocyclization was observed, as the remaining mass balance was recovered diyne **7**. Longer reaction times may be necessary for effective use of reduced catalyst loadings.

Table 8.5 – Reduction of Catalyst Loadings when Using PPG₄₂₅ for the Synthesis of a Protected Macrocylic Lipid **8**.



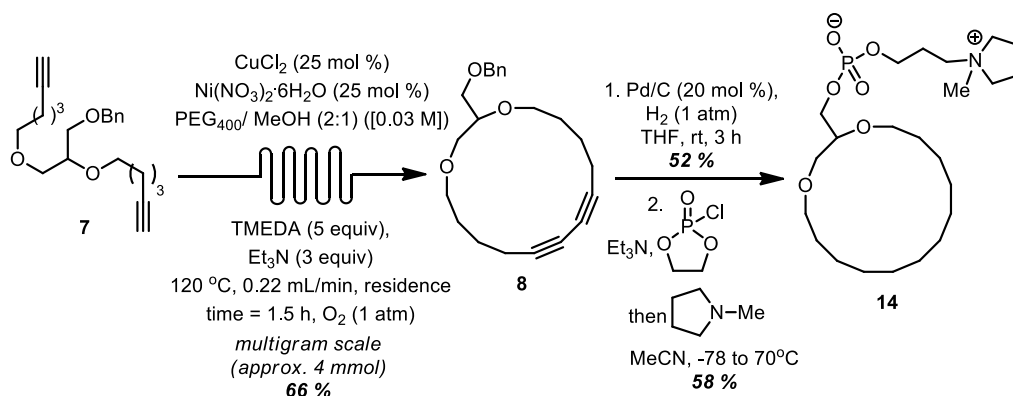
Entry	mol %	PEG	Flow Rate (mL/min); Residence Time (h)	Yield (%)
1	25	PEG ₄₀₀	0.22; 1.5	71
2	25	PPG ₄₂₅	0.22; 1.5	65
3	10	PPG ₄₂₅	0.11; 3	92
4	5	PPG ₄₂₅	0.11; 3	78

As dimeric macrocyclic lipids are found in Nature,⁶ the macrocyclization of the diyne **12** was investigated under the optimized reaction conditions (Scheme 8.2). Acyclic diyne **12** cannot undergo intramolecular cyclization due to ring strain but selectively forms the dimer **13** in 55 % yield *via* continuous flow (46 % using microwave heating).



Scheme 8.2 – Synthesis of a dimeric macrocyclic lipid **13** as a mixture of head-to-tail and head-to-head isomers.

To demonstrate the utility of the novel macrocycles prepared in Table 7.4 as lipids, the synthesis of the 16-membered macrocyclic diyne **8** was performed on a multigram scale (~4 mmol) and similar yields were obtained even when the reaction was scaled by a factor of 30X (Scheme 8.3). Upon isolation, macrocyclic lipid **8** was functionalized with a polar phosphonate group. A global hydrogenation (Pd/C, H₂ (1 atm)) of macrocycle **8** results in cleavage of the Bn protecting group and exhaustive hydrogenation of the 1,3-diyne to afford the corresponding saturated macrocycle in 52 % yield. Subsequent phosphonation provided the saturated macrocyclic lipid **14** in 58 % yield.



Scheme 8.3 – Conversion of Bn-protected macrocycle **8** into novel macrocyclic phosphonate containing lipid **14**.

8.4 – Conclusion

The above studies demonstrate that a continuous flow-macrocyclization protocol utilizing “phase separation” eliminates the need for extremely high-dilution conditions and can be used to prepare meaningful quantities of biologically relevant macrocyclic lipid structures. The combination of the “phase separation” strategy with a continuous flow synthesis presents several green advantages towards macrocycle synthesis: the precise control of reaction time

and temperature prevent the formation of unwanted oligomers and waste, 2) the high concentrations reduce the large quantities of solvents that would have to be disposed of in environmentally damaging processes and 3) the use of PEG as a solvent represents a non-volatile and non-toxic alternative to traditional organic solvents. Macrocycles could be synthesized in high yields (up to 99 %), in short reaction times (1.5 h) and on large scales without the need to alter the reactions conditions. Preliminary results demonstrate that reduced catalyst loadings may be possible when using modified PEG co-solvents. The demonstration of the viability of the phase separation/continuous flow synthetic strategy should find applicability in the synthesis of other macrocycles in academia and industry.

Acknowledgement. The authors acknowledge the Natural Sciences and Engineering Research Council of Canada (NSERC), Université de Montreal and the Centre for Green Chemistry and Catalysis (CGCC) for generous funding. A.-C. B. thanks NSERC (Vanier Graduate Scholarship) and CGCC for graduate scholarships, and S. R. thanks CGCC for an undergraduate fellowship.

Supporting Information Available: Electronic Supplementary Information (ESI) available: Experimental procedure and characterization data for all new compounds. See DOI: 10.1039/b000000x/

8.5 – Bibliography

- (1) P. Watts, and C. Wiles, *J. Chem. Res.*, 2012, **36**, 181; C. Wiles, *PharmaChem*, 2011, **10**, 15; L. Malet-Sanz, and F. Susanne, *J. Med. Chem.*, 2012, **55**, 4062.
- (2) J. C. Roxburgh, *Tetrahedron*, 1995, **51**, 9767; E. M. Driggers, S. P. Hale, J. Lee, and N. K. Terrett, *Nat. Rev. Drug Discovery*, 2008, **7**, 608; E. Marsault, and M. L. Peterson, *J. Med. Chem.*, 2011, **54**, 1961; H. Matsuda, S. Watanabe, and K. Yamamoto, *Chem. Biodiversity*, 2004, **1**, 1985.
- (3) A. R. Bogdan, S. V. Jerome, K. N. Houk, and K. James, *J. Am. Chem. Soc.*, 2012, **134**, 2127; A. R. Bogdan, and K. James, *Org. Lett.*, 2011, **13**, 4060; A. R. Bogdan, and K. James, *Chem.–Eur. J.*, 2010, **16**, 14506.
- (4) For an alternative synthetic route employing ring expansion to similar macrocycles that avoid high dilution and can be used in flow see: M. Nagel, G. Frater, and H.-J. Hansen, *Chimia*, 2003, **57**, 196.
- (5) A.-C. Bédard, and S. K. Collins, *J. Am. Chem. Soc.*, 2011, **133**, 19976; A.-C. Bédard, and S. K. Collins, *Chem. Commun.*, 2012, **48**, 6420; A.-C. Bédard, and S. K. Collins, *Chem.–Eur. J.*, 2013, **19**, 2108; A.-C. Bédard, and S. K. Collins, *ACS Catal.* 2013, **3**, 773.
- (6) M. De Rosa, and A. Gambacorta, *Prog. Lipid Res.*, 1988, **27**, 153; M. Kates, *Membrane Lipids of Archaeal*, Elsevier, Oxford, 1993, 261; P. B. Comita, R. B. Gagosian, H. Pang, and C. E. Costello, *J. Biol. Chem.*, 1984, **259**, 15234.
- (7) T. N. Glasnov, and C. O. Kappe, *Chem.–Eur. J.*, 2011, **17**, 11956.
- (8) T. P. Petersen, A. Polyzos, M. O'Brien, T. Ulven, I. R. Baxendale, and S. V. Ley, *ChemSusChem*, 2012, **5**, 274.
- (9) An E_{mac} above ~ 7.1 suggests a macrocyclization is within the top 10% of the most efficient macrocyclizations reported to date. For a discussion on grading the efficiency of macrocyclization reactions through the use of the E_{mac} factor see: J. C. Collins, and K. James, *Med. Chem. Commun.*, 2012, **3**, 1489.
- (10) T. Eguchi, T. Terachi, and K. Kakinuma, *J. Chem. Soc. Chem. Comm.*, 1994, **137**; T. Eguchi, K. Arakawa, T. Terachi, and K. Kakinuma, *J. Org. Chem.*, 1997, **62**, 1924; K. Arakawa, T. Eguchi, and K. Kakinuma, *Chem. Lett.*, 1998, **8**, 901.
- (11) H. Liu, C. E. Olsen, and S. B. Christensen, *J. Nat. Prod.*, 2004, **67**, 1439; T. Eguchi, K. Arakawa, K. Kakinuma, G. Rapp, S. Ghosh, Y. Nakatani, and G. Ourisson, *Chem.–Eur. J.*, 2000, **6**, 3351; O. Dannenmuller, K. Arakawa, T. Eguchi, K. Kakinuma, S. Blanc, A.-M. Albrecht, M. Schmutz, Y. Nakatani, and G. Ourisson, *Chem.–Eur. J.*, 2000, **6**, 645; W. P. D. Goldring, E. Jubeli, R. A. Downs, A. J. S. Johnston, N. Abdul Khaliq, L. Raju, D. Wafadari, and M. D. Pungente, *Bioorg. Med. Chem. Lett.*, 2012, **22**, 4686; M. Shibakami, S. Miyoshi, M. Nakamura, and R. Goto, *Synlett*, 2009, **16**, 2651; S. Bhattacharya, and J. Biswas, *Langmuir*, 2010, **26**, 4642; Q.-D. Huang, H. Chen, L.-H. Zhou, J. Huang, J. Wu, and X.-Q. Yu, *Chem. Biol. Drug Des.*, 2008, **71**, 224; M.-L. Miramon, N. Mignet, and J. Herscovici, *J. Org. Chem.*, 2004, **69**, 6949.

PART 3

Chapter 9 : Introduction to the Copper-Catalyzed Azide-Alkyne Cycloaddition

Since the discovery of the copper-catalyzed azide-alkyne cycloaddition (CuAAC), it has made a significant impact on the scientific community.^{1,2} The simplicity of the transformation combined with the availability of the starting materials has allowed it to influence many areas of research such as material science, medicinal chemistry and supramolecular chemistry.^{1,2} CuAAC is often referred to as “Click” chemistry, meaning that it is part of a family of very efficient chemical transformations that have the following characteristics : 1) modular, 2) broad scope, 3) high yielding, 4) generates only inoffensive byproducts, 5) stereospecific, 6) simple reaction conditions (insensitive to oxygen and water) and 7) simple product isolation (nonchromatographic).² The subsequent chapter will elaborate on the CuAAC reaction, its application in synthesis as well as insight into the reaction mechanism, ligand effects, and catalysis *via* other metals. In addition, the copper-catalyzed azide-iodoalkyne cycloaddition (CuAiAC) variant will be presented.

9.1 – Discovery and Improvement of the Azide-Alkyne Cycloaddition Reaction

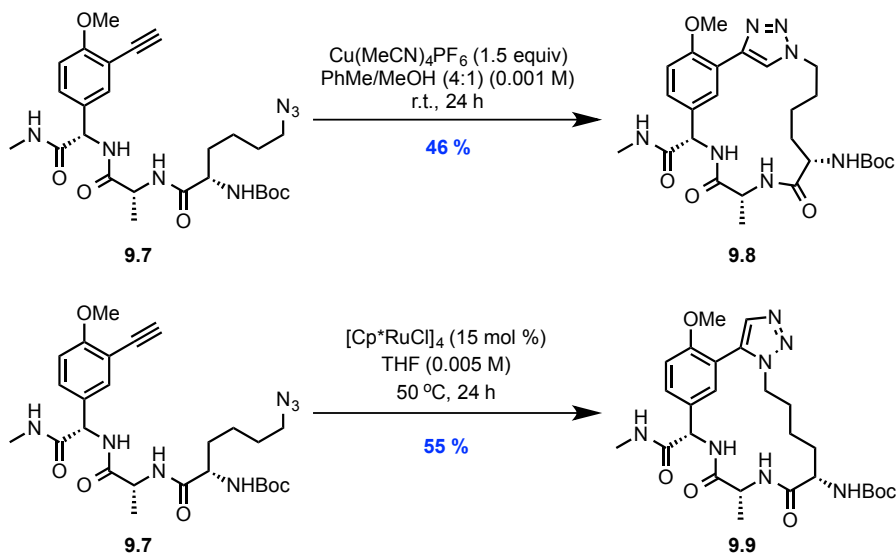
The AAC was first investigated by Huisgen for over twenty years starting in the 1950's.³ The uncatalyzed cycloaddition of alkyne and azide is a relatively slow process that requires high temperatures and long reaction times. Although the overall process is exothermic (ΔH^0 between -50 and -65 kcal/mol), it has an important calculated activation barrier of 25 kcal/mol for methyl azide and propyne.⁴ While the triazole motif is a valuable moiety in

The reaction manifold also promotes cycloaddition with internal alkynes, in contrast with the copper-catalyzed version.⁷ Besides, iridium catalysts have also been used to form 1,5-triazole products using bromoalkynes as starting materials, under mild reaction conditions.⁸

9.2 – Applications of the Copper-Catalyzed Azide-Alkyne

Cycloaddition Reaction

The versatility of the AAC has been demonstrated in various fields, particularly in medicinal chemistry⁹⁻¹². First, AAC reactions have been exploited for the synthesis of macrocyclic peptides. For example, vancomycin-inspired tripeptide mimics **9.8** and **9.9** were synthesized using the copper and ruthenium variants of the reaction starting from the same peptidic precursor **9.7** (Scheme 9.2). It was found that the regioisomeric macrocycles **9.8** and **9.9** had good overlap with balhimycin, a structural analog of vancomycin that also exhibits antibacterial properties (Figure 9.1).^{9,10} Macrocyclic CuAAC in continuous flow is also an emerging tool for the synthesis of macrocyclic drug candidates (refer to Chapter 7, Scheme 7.2 and 7.3).¹¹



Scheme 9.2 – CuAAC and RuAAC macrocyclization of vancomycin-inspired tripeptides.

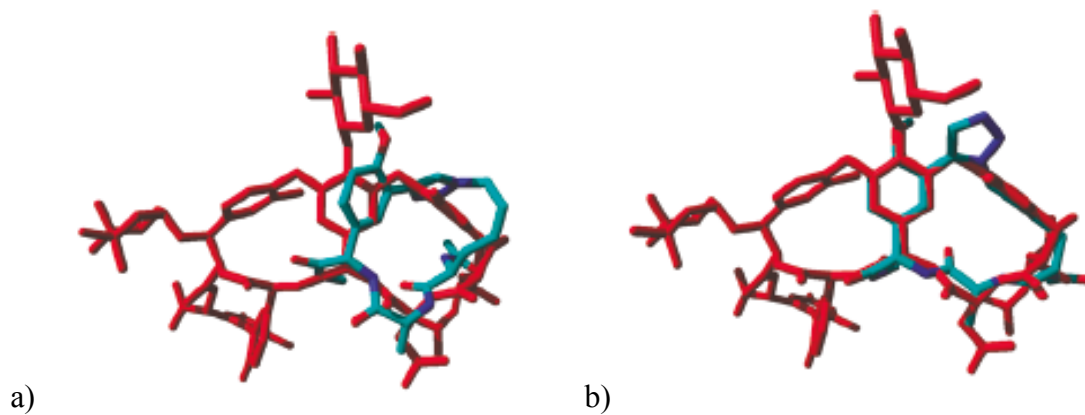
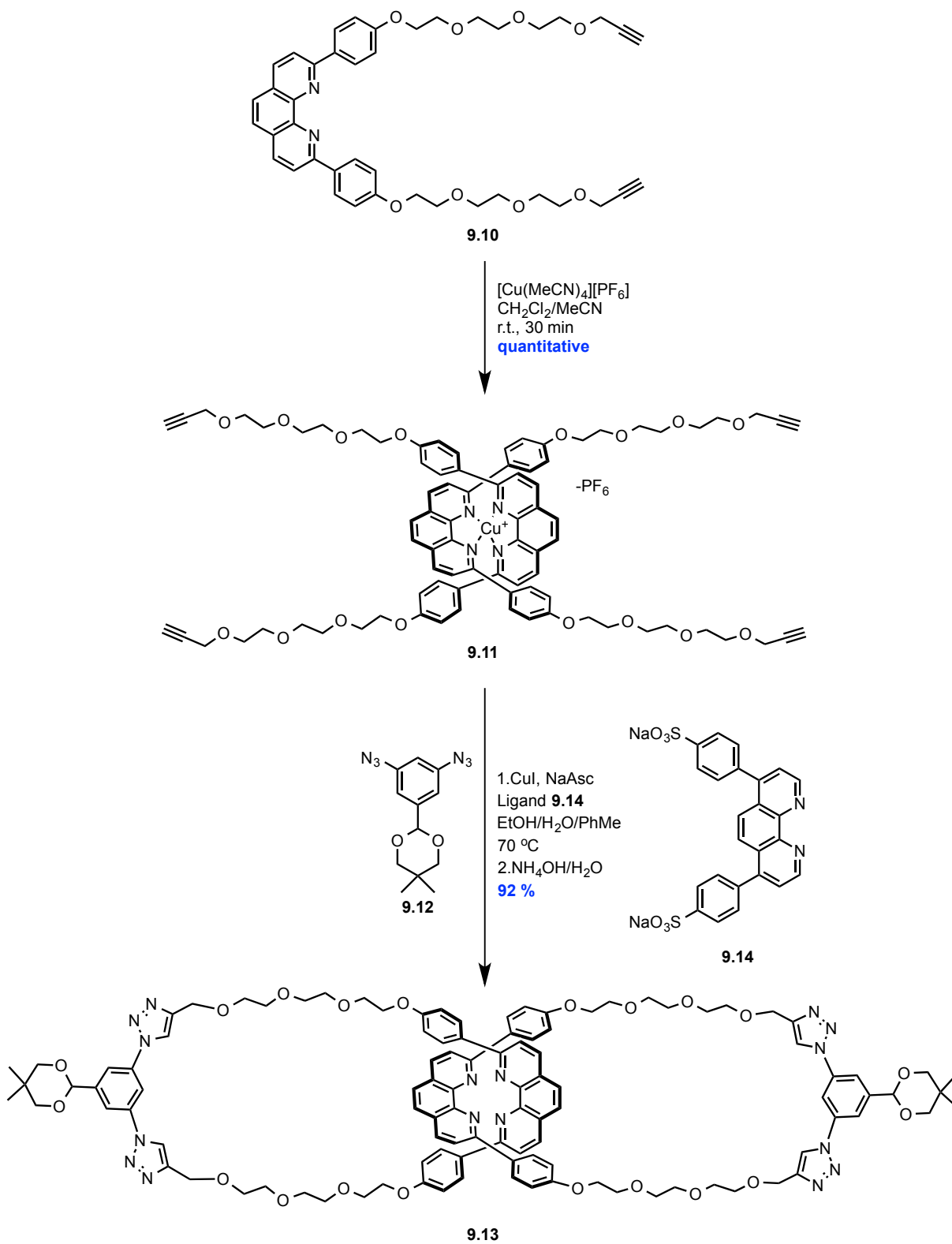


Figure 9.1 – a) Tripeptide **9.8** structure (blue) overlay with balhimycin (red), b) Tripeptide **9.9** structure (blue) overlay with balhimycin (red). (Reproduced with permission from ref 10. Copyright 2011 American Chemical Society.)

A second example of the utility of the AAC reaction in medicinal chemistry is exploring the triazole moiety as a mimic of the trans amide bond. Mindt and co-workers¹² demonstrated that a 1,4-triazole unit could be inserted into a series of biologically relevant peptides where the triazole unit increased the stability of the peptide as well as its tumor-targeting capacities.

In supramolecular chemistry, CuAAC has found myriad applications due to its functional group compatibility.^{6c} The formation of a triazole is often used as a tool for macrocyclization for the formation of rotaxanes and catenanes. For example, a copper(I)-template approach¹³ was used to synthesize catenane **9.13** in good yield.¹⁴ Macrocyclization of precursor **9.10** without the Cu(I)-template yields only oligomers (Scheme 9.3).

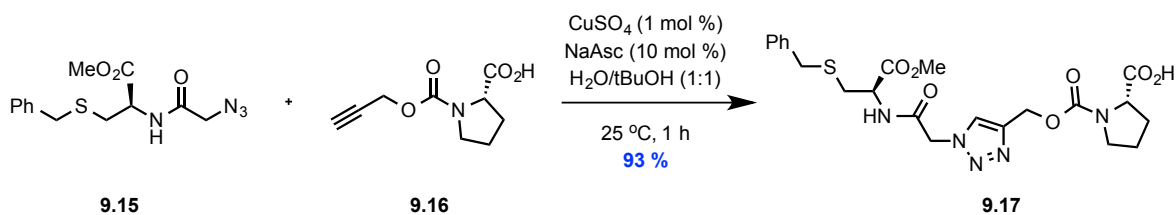


Scheme 9.3 – CuAAC macrocyclization using a template strategy.

9.3 – Mechanistic Aspects of the Copper-Catalyzed Azide-Alkyne Cycloaddition Reaction

9.3.1 – Importance of the Copper Source

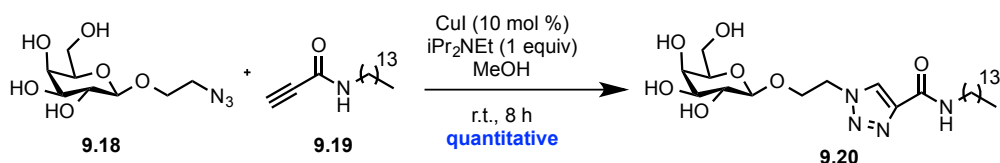
Only copper(I) salts are catalytically active in the CuAAC. Unfortunately, Cu(I) is not thermodynamically stable and prone to oxidation under atmospheric conditions.¹⁵ To maintain a source of Cu(I) in solution, the use of a stable Cu(II) salt and a reductant such as sodium ascorbate (NaAsc),^{5a} in large excess compared to the Cu(II), is often used. The strategy allows for *in situ* reduction of copper(II). Typical reaction conditions are shown in Scheme 9.4. The exclusion of oxygen is not needed under these conditions.



Scheme 9.4 – CuAAC promoted by *in situ* reduction of a Cu(II) salt.

When Cu(II) gets reduced *in situ*, the resulting catalytically active Cu(I) species rapidly forms the copper acetylide. Cu(I)-halide salts require at least an amine base and sometime high temperatures to form the copper-acetylide. The partial solubility of CuI in organic solvents such as THF or MeCN allowed for its use in anhydrous conditions.¹⁶ A range of Cu(I) salts (*e.g.* [Cu(CH₃CN)₄]PF₆) were introduced as catalysts for the CuAAC reaction due to their increased solubility in organic solvents. Importantly, Cu(I) salts can often be isolated in high purity, a desirable feature for sensitive chemistry such as bioconjugations or polymerization.¹⁷ Noteworthy, oxygen needs to be excluded from the reaction mixture when a Cu(I) source is

used. Typical reaction conditions using a Cu(I) source in combination with a ligand are shown in Scheme 8.5.¹⁸



Scheme 9.5 – CuAAC promoted by a Cu(I) salt and amine ligand.

The use of Cu(0) in the form of a powder or nanoparticles has also been reported.¹⁹ The addition of a Cu(II) salt is often needed in these conditions. Cu(0) can be used in aqueous media. It is assumed that Cu(I) is formed under the reaction conditions. Moreover, facile separation of the catalyst from the reaction mixture facilitates the product isolation step.

9.3.2 – Importance of Ligands

An efficient strategy used to promote CuAAC with Cu(I) salts is to employ ligand effects. Ligands can significantly improve the catalytic efficiency and the stability of the Cu(I) catalyst in the CuAAC reaction. During mechanistic investigations, it was found that the CuAAC reaction was autocatalytic, meaning that the formed triazole can act as a ligand for the Cu(I) metal and enhance the rate of the reaction. Fokin took advantage of the autocatalytic nature of the Click reaction and designed polytriazole ligands for copper.²⁰ In Fokin's study, TBTA **9.21** was found to be the most effective ligand (Figure 9.2). Water soluble ligand BTES **9.23** was later developed for bioconjugation chemistry.²¹ Another study showed that benzimidazole-type ligands could further improve the rate of the CuAAC.²² Ligand BimC₄A **9.24** is water soluble, and it was postulated that the pendant carboxylic acid chains of the ligand help in the proto-decupration step of the mechanism.

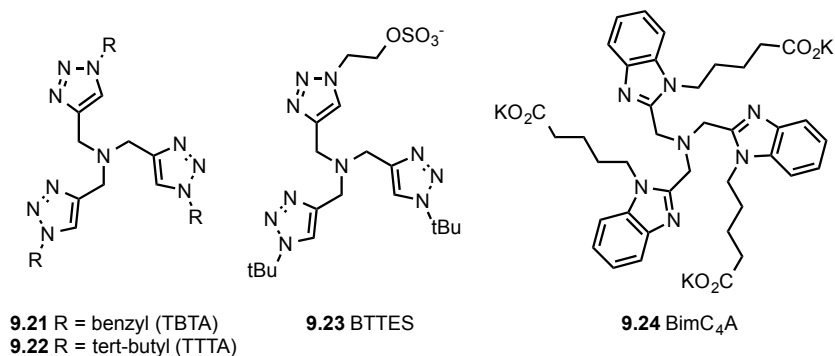
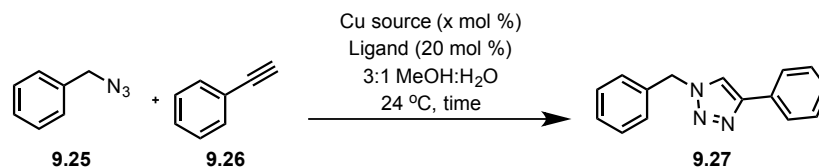


Figure 9.2 – Structure of ligands for CuAAC.

An extensive study of the ligand effects was conducted by Finn and co-workers²² The authors demonstrated the impact of the ligand for the rate of the reaction. The results are summarized in Table 9.1. Although TBTA **9.21** is known to be a good ligand to achieve efficient CuAAC, when its loading is decreased to 0.5 mol % in the presence of a Cu(I) source, the reaction only yields 47 % of the desired triazole. Due to its improved water solubility, BimC₄A **9.24** stays highly efficient even at 0.05 mol % in a 3:1 mixture of MeOH/H₂O. In comparison, simple amine ligands such as iPr₂NEt in the presence of CuI only affords 29 % of triazole **9.27** after 72 h. The role of the polytriazole ligands in improving the catalytic efficiency of the reaction will be discussed in the following section (Figure 9.3).

Table 9.1 – Comparison of ligand effects in CuAAC



Entry	Ligand (mol %)	Cu(I) source (mol %)	Time (h)	Yield (%)
1	9.21 (0.5)	CuSO ₄ (0.5), NaAsc (40 equiv)	4.5	47
2	9.24 (0.5)	CuSO ₄ (0.5), NaAsc (40 equiv)	0.2	100
3	9.24 (0.05)	CuSO ₄ (0.05), NaAsc (40 equiv)	5	98
4*	iPr ₂ NEt (5)	CuI (0.5)	72	29

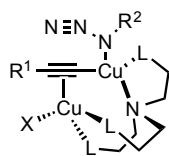
*Reaction in absolute MeOH

Although it has been demonstrated on several occasions that the CuAAC is biocompatible,²³ the rate of the reaction is still slow when the reaction is run in dilute aqueous media. Hence, high catalyst loadings need to be used and although the CuAAC reaction can be successful, the living organism is usually killed in the process. To solve the issue, a copper-free variant that relies on ring strain to activate the alkyne, typically cyclooctyne-based, was developed.²⁴ Alternatively, water soluble ligand BTES **9.23** was designed for biocompatible conjugation chemistry.²¹ It was shown to increase the rate of the cycloaddition by a factor of 10 when compared to cyclooctyne-based copper-free click chemistry and survival of the organism was achieved. The discovery of BTES **9.23** allowed for *in vivo* imaging of zebrafish embryogenesis.²¹

9.3.3 – Proposed Catalytic Cycle

Insight into the mechanism of the CuAAC reaction is important for the continued evolution of “Click” chemistry. The mechanistic study was initially challenging because of the tendency of copper acetylides to form aggregates.²⁵ Moreover, the mixture of Cu(I) with various ligands and alkynes can lead to many equilibria that can be difficult to characterize. Fokin and co-workers studied the mechanism using isotopic labeling of copper.²⁶ When benzyl azide **9.25** was reacted in the presence of cuprated alkyne **9.28** (with the naturally occurring isotope distribution; 69 % ⁶³Cu and 31 % ⁶⁵Cu) in the presence of an isotopically enriched ⁶³Cu(I) catalyst, the cuprated triazole formed was isotopically enriched in ⁶³Cu (Scheme 8.6a). It was found that neither intermediate **9.28** or **9.29** exchanged their copper atom when given the possibility (Scheme 9.6b and c). Since it had been known that two copper atoms were implied in the mechanism, shuffling of isotopes was proposed to occur *via* intermediate **9.36** (Scheme 9.7).

The now accepted catalytic cycle begins by cupration of the alkyne **9.30** to yield intermediate **9.31**. Then, π -interaction with a second copper atom **9.32** and coordination of the azide **9.34** through the internal nitrogen gives rise to reactive intermediate **9.35**. Stepwise cycloaddition can then proceed to yield the cuprated triazole **9.37**, by passing through reactive intermediate **9.36**. Proto-decupration can then provide the desired product **9.38** and regenerate the copper catalyst **9.32**.

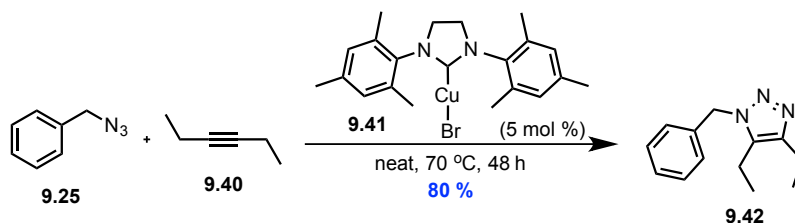


9.39

Figure 9.3 – Proposed di-copper species **9.39** that could be favored in the presence of polytriazole or benzimidazole ligands.

9.4 – Copper-Catalyzed Iodoalkyne-Azide Cycloaddition

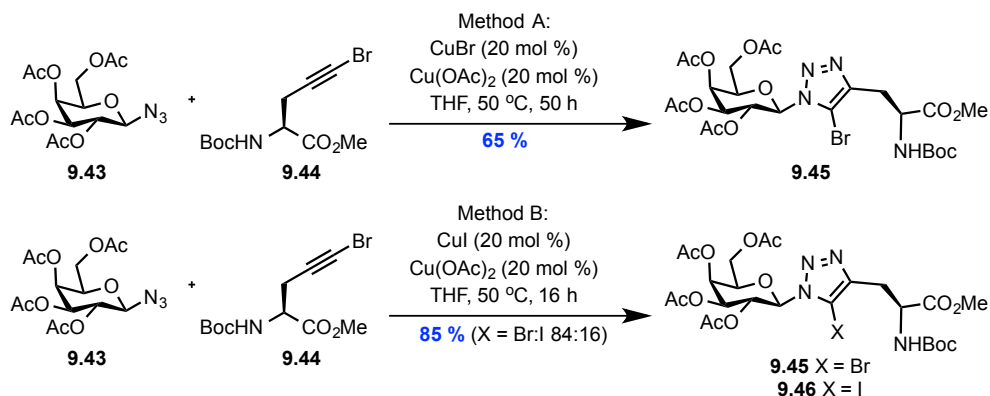
Apart from exceptions, copper-catalyzed AAC does not enable the synthesis of 1,4,5-trisubstituted triazoles using internal alkynes. Only two isolated examples of internal alkynes being used in the CuAAC have been reported and they both report solely the reaction between benzyl azide **9.25** and 3-hexyne **9.40**.²⁷ A Cu-N-heterocyclic carbene (NHC) complex has been shown to catalyze the aforementioned transformation to yield the corresponding 1,4,5-trisubstituted triazole **9.42** (Scheme 9.8).^{27a}



Scheme 9.8 – Rare example of CuAAC with an internal alkyne.

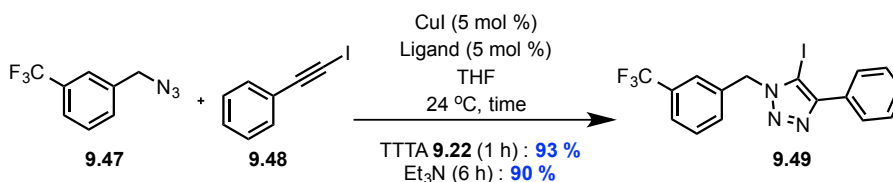
It was recently discovered that 1-haloalkynes are alternative substrates to terminal alkynes in the CuAAC. In 2005, the first report of a Cu(I) and Cu(II) co-catalyzed bromoalkyne-azide cycloaddition was reported.²⁸ Importantly, when CuI was used as the Cu(I)

source instead of CuBr the reaction rate was improved and 14 % of the iodotriazole **9.46** was observed as a side product (Scheme 9.9).



Scheme 9.9 – Copper-catalyzed cycloaddition of azides and 1-bromoalkynes

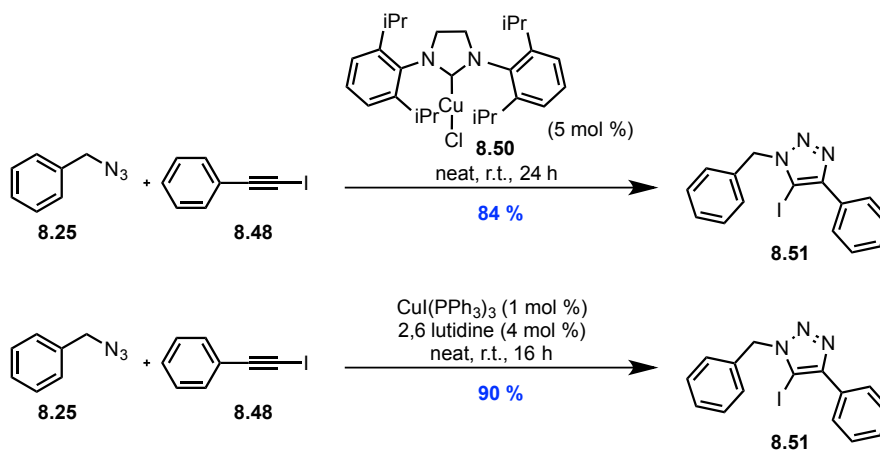
The initial report did not attract much attention until 2009 when Fokin reported 1-iodoalkynes as a viable alternative for the CuAAC reaction of internal alkynes (Scheme 9.10).²⁹ The reaction proceeded smoothly in a wide range of solvents and had an impressive functional group tolerance. Noteworthy, both TTTA **9.22** or Et₃N could be used as ligands for the Cu(I) source.



Scheme 9.10 – Copper-catalyzed cycloaddition of azide and 1-iodoalkynes.

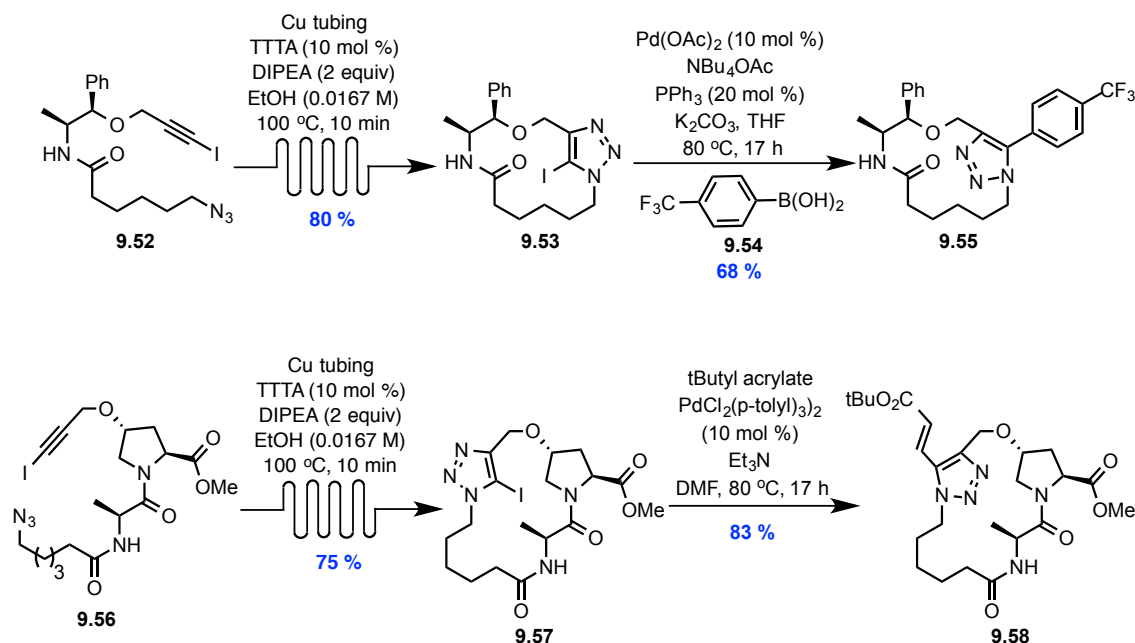
Cu-NHC and Cu-phosphine complexes are also catalytically active in the CuAAC to form 5-iodotriazoles (Scheme 9.11). In addition to the report of two new catalysts for the

CuAiAC, Diez-Gonzalez and co-workers studied the reaction mechanism by DFT (refer the Scheme 9.14).³⁰



Scheme 9.11 – Copper-NHC and copper-phosphine complex catalyzed cycloaddition of azide and 1-iodoalkynes.

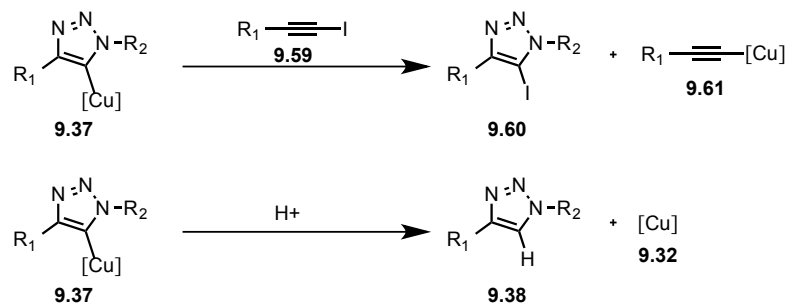
The CuAiAC reaction was later used by James in the synthesis of macrocyclic peptides in continuous flow (refer to Chapter 7, Scheme 7.3).^{11b} The resulting iodotriazole could also be readily functionalized using well established palladium cross-coupling chemistry such as the Suzuki and the Heck cross-coupling reactions (Scheme 9.12).^{11b,31}



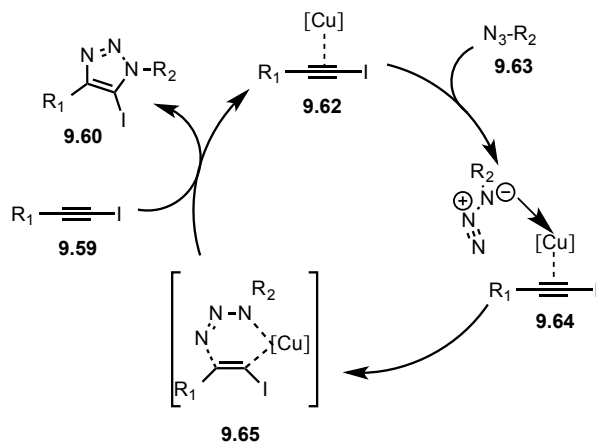
Scheme 9.12 – Synthesis and derivatization of the iodotriazole moiety .

9.4.1 – Proposed Catalytic Cycle

The postulated mechanism for the CuAiAC reaction differs from the one depicted in Scheme 9.6 for CuAAC. It was proposed that the copper catalyst does not insert in the carbon-iodide bond of the alkyne but rather interacts with the alkyne *via* π -interactions. The hypothesis is supported by the absence of prototriazole **9.38** in the reaction mixture. If cuprated triazole **9.37** was formed in the CuAiAC reaction, a mixture of iodo- and prototriazole would be expected since both paths shown in Scheme 9.13 would be possible to turn over the catalyst. In his seminal report, Fokin states that no prototriazole is observed and thus postulated a catalytic cycle where the copper only acts as a π -acid (Scheme 9.14).



Scheme 9.13 – Mechanistic postulation for CuAiAC



Scheme 9.14 – Proposed catalytic cycle for CuAiAC

9.4.2 – Application of Copper-Catalyzed Iodo-Alkyne-Azide Cycloaddition

An interesting application of the CuAiAC is the synthesis of antifungal small molecules. The corresponding triazole has been identified as a lead candidate for the inhibition of *Escherichia coli* PDHc-E1 inhibitory activity and antifungal activity but lacked selectivity toward its target.³² The addition of an iodine on the triazole allowed for increased enzyme-selectivity as well as a 6 fold increase in the potency (Figure 8.4).³² Iodotriazole **9.67** was readily synthesised using Fokin's CuI/Et₃N procedure.²⁹

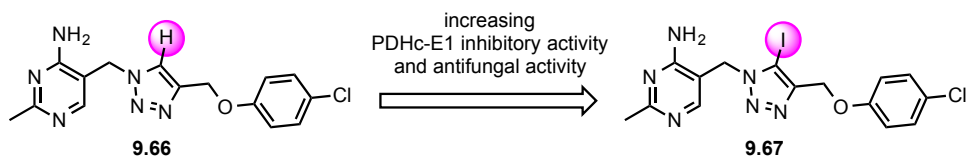


Figure 9.4 – Effect of the addition of an iodine on the triazole moiety of a *Escherichia coli* PDHc-E1 inhibitor and antifungal.

9.5 – Conclusion

The copper-catalyzed azide-alkyne cycloaddition reaction has already made a significant impact on the chemical society. It has been applied to key bond forming reaction in various context, including challenging macrocyclizations. The development of an efficient CuAAC macrocyclization at high concentration using the “phase separation” strategy would, amongst other applications, allow the efficient synthesis of various medicinally relevant compounds.

9.6 – Bibliography

- (1) Hein, J. E.; Fokin, V. V. *Chem. Soc. Rev.* **2010**, *39*, 1302-1315.
- (2) Kolb, H. C.; Finn, M. G.; Sharpless, K. B. *Angew. Chem. Int. Ed.* **2001**, *40*, 2004-2021.
- (3) Huisgen, R. *Angew. Chem. Int. Ed.* **1963**, *2*, 565-598.
- (4) Himo, F.; Lovell, T.; Hilgraf, R.; Rostovtsev, V. V.; Noodleman, L.; Sharpless, K. B.; Fokin, V. V. *J. Am. Chem. Soc.* **2005**, *127*, 210-216.
- (5) a) Rostovtsev, V. V.; Green, L. G.; Fokin, V. V.; Sharpless, K. B. *Angew. Chem. Int. Ed.* **2002**, *41*, 2596-2599; b) Tornøe, C. W.; Christensen, C.; Meldal, M. *J. Org. Chem.* **2002**, *67*, 3057-3064.
- (6) a) Tron, G. C.; Pirali, T.; Billington, R. A.; Canonico, P. L.; Sorba, G.; Genazzani, A. *A. Medicinal Research Reviews* **2008**, *28*, 278-308; b) Lutz, J.-F.; Zarafshani, Z. *Adv. Drug Del. Rev.* **2008**, *60*, 958-970; c) Moses, J. E.; Moorhouse, A. D. *Chem. Soc. Rev.* **2007**, *36*, 1249-1262; d) Bock, V. D.; Hiemstra, H.; van Maarseveen, J. H. *Eur. J. Org. Chem.* **2006**, *2006*, 51-68; e) Meldal, M.; Tornøe, C. W. *Chem. Rev.* **2008**, *108*, 2952-3015.
- (7) a) Zhang, L.; Chen, X.; Xue, P.; Sun, H. H. Y.; Williams, I. D.; Sharpless, K. B.; Fokin, V. V.; Jia, G. *J. Am. Chem. Soc.* **2005**, *127*, 15998-15999; b) Boren, B. C.; Narayan, S.; Rasmussen, L. K.; Zhang, L.; Zhao, H.; Lin, Z.; Jia, G.; Fokin, V. V. *J. Am. Chem. Soc.* **2008**, *130*, 8923-8930.
- (8) Rasolofonjatovo, E.; Theeramunkong, S.; Bouriaud, A.; Kolodych, S.; Chaumontet, M.; Taran, F. *Org. Lett.* **2013**, *15*, 4698-4701.
- (9) Chatterjee, S.; Vijayakumar, E. K. S.; Nadkarni, S. R.; Patel, M. V.; Blumbach, J.; Ganguli, B. N.; Fehlhaber, H. W.; Kogler, H.; Vertesy, L. *J. Org. Chem.* **1994**, *59*, 3480-3484.
- (10) Zhang, J.; Kemmink, J.; Rijkers, D. T. S.; Liskamp, R. M. J. *Org. Lett.* **2011**, *13*, 3438-3441.
- (11) a) Bogdan, A. R.; James, K. *Chem. Eur. J.* **2010**, *16*, 14506-14512; b) Bogdan, A. R.; James, K. *Org. Lett.* **2011**, *13*, 4060-4063; c) Bogdan, A. R.; Jerome, S. V.; Houk, K. N.; James, K. *J. Am. Chem. Soc.* **2011**, *134*, 2127-2138.
- (12) Valverde, I. E.; Bauman, A.; Kluba, C. A.; Vomstein, S.; Walter, M. A.; Mindt, T. L. *Angew. Chem. Int. Ed.* **2013**, *52*, 8957-8960.
- (13) Dietrich-Buchecker, C. O.; Sauvage, J. P. *Chem. Rev.* **1987**, *87*, 795-810.
- (14) Megiatto, J. D.; Schuster, D. I. *J. Am. Chem. Soc.* **2008**, *130*, 12872-12873.
- (15) Richardson, H. W. In *Ullmann's Encyclopedia of Industrial Chemistry*; Wiley-VCH Verlag GmbH & Co. KGaA: 2000.
- (16) a) Yoo, E. J.; Ahlquist, M.; Kim, S. H.; Bae, I.; Fokin, V. V.; Sharpless, K. B.; Chang, S. *Angew. Chem. Int. Ed.* **2007**, *46*, 1730-1733; b) Zhang, Z.; Fan, E. *Tetrahedron Lett.* **2006**, *47*, 665-669; c) Hotha, S.; Kashyap, S. *J. Org. Chem.* **2006**, *71*, 364-367.
- (17) Evans, R. A. *Aust. J. Chem.* **2007**, *60*, 384-395.
- (18) Fazio, F.; Bryan, M. C.; Blixt, O.; Paulson, J. C.; Wong, C.-H. *J. Am. Chem. Soc.* **2002**, *124*, 14397-14402.
- (19) Wan, Q.; Chen, J.; Chen, G.; Danishefsky, S. J. *J. Org. Chem.* **2006**, *71*, 8244-8249.
- (20) Chan, T. R.; Hilgraf, R.; Sharpless, K. B.; Fokin, V. V. *Org. Lett.* **2004**, *6*, 2853-2855.

- (21) Soriano del Amo, D.; Wang, W.; Jiang, H.; Besanceney, C.; Yan, A. C.; Levy, M.; Liu, Y.; Marlow, F. L.; Wu, P. *J. Am. Chem. Soc.* **2010**, *132*, 16893-16899.
- (22) a) Rodionov, V. O.; Presolski, S. I.; Díaz Díaz, D.; Fokin, V. V.; Finn, M. G. *J. Am. Chem. Soc.* **2007**, *129*, 12705-12712; b) Rodionov, V. O.; Presolski, S. I.; Gardinier, S.; Lim, Y.-H.; Finn, M. G. *J. Am. Chem. Soc.* **2007**, *129*, 12696-12704.
- (23) Thirumurugan, P.; Matosiuk, D.; Jozwiak, K. *Chem. Rev.* **2013**.
- (24) Jewett, J. C.; Bertozzi, C. R. *Chem. Soc. Rev.* **2010**, *39*, 1272-1279.
- (25) M. Mykhalichko, B.; N. Temkin, O.; G. Mys'kiv, M. *Russian Chemical Reviews* **2000**, *69*, 957-984.
- (26) Worrell, B. T.; Malik, J. A.; Fokin, V. V. *Science* **2013**, *340*, 457-460.
- (27) a) Díez-González, S.; Correa, A.; Cavallo, L.; Nolan, S. P. *Chem. Eur. J.* **2006**, *12*, 7558-7564; b) Candelon, N.; Lastecoueres, D.; Diallo, A. K.; Ruiz Aranzaes, J.; Astruc, D.; Vincent, J.-M. *Chem. Commun.* **2008**, 741-743.
- (28) Kuijpers, B. H. M. D., G. C. T.; Groothuys, S.; Quaedflieg, P. J. L. M.; Blaauw, R. H.; van Delft, F. L.; Rutjes, F. P. J. T. *Synlett* **2005**, 3059-3062.
- (29) Hein, J. E.; Tripp, J. C.; Krasnova, L. B.; Sharpless, K. B.; Fokin, V. V. *Angew. Chem. Int. Ed.* **2009**, *48*, 8018-8021.
- (30) Lal, S.; Rzepa, H. S.; Díez-González, S. *ACS Catal.* **2014**, *4*, 2274-2287.
- (31) Schulman, J. M.; Friedman, A. A.; Pantelev, J.; Lautens, M. *Chem. Commun.* **2012**, *48*, 55-57.
- (32) He, J.-B.; He, H.-F.; Zhao, L.-L.; Zhang, L.; You, G.-Y.; Feng, L.-L.; Wan, J.; He, H.-W. *Bioorg. Med. Chem.* **2015**, *23*, 1395-1401.

Chapter 10. Advanced Strategies for Efficient Macrocyclic Cu(I)-Catalyzed Cycloaddition of Azides

Anne-Catherine Bédard and Shawn K. Collins*

Département de Chimie, Center for Green Chemistry and Catalysis, Université de
Montréal, CP 6128 Station Downtown, Montréal, Québec H3C 3J7 Canada

Organic Letters **2014**, *16*, 5286-5289.

Contributions:

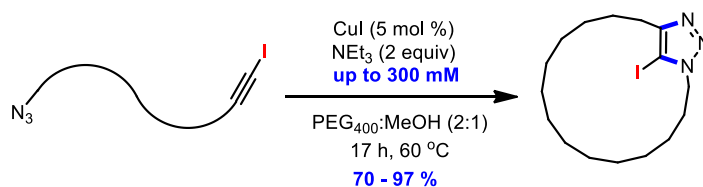
- Anne-Catherine Bédard participated in the design of the experiments, did all the experimental work and contributed to the writing of the manuscript.
- Shawn K. Collins participated in the design of the experiments and writing of the manuscript.

Reproduced by permission from the American Chemical Society

Permanent link to the article (DOI) : [10.1021/ol502415a](https://doi.org/10.1021/ol502415a)

10.1 – Abstract

An advanced strategy for efficient macrocyclic Cu(I)-catalyzed cycloaddition is described. The key features include: employing azide-iodoalkyne cycloadditions (CuAiAC), low catalyst loadings, relatively high concentrations (30 mM→300 mM) and application to continuous flow. The remarkably efficient new tool affords a variety of macrocyclic skeletons having either different alkyl, aryl or amino acid spacers in high yields, (70-97 %). The macrocyclic CuAiAC process affords macrocycles having an iodotriazole moiety that can be further functionalized using standard Pd-catalyzed cross-couplings.



CuAiAC Macrocyclization

- Wide functional group tolerance
 - Catalytic copper
- Simple experimental set-up/High concentrations
 - New sites for further functionalization
 - Applicable to Continuous Flow

10.2 – Introduction

The copper-catalyzed azide–alkyne cycloaddition reaction¹ (CuAAC or commonly referred to as a “Click” reaction) has become an important synthetic strategy for the preparation of macrocycles.^{2,3} Macrocyclic CuAAC processes have found application in medicinal chemistry for the preparation of macrocyclic carbohydrates,⁴ peptides⁵ and even rigidified drug-like macrocycles under continuous flow conditions.⁶ Macrocyclic CuAAC has also found applications in materials science in the development of novel receptors, electronic materials and molecular machines.⁷

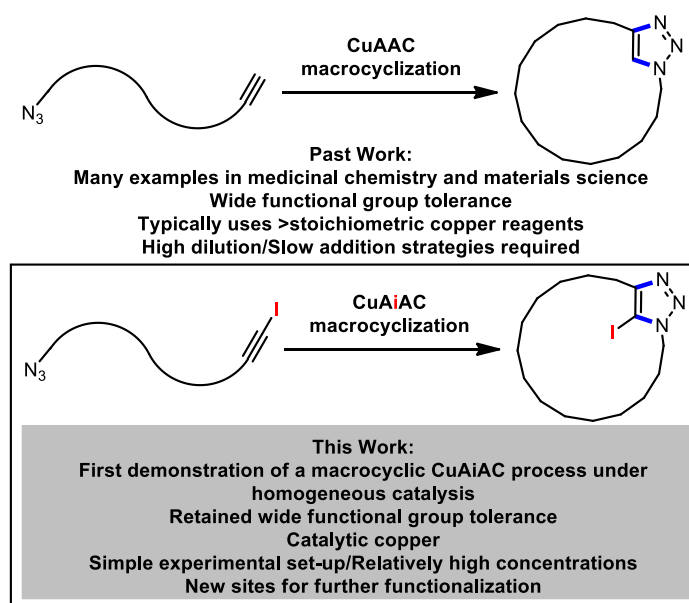


Figure 10.1 – Macrocyclic azide-alkyne cycloaddition processes.

Despite the wealth of applications, most macrocyclic CuAAC reactions still suffer from the slow rate of ring closing associated with conventional macrocyclization reactions (Figure 10.1). Consequently, long reaction times and high catalyst loadings (often super

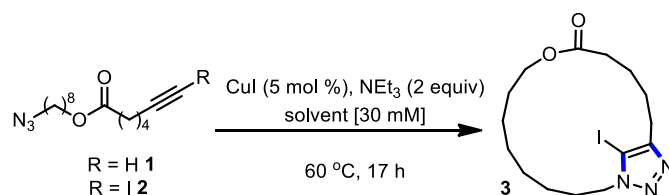
stoichiometric quantities of Cu) can be required in combination with the use of high dilution and/or slow addition techniques to slow competing oligomerization, are necessary to obtain satisfactory macrocyclization.⁸ The fact that these characteristic challenges remain prevalent in contemporary synthesis highlights the need for general reliable tools and/or strategies for efficient macrocyclization at high concentrations.⁹ In an effort to develop such a process based upon “Click” strategies, the copper-catalyzed azide-iodoalkyne cycloaddition (CuAiAC) was identified as an ideal candidate for exploration as a macrocyclization technique. The CuAiAC process was recently reported as an efficient “Click” process, with several advantages over its CuAAC analog: 1) the iodoalkyne coupling partners are stable and readily accessible internal acetylenes¹⁰ that exhibit reactivity typically greater than terminal alkynes in the cycloaddition process,^{11,12} and 2) the formation of the product iodotriazoles also provides a convenient handle for further functionalization¹³ and possibilities for diversity-oriented synthesis.¹⁴ Despite the advantages, the CuAiAC reaction remains poorly explored (Figure 10.1) and only a single report of a macrocyclic variant employing a copper tubing reactor under continuous flow conditions has been reported.¹⁵ Herein we report on an improved macrocyclic “Click” process through the development of an efficient macrocyclic Cu(I)-catalyzed azide-iodoalkyne cycloaddition process that can be performed at high concentrations using a phase separation strategy.

10.3 – Results and Discussion

The development of a CuAiAC macrocyclization protocol that could be performed at high concentrations began with the design of an appropriate model substrate. An ideal acyclic precursor would be devoid of any structural motifs (heteroatoms, aryl groups) that could

conformationally bias the molecule towards macrocyclization. Although the ring-closing of such a precursor would be challenging, successful macrocyclization could be attributed solely to control of dilution effects.

Table 10.1 – Optimization of Macrocylic CuAiAC using a Phase Separation Strategy.



entry	solvent	yield 3 (%) ^a	recovered 2 (%) ^a
1	MeOH	23	poly
2	PEG ₄₀₀	-	99 ^b
3	PEG ₄₀₀ :MeOH 1:9	29	-
4	PEG ₄₀₀ :MeOH 1:2	60	-
5	PEG ₄₀₀ :MeOH 1:1	93	-
6	PEG ₄₀₀ :MeOH 2:1	97	-
7	PEG ₄₀₀ :MeOH 4:1	40	- ^b
8	PEG ₄₀₀ :MeOH 9:1	-	99 ^b

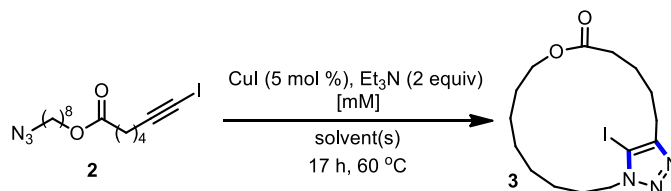
^a Yields following chromatography. ^b Product recovered was azide-alkyne **1**.
No iodinated uncyclized products were observed

Consequently, the azide-iodoalkyne **2** was selected for evaluation under phase separation conditions. The phase separation strategy has been previously reported to control dilution effects in macrocyclization reactions through the use of poly(ethylene glycol) (PEG) co-solvents.¹⁶ Reaction media consisting of high ratios of PEG₄₀₀:MeOH formed aggregated mixtures, in which lipophilic PEG aggregates preferentially solubilize organic substrates. Slow

diffusion out of a PEG aggregate into the MeOH co-solvent and subsequent cyclization is believed to mimic slow addition conditions, allowing for macrocyclization processes to be conducted at much higher concentrations while affording higher yields. Consequently, the macrocyclization of azide-iodoalkyne **2** was explored using catalytic systems previously developed for either CuAiAC intermolecular cycloaddition or CuAAC reactions in aqueous media. Initial investigations targeted a concentration of 30 mM using 1:1 mixtures of PEG₄₀₀:MeOH. First, catalyst systems using tridentate ligands were investigated, but both the CuSO₄·5H₂O/(BimC₄A)₃/NaAsc¹⁷ and CuSO₄·5H₂O/TBTA¹⁸/NaAsc conditions failed to afford any of the desired 17-membered macrocycle **3** and none of the azide-iodoalkyne **2** was recovered.¹⁹ When a catalyst system of CuI/NEt₃, previously exploited in intermolecular CuAiAC reactions,^{17,18} was evaluated in a PEG₄₀₀:MeOH 1:1 solvent system, a 93 % yield of the desired iodo-triazole macrocycle **3** was isolated (Table 10.1). The best yield (97 % of **3**) was obtained at a PEG₄₀₀:MeOH 2:1 ratio.²⁰ Control reactions in the individual reaction solvents were examined. When azide-iodoalkyne **2** was treated with CuI/NEt₃ in MeOH, a 23 % yield of macrocycle **3** was observed and extensive polymerization of the azide-iodoalkyne could be observed. When macrocyclization was attempted in PEG₄₀₀:MeOH 9:1 or just PEG₄₀₀, the de-iodinated azide-alkyne **1** was isolated quantitatively.²¹ The isolation of uncyclized azide-alkyne **1** at high PEG₄₀₀:MeOH ratios suggests that the reactivity of the catalyst system towards triazole formation was inhibited by the increasing concentrations of PEG₄₀₀, as is consistent with other reports of inhibition of transition metal catalysts by PEG solvent.^{14b}

To demonstrate the ability of the PEG₄₀₀:MeOH solvent system to control dilution effects, the macrocyclization of azide-iodoalkyne **2** was first investigated at high dilution using the optimized catalyst system in MeOH (Table 10.2, entries 1→5).

Table 10.2 – Concentration Effects of Macrocylic CuAiAC Using Both Traditional High Dilution and Phase Separation Strategies.



entry	solvent, concentration	yield 3 (%) ^a	yield 2 (%) ^a
1	MeOH, [0.2 mM]	-	99
2	MeOH, [0.2 mM] ^b	43	22
3	MeOH, [1 mM]	-	99
4	MeOH, [1 mM] ^c	56 ^d	-
5	MeOH, [2 mM]	-	99
6	MeOH, [10 mM]	15 ^d	15
7	MeOH, [30 mM]	23 ^d	-
8	PEG ₄₀₀ :MeOH 2:1, [30 mM]	97	-
9	PEG ₄₀₀ :MeOH 2:1, [100 mM]	76	-
10	PEG ₄₀₀ :MeOH 2:1, [300 mM]	58	-

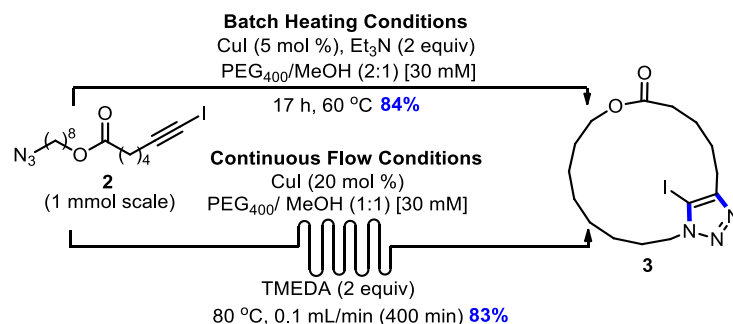
^a Yields following chromatography. ^b Using CuI (20 mol %) and NEt₃ (8 equiv), 70 °C, 3 d. ^c Using CuI (2 equiv) and NEt₃ (80 equiv). ^d Formation of insoluble polymeric materials observed.

When the macrocyclization (**2**→**3**) was conducted at high dilution (0.2, 1 or 2 mM), little reaction was observed and the azide-iodoalkyne **2** was recovered quantitatively. In an effort to promote macrocyclization, a high dilution macrocyclization (0.2 mM) with higher catalyst loadings (20 mol %) and longer reaction times (3 d) was performed and afforded low yields and unconsumed azide-iodoalkyne (43 % of **3**, 22 % recovered **2**). Increased catalyst

loadings (CuI (2 equiv.)) could also coerce macrocyclization of **2** at 1 mM affording a 56 % yield of triazole **3** and oligomerizing the remaining mass balance. It was hypothesized that increasing the concentration would help promote conversion, so the macrocyclization (**2**→**3**) was examined at higher concentrations in MeOH, but with low catalyst loading (5 mol %) (entries 6 and 7). Macrocyclization at 10 mM afforded a 15 % yield of **3** and 15 % of azide-iodoalkyne **2**. At 30 mM, only a 23 % yield of macrocycle **3** and extensive polymerization of the **2** was observed. In contrast, at the identical concentration but using the PEG₄₀₀: MeOH (2:1) mixture, a 97 % of macrocycle **3** was obtained. When employing the PEG₄₀₀:MeOH mixtures, the concentration could be further increased to 100 mM and 300 mM and good yields of macrocycle **3** were still obtained (a 58 % yield of **3** at 300 mM). These results are in stark contrast to those obtained using traditional high dilution/slow addition techniques. Indeed, phase separation afforded superior yields at higher concentrations (1500X greater) with lower catalyst loadings (5-40X lower). The above results demonstrate that the phase separation allows for both greater concentrations and, consequently, lower catalyst loadings to be employed in macrocyclization reactions.

To demonstrate that the method can be used to prepare meaningful quantities of desired macrocycles, a gram-scale macrocyclization was performed using the optimized conditions with azide-iodoalkyne **2**. Upon scale-up to 1 mmol, the desired triazole macrocycle **3** was obtained in 84 % yield. To develop a more efficient demonstration of the ability to scale-up, the “phase separation” strategy was adapted to a continuous flow protocol. Less than a handful of macrocyclizations under continuous flow conditions have been reported.^{6,15,16c} Following optimization of temperature and flow rate, it was found that the azide-iodoalkyne **2** could be cyclized in good yield (up to 83 %), in shorter reaction time than in batch (17 h vs.

~6.6 h (400 min)). Importantly, the slightly higher temperatures involved required a change in the catalyst system. The use of a bidentate TMEDA ligand, in place of NEt₃, resulted in a reaction mixture which remained homogeneous throughout the reaction time.



Scheme 10.1 – Macrocyclic CuAiAC under continuous flow conditions.

With an optimized catalyst/solvent system in hand, a substrate scope for the macrocyclization was performed (Table 10.3).²² The first acyclic precursors selected were purposely designed with flexible alkyl chains to evaluate the efficiency of the methodology with compounds having little structural or conformational bias towards cyclization. The 17-membered macrolactone **3** was obtained in 95 % isolated yield and the analogous 17-membered macrocycle **4** having different alkyl spacers was also obtained in excellent yield (93 %) when subjected the identical reaction conditions. In an attempt to prepare more challenging smaller ring sizes, the macrocyclic CuAiAC reaction to form the 12-membered ring **5b** was performed (entry 3). An excellent yield of 78 % was observed, however the macrocyclization had afforded a 1:1 ratio of two products: the desired 12-membered ring **5b** and the 11-membered ring **5a** which results from regioisomeric cycloaddition across the iodoalkyne.²³ Larger macrocycles such as the 21-membered **7** and the 25-membered **8** could also be prepared in good yields (87 and 85 % respectively, entries 5 and 6). The 16-membered

macrolactone **6** obtained from reaction with an aryl alkyne was isolated in 70 % yield (entry 4). Once again, larger macrocycles bearing an aryl spacer, such as **9**, could be isolated in 75 % using the optimized reaction conditions. The macrocyclic CuAiAC reaction was also applied to the cyclization of substrates having more complex structures including the presence of heteroatoms and chiral centers (Table 10.3, entries 8→12). Macrocycles having an embedded phenylalanine residue with different alkyl spacers were prepared in good yields: the 20-membered iodo-triazole macrocycle **10** was isolated in 91 % yield. The size of the macrocycle could be expanded while maintaining good yields as the slightly larger 24-membered analog **11** was obtained in 83 % yield. Also, the position of the azide and alkyne functionalities in the products could easily be reversed, as the 21-membered macrocycle **12** was isolated in 84 % yield. Other amino acids could be incorporated as the 24-membered isoleucine-derived macrocycle **13** was also cyclized at high concentration in high yield (86 %).

Table 10.3 – Substrate Scope of Macrocyclic CuAiAC Using a Phase Separation Strategy.^a

entry	product	yield (%)	entry	product	yield (%)
1		95	2		93
3		78 (1:1)	4		70
5		87	6		85
7		75	8		91
9		83	10		84
11		86	12		83

^a Yield following chromatography. Ring size indicated in red.

Again, to demonstrate the efficiency of the protocol on complex substrates, the synthesis of the peptidic macrocycle **17**¹⁵ was performed. Macrocycle **17** had already been prepared by Bogdan and James during the synthesis of a library of peptidic macrocycles for drug discovery efforts in good yield (75 %, [17 mM]). Bogdan and James also demonstrated further functionalization of the iodotriazole motif via Pd-catalysis. Under the optimized “phase separation” conditions, macrocycle **17** was obtained in 83 % yield ([30 mM]).

10.4 – Conclusion

In summary, a protocol for a macrocyclic Cu(I)-catalyzed azide-iodoalkyne cycloaddition (CuAiAC) is described. The CuAiAC is a remarkably efficient new tool for macrocyclization, affording high yields, at low catalyst loadings, at relatively high concentrations (30 mM→300 mM) using a phase separation strategy. A variety of macrocyclic skeletons could be prepared having either different alkyl, aryl or amino acid building blocks. The macrocyclic CuAiAC is particularly attractive for industrial purposes as: 1) the process affords macrocycles having an iodotriazole moiety that is a convenient handle for use in diversity-oriented syntheses of macrocyclic libraries,¹⁴ and 2) the ability to exploit continuous flow conditions allows for facile scale-up using non-volatile/non-toxic PEG in place of large volumes of organic solvents. The macrocyclic CuAiAC reactions presented herein further suggest that phase separation is a viable technique for improving or developing novel macrocyclization processes. The effectiveness of the CuAiAC macrocyclization should be highly useful, given the prevalence of “click”-type strategies in fields such as material science and chemical biology.

Acknowledgement. The authors acknowledge the Natural Sciences and Engineering Research Council of Canada (NSERC), Université de Montreal and the Centre for Green Chemistry and Catalysis for generous funding. A.-C. B. thanks NSERC for a Vanier graduate scholarship.

Supporting Information Available: Experimental procedures and characterization data for all new compounds. This material is available free of charge via the Internet at <http://pubs.acs.org>.

10.5 – Bibliography

- (1) (a) Rostovtsev, V. V.; Green, L. G.; Fokin, V. V.; Sharpless, K. B. *Angew. Chem., Int. Ed.* **2002**, *41*, 2596. (b) Tornøe, C. W.; Christensen, C.; Meldal, M. *J. Org. Chem.* **2002**, *67*, 3057.
- (2) (a) Weber, E.; Vögtle, F.; Burrell, A. K. *Macrocycles*; Springer-Verlag: Berlin, Germany, 1992. (b) Pasini, D. *Molecules* **2013**, 9512. (c) Caricatoa, M.; Olmoa, A.; Gargiullib, C.; Gattusob, G.; Pasinia, D. *Tetrahedron* **2012**, *68*, 7861. (d) Li, Y.; Flood, A. H. *Angew. Chem., Int. Ed.* **2008**, *47*, 2649.
- (3) (a) Wu, P.; Fokin, V. V. *Aldrichimica Acta* **2007**, *40*, 7. (b) Meldal, M.; Tornøe, C. W. *Chem. Rev.* **2008**, *108*, 2952.
- (4) (a) Jogula, S.; Dasari, B.; Khatravath, M.; Chandrasekar, G.; Kitambi, S. S.; Arya, P. *Eur. J. Org. Chem.* **2013**, 5036. (b) Potopnyk, M. A.; Jarosz, S. in *Click Chemistry in Glycoscience* (Eds.: Witezak, Z. J.; Bielski, R.) Wiley, 2013, 235.
- (5) (a) Kolb, H. C.; Sharpless, K. B. *Drug Discovery Today* **2003**, *8*, 1128. (b) Whiting, M.; Tripp, J. C.; Lin, Y. C.; Lindstrom, W.; Olson, A. J.; Elder, J. H.; Sharpless, K. B.; Fokin, V. V. *J. Med. Chem.* **2006**, *49*, 7697. (c) Wilkinson, B. L.; Bornaghi, L. F.; Houston, T. A.; Poulsen, S.-A. in *Drug Design Research Perspectives* (Ed.: Kaplan, S. P.), Nova, Hauppauge, 2007, 57. (d) Wang, Q.; Chan, T. R.; Hilgraf, R.; Fokin, V. V.; Sharpless, K. B.; Finn, M. G. *J. Am. Chem. Soc.* **2003**, *125*, 3192.
- (6) (a) Bogdan, a. R.; Jerome, S. V.; Houk, K. N.; James, K. *J. Am. Chem. Soc.* **2012**, *134*, 2127. (b) Bogdan, A. R.; James, K. *Chem.–Eur. J.* **2010**, *16*, 14506.
- (7) (a) Hawker, C. J.; Fokin, V. V.; Finn, M. G.; Sharpless, K. B. *Aust. J. Chem.* **2007**, *60*, 381. (b) Mulla, K.; Shaik, H.; Thompson, D. W.; Zhao, Y. *Org. Lett.* **2013**, *15*, 4532. (c) Hui, P.; Chandrasekar, R. *Adv. Mater.* **2013**, *25*, 2963. (d) Busseron, E.; Coutrot, F. *J. Org. Chem.* **2013**, *78*, 4099.
- (8) Chouhan, G.; James, K. *Org. Lett.* **2013**, *15*, 1206.
- (9) For some rare specific examples of macrocyclization at high concentrations, see (a) Collins, J. C.; Farley, K. A.; Limberakis, C.; Liras, S.; Price, D.; James, K. *J. Org. Chem.* **2012**, *77*, 11079. (b) Wei, X.; Shu, C.; Haddad, N.; Zeng, X.; Patel, N. D.; Tan, Z.; Liu, J.; Lee, H.; Shen, S.; Campbell, S.; Varsolona, R. J.; Busacca, C. A.; Hossain, A.; Yee, N. K.; Senanayake, C. H. *Org. Lett.* **2013**, *15*, 1016. (c) Trost, B. M.; Warner, R. W. *J. Am. Chem. Soc.* **1982**, *104*, 6112.
- (10) Ru-based catalysts can promote Click cycloaddition of internal alkynes, see: (a) Zhang, L.; Chen, X.; Xue, P.; Sun, H. H. Y.; Williams, I. D.; Sharpless, K. B.; Fokin, V. V.; Jia, G. *J. Am. Chem. Soc.* **2005**, *127*, 15998. (b) Boren, B. C.; Narayan, S.; Rasmussen, L. K.; Zhang, L.; Zhao, H.; Lin, Z.; Jia, G.; Fokin, V. V. *J. Am. Chem. Soc.* **2008**, *130*, 8923.
- (11) (a) Hein, J. E.; Tripp, J. C.; Krasnova, L. B.; Sharpless, K. B.; Fokin, V. V. *Angew. Chem., Int. Ed.* 2009, *48*, 8018. (b) For an evaluation of other reactive alkynes see: Kislukhin, A. A.; Hong, V. P.; Breitenkamp, K. E.; Finn, M. G. *Bioconjugate Chem.* **2013**, *24*, 684. For alternative uses of iodo-Click reactions in medicine see (c) Wang, C.; Yin, J.; Zhou, W.; Zhang, L.; Zhou, Z. *J. South. Med. Univ.* **2013**, *33*, 779.

- (12) Bromoalkynes require high catalyst loadings, elevated temperatures and long reaction times, see: Kuijpers, B. H. M.; Dijkmans, G. C. T.; Groothuys, S.; Quaedflieg, P. J. L. M.; Blaauw, R. H.; van Delft, F. L.; Rutjes, F. P. J. T. *Synlett* **2005**, 3059.
- (13) (a) Schulman, J. M.; Friedman, A. A.; Panteleev, J.; Lautens, M. *Chem. Commun.* **2012**, 48, 55. (b) Deng, J.; Wu, Y.-M.; Chen, Q.-Y. *Synthesis* **2005**, 16, 2730. (c) Worrell, B. T.; Hein, J. E.; Fokin, V. V. *Angew. Chem., Int. Ed.* **2012**, 51, 11791
- (14) (a) Henning S. G. Beckmann, H. S. G.; Nie1, F.; Hagerman, C. E.; Johansson, H.; Tan, Y. S.; Wilcke, D.; Spring, D. R. *Nature Chem.*, **2013**, 5, 861. (b) Bauer, R. A.; Wenderski, T. A.; Tan, D. S. *Nature Chem. Biol.* **2013**, 9, 21. (c) Kopp, F.; Stratton, C. F.; Akella, L. B.; Tan, D. S. *Nature Chem. Biol.* **2012**, 8, 358.
- (15) Bogdan, A. R.; James, K. *Org. Lett.* **2011**, 13, 4060.
- (16) (a) Bédard, A.-C.; Collins, S. K. *J. Am. Chem. Soc.* **2011**, 133, 19976. (b) Bédard, A.-C.; Collins, S. K. *ACS Catal.* **2013**, 3, 773. (c) Bédard, A.-C.; Régnier, S.; Collins, S. K. *Green Chem.* **2013**, 15, 1962.
- (17) (a) Rodionov, V. O.; Presolski, S. I.; Gardinier, S.; Lim Y.-H.; Finn, M. G. *J. Am. Chem. Soc.* **2013**, 135, 1626. (b) Presolski, S. I.; Hong, V.; Cho S.-H.; Finn, M. G. *J. Am. Chem. Soc.* **2010**, 132, 14570.
- (18) Chouhan G.; James, K. *Org. Lett.* **2011**, 13, 2754. Also see ref 6.
- (19) See Supporting Information for a full table of optimization for the macrocyclization. The TBTA and (BimC4A)₃ ligands were originally designed to promote triazole formation from terminal alkynes. See ref 17.
- (20) Critical aggregation concentration (CAC) = 28 % PEG₄₀₀:MeOH. The surface tension measurements can be used as a predictive tool to identify ratios of PEG:solvent that will be optimal for controlling dilution effects. For a graphic displaying the surface tension of the PEG₄₀₀:MeOH mixtures and yields of the macrocyclization, see the Supporting Information. For more information on the predictive use of the surface tension diagrams, see: Bédard, A.-C.; Collins, S. K. *Chem. Eur. J.* **2012**, 19, 2108.
- (21) The mechanism for the formation of the de-iodinated product is not understood at this time.
- (22) Typically, macrocyclization reactions can be run at catalyst loadings of 5 mol %. In several cases, small amounts of unreacted starting material were difficult to separate from the desired macrocycle by simple silica gel chromatography. In these cases, the catalyst loading was increased to help promote complete conversion and facilitate purification.
- (23) The lack of regioisomeric control in forming **11** and **12** is not understood at the current time. Changes in regiocontrol were not observed in strained macrocycles formed via CuAAC (see ref 6). It is possible that the lack of a Cu-acetylide intermediate may allow for changes in regiocontrol in macrocyclic CuAiAC reactions.

Chapter 11: Efficient Continuous Flow Synthesis of Macrocyclic Triazoles

Anne-Catherine Bédard, Jeffrey Santandrea and Shawn K. Collins*

Département de Chimie, Center for Green Chemistry and Catalysis, Université de
Montréal, CP 6128 Station Downtown, Montréal, Québec H3C 3J7 Canada

Journal of Flow Chemistry **2015**, Ahead of print.

Contributions:

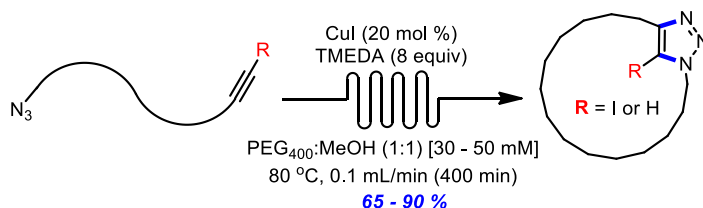
- Anne-Catherine Bédard participated in the design of the experiments, experimental work and contributed to the writing of the manuscript.
- Jeffrey Santandrea participated in the design of the experiments, the synthesis of substrates (cyclization precursor) and contributed to the writing of the manuscript.
- Shawn K. Collins participated in the design of the experiments and writing of the manuscript.

Reproduce with permission from Akadémiai Kiadó

Permanent link to the article : [10.1556/JFC-D-14-00042](https://doi.org/10.1556/JFC-D-14-00042)

11.1 – Abstract

The continuous flow synthesis of a series of 11- to 26-membered macrocycles via copper-catalyzed azide–alkyne cycloaddition is reported. The approach employs homogeneous catalysis to promote formation of triazole-containing macrocycles in good to excellent yields (65-90 %) at relatively high concentration (30-50 mM) using a phase separation strategy.



11.2 – Introduction

Macrocycles have become pharmaceutically relevant targets for drug design.¹ Despite the industrial interest, few macrocyclization reactions have been adapted to continuous flow syntheses.^{2,3} Batch macrocyclization reactions almost always require large catalyst loadings, large dilution factors and are plagued by possible precipitation of unwanted oligomers. These characteristics make the transposition of macrocyclization from batch to continuous flow challenging. Recently, James and co-workers reported the first continuous flow synthesis of macrocycles via alkyne–azide cycloaddition (CuAAC) or copper-catalyzed azide-iodoalkyne cyclo-addition (CuAiAC) chemistry.³ Their protocols employed a heterogeneous copper tubing reactor to efficiently synthesize a library of drug-like macrocycles.

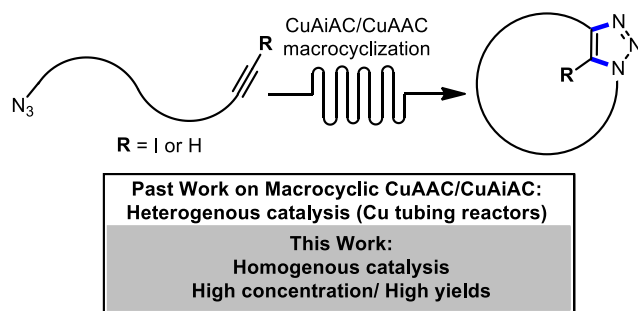


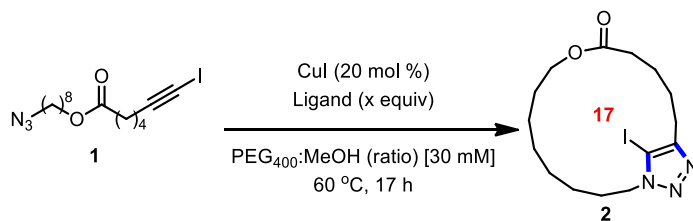
Figure 11.1 – Macrocyclic azide-alkyne cycloaddition processes in continuous flow.

Our group recently reported that a homogeneous catalysis approach could be adapted to continuous flow and allow macrocyclization *via* Glaser-Hay coupling using a stainless steel reactor. The reactions exploited a “phase separation” strategy, in which aggregated solvent mixtures employing poly(ethylene glycol) (PEG) co-solvents allowed for macrocyclization at relatively high concentrations (30 mM) and low catalyst loadings.⁴ Given the interest in “Click”-type processes for the synthesis of various macrocycles,⁵ including macrocyclic carbohydrates⁶ and peptides,⁷ our group also recently reported the application of the “phase separation” strategy to macrocyclic CuAiAC⁸ processes in batch.⁹ The resulting iodotriazole-containing macrocycles provide a convenient handle for further derivatization¹⁰ and opportunities for diversity-oriented synthesis.¹¹ Our report provided preliminary data suggesting the transposition of the macrocyclic CuAiAC process under “phase separation” conditions would be possible. Herein, we report a full account of the macrocyclic CuAiAC reactions in continuous flow at relatively high concentrations made possible via the “phase separation” strategy and disclose an extension of the substrate scope to CuAAC processes.

11.3 – Results and Discussion

The development of a CuAiAC macrocyclization using “phase separation” in continuous flow began with transposing the batch conditions.⁸ Preliminary studies explored the cyclization of ester **1**, an unconformationally biased model, at higher temperatures with a variety of ligands in batch to afford the 17-membered macrocycle **2** (Table 11.1). The batch macrocyclization conditions utilized CuI (20 mol %), NEt₃ (8 equiv) in PEG₄₀₀:MeOH (2:1) at a reaction concentration of 30 mM. While these conditions provided an excellent yield of macrocycle **2**, the reaction mixture became increasingly heterogeneous as the reaction progressed. As we had previously observed better homogeneity when using bidentate ligands in Cu-catalyzed macrocyclization reactions, we investigated TMEDA as a ligand alternative.¹² Although the resulting reaction mixture remained homogeneous, we observed no conversion of **1** to **2** (entry 2). Consequently, the ligand loading as well as the ratio of PEG₄₀₀:MeOH were decreased. When CuI (20 mol %), ligand (2 equiv.) and a PEG₄₀₀:MeOH (2:1) solvent ratio was used, a 50 % yield of **2** was observed. Other bidentate ligands such as 2,2'-bipyridine and 1,10-phenanthroline did not afford any desired product, while other alkyl bidentate ligands such as ethylenediamine and DMEDA provided low yields of **2**, but heterogeneous reaction mixtures. Given that TMEDA afforded a highly homogeneous reaction mixture and the highest yield (50 %) out of the ligands surveyed, it was chosen for optimization under continuous flow conditions.

Table 11.1 – Optimization of Macrocyclic CuAiAC using a Phase Separation Strategy in Batch.



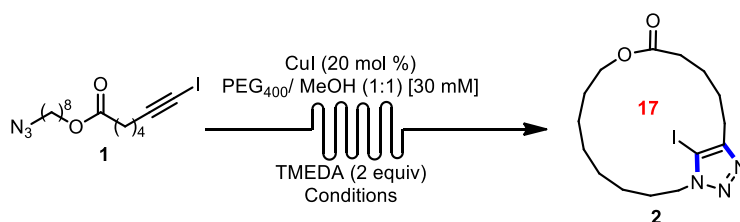
entry	ligand	equiv	solvent ratio	yield 2 (%) ^a	recovered 1 (%) ^a	homogeneity ^b
1	triethylamine	8	2:1	95	-	het
2	TMEDA	8	2:1	-	99	homo
3	TMEDA	2	2:1	33	67	homo
4	TMEDA	2	1:1	50	50	homo
5	bipy	2	1:1	-	99	homo
6	phen	2	1:1	-	99	homo
7	ethylenediamine	2	1:1	21	75	het
8	DMEDA	2	1:1	32	65	het

^a Yields following chromatography. ^b Appearance of the reaction at the end of the 17 h reaction time. The term “het” refers to a heterogeneous mixture while “homo” refers to a homogeneous reaction mixture. bipy = 2,2'-bipyridine, phen = 1,10-phenanthroline

The optimization under continuous flow conditions utilized a Vapourtec R2+ pumping module in combination with a R4 heating module and four in-line 10 mL PFA coil tube reactors (Table 11.2). Using the optimized conditions from the “batch” experiments under continuous flow led to only traces of the desired CuAiAC product **2** after a residence time of 300 minutes (entry 1). Relatively slow flow rates had to be used (0.1→0.4 ml/min) to maintain a consistent pressure due to the viscosity of PEG₄₀₀. Increasing the temperature to 80 °C smoothly afforded the desired product **2** in 74 % yield with 21 % of recovered **1**. Increasing the residence time to 400 min led to complete conversion of the starting material **1** and 83 % yield of **2**. Increasing the concentration of the reaction to 50 mM afforded a similarly high yield (entry 4). Further increasing the temperature (100 °C) did not improve the yield and

resulted in degradation of the acyclic iodoalkyne **1** (entry 5) and lowering the residence time to 100 minutes afforded low conversions. Gratifyingly, consistent yields were obtained upon scale-up (1 mmol of **1**; 81 % of **2**) (entry 7).

Table 11.2 – Optimization of Macrocylic CuAiAC under Continuous Flow Conditions.

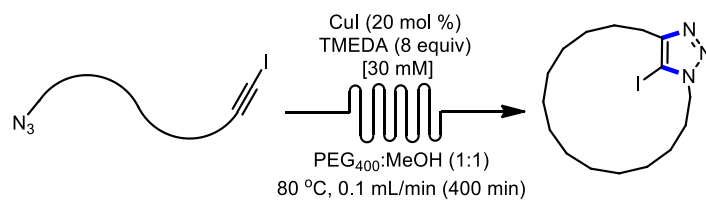


entry	temp. (°C)	flow rate (mL/min); residence time (min)	yield 2 (%) ^a	recovered 1 (%) ^a
1	60	0.13; 300	<5	95
2	80	0.13; 300	74	21
3	80	0.10; 400	83	-
4	80	0.10; 400	76 ^b	-
5	100	0.13; 300	-	-
6	100	0.4; 100	-	83
7	80	0.10:400	81 ^c	-

^a Yields following chromatography. ^b [50 mM]. ^c 1 mmol scale.

Using the optimized macrocyclization conditions employing "phase separation" at high concentrations, a series of azido-iodoalkynes were synthesized (Table 11.3). While the 17-membered macrolactone model substrate **2** cyclized in 83 % yield, the isomeric 17-membered ring **3** was cyclized in 90 % yield. The 21-membered ring phenolic ether **4** was also synthesized in 76 % yield. Amino acid containing macrocycles were also targeted. It was found that the incorporation of either isoleucine or phenylalanine was well tolerated. The 24-membered isoleucine-derived macrocycle **5** was isolated in 82 % while the phenylalanine-derived macrocycles **6** and **7** were obtained in 78 and 80 % yield respectively.

Table 11.3 – Substrate Scope of Macrocyclic CuAiAC Using a Phase Separation Strategy in Continuous Flow.^a

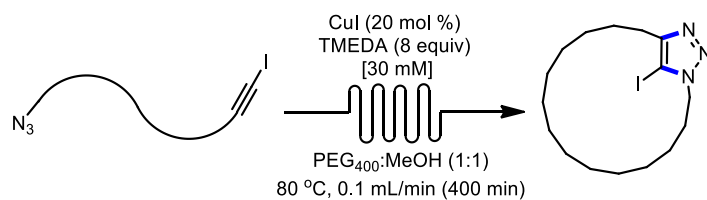


entry	product	yield (%)	entry	product	yield (%)
1		83	2		90
3		76	4		82
5		78	6		80

^a Yield following chromatography. Ring size indicated in red.

In an effort to further broaden the scope of the reaction, the optimized continuous flow reaction conditions were applied to macrocyclic CuAAC. First, we investigated the use of acyclic substrates bearing aryl azides (Table 11.4). The desired 16-membered macrocycle **8** was synthesized in 87 % yield with complete regioselectivity. Both a smaller 11-membered ring **10** and a larger 26-membered ring **11** could also be obtained (entries 3 and 4). The aryl azide moiety could be extended to afford a naphthalene-derived macrocycle **12** in good yield (81 %). Further aromatic substitutions were also possible. Macrocycle **13** bearing an electron withdrawing fluoride substituent para to the triazole was formed in 83 % yield. It was found that electron donating substituents on the aryl moiety were also well tolerated under the same conditions. The 16-membered macrocycles **13** and **14** bearing methyl and methoxy substituents could be formed in 76 % and 73 % respectively. Finally, aryl alkynes were also compatible with the continuous flow protocol, affording the 15-membered macrolactone **9** in 85 % yield (entry 2).

Table 11.4 – Substrate Scope of Macrocyclic CuAAC Using a Phase Separation Strategy in Continuous Flow.^a



entry	product	yield (%)	entry	product	yield (%)
1		87	2		85
3		66	4		61
5		81	6		83
7		76	8		73

^a Yield following chromatography. Ring size indicated in red.

11.4 – Conclusion

In conclusion, we have developed a simple and efficient method for the synthesis of triazole containing macrocycles. The method employs homogenous copper catalysis and a relatively simple catalyst system. Using a phase separation strategy under continuous flow conditions allows for reactions to be conducted at relatively high concentrations. A wide range of structurally diverse products were possible via either macrocyclic CuAiAC or CuAAC reactions. Given the interest macrocycles in various fields, we anticipate the protocols described herein to be use in a variety of applications.

Acknowledgement. The authors acknowledge the Natural Sciences and Engineering Research Council of Canada (NSERC), Université de Montreal and the Centre for Green Chemistry and Catalysis for generous funding. Funding was also provided by the NSERC CREATE program in Continuous Flow Science. A.-C. B. thanks NSERC for a Vanier graduate scholarship.

Supporting Information Available: Experimental procedures and characterization data for all new compounds

11.5 – Bibliography

- (1) (a) Driggers, E. M.; Hale, S. P.; Lee, J.; Terrett, N. K. *Nat. Rev. Drug Discovery* **2008**, *7*, 608. (b) Marsault, E.; Peterson, M. L. *J. Med. Chem.* **2011**, *54*, 1961. (c) Yudin, A. K. *Chem. Sci.* **2015**, *6*, 30.
- (2) (a) Bédard, A.-C.; Regnier, S.; Collins, S. K., *Green Chem.* **2013**, *15*, 1962. (b) Bogdan, A. R.; James, K. *Org. Lett.* **2011**, *13*, 4060.
- (3) (a) Bogdan, A. R.; Jerome, S. V.; Houk, K. N.; James, K. *J. Am. Chem. Soc.* **2012**, *134*, 2127. (b) Bogdan, A. R.; James, K. *Chem.–Eur. J.* **2010**, *16*, 14506.
- (4) Bédard, A.-C.; Collins, S. K., *J. Am. Chem. Soc.* **2011**, *133*, 19776.
- (5) (a) Pasini, D. *Molecules* **2013**, *18*, 9512. (b) Caricato, M.; Olmo, A.; Gargiulli, C.; Gattuso, G.; Pasini, D. *Tetrahedron* **2012**, *68*, 7861. (c) Yongjun Li, Y.; Flood, A. H. *Angew. Chem., Int. Ed.* **2008**, *47*, 2649.
- (6) (a) Jogula, S.; Dasari, B.; Khatravath, M.; Chandrasekar, G.; Kitambi, S. S.; Arya, P. *Eur. J. Org. Chem.* **2013**, 5036. (b) Potopnyk, M. A.; Jarosz, S. in *Click Chemistry in Glycoscience* (Eds.: Witczak, Z. J.; Bielski, R.) Wiley, 2013, 235.
- (7) (a) Kolb, H. C.; Sharpless, K. B. *Drug Discovery Today* **2003**, *8*, 1128. (b) Whiting, M.; Tripp, J. C.; Lin, Y. C.; Lindstrom, W.; Olson, A. J.; Elder, J. H.; Sharpless, K. B.; Fokin, V. V. *J. Med. Chem.* **2006**, *49*, 7697. (c) Wilkinson, B. L.; Bornaghi, L. F.; Houston, T. A.; Poulsen, S.-A. in *Drug Design Research Perspectives* (Ed.: Kaplan, S. P.), Nova, Hauppauge, 2007, 57. (d) Wang, Q.; Chan, T. R.; Hilgraf, R.; Fokin, V. V.; Sharpless, K. B.; Finn, M. G. *J. Am. Chem. Soc.* **2003**, *125*, 3192.
- (8) (a) Rostovtsev, V. V.; Green, L. G.; Fokin, V. V.; Sharpless, K. B. *Angew. Chem., Int. Ed.* **2002**, *41*, 2596. (b) Tornøe, C. W.; Christensen, C.; Meldal, M. *J. Org. Chem.* **2002**, *67*, 3057.
- (9) Bédard, A.-C.; Collins, S. K., *Org. Lett.* **2014**, *16*, 5286.
- (10) (a) Schulman, J. M.; Friedman, A. A.; Panteleev, J.; Lautens, M. *Chem. Commun.* **2012**, *48*, 55. (b) Deng, J.; Wu, Y.-M.; Chen, Q.-Y. *Synthesis* **2005**, *16*, 2730. (c) Worrell, B. T.; Hein, J. E.; Fokin, V. V. *Angew. Chem., Int. Ed.* **2012**, *51*, 11791
- (11) (a) Henning S. G. Beckmann, H. S. G.; Niel, F.; Hagerman, C. E.; Johansson, H.; Tan, Y. S.; Wilcke, D.; Spring, D. R. *Nature Chem.*, **2013**, *5*, 861. (b) Bauer, R. A.; Wenderski, T. A.; Tan, D. S. *Nature Chem. Biol.* **2013**, *9*, 21. (c) Kopp, F.; Stratton, C. F.; Akella, L. B.; Tan, D. S. *Nature Chem. Biol.* **2012**, *8*, 358.
- (12) Bédard, A.-C.; Collins, S. K. *Chem. Commun.* **2012**, *48*, 6420.

Chapter 12 : Conclusion and Perspectives

The preceding thesis describes the development of a novel approach aimed at improving the efficiency of macrocyclization reactions through the control of dilution effects. The “phase separation” strategy relies on an aggregated solvent mixture controlled by a poly(ethylene glycol) (PEG) co-solvent and allows for macrocyclization to be conducted at high concentrations.

First, macrocyclic Glaser-Hay oxidative coupling of terminal alkynes was employed in combination with the “phase separation” strategy in order to successfully synthesize a variety of structurally diverse macrocycles with varying ring sizes (16- to 28-membered rings) and functional groups. Phase separation between catalyst and substrates can be achieved either by developing hydrophilic ligands for transition metal complexes that allow for the catalysts to be sequestered in a highly polar and/or hydrophilic phase (*i.e.* PEGylated TMEDA derivative T-PEG₁₉₀₀, Scheme 12.1b) or through the use of aggregated mixtures of PEG₄₀₀ in MeOH (Scheme 12.1b). When compared to the traditional high-dilution and slow addition strategy (Scheme 12.1a), both “phase separation” strategies promoted the macrocyclization of a linear unconformationally biased precursor at a significantly higher concentration (0.0002 M → 0.03 M) with improved yields (11 % → 65 -73 %).

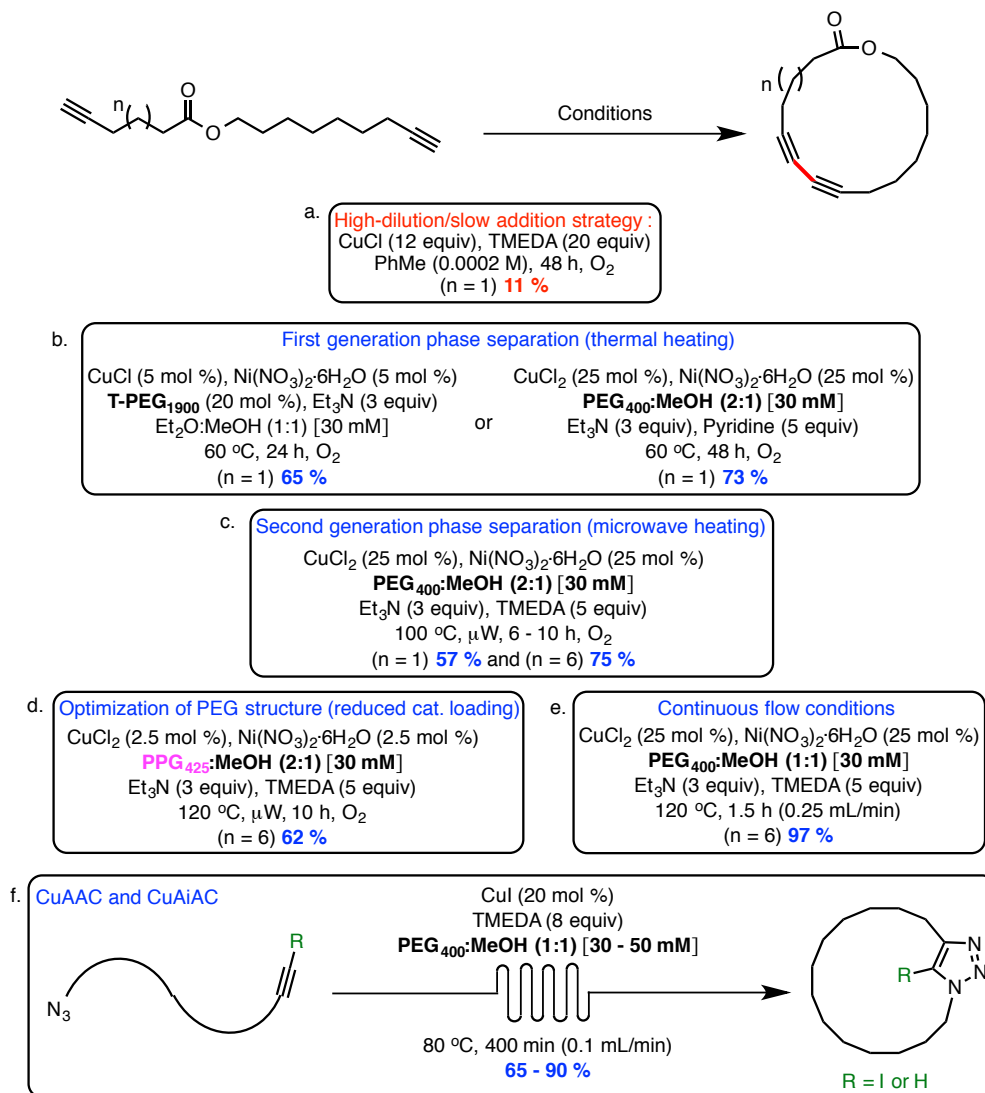
Next, a “phase separation” protocol that allows for Glaser-Hay macrocyclizations to be performed at high concentrations using microwave irradiation was developed. The reaction time was considerably reduced from 24-48 to 1-6 h and relied on a Cu/TMEDA catalyst system to maintain stability and solubility of the catalysts at higher temperatures (*vs.* thermal heating, Scheme 12.1c).

Insight into the mechanism of “phase separation” was probed using surface tension measurements, UV spectroscopy and chemical tagging. The origin of the efficiency in macrocyclic Glaser-Hay couplings that can be performed at high concentrations using the “phase separation” strategy was elucidated. The selective and high yielding macrocyclizations are due to aggregates of PEG₄₀₀ that can act to mimic phase separation normally achieved using organic/aqueous mixtures. Chemical tagging and UV measurements showed that the organic substrate preferentially resided within a PEG aggregate and can slowly diffuse to the MeOH phase where the catalysis is highly active leading to selective macrocyclization. Importantly, the degree of aggregation of the solvent was shown to greatly influence the yields of macrocyclizations.

The nature of the polymer co-solvent plays a role in controlling both aggregation and catalysis in the “phase separation” strategy. The first evaluation of the structural effects of PEG-derived polymers and their aggregation abilities for exploitation in organic synthesis was studied. Of the different structural effects studied, several important observations were made: 1) macrocyclizations exhibit greater efficiency at high ratios of PEG/MeOH, but very high ratios (>90 % PEG/MeOH) can result in catalyst inhibition, 2) the terminal hydroxyl groups are important for inducing aggregation; and 3) poly(propylene glycol)-containing PEGs (PPG₄₂₅ and Pluronic₁₁₀₀) provided good yields and are much more lipophilic than PEG, making them interesting alternatives for substrates that have problematic solubility. Moreover, it was found that catalyst activity was considerably higher in PPG₄₂₅ mixtures than in mixtures of other PEG solvents. Therefore, PPG₄₂₅ mixtures were exploited to develop macrocyclization reactions with 10-fold reduced catalyst loadings (Scheme 12.1d).

The “phase separation” strategy was also transferred to a continuous flow-macrocyclization protocol (Scheme 12.1e). The combination of the “phase separation” strategy with a continuous flow synthesis allowed for the precise control of reaction time and temperature, resulting in a reduction in the formation of unwanted oligomers and waste, high yields (up to 99 %), and short reaction times (1.5 h).

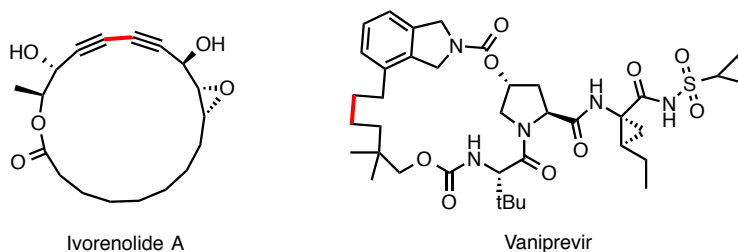
Lastly, the “phase separation” strategy was applied to the copper-catalyzed iodoalkyne-azide cycloaddition (CuAiAC) in both batch and continuous flow. The CuAiAC is an efficient new tool for macrocyclization, affording high yields, at low catalyst loadings (5 to 20 mol %) and high concentrations (up to 300 mM). A variety of macrocyclic skeletons were prepared having either different alkyl, aryl or amino acid building blocks. In addition to the advantages previously discussed that are associated with the “phase separation” strategy, the CuAiAC method developed employs a relatively simple catalyst system (*i.e.* CuI and Et₃N) and was easily transposed to continuous flow conditions (Scheme 12.1f). Given the interest in macrocycles in various fields, we anticipate the protocols described herein to be of use in a variety of applications.



Scheme 12.1 – Evolution of the “phase separation” strategy.

The “phase separation” technology has been demonstrated as a strategy for the construction of macrocycles *via* Glaser-Hay oxidative coupling of alkynes and copper-catalyzed azide-alkyne and azide-iodoalkyne cycloadditions. Despite the successful synthesis of macrocycles with various ring sizes and functional groups, and the mechanistic insight into the origin of the control of dilution, there is much research that needs to be investigated before “phase separation” can be considered a general tool for the synthesis of macrocycles. The following section describes some perspectives into possible future goals and areas of exploration with respect to the “phase separation” strategy.

One aspect of the “phase separation” strategy that would be important to investigate is expanding the limits of the substrate scope. As the Glaser-Hay coupling has to date been the most heavily investigated, it would be interesting to apply it to the total synthesis of complex macrocycles. Consequently, recent efforts in our group have identified two classes of “structurally complex” macrocycles for study: macrocyclic natural products and macrocyclic peptidic macrocycles explored in pharmaceutical drug discovery. For the former, our group has begun a total synthesis effort towards the diyne containing macrolide Ivorenolide A (Scheme 12.2). A previous synthesis utilized a Yamaguchi macrolactonization reaction at high dilution to construct the core macrocycle. Second, our group is exploring a synthesis of Vaniprevir (Scheme 12.2), a HCV protease inhibitor that was previously synthesized via an olefin metathesis reaction. In either of the synthesis projects, the key bond forming reaction will be a Glaser-Hay oxidative coupling using the “phase separation” strategy (shown in red, Scheme 12.2).

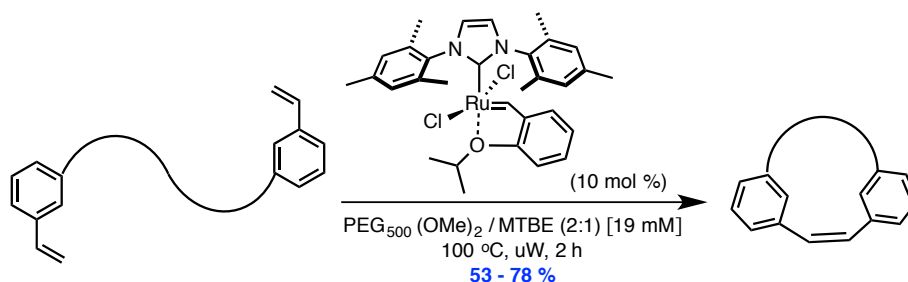


Scheme 12.2 – Structures of Ivorenolide A and Vaniprevir. Key bond forming reaction shown in red.

A second aspect of the “phase separation” strategy that could be further explored is the “scope” of the catalysis. Both of the transformations previously developed are based on copper catalysis employing alkynyl functionalities. While there are a number of other copper-catalyzed transformations of alkynes that could also be explored (*e.g.* Cadiot-Chadkowiec couplings or ynamide couplings), an alternative would be exploring copper-catalyzed oxidative transformations of other motifs. A promising application would be in the formation of disulfide bonds. First, it is well known that S-S bond formation can typically be performed under oxidative copper-catalysis. Second, given the number of biologically active macrocycles with key disulfide bridges, the development of a catalytic macrocyclic S-S bond formation at high concentrations might open avenues for exploring new macrocycles in medicinal chemistry.

In expanding the scope of catalysis of the “phase separation” strategy, the insight gained through the development of the “phase separation” strategy in the Cu-catalyzed reactions could be applied to catalysis with other metals. To date, our group has explored the application of macrocyclic olefin metathesis using a ruthenium-based catalyst to the “phase separation” strategy (Scheme 12.3).¹ The protocol was shown to allow macrocyclization at up

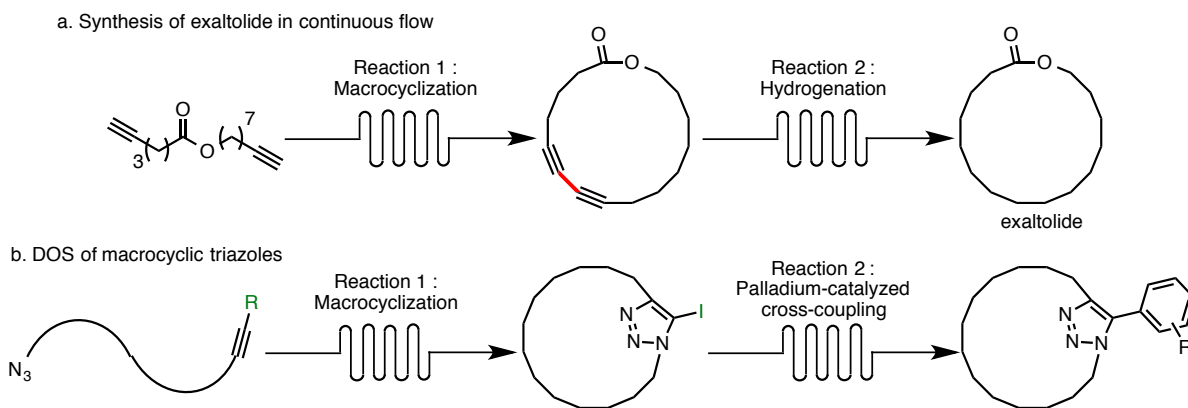
to 60 times greater concentrations than literature procedures. The key to the success of the protocol was the discovery of a mixture of both a non-protic organic solvent and poly(ethylene glycol) polymer that promoted aggregation. With the knowledge that both copper and ruthenium catalysis are tolerated under the “phase separation” conditions, it would be interesting to investigate the ruthenium-catalyzed azide-alkyne cycloaddition (RuAAC). The RuAAC methodology affords regioisomeric macrocyclic triazole products when compared to the CuAAC manifold (refer to Scheme 9.2). Given the interest in macrocyclic peptides in drug discovery, the development of such a protocol would have significant applications.



Scheme 12.3 – Macrocyclic ring-closing metathesis using the “phase separation” strategy

It should also be noted that there are a number of other macrocyclization reactions that have had considerable impact on the scientific community. Another example of a relevant class of reactions that could be investigated using the phase separation strategy are macrocyclic palladium-catalyzed cross-couplings. As palladium catalysis affords highly efficient transformations tolerant to functionality and exhibits compatibility with PEG solvents, it is reasonable to assume that new protocols for the synthesis of carbon-carbons bonds via cross-coupling could be achieved through “phase separation”.

Lastly, it is known that library generation of macrocycles is challenging due to the inefficiency of most macrocyclization reactions. Consequently, most libraries of macrocycles involved tedious diversity oriented synthesis (DOS)² of linear precursors which subsequently undergo macrocyclization as the last step in the synthetic route. Having developed efficient macrocyclization reactions at high concentration in continuous flow, one can easily obtain significant amounts of a macrocyclic core structure early in a synthetic sequence. Performing subsequent structural modifications on the core macrocycle would result in a paradigm shift in the way medicinal chemists typically perform structure-activity relationship (SAR) studies on macrocycles. Making synthetic alterations to a macrocyclic core may also allow for varying topologies that could not be obtained through macrocyclization of an already functionalized linear precursor. As such, the new strategy for DOS of macrocycles would help probe for new biological activities (SAR). As a first step towards these goals, important knowledge for performing tandem reactions in continuous flow synthesis is needed. Two possible avenues for exploration using existing technology developed in the preceding thesis involve either a tandem Glaser-Hay macrocyclization/hydrogenation sequence or a tandem CuAAC reaction/cross coupling sequence. (Scheme 12.4).



Scheme 12.4 – Examples of derivatization of macrocycles in continuous flow.

To conclude, it should be noted that the “phase separation” strategy is not without significant limitations. Some challenges are inherent to the use of PEG and MeOH as the solvent combination. First, PEGs are highly Lewis basic due to the abundance of oxygen atoms in the polymer. Therefore, Lewis acid catalysis using the “phase separation” strategy will be challenging and alternative reaction manifolds must be postulated. Second, the use of MeOH as a co-solvent allows for efficient aggregation of the PEG polymer, but as a protic solvent, MeOH is not always compatible with certain forms of catalysis and further understanding of the properties of PEG in organic solvents must be investigated in order to render the “phase separation” strategy more general. Further studies on the aggregation of PEG in organic solvents using surface tension measurements, as well as investigation of other surfactants to induce aggregation, are currently on-going in our laboratory. It is hoped that these studies will help cement the status of the “phase separation” strategy as a tool for efficient macrocyclization in the toolbox of organic synthetic chemists.

12.1 – Bibliography

- (1) Raymond, M.; Holtz-Mulholland, M.; Collins, S. K. *Chem. Eur. J.* **2014**, *20*, 12763-12767.
- (2) a) Isidro-Llobet, A.; Murillo, T.; Bello, P.; Cilibrizzi, A.; Hodgkinson, J. T.; Galloway, W. R. J. D.; Bender, A.; Welch, M.; Spring, D. R. *Proc. Nat. Acad. Sci.* **2011**; b) Bauer, R. A.; Wenderski, T. A.; Tan, D. S. *Nat Chem Biol* **2013**, *9*, 21-29; c) Beckmann, H. S. G.; Nie, F.; Hagerman, C. E.; Johansson, H.; Tan, Y. S.; Wilcke, D.; Spring, D. R. *Nat. Chem.* **2013**, *5*, 861-867.

Supporting Information

Chapter 13 : Supporting Information of Chapter 2: Phase Separation as a Strategy Towards Controlling Dilution Effects in Macrocyclic Glaser-Hay Couplings

General:

All reactions that were carried out under anhydrous conditions were performed under an inert argon or nitrogen atmosphere in glassware that had previously been dried overnight at 120 °C or had been flame dried and cooled under a stream of argon or nitrogen.² All chemical products were obtained from Sigma-Aldrich Chemical Company or Strem Chemicals and were reagent quality. Allyl 4,6-O-benzylidene-D-glucopyranoside was prepared according to literature procedures.³ Methyl-3,6-dihydroxybenzyl ester was prepared according to literature procedures.⁴ Technical solvents were obtained from VWR International Co. Anhydrous solvents (CH₂Cl₂, Et₂O, THF, DMF, Toluene, and hexanes) were dried and deoxygenated using a GlassContour system (Irvine, CA). Isolated yields reflect the mass obtained following flash column silica gel chromatography. Organic compounds were purified using the method reported by W. C. Still⁵ and using silica gel obtained from Silicycle Chemical division (40-63 nm; 230-240 mesh). Analytical thin-layer chromatography (TLC) was performed on glass-backed silica gel 60 coated with a fluorescence indicator (Silicycle Chemical division, 0.25

² Shriver, D. F.; Drezdon, M. A. in *The Manipulation of Air-Sensitive Compounds*; Wiley-VCH: New York, 1986.

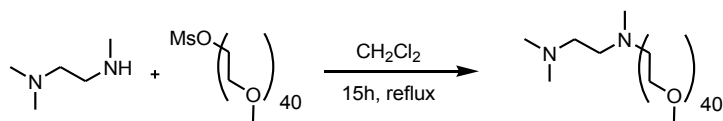
³ Tanaka, H.; Kawai, K.; Fujiwara, K.; Murai, A. *Tetrahedron* **2002**, *5*, 10017.

⁴ Zhu, J.; Beugelmans, R.; Bourdet, S.; Chastanet, J.; Roussi, G. *J. Org. Chem.* **1995**, *60*, 6389.

⁵ Still, W. C.; Kahn, M.; Mitra, A. *J. Org. Chem.* **1978**, *43*, 2923.

mm, F₂₅₄). Visualization of TLC plate was performed by UV (254 nm), KMnO₄ or *p*-anisaldehyde stains. All mixed solvent eluents are reported as v/v solutions. Concentration refers to removal of volatiles at low pressure on a rotary evaporator. All reported compounds were homogeneous by thin layer chromatography (TLC) and by ¹H NMR. NMR spectra were taken in deuterated CDCl₃ using Bruker AV-300 and AV-400 instruments unless otherwise noted. Signals due to the solvent served as the internal standard (CHCl₃: δ 7.27 for ¹H, δ 77.0 for ¹³C). The ¹H NMR chemical shifts and coupling constants were determined assuming first-order behavior. Multiplicity is indicated by one or more of the following: s (singlet), d (doublet), t (triplet), q (quartet), m (multiplet), br (broad); the list of couplings constants (*J*) corresponds to the order of the multiplicity assignment. The ¹H NMR assignments were made based on chemical shift and multiplicity and were confirmed, where necessary, by homonuclear decoupling, 2D COSY experiments. The ¹³C NMR assignments were made on the basis of chemical shift and multiplicity and were confirmed, where necessary, by two dimensional correlation experiments (HSQC). High resolution mass spectroscopy (HRMS) was done by the Centre régional de spectrométrie de masse at the Département de Chimie, Université de Montréal from an Agilent LC-MSD TOF system using ESI mode of ionization unless otherwise noted.

SYNTHESIS OF TPEG₁₉₀₀ 7 AND MACROCYCLIZATION PROTOCOL.



Polyethylene glycol 1900 monomethyl ether mesylate⁶ (5.4 g, 2.8 mmol, 1 equiv.) was placed in a sealed tube equipped with a stirring bar. Dry dichloromethane (100 mL) and trimethylethylene diamine (2.8 mL, 28 mmol, 10 equiv.) were added and the clear solution was stirred for 15 h at 60 °C. The solution was then cooled to room temperature and diethylether (100 mL) was added. The mixture was placed in a laboratory refrigerator for 5 h to induce precipitation. The solid was filtered and washed with diethylether (3X 100 mL). The solid was redissolved in dichloromethane and passed through a short pad of neutral alumina (15 % methanol in dichloromethane). T-PEG₁₉₀₀ 7 (5.7 g, 2.8 mmol) was obtained as a white solid in quantitative yield (>98 %). ¹H NMR (500 MHz, CDCl₃, 35 °C) δ ppm 5.49-5.47 (m, 2H); 4.54-4.51 (m, 2H), 4.20-4.10 (m, 6H); 3.97-3.87 (m, 8H); 3.66-3.32 (m, PEG); 3.26 (s, 55H); 3.13 (bs, 150H); 2.58-2.55 (m, 16H); 2.31 (s, 10H); 2.26 (s, 6H); 2.22 (s, 8H); ¹³C NMR (500 MHz, CDCl₃) δ ppm 72.4, 71.5, 70.9, 70.22, 70.16, 70.13 (PEG), 70.1, 69.8, 61.1, 58.6, 42.4; MALDI-TOF : m/z 1963.482.

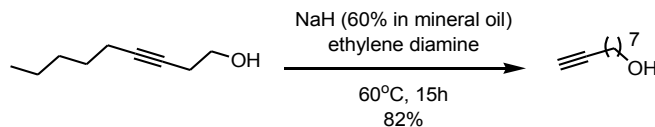
General Procedure for Macrocyclization using TPEG₁₉₀₀: The general procedure for the macrocyclization of diynes under Glaser-Hay oxidative coupling conditions using TPEG₁₉₀₀ is as follows. To a vial equipped with a stirring bar was charged with CuCl (0.065 mmol, 12 mg,

⁶ Polyethylene glycol 1900 monomethyl ether mesylate was synthesised from molecular weight 1900 PEG methyl ether purchased from Alfa Aesar. See : Zhao, X.; Janda, K. D. *Tetrahedron Lett.* **1997**, *38*, 5437-5440.

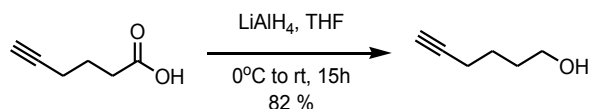
25 mol %), Ni(NO₃)₂·6H₂O (0.065 mmol, 19 mg, 25 mol %) and TPEG₁₉₀₀ (250 mg, 0.13 mmol, 50 mol %), methanol (5 mL) and triethylamine (0.36 mmol, 0.11 mL, 3 equiv.). The mixture was stirred at room temperature for 15 min or until the metals were solubilized. The diyne (0.26 mmol) was then added as an ether solution (5 mL) in one portion. Oxygen was bubbled in the solution for 5 min and the vial was then closed. The reaction was warmed to 60 °C and monitored by TLC for consumption of the starting material (oxygen was bubbled again in the solution every 12 h). When the reaction was completed by TLC, the reaction was cooled to room temperature and silica gel was added. The crude mixture was dried under reduced pressure and purified by column chromatography (100 % hexanes→10 % ethyl acetate in hexanes) to afford pure macrocycle.

SYNTHESIS OF MACROCYCLIZATION PRECURSORS.

General Procedure for Steglich Esterifications: To a stirred solution of the alcohol (1 equiv.) and the carboxylic acid (1.5 equiv.) in dry dichloromethane (0.2 M) was added N,N'-dicyclohexylcarbodiimide (DCC, 2 equiv.) and 4-dimethylaminopyridine (DMAP, 3 equiv.) at room temperature. The reaction mixture was stirred at room temperature for 15 h. Upon complete conversion of the starting material, the crude reaction mixture was placed in a freezer for 5 h to induce the precipitation of the urea, which was subsequently removed by filtration. The filtrate was concentrated *in vacuo* to provide the crude reaction mixture which was purified by column chromatography on silica-gel to afford the desired product.



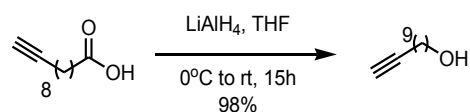
8-nonyl-1-ol: To a flask containing ethylene diamine (70 mL) at 0 °C was added NaH (60 % in mineral oil, 5.7 g, 142.6 mmol, 4 equiv.). The mixture was slowly warmed to room temperature and stirred for 1 h. Then the reaction was warmed to 60 °C and stirred for 2 h. After cooling the reaction to 45 °C, 3-nonyl-1-ol (5 mL, 35.7 mmol, 1 equiv.) was added in one portion and the solution was stirred at 60 °C for 15 h. Upon cooling to 0 °C, 1M HCl (30 mL) was added and the organic and aqueous layers were separated. The aqueous layer was extracted with ethyl acetate (2x), and the combined organic layers were dried over anhydrous Na₂SO₄. The suspension was filtered and the filtrate was concentrated *in vacuo*. Purification of the crude product by column chromatography on silica gel (20 % ethyl acetate in hexanes) afforded the product as a colorless oil (4.1 g, 82 %). The NMR data are in agreement with that obtained in the literature.⁷



5-hexyn-1-ol: To a solution of lithium aluminum hydride (676 mg, 17.8 mmol, 2 equiv.) in anhydrous tetrahydrofuran (30 mL) at 0 °C was added 5-hexynoic acid (1 mL, 8.9 mmol, 1 equiv.). The solution was warmed to room temperature and stirred for 15 h. The reaction was cooled to 0 °C and 2 M NaOH (10 mL) was added dropwise. Water and ethyl acetate were added and the organic and aqueous layers were separated. The aqueous layer was extracted

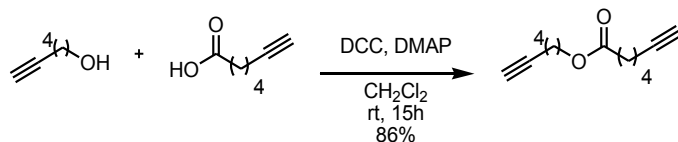
⁷ (a) Denmark, S. E.; Jones, T. K. *J. Org. Chem.* **1982**, *47*, 4595-4597. (b) Renauld, J. L.; Aubert, C.; Malacria, M. *Tetrahedron* **1999**, *55*, 5113-5128.

with ethyl acetate (2x), and the combined organic layers were dried over anhydrous Na₂SO₄. The suspension was filtered and the filtrate was concentrated *in vacuo*. Purification of the crude reaction product by column chromatography on silica gel (10→20 % ethyl acetate in hexanes) afforded the product as a colorless oil (713 mg, 82 %). ¹H NMR (300 MHz, CDCl₃) δ = 3.67 (t, *J* = 6.2 Hz, 2H), 2.23 (td, *J* = 6.8, 2.7 Hz, 2H), 1.96 (t, *J* = 2.6 Hz, 1H), 1.76 - 1.54 (m, 4H); ¹³C NMR (75 MHz, CDCl₃) δ = 84.3, 68.5, 62.3, 31.6, 24.7, 18.2 ppm; HRMS (ESI) *m/z* calculated for C₆H₁₁O [M+H]⁺, 99.0804; found: 99.0805.

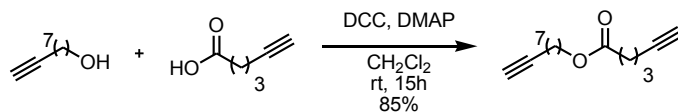


10-undecyn-1-ol: To a solution of lithium aluminum hydride (420 mg, 11.0 mmol, 2 equiv.) in anhydrous tetrahydrofuran (28 mL) at 0 °C was added 5-hexynoic acid (1 g, 5.5 mmol, 1 equiv.). The solution was warmed to room temperature and stirred for 15 h. The reaction was cooled to 0 °C and 2 M NaOH (10 mL) was added dropwise. Water and ethyl acetate were added and the organic and aqueous layers were separated. The aqueous layer was extracted with ethyl acetate (2x), and the combined organic layers were dried over anhydrous Na₂SO₄. The suspension was filtered and the filtrate was concentrated *in vacuo*. Purification of the crude reaction product by column chromatography on silica gel (10→20 % ethyl acetate in hexanes) afforded the product as a colorless oil (924 mg, >98 %). The NMR data are in agreement with that in the literature.⁸

⁸ Sharma, A.; Chattopadhyay, S. *J. Org. Chem.* **1998**, *63*, 6128.

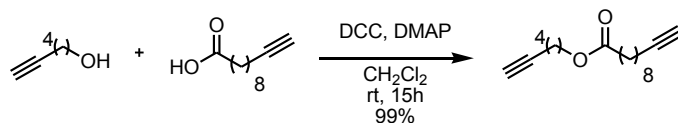


Hex-5-yn-1-yl hept-6-ynoate: Following the General Procedure, 5-hexyn-1-ol (52 mg, 0.53 mmol), 6-heptynoic acid (100 mg, 0.79 mmol), DCC (219 mg, 1.1 mmol) and DMAP (194 mg, 1.6 mmol) in anhydrous DCM (5 mL) were added to the reaction flask. Following purification by column chromatography (10 % ethyl acetate in hexanes), the desired product was obtained as a colorless oil (106 mg, 86 %). ^1H NMR (300 MHz, CDCl_3) δ = 4.09 (t, J = 6.4 Hz, 2H), 2.33 (t, J = 7.4 Hz, 2H), 2.27 - 2.15 (m, 4H), 1.95 (q, J = 2.6 Hz, 2H), 1.82 - 1.68 (m, 4H), 1.66 - 1.49 (m, 4H); ^{13}C NMR (75 MHz, CDCl_3) δ = 173.4, 83.9, 83.8, 68.7, 68.6, 63.6, 33.7, 27.8, 27.6, 24.9, 24.0, 18.1, 18.0 ppm; HRMS (ESI) m/z calculated for $\text{C}_{13}\text{H}_{19}\text{O}_2$ $[\text{M}+\text{H}]^+$, 206.1387; found: 207.1390.

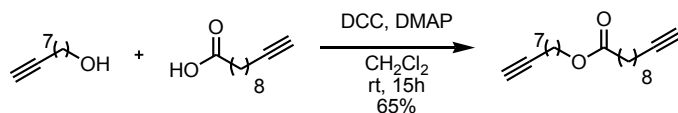


Non-8-yn-1-yl hex-5-ynoate: Following the General Procedure, 8-nonyn-1-ol (2.1 g, 14.7 mmol), 5-hexynoic acid (2.43 mL, 22.1 mmol), DCC (6.1 g, 29.4 mmol) and DMAP (5.4 g, 44.1 mmol) in anhydrous DCM (74 mL) were added to the reaction flask. Following purification by column chromatography (10 % ethyl acetate in hexanes), the desired product was obtained as a colorless oil (2.7 g, 85 %). ^1H NMR (400MHz, CDCl_3) δ = 4.05 (t, J = 6.7 Hz, 2H), 2.43 (t, J = 7.4 Hz, 2H), 2.25 (td, J = 7.0, 2.6 Hz, 2H), 2.17 (td, J = 7.0, 2.7 Hz, 2H), 1.96 (t, J = 2.7 Hz, 1H), 1.93 (t, J = 2.7 Hz, 1H), 1.87-1.81 (m, 2H), 1.65-1.58 (m, 2H), 1.53-1.48 (m, 2H), 1.43-1.28 (m, 6H); ^{13}C NMR (75 MHz, CDCl_3) δ = 173.1, 84.5, 83.2, 69.0, 68.1,

64.4, 32.9, 28.6, 28.5, 28.5, 28.3, 25.7, 23.6, 18.3, 17.8 ppm; HRMS (ESI) m/z calculated for $C_{15}H_{23}O_2$ $[M+H]^+$, 235.1693; found: 235.1698.

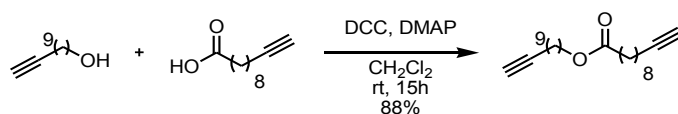


Hex-5-yn-1-yl undec-10-ynoate: Following the General Procedure, 5-hexyn-1-ol (100 mg, 1.0 mmol), 10-undecynoic acid (278 mg, 1.5 mmol), DCC (721 mg, 2.0 mmol) and DMAP (374 mg, 3.0 mmol) in anhydrous DCM (7.7 mL) were added to the reaction flask. Following purification by column chromatography (5% ethyl acetate in hexanes), the desired product was obtained as a colorless oil (280 mg, 99 %). 1H NMR (400MHz, $CDCl_3$) δ = 4.07 (t, J = 6.5 Hz, 2H), 2.27 (t, J = 7.5 Hz, 2H), 2.21 (td, J = 7.0, 2.7 Hz, 2H), 2.15 (td, J = 7.0, 2.6 Hz, 2H), 1.94 (td, J = 2.6, 0.6 Hz, 1H), 1.91 (td, J = 2.6, 0.6 Hz, 1H), 1.79 - 1.66 (m, 4H), 1.64 - 1.44 (m, 6H), 1.42 - 1.20 (m, 6H); ^{13}C NMR (75 MHz, $CDCl_3$) δ = 173.9, 84.7, 83.9, 68.7, 68.1, 63.7, 34.3, 29.08, 29.06, 28.9, 28.6, 28.4, 27.7, 24.9 (2C), 18.4, 18.1 ppm; HRMS (ESI) m/z calculated for $C_{17}H_{27}O_2$ $[M+H]^+$, 263.2006; found: 263.2013.

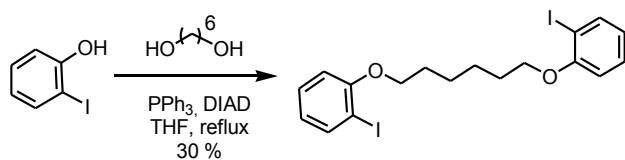


Non-8-yn-1-yl undec-10-ynoate: Following the General Procedure, 8-nonyn-1-ol (100 mg, 1.0 mmol), 10-undecynoic acid (195 mg, 1.5 mmol), DCC (294 mg, 2.0 mmol) and DMAP (260 mg, 3.0 mmol) in anhydrous DCM (5.0 mL) were added to the reaction flask. Following purification by column chromatography (5 % ethyl acetate in hexanes), the desired product was obtained as a colorless oil (196 mg, 65 %). 1H NMR (300 MHz, $CDCl_3$) δ = 4.06 (t, J = 6.7 Hz, 2H), 2.29 (t, J = 7.5 Hz, 2H), 2.22-2.15 (m, 4H), 1.94 (td, J = 2.6, 1.2 Hz, 2H), 1.65 -

1.48 (m, 8H), 1.47 - 1.23 (m, 14H); ^{13}C NMR (75 MHz, CDCl_3) δ = 173.9, 84.69, 84.59, 68.15, 68.07, 64.3, 34.4, 29.08, 29.06, 28.9, 28.7, 28.64, 28.57 (2C), 28.4, 28.3, 25.8, 25.0, 18.4, 18.3 ppm; HRMS (ESI) m/z calculated for $\text{C}_{20}\text{H}_{33}\text{O}_2$ $[\text{M}+\text{H}]^+$, 305.2475; found: 305.2462.

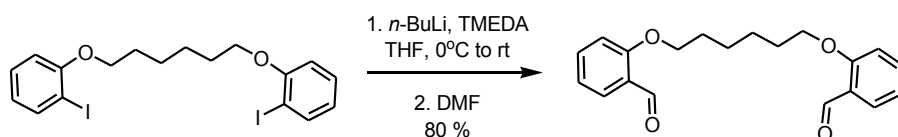


Dec-9-yn-1-yl undec-10-ynoate: Following the General Procedure, 10-undecyl-1-ol (172 mg, 1.0 mmol), 10-undecynoic acid (278 mg, 1.5 mmol), DCC (421 mg, 2.0 mmol) and DMAP (374 mg, 3.0 mmol) in anhydrous DCM (7.7 mL) were added to the reaction flask. Following purification by column chromatography (5 % ethyl acetate in hexanes), the desired product was obtained as a colorless oil (297 mg, 88 %). ^1H NMR (300 MHz, CDCl_3) δ = 4.03 (t, J = 6.7 Hz, 2H), 2.27 (t, J = 7.5 Hz, 2H), 2.18 - 2.13 (m, 4H), 1.91 (td, J = 2.6, 0.6 Hz, 2H), 1.62-1.45 (m, 8H), 1.41 - 1.29 (m, 16H); ^{13}C NMR (75 MHz, CDCl_3) δ = 173.8, 84.58, 84.56, 68.0, 64.3, 34.3, 29.3, 29.1, 29.02, 28.99, 28.9, 28.8, 28.61, 28.57 (2C), 28.56, 28.37, 28.35, 25.8, 24.9, 18.3 (2C) ppm; HRMS (ESI) m/z calculated for $\text{C}_{22}\text{H}_{37}\text{O}_2$ $[\text{M}+\text{H}]^+$, 333.2778; found: 333.2788.



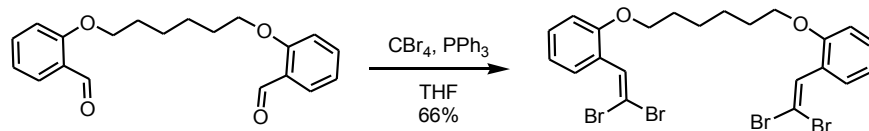
1,6-bis(2-iodophenoxy)hexane: To a stirred solution of 2-iodophenol (3.1 g, 14.1 mmol) in anhydrous THF (65 mL) was added triphenylphosphine (3.7 g, 2.2 equiv., 14.1 mmol), 1,6-hexanediol (0.76 g, 1 equiv., 6.4 mmol) and diisopropyl azodicarboxylate (2.8 mL, 2.2 equiv., 14.1 mmol) in that order under a N_2 atmosphere. The reaction mixture was heated at reflux for

15 hours. The reaction was concentrated *in vacuo* to provide a crude reaction mixture which was purified by column chromatography on silica-gel (100 hexanes→10 % ethyl acetates in hexanes) to afford the desired product as a beige solid (1.0 g, 30 %). ¹H NMR (300 MHz, CDCl₃) δ = 7.77 (dd, *J* = 7.8, 1.7 Hz, 2H), 7.33 - 7.24 (m, 2H), 6.82 (dd, *J* = 8.2, 1.3, Hz, 2H), 6.71 (td, *J* = 7.6, 1.3 Hz, 2H), 4.05 (t, *J* = 6.2 Hz, 4H), 1.95 - 1.87 (m, 4H), 1.68-1.63 (m, 4H); ¹³C NMR (75 MHz, CDCl₃) δ = 157.5, 139.3, 129.4, 122.3, 112.1, 86.7, 68.9, 29.0, 25.7 ppm; HRMS (ESI) *m/z* calculated for C₁₈H₂₀I₂NaO₂ [M+Na]⁺, 544.9445; found: 544.9447.

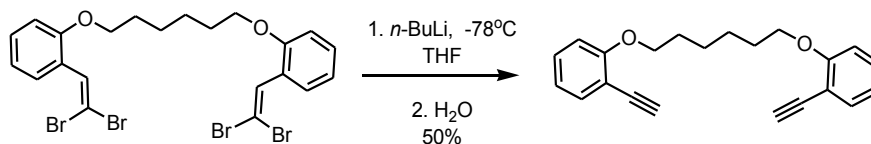


2,2'-(hexane-1,6-diylbis(oxy))dibenzaldehyde: To a solution of 1,6-bis(2-iodophenoxy)hexane (100 mg, 0.2 mmol, 1 equiv.) and tetramethylethylenediamine (22 mg, 0.2 mmol, 1 equiv.) in anhydrous tetrahydrofuran (3 mL) at 0 °C under N₂ was added freshly titrated *n*-BuLi (1.4 M in Hexanes, 0.55 mL, 0.77 mmol, 4 equiv.) dropwise. The reaction mixture was then warmed to room temperature and stirred for 1h. Anhydrous dimethylformamide (0.16 mL, 0.95 mmol, 5 equiv.) was added to the mixture in one portion at room temperature and the reaction was stirred for 1 h. Water and ethyl acetate are then added and the organic and aqueous layers were separated. The aqueous layer was extracted with ethyl acetate (2x), and the combined organic layers were washed (4x) with a saturated solution of CuSO₄, dried over anhydrous Na₂SO₄. The suspension was filtered and the filtrate was concentrated *in vacuo*. Purification by column chromatography on silica gel (5→15 % ethyl acetate in hexanes) afforded the product as a beige solid (50 mg, 80 %). ¹H NMR (300 MHz, CDCl₃) δ = 10.52 (d, *J* = 0.6 Hz, 2H), 7.83 (dd, *J* = 7.6, 1.8 Hz, 2H), 7.56 - 7.51 (m, 2H), 7.04 - 6.97 (m, 4H), 4.10 (t, *J* = 9 Hz, 4H), 1.91 (m, 4H), 1.66 - 1.55 (m, 4H); ¹³C NMR (75 MHz,

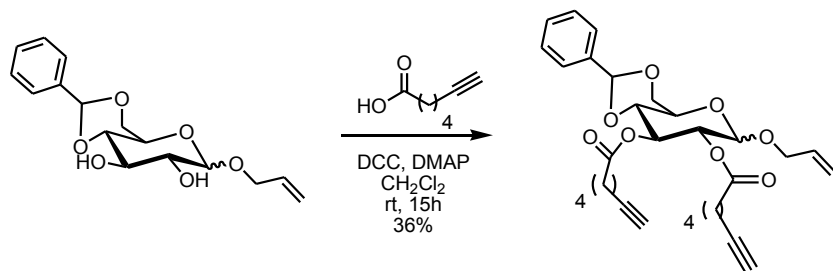
CDCl₃) δ = 189.7, 161.4, 135.9, 128.2, 124.9, 120.5, 112.4, 68.2, 29.0, 25.8 ppm; HRMS (ESI) m/z calculated for C₂₀H₂₃O₄ [M+H]⁺, 327.1591; found: 327.1595.



1,6-bis(2-(2,2-dibromovinyl)phenoxy)hexane: Carbon tetrabromide (234 mg, 0.7 mmol, 2 equiv.) and triphenylphosphine (413 mg, 1.6 mmol, 4.5 equiv.) were placed in a flask and dichloromethane (2.0 mL) was added at 0 °C. The orange mixture was stirred 10 min at 0 °C, then 2,2'-(hexane-1,6-diylbis(oxy))dibenzaldehyde (115 mg, 0.35 mmol, 1 equiv.) and 2,6-lutidine (0.1 mL, 0.7 mmol, 2 equiv.) were added as a dichloromethane solution (2.0 mL) and the reaction was stirred 2 h at 0 °C. After warming to room temperature, a saturated solution of NH₄Cl (5 mL) was added and the aqueous phase was extracted with dichloromethane (3x). The combined organic phases were dried with anhydrous Na₂SO₄. The suspension was filtered and the filtrate was concentrated *in vacuo*. Purification by column chromatography on silica gel (100 % hexanes→10 % ethyl acetate in hexanes) afforded the product as a yellow solid (147 mg, 66 %). ¹H NMR (300 MHz, CDCl₃) δ = 7.70 (dd, J = 7.7, 1.3 Hz, 2H), 7.61 (s, 2H), 7.34 - 7.28 (m, 2H), 6.94 (t, J = 7.6 Hz, 2H), 6.88 (d, J = 7.9 Hz, 2H), 4.02 (t, J = 6 Hz, 4H), 1.92 - 1.83 (m, 4H), 1.63 - 1.56 (m, 4H); ¹³C NMR (75 MHz, CDCl₃) δ = 156.0, 133.0, 129.9, 129.1, 124.6, 120.1, 111.7, 89.4, 68.3, 29.1, 25.9 ppm; HRMS (ESI) m/z calculated for C₂₂H₂₂AgBr₄O₄ [M+Ag]⁺, 740.7399; found: 740.7431.

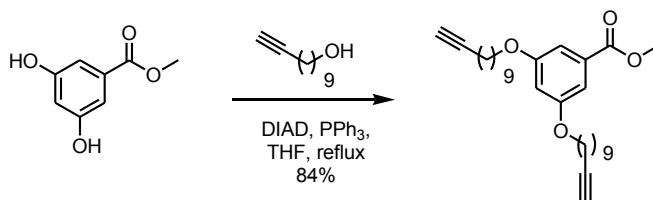


1,6-bis(2-ethynylphenoxy)hexane: To a solution of 1,6-bis(2-(2,2-dibromovinyl)phenoxy)hexane (110 mg, 0.2 mmol, 1 equiv.) in anhydrous tetrahydrofuran (3 mL) at -78 °C was added a solution of freshly titrated *n*-BuLi (1.4 M in Hexanes, 0.6 mL, 0.85 mmol, 5 equiv.) dropwise. The mixture was stirred 1 h at -78 °C then another 1 h at -20 °C. When complete consumption of the starting tetrabromide, the reaction is warmed to 0 °C and a saturated solution of NH₄Cl (3 mL) is added dropwise. The organic and aqueous phases are separated and the aqueous phase is extracted with ethyl acetate (3x). The combined organic phases are washed with brine (1x) and dried over anhydrous Na₂SO₄. The suspension was filtered and the filtrate was concentrated in vacuo. Purification by column chromatography on silica gel (10 % ethyl acetate in hexanes) afforded the product as a yellow solid (110 mg, 50 %). ¹H NMR (300 MHz, CDCl₃) δ = 7.46 (dd, *J* = 7.5, 1.6 Hz, 2H), 7.33 - 7.27 (m, 2H), 6.93 - 6.86 (m, 4H), 4.06 (t, *J* = 6.5 Hz, 4H), 3.25 (s, 2H), 1.96 - 1.82 (m, 4H), 1.67 - 1.54 (m, 4H); ¹³C NMR (75 MHz, CDCl₃) δ = 160.2, 134.1, 130.1, 120.3, 112.0, 111.6, 81.0, 80.1, 68.5, 28.9, 25.6 ppm; HRMS (ESI) *m/z* calculated for C₂₂H₂₃O₂ [M+H]⁺, 319.1683; found: 319.1695.

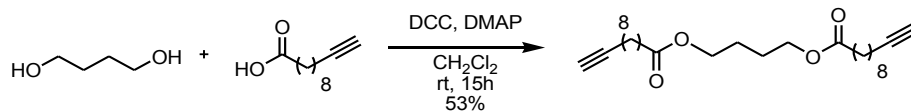


(4aR,7R,8S,8aR)-6-(allyloxy)-2-phenylhexahydropyrano[3,2-d][1,3]dioxine-7,8-diyl

bis(hept-6-ynoate): Following the General Procedure, allyl 4,6-O-benzylidene-D-glucopyranoside (150 mg, 0.5 mmol, 1 equiv.), 5-hexynoic acid (0.2 mL, 1.46 mmol, 3 equiv.), DCC (412 mg, 2.0 mmol, 4 equiv.) and DMAP (366 mg, 3.0 mmol, 6 equiv.) in anhydrous DCM (5 mL) were added to the reaction flask. Following purification by column chromatography (5 %→20 % ethyl acetate in hexanes), the desired product was obtained as a white solid (100 mg, 36 %) ¹H NMR (400 MHz, CDCl₃) (mixture of α and β anomers (0.85 :0.15), data reported for major anomer only) δ = ¹H NMR (300MHz, CDCl₃) δ = 7.46 - 7.41 (m, 2H), 7.36 - 7.32 (m, 3H), 5.94 - 5.81 (m, 1H), 5.65 (t, *J* = 9.9 Hz, 1H), 5.51 (s, 1H), 5.35 - 5.20 (m, 2H), 5.12 (d, *J* = 3.8 Hz, 1H), 4.91 (dd, *J* = 9.9, 3.8 Hz, 1H), 4.32 - 4.27 (m, 1H), 4.23 (ddt, *J* = 13.0, 5.1, 1.4 Hz, 1H), 4.04 - 3.95 (m, 2H), 3.76 (t, *J* = 10.3 Hz, 1H), 3.65 (t, *J* = 12 Hz, 1H), 2.39 - 2.31 (m, 4H), 2.22 (td, *J* = 7.0, 2.6 Hz, 2H), 2.12 (td, *J* = 7.0, 2.6 Hz, 2H), 1.96 (t, *J* = 3 Hz, 1H), 1.92 (t, *J* = 2.7 Hz, 1H), 1.78 - 1.66 (m, 4H), 1.60 - 1.45 (m, 4H); ¹³C NMR (100 MHz, CDCl₃) δ = 172.7, 172.1, 136.9, 133.19, 133.16, 129.0, 128.18, 128.15, 126.1, 118.0, 101.5, 95.6, 83.8, 83.7, 79.3, 71.4, 68.8, 68.70, 68.65 (2C), 68.6, 62.5, 33.7, 33.5, 27.6, 27.5, 24.0, 23.9, 18.04, 17.96 ppm; HRMS (ESI) *m/z* calculated for C₃₀H₃₆NaO₈ [M+Na]⁺, 547.2302; found: 547.2302.

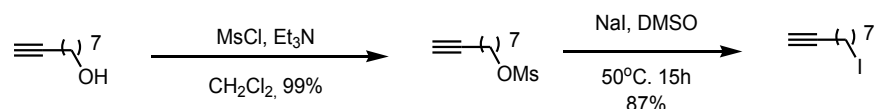


Methyl 3,5-bis(undec-10-yn-1-yloxy)benzoate: To a solution of methyl 3,6-dihydroxybenzoate (80.1 mg, 0.48 mmol) in anhydrous tetrahydrofuran (5 mL) was added triphenylphosphine (377.3 mg, 3 equiv., 1.44 mmol), 10-undecyn-1-ol (200 mg, 2.5 equiv., 1.19 mmol) and diisopropyl azodicarboxylate (0.28 mL, 3 equiv., 1.44 mmol,) in that order under a N₂ atmosphere. The reaction mixture was heated at reflux for 15 hours. The reaction was concentrated *in vacuo* to provide a crude reaction mixture which was purified by column chromatography on silica-gel (10 % ethyl acetate in hexanes) to afford the desired product as a white solid (188 mg, 84 %). ¹H NMR (300 MHz, CDCl₃) δ = 7.16 (d, *J* = 2.3 Hz, 2H), 6.64 (t, *J* = 2.3 Hz, 1H), 3.97 (t, *J* = 6.5 Hz, 4H), 3.90 (s, 3H), 2.22 - 2.16 (m, 4H), 1.95 (t, *J* = 2.7 Hz, 2H), 1.83 - 1.73 (m, 4H), 1.56 - 1.23 (m, 24H); ¹³C NMR (125 MHz, CDCl₃) δ = 167.0, 160.13, 160.11, 131.8, 107.6, 106.6, 84.8, 68.3, 68.1, 52.2, 29.4, 29.3, 29.2, 29.0, 28.7, 28.5, 26.0, 18.40, 18.38 ppm; HRMS (ESI) *m/z* calculated for C₃₀H₄₅O₄ [M+H]⁺, 469.3312; found: 469.3322.



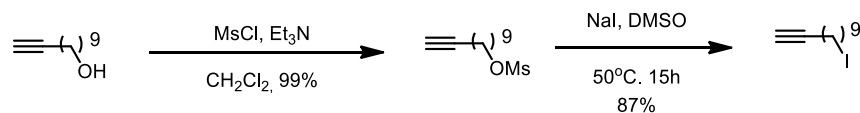
Butane-1,4-diyl bis(undec-10-ynoate): Following the General Procedure, butane-1,4-diol (250 mg, 2.8 mmol), 10-undecynoic acid (1.51 g, 8.3 mmol), DCC (2.3 g, 11.2 mmol), DMAP (2.1 g, 16.8 mmol) and anhydrous DCM (15 mL) were added to the reaction flask. Following purification by column chromatography (20 % ethyl acetate in hexanes), the desired product was obtained as a white solid (622 mg, 53 %). ¹H NMR (300 MHz, CDCl₃) δ = 4.06 - 3.87 (m,

4H), 2.16 (t, $J = 7.5$ Hz, 4H), 2.03 (td, $J = 7.0, 2.7$ Hz, 4H), 1.82 (t, $J = 2.6$ Hz, 2H), 1.66 - 1.54 (m, 4H), 1.48 (t, $J = 7.0$ Hz, 4H), 1.44 - 1.32 (m, 4H), 1.32 - 1.10 (m, 16H); ^{13}C NMR (75 MHz, CDCl_3) $\delta = 173.2, 84.1, 68.0, 63.3, 33.8, 28.74, 28.69, 28.5, 28.3, 28.1, 25.0, 24.6, 18.0$ ppm; HRMS (ESI) m/z calculated for $\text{C}_{26}\text{H}_{43}\text{O}_4$ $[\text{M}+\text{H}]^+$, 419.3156; found: 419.3154.



Non-8-yn-1-yl methanesulfonate: 9-nonyn-1-ol (1 g, 7.14 mmol, 1 equiv.) was dissolved in anhydrous dichloromethane (60 mL) and cooled to 0 °C. Triethylamine (2 mL, 15 mmol, 2.1 equiv.) was added, followed by methanesulfonyl chloride (0.6 mL, 7.8 mmol, 1.1 equiv.). The mixture was stirred at 0 °C for 1 h, then warmed to room temperature and stirred for another hour. Water (50 mL) was added and the organic and aqueous phases were separated. The aqueous phase was extracted with dichloromethane (2x), dried with anhydrous Na_2SO_4 , and the resulting suspension was filtered. The filtrate was concentrated in vacuo and the crude product purified by chromatography over a short pad of silica gel (10 % ethyl acetate in hexanes). The product was isolated as a colorless oil (1.6 g, 7.1 mmol, 99 %) and immediately used in the following reaction. **9-iodonon-1-yne:** Non-8-yn-1-yl methanesulfonate (1.6 g, 7.1 mmol, 1 equiv.) was dissolved in DMSO (15 mL) and sodium iodide was added (3.1 g, 20.5 mmol, 3 equiv.) and the mixture was stirred at 50 °C for 15 h. Ethyl acetate (30 mL) and water (30 mL) were added and the organic and aqueous phases were separated. The organic phase was washed with brine (5x), dried with anhydrous Na_2SO_4 , the suspension was filtered and the

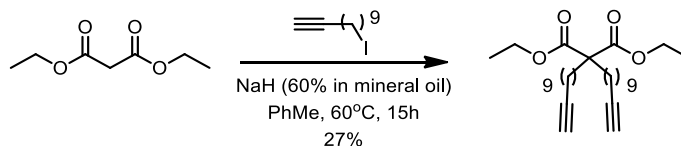
filtrate was concentrated *in vacuo* to afford the pure product as a colorless oil (1.5 g, 6.2 mmol, 87%). The NMR data were in agreement with that found in the literature.⁹



Undec-10-yn-1-yl methanesulfonate: 10-undecyn-1-ol (1 g, 5.95 mmol, 1 equiv.) was dissolved in anhydrous dichloromethane (50 mL) and cooled to 0 °C. Triethylamine (2 mL, 15 mmol, 2.5 equiv.) was added, followed by methanesulfonyl chloride (0.6 mL, 7.8 mmol, 1.3 equiv.). The mixture was stirred at 0 °C for 1 h, then warmed to room temperature and stirred for another hour. Water (50 mL) was added and the organic and aqueous phases were separated. The aqueous phase was extracted with dichloromethane (2x), dried with anhydrous Na₂SO₄, and the resulting suspension was filtered. The filtrate was concentrated *in vacuo* and the crude product purified by chromatography over a short pad of silica gel (10 % ethyl acetate in hexanes). The product was isolated as a colorless oil (1.5 g, 99 %) and immediately used in the following reaction. **10-iodoundec-1-yne:** Undec-10-yn-1-yl methanesulfonate (1.46 g, 5.95 mmol, 1 equiv.) was dissolved in DMSO (13 mL) and sodium iodide was added (3.1 g, 20.5 mmol, 3.5 equiv.) and the mixture was stirred at 50 °C for 15 h. Ethyl acetate (30 mL) and water (30 mL) were added and the organic and aqueous phases were separated. The organic phase was washed with brine (5x), dried with anhydrous Na₂SO₄, the suspension was

⁹ Knapp, Jr. F. F.; Srivastava, P. C.; Callahan, A. P.; Cunningham, E. B.; Kabalka, G. W.; Sastry, K. A. *J. Med. Chem.* **1984**, *27*, 57.

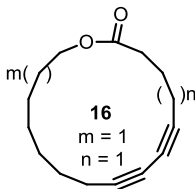
filtered and the filtrate was concentrated *in vacuo* to afford the pure product as a colorless oil (1.36 g, 4.9 mmol, 82 %). The NMR data were in agreement with that found in the literature.¹⁰



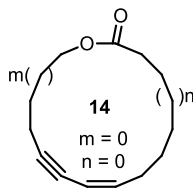
Diethyl 2,2-di(undec-10-yn-1-yl)malonate: Diethylmalonate (83.2 mg, 0.52 mmol, 1 equiv.) was dissolved in anhydrous toluene (2 mL) in a flamed dried flask equipped with a stir bar and a condenser. NaH (60 % in mineral oil, 104 mg, 2.6 mmol, 5 equiv.) was added at room temperature, then 10-iodoundec-1-yne (440 mg, 1.59 mmol, 3 equiv.) was added in one portion as a toluene solution (1 mL). The mixture was warmed to 60 °C and stirred for 15 h. The reaction was then cooled back to room temperature, quenched with H₂O and extracted with ethyl acetate (3x). The organic phases were dried over anhydrous Na₂SO₄, and the resulting suspension was filtered. The filtrate was concentrated *in vacuo* and the crude product purified by chromatography (5 % ethyl acetate in hexanes). The desired product was isolated as a colorless oil (65 mg, 27 %). ¹H NMR (300 MHz, CDCl₃) δ = 4.17 (q, *J* = 6.0 Hz, 4H), 2.17 (td, *J* = 9.0, 3.0 Hz, 4H), 1.93 (t, *J* = 3.0, 2H), 1.87 – 1.82 (m, 4H), 1.56 - 1.46 (m, 4H), 1.43 - 1.10 (m, 30H); ¹³C NMR (75 MHz, CDCl₃) δ = 172.0, 84.7, 68.0, 60.9, 57.5, 32.1, 29.8, 29.3, 29.2, 29.0, 28.7, 28.4, 23.9, 18.3, 14.1 ppm; HRMS (ESI) *m/z* calculated for C₂₉H₄₉O₄ [M+H]⁺, 461.3625; found: 461.3633.

¹⁰ Crisp, T. G.; Gore, J. *Tetrahedron* **1997**, 53, 1505-1522.

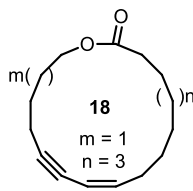
SYNTHESIS OF MACROCYCLES



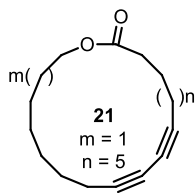
General procedure for the macrocyclization of diynes under Glaser-Hay oxidative coupling conditions: Macrocycle (**3**): To a vial equipped with a stirring bar was added CuCl_2 (5.5 mg, 0.48 mmol, 25 mol%) and $\text{Ni}(\text{NO}_3)_2 \cdot 6\text{H}_2\text{O}$ (9.3 mg, 0.48 mmol, 25 mol %). Polyethylene glycol 400 (3.33 mL), triethylamine (0.05 mL, 0.36 mmol, 3 equiv.) and pyridine (0.05 mL, 0.6 mmol, 5 equiv.) were added and the mixture was stirred at room temperature for 15 min or until the metals were solubilized. The diyne (0.12 mmol) was added to the homogenous mixture as a methanol solution (1.67 mL) in one portion. Oxygen was bubbled in the solution for 5 min and the vial was then closed with a screw cap. The reaction was warmed to 60 °C and monitored by TLC for consumption of the starting material (oxygen was bubbled again through the solution every 12 h). When the starting material was completely consumed (TLC), the reaction was cooled to room temperature and the crude mixture was loaded directly on a silica column. Purification by chromatography (100 % hexanes→10 % ethyl acetate in hexane) afforded the product as a colorless semi-solid (31 mg, 73 %). ^1H NMR (400 MHz, CDCl_3) δ = 4.09 (t, J = 8 Hz, 2H), 2.41 - 2.33 (m, 4H), 2.24 (t, J = 5.9 Hz, 2H), 1.93 - 1.87 (m, 2H), 1.77 - 1.70 (m, 2H), 1.55 - 1.50 (m, 4H), 1.46 - 1.36 (m, 4H); ^{13}C NMR (100 MHz, CDCl_3) δ ppm = 173.4, 77.7, 75.7, 67.0, 66.6, 64.3, 33.3, 26.5, 25.2, 25.1, 24.9, 23.5, 22.1, 19.0, 18.1; HRMS (ESI) m/z calculated for $\text{C}_{15}\text{H}_{21}\text{O}_2$ $[\text{M}+\text{H}]^+$, 233.1536; found: 233.1531.



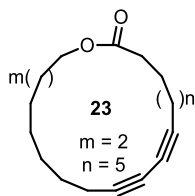
Macrocycle (8): Following the general procedure described above, macrocycle **8** was isolated. (15 mg, 62 %). ^1H NMR (300 MHz, CDCl_3) δ ppm 4.24 (t, $J = 6$ Hz, 2H); 2.69 (t, $J = 6$ Hz, 2H); 2.28 – 2.21 (m, 4H); 1.92 – 1.77 (m, 8H); ^{13}C NMR (125 MHz, CDCl_3) δ ppm = 173.9, 82.8, 82.5, 67.8, 67.7, 62.9, 32.3, 27.7, 25.8, 24.9, 23.3, 19.0, 10.1; HRMS (ESI) m/z calculated for $\text{C}_{13}\text{H}_{17}\text{O}_2$ $[\text{M}+\text{H}]^+$, 205.1223; found: 205.1225.



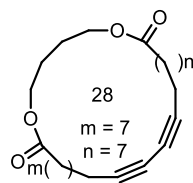
Macrocycle (9): Following the general procedure described above, macrocycle **9** was isolated. (24 mg, 74 %) ^1H NMR (300 MHz, CDCl_3) δ = 4.17 (t, $J = 6.3$ Hz, 2H), 2.36 - 2.26 (m, 8H), 1.88 - 1.78 (m, 2H), 1.68 - 1.26 (m, 12H); ^{13}C NMR (125 MHz, CDCl_3) δ ppm = 173.8, 78.0, 76.9, 66.6, 66.3, 63.6, 34.8, 28.7, 28.0, 27.8, 27.6, 27.0, 26.8, 25.0, 24.6, 18.9, 18.8; HRMS (ESI) m/z calculated for $\text{C}_{17}\text{H}_{25}\text{O}_2$ $[\text{M}+\text{H}]^+$, 261.1849; found: 261.1844.



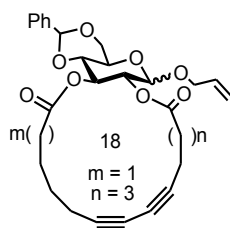
Macrocycle (10): Following the general procedure described above, macrocycle **10** was isolated. (30 mg, 0.1 mmol, 81 %). ^1H NMR (300 MHz, CDCl_3) $\delta = 4.10$ (t, $J = 6.5$ Hz, 2H), 2.36 - 2.26 (m, 6H), 1.70 - 1.61 (m, 6H), 1.50 - 1.26 (m, 14H); ^{13}C NMR (125 MHz, CDCl_3) δ ppm = 174.0, 77.6, 77.2, 66.0, 65.8, 64.2, 34.3, 29.1, 28.5, 28.23, 28.22, 28.19, 27.93, 27.91, 27.63, 27.58, 25.7, 25.0, 19.03, 19.02; HRMS (ESI) m/z calculated for $\text{C}_{20}\text{H}_{31}\text{O}_2$ $[\text{M}+\text{H}]^+$, 303.2319; found: 303.2325.



Macrocycle (11): Following the general procedure described above, macrocycle **11** was isolated. (31 mg, 78 %). ^1H NMR (300 MHz, CDCl_3) $\delta = 4.09$ (t, $J = 6.5$ Hz, 2H), 2.35 - 2.26 (m, 6H), 1.68 - 1.62 (m, 6H), 1.53 - 1.26 (m, 16H); ^{13}C NMR (125 MHz, CDCl_3) δ ppm = 174.0, 77.50, 77.46, 65.9, 65.7, 64.2, 34.2, 28.88, 28.86, 28.7, 28.4, 28.32, 28.28, 28.23, 28.1, 27.83, 27.81, 27.5, 25.7, 25.0, 19.07, 18.99, ; HRMS (ESI) m/z calculated for $\text{C}_{22}\text{H}_{35}\text{O}_2$ $[\text{M}+\text{H}]^+$, 331.2632; found: 331.2640.

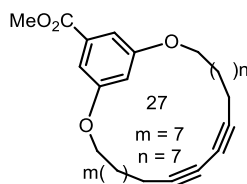


Macrocycle (12): Following the general procedure described above, macrocycle **12** was isolated. (50 mg, 98 %). ^1H NMR (400 MHz, CDCl_3) δ = 4.16 - 4.04 (m, 4H), 2.32 (t, J = 7.6 Hz, 4H), 2.27 (t, J = 6.3 Hz, 4H), 1.72 (m, 4H), 1.69 - 1.60 (m, 4H), 1.55 - 1.39 (m, 8H), 1.38 - 1.28 (m, 12H); ^{13}C NMR (75 MHz, CDCl_3) δ ppm = 173.9, 77.4, 65.6, 63.8, 34.3, 28.69, 28.68, 28.6, 28.2, 27.8, 25.4, 24.9, 19.1; HRMS (ESI) m/z calculated for $\text{C}_{26}\text{H}_{41}\text{O}_4$ $[\text{M}+\text{H}]^+$, 417.2999; found: 417.3006.

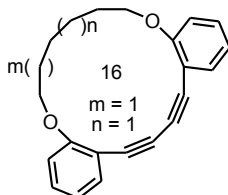


Macrocycle (13): Following the general procedure described above, macrocycle **13** was isolated. (42 mg, 0.08 mmol, 67 %). ^1H NMR (300 MHz, CDCl_3) (mixture of α and β anomers (0.75 : 0.25), data reported for major anomer only), δ = 7.49 - 7.40 (m, 2H), 7.39 - 7.31 (m, 3H), 5.86 (dddd, J = 17.0, 10.8, 5.8, 5.2 Hz, 1H), 5.70 (t, J = 10.0 Hz, 1H), 5.51 (s, 1H), 5.38 - 5.08 (m, 2 H), 4.83 (dd, J = 10.0, 3.7 Hz, 1 H), 4.30 (dd, J = 10.2, 4.8 Hz, 1H), 4.21 (ddt, J = 16.0, 8.0, 4.0 Hz, 1H), 4.06 - 3.94 (m, 2H), 3.77 (t, J = 12.0 Hz, 1H), 3.62 (t, J = 12.0 Hz, 1H), 2.85 - 2.69 (m, 1H), 2.65 - 2.51 (m, 1H), 2.43 - 2.26 (m, 6H), 1.98 - 1.64 (m, 5H), 1.63 - 1.43 (m, 4H); ^{13}C NMR (176 MHz, CDCl_3) δ ppm = 173.3, 172.4, 137.0, 133.3, 129.0, 128.2, 126.1, 117.8, 101.4, 95.6, 79.7, 78.1, 77.8, 71.9, 68.8, 68.7, 68.4, 62.6, 33.6, 33.4, 27.7, 27.5,

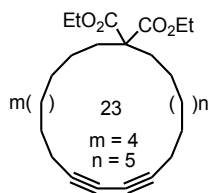
26.1, 26.0, 24.1, 23.6, 19.1, 18.7, 18.1, 18.0; HRMS (ESI) m/z calculated for $C_{30}H_{34}NaO_8$ $[M+Na]^+$, 545.2146; found: 545.2147.



Macrocycle (14): Following the general procedure described above, macrocycle **14** was isolated. (39 mg, 0.082 mmol, 69 %). ¹H NMR (300 MHz, CDCl₃) δ = 7.17 (d, J = 2.2 Hz, 2H), 6.70 (t, J = 2.2 Hz, 1H), 4.08 - 3.99 (t, J = 6.0 Hz, 4H), 3.91 (s, 3H), 2.25 (t, J = 6.4 Hz, 4H), 1.84 - 1.71 (m, 4H), 1.65 - 1.14 (m, 28H); ¹³C NMR (125 MHz, CDCl₃) δ ppm = 167.0, 160.1, 131.8, 107.6, 107.4, 77.5, 68.0, 65.5, 52.2, 29.1, 28.7, 28.73, 28.66, 28.65, 28.3, 28.1, 25.8, 19.1 ppm; HRMS (ESI) m/z calculated for $C_{30}H_{43}O_4$ $[M+H]^+$, 467.3156; found: 467.3165.



Macrocycle (16): Following the general procedure described above, macrocycle **16** was isolated. (37.3 mg, 98 %). ¹H NMR (300 MHz, CDCl₃) δ = 7.39 (dd, J = 7.6, 1.7 Hz, 2H), 7.33 - 7.28 (m, 2H), 6.96 - 6.86 (m, 4H), 4.09 (t, J = 5.3 Hz, 4H), 1.96 - 1.85 (m, 4H), 1.84 - 1.74 (m, 4H); ¹³C NMR (75 MHz, CDCl₃) δ ppm = 162.5, 132.0, 130.4, 120.8, 113.7, 112.6, 79.8, 79.2, 70.2, 30.0, 27.6 ppm; HRMS (ESI) m/z calculated for $C_{22}H_{21}O_2$ $[M+H]^+$, 317.1536; found: 317.1545.

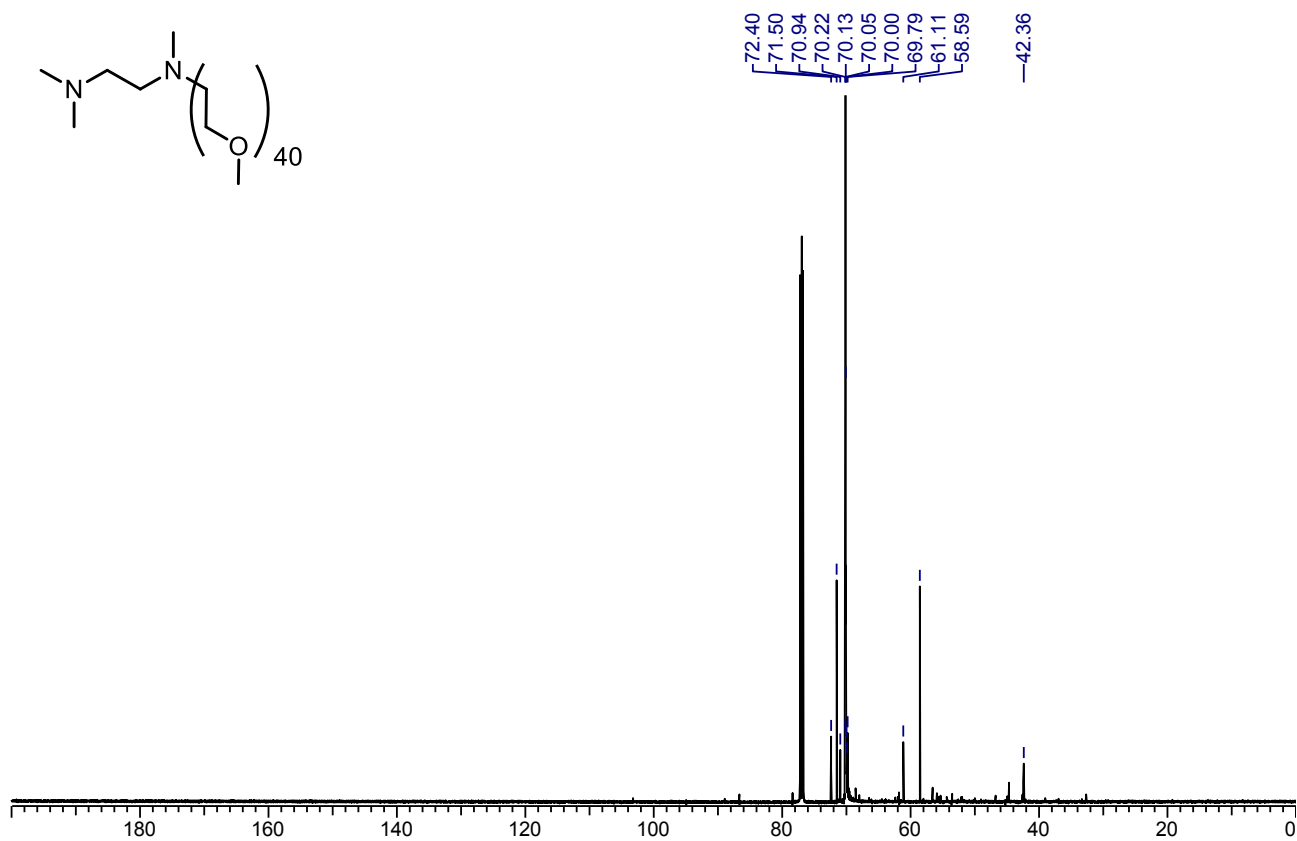
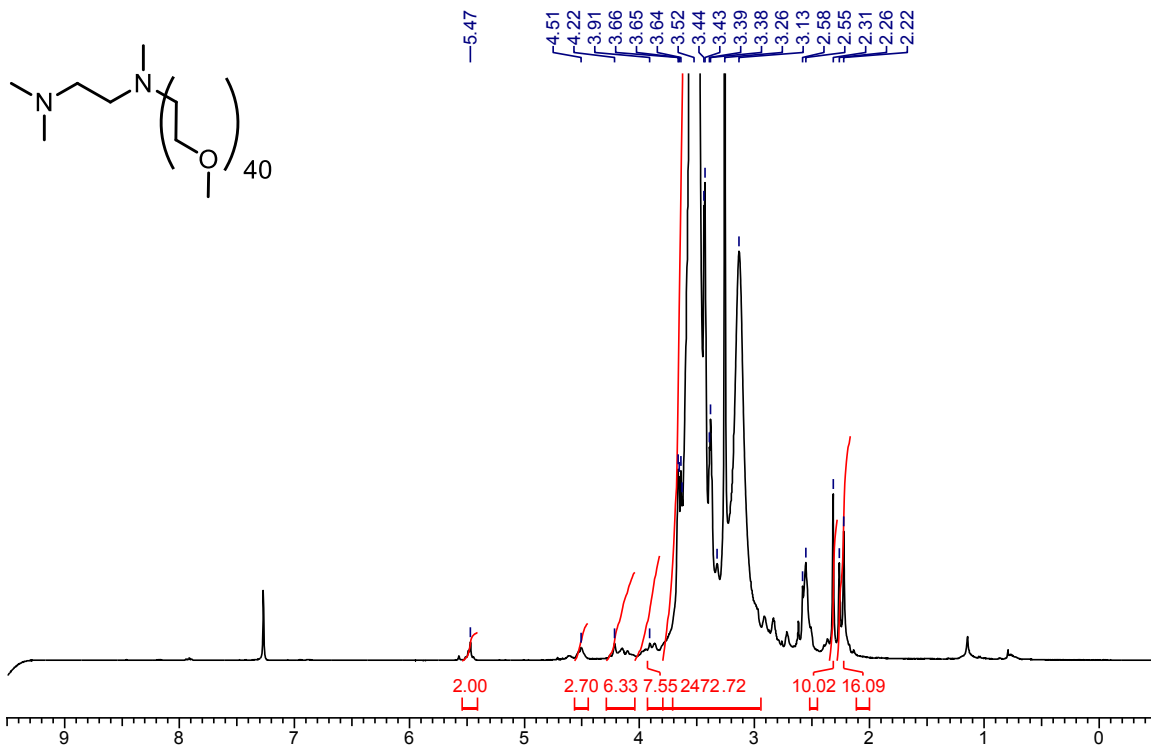


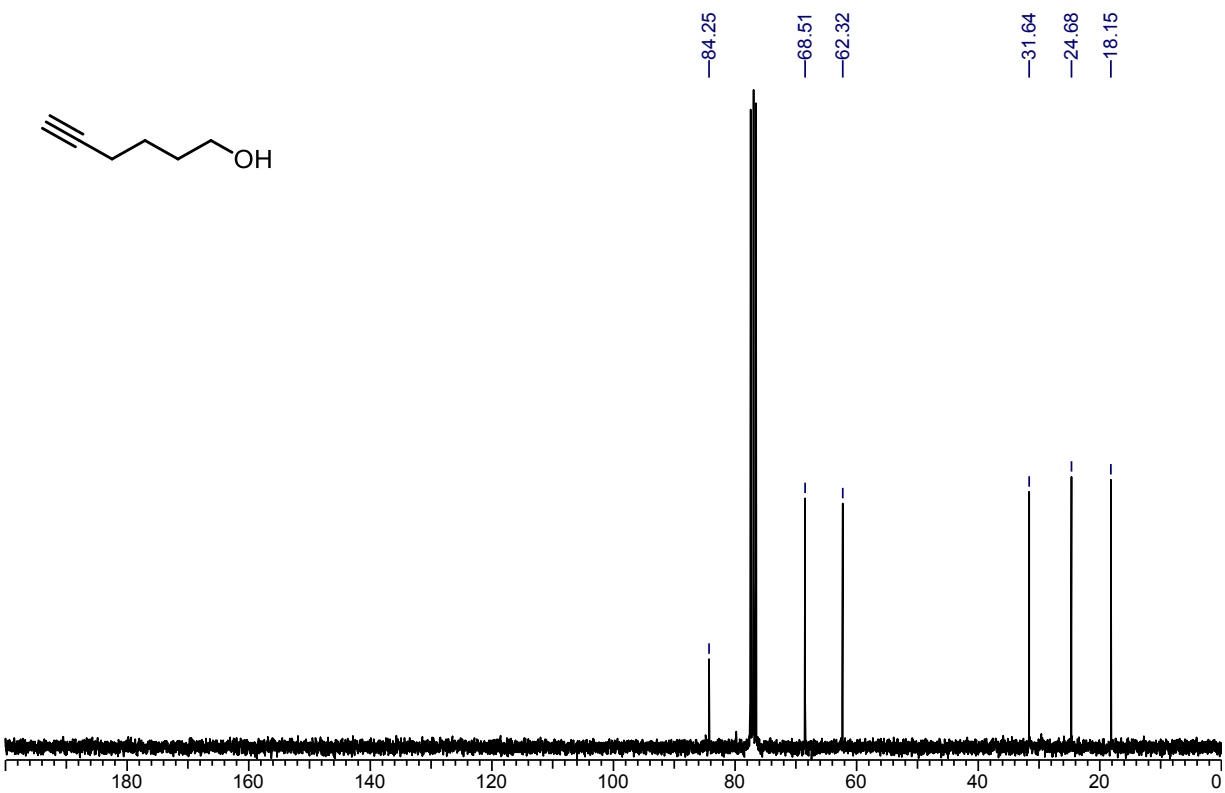
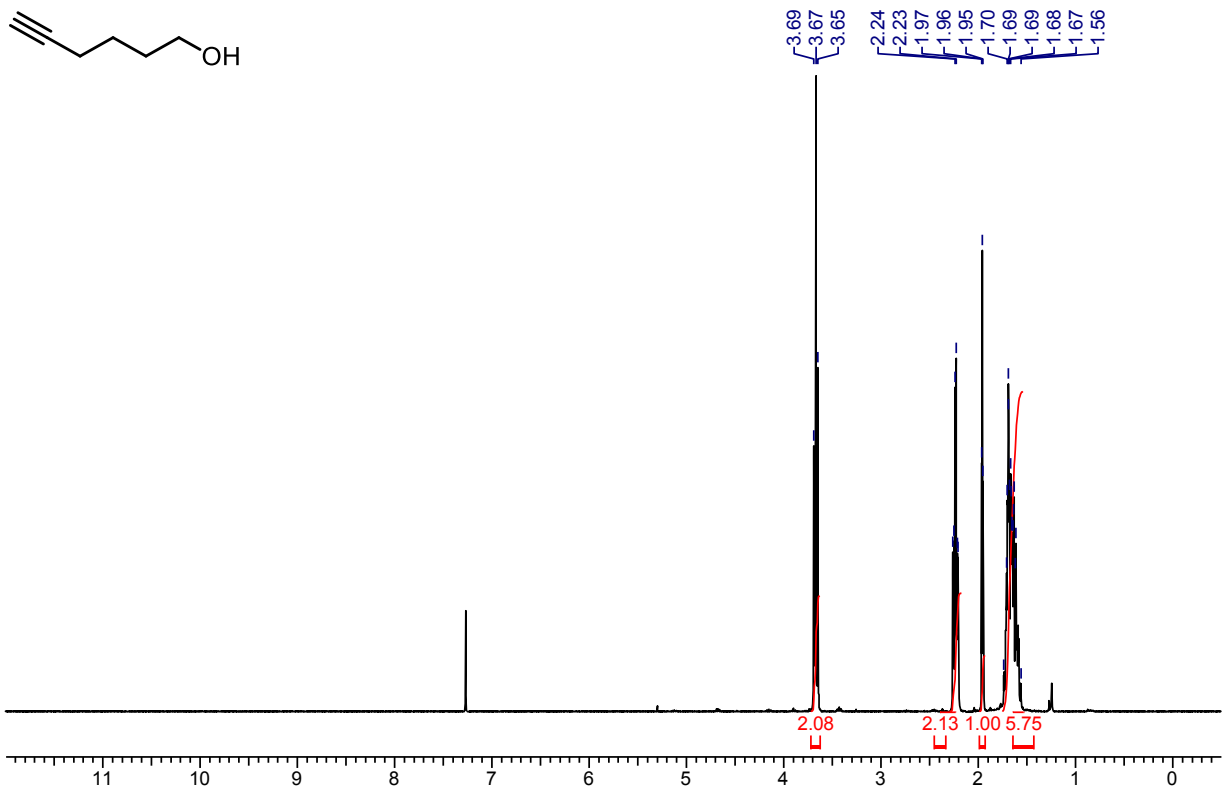
Macrocycle (15): Following the general procedure described above, macrocycle **15** was isolated. (20 mg, 0.044 mmol, 63 %). ^1H NMR (400 MHz, CDCl_3) δ = 4.18 (q, J = 8 Hz, 4H), 2.30 (t, J = 4 Hz, 4H), 1.91 -1.87 (m, 4H), 1.49-1.43 (m, 8H), 1.34-1.26 (m, 20H), 1.24 (t, J = 4 Hz, 6H); ^{13}C NMR (75 MHz, CDCl_3) δ ppm = 172.1, 77.2, 61.0, 57.6, 31.3, 29.9, 29.7, 29.1, 28.9, 28.3, 28.2, 27.9, 23.4, 19.2, 14.1 ppm; HRMS (ESI) m/z calculated for $\text{C}_{29}\text{H}_{47}\text{O}_4$ $[\text{M}+\text{H}]^+$, 459.3469; found: 459.3475.

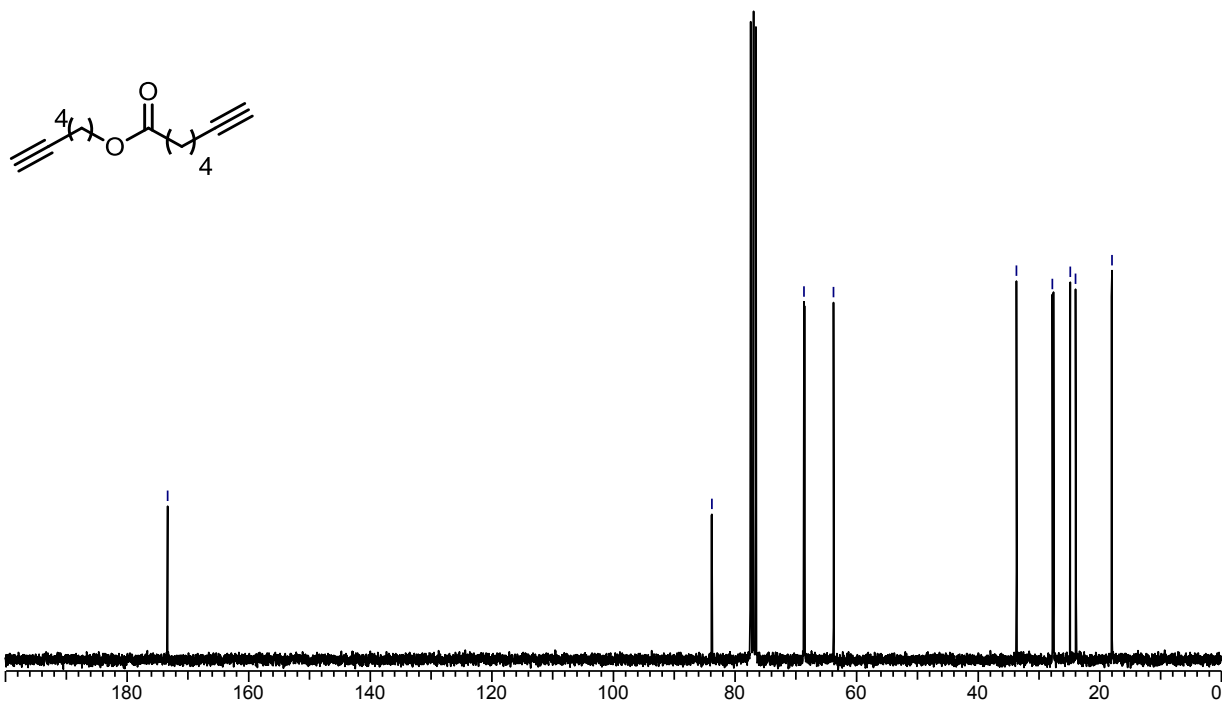
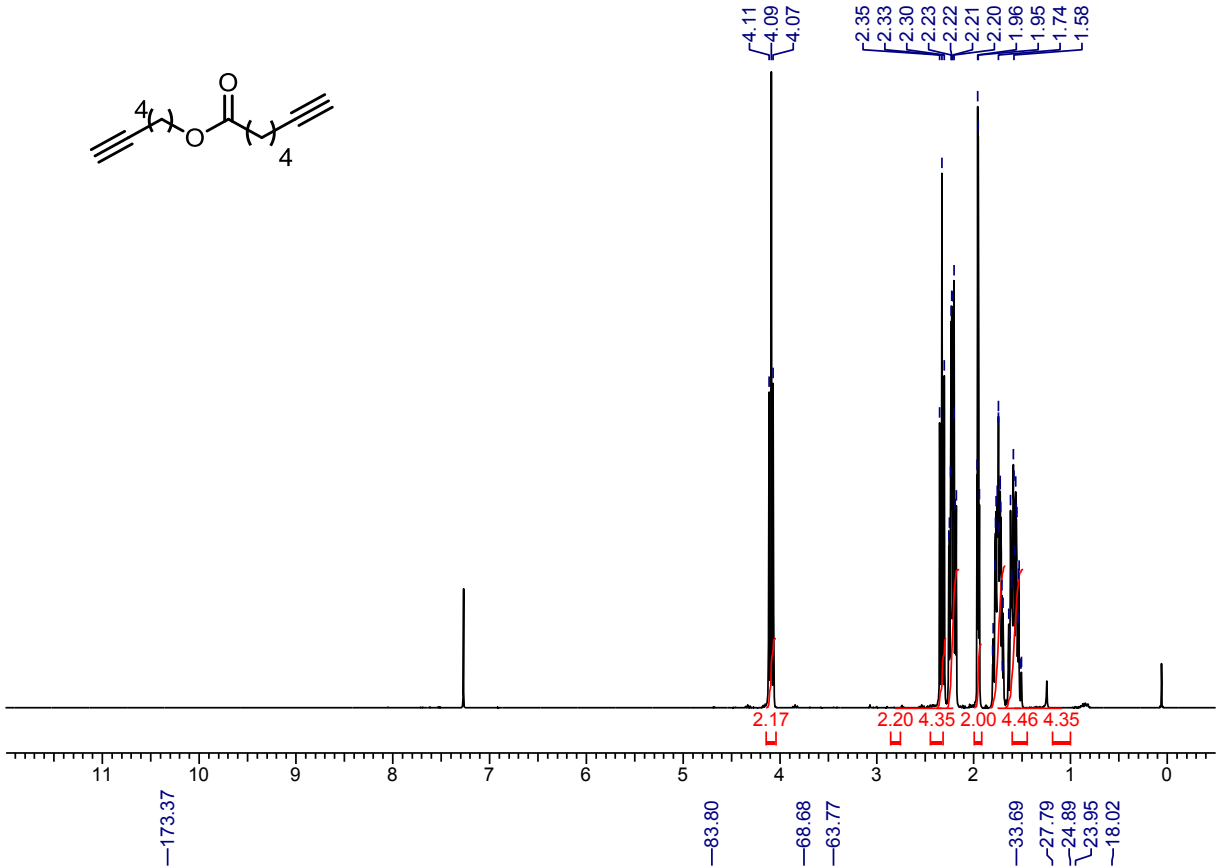
Complete Reference From Text:

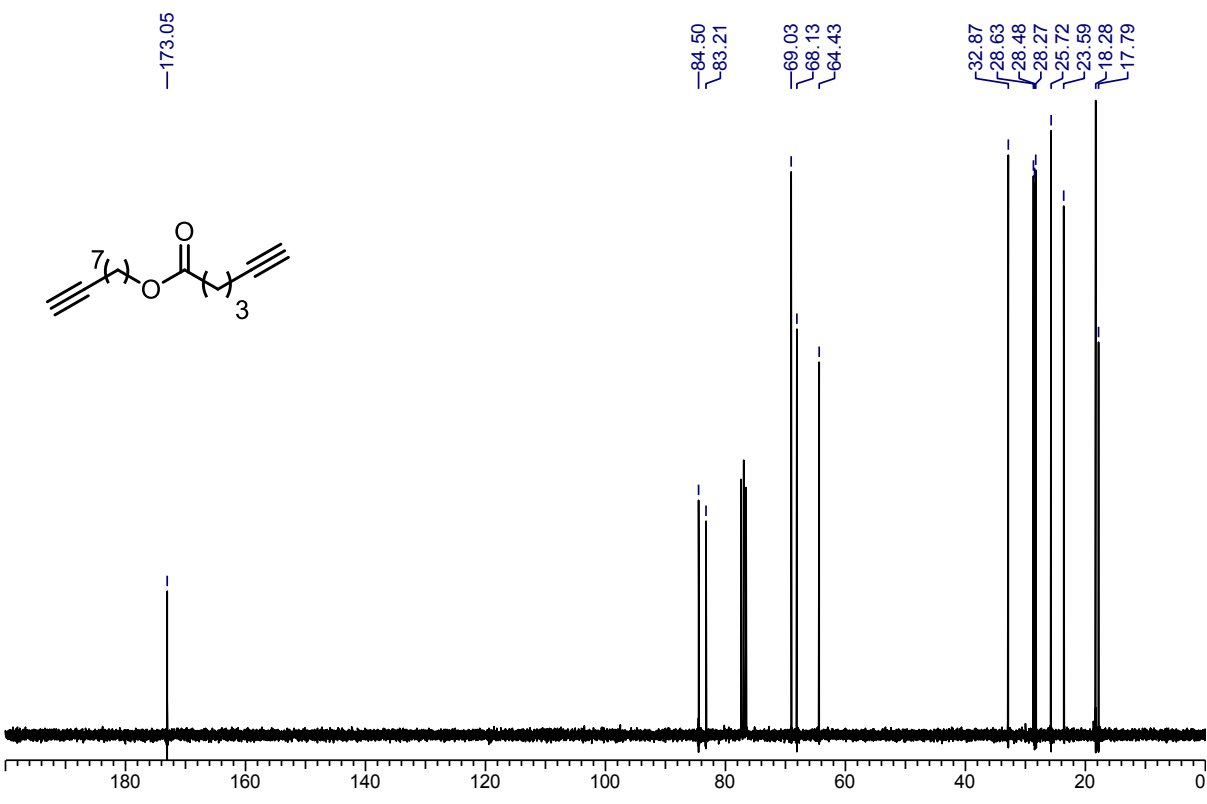
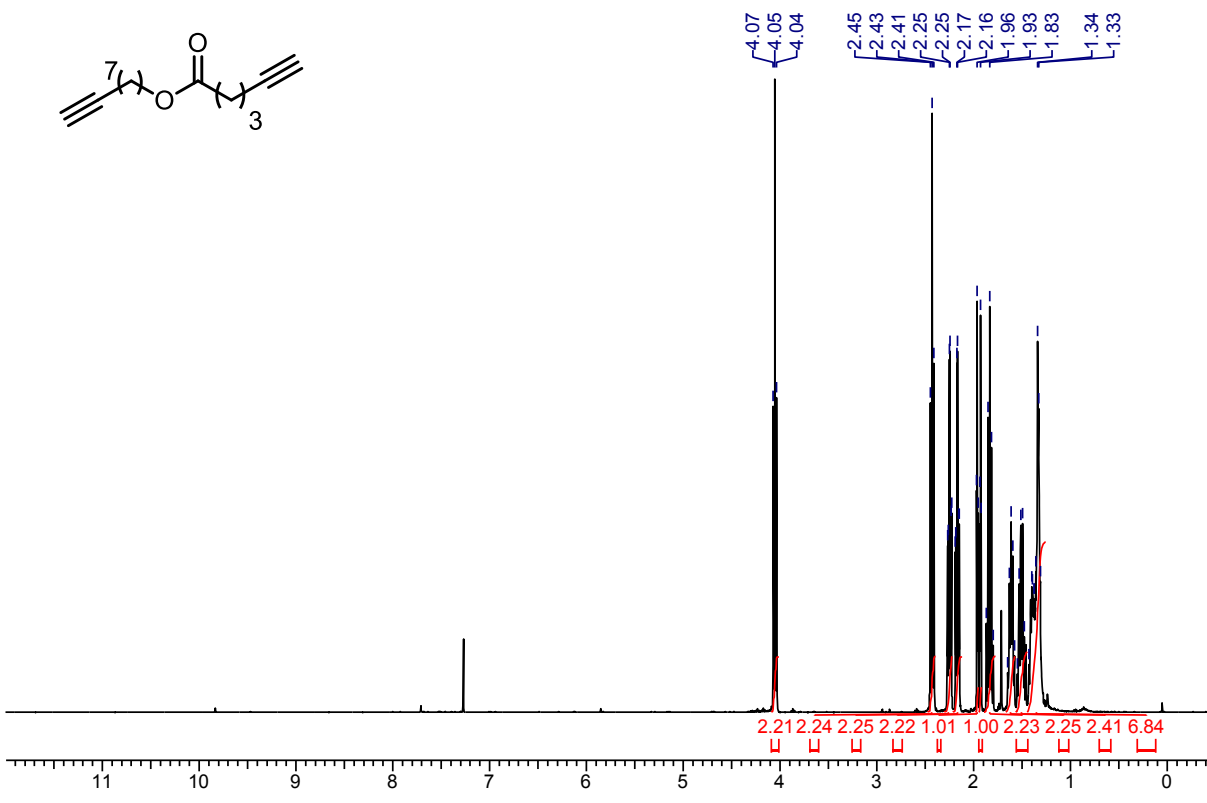
- (3) Lamarre, D.; Anderson, P. C.; Bailey, M.; Beaulieu, P.; Bolger, G.; Bonneau, P.; Bös, M.; Cameron, D. R.; Cartier, M.; Cordingley, M. G.; Faucher, A.-M.; Goudreau, N.; Kawai, S. H.; Kukulj, G.; Lagacé, L.; Laplante, S. R.; Narjes, H.; Poupart, M.-A.; Rancourt, J.; Sentjens, R. E.; St-George, R.; Simoneau, B.; Steinmann, G.; Thibeault, D.; Tsantrizos, Y. S.; Weldon, S. M.; Yong, C.-L.; Llinàs-Brunet, M. *Nature* **2003**, *426*, 186-189.

NMR SPECTRA FOR NEW COMPOUNDS

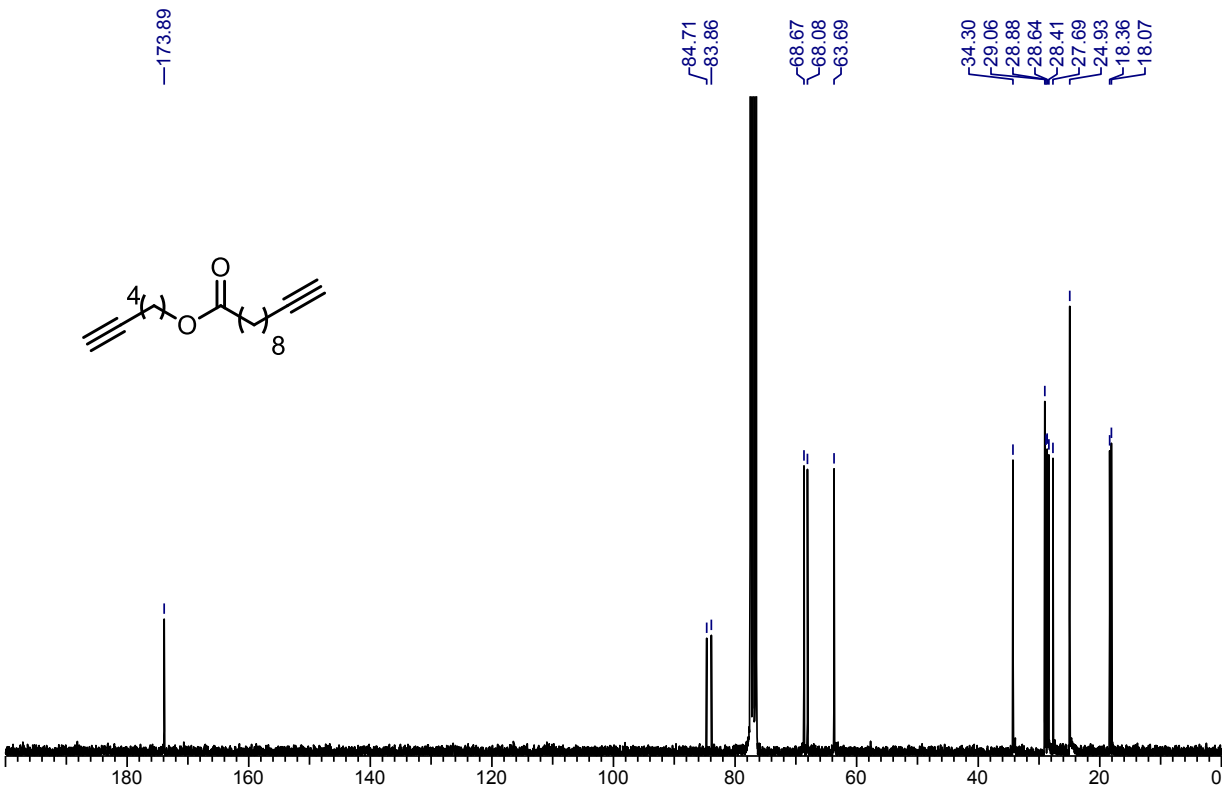
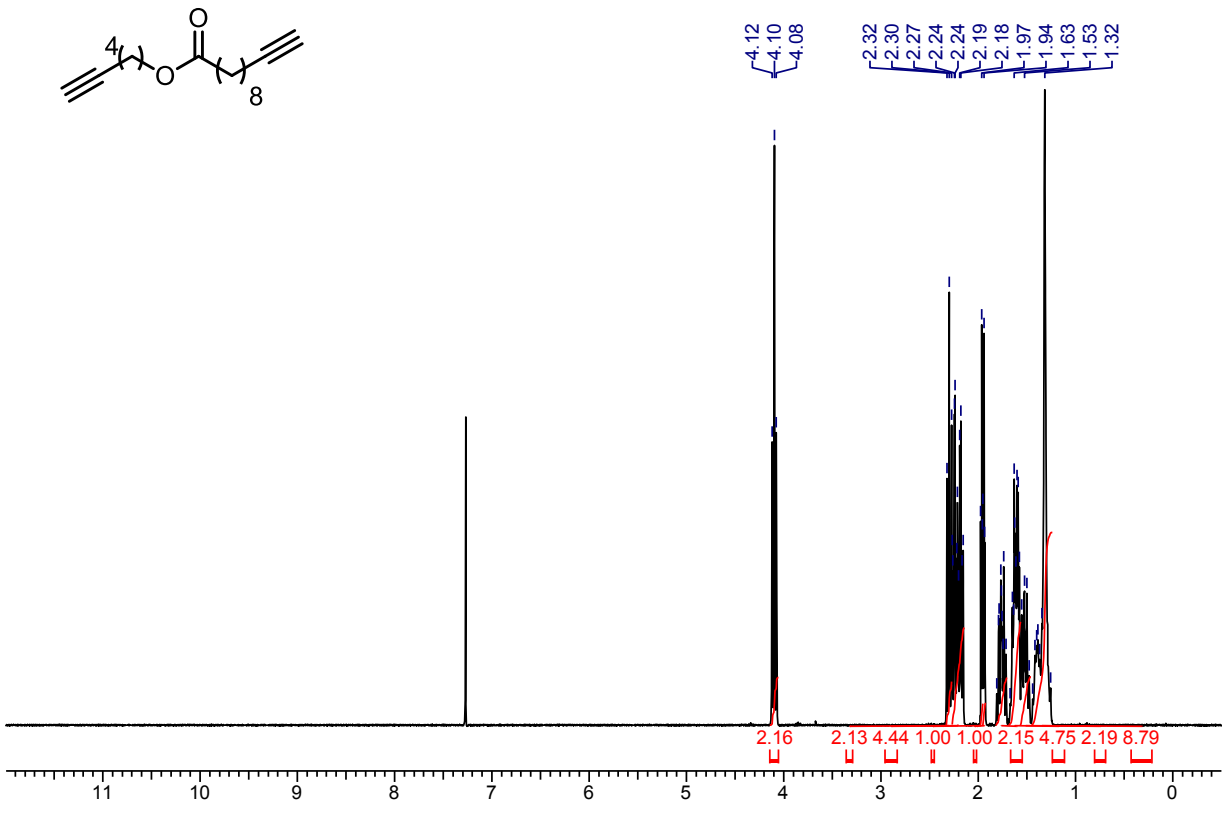


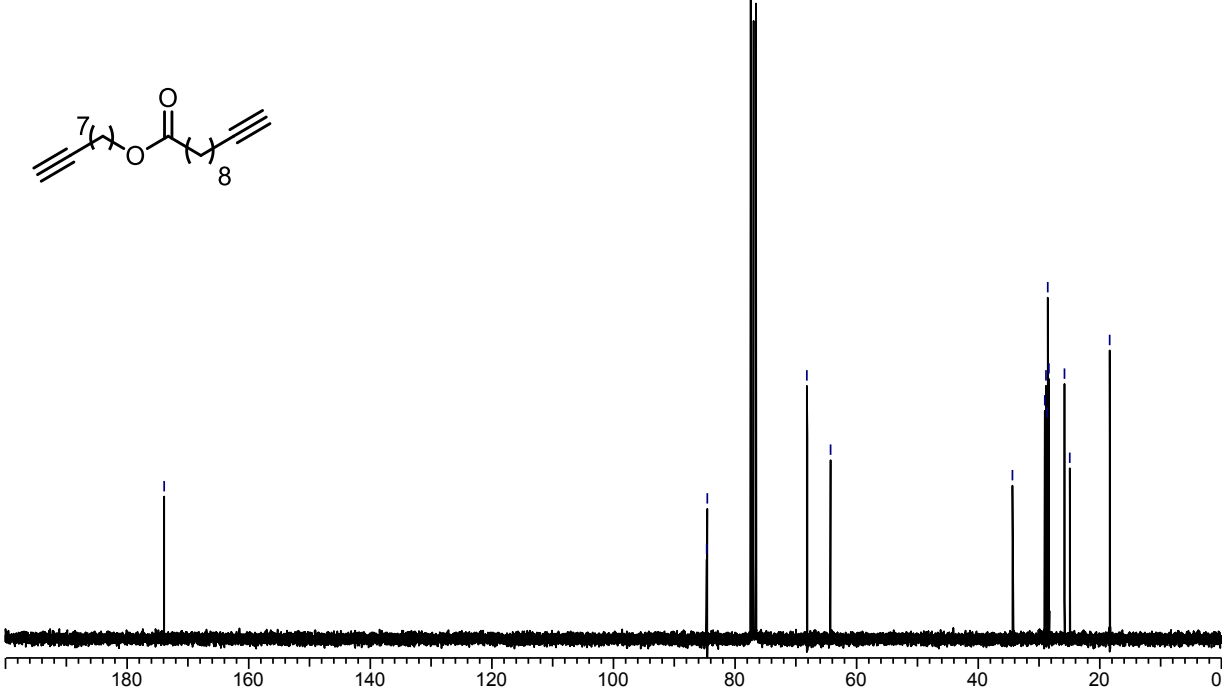
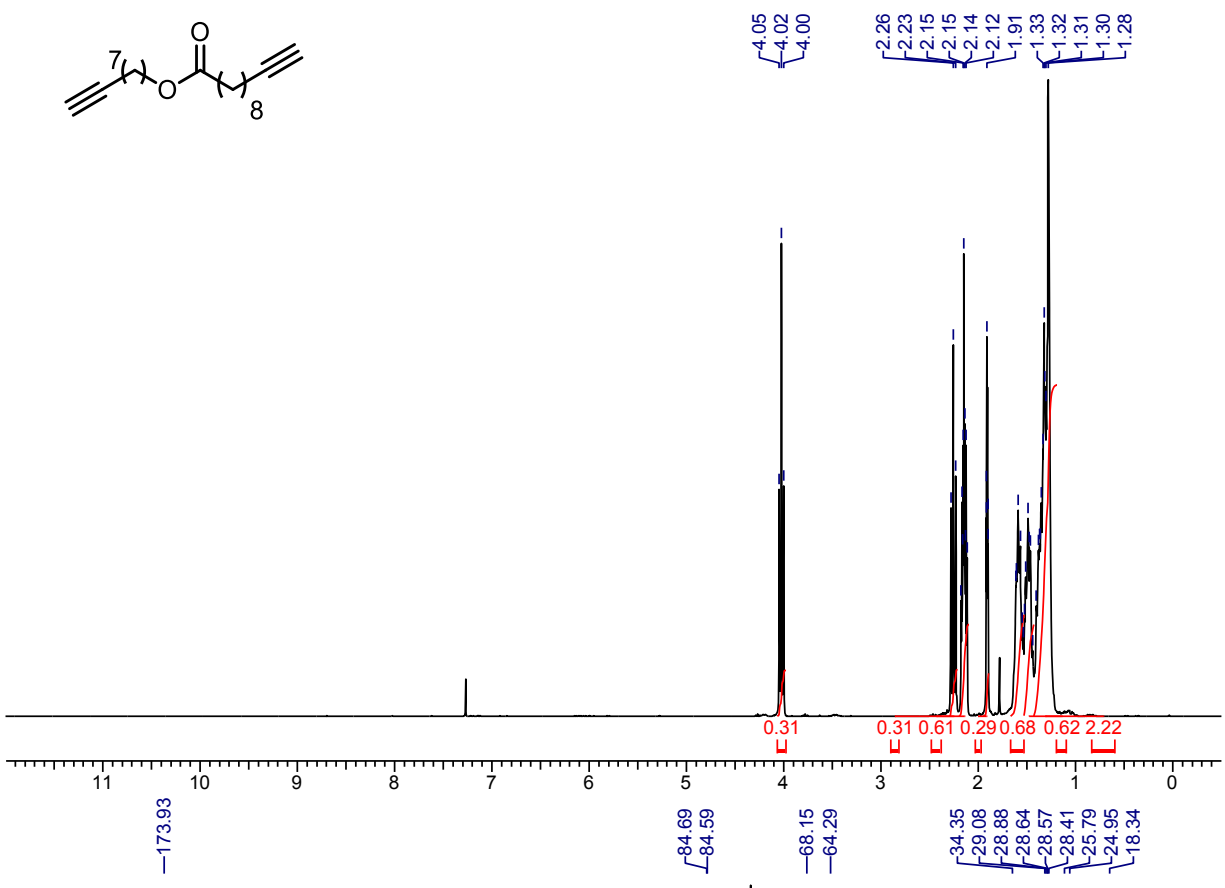




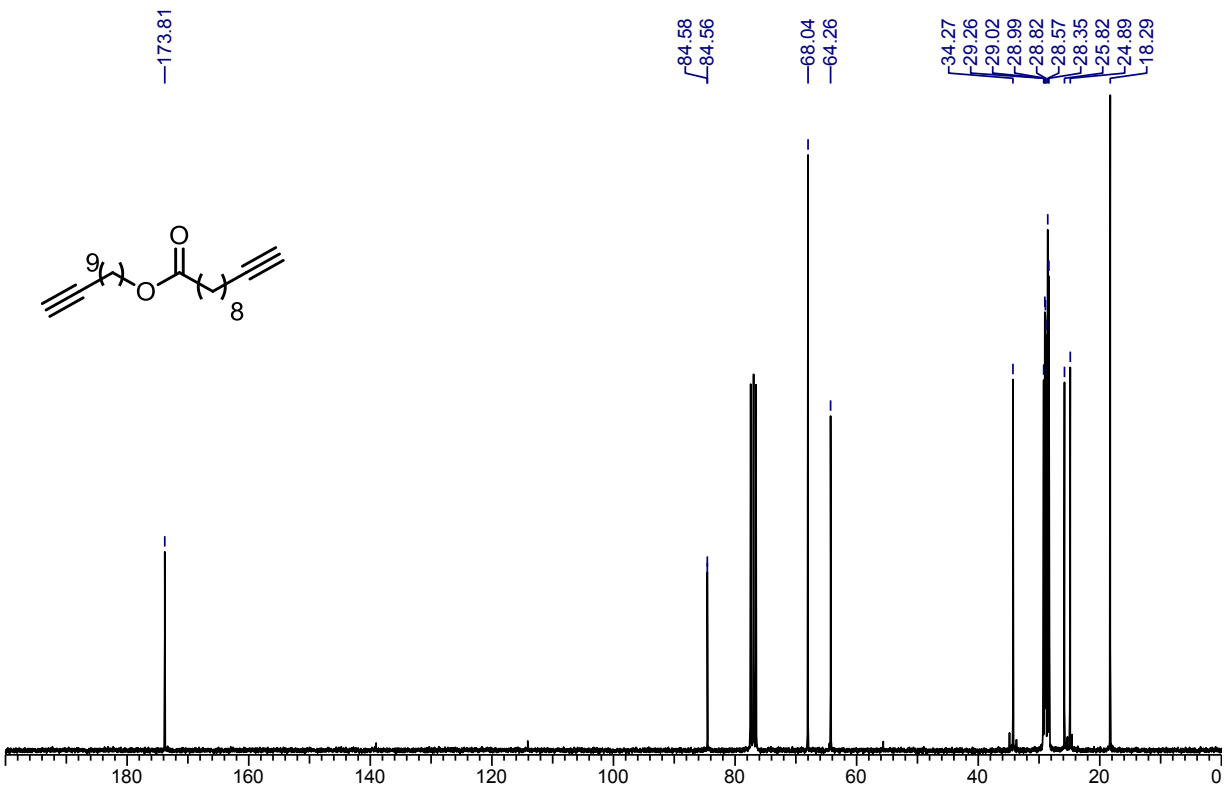
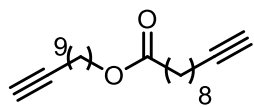
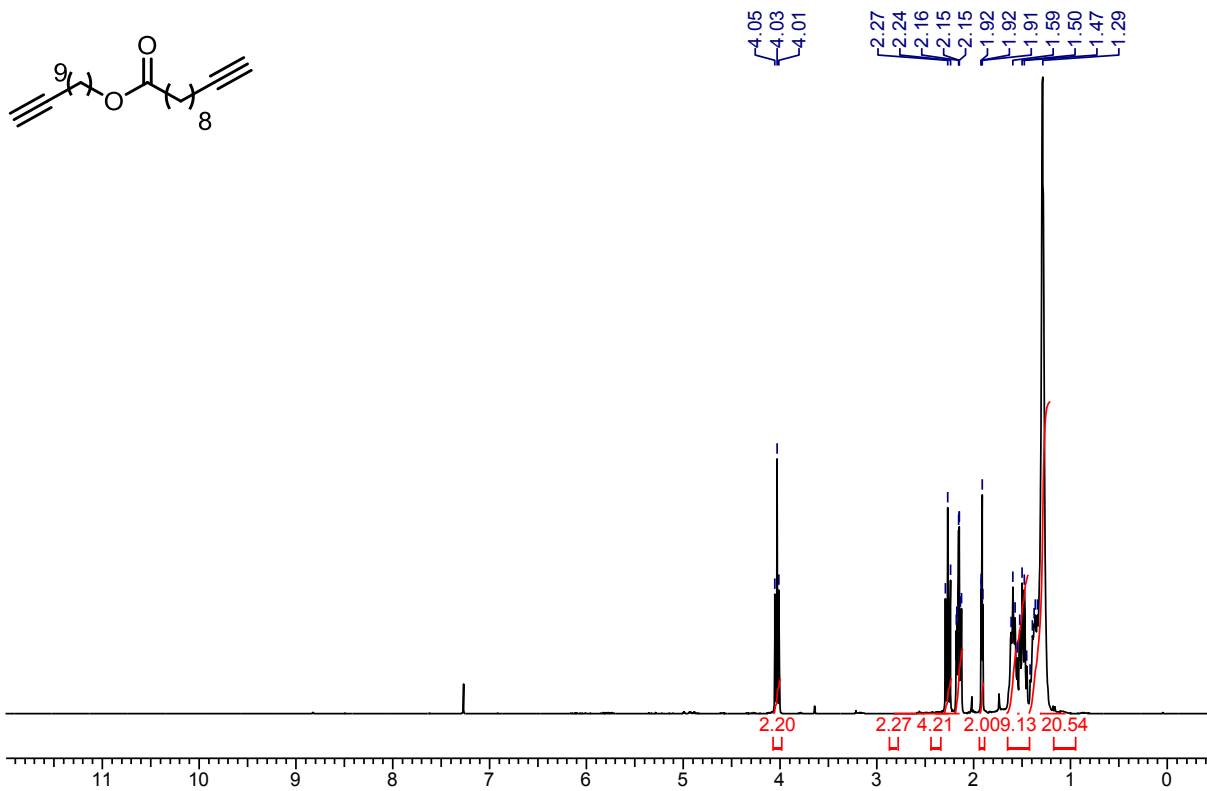
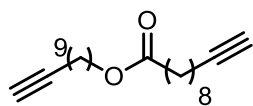


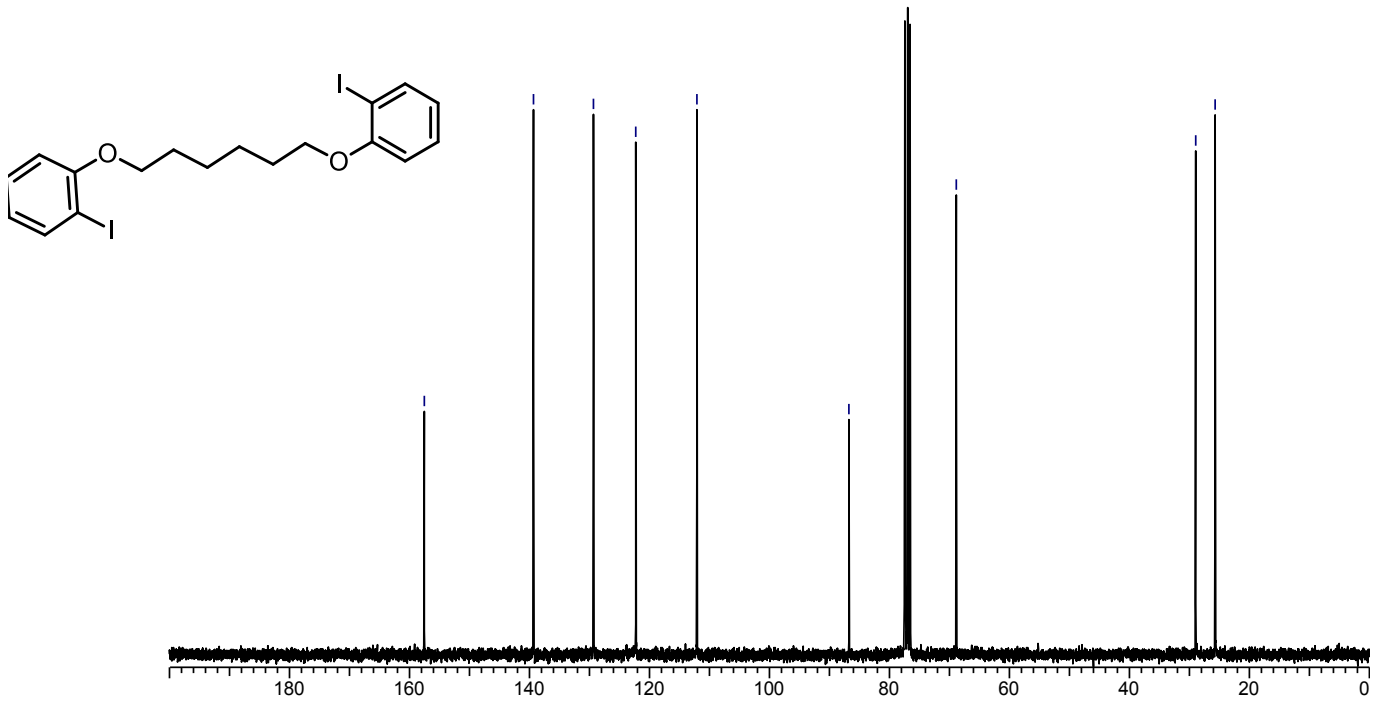
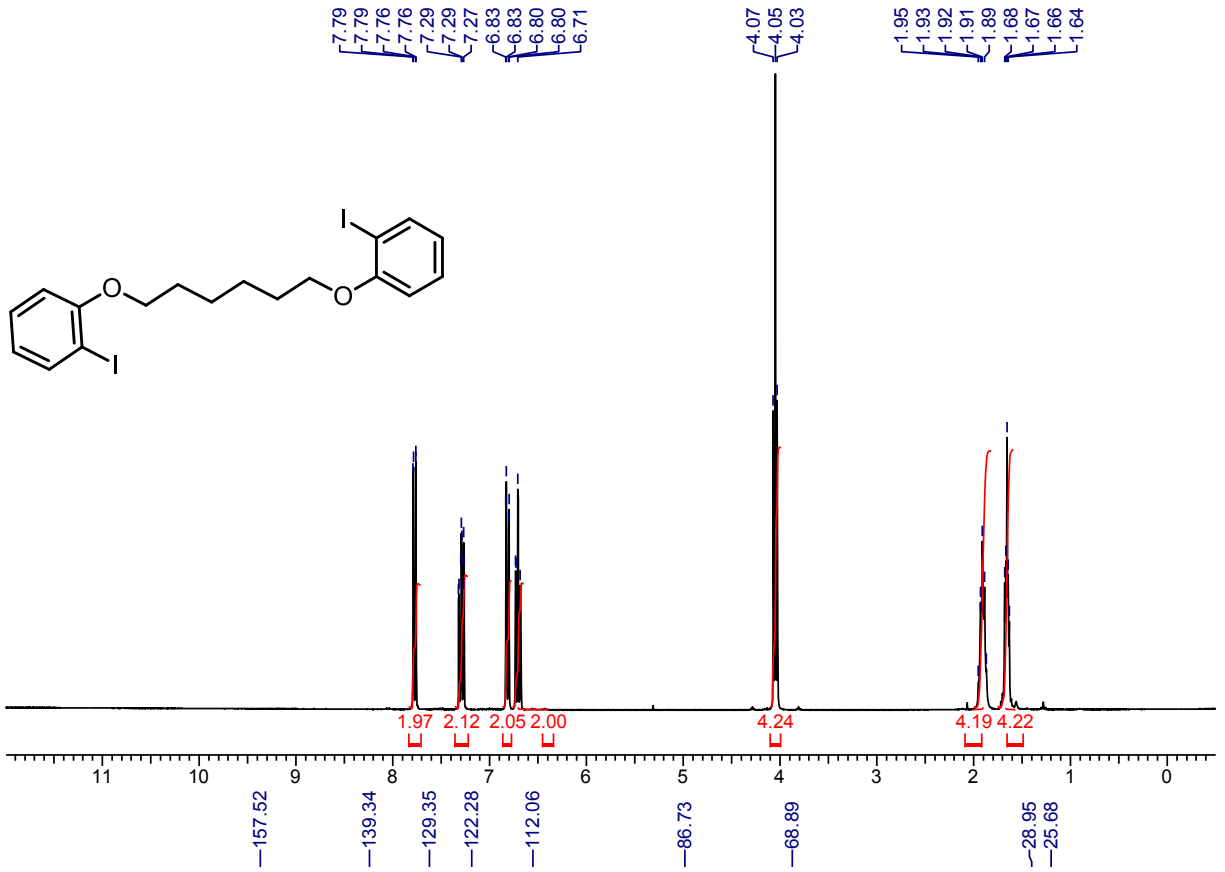
bb

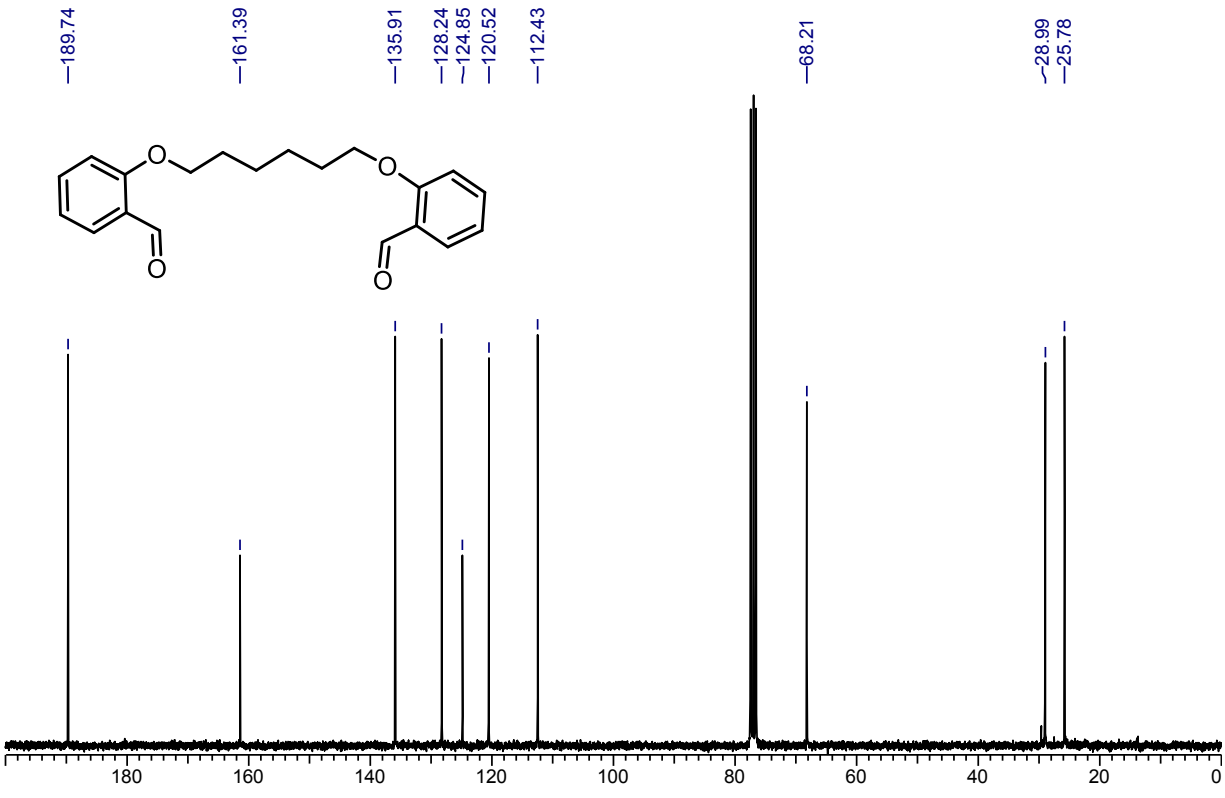
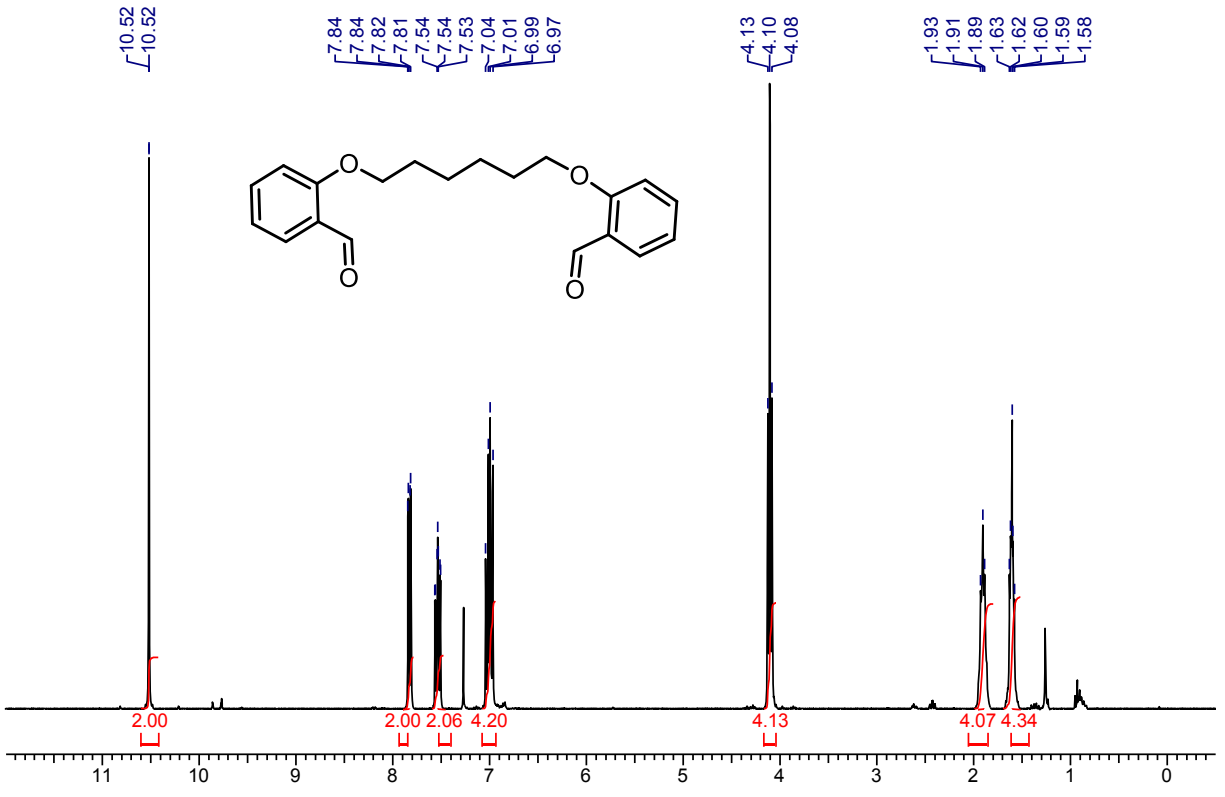


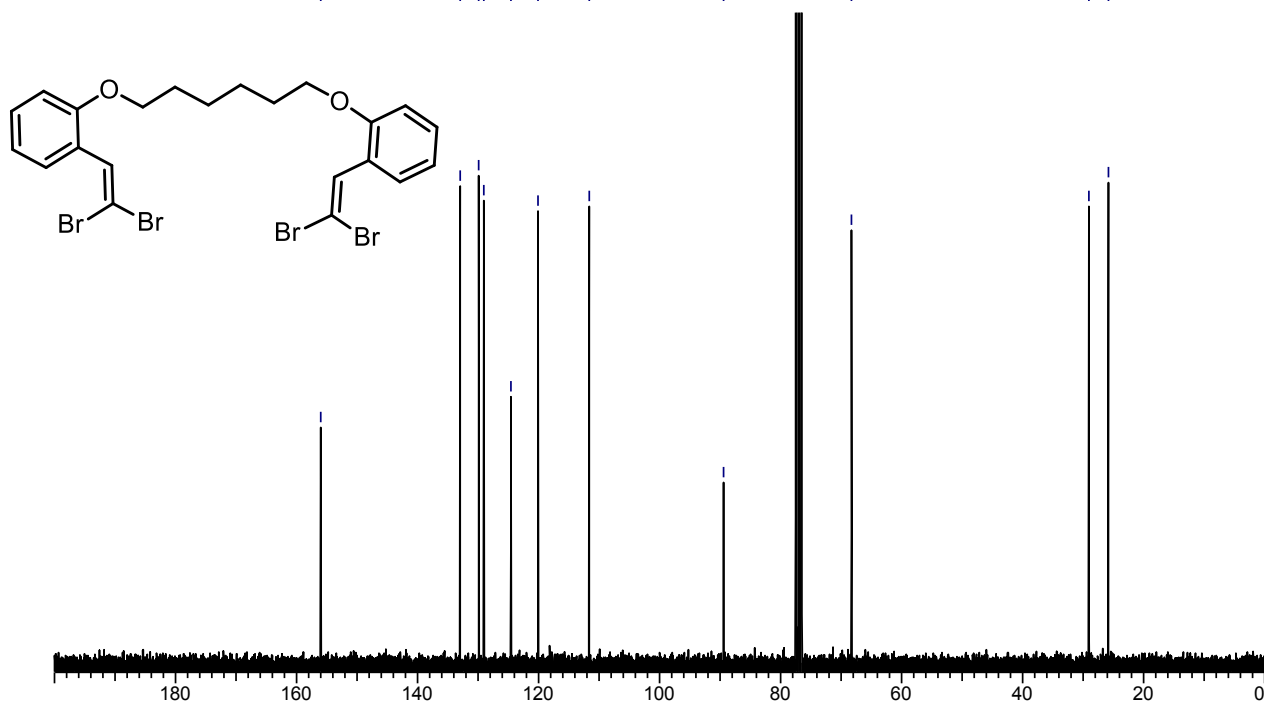
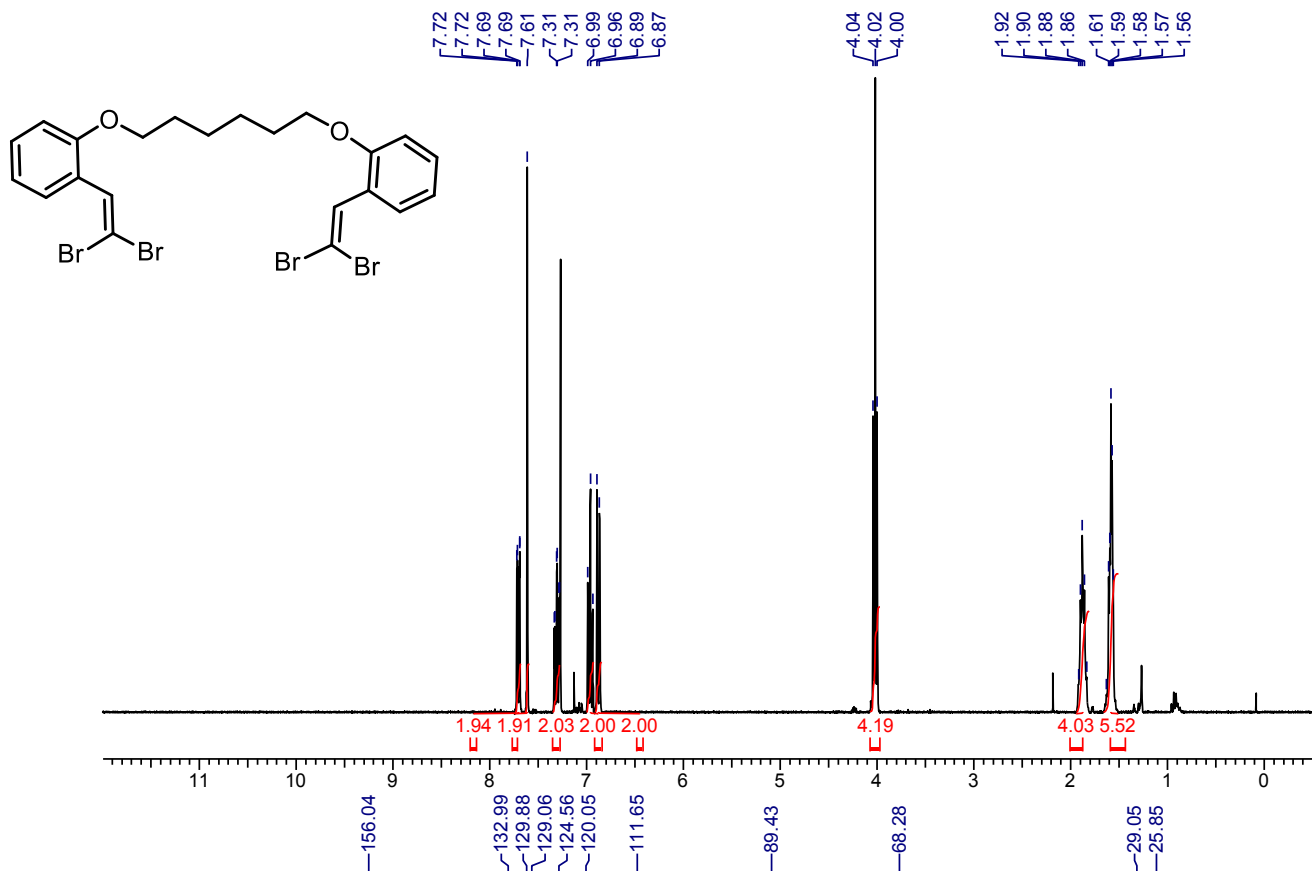


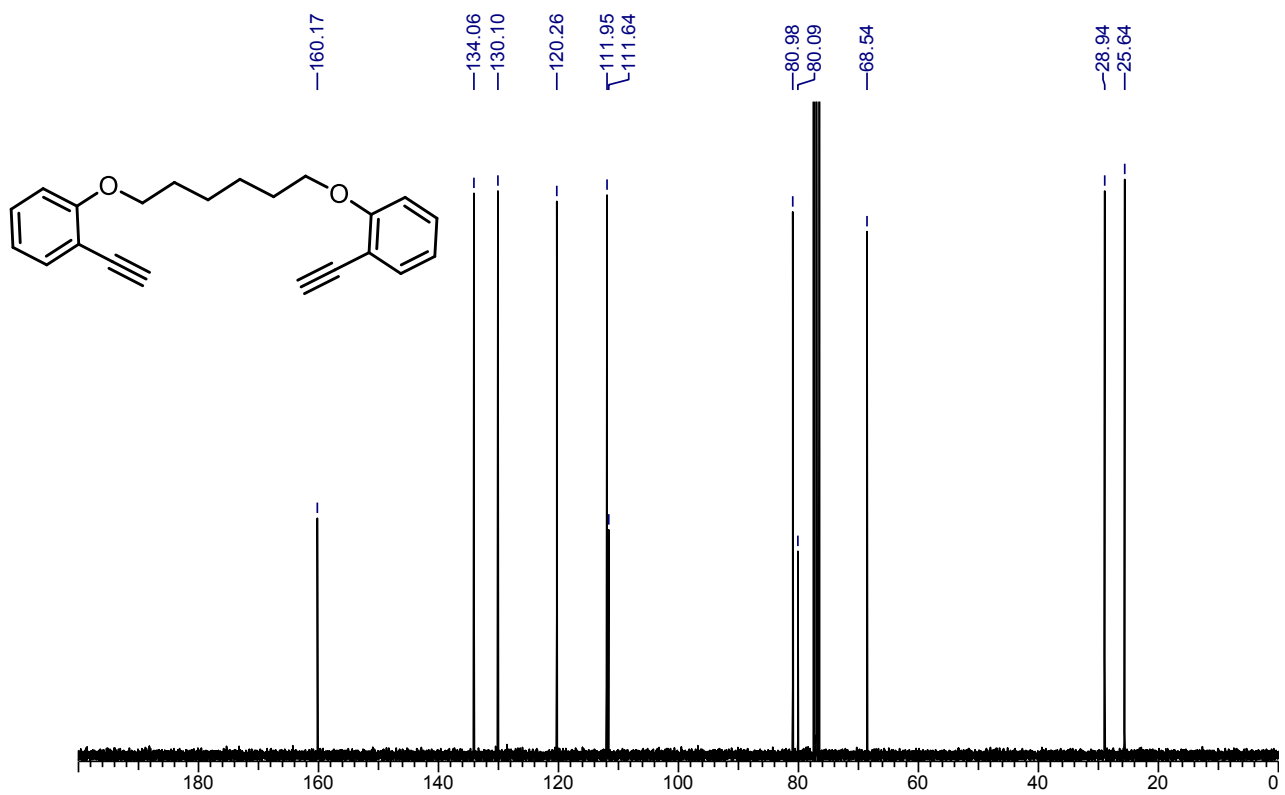
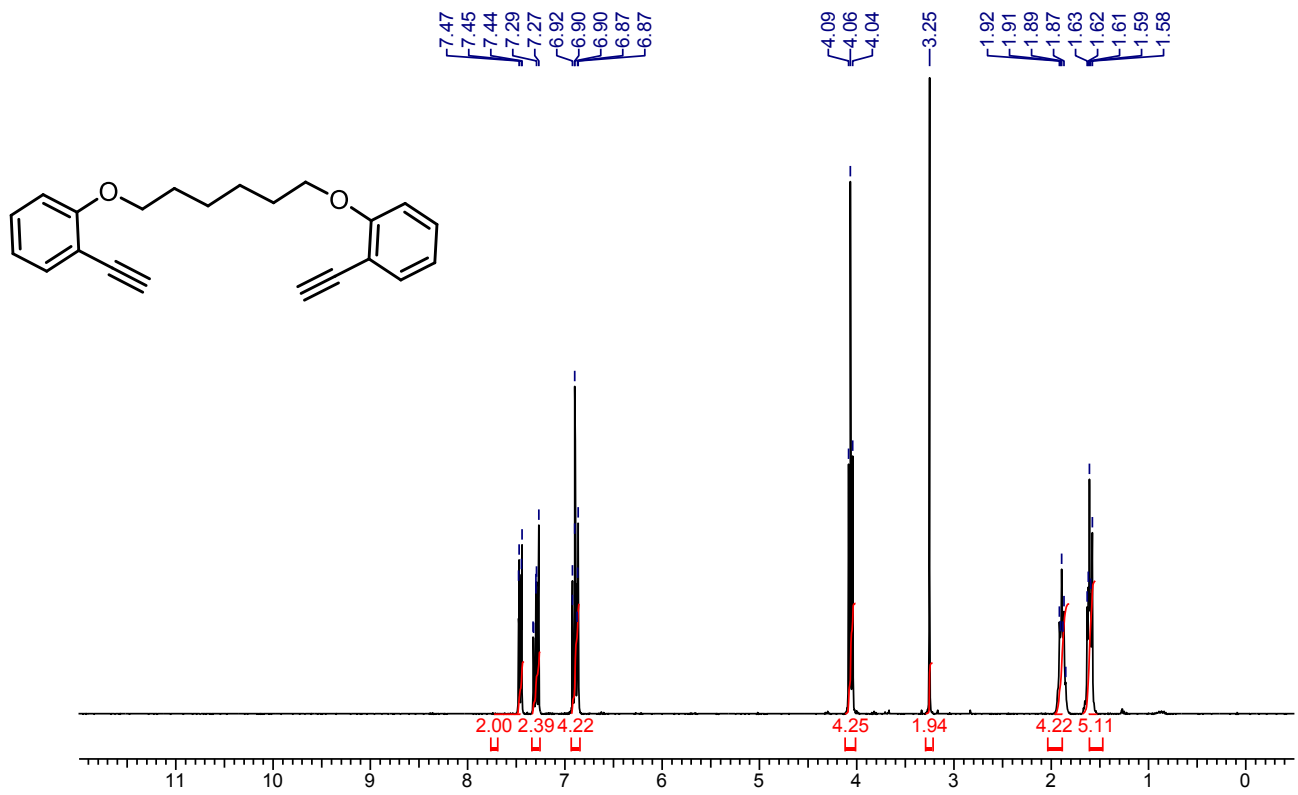
dd

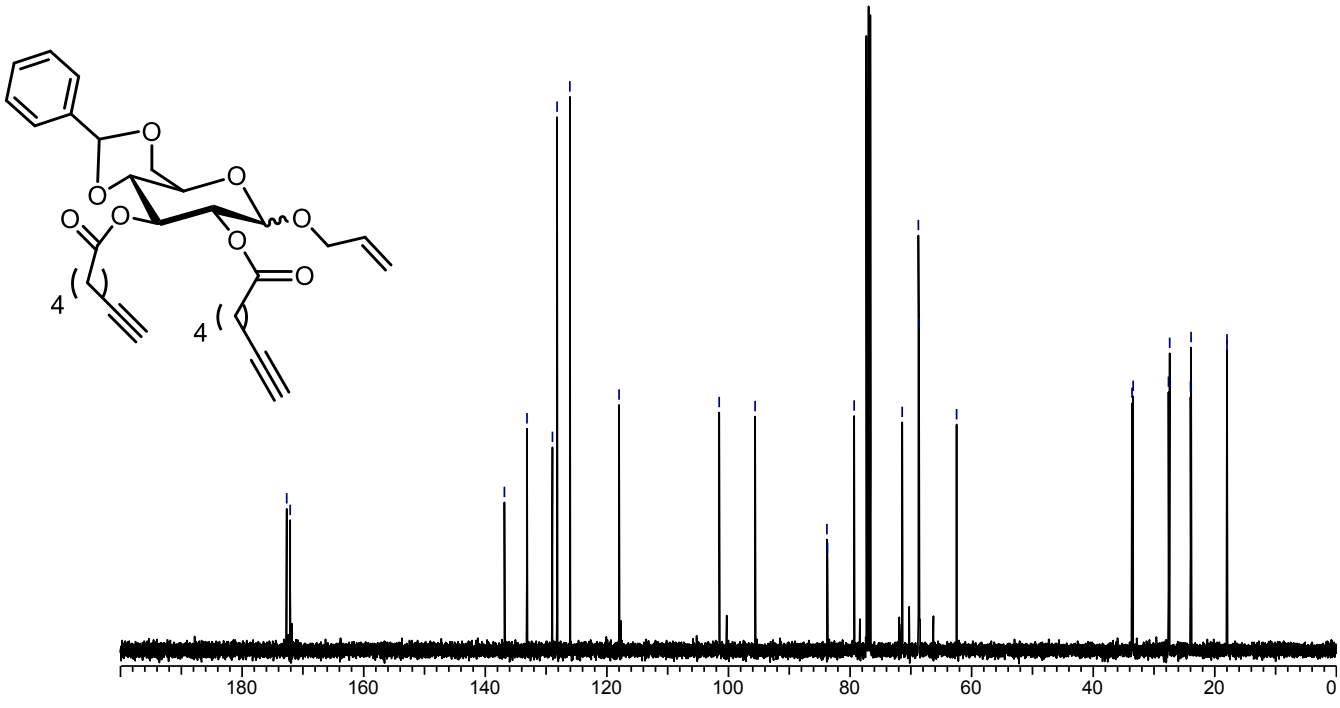
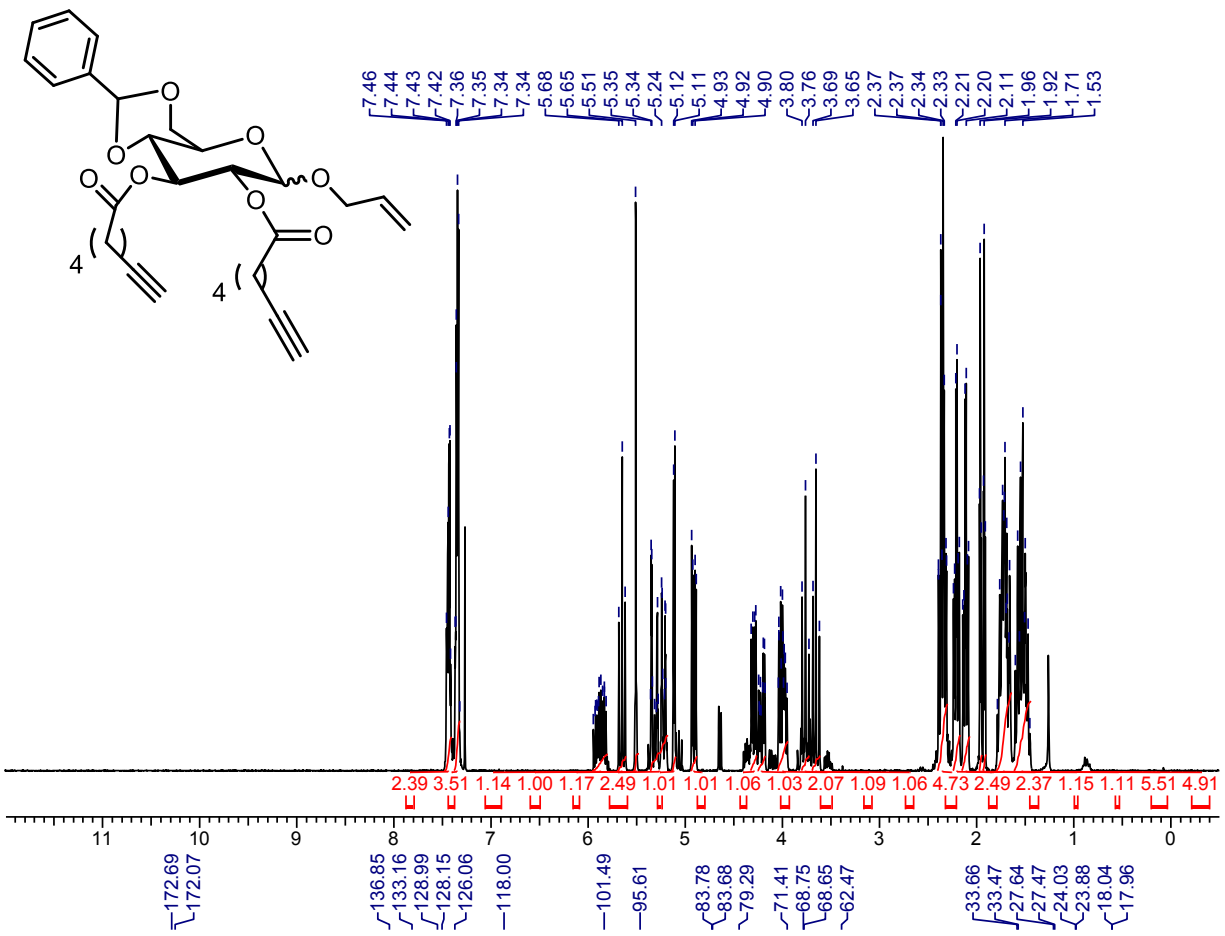


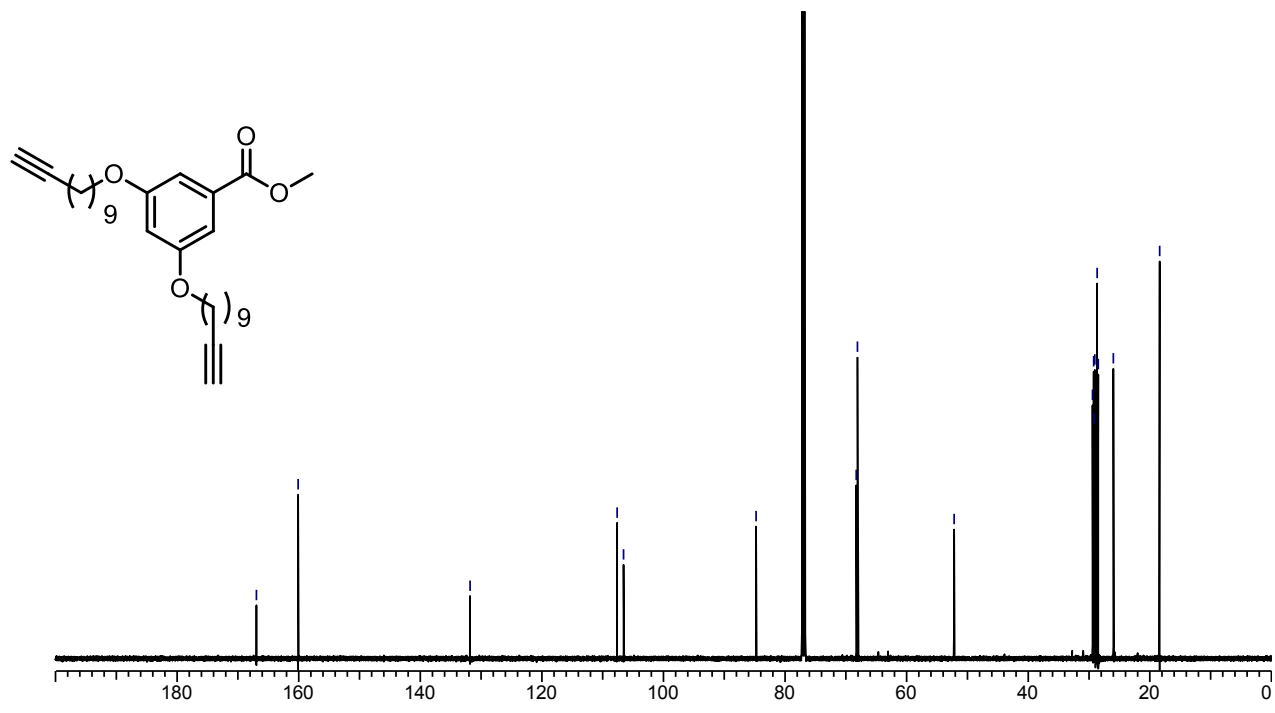
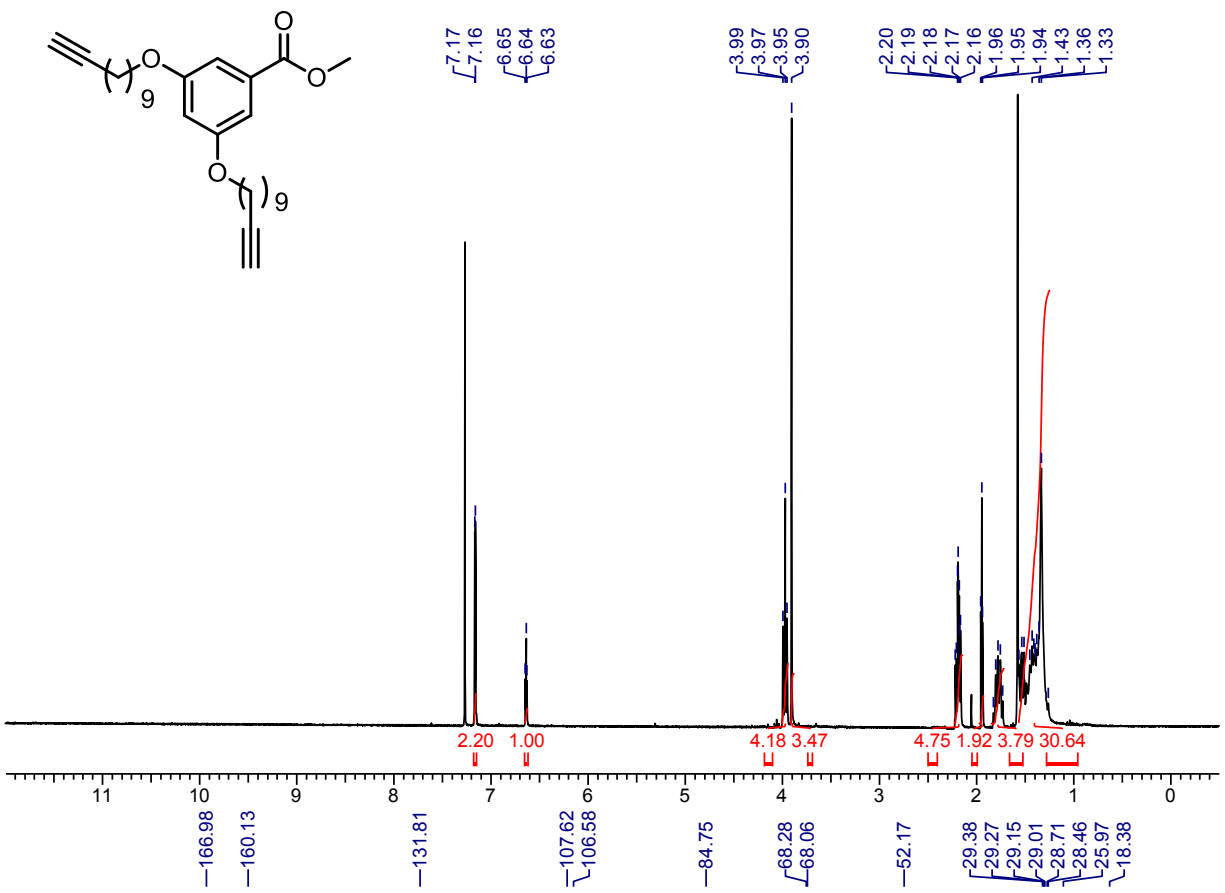


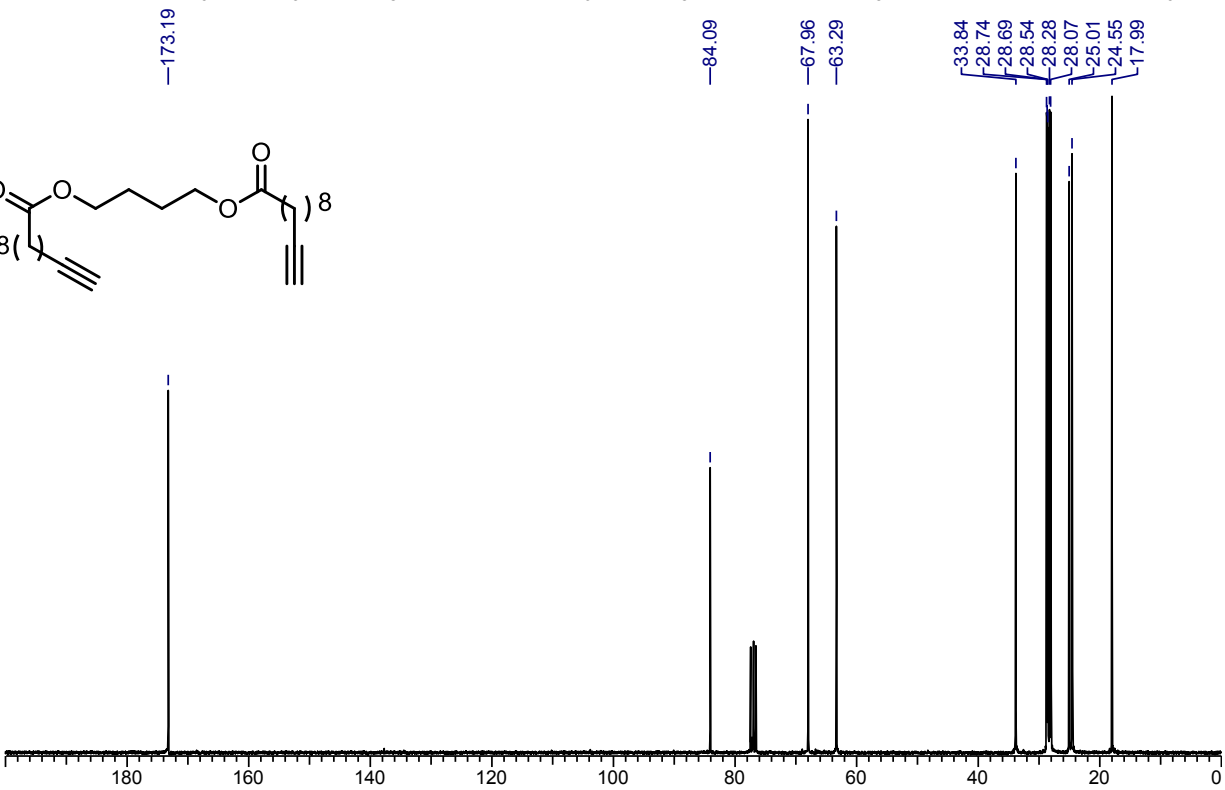
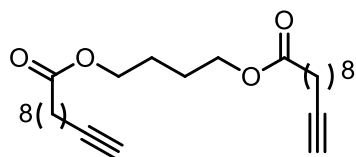
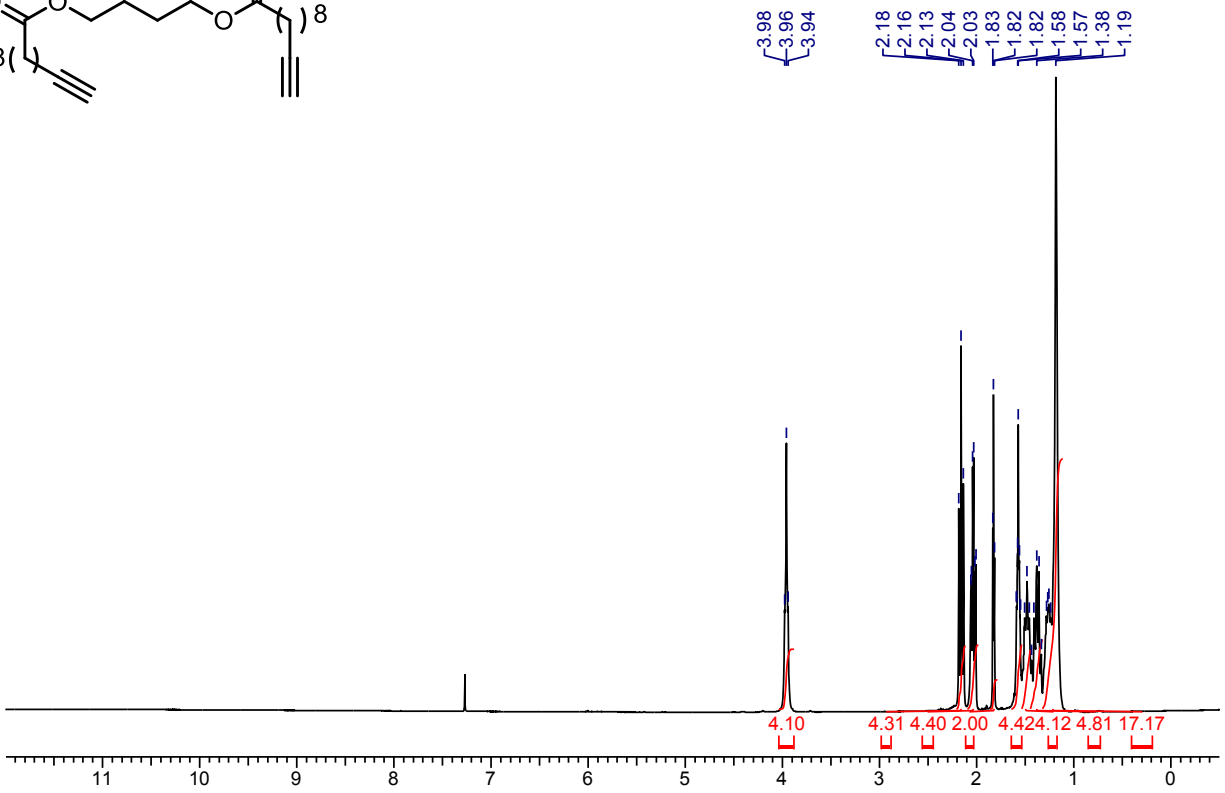
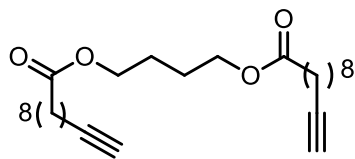


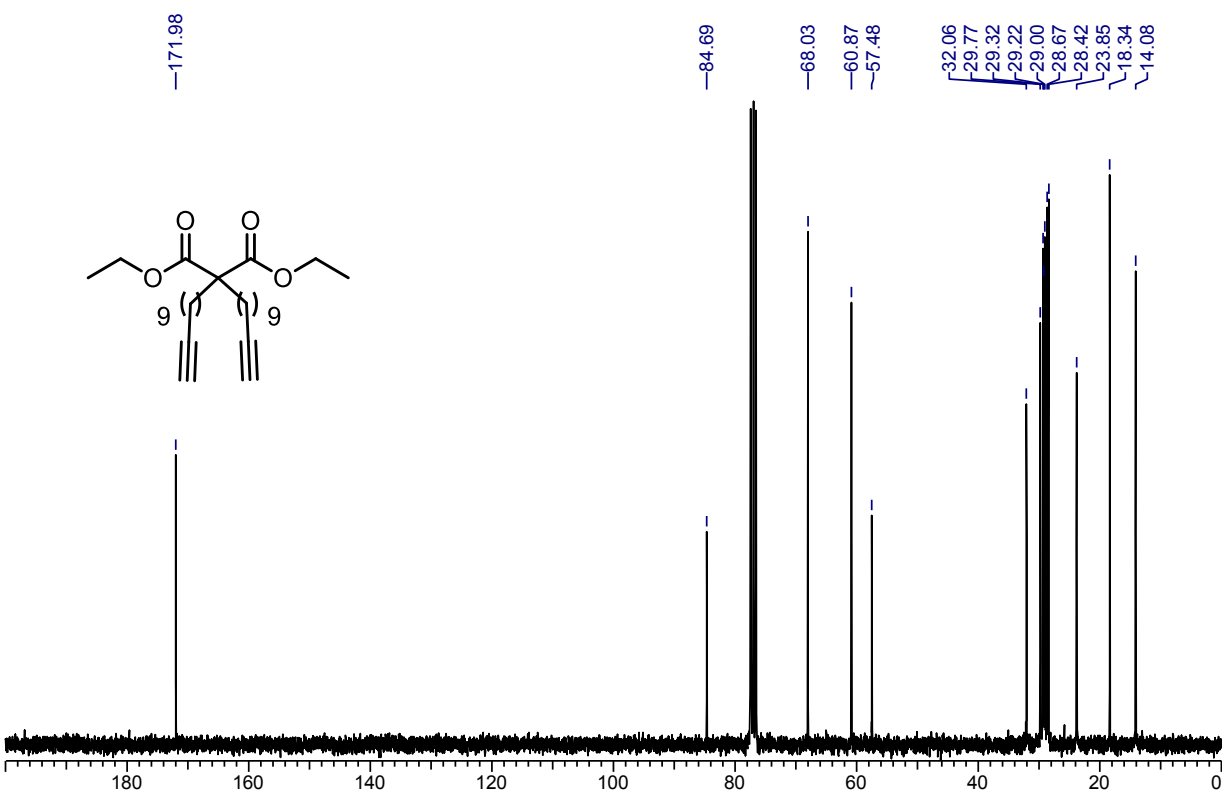
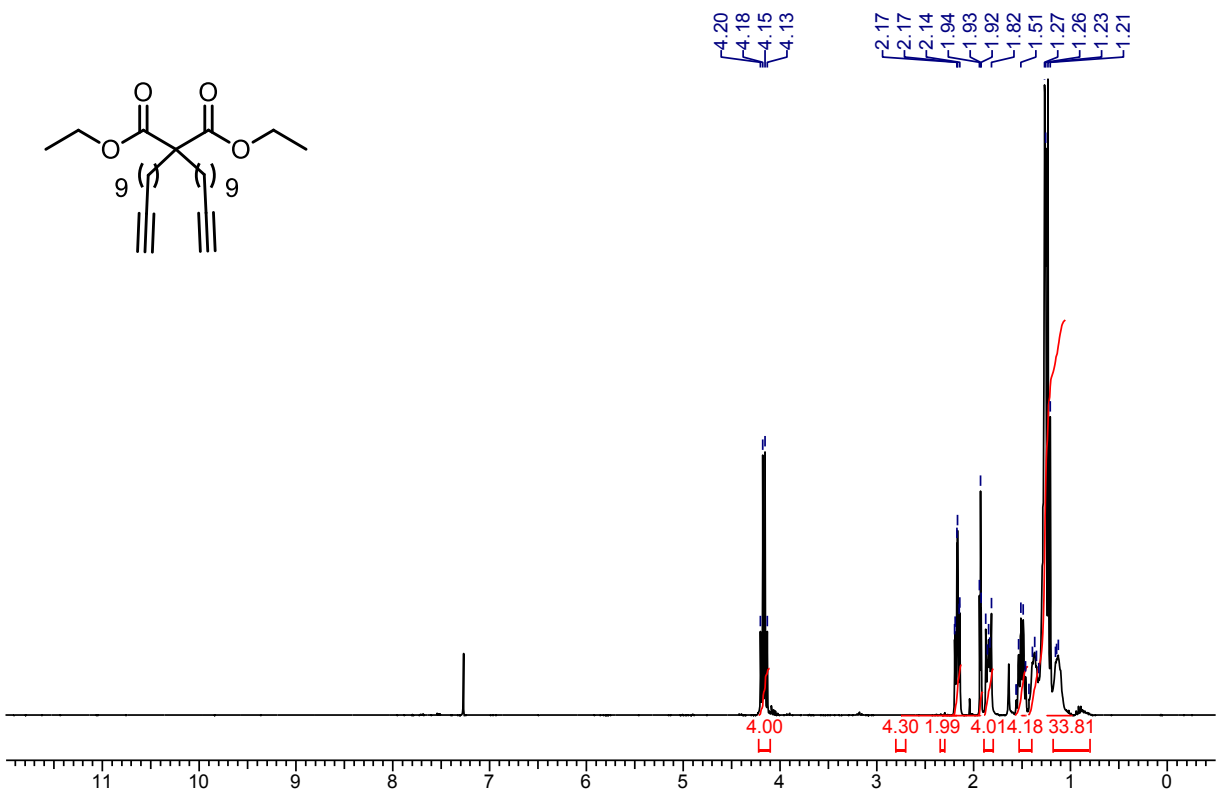




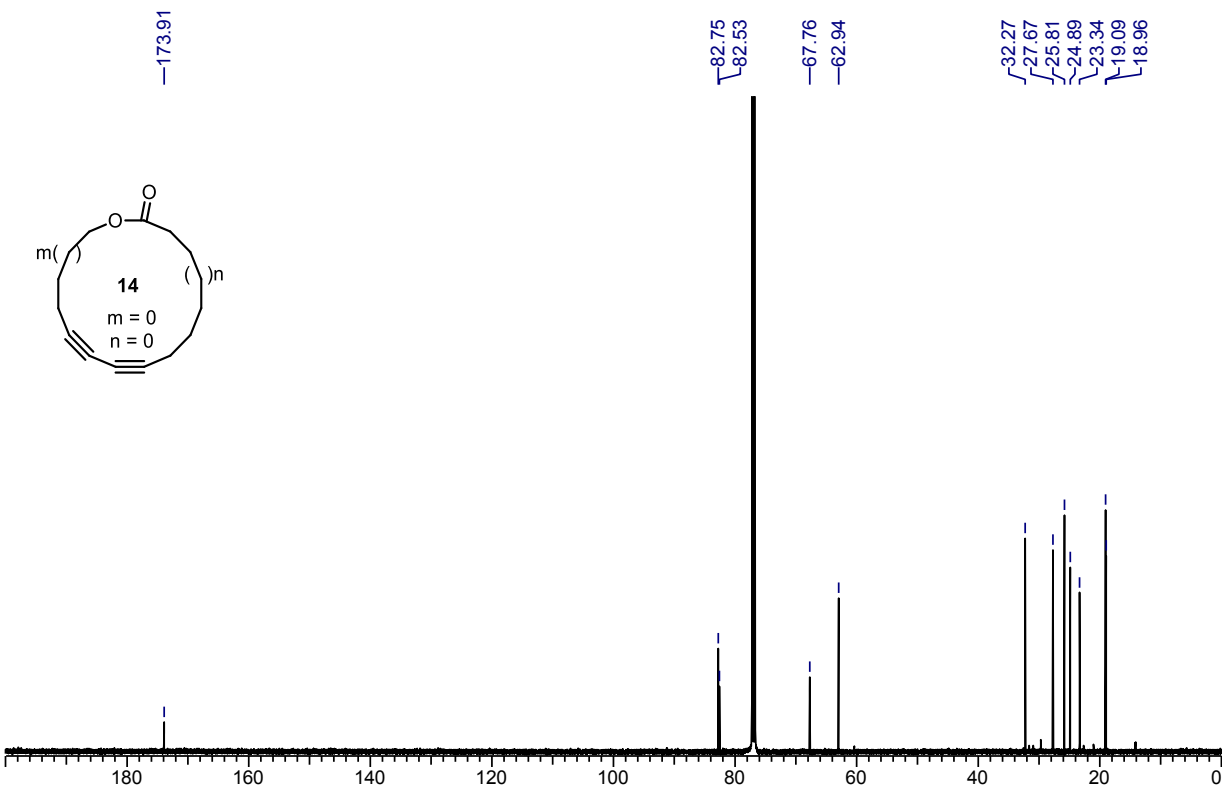
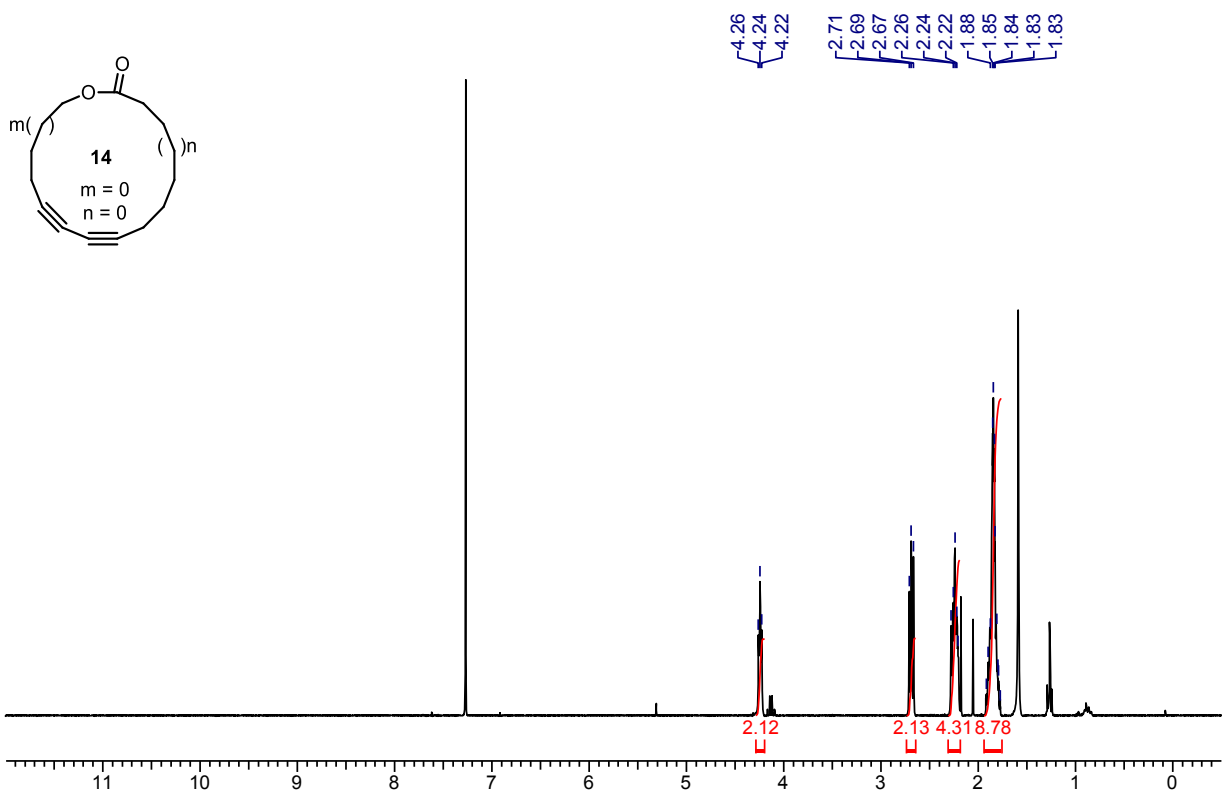




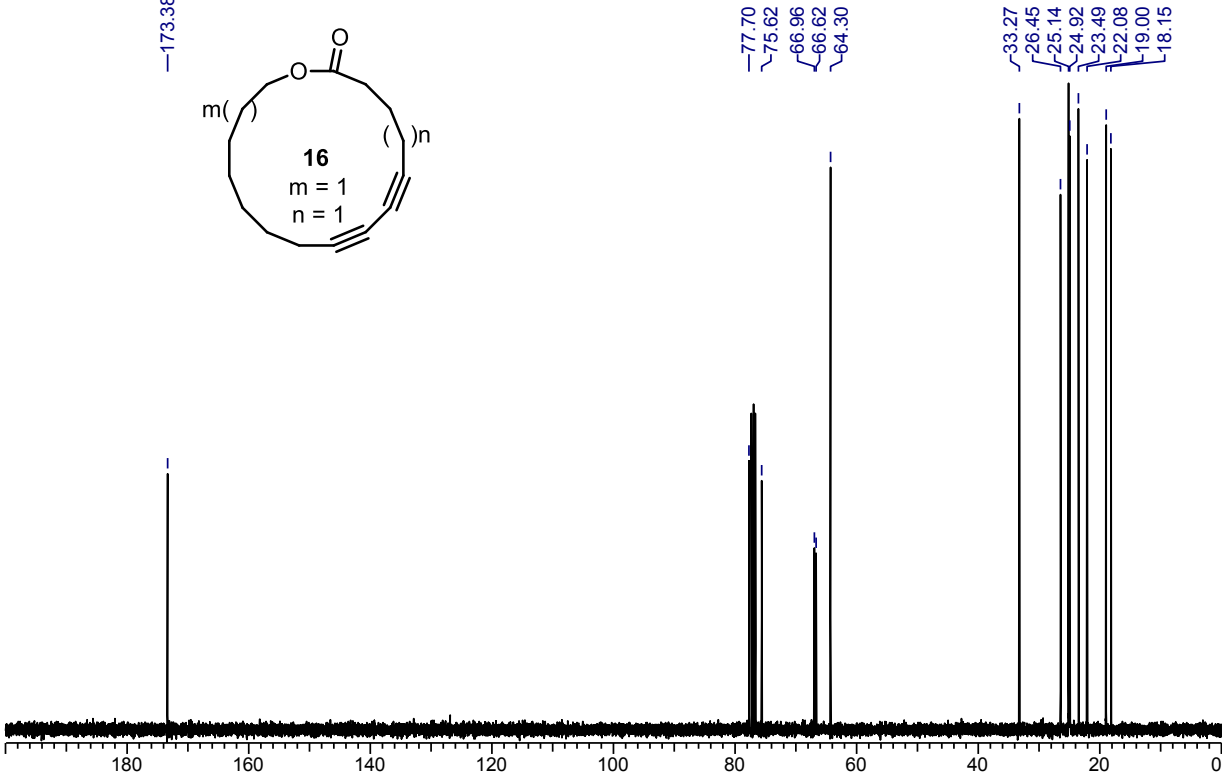
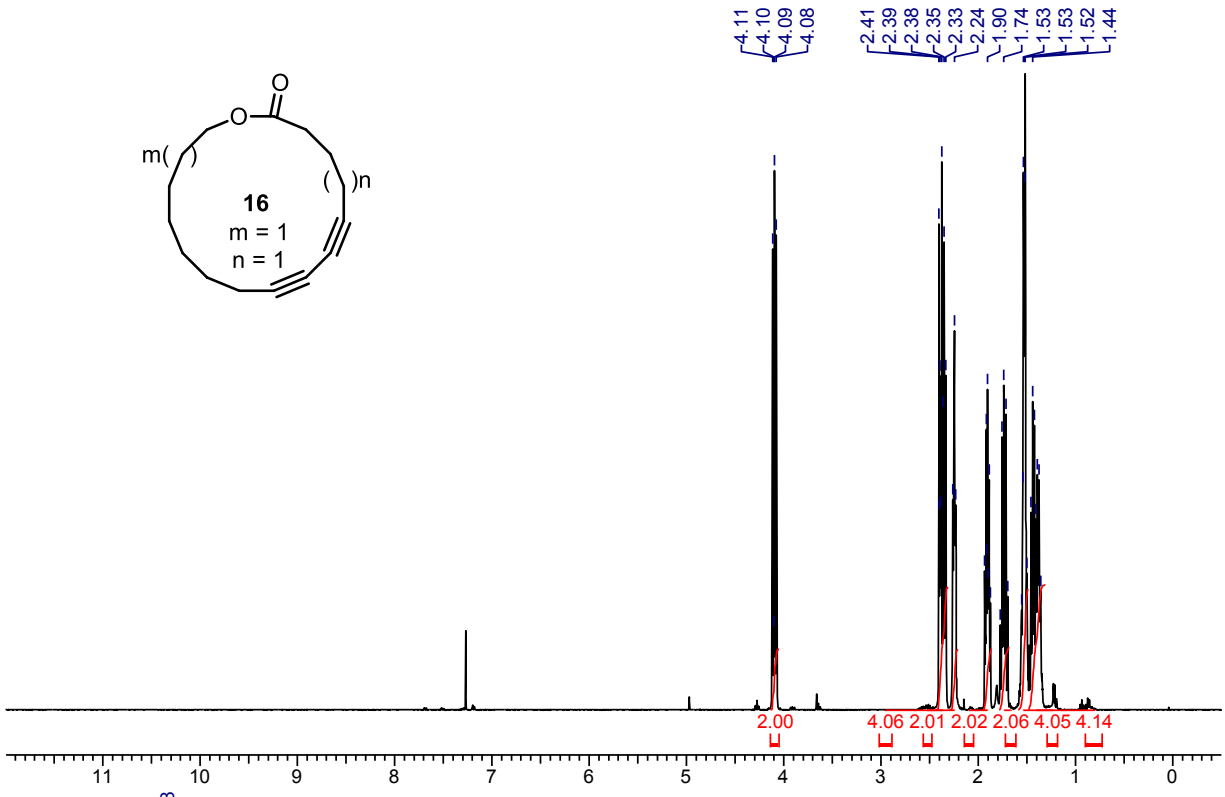


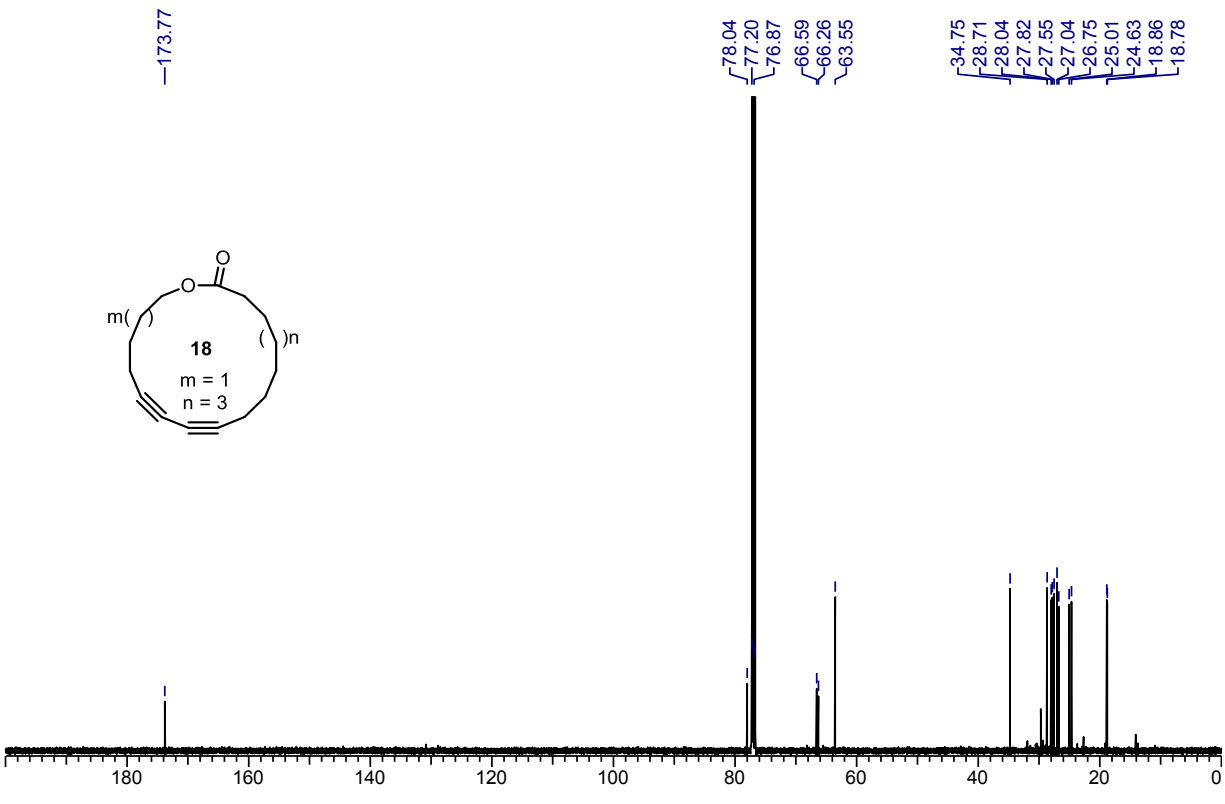
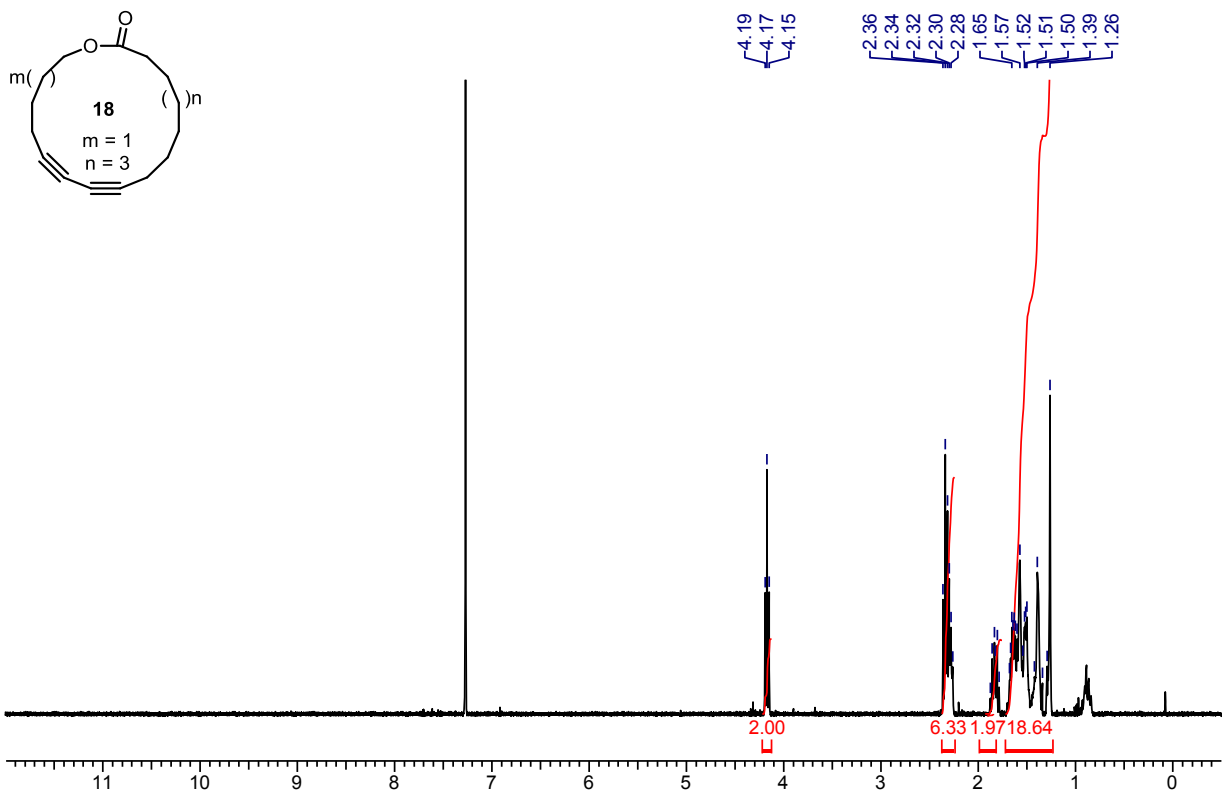


mm

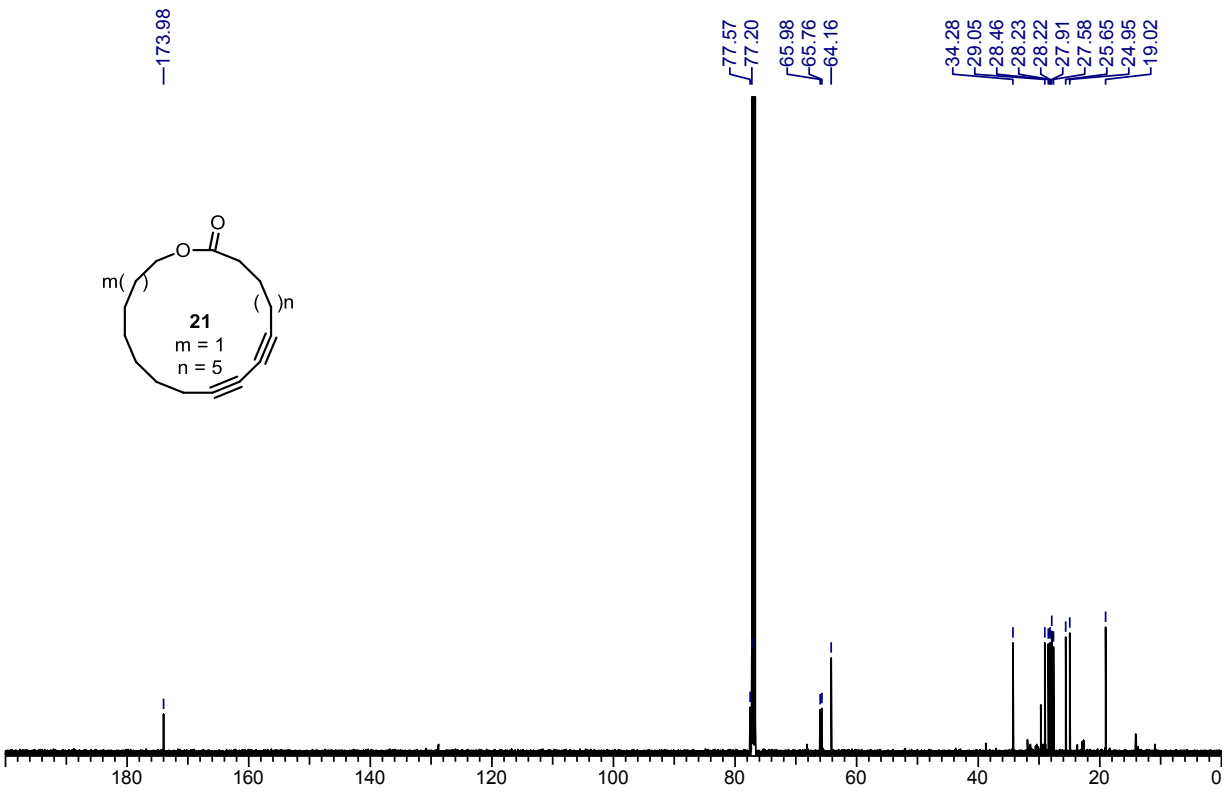
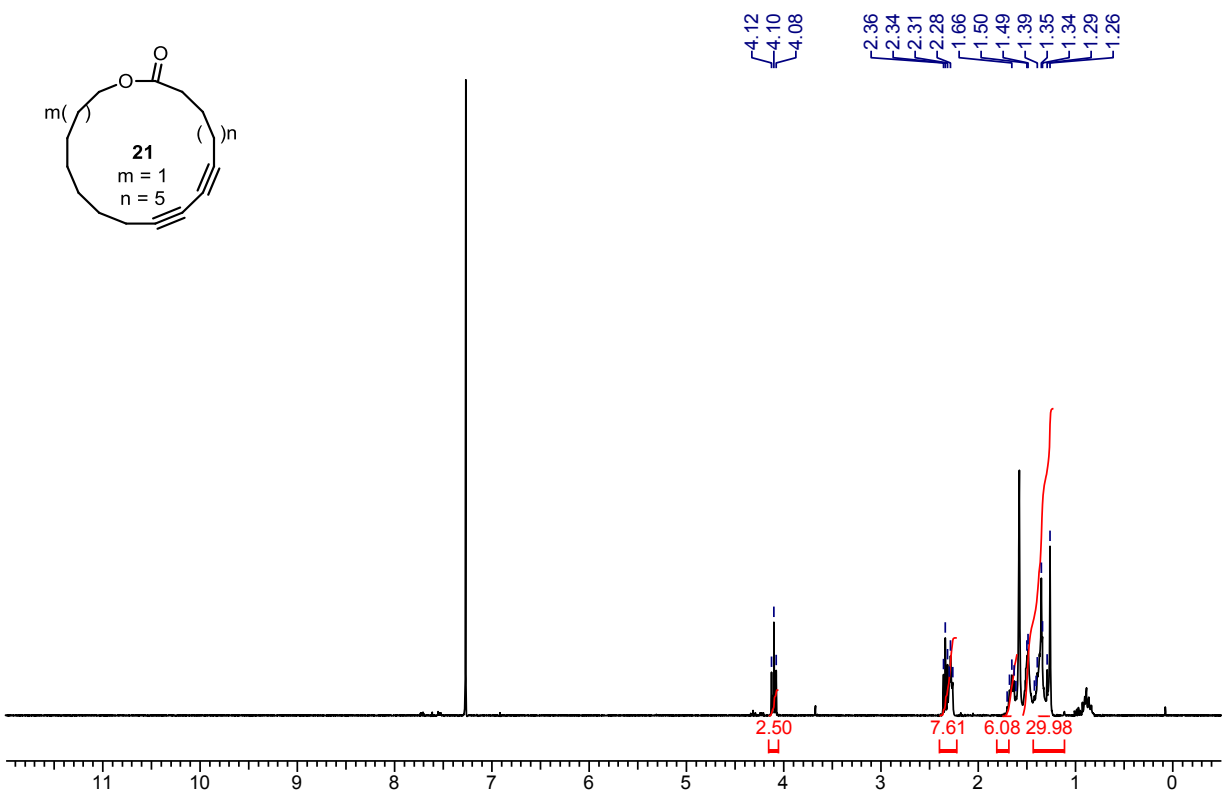


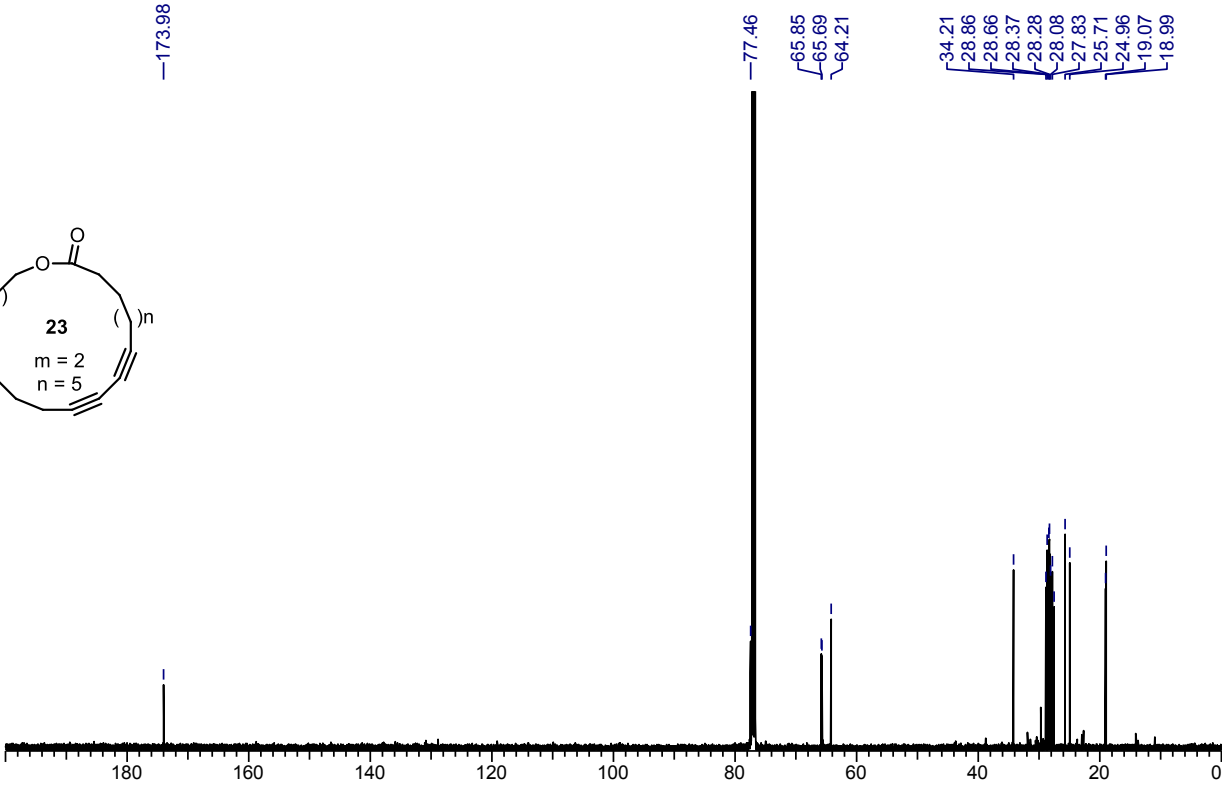
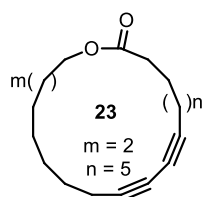
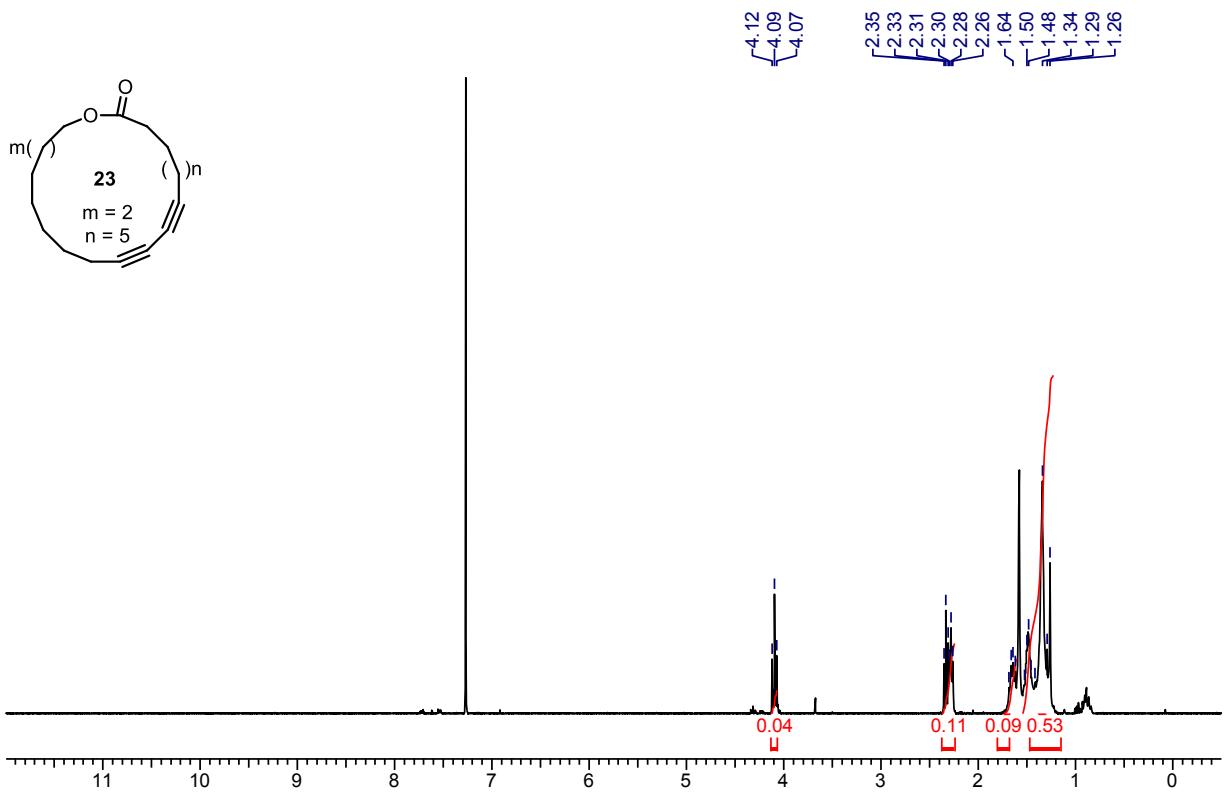
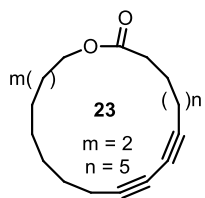
nn

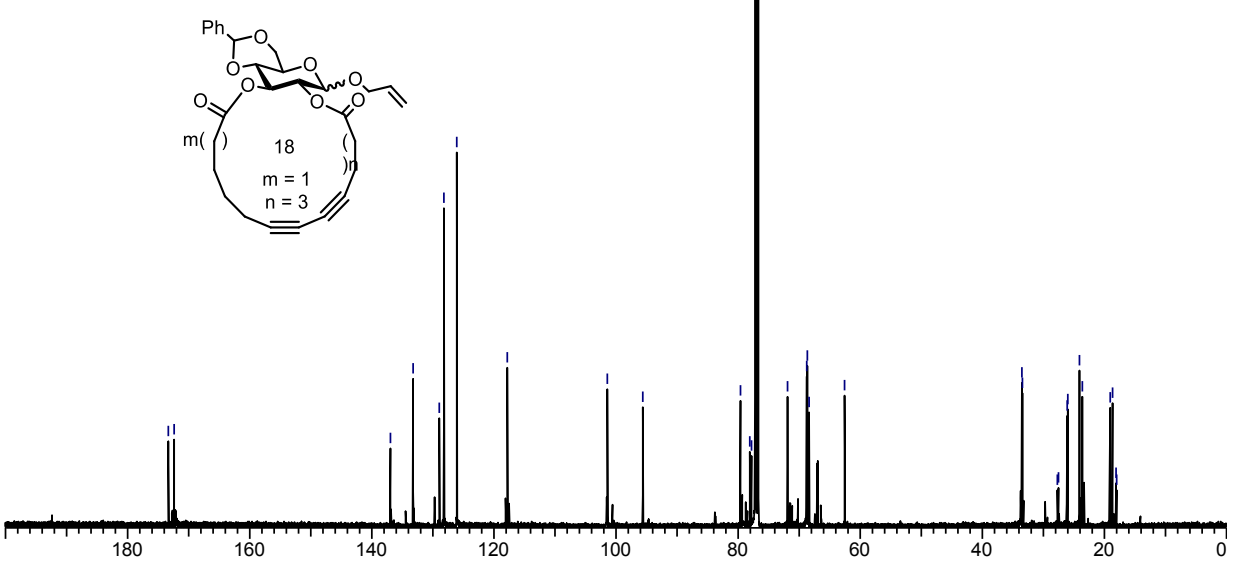
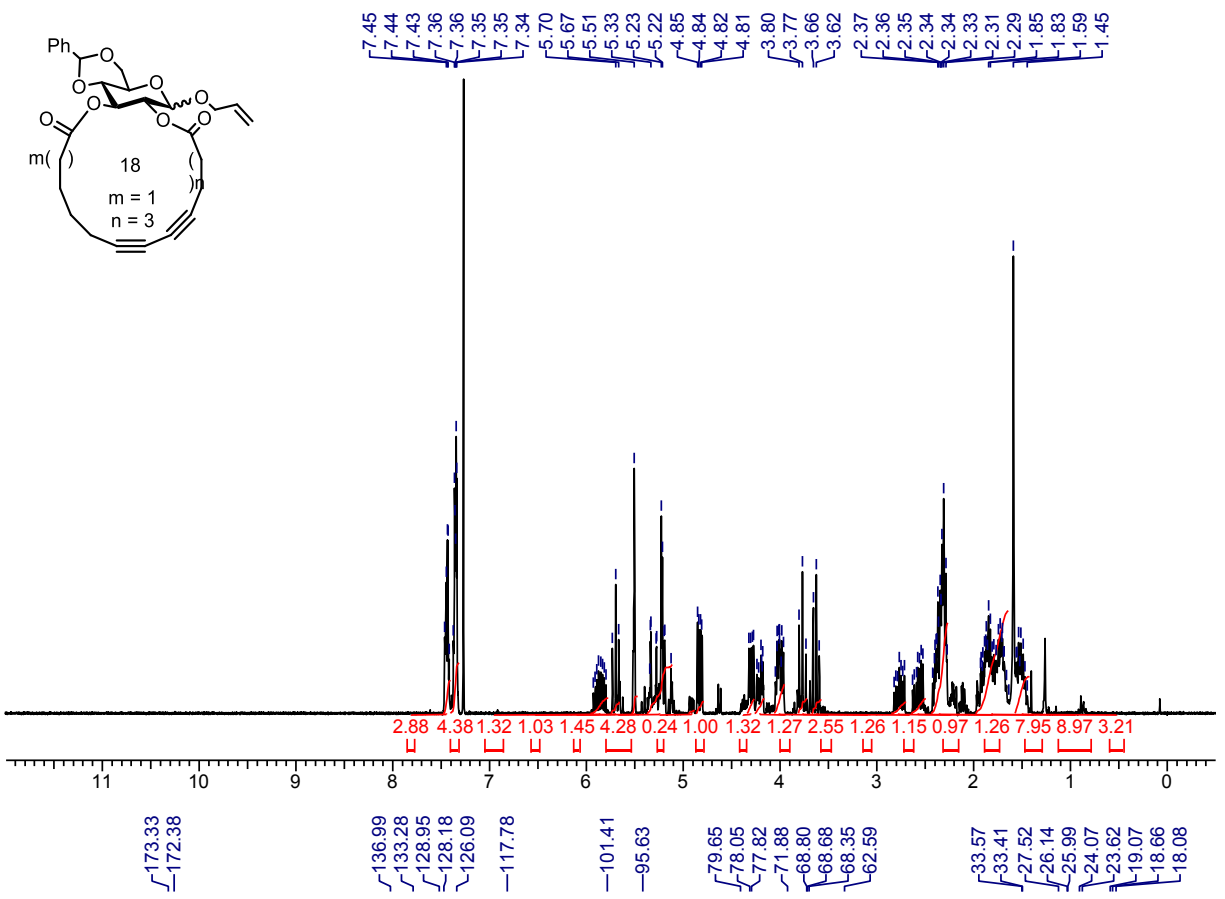


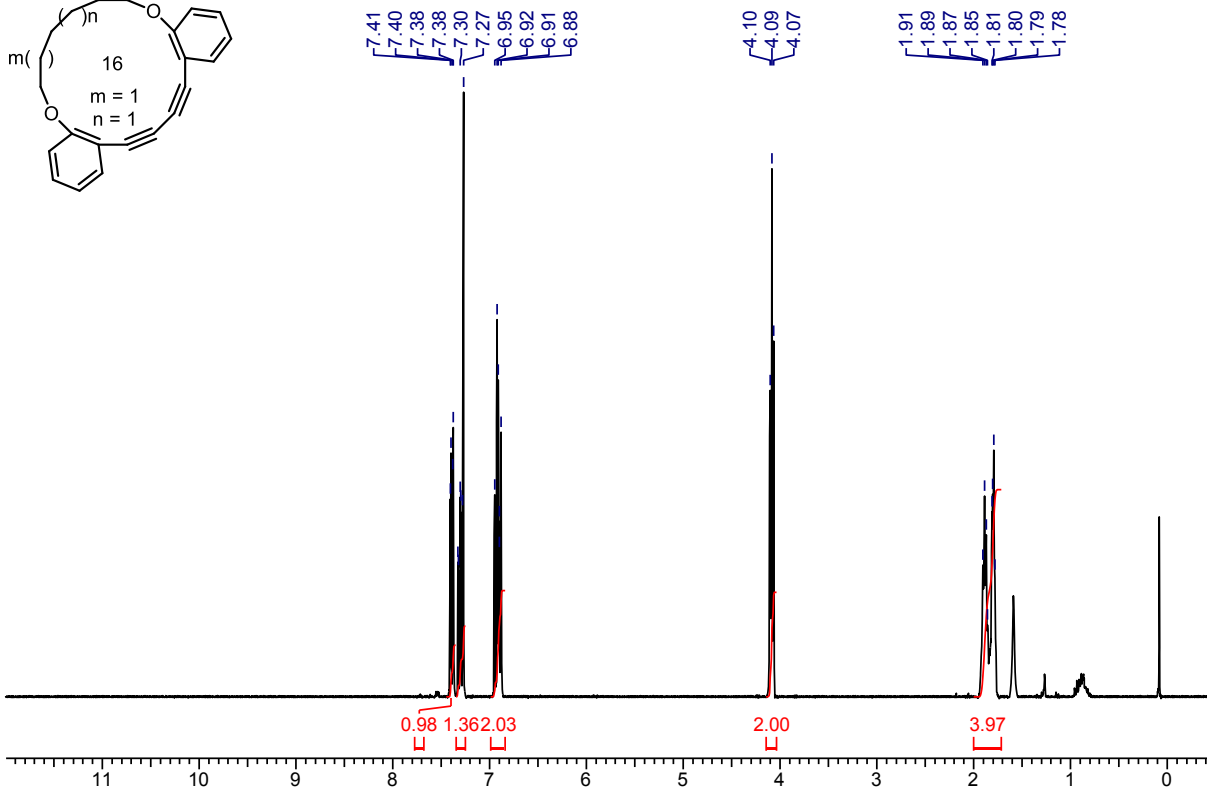
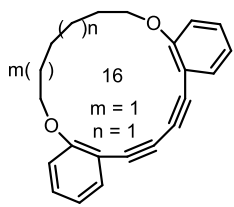


pp









-162.17

-131.59

-130.08

-120.47

-113.39

-112.27

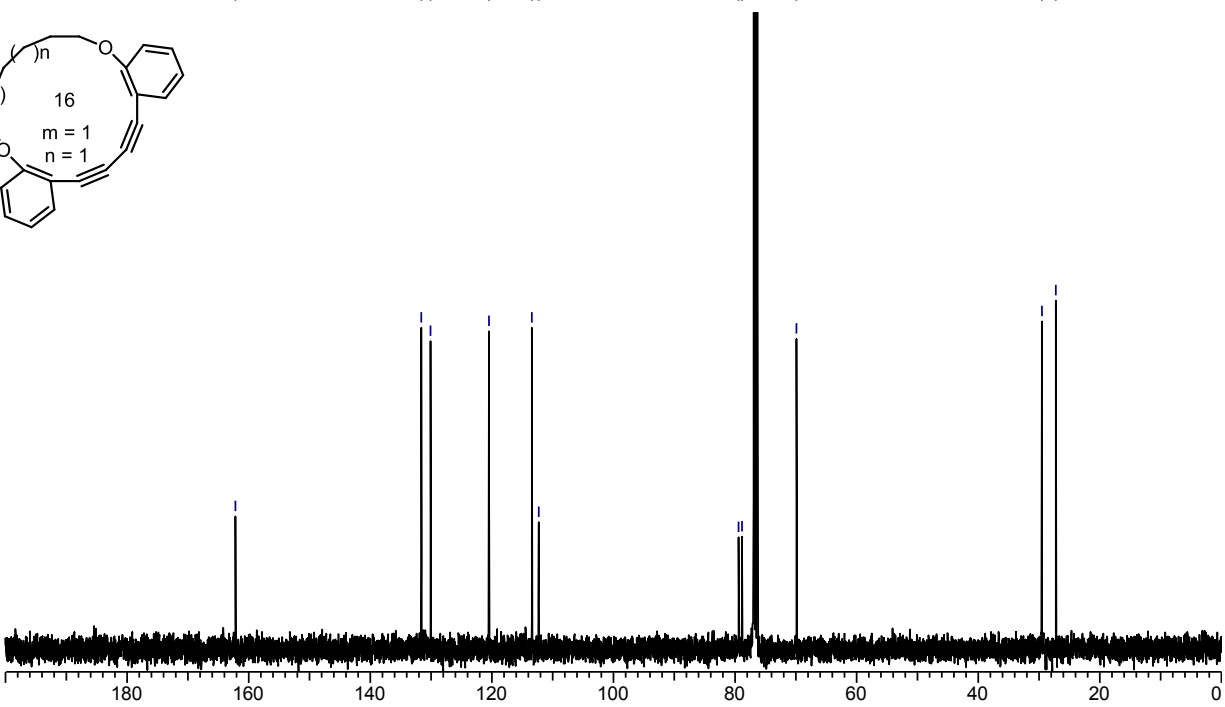
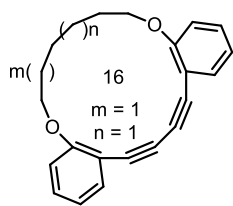
-79.40

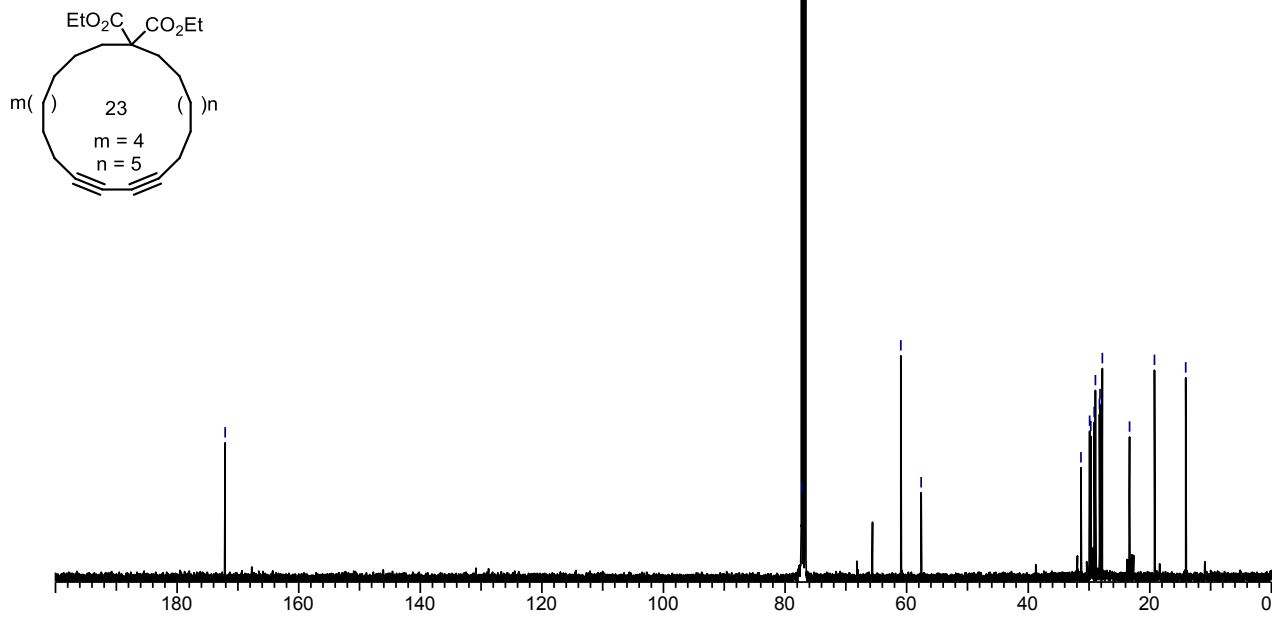
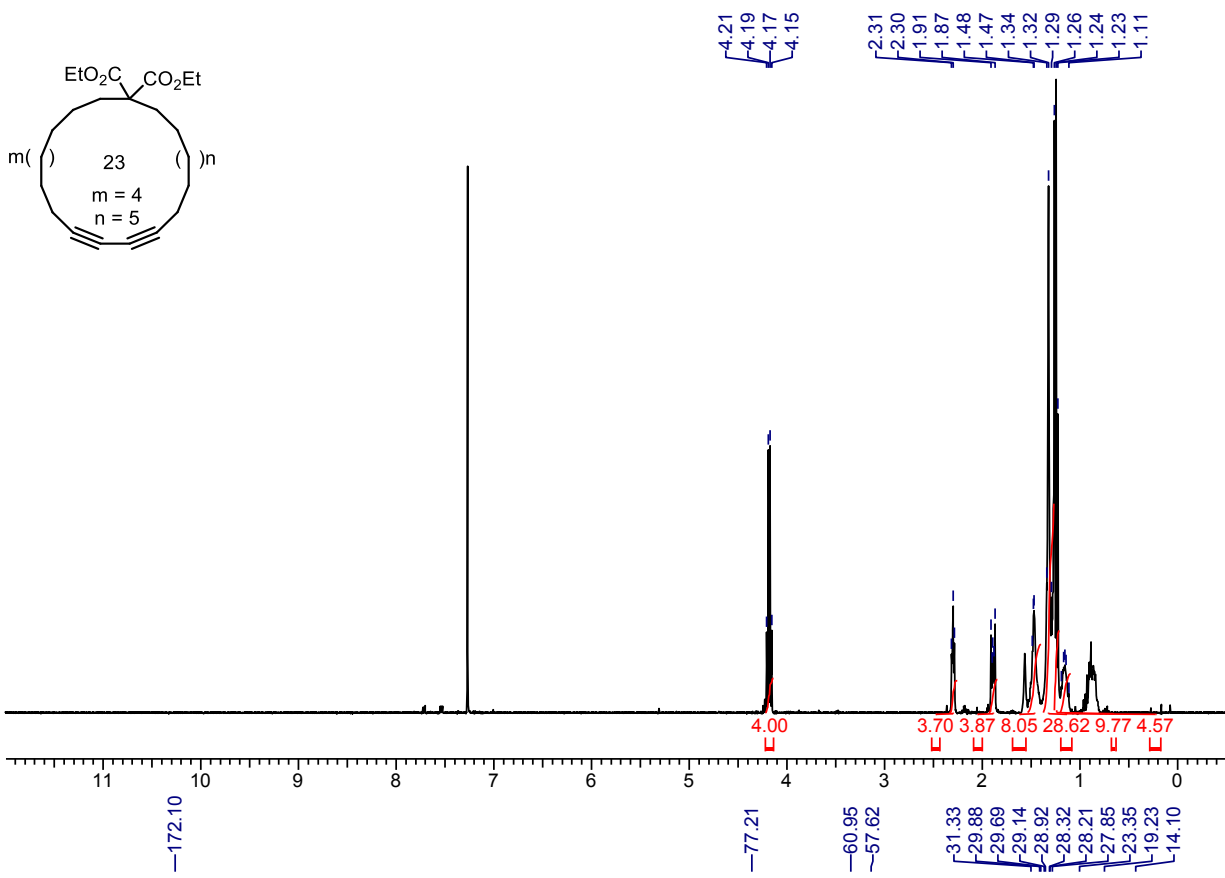
-78.84

-69.87

-29.55

-27.20





Chapter 14 : Supporting Information of Chapter 3: Microwave Accelerated Glaser-Hay Macrocyclizations at High Concentrations

General:

All reactions that were carried out under anhydrous conditions were performed under an inert argon or nitrogen atmosphere in glassware that had previously been dried overnight at 120 °C or had been flame dried and cooled under a stream of argon or nitrogen.¹¹ All chemical products were obtained from Sigma-Aldrich Chemical Company or Strem Chemicals and were reagent quality. Technical solvents were obtained from VWR International Co. Anhydrous solvents (CH₂Cl₂, Et₂O, THF, DMF, Toluene, and hexanes) were dried and deoxygenated using a GlassContour system (Irvine, CA). Isolated yields reflect the mass obtained following flash column silica gel chromatography. Organic compounds were purified using the method reported by W. C. Still¹² and using silica gel obtained from Silicycle Chemical division (40-63 nm; 230-240 mesh). Analytical thin-layer chromatography (TLC) was performed on glass-backed silica gel 60 coated with a fluorescence indicator (Silicycle Chemical division, 0.25 mm, F₂₅₄). Visualization of TLC plate was performed by UV (254 nm), KMnO₄ or *p*-anisaldehyde stains. All mixed solvent eluents are reported as v/v solutions. Concentration refers to removal of volatiles at low pressure on a rotary evaporator. All

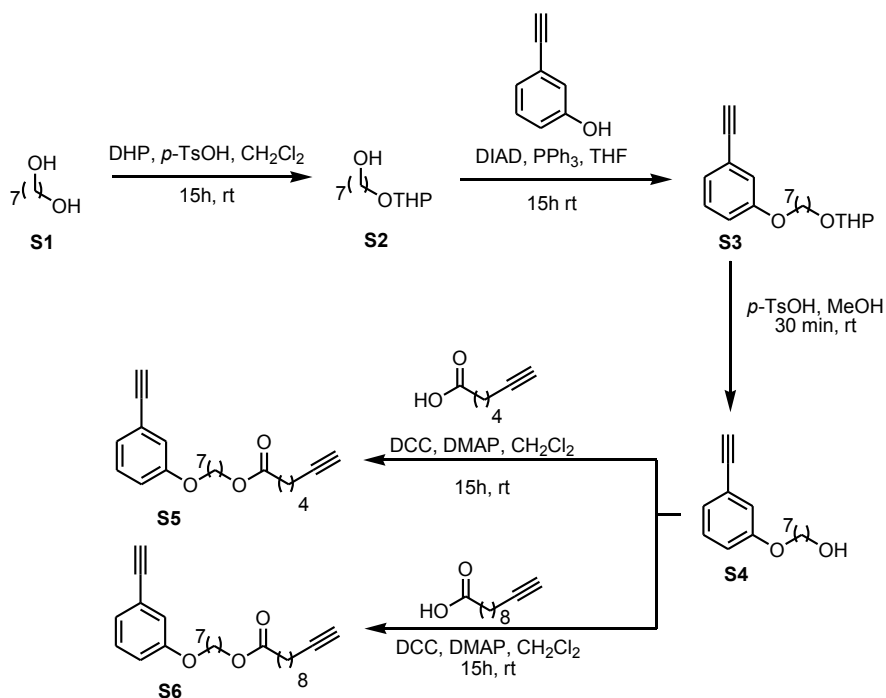
¹¹ Shriver, D. F.; Drezdon, M. A. in *The Manipulation of Air-Sensitive Compounds*; Wiley-VCH: New York, 1986.

¹² Still, W. C.; Kahn, M.; Mitra, A. *J. Org. Chem.* **1978**, *43*, 2923.

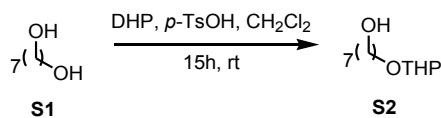
reported compounds were homogeneous by thin layer chromatography (TLC) and by ^1H NMR. NMR spectra were taken in deuterated CDCl_3 using Bruker AV-300 and AV-400 instruments unless otherwise noted. Signals due to the solvent served as the internal standard (CHCl_3 : δ 7.27 for ^1H , δ 77.0 for ^{13}C). The ^1H NMR chemical shifts and coupling constants were determined assuming first-order behavior. Multiplicity is indicated by one or more of the following: s (singlet), d (doublet), t (triplet), q (quartet), m (multiplet), br (broad); the list of couplings constants (J) corresponds to the order of the multiplicity assignment. The ^1H NMR assignments were made based on chemical shift and multiplicity. The ^{13}C NMR assignments were made on the basis of chemical shift and multiplicity. High resolution mass spectroscopy (HRMS) was done by the Centre régional de spectrométrie de masse at the Département de Chimie, Université de Montréal from an Agilent LC-MSD TOF system using ESI mode of ionization unless otherwise noted. The microwave used is a Biotage Initiator Sixty®.

SYNTHESIS OF MACROCYCLIZATION PRECURSORS.

Note that macrocyclic diyne precursors for macrocycles **3-7** have been previously prepared.¹³



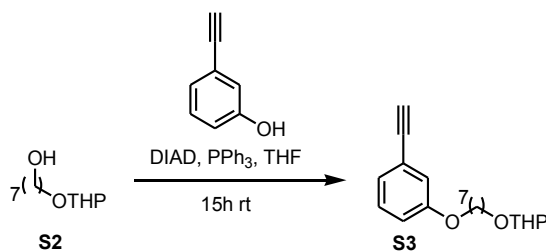
The synthesis of the acyclic precursors to macrocycles **S5** and **S6** are described below.



7-((tetrahydro-2H-pyran-2-yl)oxy)heptan-1-ol (S2): To a stirred solution of 1,7-heptanediol (2.0 g, 15.1 mmol, 1 equiv.) in dry dichloromethane (30 mL) at room temperature was added dihydropyran (1.3 g, 15.1 mmol, 1 equiv.) in one portion, followed by *p*-toluenesulfonic acid (154 mg, 0.8 mmol, 0.05 equiv.). The mixture was stirred for 20 h at room temperature. A saturated solution of NaHCO₃ was then added and the mixture was extracted with ether (3X),

¹³ Bédard, A.-C.; Collins, S. K. *J. Am. Chem. Soc.* **2011**, *133*, 19976-19981.

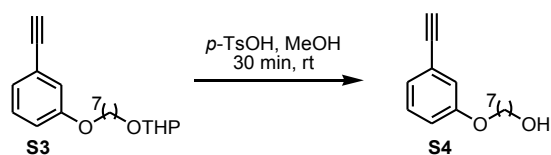
then the organic layers were combined and dried with Na₂SO₄. Following purification by column chromatography on silica gel (10 % ethyl acetates in hexanes), the product was obtained as a colorless oil (60 %, 1.9 g). The NMR data are in agreement with that obtained in the literature.¹⁴



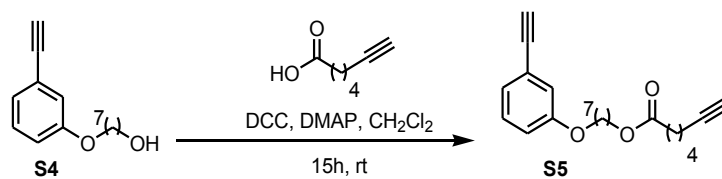
2-((7-(3-ethynylphenoxy)heptyl)oxy)tetrahydro-2H-pyran (S3): To a stirred solution of 3-hydroxyphenylacetylene (0.9 g, 7.5 mmol, 1 equiv.) in anhydrous THF (40 mL) was added triphenylphosphine (3.0 g, 11.3 mmol, 1.5 equiv.), 7-((tetrahydro-2H-pyran-2-yl)oxy)heptan-1-ol (S2) (1.9 g, 8.9 mmol, 1 equiv.) and diisopropyl azodicarboxylate (2.2 mL, 11.3 mmol, 1.5 equiv.) in that order under a N₂ atmosphere. The reaction mixture was heated at reflux for 15 hours. The reaction was concentrated *in vacuo* to provide a crude reaction mixture which was purified by silica gel column chromatography (100 % hexanes → 10 % ethyl acetates in hexanes) to afford the desired product as a colorless oil (26 %, 0.6 g). ¹H NMR (400 MHz, CDCl₃) δ = 7.25 - 7.18 (m, 1H), 7.07 (td, *J* = 7.6, 1.1 Hz, 1H), 7.01 (dd, *J* = 2.4, 1.5 Hz, 1H), 6.90 (ddd, *J* = 8.2, 2.6, 0.9 Hz, 1H), 4.58 (dd, *J* = 4.2, 2.7 Hz, 1H), 3.97 - 3.84 (m, 3H), 3.75 (td, *J* = 9.6, 6.8 Hz, 1H), 3.56 - 3.46 (m, 1H), 3.40 (td, *J* = 9.6, 6.7 Hz, 1H), 3.06 (s, 1H), 1.91 - 1.67 (m, 4H), 1.67 - 1.35 (m, 12H); ¹³C NMR (75 MHz, CDCl₃) δ = 158.8, 129.3, 124.4,

¹⁴ Poppe, L.; Hull, W. E.; Rétey, J. *Helv. Chim. Acta* **1993**, *76*, 2367-2383.

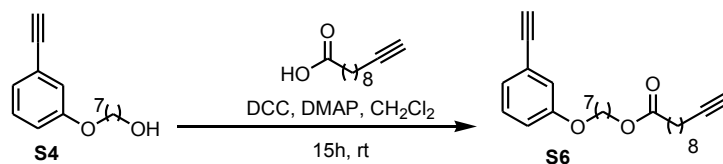
123.0, 117.6, 116.0, 98.8, 83.6, 76.8, 68.0, 67.6, 62.3, 30.8, 29.7, 29.2, 29.1, 26.2, 26.0, 25.5, 19.7 ppm; HRMS (ESI) m/z calculated for $C_{20}H_{29}O_3$ $[M+H]^+$, 317.2111; found: 317.2117.



7-(3-ethynylphenoxy)heptan-1-ol (S4): To a stirred solution of (**S3**) (0.5 g, 1.6 mmol, 1 equiv.) in methanol (10 mL) at room temperature was added *p*-toluenesulfonic acid (30 mg, 0.16 mmol, 0.1 equiv.). The mixture was stirred for 30 min at room temperature, then water and ethyl acetate were added to the mixture and the aqueous and organic layers were separated. The aqueous layer was extracted with ethyl acetate (3X). The organic phases were combined and washed with brine then dried with Na_2SO_4 . The reaction was concentrated under vacuum to provide a crude reaction mixture which was purified by silica gel column chromatography (20 % ethyl acetate in hexanes \rightarrow 50 % ethyl acetate in hexanes) to afford the desired product as a colorless oil (99 %, 0.46 g). 1H NMR (400 MHz, $CDCl_3$) δ = 7.26 - 7.18 (m, 1H), 7.08 (td, J = 7.6, 1.1 Hz, 1H), 7.02 (dd, J = 2.5, 1.4 Hz, 1H), 6.90 (ddd, J = 8.2, 2.6, 0.9 Hz, 1H), 3.95 (t, J = 6.5 Hz, 2H), 3.66 (t, J = 6.6 Hz, 2H), 3.06 (s, 1H), 1.87 - 1.72 (m, 2H), 1.66 - 1.53 (m, 2H), 1.52 - 1.31 (m, 6H); ^{13}C NMR (75 MHz, $CDCl_3$) δ = 158.8, 129.3, 124.5, 123.0, 117.6, 115.9, 83.6, 76.8, 68.0, 63.0, 32.7, 29.11, 29.08, 26.0, 25.6 ppm; HRMS (ESI) m/z calculated for $C_{15}H_{21}O_2$ $[M+H]^+$, 233.1536; found: 233.1529.



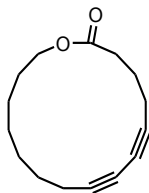
7-(3-ethynylphenoxy)heptyl hept-6-ynoate (S5): To a stirred solution of 7-(3-ethynylphenoxy)heptan-1-ol (S4) (210 mg, 0.92 mmol, 1 equiv.) and the 6-heptynoic acid (232 mg, 1.84 mmol, 2.0 equiv.) in dry dichloromethane (5 mL) was added *N,N*-dicyclohexylcarbodiimide (590 mg, 2.76 mmol, 3 equiv.) and 4-dimethylaminopyridine (337 mg, 2.76 mmol, 3 equiv.) at room temperature. The reaction mixture was stirred at room temperature for 15 h. The crude reaction mixture was placed in a freezer for 5 h to induce the precipitation of the urea, which was subsequently removed by filtration. The filtrate was concentrated under vacuum to provide the crude reaction mixture which was purified by silica gel column chromatography (100 % hexanes \rightarrow 10 % ethyl acetates in hexanes) to afford the desired product as a colorless oil (15 %, 53 mg). ^1H NMR (300 MHz, CDCl_3) δ = 7.25 - 7.19 (m, 1H), 7.08 (td, J = 7.6, 1.1 Hz, 1H), 7.01 (dd, J = 2.6, 1.5 Hz, 1H), 6.90 (ddd, J = 8.3, 2.6, 1.0 Hz, 1H), 4.08 (t, J = 6.7 Hz, 2H), 3.95 (t, J = 6.5 Hz, 2H), 3.06 (s, 1H), 2.34 (t, J = 7.4 Hz, 2H), 2.27 - 2.19 (m, 2H), 1.96 (t, J = 2.7 Hz, 1H), 1.84 - 1.71 (m, 4H), 1.70 - 1.53 (m, 4H), 1.53 - 1.36 (m, 6H); ^{13}C NMR (75 MHz, CDCl_3) δ = 173.5, 158.8, 129.4, 124.5, 123.0, 117.6, 115.9, 84.0, 83.6, 76.8, 68.6, 67.4, 64.4, 33.8, 29.1, 29.0, 28.6, 27.9, 25.9 (2C), 24.0, 18.1 ppm; HRMS (ESI) m/z calculated for $\text{C}_{22}\text{H}_{29}\text{O}_3$ $[\text{M}+\text{H}]^+$, 341.2111; found: 341.2126.



7-(3-ethynylphenoxy)heptyl undec-10-ynoate (S6) : To a stirred solution of 7-(3-ethynylphenoxy)heptan-1-ol (**S4**) (210 mg, 0.92 mmol, 1 equiv.) and the 10-undecynoic acid (335 mg, 1.84 mmol, 2.0 equiv.) in dry dichloromethane (5 mL) was added *N,N'*-dicyclohexylcarbodiimide (590 mg, 2.76 mmol, 3 equiv.) and 4-dimethylaminopyridine (337 mg, 2.76 mmol, 3 equiv.) at room temperature. The reaction mixture was stirred at room temperature for 15 h. The crude reaction mixture was placed in a freezer for 5 h to induce the precipitation of the urea, which was subsequently removed by filtration. The filtrate was concentrated under vacuum to provide the crude reaction mixture which was purified by silica gel column chromatography (100 % hexanes → 10 % ethyl acetates in hexanes) to afford the desired product as a colorless oil (50 %, 97 mg). ¹H NMR (400 MHz, CDCl₃) δ = 7.26 - 7.19 (m, 1H), 7.08 (td, *J* = 7.6, 1.1 Hz, 1H), 7.01 (dd, *J* = 2.4, 1.5 Hz, 1H), 6.90 (ddd, *J* = 8.3, 2.7, 0.9 Hz, 1H), 4.07 (t, *J* = 6.8 Hz, 2H), 3.94 (t, *J* = 6.5 Hz, 2H), 3.06 (s, 1H), 2.30 (t, *J* = 7.5 Hz, 2H), 2.22 - 2.13 (m, 3H), 1.94 (t, *J* = 2.7 Hz, 1H), 1.83 - 1.73 (m, 3H), 1.68 - 1.57 (m, 4H), 1.57 - 1.44 (m, 4H), 1.44 - 1.22 (m, 10H); ¹³C NMR (75 MHz, CDCl₃) δ = 173.9, 158.8, 129.3, 124.5, 123.0, 117.6, 115.9, 84.7, 83.6, 76.8, 68.1, 67.9, 64.3, 34.3, 29.08 (2C), 29.06, 29.0, 28.9, 28.64, 28.57, 28.4, 25.9, 25.0, 18.4 (2C) ppm; HRMS (ESI) *m/z* calculated for C₂₆H₃₇O₃ [M+H]⁺, 397.2737; found: 397.2746.

SYNTHESIS OF MACROCYCLES

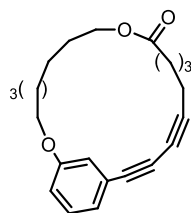
Note that macrocycles **3**, **4**, **5**, **6** and **7** have been previously prepared.³



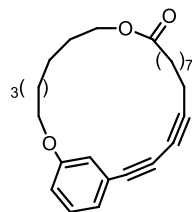
General procedure for the macrocyclization of diynes under Glaser-Hay oxidative coupling conditions using thermal heating: Macrocycle (**2**): To a vial equipped with a stirring bar was added CuCl_2 (5.5 mg, 0.48 mmol, 25 mol %) and $\text{Ni}(\text{NO}_3)_2 \cdot 6\text{H}_2\text{O}$ (9.3 mg, 0.48 mmol, 25 mol %). Polyethylene glycol 400 (3.33 mL), triethylamine (0.05 mL, 0.36 mmol, 3 equiv.) and pyridine (0.05 mL, 0.6 mmol, 5 equiv.) were added and the mixture was stirred at room temperature for 15 min or until the metals were solubilized. The diyne (28 mg, 0.12 mmol) was added to the homogenous mixture as a methanol solution (1.67 mL) in one portion. Oxygen was bubbled in the solution for 5 min and the vial was then closed with a screw cap. The reaction was warmed to 60 °C and monitored by TLC for consumption of the starting material (oxygen was bubbled again through the solution every 12 h). When the starting material was completely consumed (TLC), the reaction was cooled to room temperature and the crude mixture was loaded directly on a silica column. Purification by silica gel chromatography (100 % hexanes \rightarrow 10 % ethyl acetate in hexanes) afforded the product as a colorless semi-solid (31 mg, 73 %).

General procedure for the macrocyclization of diynes under Glaser-Hay oxidative coupling conditions using microwave irradiation: Macrocycle (**2**): To a microwave vial equipped with a stirring bar was added CuCl_2 (5.5 mg, 0.48 mmol, 25 mol %) and

Ni(NO₃)₂·6H₂O (9.3 mg, 0.48 mmol, 25 mol %). Polyethylene glycol 400 (3.33 mL), triethylamine (0.05 mL, 0.36 mmol, 3 equiv.) and tetramethylethylene diamine (0.09 mL, 0.6 mmol, 5 equiv.) were added and the mixture was stirred at room temperature for 15 min or until the metals were solubilized. The diyne (28 mg, 0.12 mmol) was added to the homogenous mixture as a methanol solution (1.67 mL) in one portion. Oxygen was bubbled in the solution for 5 min and the vial was then sealed with a microwave cap. The reaction was warmed to 120 °C for 3 to 6 h. The crude mixture was loaded directly onto silica gel for purification by chromatography (100 % hexanes → 10 % ethyl acetate in hexanes) and afforded the product as a colorless semi-solid (16 mg, 57 %).



Macrocycle (8): Following the general procedure described above, macrocycle **8** was isolated. (25 mg, 62 %). ¹H NMR (400 MHz, CDCl₃) δ 7.23 - 7.17 (m, 1H), 7.08 - 7.02 (m, 2H), 6.89 (ddd, *J* = 8.3, 2.6, 1.0 Hz, 1H), 4.08 (t, *J* = 6.4 Hz, 2H), 4.03 (t, *J* = 6.9 Hz, 2H), 2.42 - 2.38 (m, 2H), 2.35 (t, *J* = 7.5 Hz, 2H), 1.78 (quin, *J* = 6.9 Hz, 2H), 1.72 - 1.60 (m, 4H), 1.60 - 1.44 (m, 4H), 1.44 - 1.33 (m, 4H); ¹³C NMR (125 MHz, CDCl₃) δ ppm = 173.9, 158.6, 129.5, 124.2, 123.0, 118.3, 117.3, 85.1, 75.0, 74.3, 68.2, 64.1, 34.1, 28.5, 28.4, 28.1, 28.0, 27.6, 25.9, 25.6, 24.8, 19.5; HRMS (ESI) *m/z* calculated for C₂₂H₂₇O₃ [M+H]⁺, 339.1955; found: 339.1964.

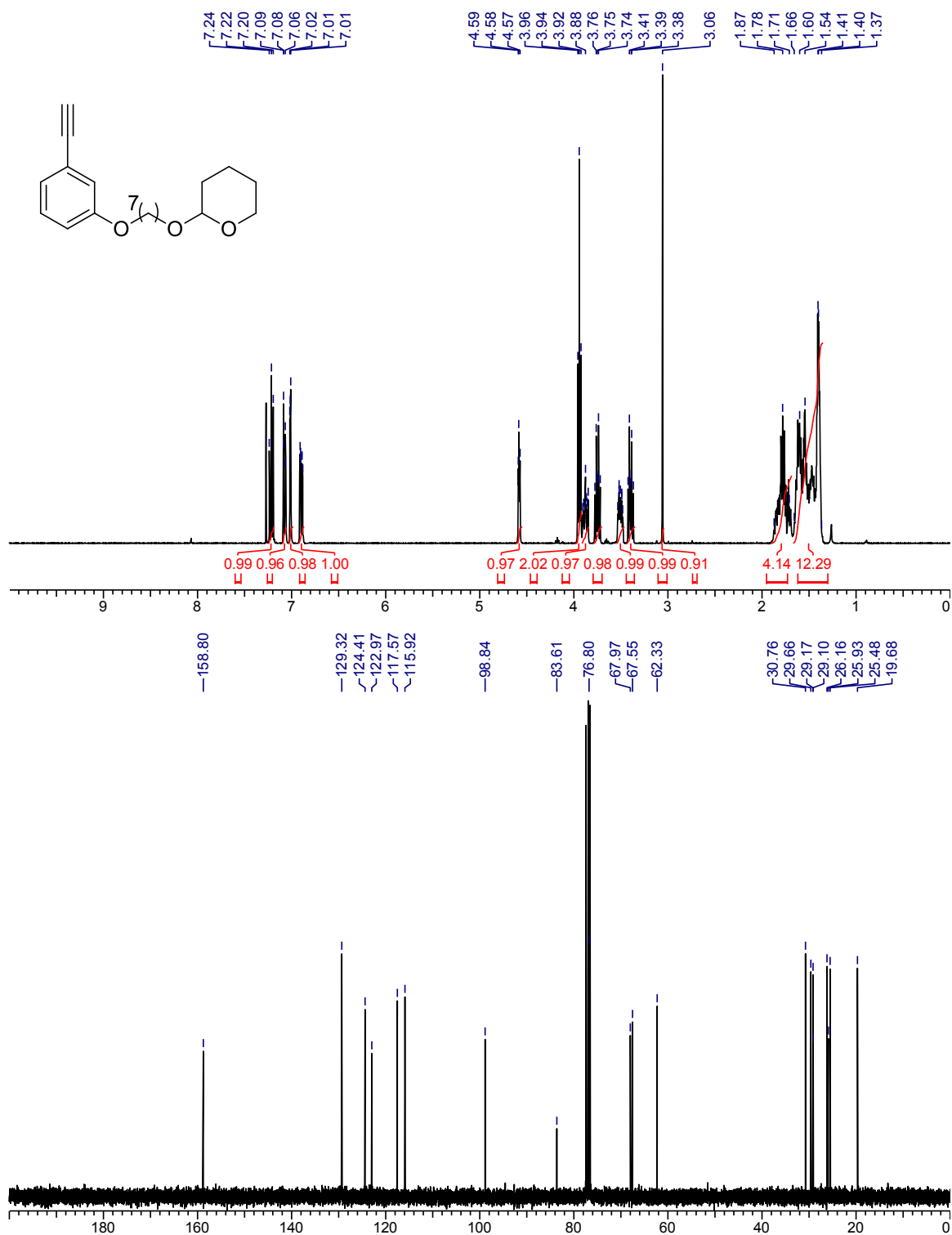


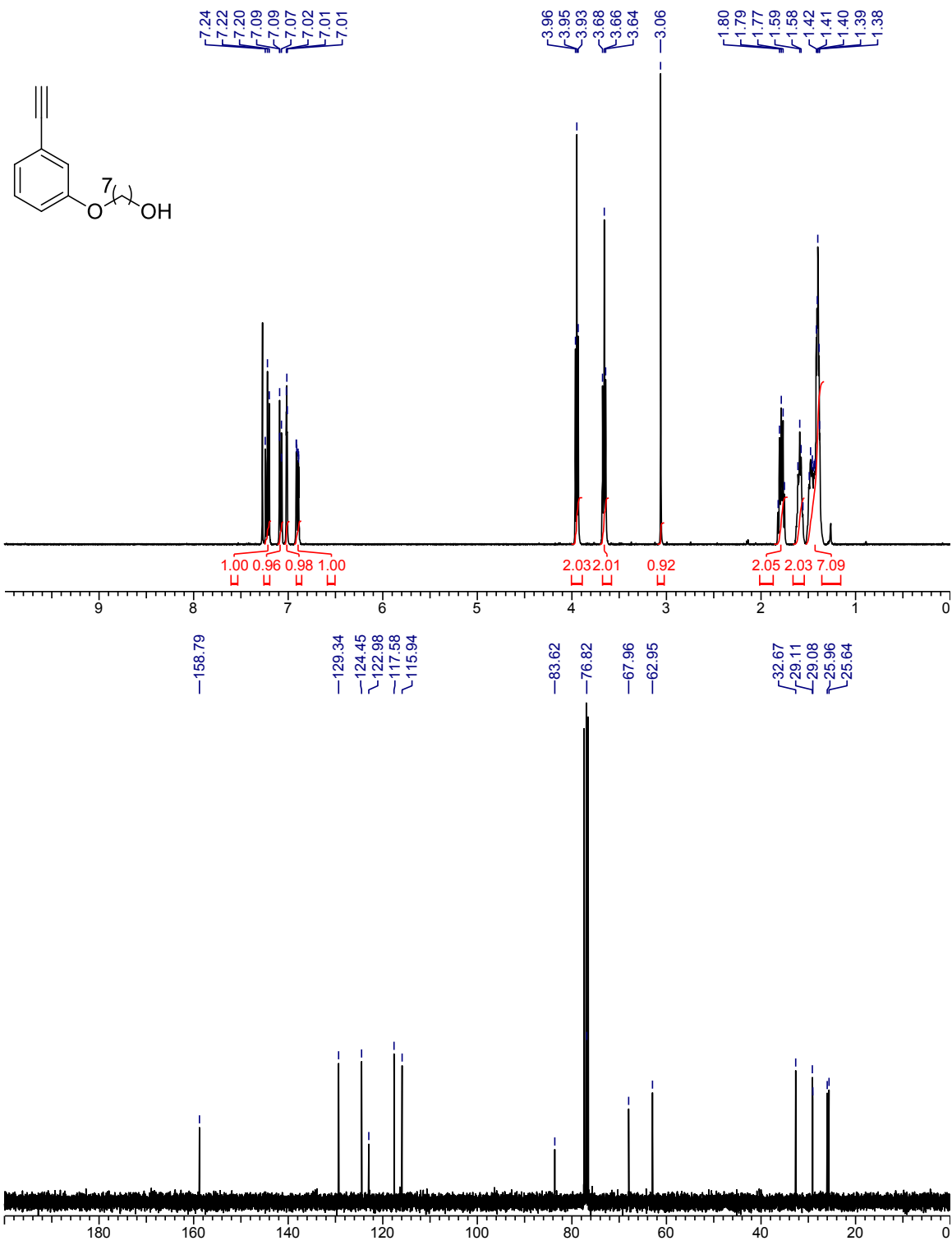
Macrocycle (9): Following the general procedure described above, macrocycle **9** was isolated. (32 mg, 64 %). ^1H NMR (400 MHz, CDCl_3) δ 7.23 - 7.16 (m, 1H), 7.09 - 7.01 (m, 2H), 6.89 (dd, $J = 8.3, 1.7$ Hz, 1H), 4.08 (t, $J = 6.4$ Hz, 2H), 4.03 (t, $J = 6.9$ Hz, 2H), 2.42 - 2.37 (m, 2H), 2.35 (t, $J = 7.5$ Hz, 2H), 1.78 (quin, $J = 6.8$ Hz, 2H), 1.71 - 1.60 (m, 4H), 1.60 - 1.45 (m, 4H), 1.45 - 1.34 (m, 12H); ^{13}C NMR (125 MHz, CDCl_3) δ ppm = 173.9, 158.6, 129.5, 124.2, 123.0, 118.3, 117.3, 85.1, 74.9, 74.3, 68.2, 65.6, 64.1, 34.1, 29.0, 28.5 (2C), 28.42, 28.40, 28.1, 27.6, 25.9, 25.5, 19.5; HRMS (ESI) m/z calculated for $\text{C}_{24}\text{H}_{34}\text{NaO}_3$ $[\text{M}+\text{Na}]^+$, 417.2400; found: 417.2408.

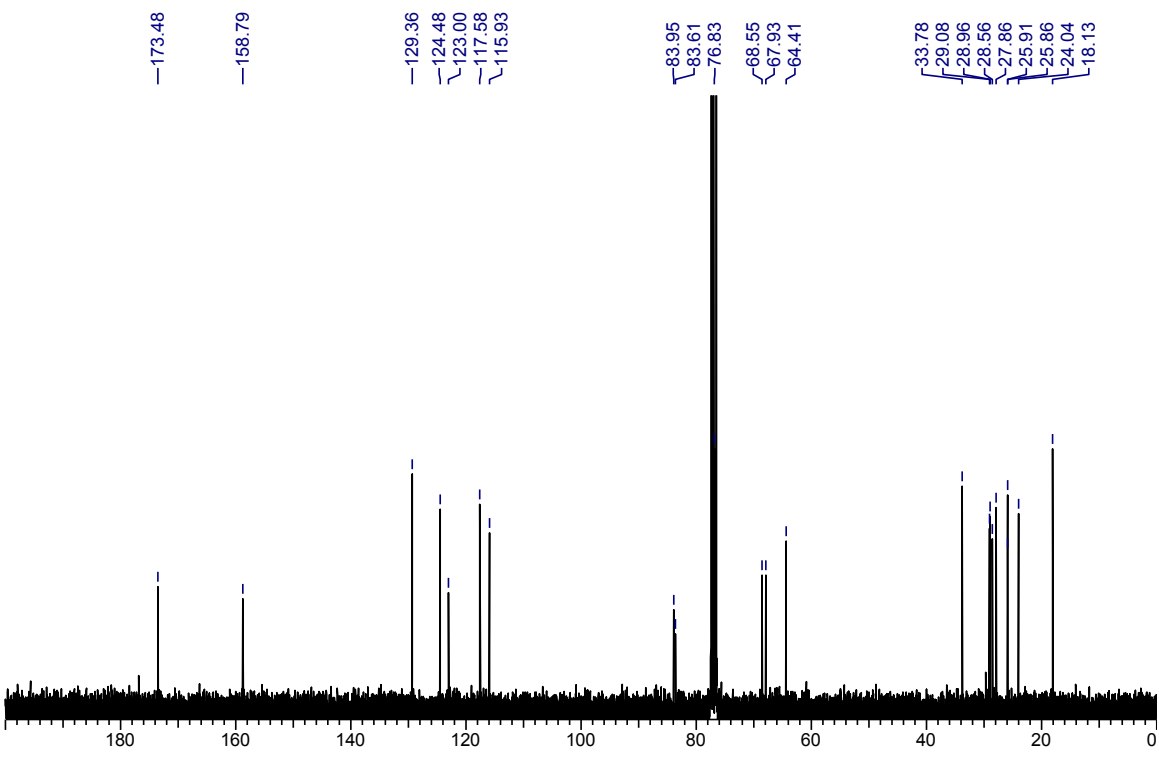
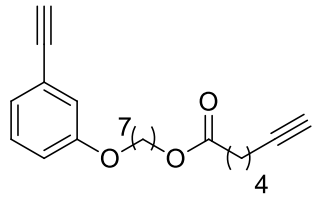
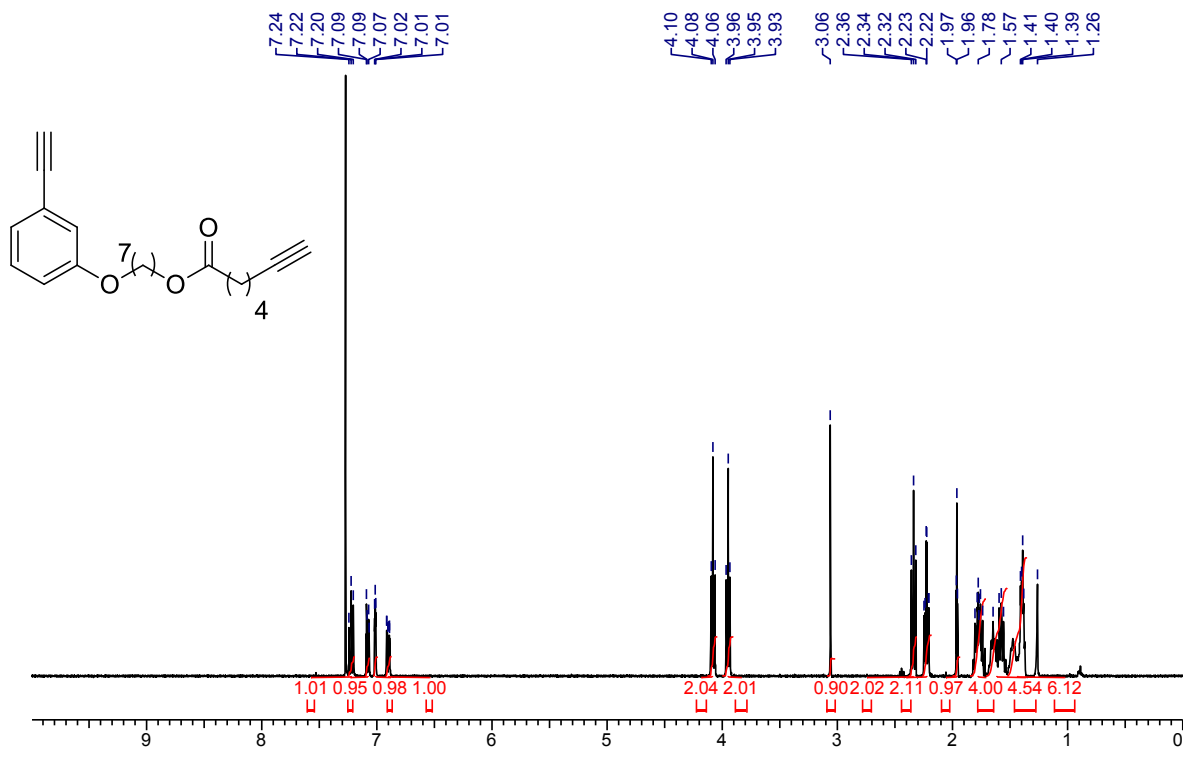
Complete Reference From Text:

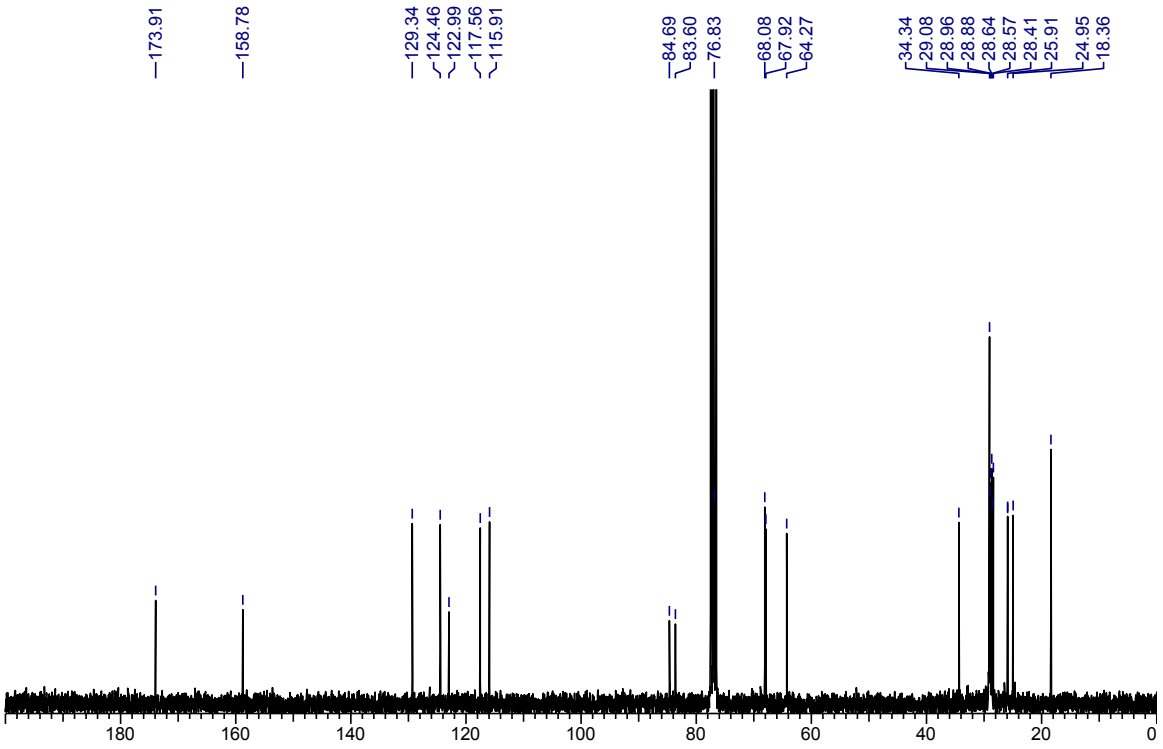
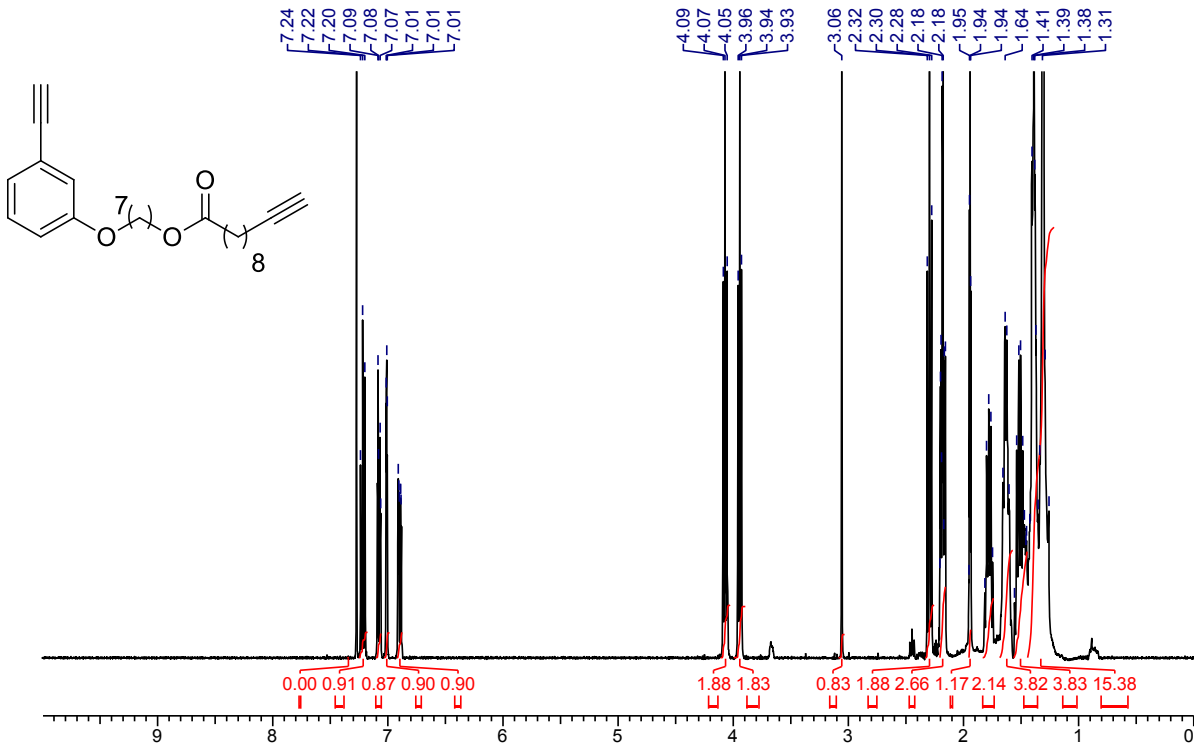
- (3) Lamarre, D.; Anderson, P. C.; Bailey, M.; Beaulieu, P.; Bolger, G.; Bonneau, P.; Bös, M.; Cameron, D. R.; Cartier, M.; Cordingley, M. G.; Faucher, A.-M.; Goudreau, N.; Kawai, S. H.; Kukolj, G.; Lagacé, L.; Laplante, S. R.; Narjes, H.; Poupart, M.-A.; Rancourt, J.; Sentjens, R. E.; St-George, R.; Simoneau, B.; Steinmann, G.; Thibeault, D.; Tsantrizos, Y. S.; Weldon, S. M.; Yong, C.-L.; Llinàs-Brunet, M. *Nature* 2003, 426, 186-189.

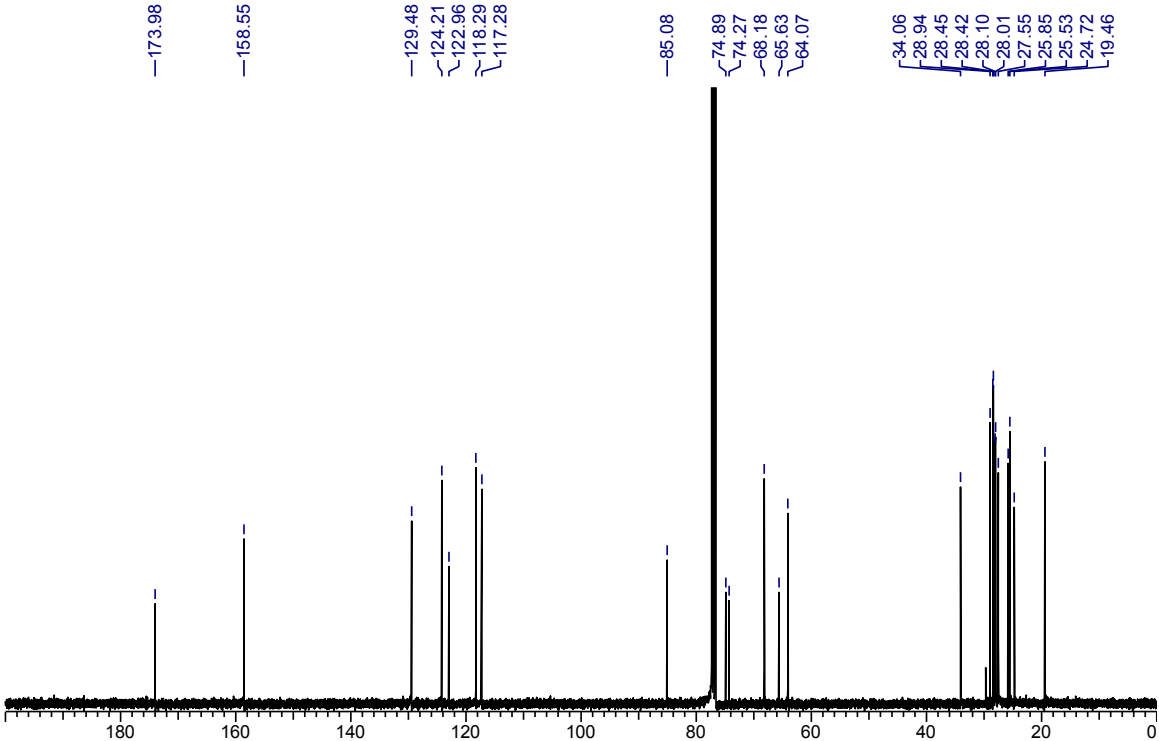
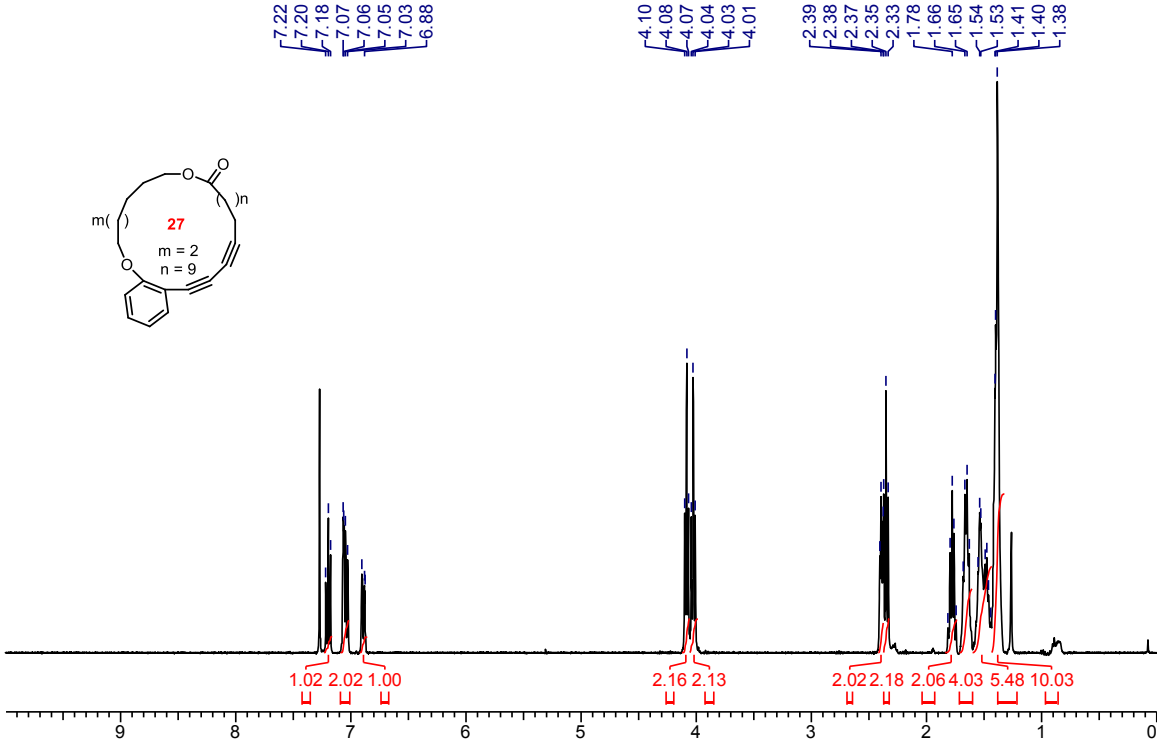
NMR SPECTRA FOR NEW COMPOUNDS











mmm

Chapter 15 : Supporting Information of Chapter 4: Exploiting Aggregation to Achieve Phase Separation in Macrocyclization

General:

All reactions that were carried out under anhydrous conditions were performed under an inert argon or nitrogen atmosphere in glassware that had previously been dried overnight at 120 °C or had been flame dried and cooled under a stream of argon or nitrogen.¹⁵ All chemical products were obtained from Sigma-Aldrich Chemical Company or Strem Chemicals and were reagent quality. Methyl-3,6-dihydroxybenzoate was prepared according to literature procedures.¹⁶ (3,4,5-Tris(2-(2-methoxyethoxy)ethoxy)-phenyl)methanol and 1-chloro-2-(2-methoxyethoxy)ethane were prepared according to literature procedures.¹⁷ Acyclic diynes **3** and **5** and the macrocycles **4** and **6** were prepared as reported in the literature.¹⁸ Technical solvents were obtained from VWR International Co. Anhydrous solvents (CH₂Cl₂, Et₂O, THF, DMF, Toluene, and hexanes) were dried and deoxygenated using a GlassContour system (Irvine, CA). Isolated yields reflect the mass obtained following flash column silica gel chromatography. Organic compounds were purified using the method reported by W. C. Still¹⁹ and using silica gel obtained from Silicycle Chemical division (40-63 nm; 230-240 mesh).

¹⁵ Shriver, D. F.; Drezdon, M. A. in *The Manipulation of Air-Sensitive Compounds*; Wiley-VCH: New York, 1986.

¹⁶ Zhu, J.; Beugelmans, R.; Bourdet, S.; Chastanet, J.; Roussi, G. *J. Org. Chem.* **1995**, *60*, 6389.

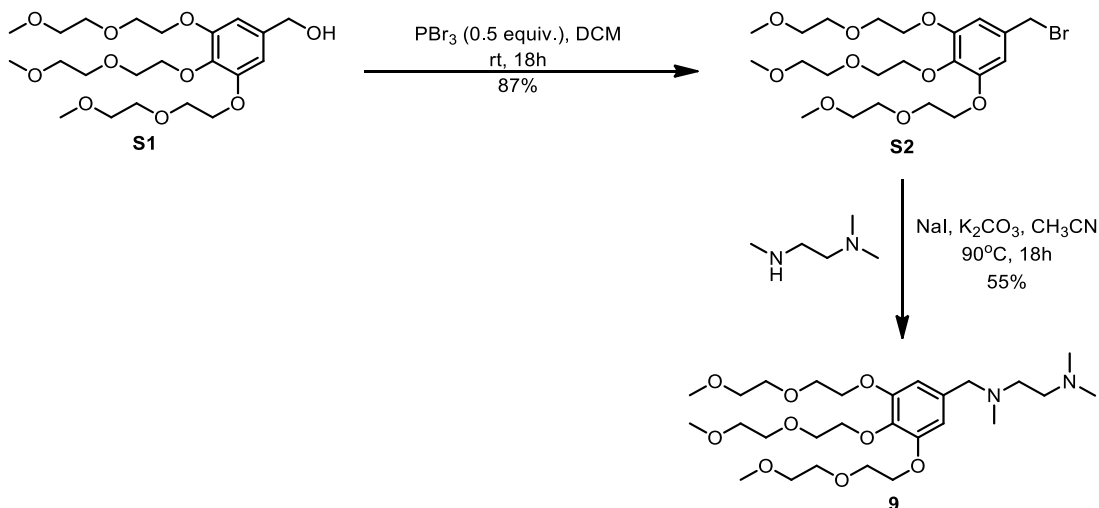
¹⁷ Gudipati, V.; Curran, D. P.; Wilcox, C. S. *J. Org. Chem.* **2006**, *71*, 3599.

¹⁸ Bédard, A.-C.; Collins, S. K. *J. Am. Chem. Soc.* **2011**, *133*, 19976.

¹⁹ Still, W. C.; Kahn, M.; Mitra, A. *J. Org. Chem.* **1978**, *43*, 2923.

Analytical thin-layer chromatography (TLC) was performed on glass-backed silica gel 60 coated with a fluorescence indicator (Silicycle Chemical division, 0.25 mm, F₂₅₄). Visualization of TLC plate was performed by UV (254 nm), KMnO₄ or *p*-anisaldehyde stains. All mixed solvent eluents are reported as v/v solutions. Concentration refers to removal of volatiles at low pressure on a rotary evaporator. All reported compounds were homogeneous by thin layer chromatography (TLC) and by ¹H NMR. NMR spectra were taken in deuterated CDCl₃ using Bruker AV-300 and AV-400 instruments unless otherwise noted. Signals due to the solvent served as the internal standard (CHCl₃: δ 7.27 for ¹H, δ 77.0 for ¹³C). The ¹H NMR chemical shifts and coupling constants were determined assuming first-order behavior. Multiplicity is indicated by one or more of the following: s (singlet), d (doublet), t (triplet), q (quartet), m (multiplet), br (broad); the list of couplings constants (*J*) corresponds to the order of the multiplicity assignment. The ¹H NMR assignments were made based on chemical shift and multiplicity. The ¹³C NMR assignments were made on the basis of chemical shift and multiplicity. High resolution mass spectroscopy (HRMS) was done by the Centre régional de spectrométrie de masse at the Département de Chimie, Université de Montréal from an Agilent LC-MSD TOF system using ESI mode of ionization unless otherwise noted.

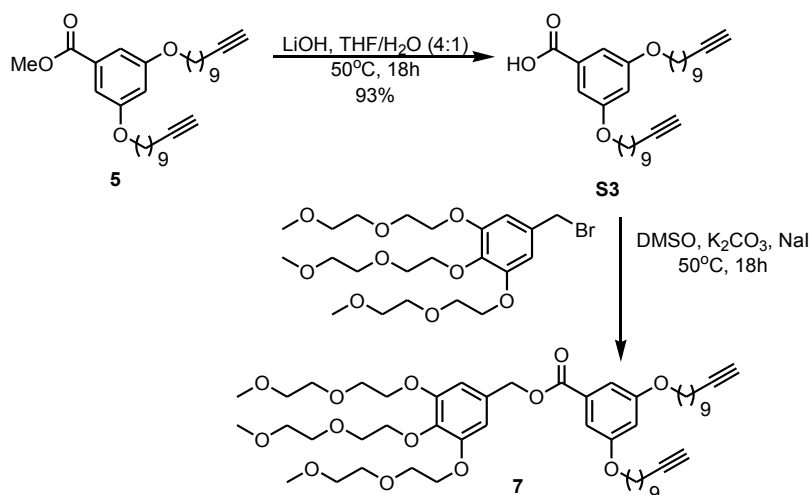
SYNTHESIS OF TAGGED LIGAND AND SUBSTRATE



N^1 -(3,4,5-tris(2-(2-methoxyethoxy)ethoxy)benzyl)- N^1,N^2,N^2 -trimethylethane-1,2-diamine

(9): To a stirring solution of (3,4,5-tris(2-(2-methoxyethoxy)ethoxy)phenyl)methanol³ **S1** (1.0 g, 2.2 mmol) in anhydrous dichloromethane (7 mL) at 0°C was added PBr_3 (0.1 mL, 1.1 mmol) dropwise. The mixture was left to stir for 1 h at 0°C then warmed to room temperature and stirred for 18 h. Distilled water was added to the reaction mixture and the phases were separated. The aqueous phase was extracted with dichloromethane (2X). The organic phases were combined, washed with brine and dried over anhydrous Na_2SO_4 . The suspension was filtered and the filtrate was concentrated in vacuo. The product 1,2,3-tris(2-(2-methoxyethoxy)ethoxy)-5-(bromomethyl)benzene **S2** was obtained as a brown oil (1.0 g, 87 %) and was used crude directly in the next step. ^1H NMR (400 MHz, CDCl_3) δ = 6.52 (s, 2 H), 4.30 (s, 2 H), 4.05 (t, J = 4.8 Hz, 6 H), 3.74 (t, J = 4.8 Hz, 4 H), 3.69 (t, J = 5.0 Hz, 2 H), 3.60 (dd, J = 3.7, 5.5 Hz, 6 H), 3.44 (dd, J = 3.4, 5.6 Hz, 6 H), 3.26 (s, 9 H). Benzyl bromide **S2** (200 mg, 0.38 mmol), anhydrous acetonitrile (2 mL) and N,N,N -trimethylethylamine (39 mg, 0.38 mmol) were placed in a sealed tube. NaI (3 mg, 0.02 mmol) and K_2CO_3 (52 mg, 0.38

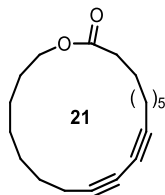
mmol) were added to the mixture. The tube was sealed and the reaction was warmed to 90 °C (oil bath) for 18 h. The reaction was then cooled to room temperature and the crude mixture was purified by chromatography on neutral alumina (100 % CH₂Cl₂ to 15 % MeOH in CH₂Cl₂). The product was obtained as a colorless oil (114 mg, 55 %). ¹H NMR (400 MHz, CDCl₃) δ = 6.87 (s, 2 H), 4.26 - 4.21 (m, 4 H), 4.21 - 4.16 (m, 2 H), 3.93 (s, 2 H), 3.89 - 3.83 (m, 4 H), 3.83 - 3.78 (m, 2 H), 3.75 - 3.69 (m, 7 H), 3.68 - 3.63 (m, 3 H), 3.58 - 3.52 (m, 7 H), 3.38 (s, 3 H), 3.38 (s, 6 H), 2.64 (s, 6 H); ¹³C NMR (75 MHz, CDCl₃) δ = 153.0, 139.2, 125.5, 110.1, 77.2, 72.4, 72.0, 71.9, 70.6 (2C), 70.5, 70.42, 70.35, 69.2, 62.2, 59.0, 42.9 ppm; HRMS (ESI) m/z calculated for C₂₇H₅₀N₂NaO₉ [M+Na]⁺, 569.3409; found: 569.3406.



3,4,5-Tris(2-(2-methoxyethoxy)ethoxy)benzyl 3,5-bis(undec-10-ynyloxy)benzoate (7): To a solution of methyl 3,5-bis(undec-10-yn-1-yloxy)benzoate⁴ **5** (852 mg, 1.82 mmol) in THF (8 mL) and H₂O (2 mL) was added LiOH (237 mg, 9.11 mmol). The mixture was warmed to 50 °C and stirred for 18 h. The reaction was cooled to room temperature and EtOAc and H₂O were added. The phases were separated and the aqueous phase's pH was adjusted to 2 using 1 N HCl. The aqueous phase was extracted with EtOAc (3X), the organic phases were combined, washed with brine and dried with anhydrous Na₂SO₄. The suspension was filtered

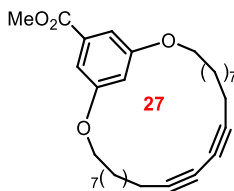
and the filtrate was concentrated in vacuo. The product 3,5-bis(undec-10-ynyloxy)benzoic acid **S3** was obtained as a pale yellow solid (770 mg, 93%) and was used crude in the next step. ^1H NMR (400MHz, acetone-*d*6) δ = 7.15 (d, J = 2.2 Hz, 2H), 6.70 (t, J = 2.3 Hz, 1H), 4.02 (t, J = 6.4 Hz, 4H), 3.54 (t, J = 6.5 Hz, 1H), 2.28 (t, J = 2.7 Hz, 2H), 2.16 (dt, J = 6.9, 2.7, 4H), 1.83 - 1.73 (m, 4H), 1.56 - 1.23 (m, 24H); HRMS (ESI) m/z calculated for $\text{C}_{29}\text{H}_{43}\text{O}_4$ $[\text{M}+\text{H}]^+$, 455.3156; found: 455.3151. Bis(undec-10-ynyloxy)benzoic acid **S3** (250 mg, 0.55 mmol) and benzyl bromide **S2** (317 mg, 0.61 mmol) were dissolved in anhydrous DMSO (3 mL). K_2CO_3 (114 mg, 0.83 mmol) and NaI (9 mg, 0.06 mmol) were added and the resulting mixture was warmed to 50 °C and stirred for 18 h. The reaction was cooled back to room temperature and EtOAc and H_2O were added. The phases were separated. The aqueous phase was then extracted with EtOAc (5X). The organic phases were combined and dried with anhydrous Na_2SO_4 . The suspension was filtered and the filtrate was concentrated in vacuo. The crude mixture was purified by silica gel column chromatography (100 % DCM to 15 % MeOH in DCM). The product was isolated as a brown oil (106 mg, 21 %) ^1H NMR (300 MHz, CDCl_3) δ = 7.15 (d, J = 2.3 Hz, 2H), 6.69 - 6.60 (m, 3H), 5.20 (s, 1H), 4.25 - 4.09 (m, 6H), 3.95 (m, 4H), 3.82 (m, 6H), 3.75 - 3.63 (m, 8H), 3.59 - 3.49 (m, 6H), 3.37 (s, 9H), 2.17 (td, J = 7.0, 2.6 Hz, 4H), 1.93 (t, J = 2.6 Hz, 2H), 1.82 - 1.70 (m, 4H), 1.58 - 1.23 (m, 23H); ^{13}C NMR (75 MHz, CDCl_3) δ = 169.5, 166.2, 160.1 (2C), 152.6 (2C), 138.3, 131.7 (2C), 131.4 (2C), 131.3, 108.0, 107.9, 107.7, 107.0, 106.4, 84.7 (2C), 72.3, 71.9 (2C), 70.6, 70.5, 70.3 (2C), 69.7 (2C), 68.8, 68.2 (2C), 68.0 (2C), 66.8, 59.0, 29.3 (2C), 29.2 (2C), 29.1 (2C), 28.9 (2C), 28.6 (2C), 28.4 (2C), 25.9 (2C), 18.3 (2C) ppm; HRMS (ESI) m/z calculated for $\text{C}_{51}\text{H}_{78}\text{NaO}_{13}$ $[\text{M}+\text{Na}]^+$, 921.5335; found: 921.5373.

SYNTHESIS OF MACROCYCLES



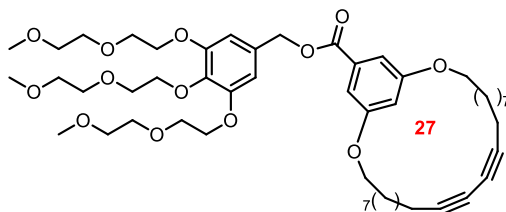
General procedure A for the macrocyclization of diynes under Glaser-Hay oxidative coupling conditions using microwave irradiation: Macrocycle (2): To a microwave vial equipped with a stirring bar was added CuCl_2 (5.5 mg, 0.03 mmol, 25 mol %) and $\text{Ni}(\text{NO}_3)_2 \cdot 6\text{H}_2\text{O}$ (9.3 mg, 0.03 mmol, 25 mol %). Polyethylene glycol 400 (3.33 mL), triethylamine (0.05 mL, 0.36 mmol, 3 equiv.) and tetramethylethylene diamine (0.09 mL, 0.6 mmol, 5 equiv.) were added and the mixture was stirred at room temperature for 15 min or until the metals were solubilized. The diyne (28 mg, 0.12 mmol) was added to the homogenous mixture as a methanol solution (1.67 mL) in one portion. Oxygen was bubbled in the solution for 5 min and the vial was then sealed with a microwave cap. The reaction was warmed to 120 °C for 6 h. The crude mixture was loaded directly onto silica gel for purification by chromatography (100 % hexanes \rightarrow 10 % ethyl acetate in hexanes) and afforded the product as a colorless semi-solid (23 mg, 81 %). ^1H NMR (300 MHz, CDCl_3) δ = 4.10 (t, J = 6.5 Hz, 2H), 2.36 - 2.26 (m, 6H), 1.70 - 1.61 (m, 6H), 1.50 - 1.26 (m, 14H); ^{13}C NMR (125 MHz, CDCl_3) δ ppm = 174.0, 77.6, 77.2, 66.0, 65.8, 64.2, 34.3, 29.1, 28.5, 28.23, 28.22, 28.19, 27.93, 27.91, 27.63, 27.58, 25.7, 25.0, 19.03, 19.02; HRMS (ESI) m/z calculated for $\text{C}_{20}\text{H}_{31}\text{O}_2$ $[\text{M}+\text{H}]^+$, 303.2319; found: 303.2325.

General procedure B for the macrocyclization of diynes under Glaser-Hay oxidative coupling conditions using thermal heating: Macrocycle (**2**): To a vial equipped with a stirring bar was added CuCl_2 (5.5 mg, 0.03 mmol, 25 mol %) and $\text{Ni}(\text{NO}_3)_2 \cdot 6\text{H}_2\text{O}$ (9.3 mg, 0.03 mmol, 25 mol %). Polyethylene glycol 400 (3.33 mL), triethylamine (0.05 mL, 0.36 mmol, 3 equiv.) and pyridine (0.05 mL, 0.6 mmol, 5 equiv.) were added and the mixture was stirred at room temperature for 15 min or until the metals were solubilized. The diyne (28 mg, 0.12 mmol) was added to the homogenous mixture as a methanol solution (1.67 mL) in one portion. Oxygen was bubbled in the solution for 5 min and the vial was then closed with a screw cap. The reaction was warmed to 60 °C and monitored by TLC for consumption of the starting material (oxygen was bubbled again through the solution every 12 h). When the starting material was completely consumed (TLC), the reaction was cooled to room temperature and the crude mixture was loaded directly on a silica column. Purification by silica gel chromatography (100 % hexanes \rightarrow 10 % ethyl acetate in hexanes) afforded the product as a colorless semi-solid (21 mg, 0.09 mmol, 73 %).



Macrocycle (6): Following the general procedure B described above, macrocycle **6** was isolated. (38 mg, 0.080 mmol, 65 %). ^1H NMR (300 MHz, CDCl_3) δ = 7.17 (d, J = 2.2 Hz, 2H), 6.70 (t, J = 2.2 Hz, 1H), 4.08 - 3.99 (t, J = 6.0 Hz, 4H), 3.91 (s, 3H), 2.25 (t, J = 6.4 Hz, 4H), 1.84 - 1.71 (m, 4H), 1.65 - 1.14 (m, 28H); ^{13}C NMR (125 MHz, CDCl_3) δ ppm = 167.0, 160.1, 131.8, 107.6, 107.4, 77.5, 68.0, 65.5, 52.2, 29.1, 28.7, 28.73, 28.66, 28.65, 28.3, 28.1,

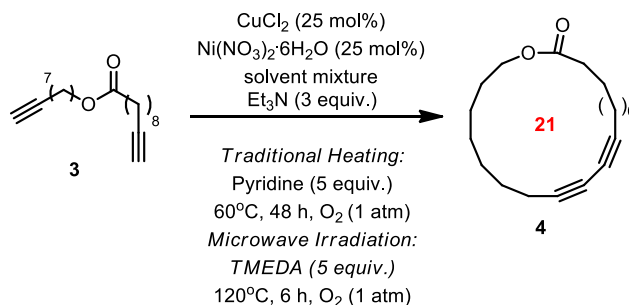
25.8, 19.1 ppm; HRMS (ESI) m/z calculated for $C_{30}H_{43}O_4$ $[M+H]^+$, 467.3156; found: 467.3165.



Macrocycle (8): Following the general procedure B described above, macrocycle **8** was isolated. (68 mg, 0.077 mmol, 64 %). 1H NMR (400 MHz, $CDCl_3$) δ = 7.18 (d, J = 2.2 Hz, 2H), 6.70 (t, J = 2.2 Hz, 1H), 6.67 (s, 2H), 5.22 (s, 2H), 4.23 - 4.14 (m, 6H), 4.02 (t, J = 6.1 Hz, 4H), 3.86 (t, J = 4.9 Hz, 4H), 3.81 (t, J = 5.0 Hz, 2H), 3.72 (m, 6H), 3.60 - 3.54 (m, 6H), 3.39 (s, 9H), 2.25 (t, J = 6.4 Hz, 4H), 1.82 - 1.73 (m, 4H), 1.65 - 1.23 (m, 24H); ^{13}C NMR (125 MHz, $CDCl_3$) δ ppm = 166.3, 160.1(2C), 152.7 (2C), 131.8, 131.4, 108.1 (2C), 107.8 (2C), 107.3, 77.5, 77.2, 72.4, 72.03 (2C), 71.98 (2C), 70.7 (2C), 70.6, 70.4 (2C), 69.7 (2C), 68.9, 68.1, 66.9 (2C), 65.5 (2C), 59.04 (2C), 59.01 (2C), 29.1(2C), 28.74 (2C), 28.66 (2C), 28.3 (2C), 28.1(2C), 25.8 (2C), 19.1 (2C) ppm; HRMS (ESI) m/z calculated for $C_{51}H_{76}NaO_{13}$ $[M+Na]^+$, 919.5178; found: 919.5191.

COMPLETE TABLE 1

Table 1 - Yields of macrocycle **4** at various ratios of PEG₄₀₀ or ethylene glycol in MeOH using both traditional heating and microwave heating.



entry	solvent	% solvent/ MeOH	Traditional Heating	Microwave Heating
			yield 4 (%) ^a	yield 4 (%) ^a
1		0	24	22
2		10	45	44
3	PEG ₄₀₀	33	62	54
4		66	81	75
5		90	69 ^{b,c}	56 ^{b,c}
6		100	<5 ^{b,c}	<5 ^{b,c}
7		0	24	22
8		10	24	27
9	ethylene	33	34	24
10	glycol	66	26 ^b	24 ^b
11		90	27 ^b	20 ^b
12		100	16 ^b	14 ^b

^a All compounds were isolated by silica gel flash chromatography. Unless otherwise stated, all remaining starting material **3** was oligomerized, see ref 13. ^b Some precipitation of the catalyst mixture was observed during the course of the reaction. ^c Remaining mass balance was recovered **3**.

SURFACE TENSION DATA

A solution of MeOH (40 mL) was placed at 60 °C in a Dataphysics DCAT11 surface tension analyser. Various amounts of PEG₄₀₀ were added and the mixture was stirred until homogenous (the stirring was stopped during the time of the measurement). The surface tension was measured using a rectangular Wilhemy plate for every % PEG₄₀₀ in MeOH following the same procedure.

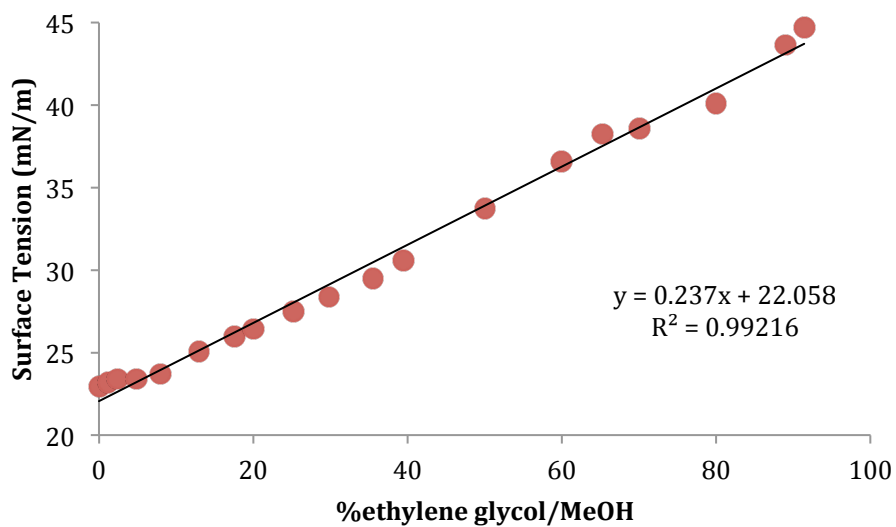
Table S1: Surface tension measurement for PEG₄₀₀/MeOH

%PEG ₄₀₀ in MeOH	Surface Tension (mN/m)	±
0	20.151	0.022
1.2	20.012	0.023
2.4	20.135	0.026
4.8	20.255	0.029
8.0	20.49	0.026
13.0	20.957	0.026
17.5	21.521	0.028
20.0	21.828	0.018
25.0	22.979	0.030
29.3	23.861	0.023
35.5	25.364	0.026
39.4	26.451	0.022
44.4	27.924	0.025
50.0	32.716	0.022
60.0	38.736	0.028
65.2	40.523	0.027
69.0	41.343	0.029
89.0	41.223	0.024
91.4	41.868	0.026

Table S2: Surface tension measurement for ethylene glycol/MeOH

%ethylene glycol in MeOH	Surface Tension (mN/m)	±
0.0	20.583	0.023
1.2	20.696	0.025
2.4	20.924	0.026
4.8	20.963	0.022
8.0	21.996	0.027
13.0	23.568	0.029
17.5	25.065	0.021
20.0	26.422	0.024
25.0	27.483	0.056
29.3	28.377	0.060
35.5	29.477	0.054
39.4	30.569	0.039
50.0	32.168	0.071
60.0	33.593	0.039
65.2	34.268	0.029
69.2	35.366	0.059
80.0	37.554	0.030
89.0	38.850	0.029
91.4	38.999	0.025

Linear regression for the surface tension graph of %ethylene glycol/MeOH



UV-VIS DATA

Macrocyclization precursor **3** (36.3 mg, 0.12 mmol) was dissolved to make a stock solutions in PEG₄₀₀ (5 mL) and in MeOH (5 mL). Aliquots from the stock solutions were used to prepare solutions of varying ratios of PEG₄₀₀/MeOH (25 %, 50 %, 75 %). Each solution was stirred for 30 min at room temperature before the absorbance was recorded. The absorbance was recorded on a Cary100 using a 1 cm trajectory and a blank (appropriate solvent or solvent mixture) for each solution.

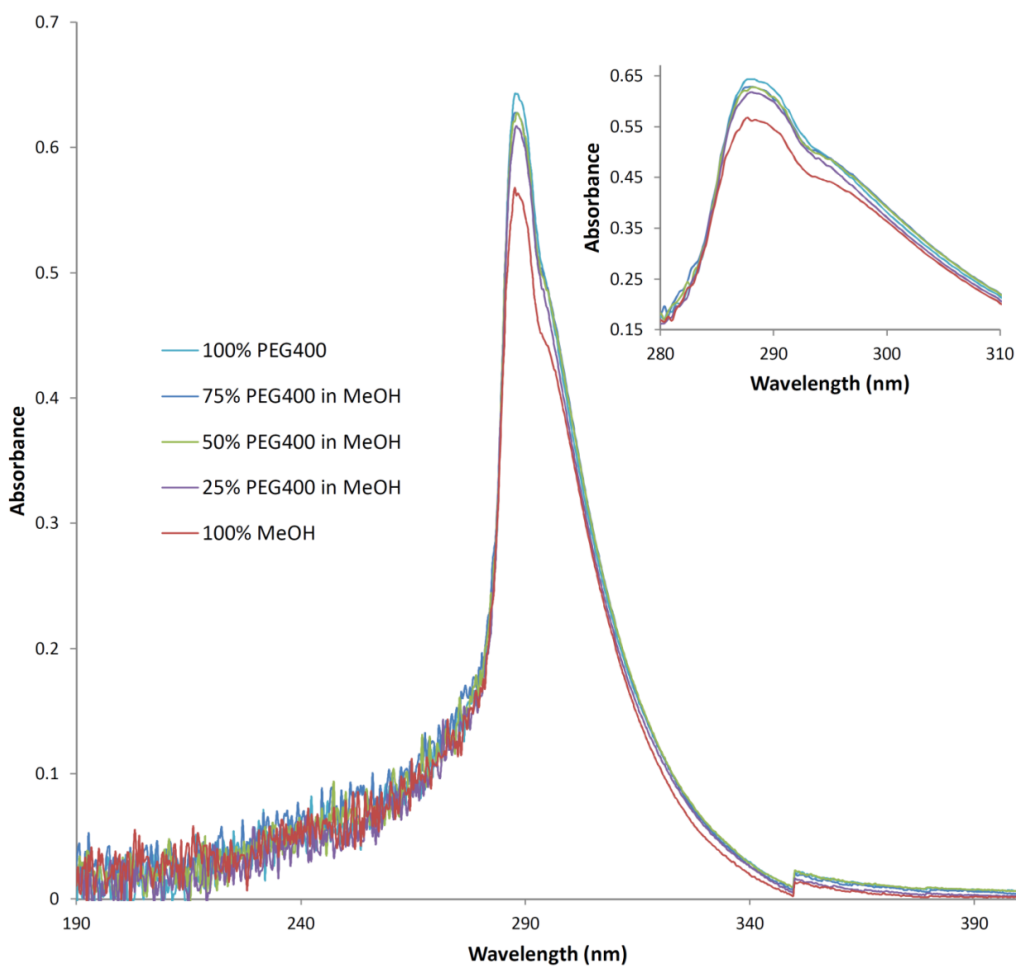
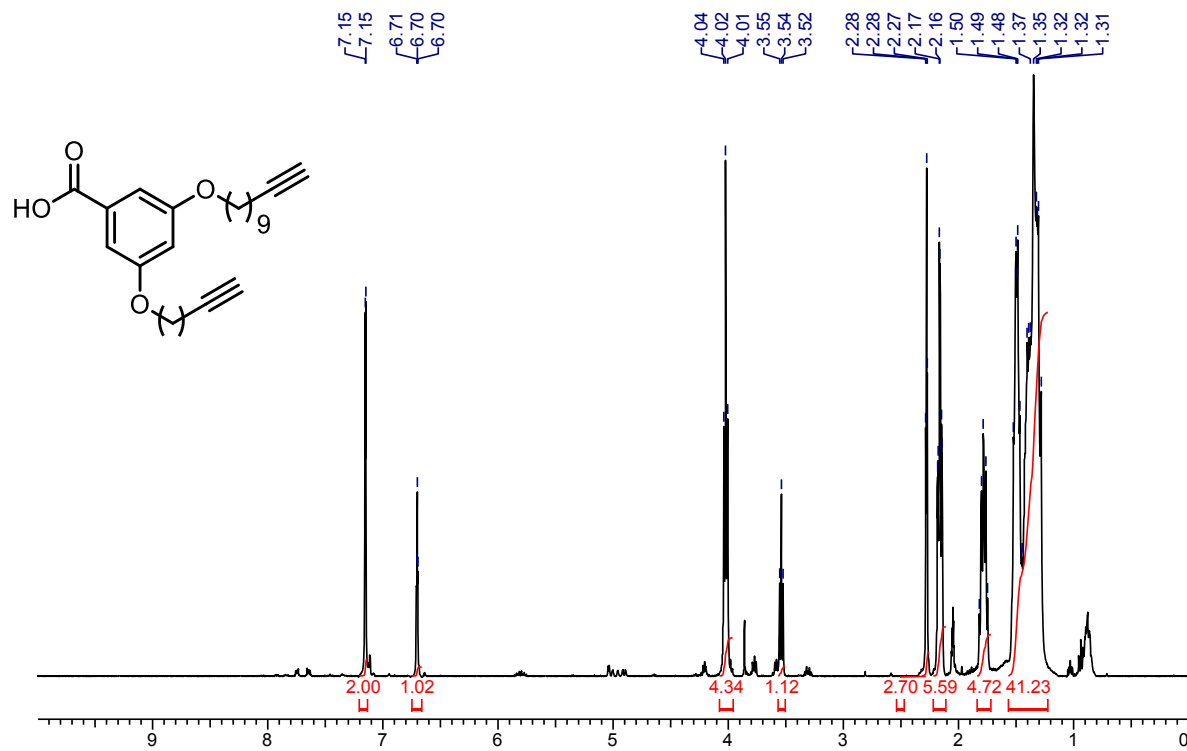
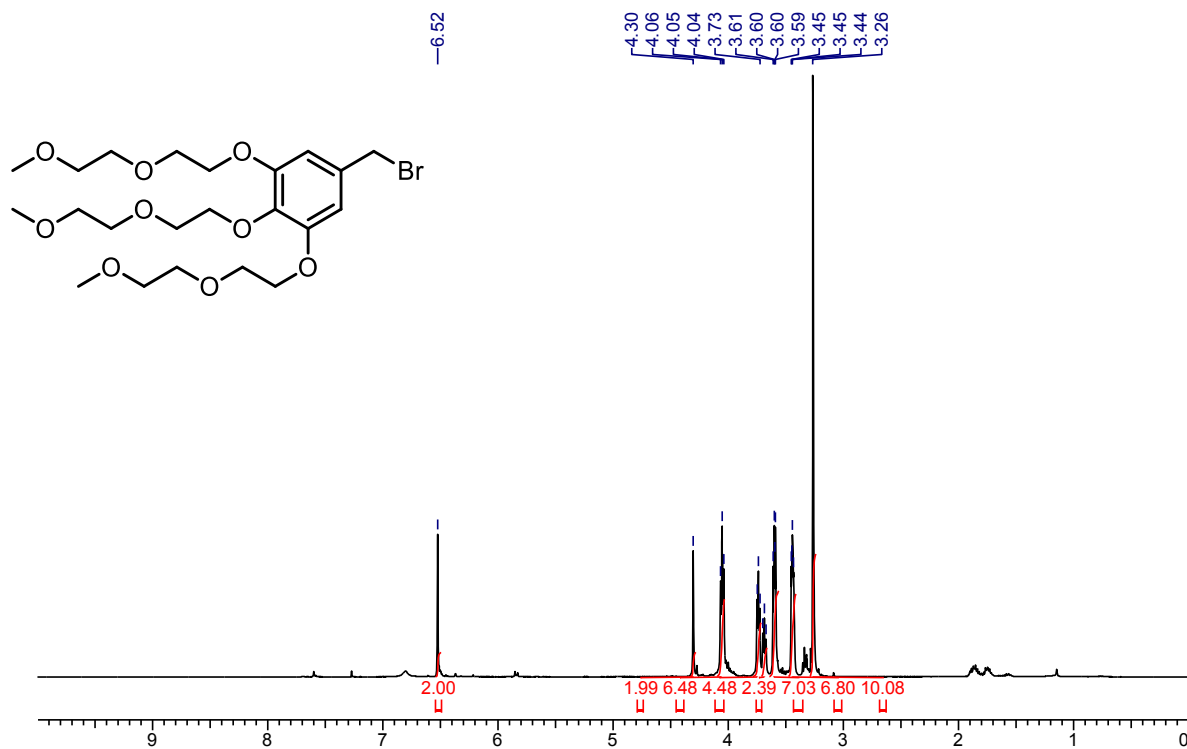
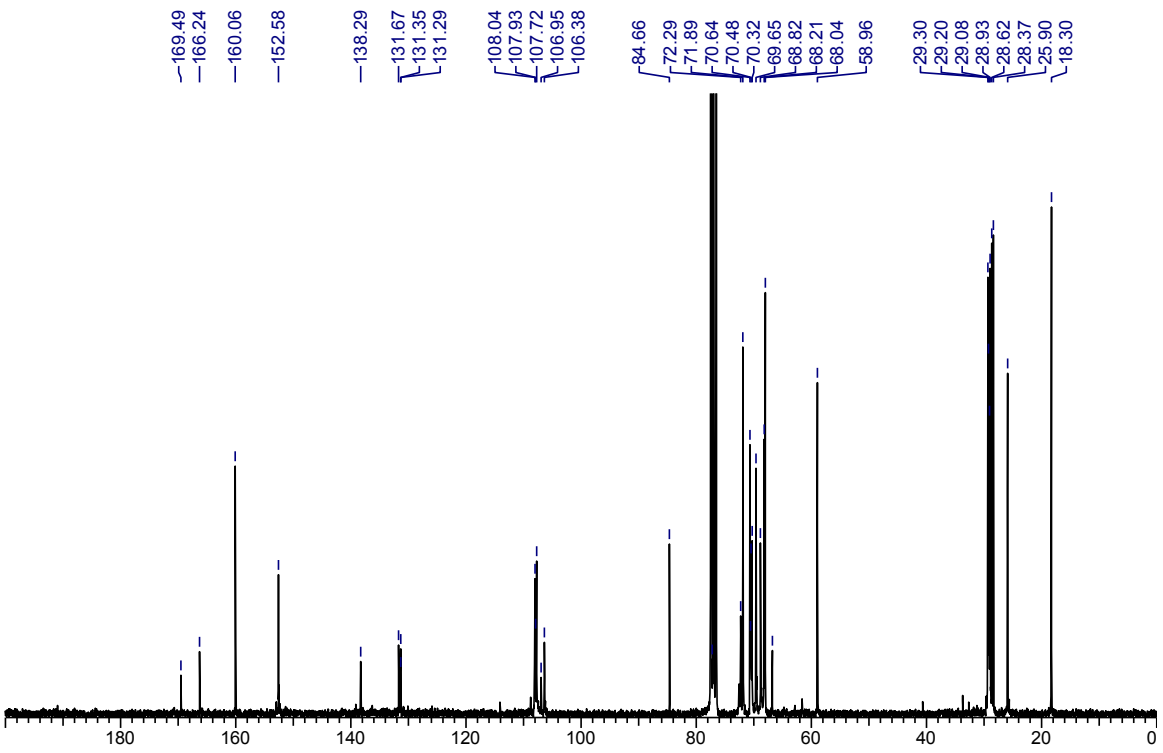
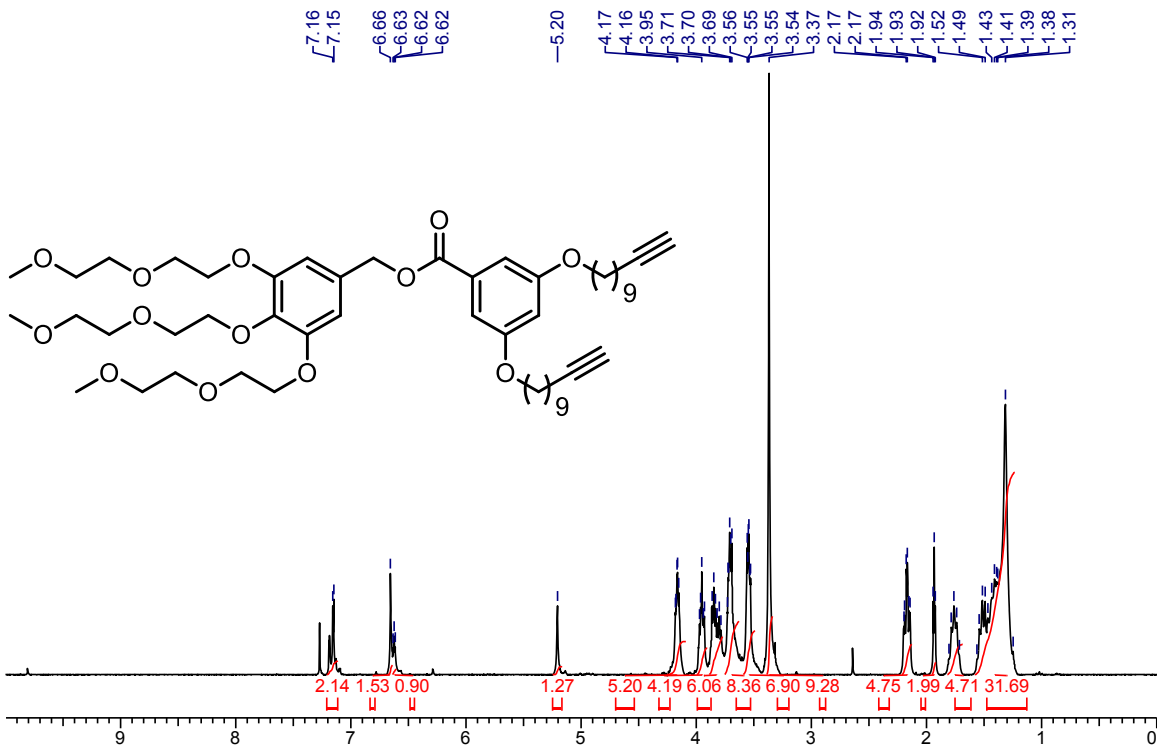


Table S3: Absorbance at maximum wavelength for various solutions of **3**

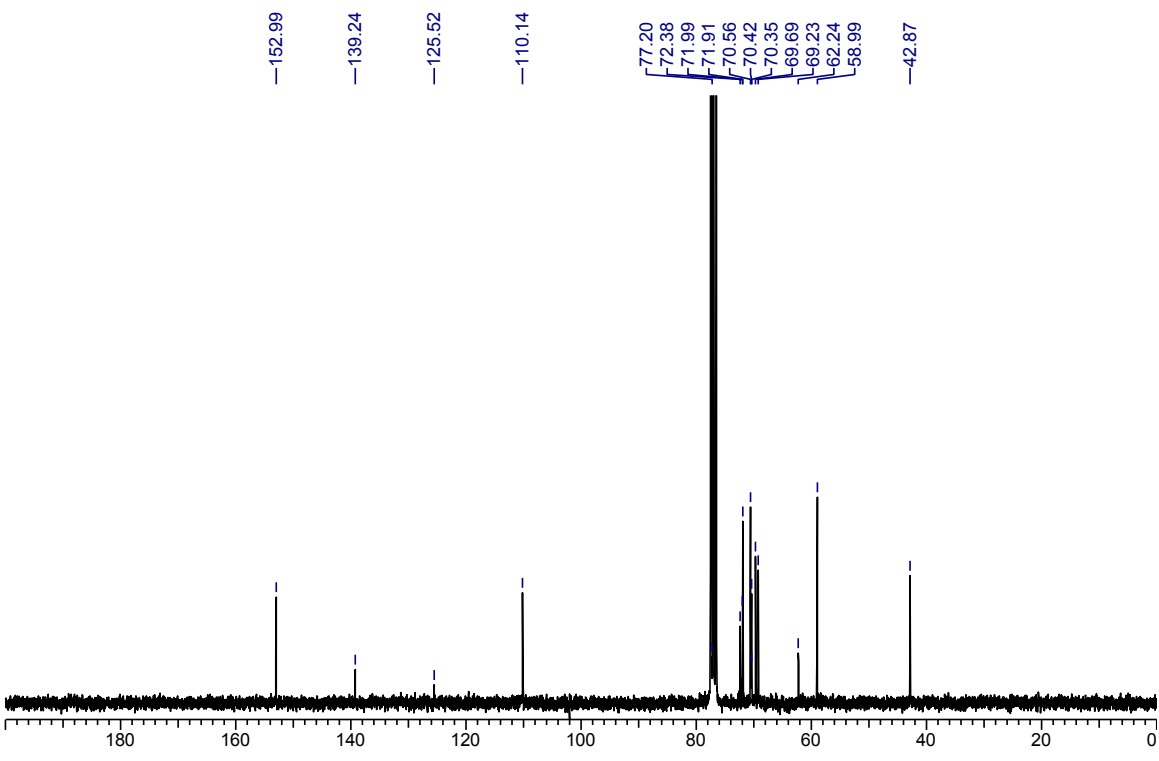
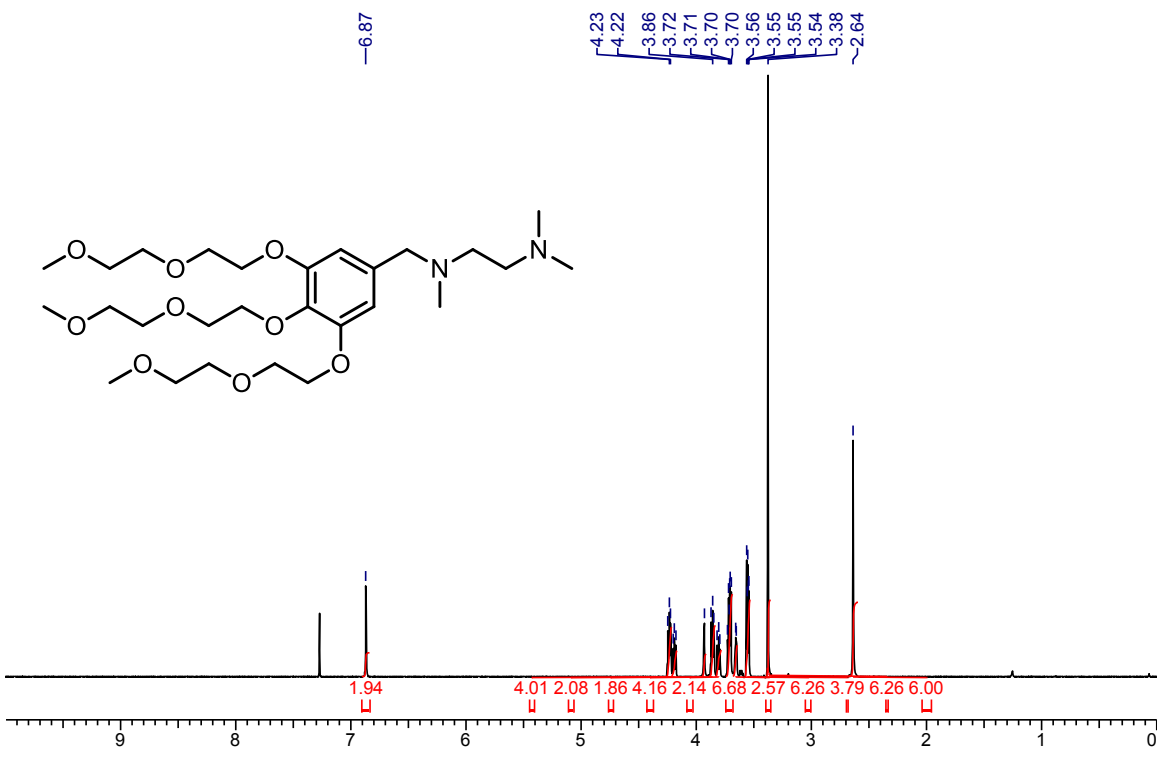
%PEG ₄₀₀ in MeOH	λ max (nm)	Absorbance
100	287.7	0.642913
75	288.0	0.627845
50	288.3	0.627310
25	288.0	0.617332
0	287.7	0.567752

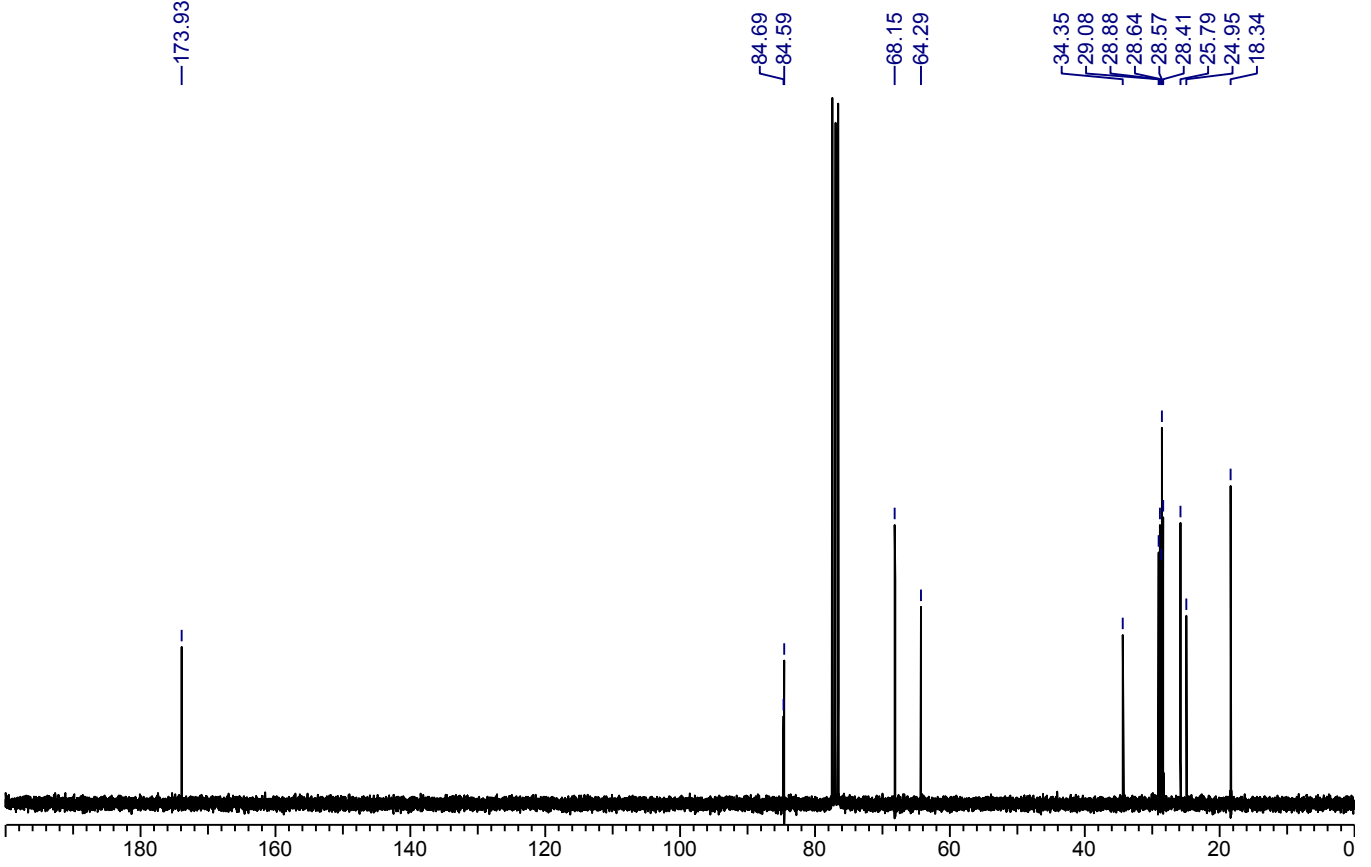
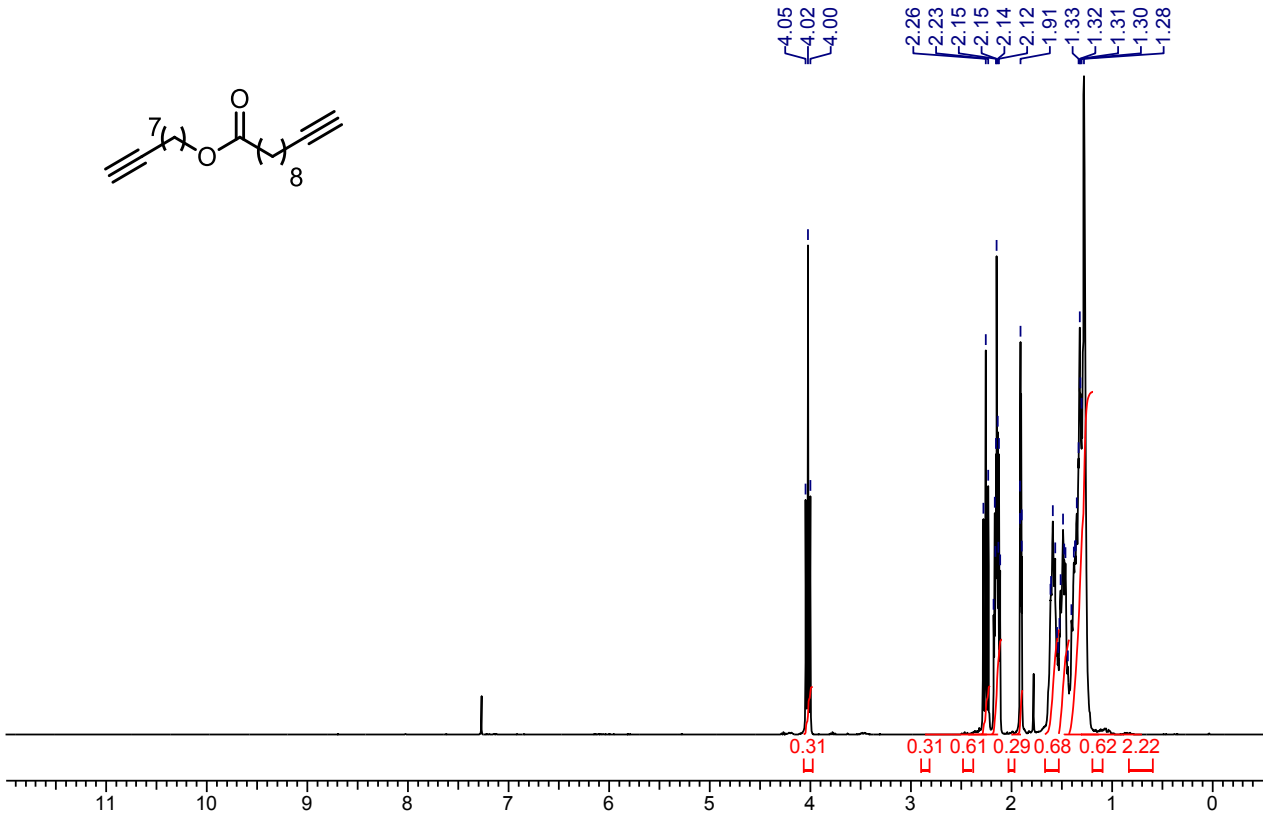
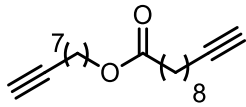
NMR SPECTRA FOR NEW COMPOUNDS



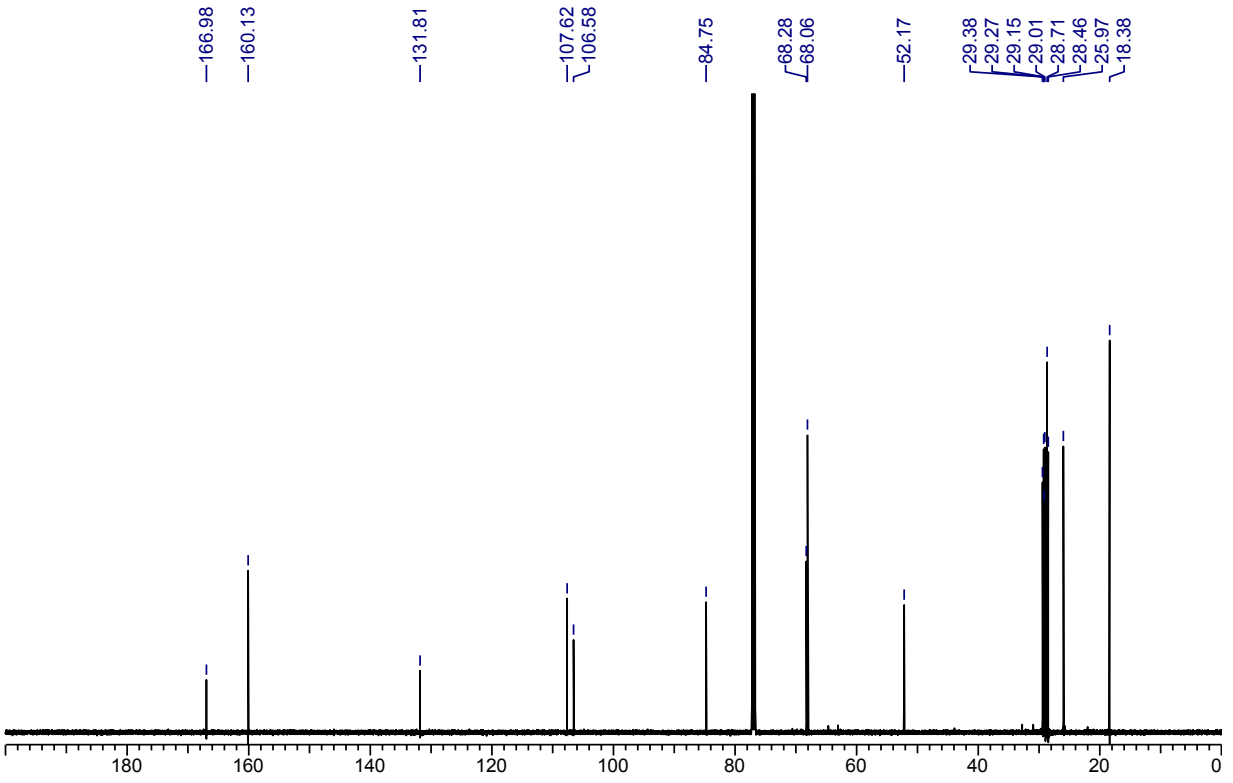
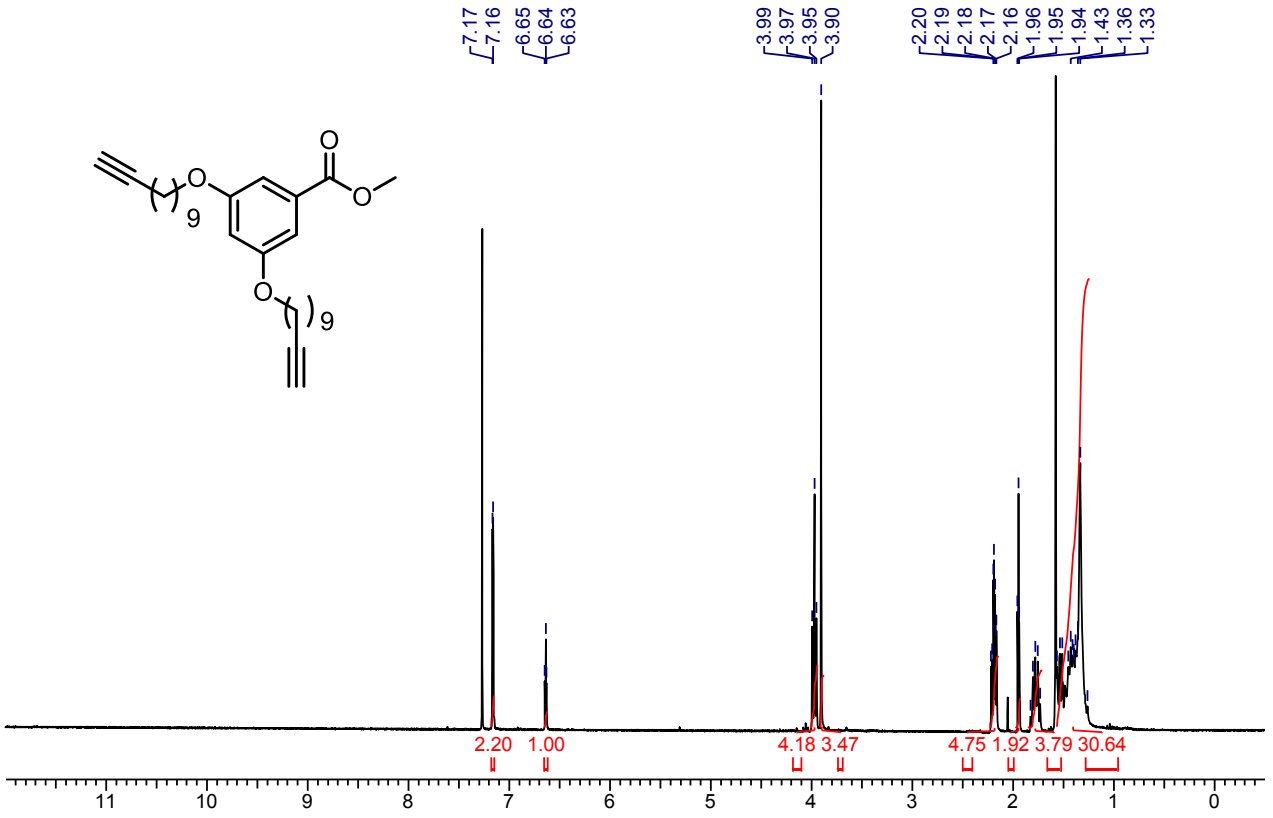


bbbb

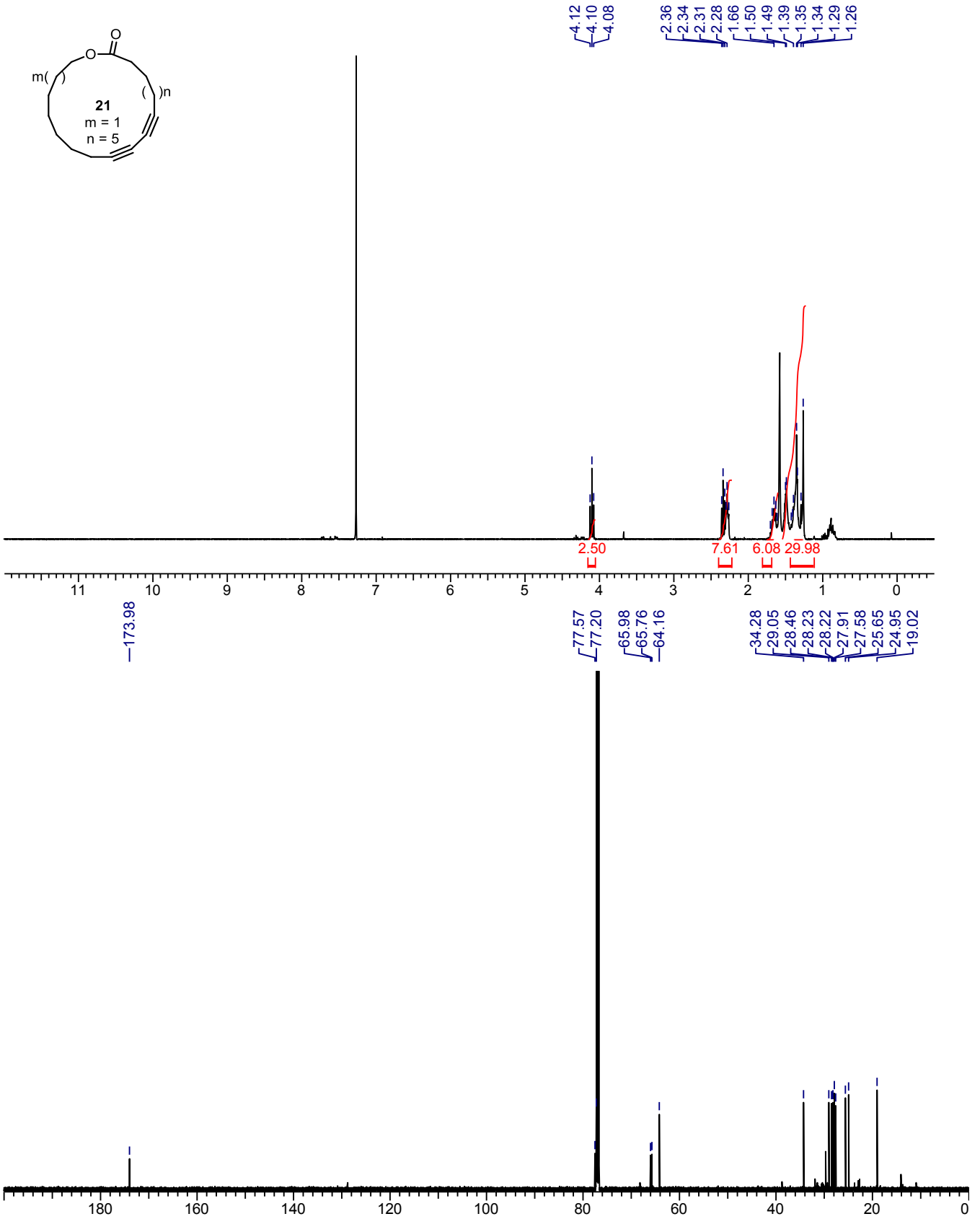
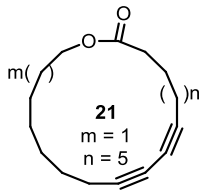




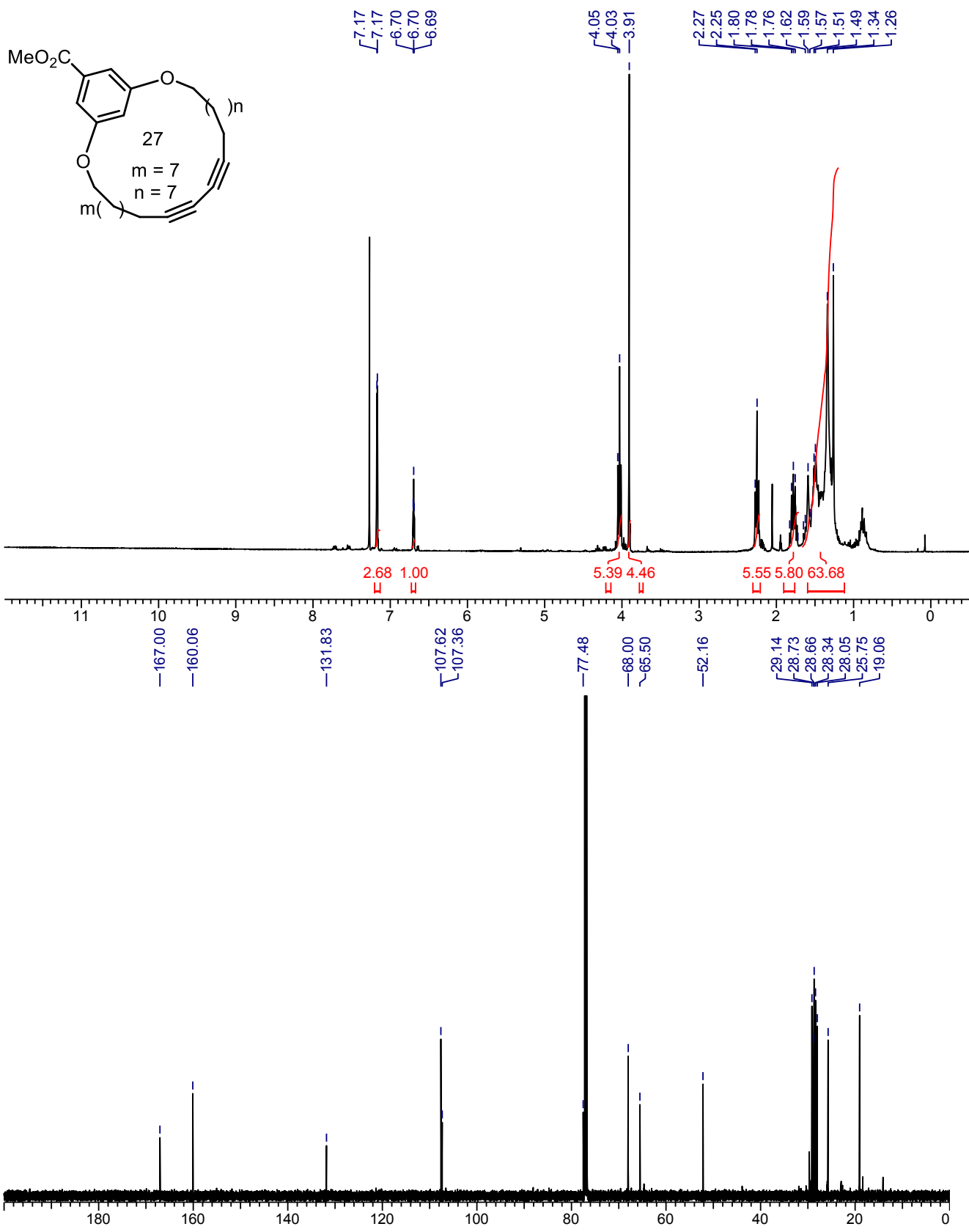
dddd

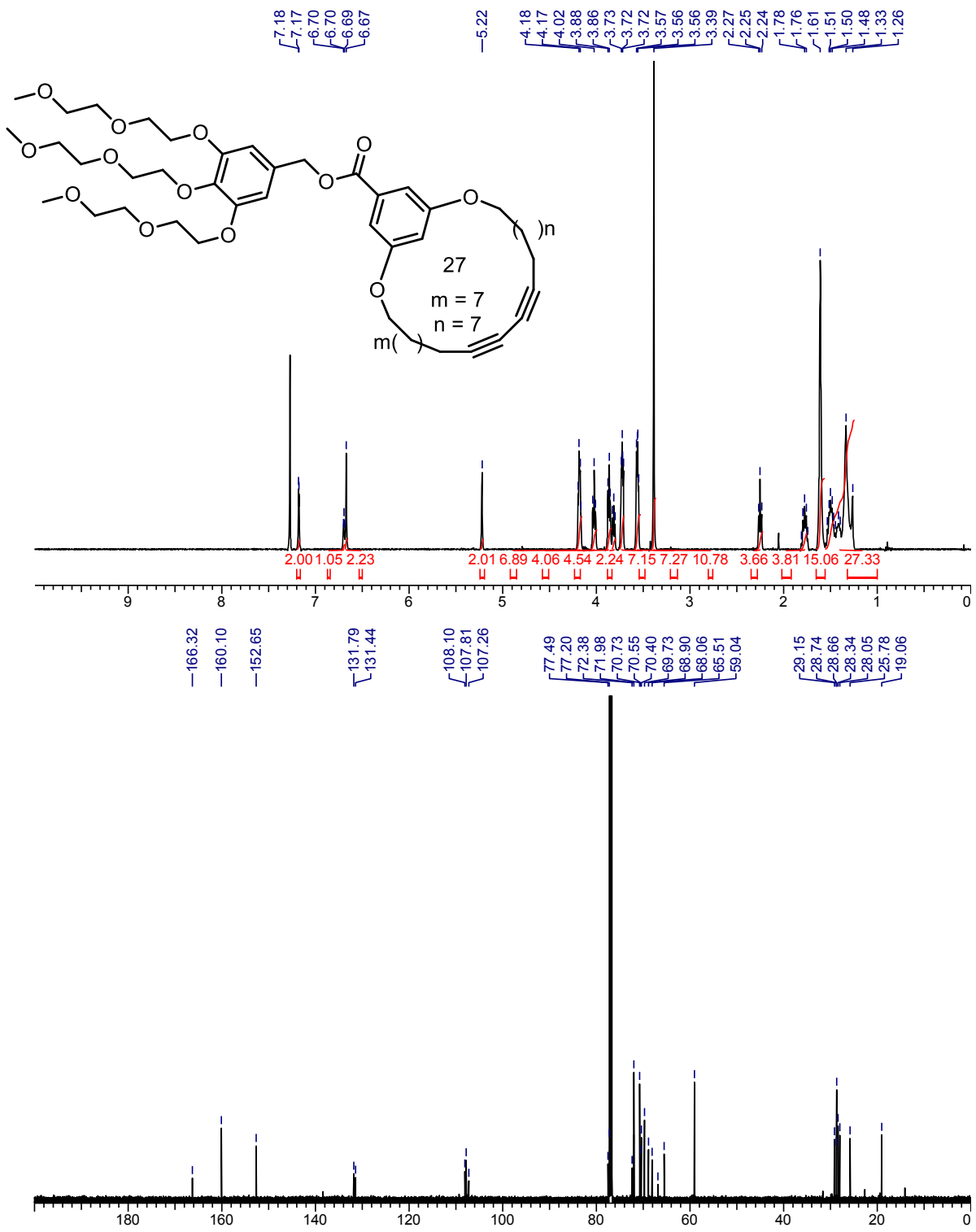


eeee



ffff





hhhh

Chapter 16 : Supporting Information of Chapter 5: Influence of Poly(ethylene glycol) Structure in Catalytic Macrocyclization Reactions

General:

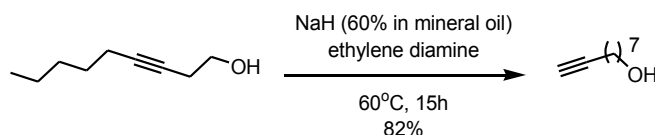
All reactions that were carried out under anhydrous conditions were performed under an inert argon or nitrogen atmosphere in glassware that had previously been dried overnight at 120 °C or had been flame dried and cooled under a stream of argon or nitrogen.²⁰ All chemical products were obtained from Sigma-Aldrich Chemical Company or Strem Chemicals and were reagent quality. Technical solvents were obtained from VWR International Co. Anhydrous solvents (CH₂Cl₂, Et₂O, THF, DMF, Toluene, and hexanes) were dried and deoxygenated using a GlassContour system (Irvine, CA). Isolated yields reflect the mass obtained following flash column silica gel chromatography. Organic compounds were purified using the method reported by W. C. Still²¹ and using silica gel obtained from Silicycle Chemical division (40-63 nm; 230-240 mesh). Analytical thin-layer chromatography (TLC) was performed on glass-backed silica gel 60 coated with a fluorescence indicator (Silicycle Chemical division, 0.25 mm, F₂₅₄). Visualization of TLC plate was performed by UV (254 nm), KMnO₄ or *p*-anisaldehyde stains. All mixed solvent eluents are reported as v/v solutions. Concentration refers to removal of volatiles at low pressure on a rotary evaporator. All reported compounds were homogeneous by thin layer chromatography (TLC) and by ¹H

²⁰ Shriver, D. F.; Drezdon, M. A. in *The Manipulation of Air-Sensitive Compounds*; Wiley-VCH: New York, 1986.

²¹ Still, W. C.; Kahn, M.; Mitra, A. *J. Org. Chem.* **1978**, *43*, 2923.

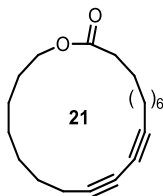
NMR. NMR spectra were taken in deuterated CDCl_3 using Bruker AV-300 and AV-400 instruments unless otherwise noted. Signals due to the solvent served as the internal standard (CHCl_3 : δ 7.27 for ^1H , δ 77.0 for ^{13}C). The ^1H NMR chemical shifts and coupling constants were determined assuming first-order behavior. Multiplicity is indicated by one or more of the following: s (singlet), d (doublet), t (triplet), q (quartet), m (multiplet), br (broad); the list of couplings constants (J) corresponds to the order of the multiplicity assignment. The ^1H NMR assignments were made based on chemical shift and multiplicity. The ^{13}C NMR assignments were made on the basis of chemical shift and multiplicity. High resolution mass spectroscopy (HRMS) was done by the Centre régional de spectrométrie de masse at the Département de Chimie, Université de Montréal from an Agilent LC-MSD TOF system using ESI mode of ionization unless otherwise noted.

SYNTHESIS OF SUBSTRATE AND MACROCYCLE.



8-nonyl-1-ol: To a flask containing ethylene diamine (70 mL) at 0 °C was added NaH (60% in mineral oil, 5.7 g, 142.6 mmol, 4 equiv.). The mixture was slowly warmed to room temperature and stirred for 1h. Then the reaction was warmed to 60 °C and stirred for 2 h. After cooling the reaction to 45 °C, 3-nonyl-1-ol (5 mL, 35.7 mmol, 1 equiv.) was added in one portion and the solution was stirred at 60 °C for 15 h. Upon cooling to 0 °C, 1M HCl (30 mL) was added and the organic and aqueous layers were separated. The aqueous layer was extracted with ethyl acetate (2x), and the combined organic layers were dried over anhydrous Na_2SO_4 . The suspension was filtered and the filtrate was concentrated in vacuo. Purification of

29.06, 28.9, 28.6, 28.4, 27.7, 24.9 (2C), 18.4, 18.1 ppm; HRMS (ESI) m/z calculated for $C_{17}H_{27}O_2$ $[M+H]^+$, 263.2006; found: 263.2013.



General procedure for the macrocyclization of 3 under Glaser-Hay oxidative coupling conditions using microwave irradiation: Macrocycle (4): To a microwave vial equipped with a stirring bar was added $CuCl_2$ (5.5 mg, 0.03 mmol, 25 mol %) and $Ni(NO_3)_2 \cdot 6H_2O$ (9.3 mg, 0.03 mmol, 25 mol %). Polyethylene glycol 400 (3.33 mL), triethylamine (0.05 mL, 0.36 mmol, 3 equiv.) and tetramethylethylene diamine (0.09 mL, 0.6 mmol, 5 equiv.) were added and the mixture was stirred at room temperature for 15 min or until the metals were solubilized. The diyne (28 mg, 0.12 mmol) was added to the homogenous mixture as a methanol solution (1.67 mL) in one portion. Oxygen was bubbled in the solution for 5 min and the vial was then sealed with a microwave cap. The reaction was warmed to 120 °C for 6 h. The crude mixture was loaded directly onto silica gel for purification by chromatography (100 % hexanes \rightarrow 10 % ethyl acetate in hexanes) and afforded the product as a colorless semi-solid (23 mg, 81 %). 1H NMR (300 MHz, $CDCl_3$) δ = 4.10 (t, J = 6.5 Hz, 2H), 2.36 - 2.26 (m, 6H), 1.70 - 1.61 (m, 6H), 1.50 - 1.26 (m, 14H); ^{13}C NMR (125 MHz, $CDCl_3$) δ ppm = 174.0, 77.6, 77.2, 66.0, 65.8, 64.2, 34.3, 29.1, 28.5, 28.23, 28.22, 28.19, 27.93, 27.91, 27.63, 27.58, 25.7, 25.0, 19.03, 19.02; HRMS (ESI) m/z calculated for $C_{20}H_{31}O_2$ $[M+H]^+$, 303.2319; found: 303.2325.

SURFACE TENSION DATA

A solution of MeOH (40 mL) was placed at 60 °C in a dataphysics DCAT11 surface tension analyser. Various amounts of the appropriate polymer were added and the mixture was stirred until homogenous (the stirring was stopped during the time of the measurement). The surface tension was measured using a rectangular Wilhemy plate for every %polymer in MeOH following the same procedure.

Table S1: Surface tension measurement for PEG₁₉₀/MeOH

%PEG ₁₉₀ in MeOH	Surface Tension (mN/m)	±
0	20.027	0.012
1.2	20.121	0.028
2.4	20.194	0.027
4.8	20.338	0.020
8.0	20.806	0.021
13.0	21.603	0.023
17.5	22.486	0.027
20.0	23.369	0.029
25.0	24.449	0.029
29.3	25.888	0.028
35.5	27.702	0.030
39.4	28.727	0.030
44.4	31.593	0.029
50.0	34.322	0.029
60.0	35.722	0.027
65.2	37.169	0.030
69.0	38.157	0.063
89.0	40.749	0.025
91.4	41.406	0.027

Table S2: Surface tension measurement for PEG₂₅₀(OMe)/MeOH

% PEG ₂₅₀ (OMe) in MeOH	Surface Tension	
	(mN/m)	±
0.0	20.365	0.020
1.2	20.404	0.010
2.4	20.464	0.027
4.8	20.630	0.027
8.0	20.880	0.013
13.0	21.380	0.220
17.5	22.000	0.028
20.0	22.249	0.024
25.0	23.267	0.003
29.3	23.225	0.025
35.5	24.291	0.003
39.4	25.012	0.023
50.0	27.049	0.028
60.0	27.091	0.018
65.2	27.530	0.017
69.2	29.001	0.017
79.0	29.165	0.018
89.0	31.047	0.026
91.4	31.836	0.022

Table S3: Surface tension measurement for PEG₄₀₀/MeOH

%PEG ₄₀₀ in MeOH	Surface Tension (mN/m)	±
0	20.151	0.022
1.2	20.012	0.023
2.4	20.135	0.026
4.8	20.255	0.029
8.0	20.49	0.026
13.0	20.957	0.026
17.5	21.521	0.028
20.0	21.828	0.018
25.0	22.979	0.030
29.3	23.861	0.023
35.5	25.364	0.026
39.4	26.451	0.022
44.4	27.924	0.025
50.0	32.716	0.022
60.0	38.736	0.028
65.2	40.523	0.027
69.0	41.343	0.029
89.0	41.223	0.024
91.4	41.868	0.026

Table S4: Surface tension measurement for PEG₁₄₅₀/MeOH

% PEG ₁₄₅₀ in MeOH	Surface Tension	
	(mN/m)	±
0.0	19.883	0.015
1.2	20.085	0.027
2.4	20.169	0.026
4.8	20.262	0.013
8.0	20.907	0.027
13.0	21.370	0.028
17.5	21.884	0.021
20.0	22.562	0.028
25.0	23.512	0.027
29.3	25.530	0.028
35.5	27.401	0.015
39.4	29.475	0.023
50.0	32.683	0.027
60.0	36.923	0.026
65.2	39.112	0.061
69.2	40.678	0.024

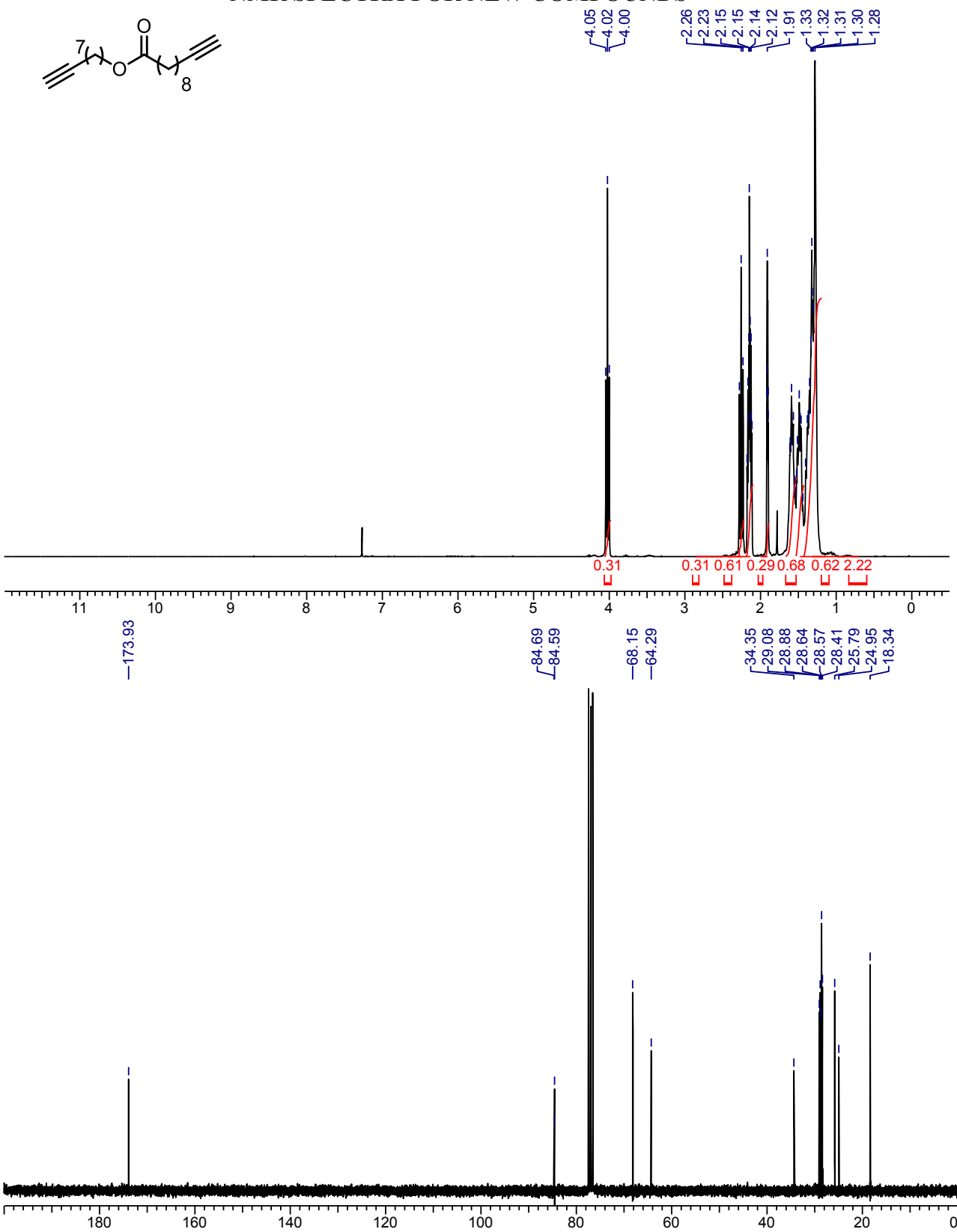
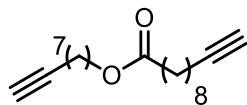
Table S5: Surface tension measurement for PPG₄₂₅/MeOH

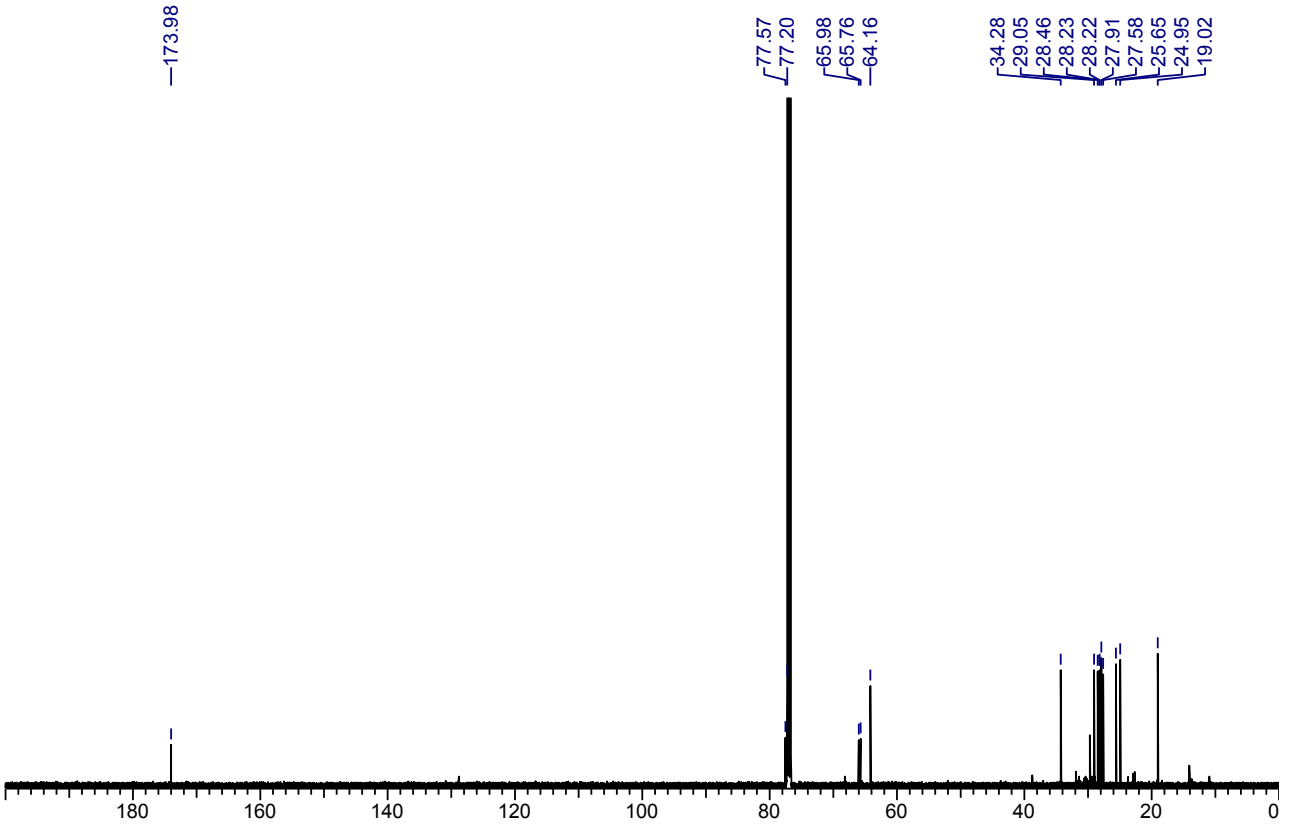
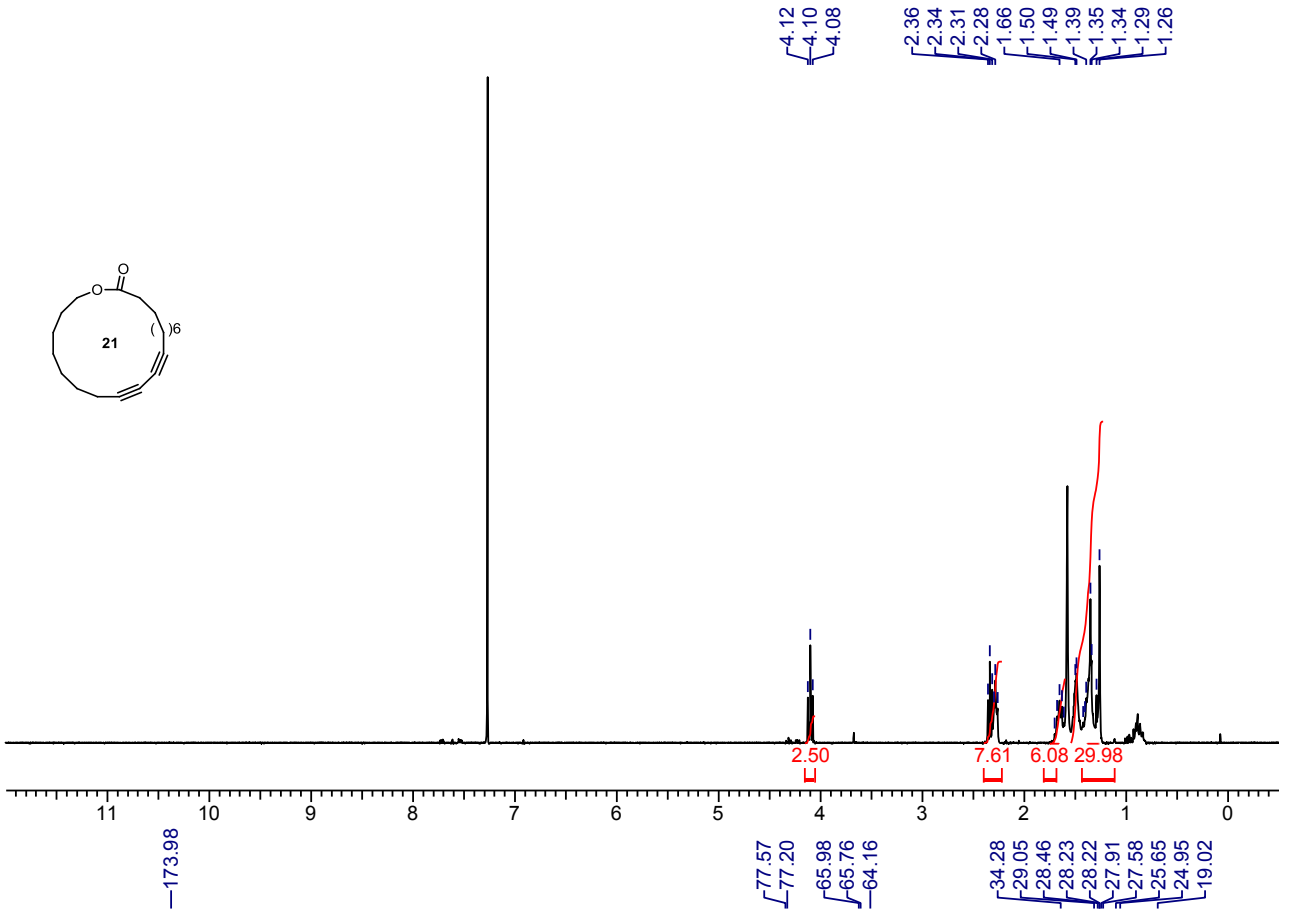
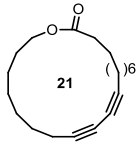
%PPG ₄₂₅ in MeOH	Surface Tension (mN/m)	±
0	20.237	0.020
1.2	20.467	0.030
2.4	20.508	0.020
4.8	20.795	0.028
8.0	20.992	0.023
13.0	21.615	0.016
17.5	22.120	0.025
20.0	22.423	0.029
25.0	23.217	0.029
29.3	24.571	0.030
35.5	25.691	0.028
39.4	25.804	0.027
44.4	27.655	0.026
50.0	28.633	0.025
60.0	29.145	0.022
65.2	30.009	0.028
69.0	30.617	0.029
79.0	30.679	0.028
89.0	30.928	0.029
91.4	30.928	0.029

Table S6: Surface tension measurement for Pluronic₁₁₀₀/MeOH

%Pluronic ₁₁₀₀ in MeOH	Surface Tension	
	(mN/m)	±
0.0	20.385	0.010
1.2	20.294	0.010
2.4	20.386	0.015
4.8	20.371	0.027
8.0	20.595	0.027
13.0	20.861	0.028
17.5	21.127	0.025
20.0	21.402	0.018
25.0	22.070	0.020
29.3	22.656	0.028
35.5	24.042	0.027
39.4	24.766	0.028
50.0	25.440	0.027
60.0	26.684	0.022
65.2	28.584	0.029
69.2	30.174	0.029
79.0	30.899	0.029
89.0	31.336	0.028
91.4	32.043	0.030

NMR SPECTRA FOR NEW COMPOUNDS





tttt

Chapter 17 : Supporting Information of Chapter 7: Continuous Flow Macrocyclization at High Concentrations: Synthesis of Macrocyclic Lipids

General:

All reactions that were carried out under anhydrous conditions were performed under an inert argon or nitrogen atmosphere in glassware that had previously been dried overnight at 120 °C or had been flame dried and cooled under a stream of argon or nitrogen.²³ All chemical products were obtained from Sigma-Aldrich Chemical Company or Strem Chemicals and were reagent quality. 10-Undecyn-1-ol²⁴ and 1-*O*-benzyl-*rac*-glycerol²⁵ were prepared according to literature procedures. The macrocyclic precursors non-8-yn-1-yl hex-5-ynoate (**1**), non-8-yn-1-yl undec-10-ynoate (**3**) and methyl 3,5-bis(undec-10-yn-1-yloxy)benzoate as well as macrocycles **4**, **5** and **7** have been previously reported in the literature.²⁶ Technical solvents were obtained from VWR International Co. Anhydrous solvents (CH₂Cl₂, Et₂O, THF, DMF, Toluene, and hexanes) were dried and deoxygenated using a GlassContour system (Irvine, CA). Isolated yields reflect the mass obtained following flash column silica gel chromatography. Organic compounds were purified using the method reported by W. C. Still²⁷ and using silica gel obtained from Silicycle Chemical division (40-63 nm; 230-240 mesh).

²³ Shriver, D. F.; Drezdon, M. A. in *The Manipulation of Air-Sensitive Compounds*; Wiley-VCH: New York, 1986.

²⁴ Sharma, A.; Chattopadhyay, S. *J. Org. Chem.* **1998**, *63*, 6128.

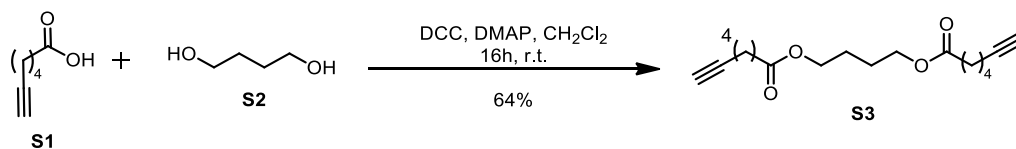
²⁵ Karmee, K. S. *Synth. Comm.* **2013**, *43*, 450.

²⁶ Bédard, A.-C.; Collins, S. K. *J. Am. Chem. Soc.* **2011**, *133*, 19976.

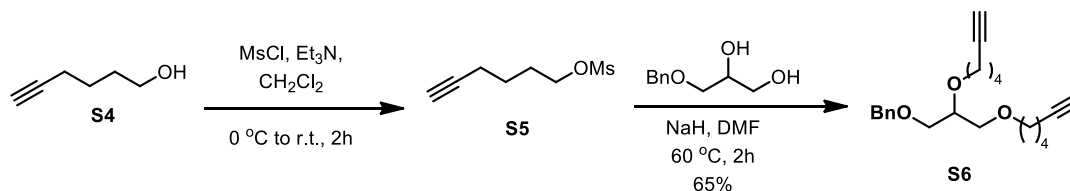
²⁷ Still, W. C.; Kahn, M.; Mitra, A. *J. Org. Chem.* **1978**, *43*, 2923.

Analytical thin-layer chromatography (TLC) was performed on glass-backed silica gel 60 coated with a fluorescence indicator (Silicycle Chemical division, 0.25 mm, F₂₅₄). Visualization of TLC plate was performed by UV (254 nm), KMnO₄ or *p*-anisaldehyde stains. All mixed solvent eluents are reported as v/v solutions. Concentration refers to removal of volatiles at low pressure on a rotary evaporator. All reported compounds were homogeneous by thin layer chromatography (TLC) and by ¹H NMR. NMR spectra were taken in deuterated CDCl₃ using Bruker AV-300 and AV-400 instruments unless otherwise noted. Signals due to the solvent served as the internal standard (CHCl₃: δ 7.27 for ¹H, δ 77.0 for ¹³C). The ¹H NMR chemical shifts and coupling constants were determined assuming first-order behavior. Multiplicity is indicated by one or more of the following: s (singlet), d (doublet), t (triplet), q (quartet), m (multiplet), br (broad); the list of couplings constants (*J*) corresponds to the order of the multiplicity assignment. The ¹H NMR assignments were made based on chemical shift and multiplicity and were confirmed, where necessary, by homonuclear decoupling, 2D COSY experiments. The ¹³C NMR assignments were made on the basis of chemical shift and multiplicity and were confirmed, where necessary, by two dimensional correlation experiments (HSQC). High resolution mass spectroscopy (HRMS) was done by the Centre régional de spectrométrie de masse at the Département de Chimie, Université de Montréal from an Agilent LC-MSD TOF system using ESI mode of ionization unless otherwise noted.

SYNTHESIS OF MACROCYCLIZATION PRECURSORS.

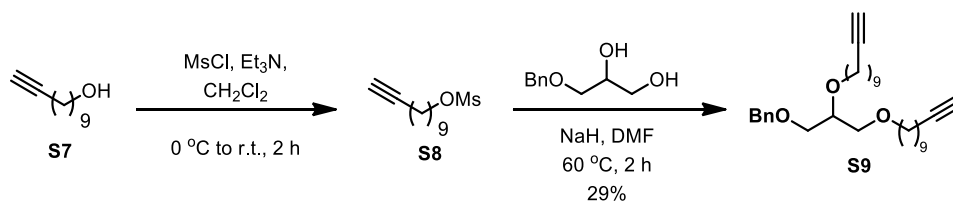


Butane-1,4-diyl dibut-3-ynoate (S3): To a stirred solution of the 1,4-butanediol (0.56 mL, 6.3 mmol, 1 equiv.) and 6-heptynoic acid (1.6 g, 13 mmol, 2.0 equiv.) in anhydrous CH₂Cl₂ (63 mL, 0.1 M) was added *N,N*-dicyclohexylcarbodiimide (5.23 g, 25.4 mmol, 4.0 equiv.) and 4-dimethylaminopyridine (3.88 g, 38 mmol, 6.0 equiv.) at room temperature. The reaction mixture was stirred at room temperature for 15 h. Upon complete conversion of the starting material (TLC), the crude reaction mixture was placed in a freezer for 5 h to induce the precipitation of the urea, which was subsequently removed by filtration. The filtrate was concentrated *in vacuo* to provide the crude reaction mixture, which was purified by silica gel column chromatography (100 % Hexanes to 20 % EtOAc/Hexanes) to afford the desired product **S3** as a colorless semi-solid (1.24 g, 64 %). ¹H NMR (300 MHz, CDCl₃) δ = 4.19 - 4.01 (m, 4H), 2.33 (t, *J* = 7.4 Hz, 4H), 2.21 (dt, *J* = 7.0, 2.6 Hz, 4H), 1.95 (t, *J* = 2.6 Hz, 2H), 1.83 - 1.64 (m, 8H), 1.62 - 1.49 (m, 4H); ¹³C NMR (75 MHz, CDCl₃) δ ppm = 173.3, 83.9, 68.6, 63.8, 33.7, 27.8, 25.3, 24.0, 18.1; HRMS (ESI) *m/z* calculated for C₁₈H₃₀NO₄ [M+NH₄]⁺, 324.2169; found: 324.2172.



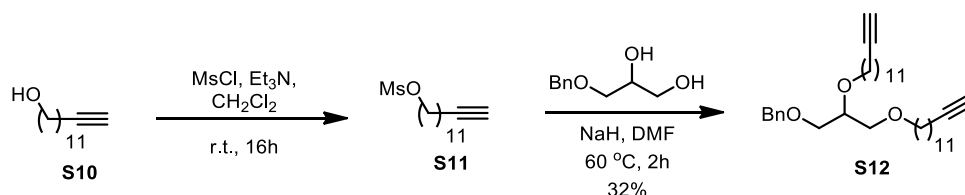
((2,3-bis(prop-2-ynyloxy)propoxy)methyl)benzene (S6): In a flamed-dried flask, 1-hexyn-1-ol (2.0 g, 20.4 mmol, 1 equiv.) was dissolved in anhydrous CH₂Cl₂ (100 mL) and Et₃N (4.9

mL, 22.4 mmol, 1.1 equiv.) was added. The mixture was cooled to 0 °C and methanesulfonyl chloride (2.8 mL, 24.5 mmol, 1.2 equiv.) was added dropwise. The mixture was slowly warmed to room temperature and stirred for 2 h. Water was added to the mixture and the organic and aqueous phases were separated. The aqueous phase was extracted 2x with CH₂Cl₂ and the organic phases were combined, dried over Na₂SO₄, filtered and concentrated *in vacuo*. The product prop-2-ynyl methanesulfonate **S5** was obtained as a crude pale yellow oil was used directly in the next step. To a stirred solution of 1-*O*-benzyl-*rac*-glycerol (570 mg, 3.1 mmol, 1 equiv.) at 0 °C in anhydrous DMF (20 mL) was added NaH (60 % in oil, 313 mg, 7.8 mmol, 2.5 equiv.) in 5 portions. The mixture was warmed slowly to r.t. and prop-2-ynyl methanesulfonate **S5** (1.38 g, 7.8 mmol, 2.5 equiv.) was added in one portion. The reaction was then warmed to 60 °C for 2 h (or until judged complete by TLC) and then cooled back to room temperature. Water and ethyl acetate were added and the organic and aqueous layers were separated. The aqueous phase was extracted with EtOAc (3x) and the combined organic layers were washed with brine (3x). The organic layer was dried with Na₂SO₄, filtered and concentrated *in vacuo*. The crude oil was purified by silica gel column chromatography (20 % EtOAc/Hexanes). The desired product **S6** was obtained as a colorless oil (0.72 g, 65 %). ¹H NMR (400 MHz, CDCl₃) δ = 7.38 - 7.22 (m, 5H), 4.60 - 4.49 (m, 2H), 3.67 - 3.39 (m, 9H), 2.24 - 2.15 (m, 4H), 2.00 - 1.96 (m, 2H), 1.73 - 1.52 (m, 8H); ¹³C NMR (75 MHz, CDCl₃) δ ppm = 138.3, 128.3, 127.6, 127.5, 84.4, 84.3, 78.0, 73.4, 70.9, 70.8, 70.2, 69.8, 68.4, 68.3, 29.1, 28.6, 25.2, 25.1, 18.18, 18.17; HRMS (ESI) m/z calculated for C₂₂H₃₁O₃ [M+H]⁺, 343.2268; found: 343.2269.



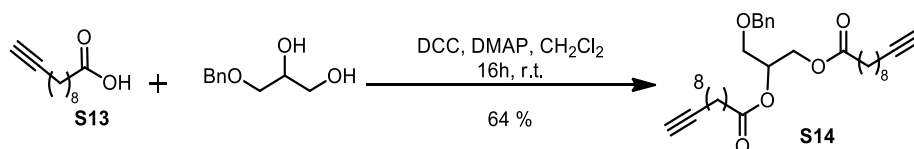
((2,3-bis(non-2-ynyloxy)propoxy)methyl)benzene (S9): In a flamed-dried flask, 1-undecyn-1-ol (1.5g, 8.9 mmol, 1 equiv.) was dissolved in anhydrous CH₂Cl₂ (45 mL) and Et₃N (2.5 mL, 13.2 mmol, 1.5 equiv.) was added. The mixture was cooled to 0 °C and methanesulfonyl chloride (0.75 mL, 9.7 mmol, 1.1 equiv.) was added dropwise. The mixture was slowly warmed to room temperature and stirred for 2 h. Water was added to the mixture and the organic and aqueous phases were separated. The aqueous phase was extracted with CH₂Cl₂ (2x) and the organic phases were combined, dried over Na₂SO₄, filtered and concentrated *in vacuo*. The non-2-ynyl methanesulfonate **S8** was obtained as a yellow oil and was used crude directly in the next step. To a stirred solution of 1-*O*-benzyl-*rac*-glycerol (277 mg, 1.63 mmol, 1 equiv.) at 0 °C in anhydrous DMF (10 mL) was added NaH (60 % in oil, 163 mg, 4.1 mmol, 2.5 equiv.) in 5 portions. The mixture was warmed slowly to r.t. and non-2-ynyl methanesulfonate (883 mg, 3.6 mmol, 2.2 equiv.) was added in one portion. The reaction was then warmed to 60 °C for 2 h (or until complete as judged by TLC) and then cooled back to room temperature. Water and ethyl acetate were added and the organic and aqueous layers were separated. The aqueous phase was extracted with EtOAc (3x) and the combined organic layers were washed with brine (3x). The organic layer was dried over Na₂SO₄, filtered and concentrated *in vacuo*. The crude oil was purified by silica gel column chromatography (15 % EtOAc/Hexanes) and the desired product **S9** was obtained as a colorless oil (200 mg, 29 %). ¹H NMR (300 MHz, CDCl₃) δ = 7.41 - 7.23 (m, 5H), 4.56 (s, 2H), 3.68 - 3.47 (m, 7H), 3.43 (t, *J* = 6.7 Hz, 2H), 2.18 (dt, *J* = 6.9, 2.5 Hz, 4H), 1.94 (t, *J* = 2.5 Hz, 2H), 1.64 - 1.46 (m, 8H),

1.46 - 1.23 (m, 20H); ^{13}C NMR (75 MHz, CDCl_3) δ ppm = 138.4, 128.3, 127.5, 84.7, 77.9, 73.3, 71.6, 70.7, 70.5, 70.3, 68.4 (2C), 30.1, 29.6, 29.41 (2C), 29.39 (2C), 29.0 (2C), 28.7 (2C), 28.4 (2C), 26.1 (2C), 26.0 (2C), 18.4 (2C); HRMS (ESI) m/z calculated for $\text{C}_{32}\text{H}_{51}\text{O}_3$ $[\text{M}+\text{H}]^+$, 483.3833; found: 483.3844.



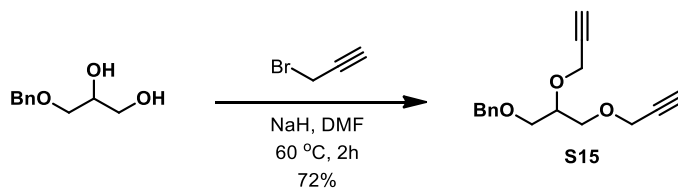
((2,3-bis(undec-2-ynyloxy)propoxy)methyl)benzene (S12): In a flamed-dried flask, 1-tridecyn-1-ol (2.30 g, 11.7 mmol, 1 equiv.) was dissolved in anhydrous DCM (60 mL) and Et_3N (1.9 mL, 14.0 mmol, 1.2 equiv.) was added. The mixture was cooled to $0\text{ }^\circ\text{C}$ and methanesulfonyl chloride (1.0 mL, 12.9 mmol, 1.1 equiv.) was added dropwise. The mixture was slowly warmed to room temperature and stirred for 2 h. Water was added to the mixture and the organic and aqueous phases were separated. The aqueous phase was extracted with CH_2Cl_2 (2x) and the organic phases were combined, dried over Na_2SO_4 , filtered and concentrated *in vacuo*. The product undec-2-ynyl methanesulfonate **S11** was obtained as a crude yellow oil which was used directly in the next step. To a stirred solution of 1-*O*-benzyl-*rac*-glycerol (0.85 g, 4.7 mmol, 1 equiv.) at $0\text{ }^\circ\text{C}$ in anhydrous DMF (60 mL) was added NaH (60 % in oil, 468 mg, 11.7 mmol, 2.5 equiv.) in 5 portions. The mixture was warmed slowly to r.t. and undec-2-ynyl methanesulfonate (3.2 g, 11.7 mmol, 2.5 equiv.) was added in one portion. The reaction was then warmed to $60\text{ }^\circ\text{C}$ for 2 h (or until judged complete by TLC) and then cooled back to room temperature. Water and ethyl acetate were added and the organic and aqueous layers were separated. The aqueous phase was extracted with EtOAc (3x) and the combined organic layers were washed with brine (3x). The organic layer was dried over

Na₂SO₄, filtered and concentrated *in vacuo*. The crude oil was purified by silica gel column chromatography (10 % EtOAc/Hexanes). The desired product **S12** was obtained as a pale yellow oil (2.0 g, 32 %). ¹H NMR (400 MHz, CDCl₃) δ = 7.36 – 7.35 (m, 4H), 7.33 - 7.26 (m, 1H), 4.58 (s, 2H), 3.68 - 3.49 (m, 7H), 3.45 (t, *J* = 6.6 Hz, 2H), 2.20 (dt, *J* = 7.1, 2.7 Hz, 4H), 1.96 (t, *J* = 2.7 Hz, 2H), 1.66 - 1.49 (m, 8H), 1.46 - 1.23 (m, 28H); ¹³C NMR (75 MHz, CDCl₃) δ ppm = 138.4, 128.3, 127.54, 127.47, 84.8, 77.9 (2C), 73.3, 71.6, 70.7, 70.6, 70.3, 68.0 (2C), 30.1 (2C), 29.63 (2C), 29.57 (2C), 29.53 (2C), 29.47 (2C), 29.1 (2C), 28.7 (2C), 28.5 (2C), 26.10 (2C), 26.07 (2C); HRMS (ESI) *m/z* calculated for C₃₆H₅₉O₃ [M+H]⁺, 539.4459; found: 539.4443.



1,2-Bis(10-undecynoyl)-3-O-benzylglycerol (S14): To a stirred solution of 1-*O*-benzyl-*rac*-glycerol (0.56 mL, 6.3 mmol, 1 equiv.) and undecynoic acid (1.6 g, 13 mmol, 2 equiv.) in anhydrous dichloromethane (63 mL) was added *N,N'*-dicyclohexylcarbodiimide (5.23 g, 25.4 mmol, 4 equiv.) and 4-dimethylaminopyridine (3.88 g, 38 mmol, 6 equiv.) at room temperature. The reaction mixture was stirred at room temperature for 15 h. Upon complete conversion of the starting material (TLC), the crude reaction mixture was placed in a freezer for 5 h to induce the precipitation of the urea, which was subsequently removed by filtration. The filtrate was concentrated *in vacuo* to provide the crude reaction mixture, which was purified by silica gel column chromatography to afford the desired product **S14** as a colorless

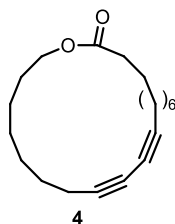
semi-solid (1.24 g, 64 %). The NMR data are in agreement with that obtained in the literature.²⁸



((2,3-bis(prop-2-ynoxy)propoxy)methyl)benzene (S15): To a stirred solution of 1-*O*-benzyl-*rac*-glycerol (600 mg, 3.3 mmol) at 0 °C in anhydrous DMF (17 mL) was added NaH (60 % in oil, 330 mg, 8.2 mmol) in 5 portions. The mixture was warmed slowly to room temperature and propargyl bromide (0.75 mL, 7.2 mmol) was added in one portion. The reaction was then warmed to 60 °C for 2 h and then cooled back to room temperature. Water and ethyl acetate were added and the organic and aqueous layers were separated. The aqueous phase was extracted with EtOAc (3x) and the combined organic layers were washed with brine (3x). The organic layer was dried over Na₂SO₄, filtered and concentrated *in vacuo*. The crude oil was purified by silica gel column chromatography (10 % EtOAc/Hexanes). The desired product **S15** was obtained as a colorless oil in (612 mg, 72 %). ¹H NMR (300 MHz, CDCl₃) δ = 7.41 - 7.22 (m, 5H), 4.55 (s, 2H), 4.33 (d, *J* = 2.4 Hz, 2H), 4.16 (d, *J* = 2.4 Hz, 2H), 3.93 (m, 1H), 3.74 - 3.57 (m, 4H), 2.47 (m, 2H); ¹³C NMR (75 MHz, CDCl₃) δ ppm = 137.8, 128.0, 127.2 (2C), 79.7, 79.2, 76.0, 74.5, 74.2, 72.9, 69.5, 69.3, 58.1, 57.1; HRMS (ESI) *m/z* calculated for C₁₆H₁₉O₃ [M+H]⁺, 259.1329; found: 259.1340.

²⁸ Bhattacharya, S.; Ghosh, S.; Easwaran, K. R. K. *J. Org. Chem.* **1998**, *63*, 9232.

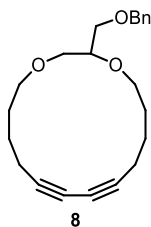
SYNTHESIS OF MACROCYCLES



General procedure A for the macrocyclization of diynes under Glaser-Hay oxidative coupling conditions using microwave irradiation: Macrocycle (4): To a microwave vial equipped with a stirring bar was added CuCl_2 (5.5 mg, 0.03 mmol, 25 mol %) and $\text{Ni}(\text{NO}_3)_2 \cdot 6\text{H}_2\text{O}$ (9.3 mg, 0.03 mmol, 25 mol %). Polyethylene glycol 400 (3.33 mL), triethylamine (0.05 mL, 0.36 mmol, 3 equiv.) and TMEDA (0.07 mL, 0.6 mmol, 5 equiv.) were added and the mixture was stirred at room temperature for 15 min or until the solution was homogenous. The diyne (0.12 mmol) was added to the mixture as a methanol solution (1.67 mL) in one portion. Oxygen was bubbled in the solution for 5 min and the vial was then closed with a microwave cap. The reaction was warmed to 120 °C for 6 h using a Biotage Initiator microwave reactor. The crude mixture was loaded directly on a silica column. Purification by chromatography (100 % Hexanes \rightarrow 20 % EtOAc/Hexanes) afforded the product **4** as a colorless semi-solid (31 mg, 81 %).

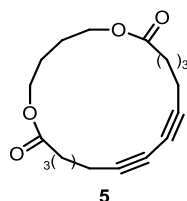
General procedure B for the macrocyclization of diynes under Glaser-Hay oxidative coupling conditions using continuous-flow: Macrocycle (4): To a pear shaped flask equipped with a stirring bar was added CuCl_2 (11 mg, 0.06 mmol, 25 mol %) and $\text{Ni}(\text{NO}_3)_2 \cdot 6\text{H}_2\text{O}$ (19 mg, 0.06 mmol, 25 mol %). Polyethylene glycol 400 (5 mL), triethylamine (0.1 mL, 0.72 mmol, 3 equiv.) and TMEDA (0.14 mL, 1.2 mmol, 5 equiv.) were

added and the mixture was stirred at room temperature for 15 min or until the solution was homogenous. The diyne (0.24 mmol) was added to the mixture as a methanol solution (5 mL) in one portion. The reaction was then passed through a 5 mL stainless-steel coil at 1 mL/min at 120 °C using a VapourTech R4 reactor and a R2+ pumping module. The solution was cycled for a total residence time of 1.5 h (which for a 10 mL reaction mixture and a 5 mL coil takes a total reaction time of 3 h). To the crude reaction mixture, silica gel was added and the solvent was removed *in vacuo*. Purification by silica gel chromatography (100 % Hexanes→20 % EtOAc/Hexanes) afforded the product as a colorless semi-solid (66 mg, 91 %).

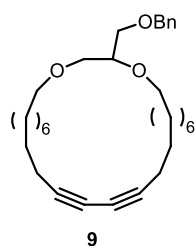


General procedure C for the large scale macrocyclization of diynes under Glaser-Hay oxidative coupling conditions using continuous-flow: Macrocycle (8): To a pear shaped flask equipped with a stirring bar was added CuCl_2 (160 mg, 0.94 mmol, 25 mol %) and $\text{Ni}(\text{NO}_3)_2 \cdot 6\text{H}_2\text{O}$ (273 mg, 0.94 mmol, 25 mol %). Polyethylene glycol 400 (96 mL), triethylamine (1.47 mL, 11.25 mmol, 3 equiv.) and TMEDA (3.0 mL, 18.75 mmol, 5 equiv.) were added and the mixture was stirred at room temperature for 15 min or until the metals were solubilized. The diyne (1.3g, 3.75 mmol) was added to the homogenous mixture as a methanol solution (48 mL) in one portion. The reaction was then passed through two 10 mL stainless-steel coil placed in series (connected with a short isolated stainless steel tube) at 0.22 mL/min at 120 °C using a VapourTech R4 reactor and a R2+ pumping module. After collection of the reaction mixture, silica gel was added and the solvent was removed *in vacuo*.

Purification by chromatography (100 % Hexanes→20 % EtOAc/Hexanes) afforded the product **8** as a colorless semi-solid (860 mg, 66 %). ^1H NMR (300 MHz, CDCl_3) δ =7.42 - 7.22 (m, 5H), 4.61 (s, 2H), 3.96 - 3.33 (m, 9H), 2.48 - 2.31 (m, 2H), 2.25 - 2.06 (m, 2H), 1.90 - 1.53 (m, 6H), 1.26 (s, 2H); ^{13}C NMR (125 MHz, CDCl_3) δ ppm = 138.7, 128.3, 127.6, 127.4, 79.5, 79.3, 73.3, 71.2, 69.5, 69.2, 69.0, 66.6, 66.3, 29.7, 29.1, 28.4, 23.5, 23.3, 19.3, 19.1; HRMS (ESI) m/z calculated for $\text{C}_{22}\text{H}_{28}\text{NaO}_3$ $[\text{M}+\text{Na}]^+$, 363.1931; found: 363.1930.

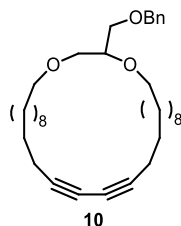


Macrocycle (5): Following the general procedure B described above, macrocycle **5** was isolated as a colorless oil. (71 mg, 72 %). ^1H NMR (300 MHz, CDCl_3) δ ppm: 4.12 (m, 4H), 2.46 - 2.24 (m, 8H), 1.95 - 1.44 (m, 12H); ^{13}C NMR (75 MHz, CDCl_3) δ ppm = 173.4, 76.7, 66.2, 64.0, 34.6, 27.2, 25.4, 24.4, 18.8; HRMS (ESI) m/z calculated for $\text{C}_{18}\text{H}_{24}\text{NaO}_4$ $[\text{M}+\text{Na}]^+$, 327.1567; found: 327.1572.

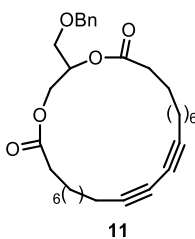


Macrocycle (9): Following the general procedure B described above, macrocycle **9** was isolated as a colorless oil (90 mg, 78 %). ^1H NMR (300 MHz, CDCl_3) δ ppm: 7.40 - 7.23 (m, 5H), 4.56 (s, 2H), 3.73 - 3.35 (m, 9H), 2.33 - 2.22 (m, 4H), 1.71 - 1.19 (m, 28H); ^{13}C NMR (75 MHz, CDCl_3) δ ppm = 138.4, 128.3, 127.6, 127.5, 77.9, 77.2, 73.3, 71.53, 71.45, 70.5,

70.3, 70.1, 65.7 (2C), 29.9, 29.7, 29.5 (2C), 29.3 (2C), 29.0, 28.9, 28.8, 28.28, 28.25, 27.82, 27.81, 26.09, 26, 07, 19.1; HRMS (ESI) m/z calculated for $C_{32}H_{49}O_3$ $[M+H]^+$, 481.3676; found: 481.3678.

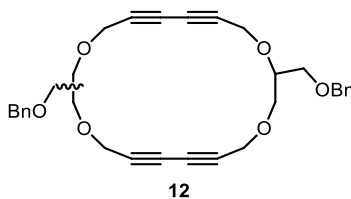


Macrocycle (10): Following the general procedure B described above, macrocycle **10** was isolated as a colorless oil (64 mg, 99 %). 1H NMR (300 MHz, $CDCl_3$) δ ppm: 7.41 - 7.25 (m, 5H), 4.56 (s, 2H), 3.74 - 3.36 (m, 9H), 2.27 (t, $J = 6.2$ Hz, 4H), 1.68 - 1.20 (m, 16H); ^{13}C NMR (75 MHz, $CDCl_3$) δ ppm = 138.4, 128.3, 127.6, 127.5, 78.0, 77.49, 77.48, 73.3 (2C), 71.6, 71.3 (2C), 70.6, 70.2 (2C), 65.594, 65.587, 30.0, 29.6, 29.50, 29.48, 29.3, 29.24, 29.214, 29.207, 28.95, 28.94, 28.40, 28.38, 28.0, 26.09, 26.07, 19.14, 19.12; HRMS (ESI) m/z calculated for $C_{36}H_{56}NaO_3$ $[M+Na]^+$, 559.4122; found: 559.4130.



Macrocycle (11): Following the general procedure B described above, macrocycle **11** was isolated as a colorless semi-solid (55 mg, 45 %). The NMR data are in agreement with that

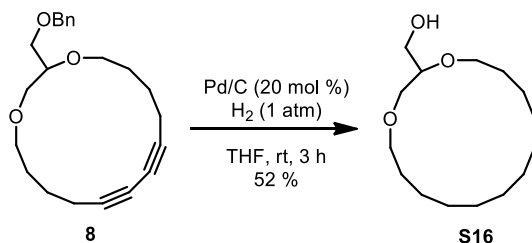
obtained in the literature.²⁹



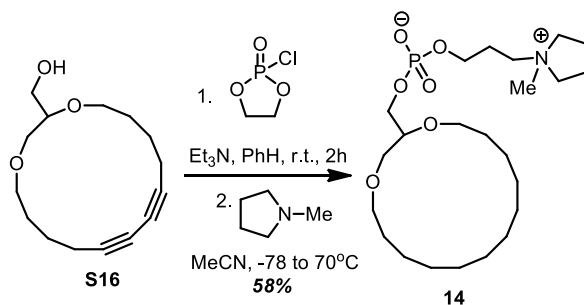
Macrocycle (12): Following the general procedure B described above, macrocycle **13** was isolated as a colorless semi-solid as a mixture of head-to-head and head-to-tail dimers (44 mg, 55 %). ¹H NMR (400 MHz, CDCl₃) δ = 7.40 - 7.28 (m, 10H), 4.58 - 4.51 (m, 6H), 4.37 - 4.26 (m, 6H), 3.99 - 3.88 (m, 2H), 3.81 - 3.65 (m, 4 H), 3.62 - 3.50 (m, 4 H); ¹³C NMR (100 MHz, CDCl₃, signal for both dimer reported) δ ppm = 138.1, 128.4, 127.7, 127.6 (2C), 78.1, 77.6, 77.20, 77.16, 75.96, 75.91, 75.86, 75.8, 75.4, 75.3, 75.1, 73.5, 70.9, 70.8, 70.74, 70.72, 70.6, 70.4, 70.34, 70.32, 70.25, 70.24, 70.21, 69.73, 69.72, 69.51, 69.45, 59.24, 59.18, 59.15, 59.09, 58.96, 58.85, 58.82. All attempts to characterize macrocycle **12** by ESI-MS failed. As such macrocycle **12** (44 mg) was completely hydrogenated (THF (5 mL), Pd/C (10 %w/w, 4.4 mg), H₂ (1 atm), 3 h, rt) to afford a single compound as a colorless oil. HRMS (ESI) m/z calculated for C₁₈H₃₆NaO₆ [M+Na]⁺ 371.2404; found: 371.2410.

²⁹ Bhattacharya, S.; Ghosh, S.; Easwaran, K. R. K. *J. Org. Chem.* **1998**, *63*, 9232.

SYNTHESIS OF PHOSPHOLIPID 14



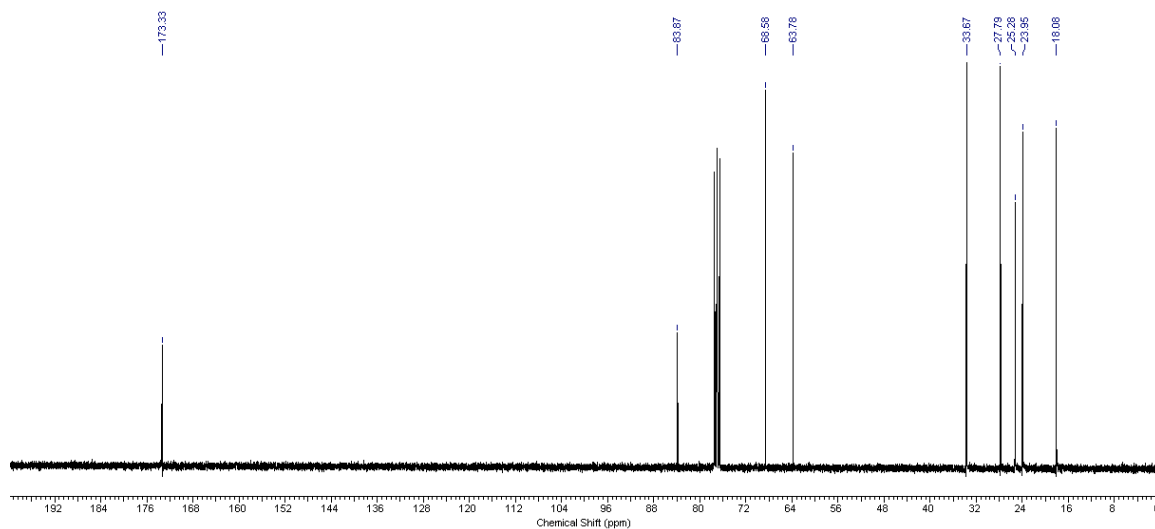
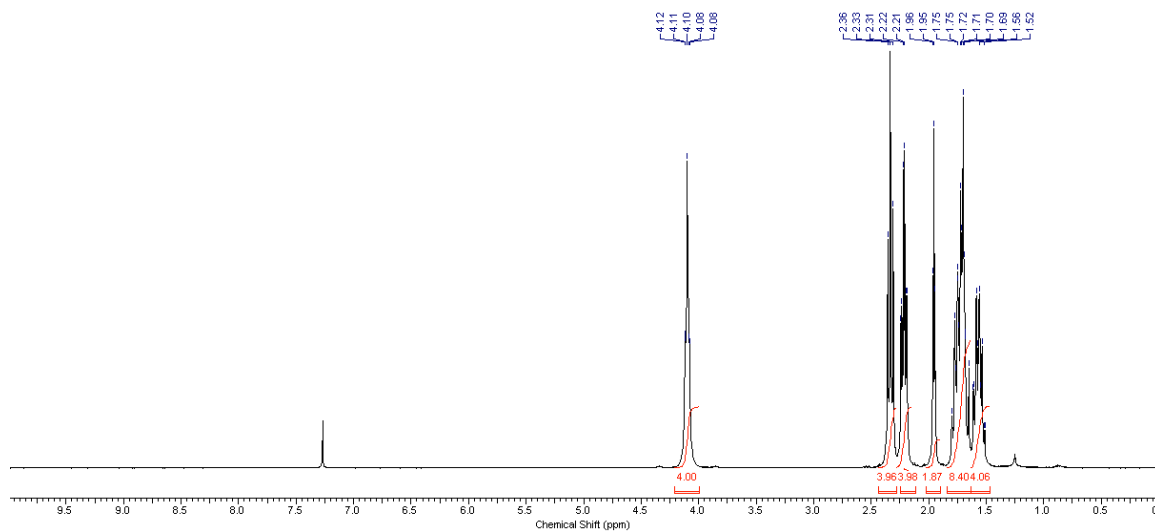
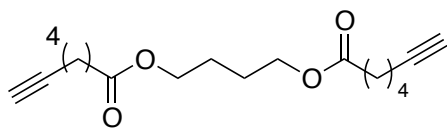
(1,4-dioxacyclohexadecan-2-yl)methanol (S16): A stirring solution of macrocycle **8** (150 mg, 0.44 mmol) in THF (5 mL) at room temperature was degassed with N₂ for 5 minutes. Pd/C (15 mg, 10 % w/w) was added and hydrogen was bubbled through the mixture for 5 minutes. The reaction was then stirred at room temperature for 3-4 h under an H₂ atmosphere (or until complete by TLC). Nitrogen was bubbled again through the reaction mixture for 5 minutes and the crude mixture was then filtered on Celite® and washed with THF (3x). The filtrate was concentrated *in vacuo* and purified by column chromatography (50 % EtOAc/Hexanes→100 % EtOAc) to afford the hydrogenated product **S16** as a colorless oil (60 mg, 52 %). ¹H NMR (400 MHz, CDCl₃) δ = 3.84 - 3.40 (m, 9H), 2.12 (dd, *J* = 6.6, 5.1 Hz, 1H), 1.72 - 1.21 (m, 20H). ¹³C NMR (100 MHz, CDCl₃) δ ppm = 78.7, 71.9, 71.0, 69.8, 62.4, 29.2, 29.0, 26.93, 26.88, 26.75, 26.72, 25.67, 25.66, 24.63, 24.55; HRMS (ESI) *m/z* calculated for C₁₅H₃₀NaO₃ [M+Na]⁺, 281.2087; found: 281.2095.

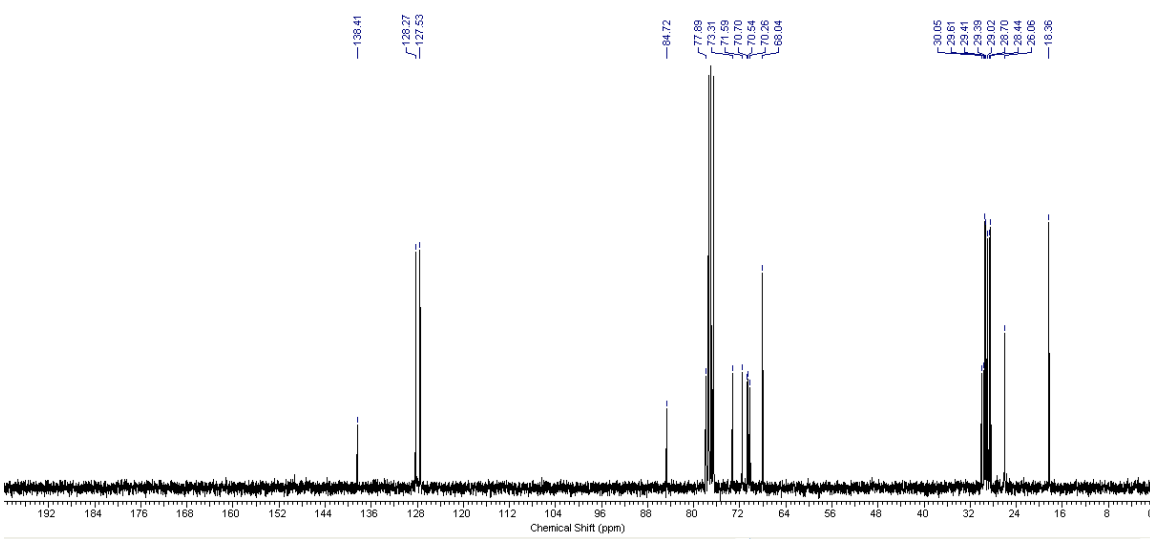
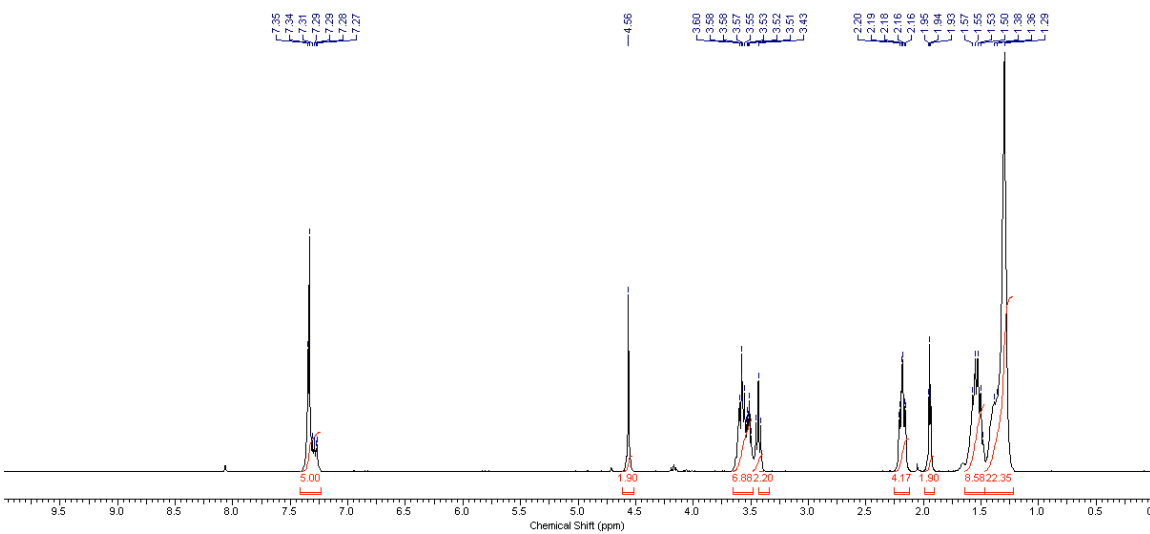
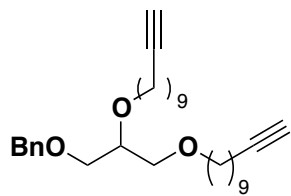


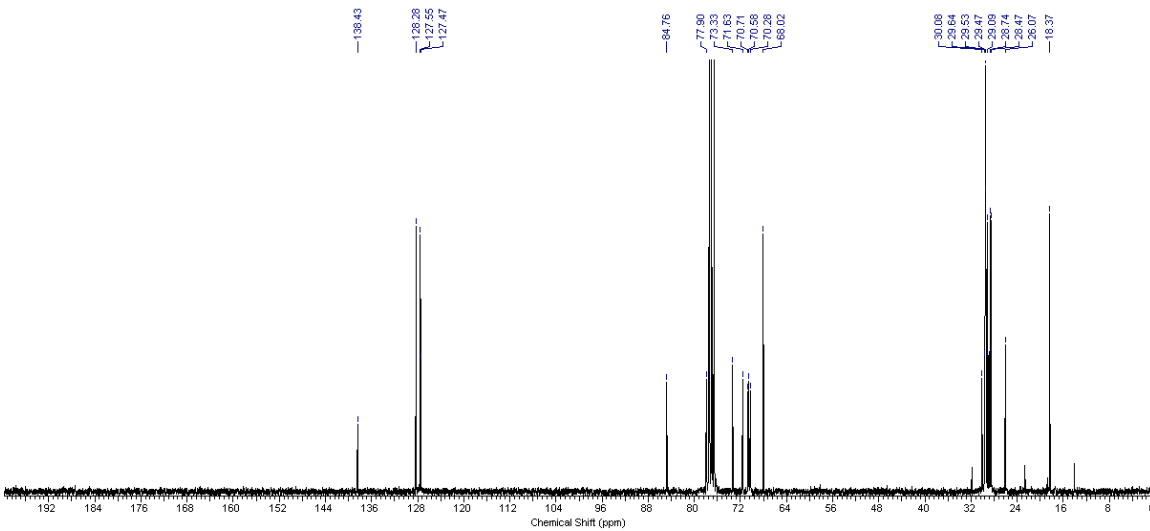
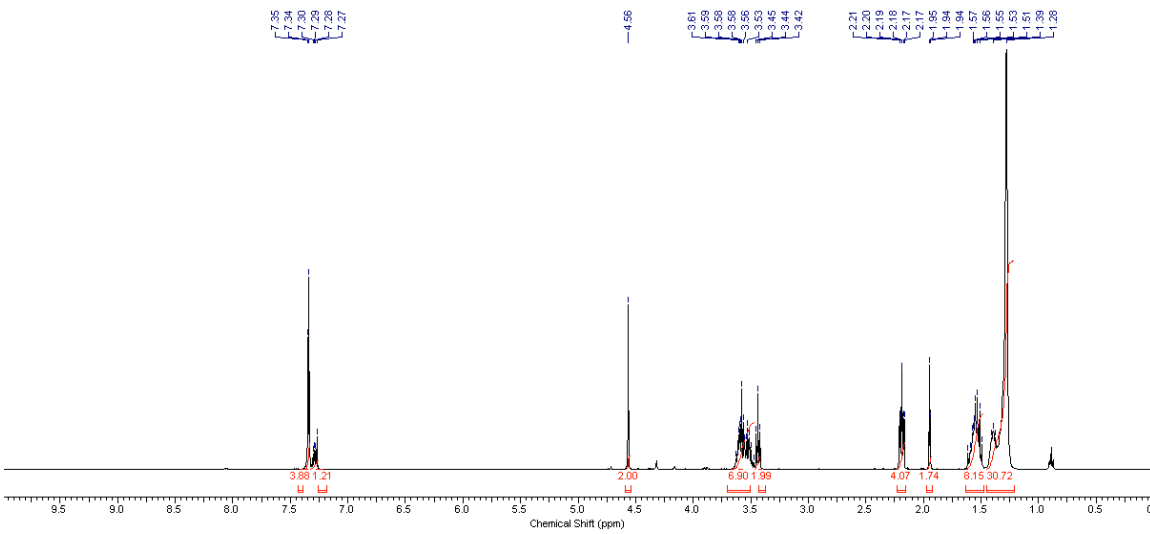
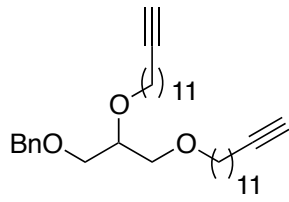
(1,4-dioxacyclohexadecan-2-yl)methyl-2-(1-methylpyrrolidinium-1-yl)ethyl phosphate

(14): To a solution of (1,4-dioxacyclohexadecan-2-yl)methanol (25 mg, 0.1 mmol) in anhydrous benzene (1 mL) was added triethylamine (0.02 mL, 0.14 mmol). The solution was cooled to 0 °C and 2-chloro-1,3,2-dioxaphospholane-2-oxide (0.011 mL, 0.12 mmol) was added. The resulting mixture was stirred at 0 °C for 5 min, warmed to room temperature and stirred another 2 h. The crystalline Et₃NHCl was removed by filtration and the filtrate was concentrated to afford a crude pale yellow oil. The crude oil was placed in a sealed tube, redissolved in anhydrous acetonitrile (2.4 mL) and cooled to -78 °C. *N*-Methylpyrrolidine (0.32 mL) was added in one portion. The tube was then sealed and warmed to 70 °C for 24 h. The reaction mixture was then concentrated in *vacuo* until the excess *N*-Methylpyrrolidine was completely removed. Lipid **14** was obtained as a pale brown semi-solid in 58 % yield. ¹H NMR (400 MHz, CDCl₃) δ = 4.53 - 4.06 (m, 9H), 3.83 - 3.49 (m, 12H), 3.17 - 3.13 (m, 2H), 1.55 - 1.26 (m, 22H). ¹³C NMR (125 MHz, CDCl₃) δ ppm = 78.7, 77.2, 71.8 (2C), 71.03, 70.99 (2C), 70.3, 69.8, 62.3, 30.3, 29.7, 29.2, 29.0, 26.93, 26.89, 26.75, 26.73, 26.69, 25.67, 24.63, 24.55; ³¹P NMR (162 MHz, CDCl₃) δ ppm = 3.31. HRMS (ESI) *m/z* calculated for C₂₃H₄₇NO₆P [M+H]⁺, 464.3141; found: 464.3175.

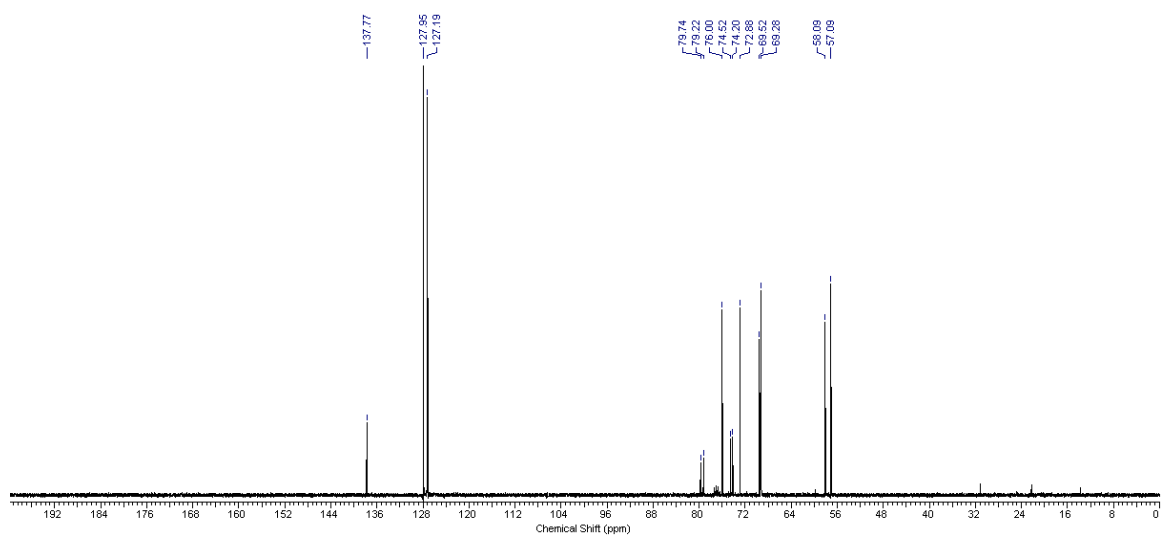
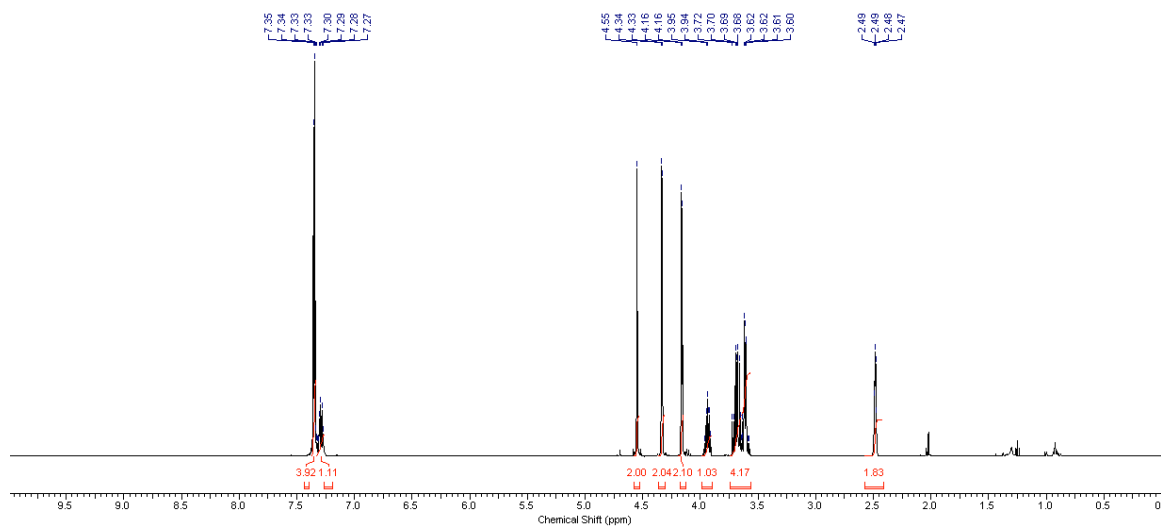
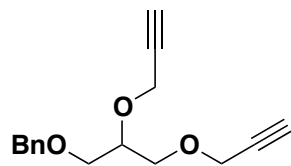
NMR SPECTRA FOR ALL NEW COMPOUNDS



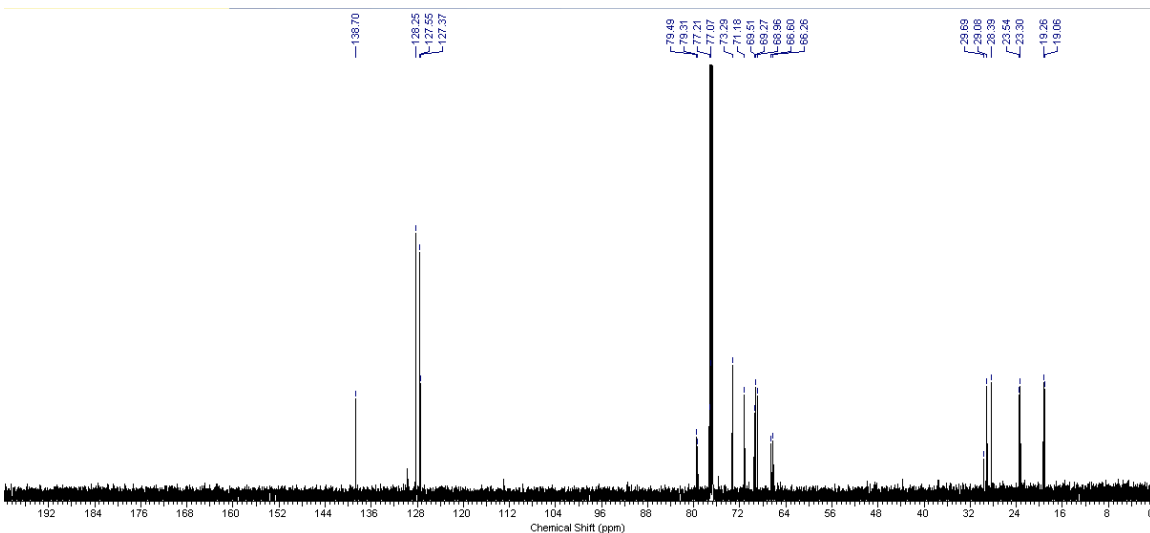
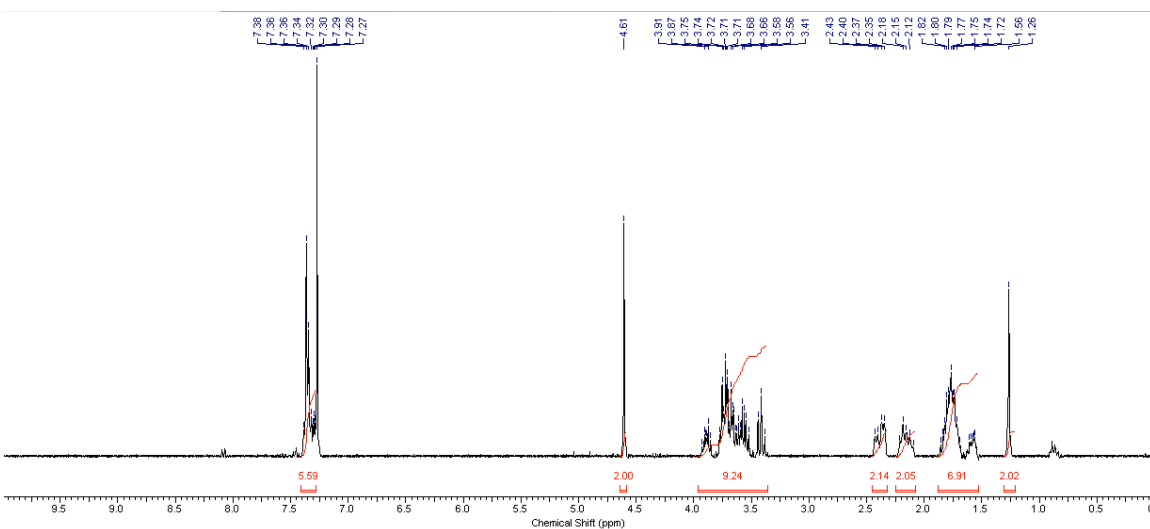
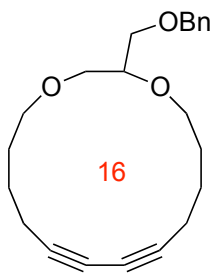




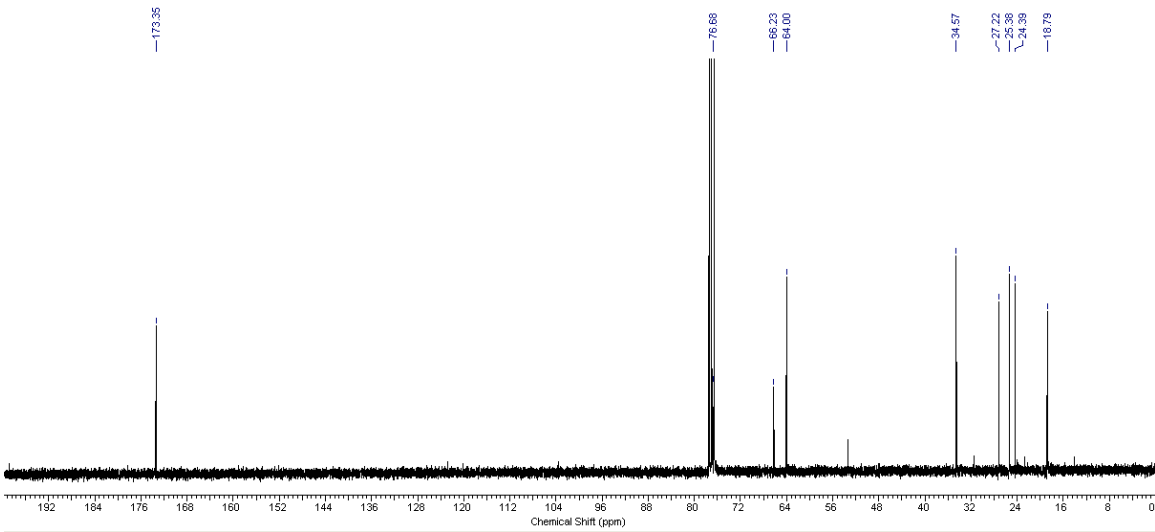
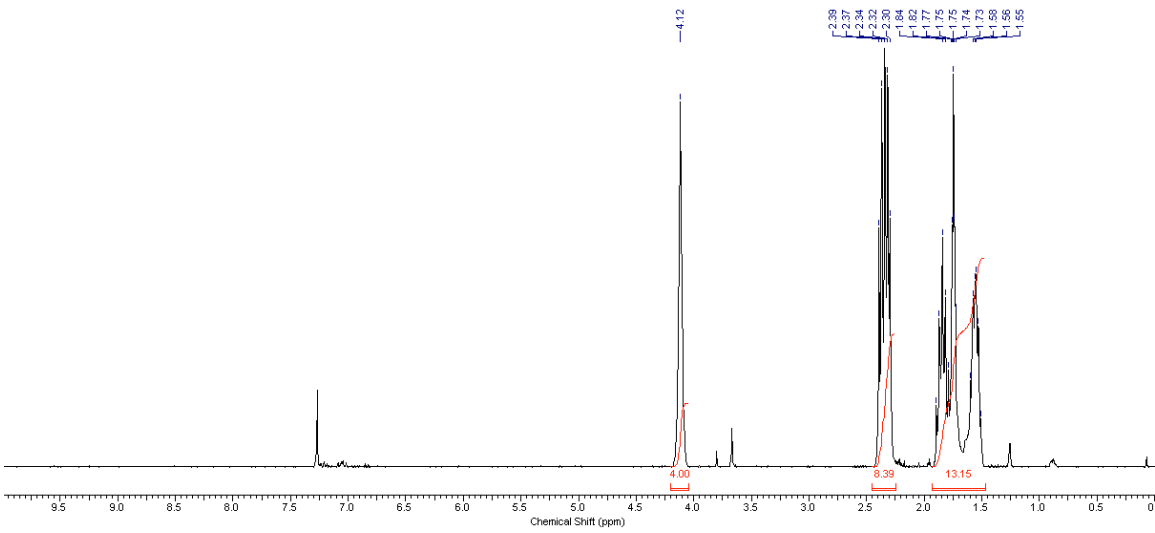
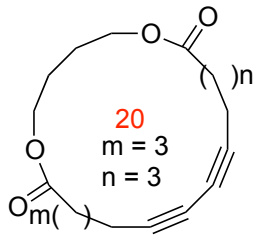
mmmmmm



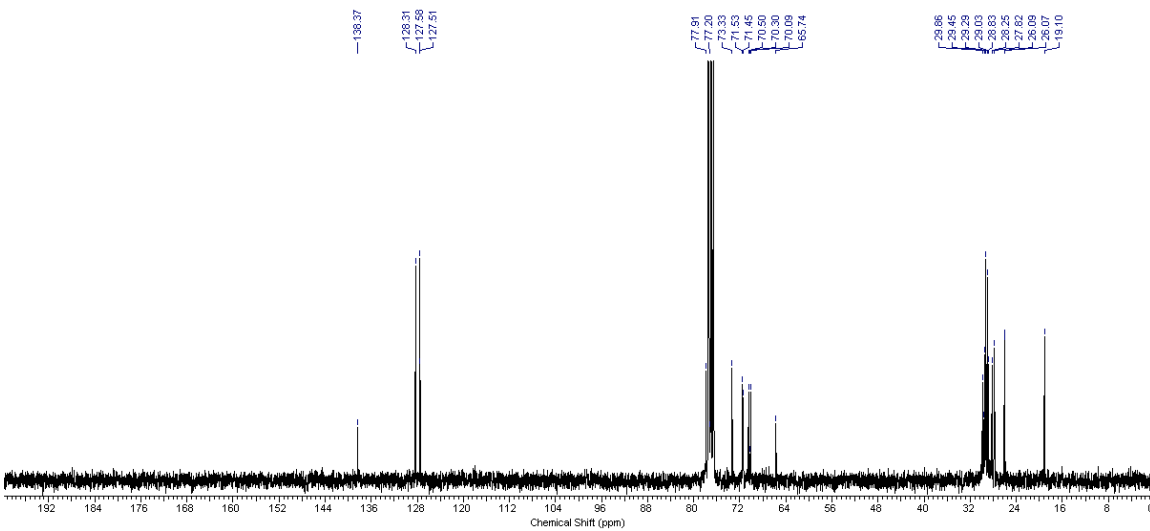
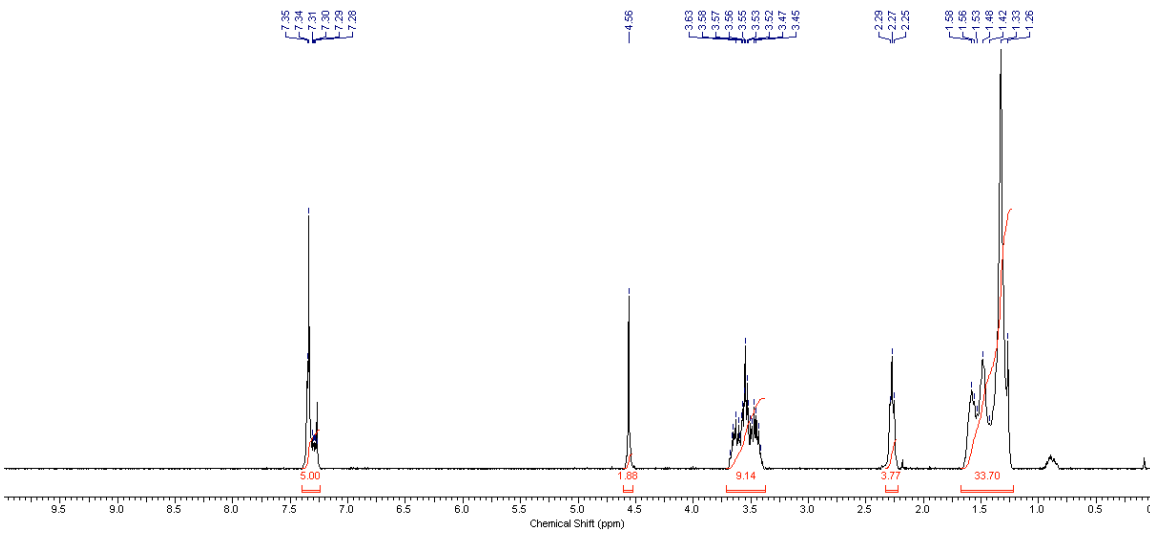
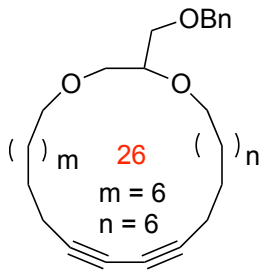
nnnnnn

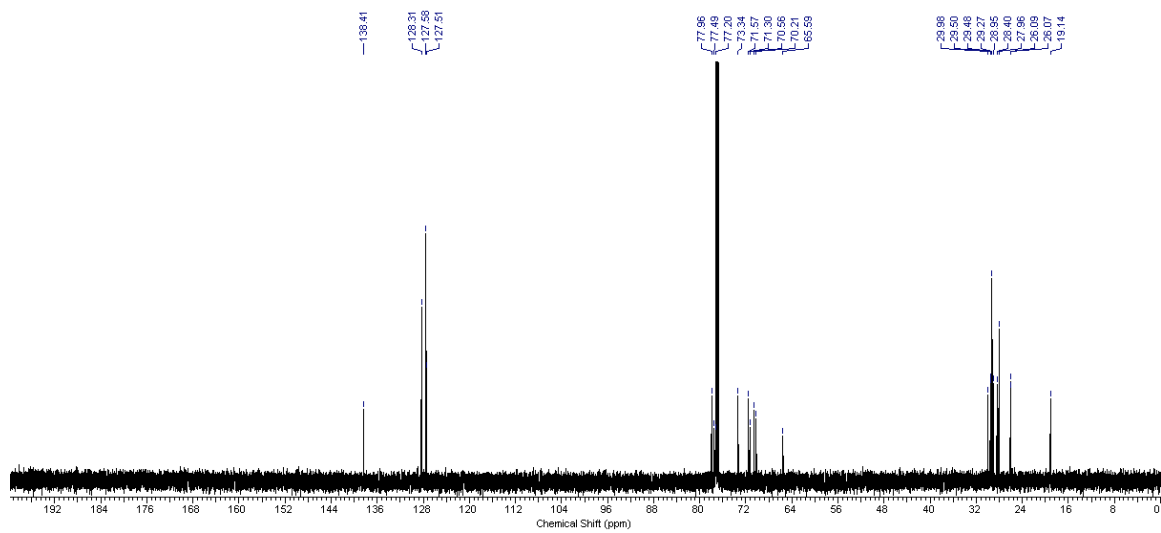
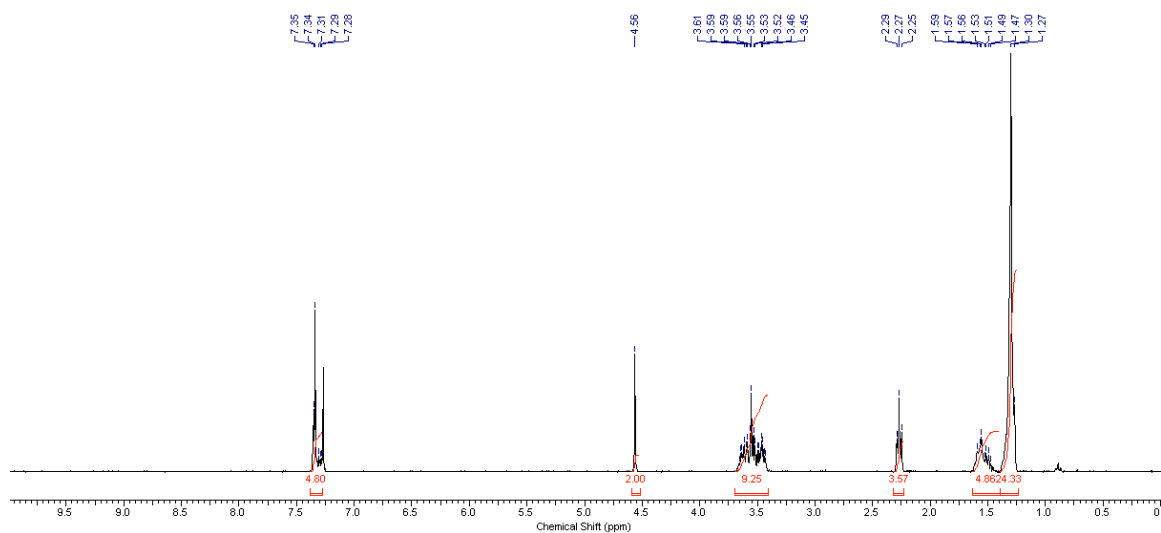
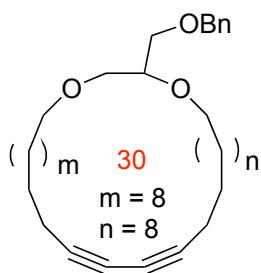


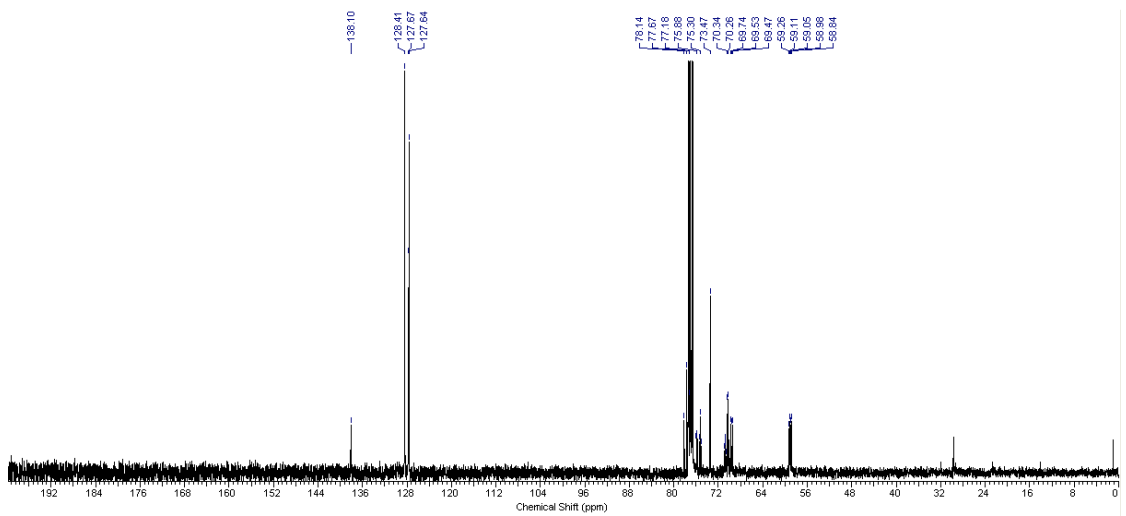
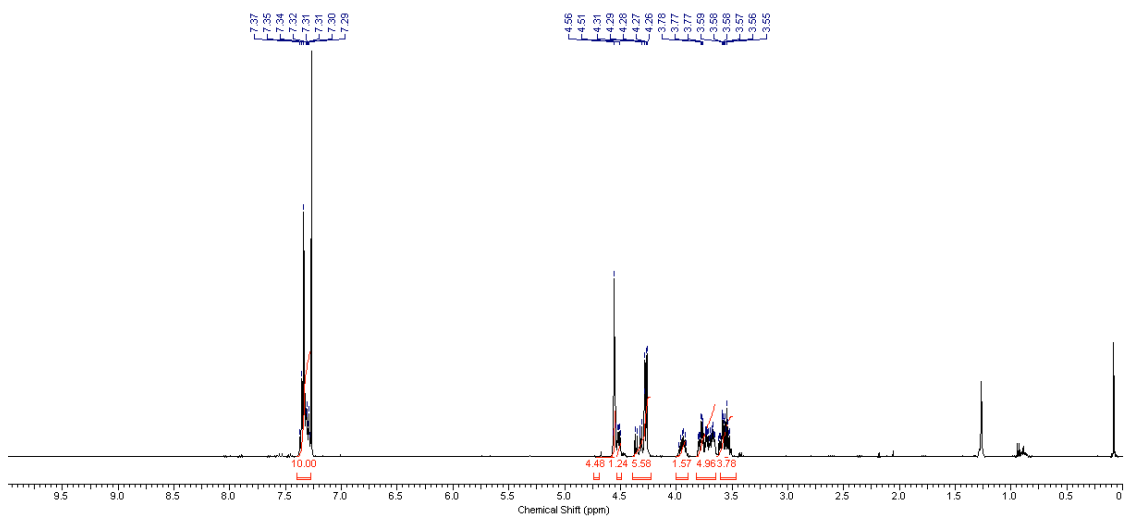
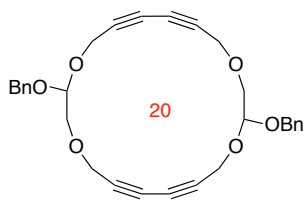
00000

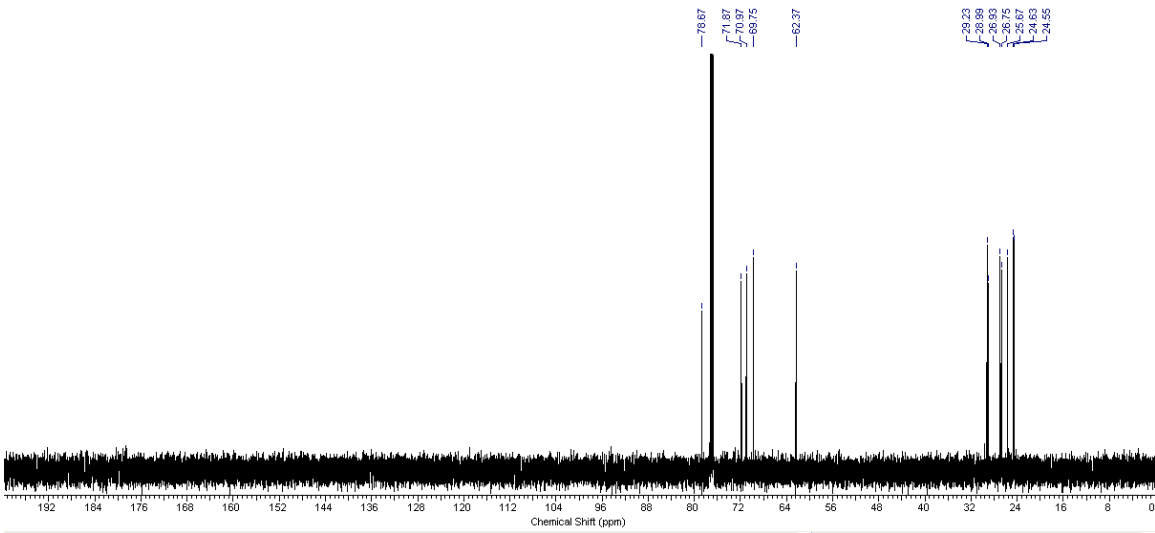
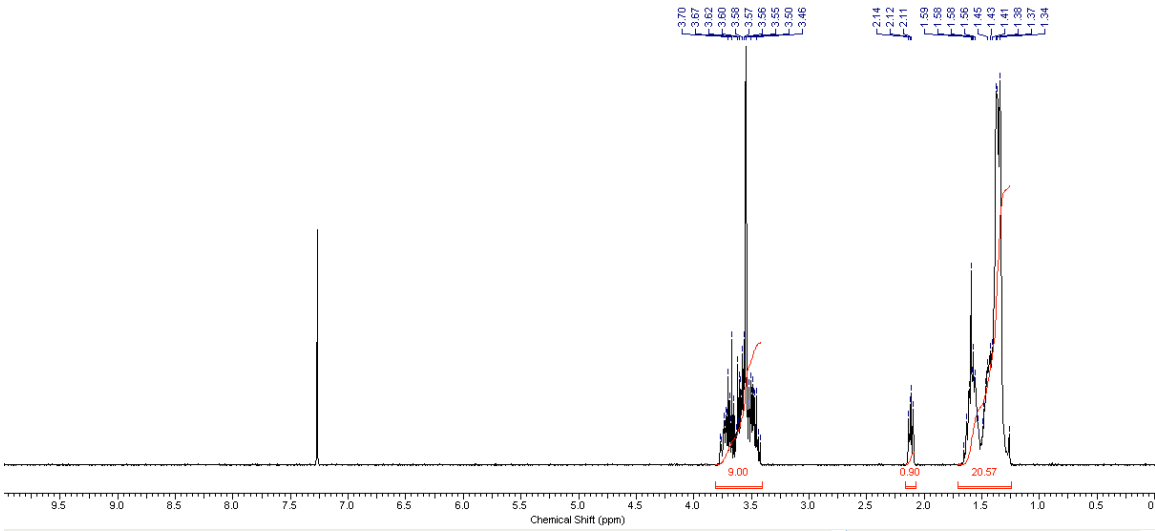
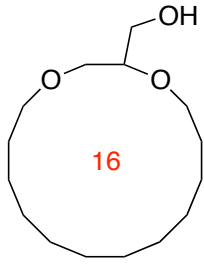


ppppp

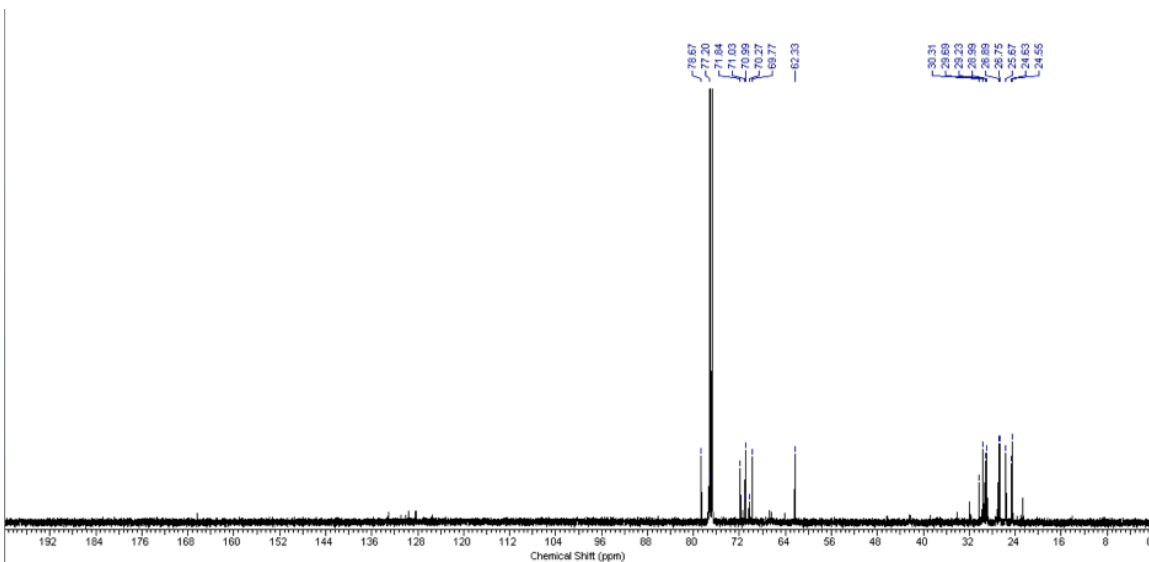
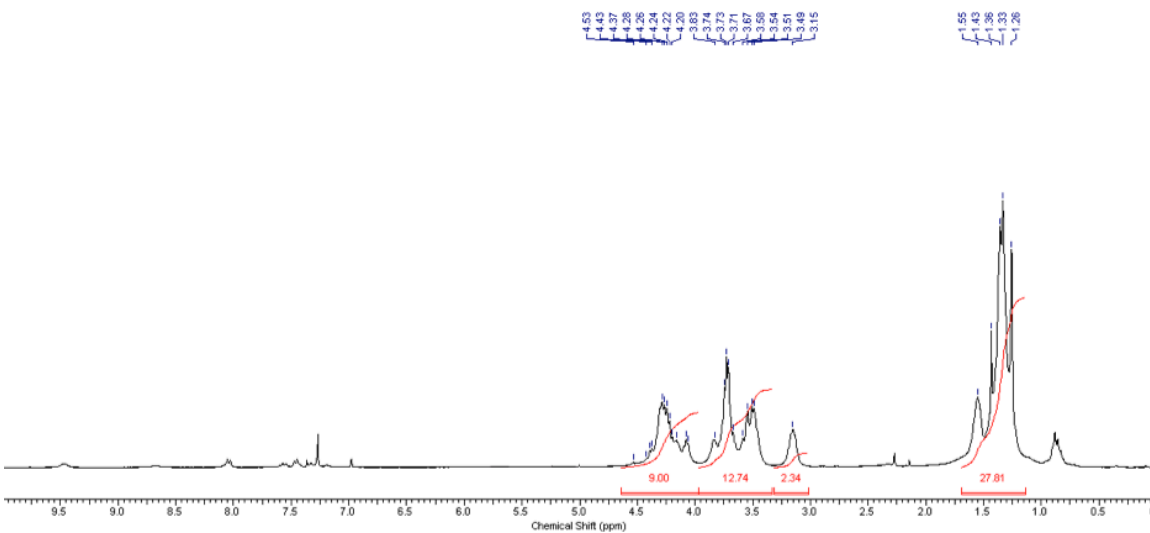
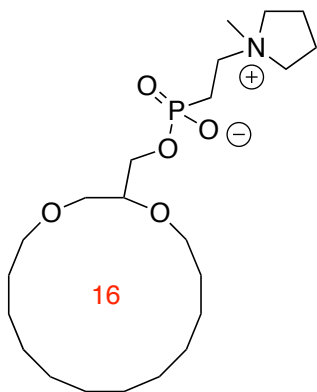


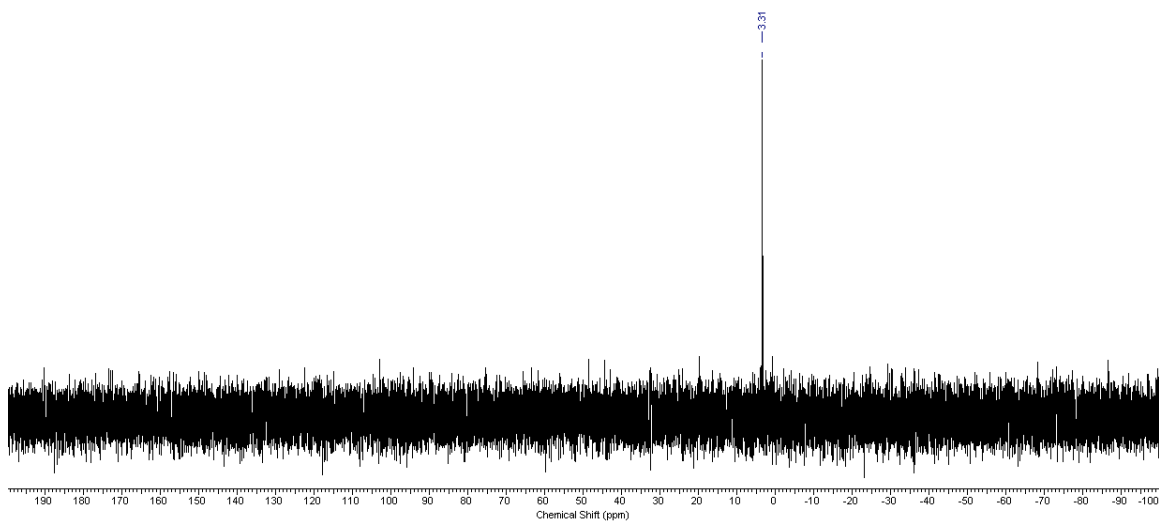
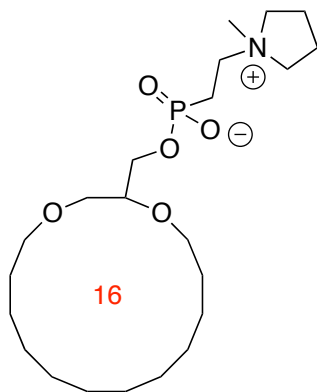






ttttt





VVVVV

Chapter 18 : Supporting Information of Chapter 9: Advanced Strategies for Efficient Macrocyclic Cu(I)- Catalyzed Cycloaddition of Azides

General:

All reactions that were carried out under anhydrous conditions were performed under an inert argon or nitrogen atmosphere in glassware that had previously been dried overnight at 120 °C or had been flame dried and cooled under a stream of argon or nitrogen.³⁰ All chemical products were obtained from Sigma-Aldrich Chemical Company or Strem Chemicals and were reagent quality. 8-azidooctan-1-ol³¹, 4-azidobutan-1-ol³², 12-azidododecan-1-ol³³ were prepared according to literature procedures. Technical solvents were obtained from VWR International Co. Anhydrous solvents (CH₂Cl₂, Et₂O, THF, DMF, Toluene, and hexanes) were dried and deoxygenated using a GlassContour system (Irvine, CA). Isolated yields reflect the mass obtained following flash column silica gel chromatography. Organic compounds were purified using the method reported by W. C. Still³⁴ and using silica gel obtained from Silicycle Chemical division (40-63 nm; 230-240 mesh). Analytical thin-layer chromatography (TLC) was performed on glass-backed silica gel 60 coated with a fluorescence indicator (Silicycle Chemical division, 0.25 mm, F₂₅₄). Visualization of TLC plate was performed by UV (254

³⁰ Shriver, D. F.; Drezdon, M. A. in *The Manipulation of Air-Sensitive Compounds*; Wiley-VCH: New York, 1986.

³¹ Kang, Y.; Lou, C.; Begam, K.; Ahmed, R.; Huang, H.; Jin, Z. *Bioorg. Med. Chem. Lett.* **2009**, *19*, 5166.

³² Kotsuki, H.; Sakai, H.; Sugino, A.; Yasuda, H. *Heterocycles* **2000**, *53*, 2561.

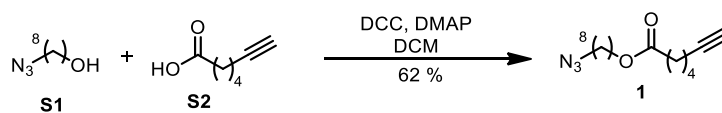
³³ Fujita, S.; Sato, T.; Hatanaka, K.; Kasuya, Maria C. Z.; Yamagata, T. *Chem. Lett.* **2004**, *33*, 580.

³⁴ Still, W. C.; Kahn, M.; Mitra, A. *J. Org. Chem.* **1978**, *43*, 2923.

nm), KMnO_4 or *p*-anisaldehyde stains. All mixed solvent eluents are reported as v/v solutions. Concentration refers to removal of volatiles at low pressure on a rotary evaporator. All reported compounds were homogeneous by thin layer chromatography (TLC) and by ^1H NMR. NMR spectra were taken in deuterated CDCl_3 using Bruker AV-300 and AV-400 instruments unless otherwise noted. Signals due to the solvent served as the internal standard (CHCl_3 : δ 7.27 for ^1H , δ 77.0 for ^{13}C). The ^1H NMR chemical shifts and coupling constants were determined assuming first-order behavior. Multiplicity is indicated by one or more of the following: s (singlet), d (doublet), t (triplet), q (quartet), m (multiplet), br (broad); the list of couplings constants (J) corresponds to the order of the multiplicity assignment. The ^1H NMR assignments were made based on chemical shift and multiplicity. The ^{13}C NMR assignments were made on the basis of chemical shift. High resolution mass spectroscopy (HRMS) was done by the Centre régional de spectrométrie de masse at the Département de Chimie, Université de Montréal from an Agilent LC-MSD TOF system using ESI mode of ionization unless otherwise noted.

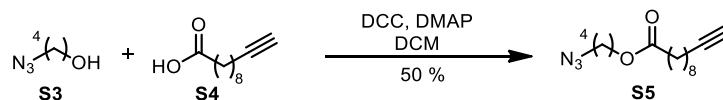
SYNTHESIS OF MACROCYCLIZATION PRECURSORS.

General Procedure A for Steglich Esterifications: To a stirred solution of the alcohol (1 equiv.) and the carboxylic acid (1.5 equiv.) in dry dichloromethane (0.2 M) was added N,N'-dicyclohexylcarbodiimide (DCC, 2 equiv.) and 4-dimethylaminopyridine (DMAP, 3 equiv.) at room temperature. The reaction mixture was stirred at room temperature for 15 h. Upon complete conversion of the starting material (by TLC analysis), the crude reaction mixture was placed in a freezer for 5 h to induce the precipitation of the urea, which was subsequently removed by filtration. The filtrate was concentrated *in vacuo* to provide the crude reaction mixture, which was purified by column chromatography on silica gel to afford the desired product.

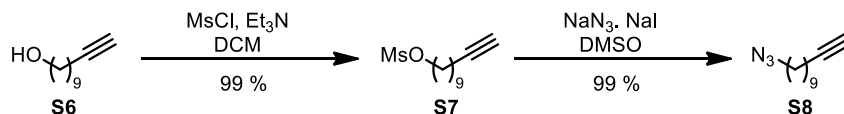


8-azidooctyl hept-6-ynoate (1): Following the General Procedure A, 8-azido-1-octanol (3.96 g, 23.1 mmol), 6-heptynoic acid (2.45 g, 19.4 mmol), DCC (7.90 g, 38.3 mmol) and DMAP (7.00 g, 57.3 mmol) in anhydrous DCM (100 mL) were added to the reaction flask. The reaction mixture was stirred at room temperature for 15 h. Upon complete conversion of the starting material, the crude reaction mixture was placed in a freezer for 5 h to induce the precipitation of the urea, which was subsequently removed by filtration. The filtrate was concentrated *in vacuo* to provide the crude reaction mixture. Following purification by column chromatography (10 % ethyl acetate in hexanes), the desired product was obtained as a colorless oil (3.36 g, 62 %). ^1H NMR (300 MHz, CDCl_3) δ = 4.06 (t, J = 6.7 Hz, 2H), 3.26 (t, J = 6.9 Hz, 2H), 2.33 (t, J = 7.4 Hz, 2H), 2.22 (td, J = 7.0, 2.7 Hz, 2H), 1.95 (t, J = 2.6 Hz, 1H), 1.85 - 1.47 (m, 8H), 1.47 - 1.20 (m, 8H); ^{13}C NMR (75 MHz, CDCl_3) δ = 173.5, 83.9, 68.5,

64.4, 51.4, 33.8, 30.0, 29.0, 28.8, 28.6, 27.8, 26.6, 25.8, 24.0, 18.1 ppm; HRMS (ESI) m/z calculated for $C_{15}H_{25}N_3NaO_2$ $[M+Na]^+$, 302.1839; found: 302.1836.

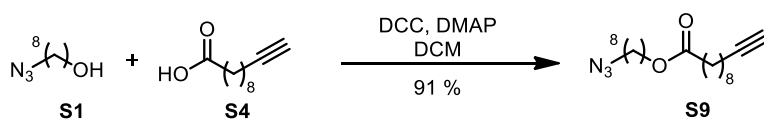


4-azidobutyl undec-10-ynoate (S5): Following the General Procedure A, 4-azidobutan-1-ol (500 mg, 4.4 mmol), 10-undecynoic acid (528 mg, 2.9 mmol), DCC (1.20 g, 5.8 mmol) and DMAP (1.06 g, 8.7 mmol) in anhydrous DCM (15 mL) were added to the reaction flask. The reaction mixture was stirred at room temperature for 15 h. Upon complete conversion of the starting material, the crude reaction mixture was placed in a freezer for 5 h to induce the precipitation of the urea, which was subsequently removed by filtration. The filtrate was concentrated *in vacuo* to provide the crude reaction mixture. Following purification by column chromatography (10 % ethyl acetate in hexanes), the desired product was obtained as a colorless oil (406 mg, 50 %). ^1H NMR (300 MHz, CDCl_3) δ = 4.10 (t, J = 6.1 Hz, 2H), 3.32 (t, J = 6.4 Hz, 2H), 2.30 (t, J = 7.5 Hz, 2H), 2.18 (td, J = 7.0, 2.6 Hz, 2H), 1.94 (t, J = 2.7 Hz, 1H), 1.78 - 1.46 (m, 8H), 1.43 - 1.26 (m, 8H); ^{13}C NMR (75 MHz, CDCl_3) δ = 173.8, 84.7, 68.1, 63.5, 51.0, 34.3, 29.07, 29.05, 28.9, 28.6, 28.4, 25.9, 25.6, 24.9, 18.4 ppm; HRMS (ESI) m/z calculated for $C_{15}H_{25}N_3NaO_2$ $[M+Na]^+$, 302.1839; found: 302.1837.



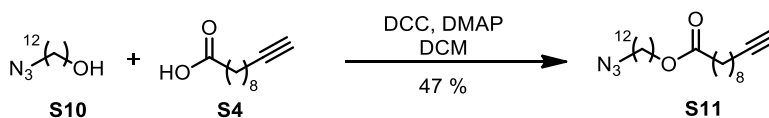
Undec-10-yn-1-yl methanesulfonate (S7): To a stirred solution of undec-10-yn-1-ol (500 mg, 2.97 mmol) in anhydrous DCM (15 mL) was added Et_3N (0.83 mL, 5.94 mmol) followed by MsCl (0.28 mL, 3.56 mmol). The solution was stirred at room temperature for 2 h. Upon complete conversion of the starting material, water was added to the the crude reaction

mixture. Following extraction (3X) with DCM, the organic phase was dried with Na₂SO₄ and filtered. The filtrate was concentrated *in vacuo* to provide the crude reaction mixture that was taken to the next step without further purification. **11-azidoundec-1-yne (S8)**: To a stirred solution of undec-10-yn-1-yl methanesulfonate (732 mg, 2.97 mmol) in DMSO (15 mL) was added NaN₃ (966 mg, 14.85 mmol) followed by NaI (222 mg, 1.5 mmol). The solution was stirred at room temperature for 16 h. Upon complete conversion of the starting material, water was added to the the crude reaction mixture. Following extraction (3X) with EtOAc, the organic phase was washed with brine, dried with Na₂SO₄ and filtered. The filtrate was concentrated *in vacuo* to provide the crude reaction mixture Following purification by column chromatography (5 % ethyl acetate in hexanes), the desired product was obtained as a colorless oil (555 mg, 97 %). ¹H NMR (400 MHz, CDCl₃) δ = 3.25 (t, *J* = 6.9 Hz, 2 H), 2.17 (dt, *J* = 7.0, 2.7 Hz, 2 H), 1.93 (t, *J* = 2.6 Hz, 1 H), 1.64 - 1.55 (m, 2 H), 1.54 - 1.45 (m, 2 H), 1.43 - 1.23 (m, 10 H); ¹³C NMR (100 MHz, CDCl₃) δ = 84.6, 68.0, 51.4, 29.2, 29.0, 28.9, 28.8, 28.6, 28.4, 28.3, 26.6 ppm; HRMS (ESI) *m/z* calculated for C₁₁H₂₀N₃ [M+H]⁺, 194.1657; found: 194.1654.



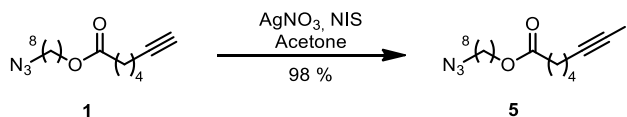
8-azidooctyl undec-10-ynoate (S9): Following the General Procedure A, 8-azidooctan-1-ol (250 mg, 1.8 mmol), 10-undecynoic acid (181 mg, 1.0 mmol), DCC (410 mg, 2.0 mmol) and DMAP (380 mg, 3.1 mmol) in anhydrous DCM (5 mL) were added to the reaction flask. The reaction mixture was stirred at room temperature for 15 h. Upon complete conversion of the starting material, the crude reaction mixture was placed in a freezer for 5 h to induce the precipitation of the urea, which was subsequently removed by filtration. The filtrate was

concentrated *in vacuo* to provide the crude reaction mixture. Following purification by column chromatography (5 % ethyl acetate in hexanes), the desired product was obtained as a colorless oil (305 mg, 91 %). ¹H NMR (300 MHz, CDCl₃) δ = 4.05 (t, *J* = 6.7 Hz, 2H), 3.26 (t, *J* = 6.9 Hz, 2H), 2.29 (t, *J* = 7.5 Hz, 2H), 2.17 (td, *J* = 7.0, 2.6 Hz, 2H), 1.93 (t, *J* = 2.6 Hz, 1H), 1.66 – 1.49 (m, 8H), 1.44 - 1.18 (m, 16H); ¹³C NMR (75 MHz, CDCl₃) δ = 173.9, 84.7, 68.1, 64.2, 51.4, 34.3, 29.1, 29.03 (2C), 28.98, 28.9, 28.8, 28.61, 28.56, 28.4, 26.6, 25.8, 24.9, 18.3 ppm; HRMS (ESI) *m/z* calculated for C₁₉H₃₃N₃NaO₂ [M+Na]⁺, 358.2465; found: 358.2465.

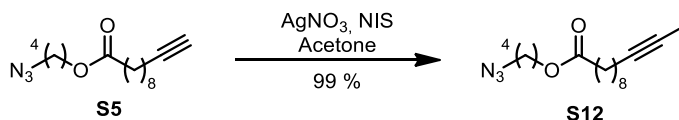


12-azidodecyl undec-10-ynoate (S11): Following the General Procedure A, 8-azidooctan-1-ol (150 mg, 0.7 mmol), 10-undecynoic acid (145 mg, 0.8 mmol), DCC (272 mg, 1.3 mmol) and DMAP (242 mg, 2.0 mmol) in anhydrous DCM (3.5 mL) were added to the reaction flask. The reaction mixture was stirred at room temperature for 15 h. Upon complete conversion of the starting material, the crude reaction mixture was placed in a freezer for 5 h to induce the precipitation of the urea, which was subsequently removed by filtration. The filtrate was concentrated *in vacuo* to provide the crude reaction mixture. Following purification by column chromatography (5 % ethyl acetate in hexanes), the desired product was obtained as a white solid (122 mg, 47 %). ¹H NMR (400 MHz, CDCl₃) δ = 4.05 (t, *J* = 6.7 Hz, 2H), 3.25 (t, *J* = 7.0 Hz, 2H), 2.29 (t, *J* = 7.5 Hz, 2H), 2.17 (td, *J* = 7.0, 2.6 Hz, 2H), 1.93 (d, *J* = 2.8 Hz, 1H), 1.65 - 1.48 (m, 8H), 1.45 - 1.18 (m, 24H); ¹³C NMR (100 MHz, CDCl₃) δ = 173.9, 84.6, 68.0, 64.3, 51.4, 34.3, 31.6, 29.45, 29.42, 29.2, 29.11, 29.07, 29.0, 28.9, 28.80, 28.6, 28.4, 26.7, 25.9,

24.9, 22.6, 18.3 ppm; HRMS (ESI) m/z calculated for $C_{23}H_{41}N_3NaO_2$ $[M+Na]^+$, 414.3091; found: 414.3079.

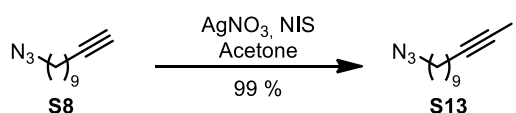


8-azidohept-6-yn-7-yl iodide (5): To a stirred solution of 8-azidohept-6-ynoate (2.00 g, 7.2 mmol) in acetone (36 mL) was added N-iodosuccinimide (1.77 g, 7.9 mmol) followed by silver nitrate (121.5 mg, 0.7 mmol). The solution was stirred in the dark for 17 h. The crude mixture was reduced *in vacuo* and purified on silica gel (10 % ethyl acetate in hexanes) to afford the desired product as a colorless oil (1.02 g, 98 %). ^1H NMR (400 MHz, CDCl_3) δ = 4.03 (t, J = 6.7 Hz, 2H), 3.23 (t, J = 6.9 Hz, 2H), 2.36 (t, J = 7.2 Hz, 2H), 2.29 (t, J = 7.2 Hz, 2H), 1.70 (m, 2H), 1.65 (m, 6H), 1.32 (m, 8H); ^{13}C NMR (75 MHz, CDCl_3) δ = 173.3, 93.9, 64.3, 51.3, 33.7, 28.97 (2C), 28.91, 28.7, 28.5, 27.8, 26.5, 25.7, 24.0, 20.4 ppm; HRMS (ESI) m/z calculated for $C_{15}H_{24}IN_3NaO_2$ $[M+Na]^+$, 428.0805; found: 428.0806.

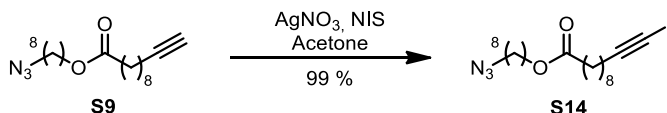


4-azidobutyl 11-iodoundec-10-ynoate (S12): To a stirred solution of the 4-azidobutyl undec-10-ynoate (400 mg, 1.4 mmol) in acetone (7 mL) was added N-iodosuccinimide (354 mg, 1.6 mmol) followed by silver nitrate (24.3 mg, 0.14 mmol). The solution was stirred in the dark for 17 h. The crude mixture was reduced *in vacuo* and purified on silica-gel (10 % ethyl acetate in hexanes) to afford the desired product as a colorless oil (580 mg, 99 %). ^1H NMR (400 MHz, CDCl_3) δ = 4.10 (t, J = 6.0 Hz, 2H), 3.33 (t, J = 6.4 Hz, 2H), 2.35 (t, J = 7.1 Hz, 2H), 2.30 (t, J = 7.5 Hz, 2H), 1.78 - 1.45 (m, 8H), 1.43 - 1.24 (m, 8H); ^{13}C NMR (100 MHz, CDCl_3) δ = 173.8, 94.7, 63.5, 51.0, 34.3, 29.0 (2C), 28.8, 28.6, 28.4, 25.9 (2C), 25.6, 24.9,

20.8 ppm; HRMS (ESI) m/z calculated for $C_{15}H_{28}IN_4O_2$ $[M+NH_4]^+$, 423.1252; found: 423.1253.

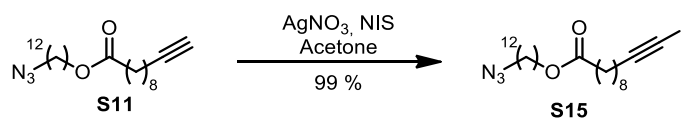


11-azido-1-iodoundec-1-yne (S13): To a stirred solution of 11-azidoundec-1-yne (500 mg, 2.6 mmol) in acetone (13 mL) was added *N*-iodosuccinimide (484 mg, 2.9 mmol) followed by silver nitrate (59 mg, 0.26 mmol). The solution was stirred in the dark for 17 h. The crude mixture was reduced *in vacuo* and purified on silica-gel (5 % ethyl acetate in hexanes) to afford the desired product as a colorless oil (832 mg, 99 %). ¹H NMR (300 MHz, CDCl₃) δ = 3.25 (t, J = 6.8 Hz, 2H), 2.34 (t, J = 7.0 Hz, 2H), 1.65 - 1.54 (m, 2H), 1.53 - 1.43 (m, 2H), 1.43 - 1.23 (m, 10H); ¹³C NMR (75 MHz, CDCl₃) δ = 94.6, 51.3, 29.1, 28.9 (2C), 28.8, 28.7, 28.5 (2C), 28.3, 26.5 ppm; HRMS (ESI) m/z calculated for $C_{11}H_{19}IN_3$ $[M+H]^+$, 320.0624; found: 320.0627.

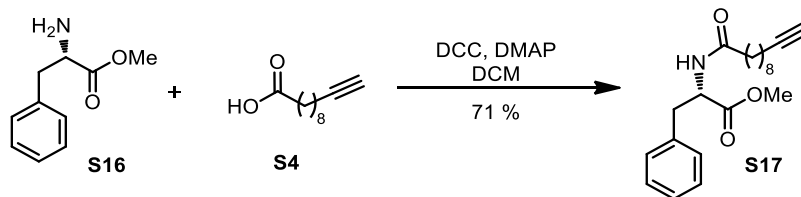


8-azido-11-iodoundec-10-yne (S14): To a stirred solution of the 8-azido-11-undecynoate (306 mg, 0.9 mmol) in acetone (5 mL) was added *N*-iodosuccinimide (225.2 mg, 1.0 mmol) followed by silver nitrate (15.4 mg, 0.091 mmol). The solution was stirred in the dark for 17 h. The crude mixture was reduced *in vacuo* and purified on silica-gel (5 % ethyl acetate in hexanes) to afford the desired product. The desired product was obtained as a colorless oil (415 mg, 99 %). ¹H NMR (300 MHz, CDCl₃) δ = 4.04 (t, J = 6.7 Hz, 2H), 3.24 (t, J = 6.9 Hz, 2H), 2.33 (t, J = 7.0 Hz, 2H), 2.27 (t, J = 7.5 Hz, 2H), 1.69 - 1.42 (m, 8H), 1.42 - 1.22 (m, 16H); ¹³C NMR (75 MHz, CDCl₃) δ = 173.8, 94.6, 64.2, 51.3, 34.3, 28.98 (2C), 28.97

(2C), 28.93, 28.8, 28.7, 28.6, 28.5, 28.3, 26.5, 25.7, 24.9, 20.7 ppm; HRMS (ESI) m/z calculated for $C_{19}H_{36}IN_4O_2 [M+NH_4]^+$, 479.1878; found: 479.1877.

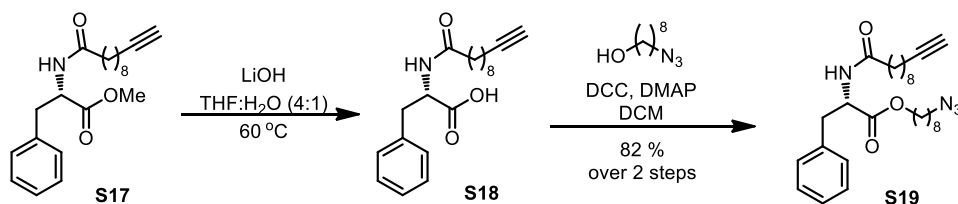


12-azidodecyl 11-iodoundec-10-ynoate (S15): To a stirred solution of the 12-azidodecyl undec-10-ynoate (130 mg, 0.3 mmol) in acetone (2 mL) was added N-iodosuccinimide (82 mg, 0.4 mmol) followed by silver nitrate (5.6 mg, 0.03 mmol). The solution was stirred in the dark for 17 h. The crude mixture was reduced *in vacuo* and purified on silica-gel (5 % ethyl acetate in hexanes) to afford the desired product. The desired product was obtained as a white solid (170 mg, 99 %). 1H NMR (400 MHz, $CDCl_3$) δ = 4.06 (t, J = 6.7 Hz, 2H), 3.26 (t, J = 6.9 Hz, 2H), 2.35 (t, J = 7.0 Hz, 2H), 2.29 (t, J = 7.5 Hz, 2H), 1.64 – 1.49 (m, 8H), 1.42 - 1.22 (m, 24H); ^{13}C NMR (100 MHz, $CDCl_3$) δ = 173.9, 94.7, 64.4, 51.4, 34.3, 29.48, 29.46, 29.43, 29.41, 29.2, 29.11, 29.10, 29.05, 29.0, 28.84, 28.79, 28.7, 28.6, 28.4, 26.7, 25.9, 24.9, 20.8 ppm; HRMS (ESI) m/z calculated for $C_{23}H_{40}IN_3NaO_2 [M+Na]^+$, 540.2057; found: 540.2049.



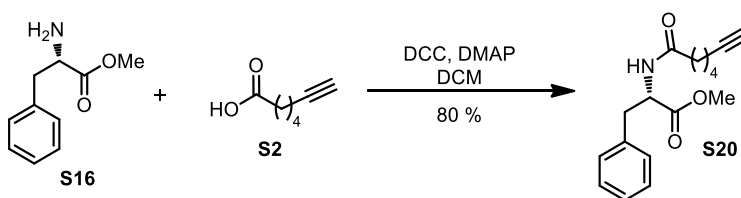
(S)-methyl-2-(undec-10-ynamido)-3-phenylpropanoate (S17): Following the General Procedure A, L-phenylalanine methyl ester hydrochloride (500 mg, 2.8 mmol), 10-undecynoic acid (340 mg, 1.9 mmol), DCC (783 mg, 3.8 mmol) and DMAP (695 mg, 5.7 mmol) in anhydrous DCM (10 mL) were added to the reaction flask. The reaction was stirred for 17 h. Upon complete conversion of the starting material, the crude reaction mixture was placed in a freezer for 5 h to induce the precipitation of the urea, which was subsequently removed by

filtration. The filtrate was concentrated *in vacuo* to provide the crude reaction mixture, which was purified by column chromatography on silica-gel (30 % ethyl acetate in hexanes). The desired product was obtained as a white solid (688 mg, 71 %). ¹H NMR (300 MHz, CDCl₃) δ = 7.33 - 7.18 (m, 3 H), 7.14 - 7.04 (m, 2 H), 6.00 (d, *J* = 7.8 Hz, 1 H), 4.91 - 4.85 (m, 1 H), 3.71 (s, 3 H), 3.21 - 2.98 (m, 2 H), 2.21 - 2.09 (m, 4 H), 1.92 (t, *J* = 3.0 Hz, 1 H), 1.66 - 1.18 (m, 12 H); ¹³C NMR (75 MHz, CDCl₃) δ = 172.5, 172.1, 135.8, 129.1, 128.4, 126.9, 84.5, 68.0, 52.8, 52.1, 37.8, 36.3, 29.02, 28.96, 28.7, 28.3, 28.5, 25.4, 18.2 ppm; HRMS (ESI) *m/z* calculated for C₂₁H₃₀NO₃ [M+H]⁺, 344.2220; found: 344.2221.



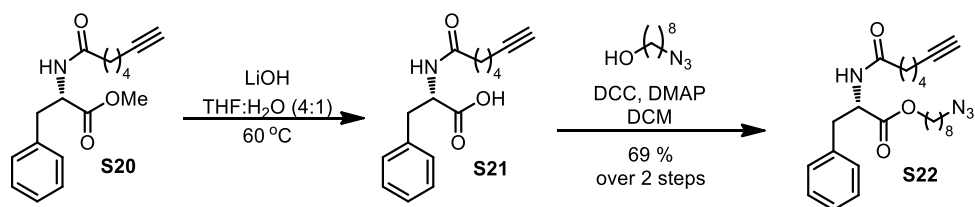
(S)-methyl-2-(undec-10-ynamido)-3-phenylpropanoic acid (S18): To a solution of (S)-methyl-2-(undec-10-ynamido)-3-phenylpropanoate (688 mg, 2 mmol) in THF:H₂O (4:1, 10 mL and 3 mL) was added LiOH (240 mg, 10 mmol). The mixture was stirred at 60 °C for 2 h and then cooled to ambient temperature. EtOAc and HCl 1 N were added to the mixture and the aqueous and organic phases were separated. The aqueous phase was extracted (2x) with EtOAc. The organic phases were combined, dried with Na₂SO₄, filtered and concentrated *in vacuo*. The crude solid was directly used in the following reaction. **(S)-azido-octan-2-(undec-10-ynamido)-3-phenylpropanoate (S19):** Following the General Procedure A, 8-azido-octan-1-ol (100 mg, 0.6 mmol), (S)-methyl-2-(undec-10-ynamido)-3-phenylpropanoic acid (234 mg, 0.7 mmol), DCC (243 mg, 1.2 mmol) and DMAP (216 mg, 1.8 mmol) in anhydrous DCM (3 mL) were added to the reaction flask. Upon complete conversion of the starting material, the crude reaction mixture was placed in a freezer for 5 h to induce the precipitation of the urea,

which was subsequently removed by filtration. The filtrate was concentrated *in vacuo* to provide the crude reaction mixture, which was purified by column chromatography on silica-gel (20 to 50 % ethyl acetate in hexanes). The desired product was obtained as a white solid (234 mg, 82 % over 2 steps). ¹H NMR (300 MHz, CDCl₃) δ = 7.29 - 7.15 (m, 3 H), 7.10 - 7.03 (m, 2 H), 5.85 (d, *J* = 7.8 Hz, 1 H), 4.88 - 4.81 (m, 1 H), 4.14 - 3.97 (m, 2 H), 3.22 (t, *J* = 6.9 Hz, 2 H), 3.16 - 2.99 (m, 2 H), 2.19 - 2.08 (m, 4 H), 1.89 (t, *J* = 2.6 Hz, 1 H), 1.66 - 1.14 (m, 24 H); ¹³C NMR (75 MHz, CDCl₃) δ = 172.5, 171.8, 135.9, 129.2, 128.4, 127.0, 84.7, 68.1, 65.5, 52.9, 51.4, 38.0, 36.5, 29.11, 29.06, 28.97, 28.93, 28.8, 28.7, 28.6, 28.37, 28.36, 26.6, 25.7, 25.5, 18.3 ppm; HRMS (ESI) *m/z* calculated for C₂₈H₄₃N₄O₃ [M+H]⁺, 483.3330; found: 483.3335.



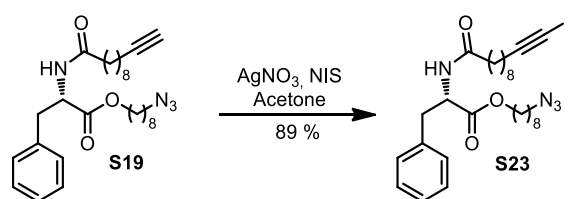
(S)-methyl-2-(hept-6-ynamido)-3-phenylpropanoate (S20): Following the General Procedure A, L-phenylalanine methyl ester hydrochloride (500 mg, 2.8 mmol), 6-heptynoic acid (240 mg, 1.9 mmol), DCC (783 mg, 3.8 mmol) and DMAP (695 mg, 5.7 mmol) in anhydrous DCM (10 mL) were added to the reaction flask. The reaction was stirred for 17 h. Upon complete conversion of the starting material, the crude reaction mixture was placed in a freezer for 5 h to induce the precipitation of the urea, which was subsequently removed by filtration. The filtrate was concentrated *in vacuo* to provide the crude reaction mixture, which was purified by column chromatography on silica-gel (30 % ethyl acetate in hexanes). The desired product was obtained as a white solid (646 mg, 80 %). ¹H NMR (300 MHz, CDCl₃) δ = 7.35 - 7.19 (m, 3 H), 7.15 - 7.06 (m, 2 H), 6.01 (d, *J* = 7.8 Hz, 1 H), 4.94 - 4.87 (m, 1 H),

3.73 (s, 3 H), 3.20 – 3.06 (m, 2 H), 2.25 - 2.13 (m, 4 H), 1.95 (t, $J = 2.6$ Hz, 1 H), 1.79 - 1.65 (m, 2 H), 1.58 - 1.44 (m, 2 H); ^{13}C NMR (75 MHz, CDCl_3) $\delta = 172.1$ (2C), 135.8, 129.1, 128.5, 127.0, 83.9, 68.6, 52.8, 52.2, 37.8, 35.7, 27.7, 24.5, 18.0 ppm; HRMS (ESI) m/z calculated for $\text{C}_{17}\text{H}_{21}\text{NNaO}_3$ $[\text{M}+\text{Na}]^+$, 310.1414; found: 310.1413.

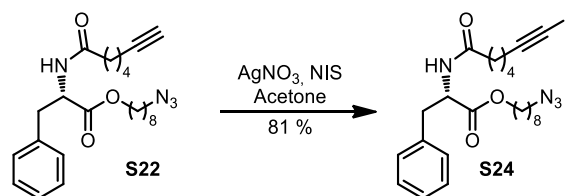


(S)-methyl-2-(hept-6-ynamido)-3-phenylpropanoic acid (S21): To a solution of (S)-methyl-2-(hept-6-ynamido)-3-phenylpropanoate (646 mg, 2.3 mmol) in THF:H₂O (4:1, 9 mL and 2.3 mL) was added LiOH (270 mg, 11 mmol). The mixture was stirred at 60 °C for 2 h and then cooled to ambient temperature. EtOAc and HCl 1 N were added to the mixture and the aqueous and organic phases were separated. The aqueous phase was extracted (2x) with EtOAc. The organic phases were combined, dried with Na₂SO₄, filtered and concentrated *in vacuo*. The crude solid was directly used in the following reaction. **(S)-azido-octan-2-(hept-6-ynamido)-3-phenylpropanoate (S22):** Following the General Procedure A, 8-azido-octan-1-ol (100 mg, 0.6 mmol), (S)-methyl-2-(hept-7-ynamido)-3-phenylpropanoic acid (193 mg, 0.7 mmol), DCC (243 mg, 1.2 mmol) and DMAP (215.9 mg, 1.8 mmol) in anhydrous DCM (3 mL) were added to the reaction flask. Upon complete conversion of the starting material, the crude reaction mixture was placed in a freezer for 5 h to induce the precipitation of the urea, which was subsequently removed by filtration. The filtrate was concentrated *in vacuo* to provide the crude reaction mixture, which was purified by column chromatography on silica-gel (20 to 50 % ethyl acetate in hexanes). The desired product was obtained as a white solid (173 mg, 69 % over 2 steps). ^1H NMR (300 MHz, CDCl_3) $\delta = 7.30 - 7.16$ (m, 3 H), 7.12 - 6.98

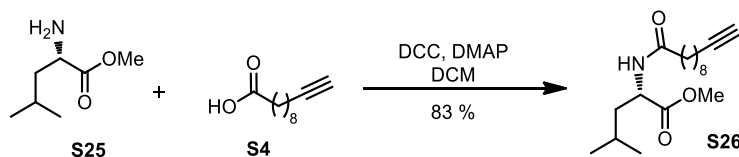
(m, 2 H), 5.86 (d, $J = 7.8$ Hz, 1 H), 4.87 – 4.81 (m, 1 H), 4.16 - 3.95 (m, 2 H), 3.21 (t, $J = 6.9$, 2 H), 3.15 - 2.99 (m, 2 H), 2.21 - 2.07 (m, 4 H), 1.90 (t, $J = 2.6$ Hz, 1 H), 1.80 - 1.13 (m, 16 H); ^{13}C NMR (75 MHz, CDCl_3) $\delta = 172.1, 171.8, 135.9, 129.3, 128.5, 127.1, 84.0, 68.6, 65.6, 52.9, 51.4, 38.0, 35.8, 29.2, 29.0, 28.8, 28.4, 27.7, 26.6, 25.7, 24.5, 18.1$ ppm; HRMS (ESI) m/z calculated for $\text{C}_{24}\text{H}_{35}\text{N}_4\text{O}_3$ $[\text{M}+\text{H}]^+$, 427.2701; found: 427.2704.



(S)-azido-octan-2-(11-iodoundec-10-ynamido)-3-phenylpropanoate (S23): To a stirred solution of the (S)-azido-octan-2-(undec-10-ynamido)-3-phenylpropanoate (82 mg, 0.17 mmol) in acetone (2 mL) was added N-iodosuccinimide (42 mg, 0.19 mmol) followed by silver nitrate (3 mg, 0.017 mmol). The solution was stirred in the dark for 17 h. The crude mixture was reduced *in vacuo* and purified on silica-gel (20 to 50 % ethyl acetate in hexanes) to afford the desired product as a colorless oil (92 mg, 89 %). ^1H NMR (300 MHz, CDCl_3) $\delta = 7.40 - 7.22$ (m, 3H), 7.11 (dd, $J = 7.6, 1.8$ Hz, 2H), 5.89 (d, $J = 7.8$ Hz, 1H), 4.90 (dt, $J = 7.9, 5.9$ Hz, 1H), 4.15 – 4.06 (m, 2H), 3.27 (t, $J = 6.9$ Hz, 2H), 3.13 (t, $J = 5.3$ Hz, 2H), 2.36 (t, $J = 7.0$ Hz, 2H), 2.18 (t, $J = 7.6$ Hz, 2H), 1.76 - 1.09 (m, 24H); ^{13}C NMR (75 MHz, CDCl_3) $\delta = 172.5, 171.8, 135.9, 129.2, 128.5, 127.0, 94.7, 65.5, 52.9, 51.4, 38.0, 36.5, 29.09, 29.07, 29.00, 28.95$ (2C), 28.81, 28.77, 28.6, 28.4 (2C), 26.6, 25.7, 25.5, 20.8 ppm; HRMS (ESI) m/z calculated for $\text{C}_{28}\text{H}_{41}\text{I}\text{N}_4\text{NaO}_3$ $[\text{M}+\text{Na}]^+$, 631.2116; found: 631.2110.

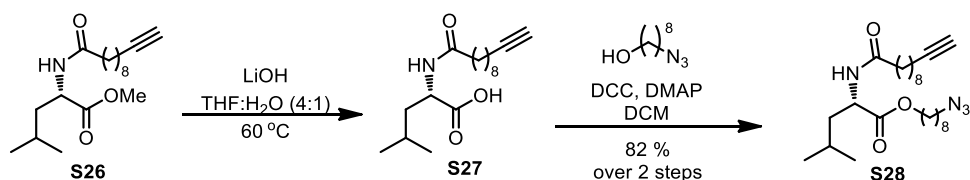


(S)-azido-octan-2-(7-iodohept-6-ynamido)-3-phenylpropanoate (S24): To a stirred solution of the (S)-azido-octan-2-(hept-6-ynamido)-3-phenylpropanoate (31 mg, 0.073 mmol) in acetone (2 mL) was added N-iodosuccinimide (18 mg, 0.08 mmol) followed by silver nitrate (1.2 mg, 0.0073 mmol). The solution was stirred in the dark for 17 h. The crude mixture was reduced *in vacuo* and purified on silica-gel (20 to 50 % ethyl acetate in hexanes) to afford the desired product as a colorless oil (33 mg, 81 %). ¹H NMR (300 MHz, CDCl₃) δ = 7.28 - 7.12 (m, 3H), 7.07 - 6.96 (m, 2H), 5.79 (d, *J* = 7.9 Hz, 1H), 4.87 - 4.75 (m, 1H), 4.16 - 3.95 (m, 2H), 3.19 (t, *J* = 6.9, 2H), 3.05 (t, *J* = 6.9 Hz, 2H), 2.29 (t, *J* = 7.0 Hz, 2H), 2.12 (t, *J* = 7.5 Hz, 2H), 1.65 - 1.40 (m, 8H), 1.35 - 1.16 (m, 8H); ¹³C NMR (75 MHz, CDCl₃) δ = 172.0, 171.8, 135.9, 129.3, 128.6, 127.1, 94.0, 65.6, 52.9, 51.5, 38.0, 35.9, 29.2 (2C), 29.1, 29.0, 28.8, 27.8, 26.6, 25.7, 25.6, 20.6 ppm; HRMS (ESI) *m/z* calculated for C₂₄H₃₄IN₄O₃ [M+H]⁺, 553.1670; found: 553.1669.



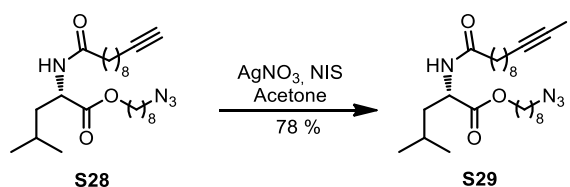
(S)-methyl 2-(undec-10-ynamido)-4-methylpentanoate (S26): Following the General Procedure A, L-isoleucine methyl ester hydrochloride (800 mg, 4.8 mmol), 10-undecynoic acid (726 mg, 3.98 mmol), DCC (1.64 g, 8.0 mmol) and DMAP (1.46 g, 12.0 mmol) in anhydrous DCM (20 mL) were added to the reaction flask. The reaction was stirred for 17 h. Upon complete conversion of the starting material, the crude reaction mixture was placed in a

freezer for 5 h to induce the precipitation of the urea, which was subsequently removed by filtration. The filtrate was concentrated *in vacuo* to provide the crude reaction mixture, which was purified by column chromatography on silica-gel (30 % ethyl acetate in hexanes). The desired product was obtained as a white solid (1.24 g, 83 %). ¹H NMR (400 MHz, CDCl₃) δ = 6.63 (d, *J* = 8.2 Hz, 1H), 5.16 (m, 1H), 4.52 - 4.32 (m, 1H), 3.95 – 3.89 (m, 1H), 3.52 (s, 3H), 2.04 (t, *J* = 7.6 Hz, 2H), 1.96 (t, *J* = 7.5 Hz, 2H), 1.84 (s, 1H), 1.78 (s, 1H), 1.56 - 1.26 (m, 6H), 1.19 – 1.06 (m, 6H), 0.74 (d, *J* = 6.4 Hz, 6H); ¹³C NMR (100 MHz, CDCl₃) δ = 173.2, 172.7, 84.0, 67.9, 51.5, 50.1, 40.7, 35.7, 28.7, 28.5, 28.2, 28.0, 25.2, 24.3, 22.4, 21.3, 17.8 ppm; HRMS (ESI) *m/z* calculated for C₁₈H₃₂NO₃ [M+H]⁺, 310.2377; found: 310.2376.



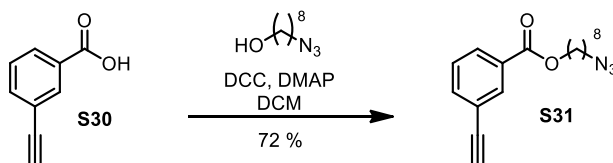
(S)-methyl 2-(undec-10-ynamido)-4-methylpentanoic acid (S27): To a solution of (S)-methyl 2-(undec-10-ynamido)-4-methylpentanoate (1.24 g, 3.74 mmol) in THF:H₂O (4:1, 16 mL and 4 mL) was added LiOH (449 mg, 18.7 mmol). The mixture was stirred at 60 °C for 2 h and then cooled to ambient temperature. EtOAc and HCl 1N were added to the mixture and the aqueous and organic phases were separated. The aqueous phase was extracted (2x) with EtOAc. The organic phases were combined, dried with Na₂SO₄, filtered and concentrated *in vacuo*. The crude solid was directly used in the following reaction. **(S)-azido-octan-2-(undec-10-ynamido)-4-methylpentanoate (S28):** Following the General Procedure A, 8-azido-octan-1-ol (500 mg, 2.9 mmol), (S)-methyl 2-(undec-10-ynamido)-4-methylpentanoic acid (929 mg, 2.9 mmol), DCC (1.2 g, 5.8 mmol) and DMAP (1.1 mg, 8.8 mmol) in anhydrous DCM (15 mL) were added to the reaction flask. Upon complete conversion of the starting material,

the crude reaction mixture was placed in a freezer for 5 h to induce the precipitation of the urea, which was subsequently removed by filtration. The filtrate was concentrated *in vacuo* to provide the crude reaction mixture, which was purified by column chromatography on silica-gel (20 to 50 % ethyl acetate in hexanes). The desired product was obtained as a white solid (720 mg, 55 % over 2 steps). ¹H NMR (400 MHz, CDCl₃) δ = 5.84 (d, *J* = 8.4 Hz, 1 H), 4.69 - 4.56 (m, 1 H), 4.11 (t, *J* = 6.8 Hz, 2 H), 3.26 (t, *J* = 7.0 Hz, 2 H), 2.26 - 2.11 (m, 4 H), 1.96 - 1.91 (m, 1 H), 1.75 - 1.45 (m, 10 H), 1.42 - 1.24 (m, 17 H), 0.94 (d, *J* = 6.1 Hz, 6 H); ¹³C NMR (100 MHz, CDCl₃) δ = 173.3, 172.7, 84.7, 68.1, 65.3, 51.4, 50.6, 41.9, 36.5, 29.13, 29.11, 29.0, 28.9, 28.8, 28.6, 28.42, 28.39, 26.6, 25.7, 25.5, 24.9, 22.8, 22.1, 18.3 ppm; HRMS (ESI) *m/z* calculated for C₂₅H₄₅N₄O₃ [M+H]⁺, 449.3486; found: 449.3507.

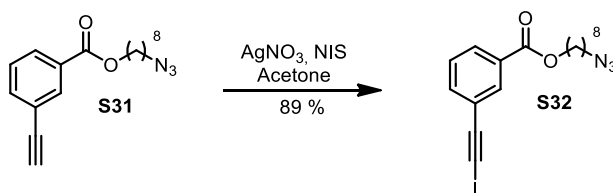


(S)-azido-octan-2-(11-iodoundec-10-ynamido)-4-methylpentanoate (S29): To a stirred solution of the (S)-azido-octan-2-(undec-10-ynamido)-4-methylpentanoate (164 mg, 0.35 mmol) in acetone (2 mL) was added N-iodosuccinimide (87 mg, 0.39 mmol) followed by silver nitrate (6 mg, 0.04 mmol). The solution was stirred in the dark for 17 h. The crude mixture was reduced *in vacuo* and purified on silica-gel (20 to 50 % ethyl acetate in hexanes) to afford the desired product as a yellow solid (156 mg, 78 %). ¹H NMR (300 MHz, CDCl₃) δ = 5.82 (d, *J* = 8.4 Hz, 1H), 4.64 (dt, *J* = 8.5, 5.2 Hz, 1H), 4.11 (t, *J* = 6.7 Hz, 2H), 3.26 (t, *J* = 6.9 Hz, 2H), 2.35 (t, *J* = 7.0 Hz, 2H), 2.26 - 2.15 (m, 2H), 1.76 - 1.43 (m, 10H), 1.35 - 1.27 (m, 17H), 0.95 (d, *J* = 6.1, 6H); ¹³C NMR (75 MHz, CDCl₃) δ = 173.3, 172.7, 94.7, 65.3, 51.4, 50.6, 41.9, 36.5, 31.6, 29.1, 29.0, 28.84, 28.77, 28.6, 28.4, 28.4, 26.6, 25.7, 25.5, 24.9, 22.8,

22.1, 20.8, 14.1; HRMS (ESI) m/z calculated for $C_{25}H_{44}IN_4O_3$ $[M+H]^+$, 575.2453; found: 575.2459.

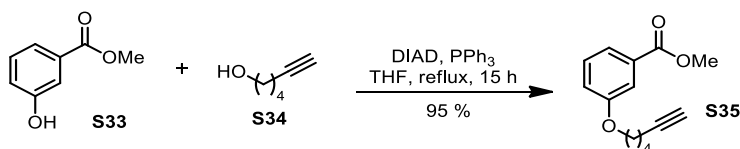


azidooctan 3-ethynylbenzoate (S31): Following the General Procedure A, 8-azidooctan-1-ol (250 mg, 1.47 mmol), 3-ethynylbenzoic acid (258 mg, 1.76 mmol), DCC (606 mg, 2.94 mmol) and DMAP (538 mg, 4.41 mmol) in anhydrous DCM (8 mL) were added to the reaction flask. Upon complete conversion of the starting material, the crude reaction mixture was placed in a freezer for 5 h to induce the precipitation of the urea, which was subsequently removed by filtration. The filtrate was concentrated *in vacuo* to provide the crude reaction mixture, which was purified by column chromatography on silica-gel (15 % ethyl acetate in hexanes). The desired product was obtained as a colorless oil (318 mg, 72 %). ¹H NMR (300 MHz, CDCl₃) δ = 8.16 - 8.10 (m, 1 H), 7.99 (td, J = 7.9, 1.4 Hz, 1 H), 7.63 (td, J = 7.8, 1.2 Hz, 1 H), 7.38 (t, J = 7.8 Hz, 1 H), 4.29 (t, J = 6.7 Hz, 2 H), 3.22 (t, J = 7.0 Hz, 2 H), 3.13 (s, 1 H), 1.81 - 1.68 (m, 2 H), 1.63 - 1.50 (m, 2 H), 1.48 - 1.27 (m, 8 H); ¹³C NMR (75 MHz, CDCl₃) δ = 165.5, 136.0, 133.0, 130.6, 129.6, 128.3, 122.4, 82.4, 78.1, 65.1, 51.2, 29.0, 28.8, 28.6, 28.4, 26.5, 25.7 ppm; HRMS (ESI) m/z calculated for $C_{17}H_{22}N_3O_2$ $[M+H]^+$, 300.1707; found: 300.1711.



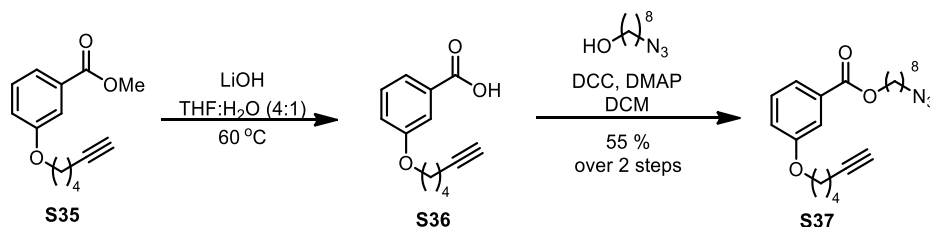
azidooctan 3-(iodoethynyl)benzoate (S32): To a stirred solution of the azidooctan 3-ethynylbenzoate (318 mg, 1.1 mmol) in acetone (6 mL) was added N-iodosuccinimide (263

mg, 1.2 mmol) followed by silver nitrate (18 mg, 0.11 mmol). The solution was stirred in the dark for 17 h. The crude mixture was reduced *in vacuo* and purified on silica-gel (10 % ethyl acetate in hexanes) to afford the desired product. The desired product was obtained as a colorless oil (305 mg, 89 %). ¹H NMR (300 MHz, CDCl₃) δ = 8.07 (t, *J* = 1.7 Hz, 1H), 7.97 (dt, *J* = 7.9, 1.5 Hz, 1H), 7.58 (dt, *J* = 7.7, 1.5 Hz, 1H), 7.38 (t, *J* = 7.8 Hz, 1H), 4.29 (t, *J* = 6.7 Hz, 2H), 3.24 (t, *J* = 6.9 Hz, 2H), 1.84 - 1.67 (m, 2H), 1.61 - 1.54 (m, 2H), 1.51 - 1.29 (m, 8H); ¹³C NMR (75 MHz, CDCl₃) δ = 165.5, 136.2, 133.2, 130.5, 129.6, 128.2, 123.6, 93.0, 65.2, 51.3, 29.0, 28.9, 28.7, 28.5, 26.5, 25.8, 8.2 ppm; HRMS (ESI) *m/z* calculated for C₁₇H₂₀IN₃NaO₂ [M+Na]⁺, 448.0492; found: 448.0490.



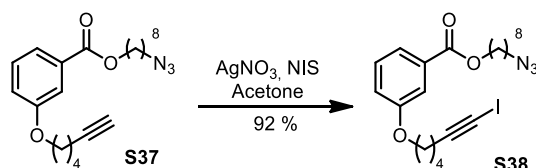
methyl 3-(hex-5-yn-1-yloxy)benzoate (S35): To a stirred solution of methyl-3-hydroxybenzoate (1.0 g, 6.6 mmol) in anhydrous THF (33 mL) was added triphenylphosphine (3.0 g, 12 mmol), 5-hexyn-1-ol (1.3 g, 12 mmol) and di-isopropyl azodicarboxylate (2.3 mL, 12 mmol) in that order under a N₂ atmosphere. The reaction mixture was heated at reflux for 15 hours. The reaction was concentrated *in vacuo* to provide a crude reaction mixture which was purified by column chromatography on silica-gel (100 % hexanes to 10 % ethyl acetates in hexanes) to afford the desired product as a colorless oil (1.8 g, 95 %). ¹H NMR (400 MHz, CDCl₃) δ = 7.62 (dd, *J* = 7.5, 1.5 Hz, 1H), 7.57 - 7.52 (m, 1H), 7.32 (t, *J* = 8.0 Hz, 1H), 7.12 - 7.05 (m, 1H), 4.02 (t, *J* = 6.2 Hz, 2H), 3.90 (d, *J* = 2.6 Hz, 3H), 2.28 (td, *J* = 7.0, 2.7 Hz, 2H), 1.98 (t, *J* = 2.7 Hz, 1H), 1.96 - 1.85 (m, 2H), 1.76 - 1.69 (m, 2H); ¹³C NMR (100 MHz,

CDCl₃) d = 166.8, 158.9, 131.3, 129.3, 121.8, 119.8, 114.5, 83.9, 68.7, 67.4, 52.1, 28.1, 24.9, 18.1 ppm; HRMS (ESI) m/z calculated for C₁₄H₁₇O₃ [M+H]⁺, 233.1172; found: 233.1161.

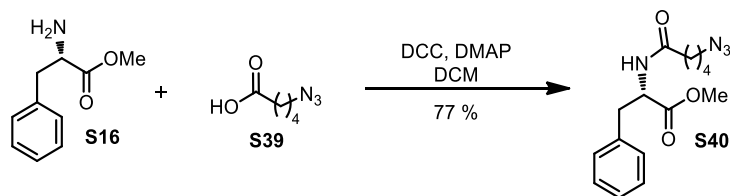


methyl 3-(hex-5-yn-1-yloxy)benzoic acid (S36): To a solution of methyl 3-(hex-5-yn-1-yloxy)benzoate (1.8 g, 7.6 mmol) in THF:H₂O (4:1, 31 mL and 8 mL) was added LiOH (914 mg, 38 mmol). The mixture was stirred at 60 °C for 2 h and then cooled to ambient temperature. EtOAc and HCl 1 N were added to the mixture and the aqueous and organic phases were separated. The aqueous phase was extracted (2x) with EtOAc. The organic phases were combined, dried with Na₂SO₄, filtered and concentrated *in vacuo*. The crude solid was directly used in the following reaction. **azidooctyl 3-(hex-5-yn-1-yloxy)benzoate (S37):** Following the General Procedure A, 8-azidooctan-1-ol (250 mg, 1.5 mmol), methyl 3-(hex-5-yn-1-yloxy)benzoic acid (391 mg, 1.8 mmol), DCC (606 mg, 2.9 mmol) and DMAP (538 mg, 4.4 mmol) in anhydrous DCM (8 mL) were added to the reaction flask. Upon complete conversion of the starting material, the crude reaction mixture was placed in a freezer for 5 h to induce the precipitation of the urea, which was subsequently removed by filtration. The filtrate was concentrated *in vacuo* to provide the crude reaction mixture, which was purified by column chromatography on silica-gel (20 % ethyl acetate in hexanes). The desired product was obtained as a colorless oil (305 mg, 55 % over 2 steps). ¹H NMR (300 MHz, CDCl₃) d = 7.61 (d, *J* = 7.7 Hz, 1 H), 7.54 (s, 1 H), 7.32 (t, *J* = 7.9 Hz, 1 H), 7.12 - 7.03 (m, 1 H), 4.29 (t, *J* = 6.7 Hz, 2 H), 4.02 (t, *J* = 6.2 Hz, 2 H), 3.24 (t, *J* = 7.0 Hz, 2 H), 2.27 (td, *J* = 7.0, 2.6, 2 H),

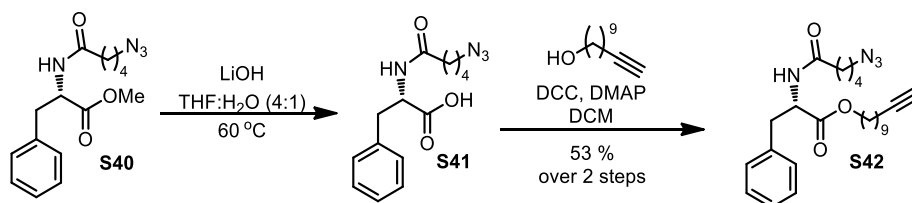
2.01 - 1.96 (m, 1 H), 1.96 - 1.86 (m, 2 H), 1.77 - 1.70 (m, 4 H), 1.65 - 1.52 (m, 2 H), 1.50 - 1.20 (m, 8 H); ^{13}C NMR (75 MHz, CDCl_3) δ = 165.4, 158.8, 131.6, 129.2, 121.7, 119.4, 114.7, 83.8, 68.6, 67.3, 65.0, 51.3, 29.0, 28.9, 28.7, 28.5, 28.1, 26.5, 25.8, 24.9, 18.0 ppm; HRMS (ESI) m/z calculated for $\text{C}_{21}\text{H}_{30}\text{N}_3\text{O}_3$ $[\text{M}+\text{H}]^+$, 372.2282; found: 372.2283.



azidoethyl 3-(6-iodohex-5-yn-1-yloxy)benzoate (S38): To a stirred solution of the azidoethyl 3-(hex-5-yn-1-yloxy)benzoate (305 mg, 0.8 mmol) in acetone (4 mL) was added N-iodosuccinimide (200 mg, 0.9 mmol) followed by silver nitrate (14 mg, 0.08 mmol). The solution was stirred in the dark for 17 h. The crude mixture was reduced *in vacuo* and purified on silica-gel (20 % ethyl acetate in hexanes) to afford the desired product as a colorless oil (371 mg, 92 %). ^1H NMR (300 MHz, CDCl_3) δ = 7.59 (dt, J = 7.7, 1.2 Hz, 1H), 7.52 (dd, J = 2.7, 1.5 Hz, 1H), 7.30 (t, J = 7.9 Hz, 1H), 7.05 (ddd, J = 8.2, 2.7, 1.0 Hz, 1H), 4.28 (t, J = 6.6 Hz, 2H), 3.99 (t, J = 6.2 Hz, 2H), 3.22 (t, J = 6.9 Hz, 2H), 2.43 (t, J = 7.0 Hz, 2H), 1.88 (m, 2H), 1.80 - 1.50 (m, 6H), 1.37 (m, 8H); ^{13}C NMR (75 MHz, CDCl_3) δ = 166.2, 158.7, 131.5, 129.2, 121.6, 119.4, 114.6, 93.9, 67.2, 64.9, 51.2, 28.9, 28.9, 28.8, 28.6, 28.5, 28.1, 26.4, 25.7, 24.9, 20.4 ppm; HRMS (ESI) m/z calculated for $\text{C}_{21}\text{H}_{28}\text{I}\text{N}_3\text{NaO}_3$ $[\text{M}+\text{Na}]^+$, 520.1068; found: 520.1064.

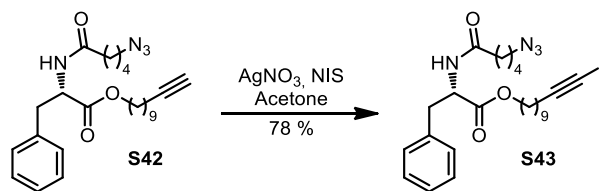


(S)-methyl 2-(5-azidopentamido)-3-phenylpropanoate (S40): Following the General Procedure A, L-Phenylalanine methyl ester hydrochloride (1 g, 5.6 mmol), 5-azidopentanoic acid (798 mg, 5.6 mmol), DCC (2.3 g, 11.2 mmol) and DMAP (2.0 mg, 16.7 mmol) in anhydrous DCM (30 mL) were added to the reaction flask. The reaction was stirred for 17 h. Upon complete conversion of the starting material, the crude reaction mixture was placed in a freezer for 5 h to induce the precipitation of the urea, which was subsequently removed by filtration. The filtrate was concentrated *in vacuo* to provide the crude reaction mixture, which was purified by column chromatography on silica-gel (30 % ethyl acetate in hexanes). The desired product was obtained as a white solid (1.3 g, 77 %). ¹H NMR (400 MHz, CDCl₃) δ = 7.36 - 7.16 (m, 3 H), 7.16 - 7.03 (m, 2 H), 6.46 (d, *J* = 7.9 Hz, 1 H), 4.96 - 4.74 (m, 1 H), 3.70 (s, 3 H), 3.21 (t, *J* = 6.7 Hz, 2 H), 3.18 - 2.97 (m, 2 H), 2.94 - 2.80 (m, 1 H), 2.23 - 2.13 (m, 2 H), 1.70 - 1.57 (m, 2 H), 1.57 - 1.45 (m, 2 H); ¹³C NMR (100 MHz, CDCl₃) δ = 171.94, 171.86, 135.8, 128.9, 128.2, 129.7, 52.7, 52.0, 50.7, 37.5, 35.1, 27.8, 22.3 ppm; HRMS (ESI) *m/z* calculated for C₁₅H₂₁N₄O₃ [M+H]⁺, 305.1608; found: 305.1598.



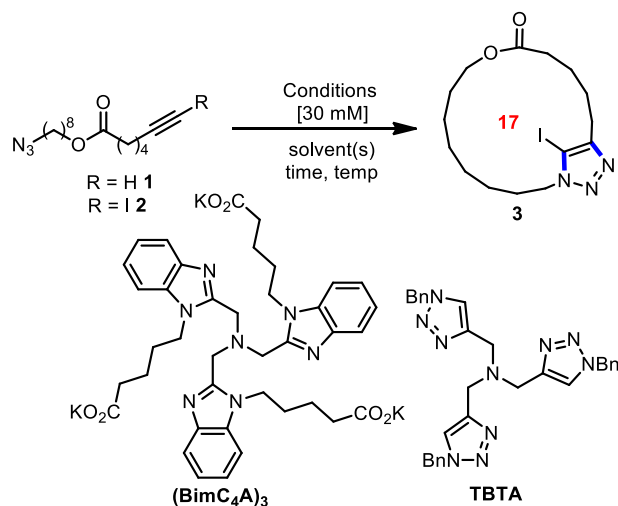
(S)-methyl 2-(5-azidopentamido)-3-phenylpropanoic acid (S41): To a solution of (S)-methyl 2-(5-azidopentamido)-3-phenylpropanoate (4.0 g, 13 mmol) in THF:H₂O (4:1, 53 mL

and 13 mL) was added LiOH (1.6 g, 65 mmol). The mixture was stirred at 60 °C for 2 h and then cooled to ambient temperature. EtOAc and HCl 1 N were added to the mixture and the aqueous and organic phases were separated. The aqueous phase was extracted (2x) with EtOAc. The organic phases were combined, dried with Na₂SO₄, filtered and concentrated *in vacuo*. A fraction of the crude solid was directly used in the following reaction. **(S)-undec-11-yn-1-yl 2-(5-azidopentamido)-3-phenylpropanoate (S42)**: Following the General Procedure A, 10-undecyn-1-ol (370 mg, 2.2 mmol), (S)-methyl 2-(5-azidopentamido)-3-phenylpropanoic acid (638 mg, 2.2 mmol), DCC (906 mg, 4.4 mmol) and DMAP (805 mg, 6.6 mmol) in anhydrous DCM (11 mL) were added to the reaction flask. Upon complete conversion of the starting material, the crude reaction mixture was placed in a freezer for 5 h to induce the precipitation of the urea, which was subsequently removed by filtration. The filtrate was concentrated *in vacuo* to provide the crude reaction mixture, which was purified by column chromatography on silica-gel (20 to 50 % ethyl acetate in hexanes). The desired product was obtained as a white solid (813 mg, 53 % over 2 steps). ¹H NMR (400 MHz, CDCl₃) δ = 7.35 - 7.21 (m, 3H), 7.14 - 7.07 (m, 2H), 5.89 (d, *J* = 7.9 Hz, 1H), 4.89 (dt, *J* = 7.9, 6.0 Hz, 1H), 4.10 (tt, *J* = 10.7, 5.3 Hz, 2H), 3.27 (t, *J* = 6.7 Hz, 2H), 3.13 (dd, *J* = 13.6, 5.9 Hz, 2H), 2.27 - 2.12 (m, 4H), 1.97 - 1.94 (m, 1H), 1.75 - 1.48 (m, 8H), 1.31 (d, *J* = 6.1 Hz, 10H); ¹³C NMR (100 MHz, CDCl₃) δ = 171.8, 171.7, 135.9, 129.2, 128.5, 127.1, 84.7, 68.1, 65.7, 52.9, 51.1, 38.0, 35.7, 29.4, 29.3, 29.1, 29.0, 28.7, 28.4, 28.2, 25.8, 22.6, 18.4 ppm. HRMS (ESI) *m/z* calculated for C₂₅H₃₇N₄O₃ [M+H]⁺, 441.2860; found: 441.2840.



(S)-10-iodoundec-11-yn-1-yl 2-(5-azidopentamido)-3-phenylpropanoate (S43): To a stirred solution of the (*S*)-undec-11-yn-1-yl 2-(5-azidopentamido)-3-phenylpropanoate (813 mg, 1.9 mmol) in acetone (10 mL) was added N-iodosuccinimide (457 mg, 2.0 mmol) followed by silver nitrate (31 mg, 0.2 mmol). The solution was stirred in the dark for 17 h. The crude mixture was reduced *in vacuo* and purified on silica-gel (20 to 50 % ethyl acetate in hexanes) to afford the desired product as a yellow solid (817 mg, 78 %). ¹H NMR (400 MHz, CDCl₃) δ = 7.35 - 7.20 (m, 3H), 7.13 - 7.06 (m, 2H), 6.15 - 6.02 (m, 1H), 4.93 - 4.80 (m, 1H), 4.08 (td, *J* = 6.7, 3.7 Hz, 2H), 3.24 (t, *J* = 6.7 Hz, 2H), 3.18 - 3.00 (m, 2H), 2.33 (td, *J* = 7.1, 2.1 Hz, 2H), 2.19 (t, *J* = 7.6 Hz, 2H), 1.72 - 1.43 (m, 8H), 1.64 - 1.28 (m, 10H); ¹³C NMR (100 MHz, CDCl₃) δ = 171.72, 171.66, 135.8, 129.1, 128.4, 126.9, 94.6, 65.5, 62.7, 52.8, 50.9, 37.9, 35.5, 29.2, 29.1, 28.9, 28.8, 28.5, 28.3, 28.1, 25.6, 22.5, 20.6 ppm; HRMS (ESI) *m/z* calculated for C₂₅H₃₅N₄IO₃ [M+H]⁺ 567.1827; found: 567.1831.

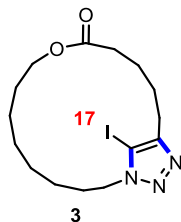
Table S1. Full Optimization of Macrocylic CuAiAC using a Phase Separation Strategy.



entry	conditions		
	solvent	yield 3 (%) ^a	recovered 2 (%) ^a
CuSO ₄ ·5H ₂ O (10 mol %), (BimC ₄ A) ₃ (20 mol %), NaAsc (4.5 eq.) 21°C, 17 h			
1	PEG ₄₀₀ :MeOH 1:1	-	-
CuSO ₄ ·5H ₂ O (10 mol %), TBTA (20 mol %), NaAsc (4.5 eq.) 21°C, 17 h			
2	PEG ₄₀₀ :MeOH 1:1	-	-
CuI (5 mol %), NEt ₃ (2 eq.), 60°C, 17 h			
3	MeOH	23	poly
4	PEG ₄₀₀	-	99 ^b
5	PEG ₄₀₀ :MeOH 1:9	29	-
6	PEG ₄₀₀ :MeOH 1:2	60	-
7	PEG ₄₀₀ :MeOH 1:1	93	-
8	PEG ₄₀₀ :MeOH 2:1	97	-
9	PEG ₄₀₀ :MeOH 4:1	40	- ^b
10	PEG ₄₀₀ :MeOH 9:1	-	99 ^b

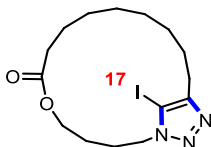
^a Yields following chromatography. ^b Product recovered was azide-alkyne **1**. No iodinated uncyclized products were observed.

SYNTHESIS OF MACROCYCLES



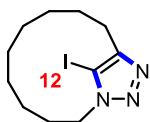
General procedure B for the click macrocyzation using phase separation conditions:

macrocycle (3): To a sealed tube equipped with a stirring bar was added the precursor (49 mg, 0.12 mmol, 1 equiv), polyethylene glycol 400 (3.33 mL) and methanol (1.67 mL). The mixture was stirred 30 seconds to mix the two solvents. Triethylamine (0.13 mL, 0.96 mmol, 8 equiv) and CuI (4.6 mg, 0.024 mmol, 20 mol %) were added to the mixture. The tube was closed and heated at 60 °C for 17 h (no precaution was taken to remove air or moisture). The reaction was then cooled back to room temperature and the crude mixture was loaded directly on a silica column. Purification by chromatography (20→50 % ethyl acetate in hexane) afforded the product as a colorless semi-solid (47 mg, 95 %). ¹H NMR (400 MHz, CDCl₃) δ = 4.53-4.39 (m, 2H), 4.07-3.96 (m, 2H), 2.77 (t, *J* = 6.4 Hz, 2H), 2.32-2.20 (m, 2H), 2.00–1.93 (m, 2H), 1.85–1.77 (m, 2H), 1.51–1.43 (m, 4H), 1.28-1.03 (m, 8H); ¹³C NMR (100 MHz, CDCl₃) δ ppm = 173.4, 150.9, 79.0, 64.2, 50.4, 35.4, 29.2, 28.4, 28.3, 27.6, 27.4, 25.1, 24.6, 24.4, 24.1 ppm; HRMS (ESI) *m/z* calculated for C₁₅H₂₄N₃NaO₂ [M+Na]⁺, 428.0805; found: 428.0815.

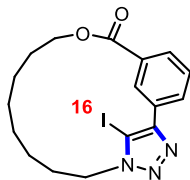


Macrocycle (4): Following the general procedure B described above, macrocycle **4** was isolated as a colorless semi-solid (46 mg, 93 %). ¹H NMR (400 MHz, CDCl₃) δ = 4.49 (t, *J* = 6.2 Hz, 2H), 4.07 (t, *J* = 6.6 Hz, 2H), 2.80 - 2.72 (m, 2H), 2.30 - 2.23 (m, 2H), 2.00 - 1.96 (m,

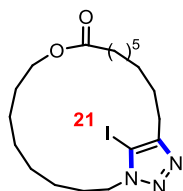
2H), 1.80 - 1.77 (m, 2H), 1.61 - 1.37 (m, 4H), 1.29 - 1.01 (m, 8H); ^{13}C NMR (100 MHz, CDCl_3) δ ppm = 173.5, 151.6, 79.05, 62.9, 49.7, 34.7, 28.6, 28.2, 28.1, 27.7, 26.63, 26.56, 25.8, 25.4, 25.1; HRMS (ESI) m/z calculated for $\text{C}_{15}\text{H}_{24}\text{IN}_3\text{NaO}_2$ $[\text{M}+\text{Na}]^+$, 428.0805; found: 428.0804.



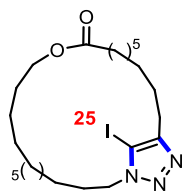
Macrocycle (5b): Following the general procedure B described above, macrocycle **5a** and **5b** were isolated as a 1:1 mixture as a colorless semi-solid (30 mg, 78 %). As a pure sample of **5b** could be obtained by silica gel chromatography. ^1H NMR (700 MHz, CDCl_3) δ = 4.38 (t, J = 6.7 Hz, 2H), 2.67 (t, J = 7.0 Hz, 2H), 1.93 - 1.84 (m, 2H), 1.73 - 1.65 (m, 2H), 1.32 - 1.25 (m, 2H), 1.23 - 1.16 (m, 4H); ^{13}C NMR (175 MHz, CDCl_3) δ ppm = 151.7, 78.6, 50.3, 29.5, 28.71, 28.68, 28.53, 28.49, 28.1, 25.7, 25.4; HRMS (ESI) m/z calculated for $\text{C}_{11}\text{H}_{18}\text{IN}_3\text{Na}$ $[\text{M}+\text{Na}]^+$, 342.0443; found: 342.0439.



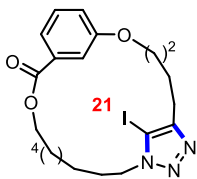
Macrocycle (6): Following the general procedure B described above, macrocycle **6** was isolated. (36 mg, 70 %). ^1H NMR (400 MHz, CDCl_3) δ = 8.21 (t, J = 1.5 Hz, 1H), 8.06 (dd, J = 7.9, 1.5 Hz, 1H), 7.72 (dd, J = 7.7, 1.4 Hz, 1H), 7.45 (t, J = 7.8 Hz, 1H), 4.35 (d, J = 6.6 Hz, 2H), 3.28 (t, J = 6.9 Hz, 2H), 1.88 - 1.73 (m, 2H), 1.64 - 1.59 (m, 2H), 1.51 - 1.32 (m, 6H); ^{13}C NMR (100 MHz, CDCl_3) δ ppm = 165.6, 136.4, 133.6, 131.0, 130.3, 128.7, 122.0, 80.9, 74.4, 65.4, 51.4, 29.1, 29.0, 28.8, 28.62, 26.64, 25.9; HRMS (ESI) m/z calculated for $\text{C}_{17}\text{H}_{21}\text{IN}_3\text{O}_2$ $[\text{M}+\text{H}]^+$, 425.0600; found: 425.0609.



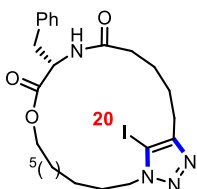
Macrocycle (7): Following the general procedure B described above, macrocycle **7** was isolated. (48 mg, 87 %). ^1H NMR (700 MHz, CDCl_3) δ ppm = 4.41 (t, J = 6.5 Hz, 2 H), 4.09 (t, J = 5.8 Hz, 2 H), 2.69 (t, J = 7.2 Hz, 2 H), 2.29 (t, J = 7.5 Hz, 2 H), 1.93 (m, 2 H), 1.77 - 1.67 (m, 2 H), 1.67 - 1.57 (m, 4 H), 1.37 - 1.16 (m, 16 H); ^{13}C NMR (175 MHz, CDCl_3) δ ppm = 174.0, 151.7, 78.3, 64.3, 50.5, 33.9, 29.5, 28.9 (2C), 28.8, 28.41, 28.38, 28.3, 27.9, 27.5, 26.0, 25.7, 25.4, 24.7; HRMS (ESI) m/z calculated for $\text{C}_{19}\text{H}_{32}\text{IN}_3\text{O}_2$ $[\text{M}+\text{H}]^+$, 461.1539; found: 461.1534



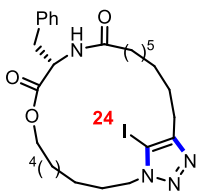
Macrocycle (8): Following the general procedure B described above, macrocycle **8** was isolated. (53 mg, 85 %). ^1H NMR (400 MHz, CDCl_3) δ ppm = 4.41 (t, J = 6.5 Hz, 2 H), 4.12 - 4.05 (m, 2 H), 2.69 (t, J = 7.1 Hz, 2 H), 2.29 (t, J = 7.4 Hz, 2 H), 1.93 (m, 2 H), 1.76 - 1.67 (m, 2 H), 1.67 - 1.54 (m, 4 H), 1.38 - 1.14 (m, 24 H); ^{13}C NMR (125 MHz, CDCl_3) δ ppm = 173.9, 151.7, 78.3, 64.3, 50.5, 31.7, 31.6, 29.7, 29.5, 29.08, 29.05, 29.01, 28.96, 28.9, 28.80, 28.81, 28.6, 28.5, 28.4, 26.0, 25.7, 25.2, 14.1; HRMS (ESI) m/z calculated for $\text{C}_{23}\text{H}_{41}\text{IN}_3\text{O}_2$ $[\text{M}+\text{H}]^+$, 518.2244; found: 518.2251.



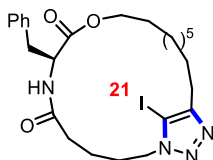
Macrocycle (9): Following the general procedure B described above, macrocycle **9** was isolated. (45 mg, 75 %). ^1H NMR (400 MHz, CDCl_3) δ 7.63 (d, $J = 7.7$ Hz, 1 H), 7.55 (s, 1 H), 7.34 (t, $J = 8.0$ Hz, 1 H), 7.09 (dd, $J = 2.6, 8.2$ Hz, 1 H), 4.32 (t, $J = 6.7$ Hz, 2 H), 4.03 (t, $J = 6.1$ Hz, 2 H), 3.27 (t, $J = 7.0$ Hz, 2 H), 2.36 (t, $J = 6.9$ Hz, 2 H), 1.97 - 1.88 (m, 2 H), 1.76 (m, 4 H), 1.66 - 1.58 (m, 2 H), 1.49 - 1.33 (m, 8 H); ^{13}C NMR (100 MHz, CDCl_3) δ ppm = 166.3, 158.6, 147.9, 131.8, 129.6, 122.1, 121.0, 118.3, 116.9, 68.0, 65.2, 50.3, 29.9, 28.94, 28.85, 28.6, 27.5, 26.3, 26.0, 25.6, 24.8 ppm; HRMS (ESI) m/z calculated for $\text{C}_{21}\text{H}_{28}\text{IN}_3\text{NaO}_3$ $[\text{M}+\text{Na}]^+$, 520.1068; found: 520.1073.



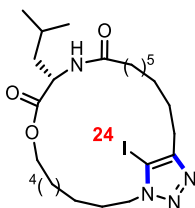
Macrocycle (10): Following the general procedure B described above, macrocycle **10** was isolated. (62 mg, 91 %). ^1H NMR (400 MHz, CDCl_3) δ = 7.35 - 7.26 (m, 3 H), 7.22 - 7.15 (m, 2 H), 6.24 (d, $J = 7.9$ Hz, 1 H), 4.90 - 4.76 (m, 1 H), 4.57 - 4.29 (m, 2 H), 4.22 - 3.97 (m, 2 H), 3.16 (m, 2 H), 2.82 - 2.63 (m, 2 H), 2.20 (t, $J = 7.4$ Hz, 2 H), 1.94 (d, $J = 7.0$ Hz, 2 H), 1.85 - 0.96 (m, 14 H); ^{13}C NMR (100 MHz, CDCl_3) δ ppm = 172.5, 171.3, 151.2, 136.5, 129.3, 128.6, 127.0, 78.4, 65.1, 53.6, 50.6, 37.6, 36.1, 29.0, 28.6, 28.5, 28.2, 27.6, 25.3, 25.08, 25.05, 24.5; HRMS (ESI) m/z calculated for $\text{C}_{24}\text{H}_{33}\text{IN}_4\text{NaO}_3$ $[\text{M}+\text{Na}]^+$, 575.1490; found: 575.1491.



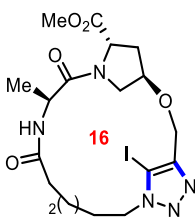
Macrocycle (11): Following the general procedure B described above, macrocycle **11** was isolated. (61 mg, 83 %). ^1H NMR (400 MHz, CDCl_3) δ = 7.30 – 7.25 (m, 3H), 7.15 – 7.13 (m, 2H), 5.77 (d, J = 8.1 Hz, 1 H), 4.86 (td, J = 6.2, 8.3 Hz, 1 H), 4.44 - 4.26 (m, 2 H), 4.17 - 3.98 (m, 2 H), 3.12 – 3.11 (m, 2 H), 2.80 - 2.68 (m, 2 H), 2.27 - 2.07 (m, 2 H), 1.94 - 1.81 (m, 2 H), 1.75 - 1.46 (m, 8 H), 1.41 - 1.14 (m, 14 H); ^{13}C NMR (175 MHz, CDCl_3) δ ppm = 172.8, 172.4, 148.1, 136.1, 129.3, 128.6, 127.1, 120.8, 65.1, 53.2, 49.9, 37.7, 36.4, 29.9, 28.8, 28.7, 28.51, 28.49, 28.4, 28.3, 28.2, 27.9, 25.9, 25.5, 25.2, 25.1 ppm; HRMS (ESI) m/z calculated for $\text{C}_{28}\text{H}_{42}\text{IN}_4\text{O}_3$ $[\text{M}+\text{H}]^+$, 609.2296; found: 609.2303.



Macrocycle (12): Following the general procedure B described above, macrocycle **12** was isolated. (57 mg, 84 %). ^1H NMR (400 MHz, CDCl_3) δ = 7.36 - 7.28 (m, 3 H), 7.18 - 7.12 (m, 2 H), 5.79 (d, J = 7.7 Hz, 1 H), 4.85 - 4.75 (m, 1 H), 4.39 – 4.35 (m, 2 H), 4.24 (td, J = 6.9, 10.8 Hz, 2 H), 3.97 (td, J = 6.4, 10.7 Hz, 2 H), 3.16 - 3.03 (m, 2 H), 2.73 - 2.63 (m, 2 H), 2.25 - 2.11 (m, 2 H), 1.97 - 1.88 (m, 2 H), 1.73 - 1.52 (m, 6 H), 1.42 - 1.07 (m, 8H); ^{13}C NMR (100 MHz, CDCl_3) δ ppm = 171.7, 171.5, 151.7, 136.0, 129.2, 128.6, 127.1, 78.7, 65.0, 53.3, 50.0, 37.6, 35.5, 29.2, 27.9, 27.8, 27.7, 27.19, 27.17, 25.3, 24.6, 22.1 ppm; HRMS (ESI) m/z calculated for $\text{C}_{24}\text{H}_{36}\text{IN}_4\text{O}_3$ $[\text{M}+\text{H}]^+$, 567.1827; found: 567.1833.

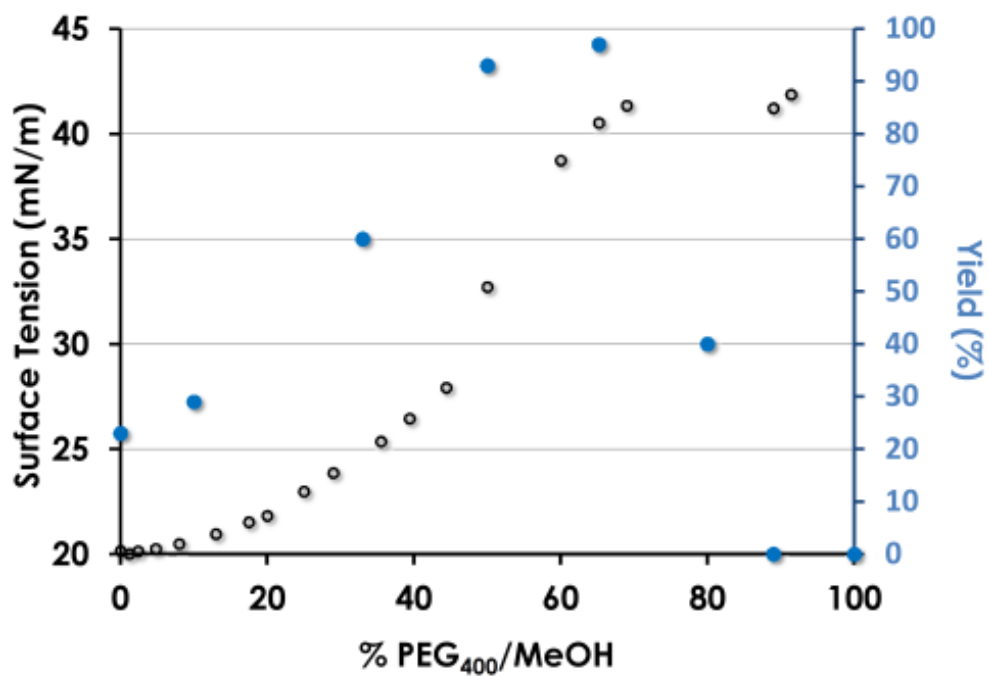
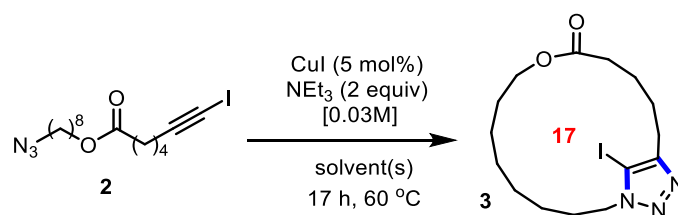


Macrocycle (13): Following the general procedure B described above, macrocycle **13** was isolated. (59 mg, 86 %). ^1H NMR (400 MHz, CDCl_3) δ = 5.80 (d, J = 8.5 Hz, 1H), 4.62–4.56 (m, 1H), 4.43–4.38 (m, 2H), 4.15–4.05 (m, 2H), 2.77–2.65 (m, 2H), 2.27–2.11 (m, 2H), 1.94–1.87 (m, 2H), 1.74–1.51 (m, 10H), 1.34–1.21 (m, 15H), 0.94 (d, J = 5.6 Hz, 6H); ^{13}C NMR (100 MHz, CDCl_3) δ ppm = 173.1, 172.7, 151.8, 78.7, 77.2, 64.9, 51.0, 50.3, 41.3, 36.4, 29.5, 28.7, 28.47, 28.46, 28.4, 28.3, 27.6, 25.7, 25.5, 25.24, 25.21, 24.9, 22.9, 21.8 ppm; HRMS (ESI) m/z calculated for $\text{C}_{25}\text{H}_{43}\text{N}_4\text{O}_3$ $[\text{M}+\text{H}]^+$, 575.2453; found: 575.2467.



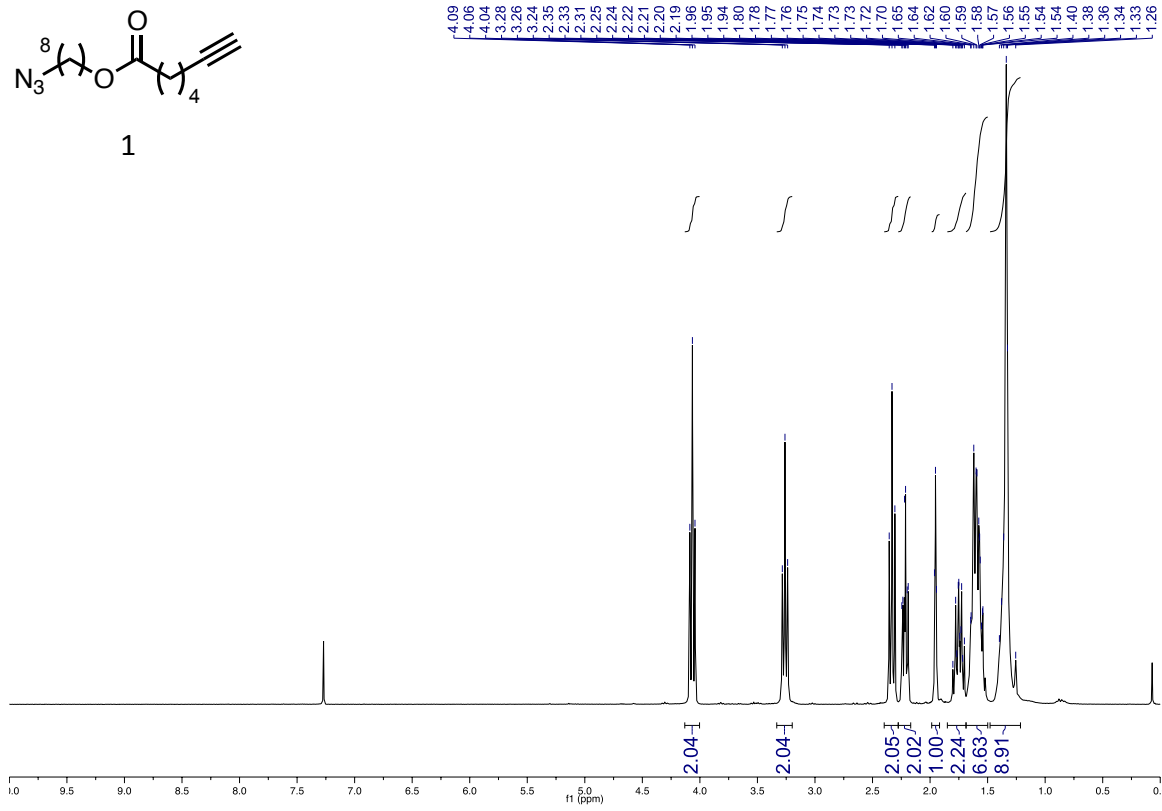
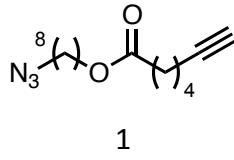
Macrocycle (14): Following the general procedure B described above, macrocycle **14** was isolated. (52 mg, 83 %). ^1H NMR (400 MHz, CDCl_3) δ = 6.69 (d, J = 7.2 Hz, 1 H), 5.18 - 5.14 (m, 1 H), 4.74 - 4.65 (m, 3 H), 4.58 (s, 1 H), 4.37 (m, 2 H), 4.20 (s, 1 H), 3.97 (d, J = 11.0 Hz, 1 H), 3.74 (s, 3 H), 3.71 (dd, J = 11.3, 3.7 Hz, 1 H), 3.28 (s, 1 H), 2.46 - 2.34 (m, 1 H), 2.26 - 2.10 (m, 2 H), 2.03 (m, 1 H), 1.90 (m, 2 H), 1.60 (dt, J = 4.3, 7.3 Hz, 1 H), 1.34 (d, J = 6.9 Hz, 3 H), 1.32 - 1.25 (m, 1 H); ^{13}C NMR (100 MHz, CDCl_3) δ ppm = 172.5, 172.4, 171.8, 129.0, 128.2, 77.2, 70.5, 57.8, 56.3, 55.4, 52.3, 50.4, 46.7, 37.7, 35.8, 28.9, 25.2, 24.0 ppm; HRMS (ESI) m/z calculated for $\text{C}_{18}\text{H}_{27}\text{N}_5\text{O}_5$ $[\text{M}+\text{H}]^+$, 520.1051; found: 520.1012.

FIGURE S1. THE EFFECTS OF AGGREGATION OF PEG₄₀₀:MeOH MIXTURES ON A CuAiac MACROCYCLIZATION.

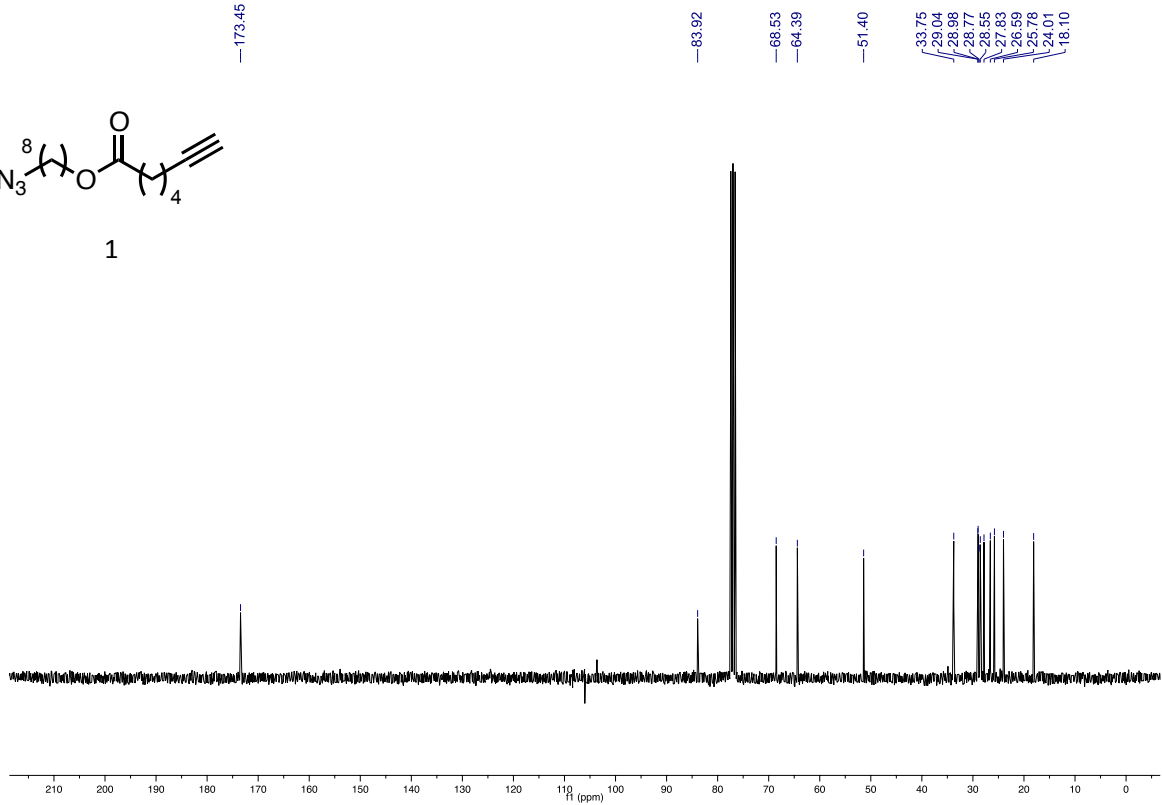
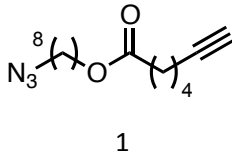


Surface tension measurements (black) observed at 60 °C. Yields (blue) of **3** are following purification by flash chromatography.

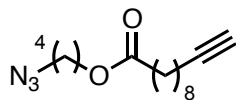
NMR DATA FOR ALL NEW COMPOUNDS



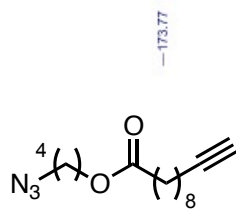
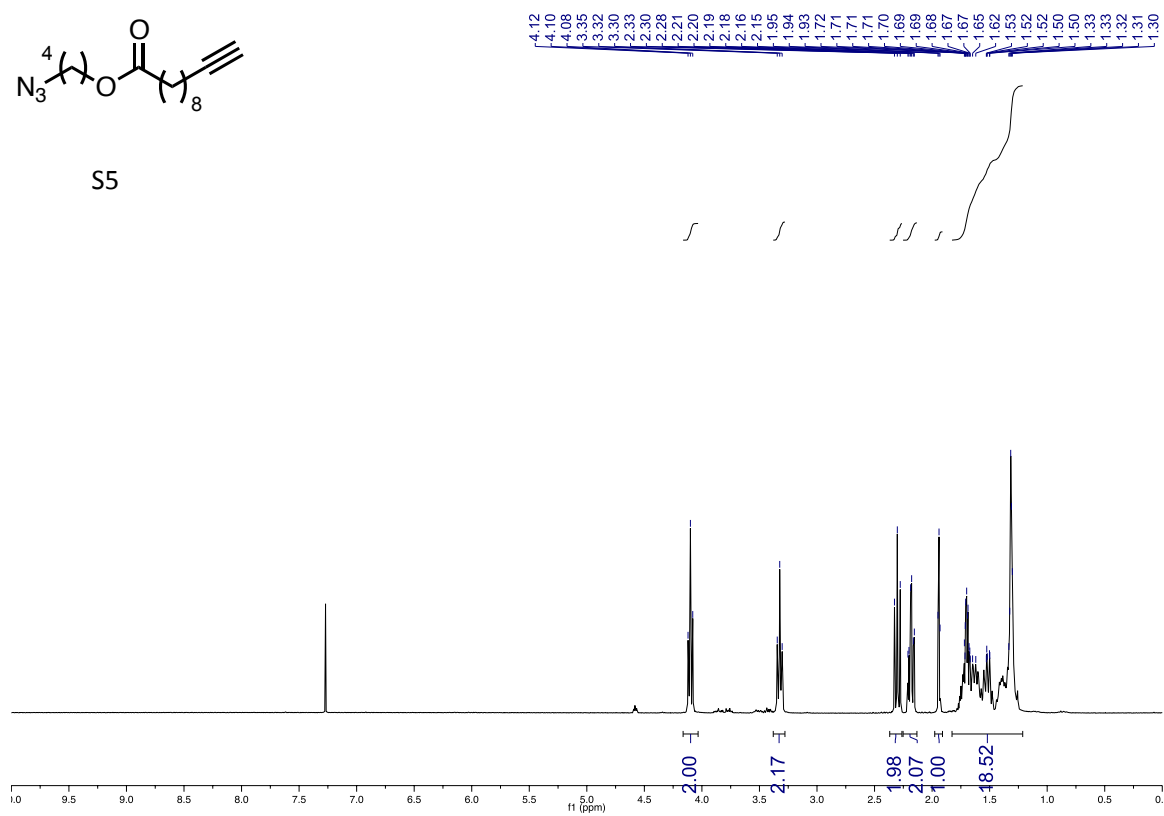
4.09
 4.06
 4.04
 3.28
 3.26
 3.24
 2.35
 2.33
 2.31
 2.25
 2.24
 2.22
 2.21
 2.20
 2.19
 1.96
 1.95
 1.94
 1.80
 1.78
 1.77
 1.76
 1.74
 1.73
 1.73
 1.72
 1.70
 1.65
 1.64
 1.60
 1.60
 1.59
 1.58
 1.57
 1.56
 1.55
 1.54
 1.54
 1.40
 1.38
 1.36
 1.34
 1.33
 1.26



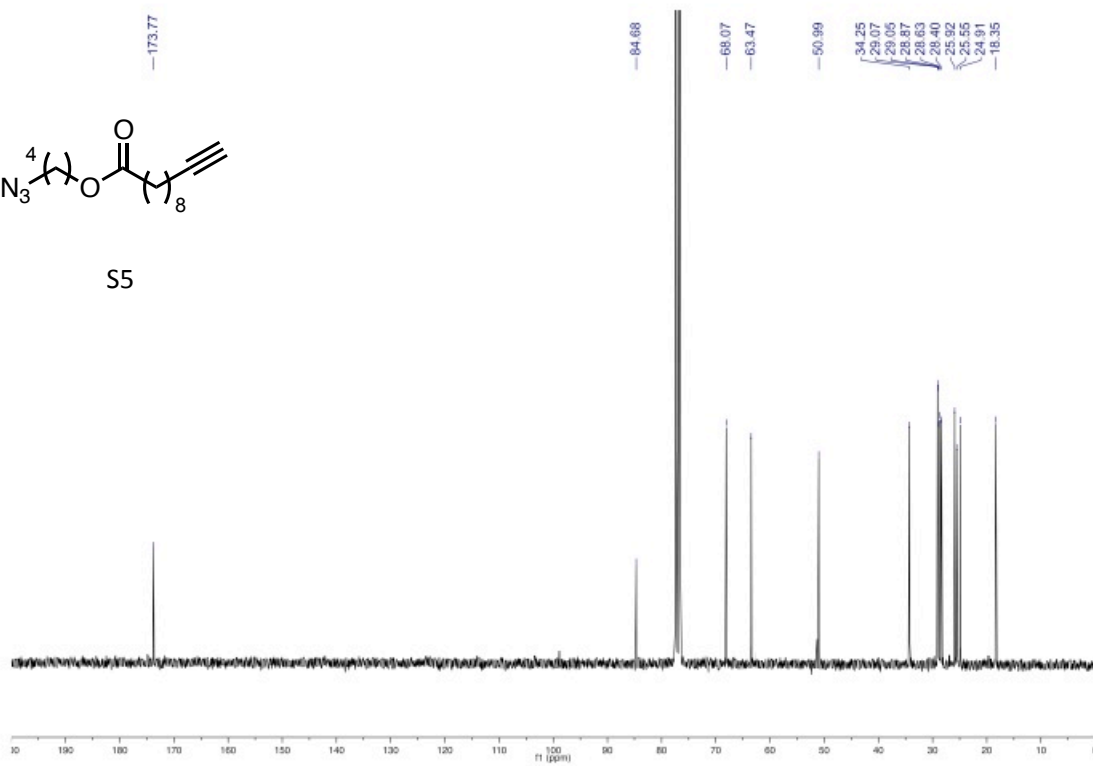
bsbbbb



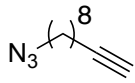
S5



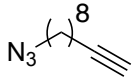
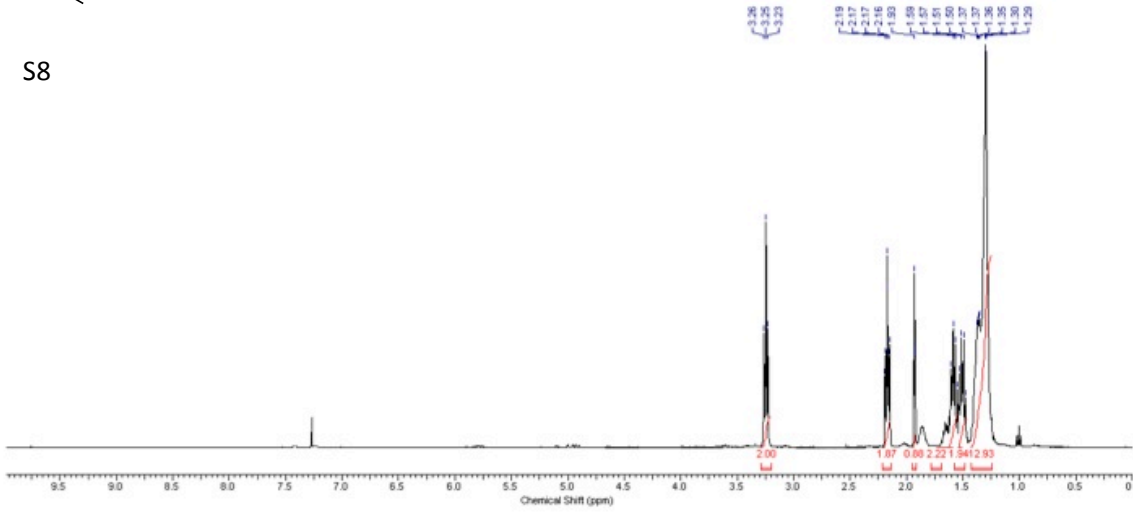
S5



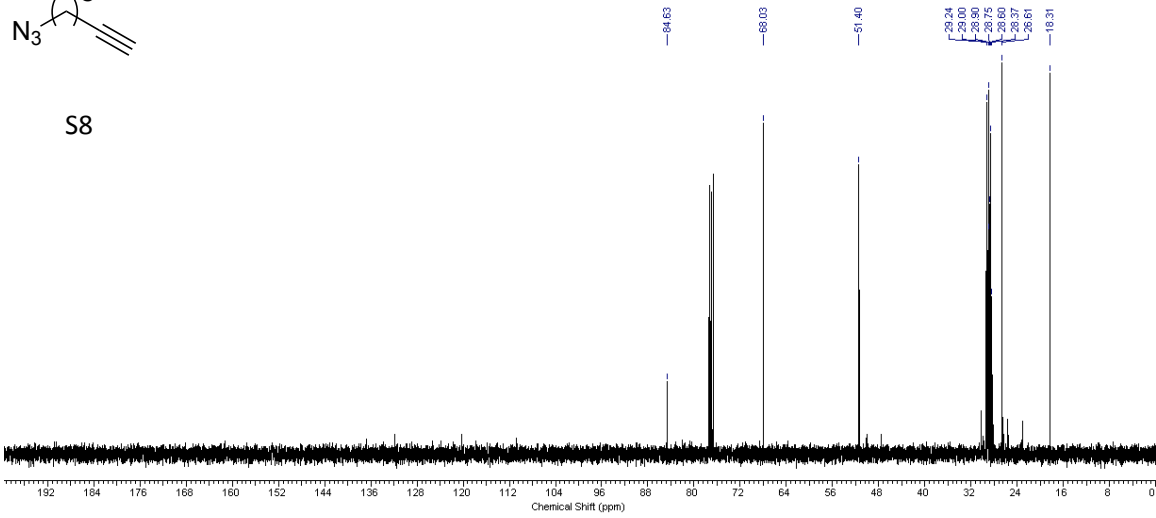
c6cccc



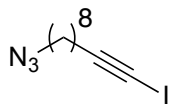
58



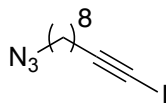
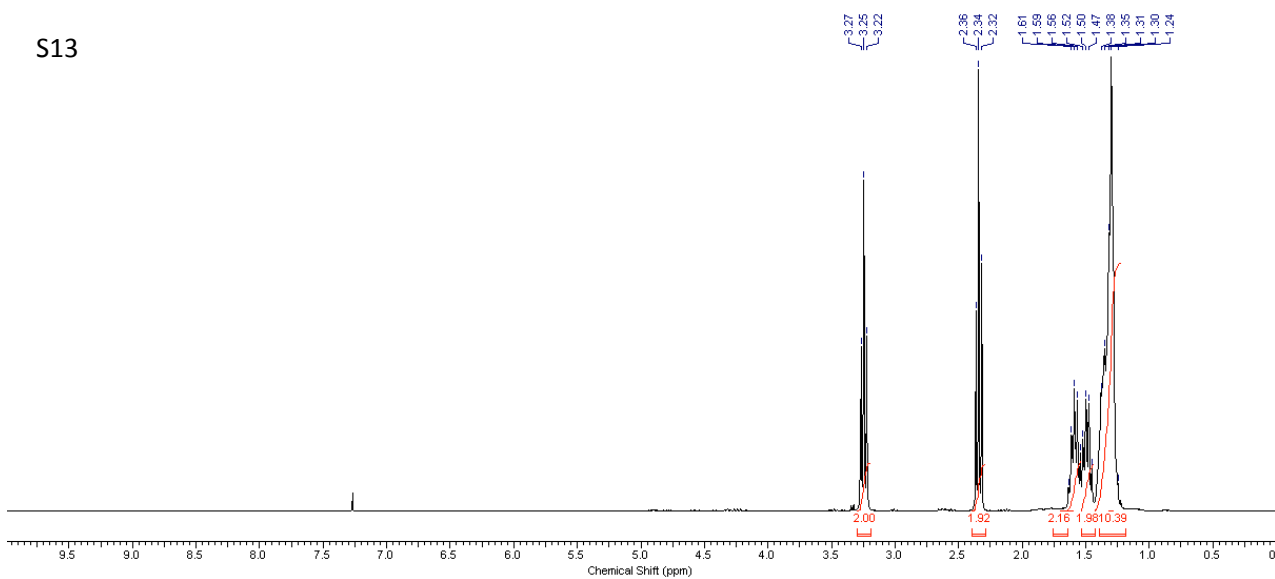
S8



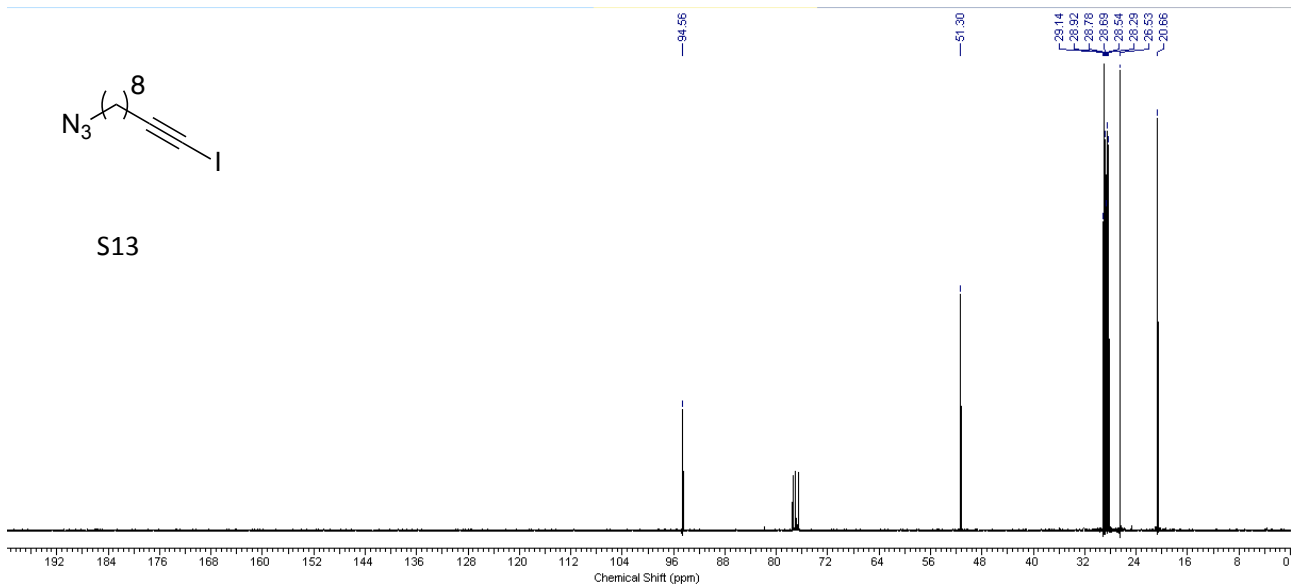
d6d6d6d6d6

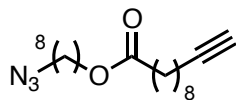


S13

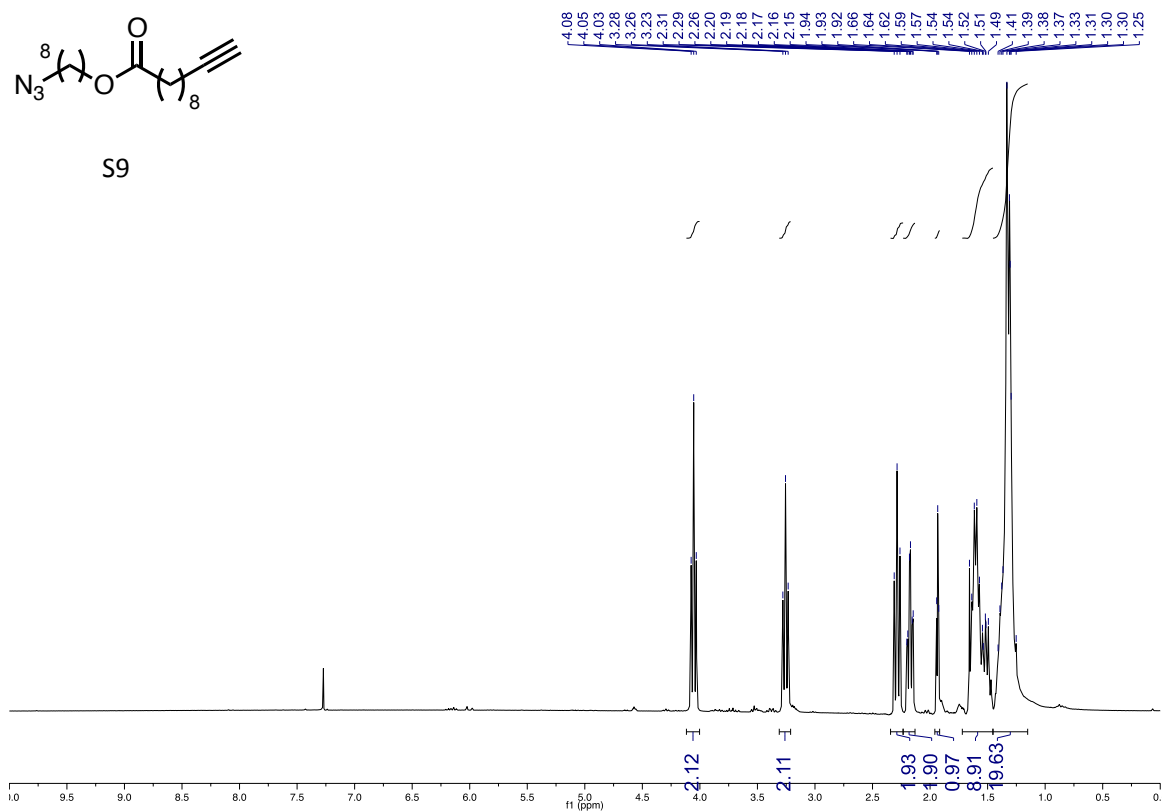


S13

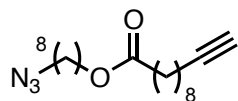




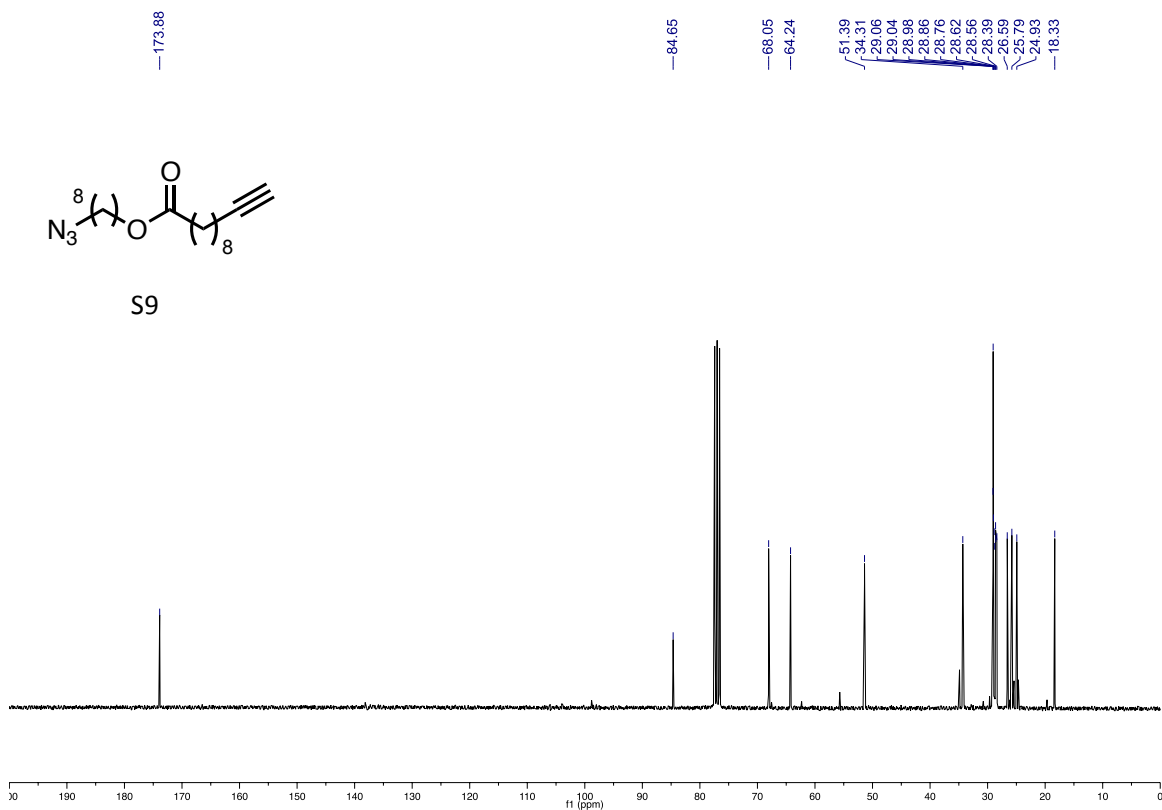
S9



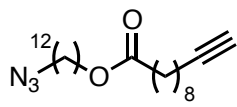
-173.88



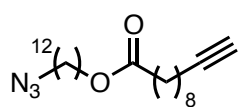
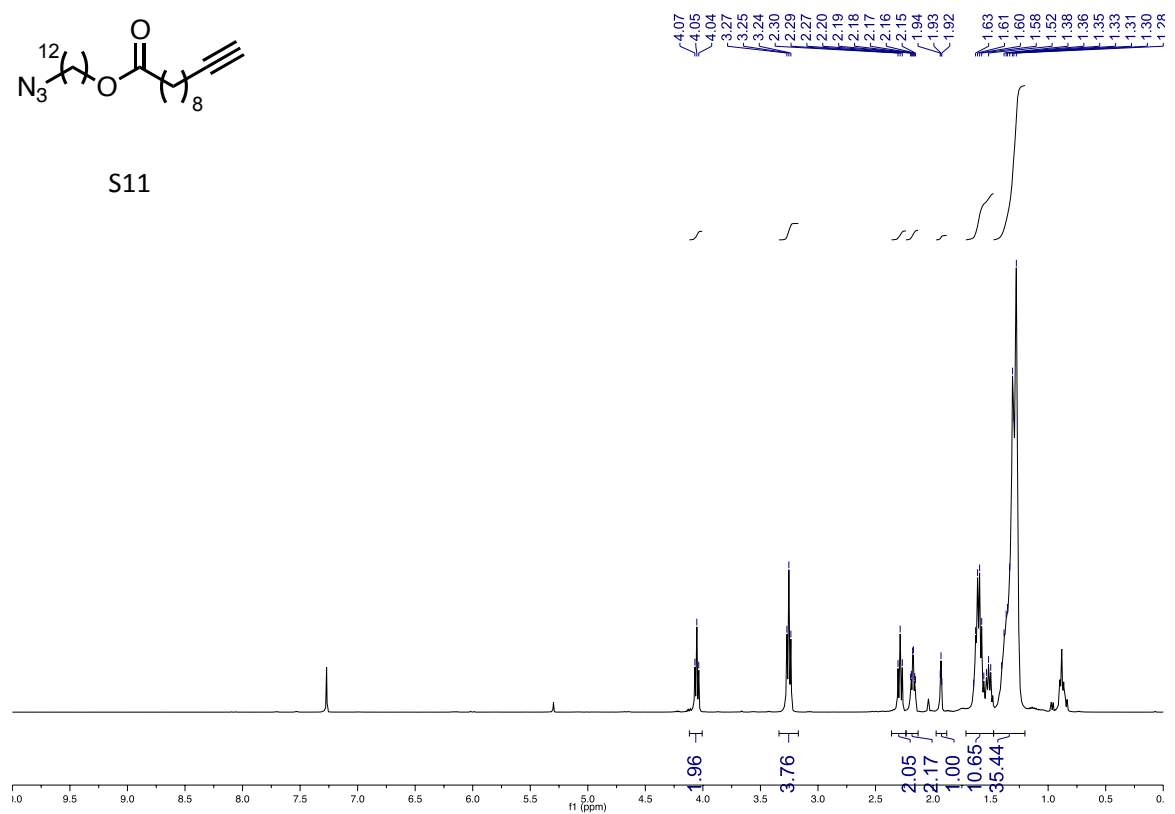
S9



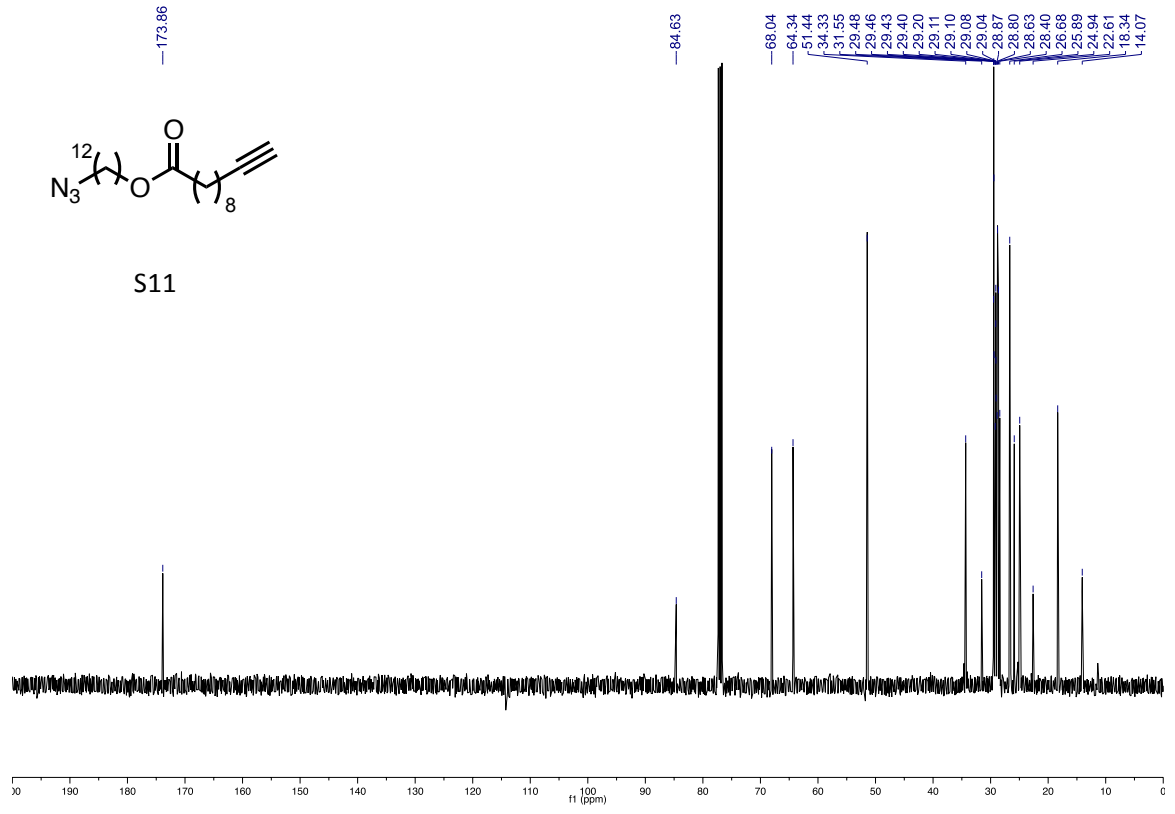
8fffff



S11

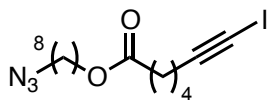


S11

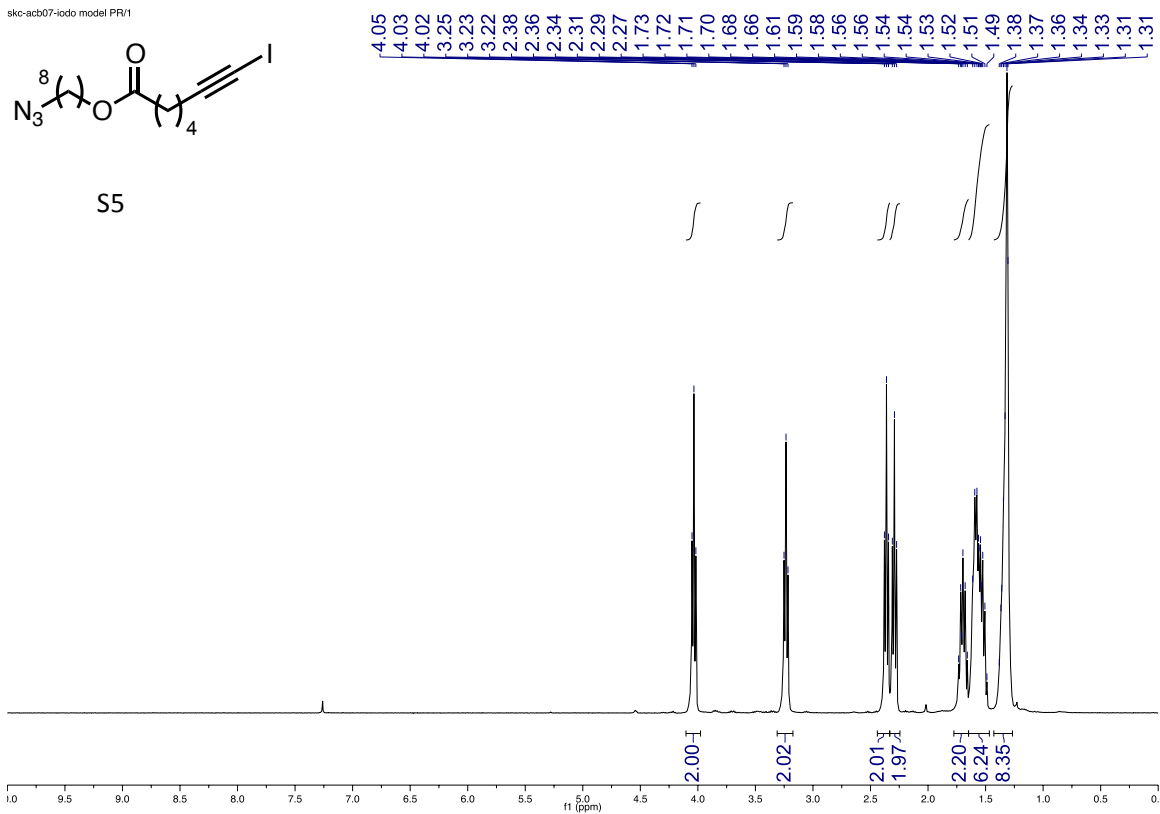


ggggggg

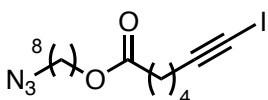
skc-acb07-iodo model PR/1



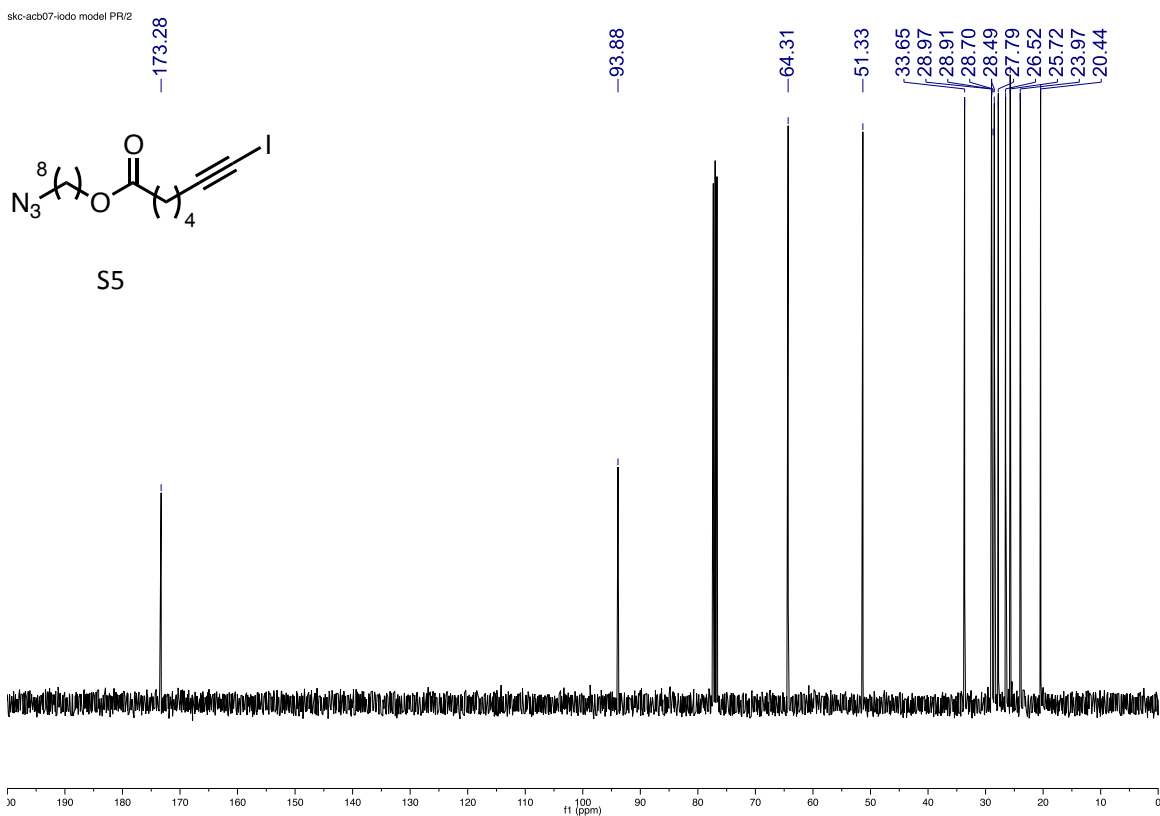
S5



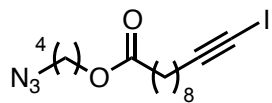
skc-acb07-iodo model PR/2



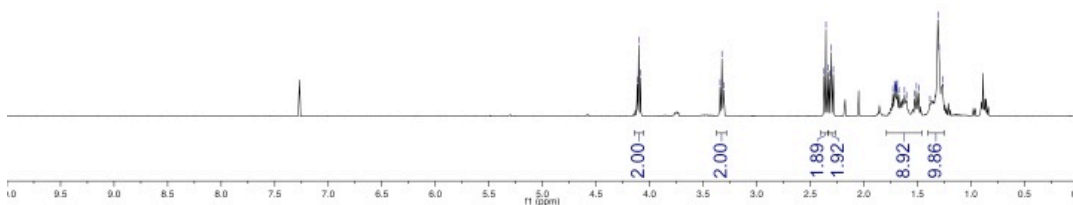
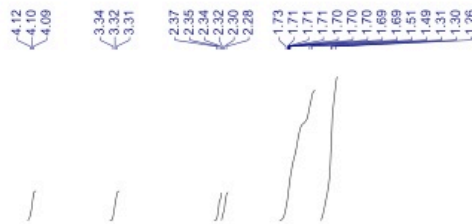
S5



hfhhhhh



S12



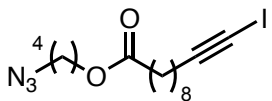
-173.77

-94.73

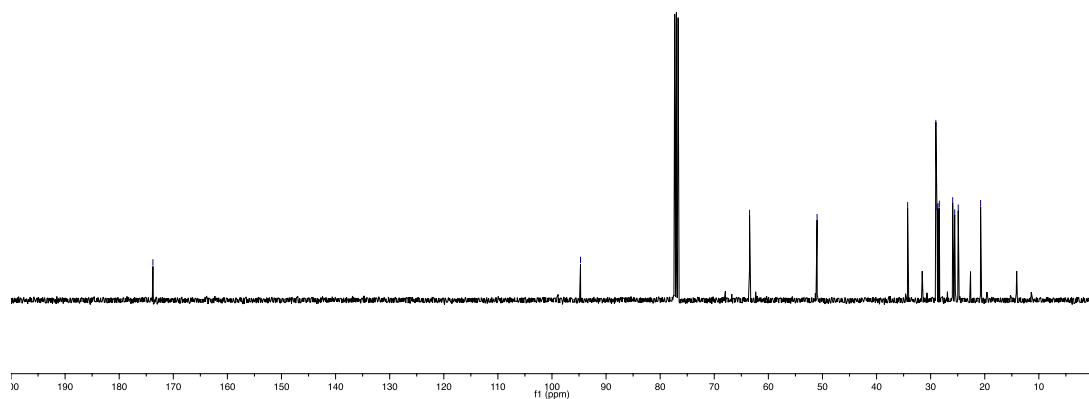
-63.47

-51.00

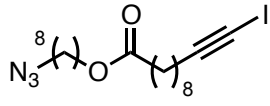
34.26
29.04
28.83
28.64
28.39
25.92
25.66
24.90
20.77



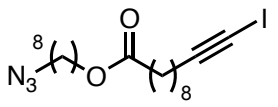
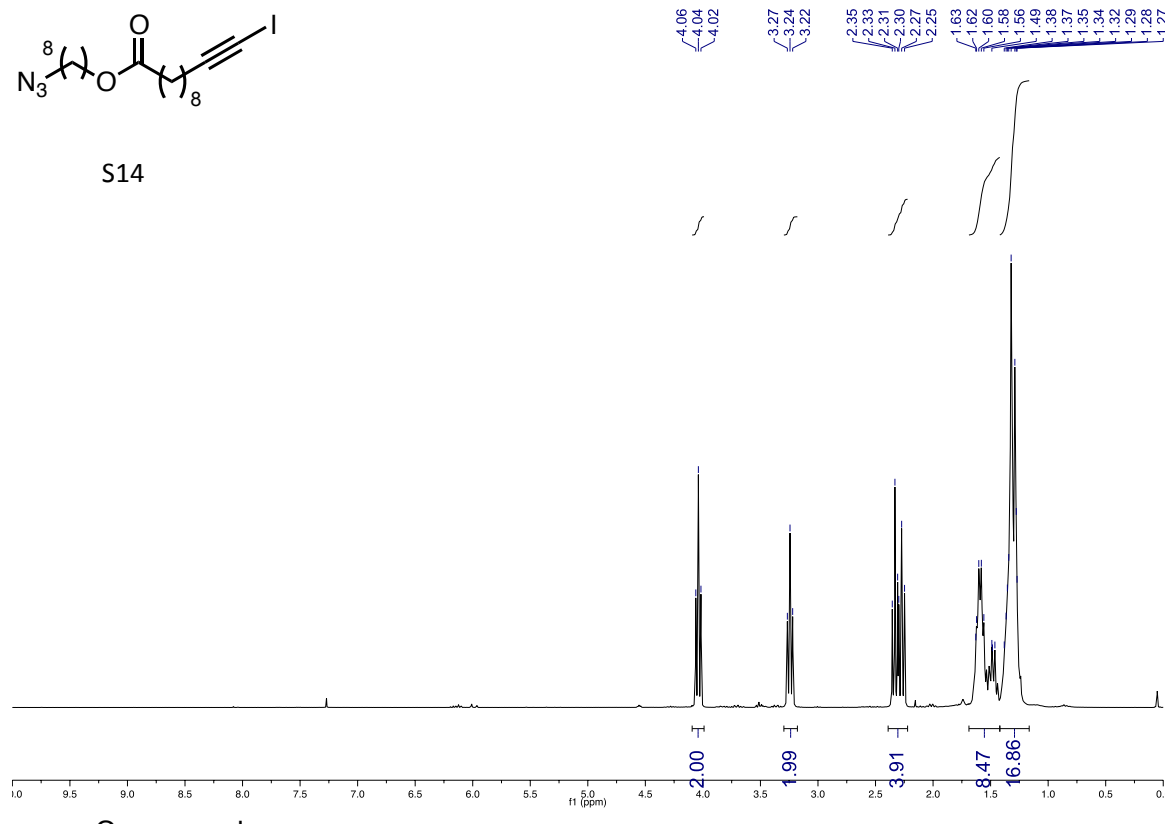
S12



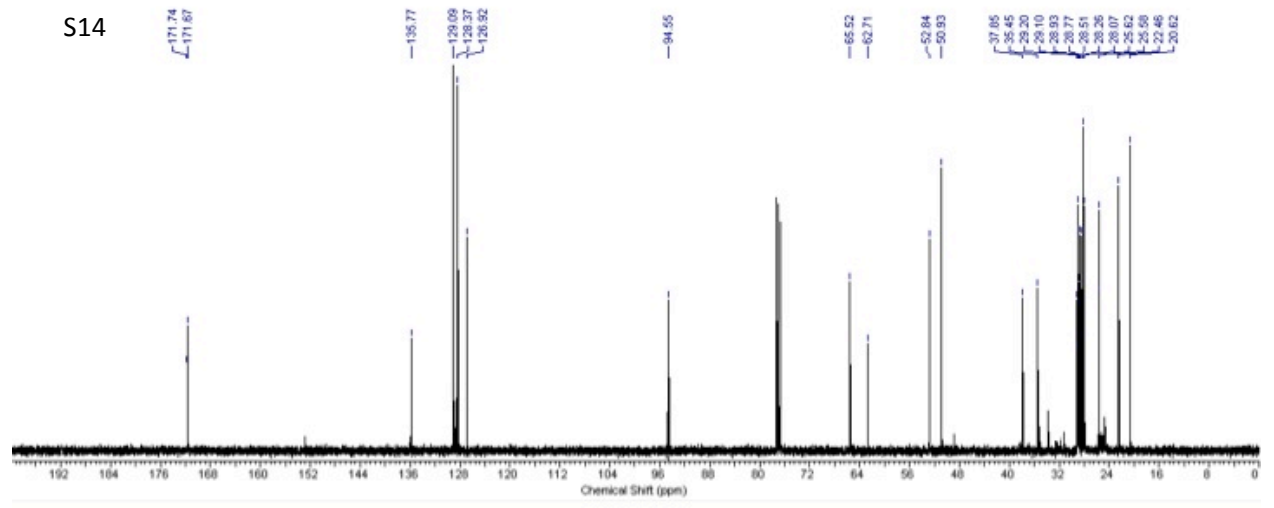
Siiiiii

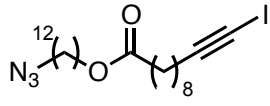


S14

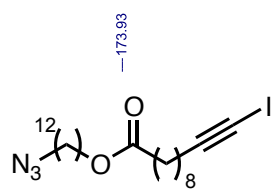
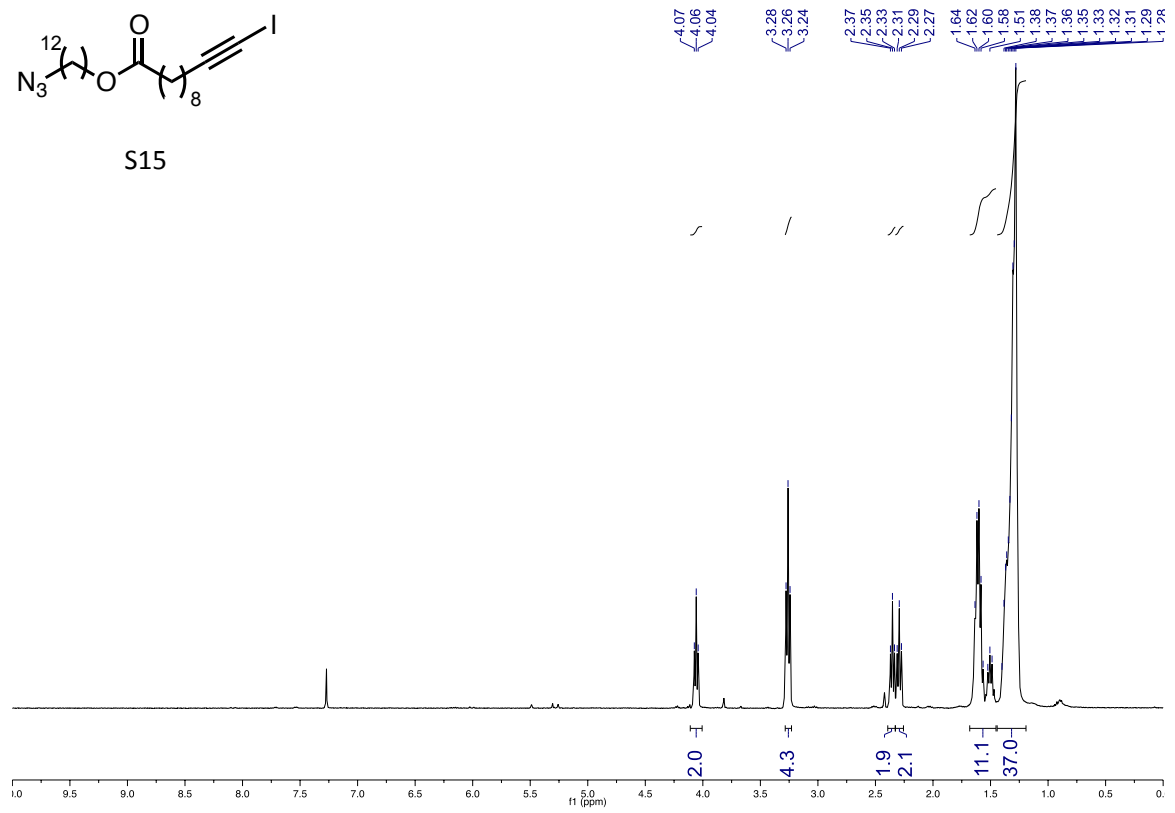


S14

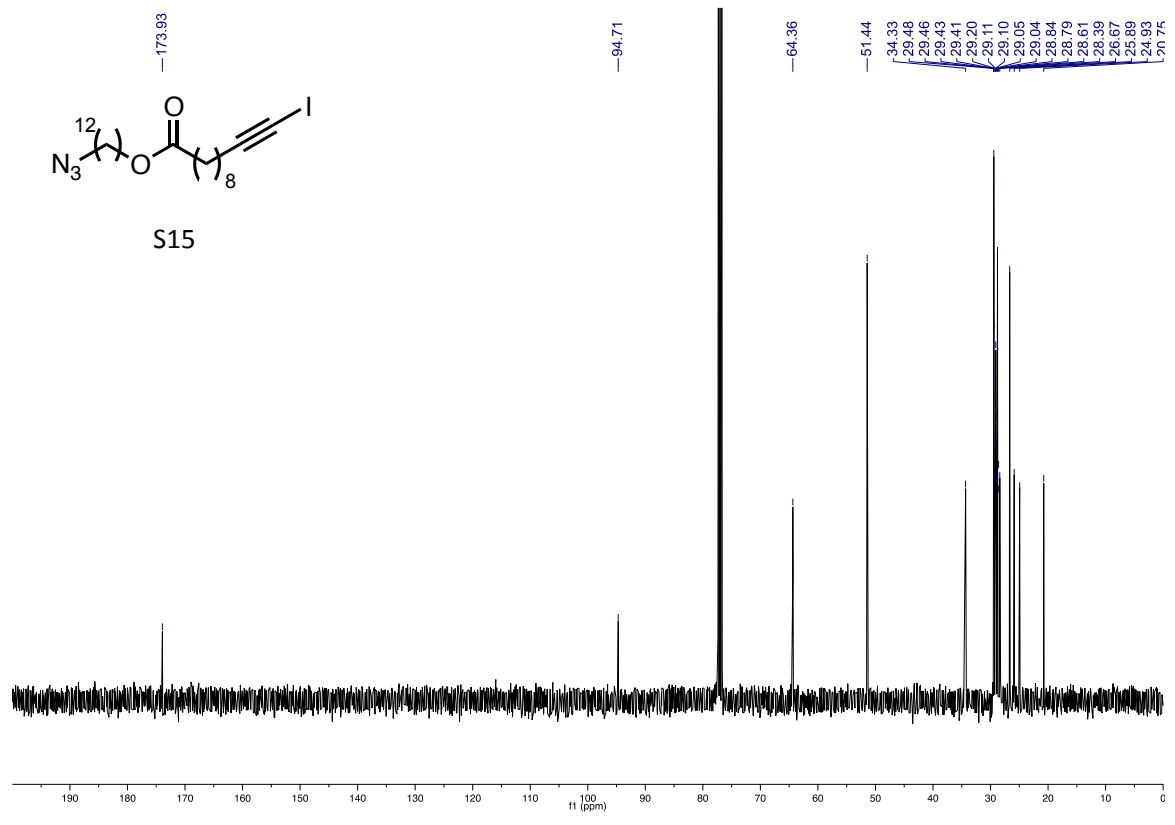




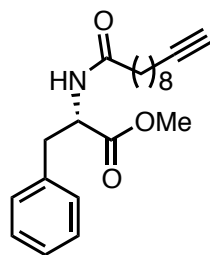
S15



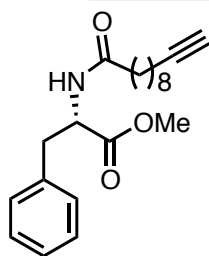
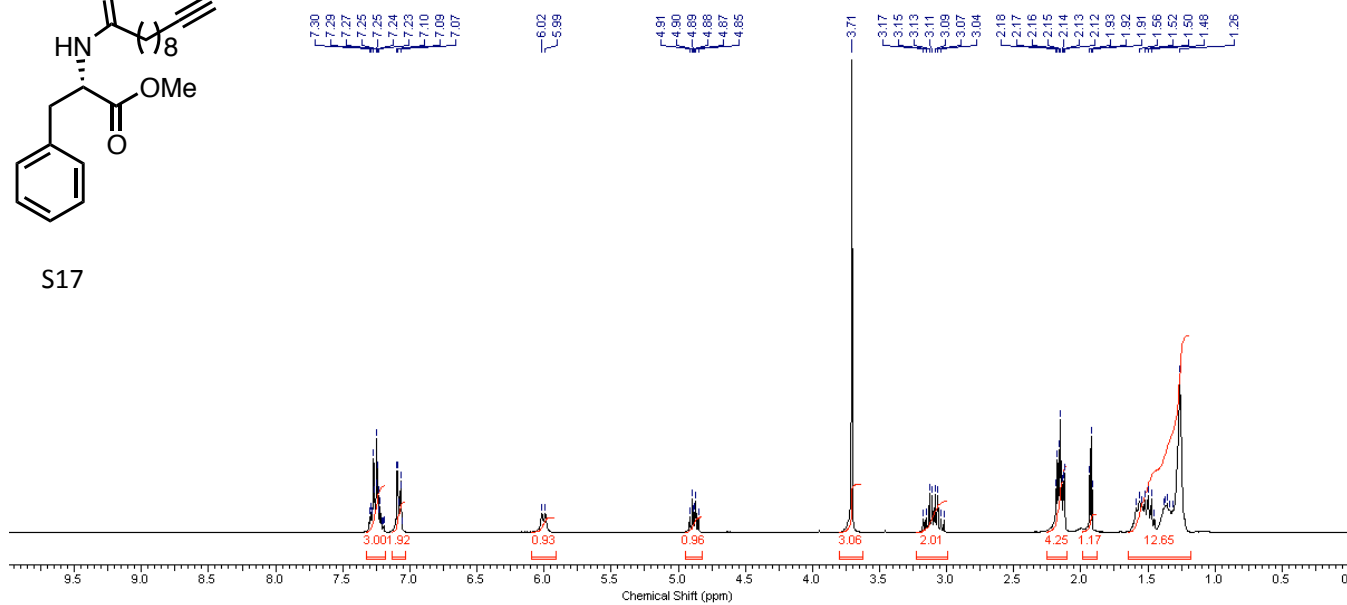
S15



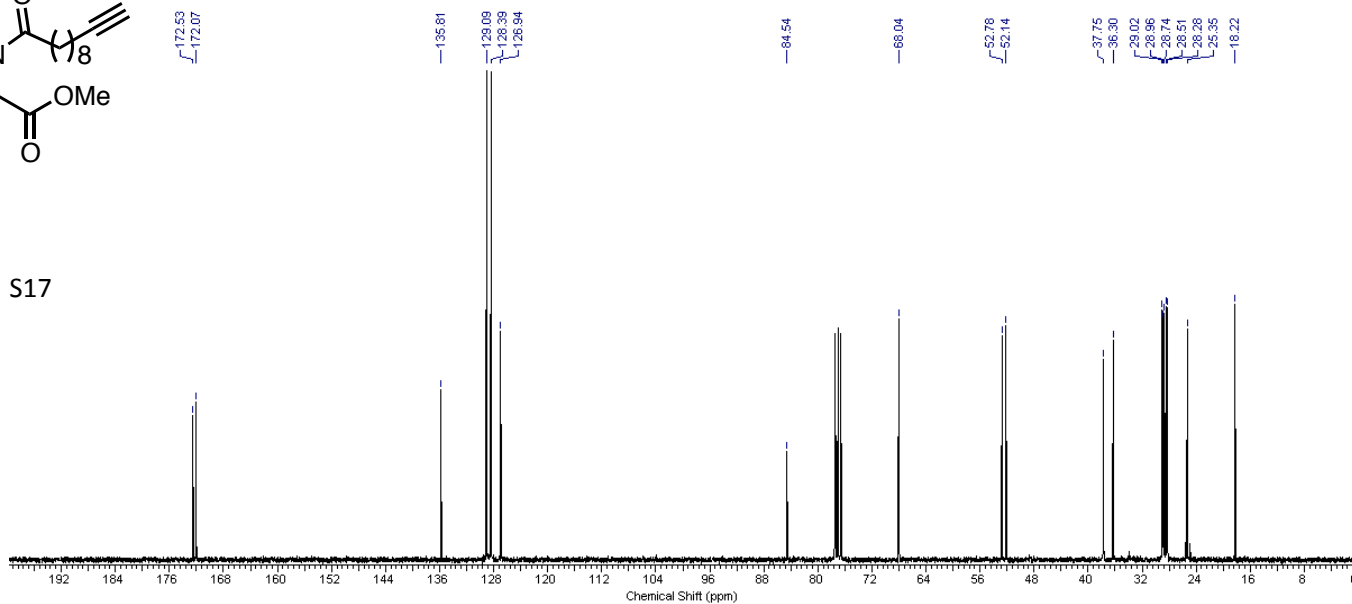
k8kkkkk



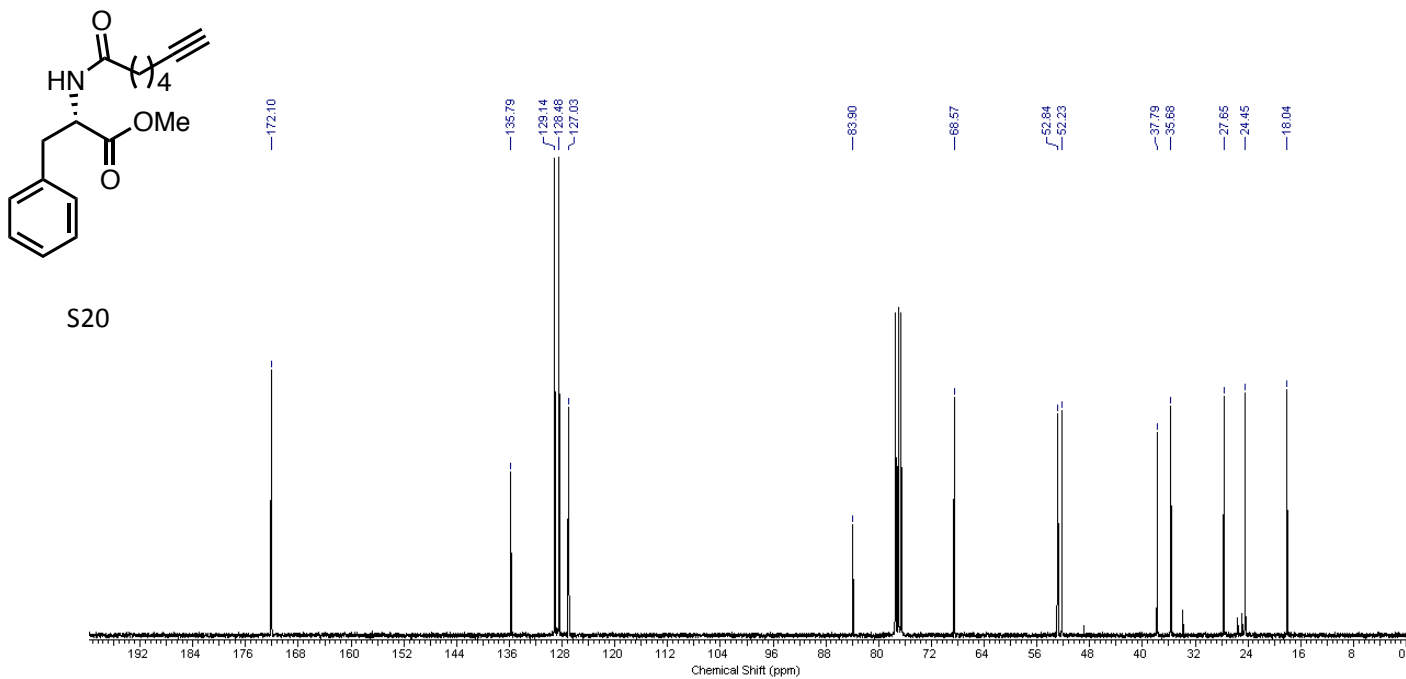
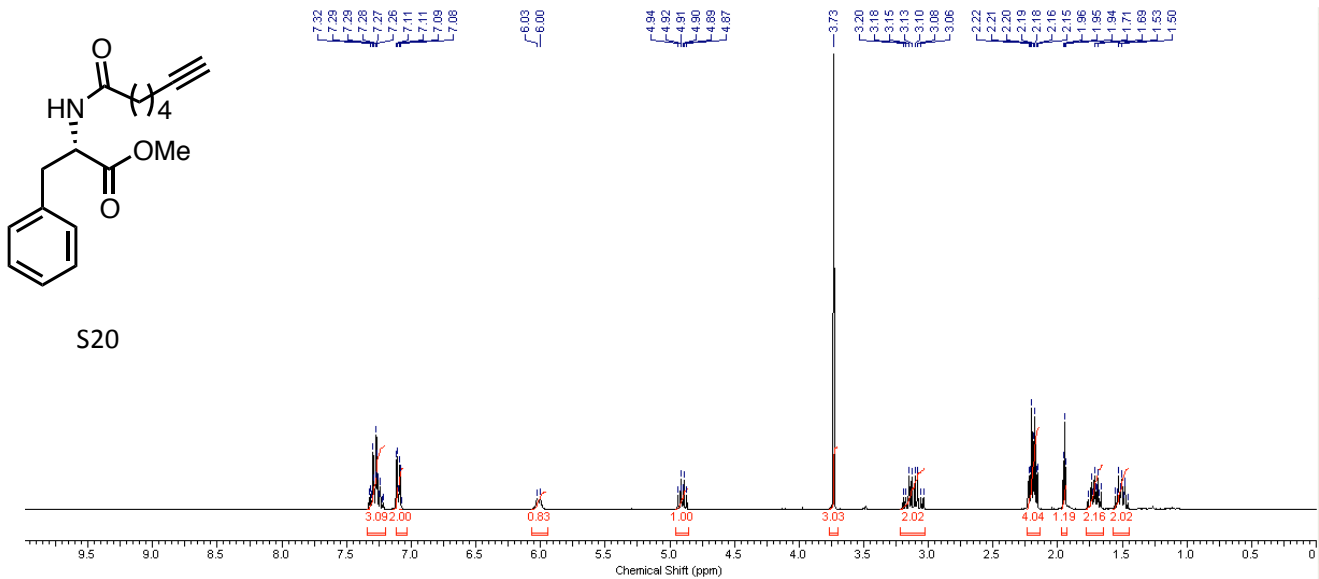
S17



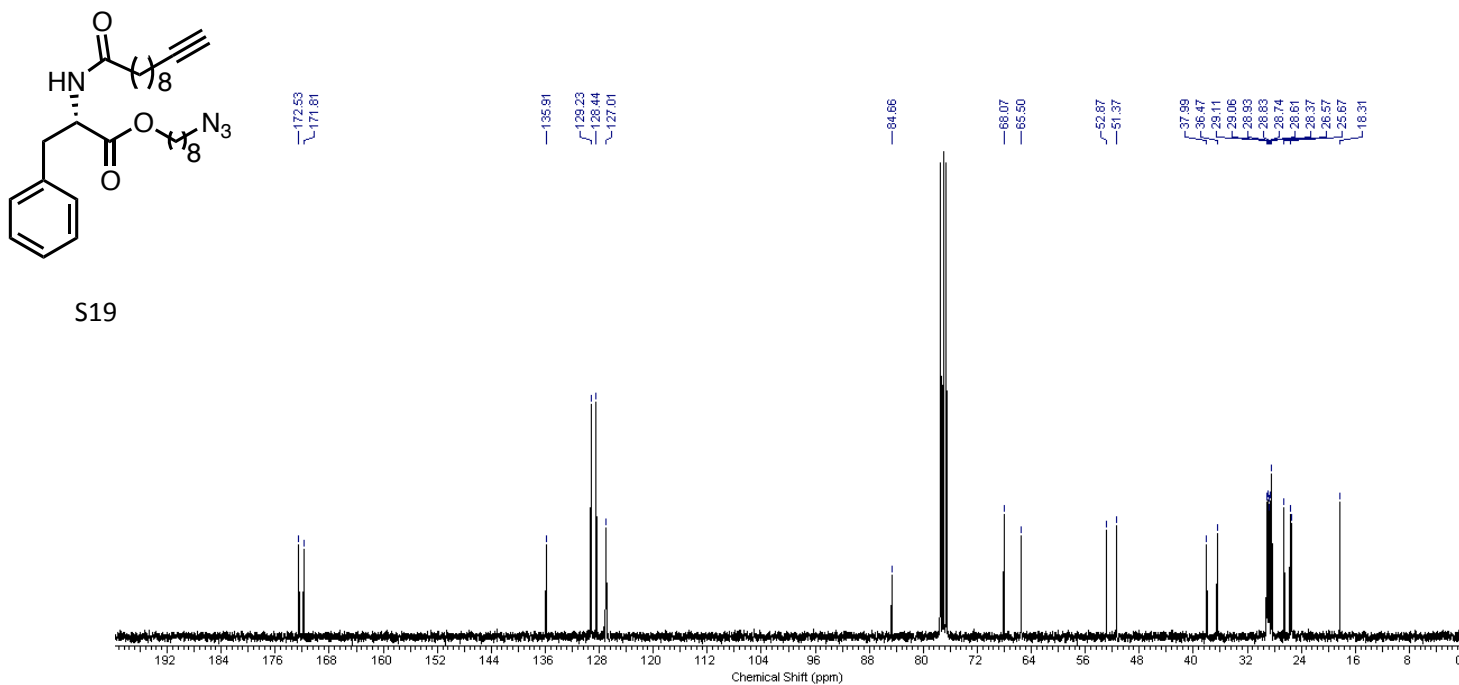
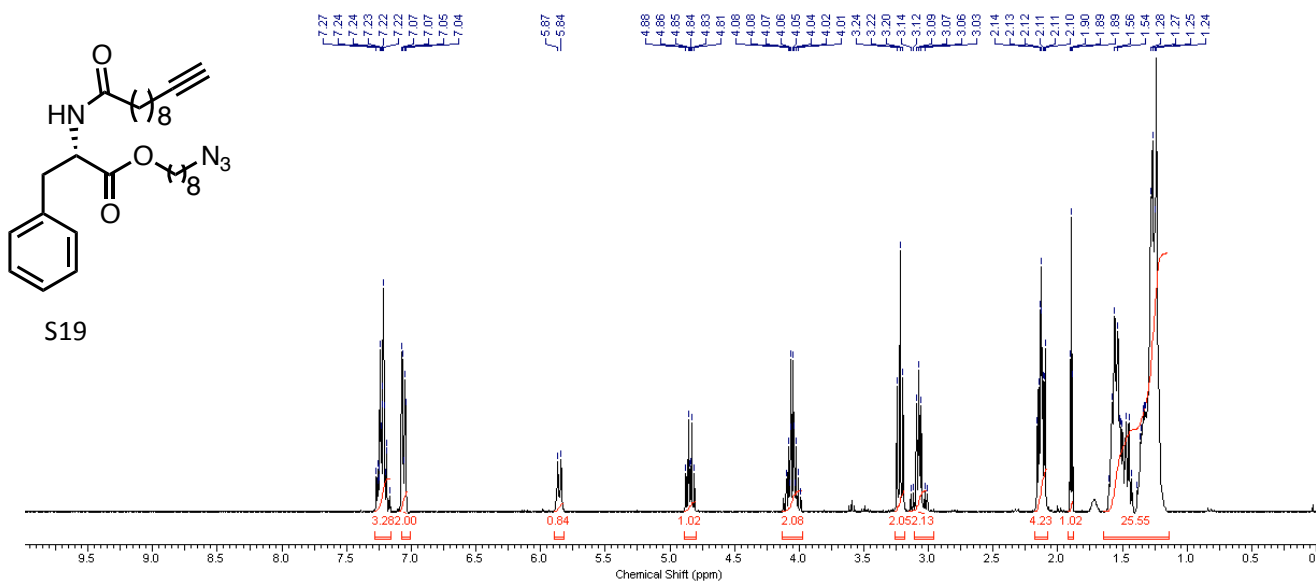
S17



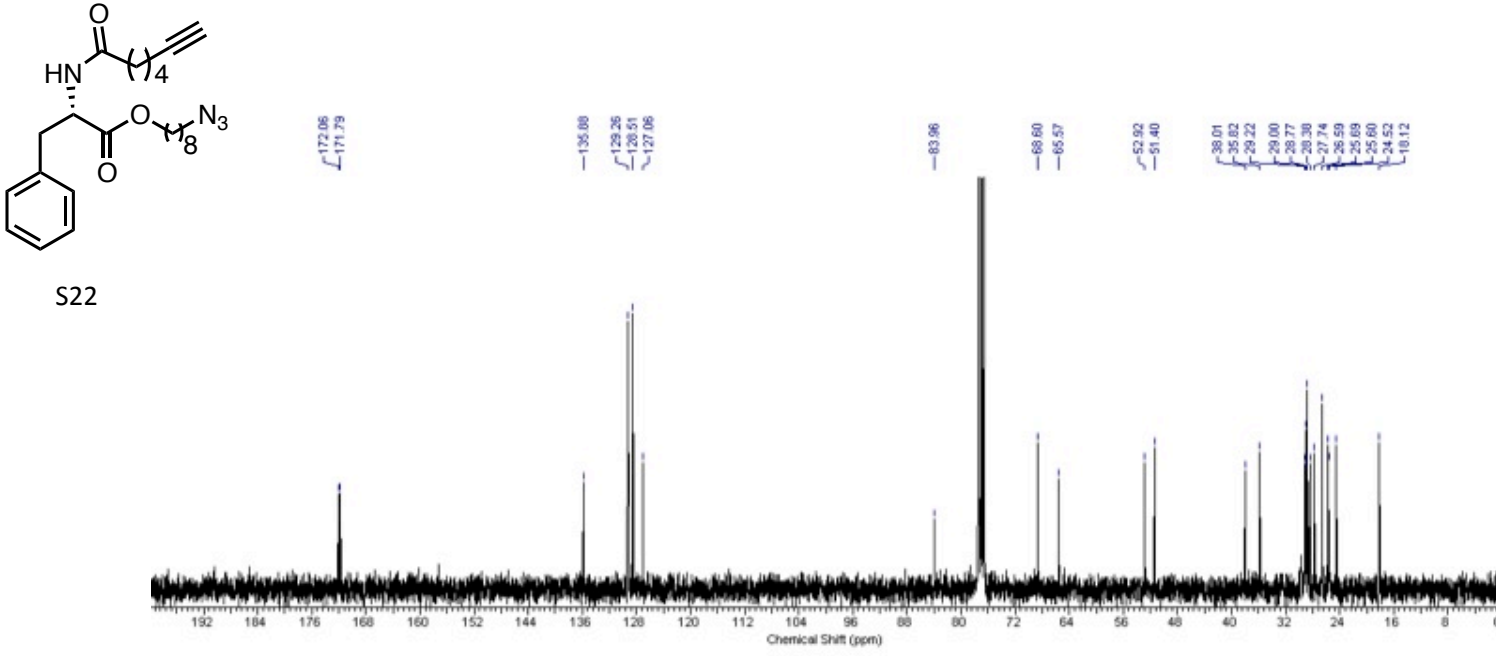
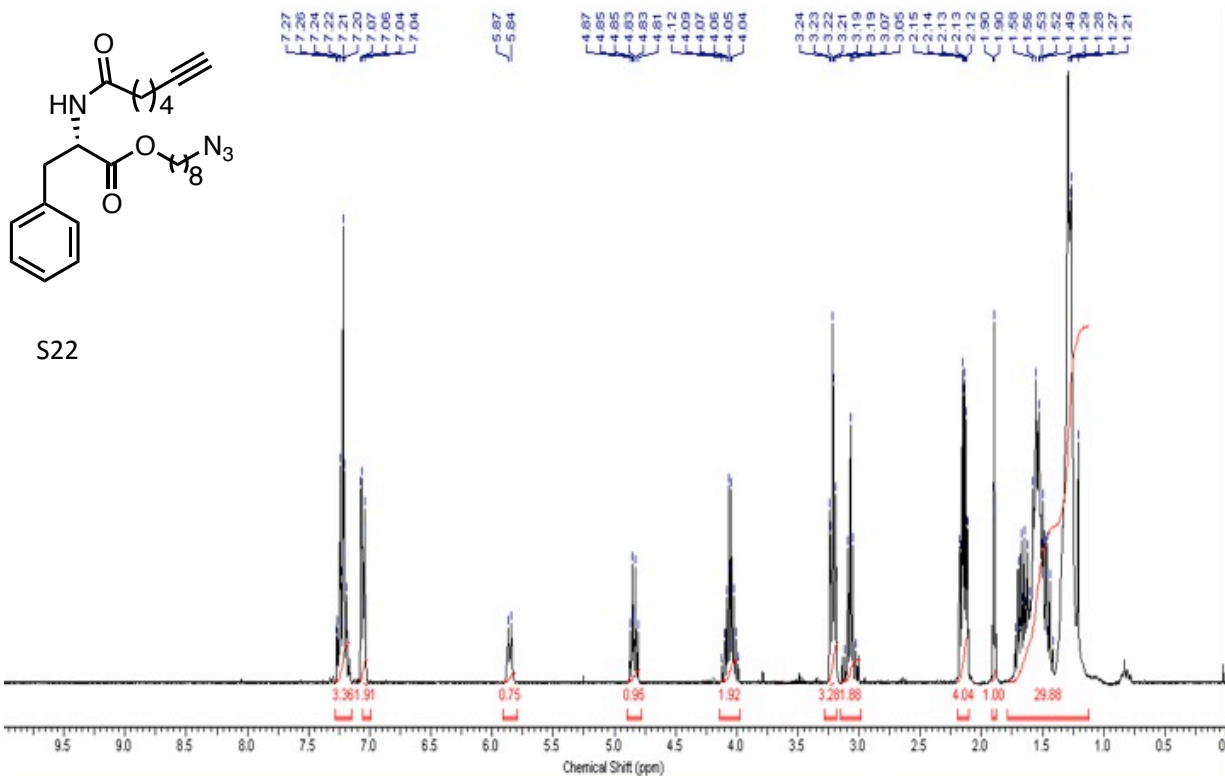
SIIIIII



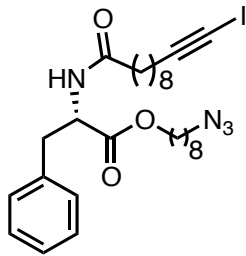
mmmmmm



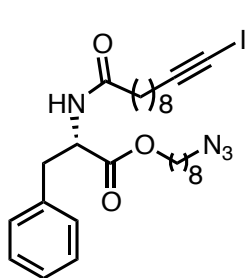
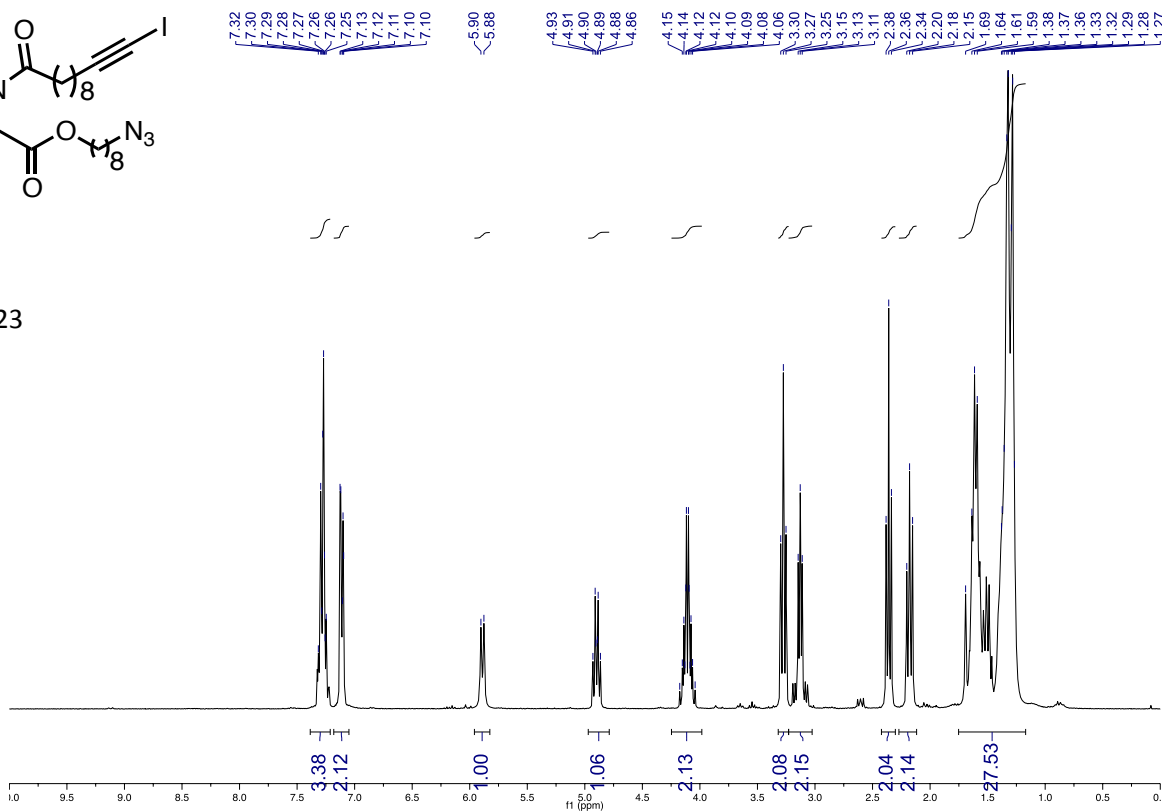
nnnnnn



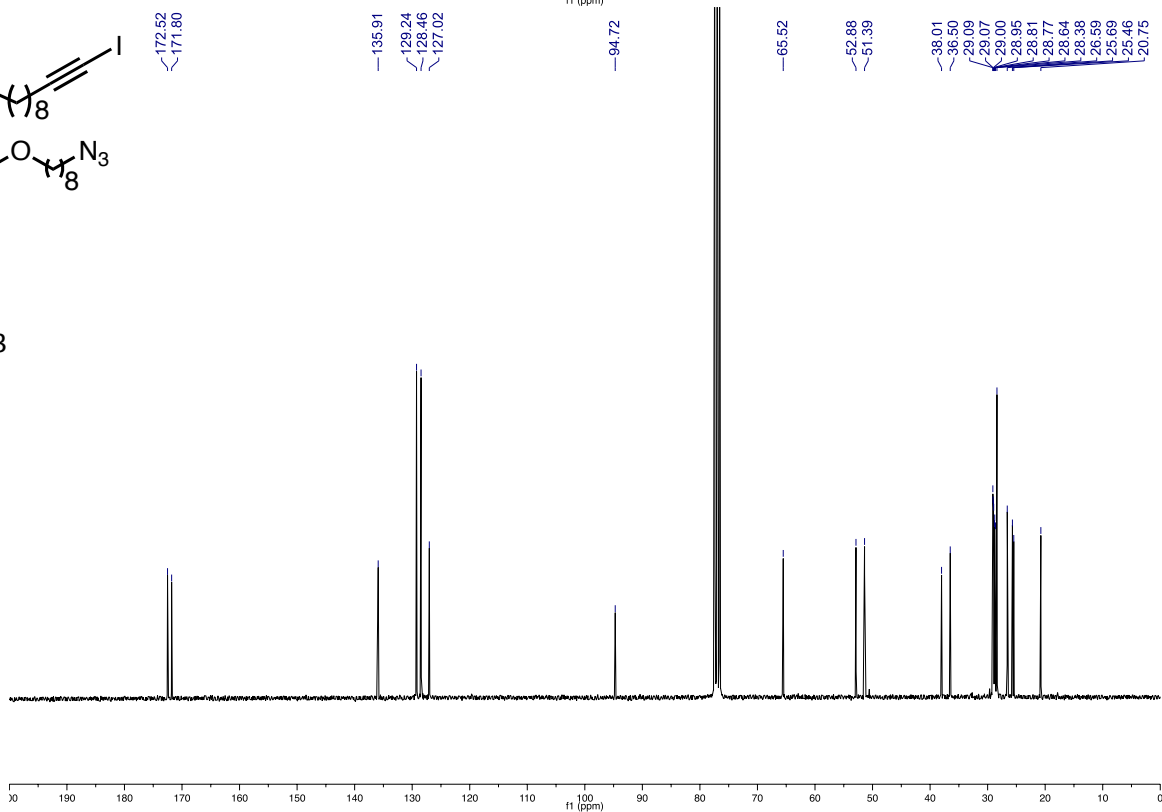
000000



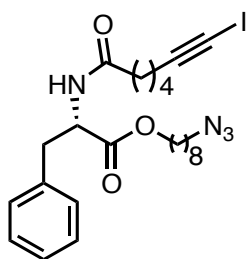
S23



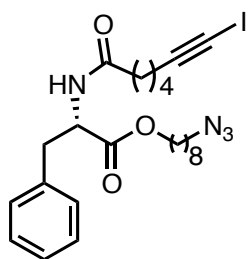
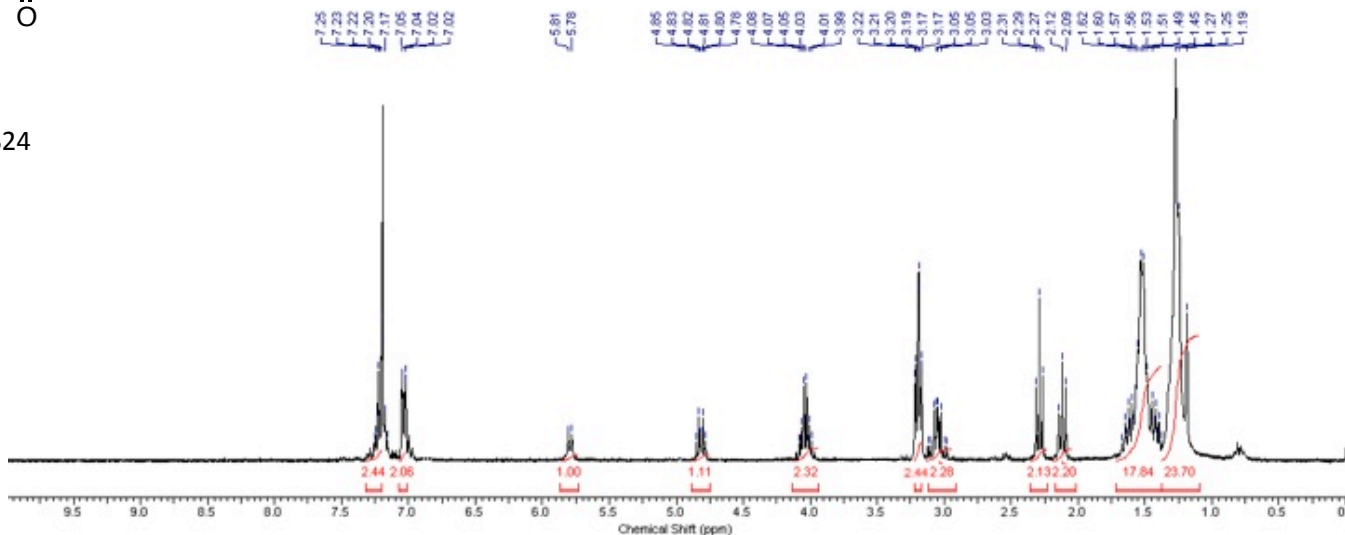
S23



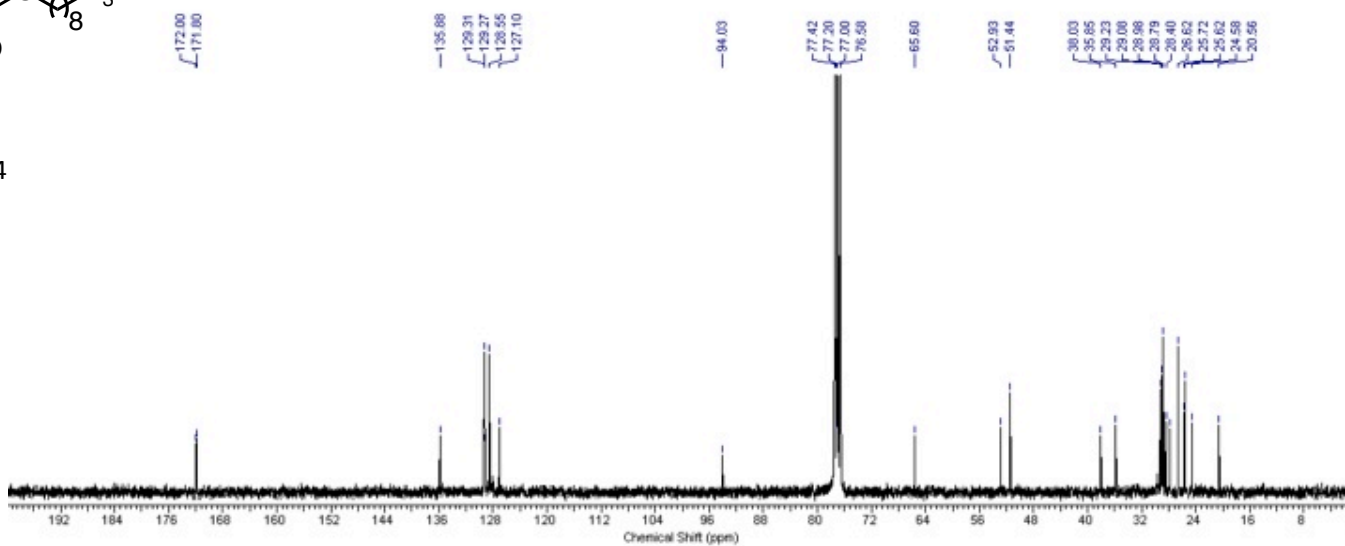
pppppp



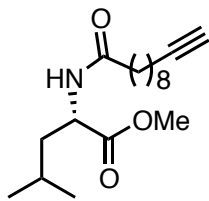
S24



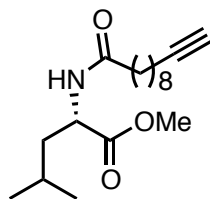
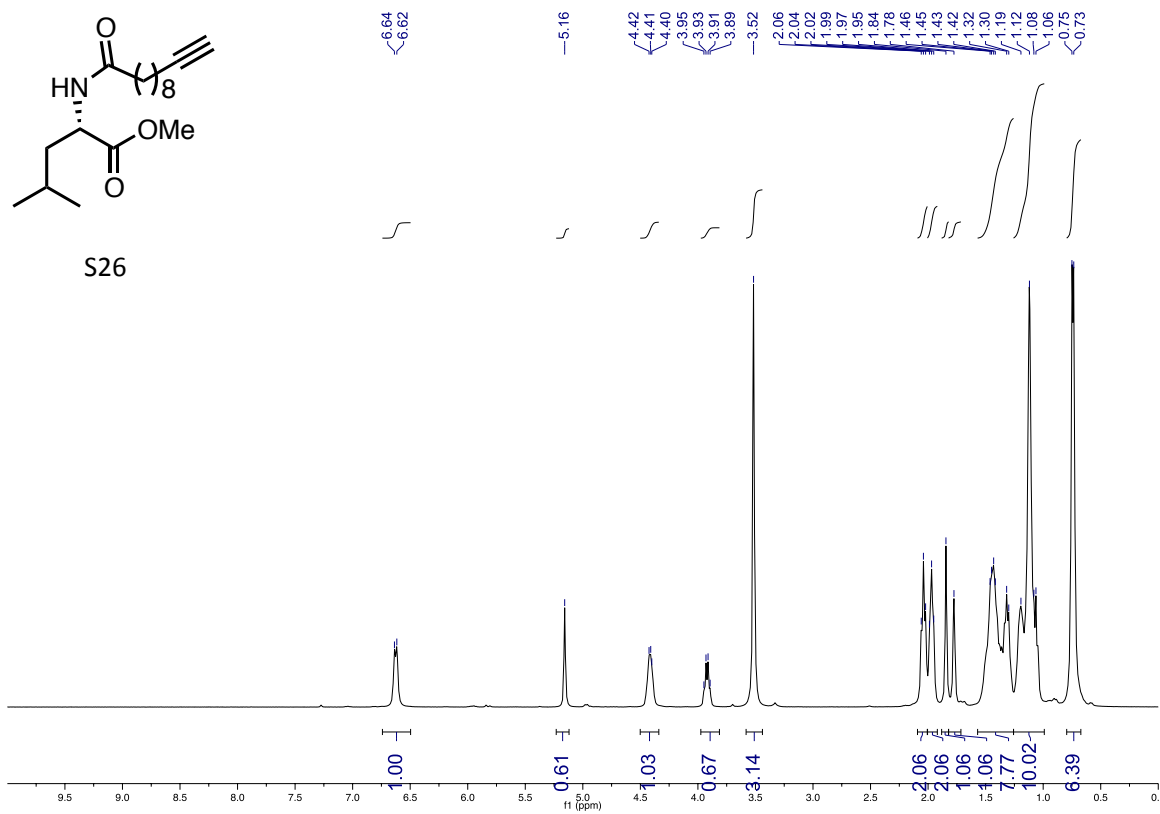
S24



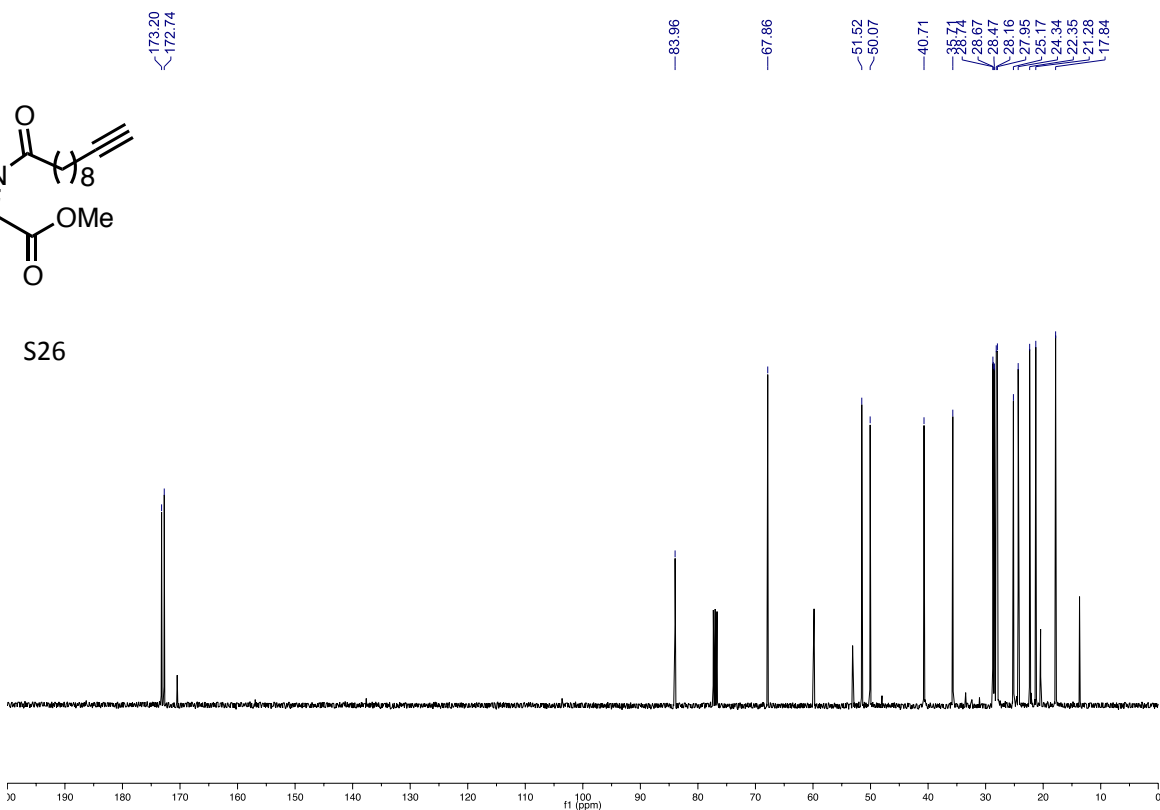
qfqqqq



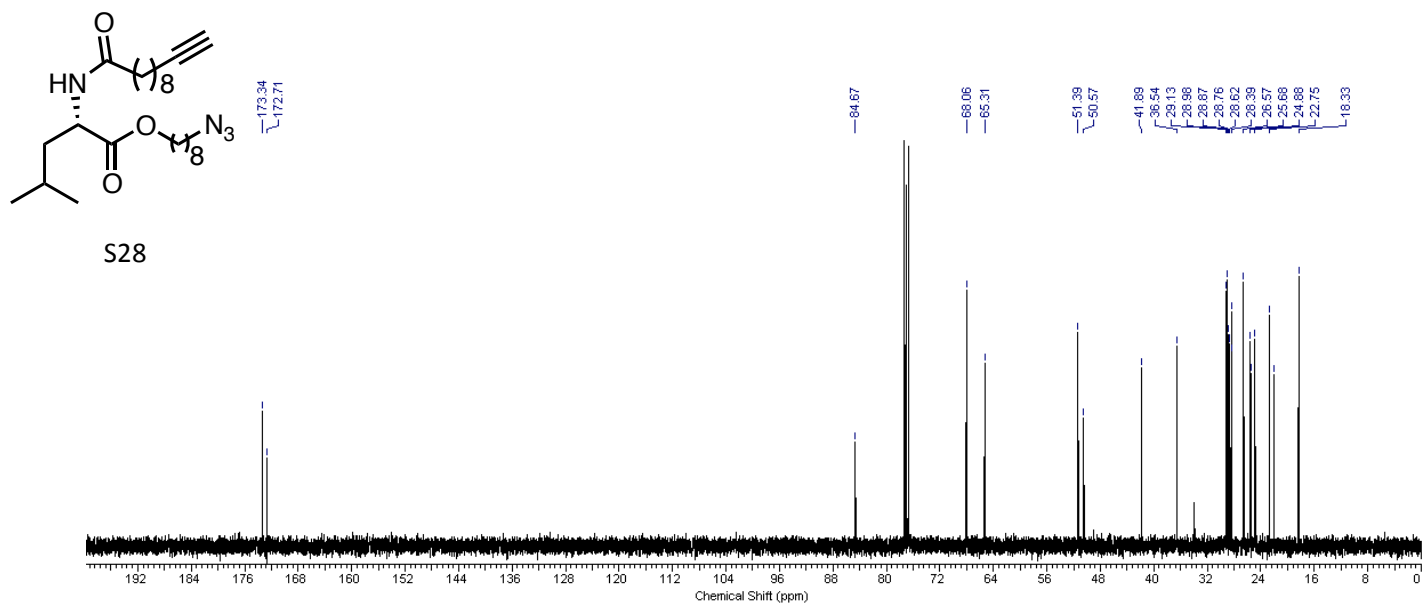
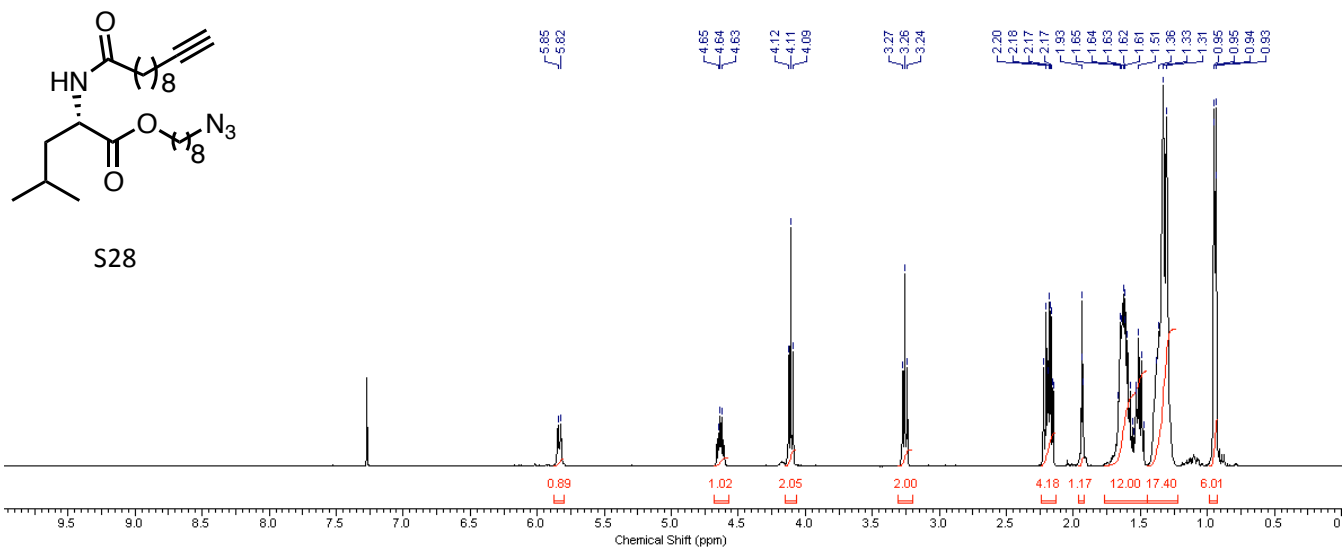
S26

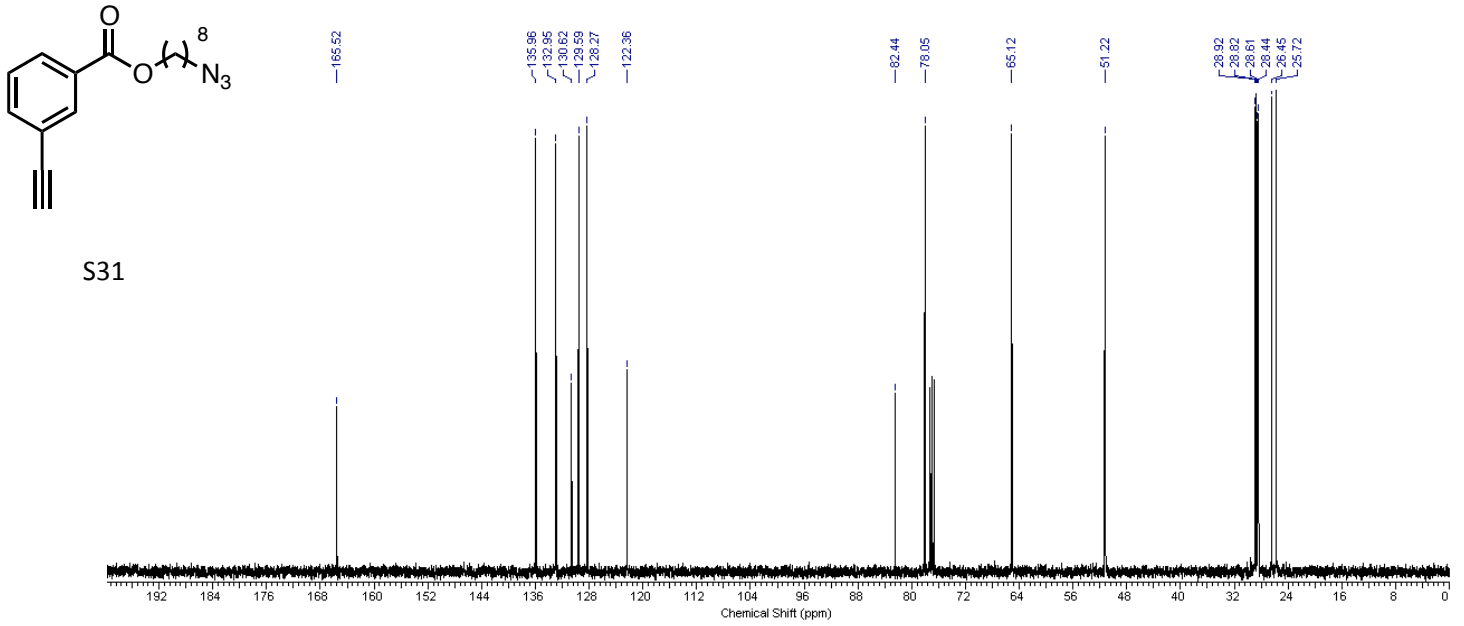
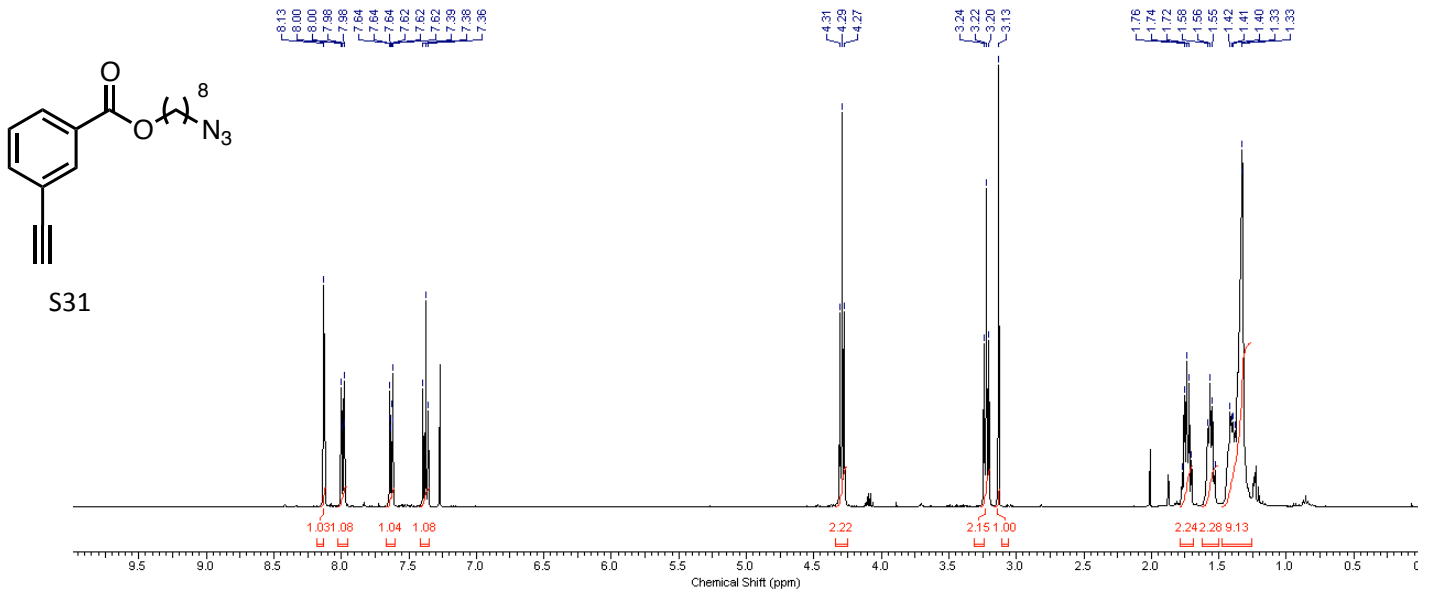


S26

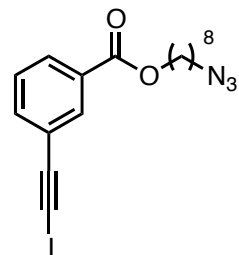


5rrrrr

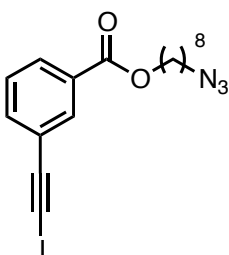
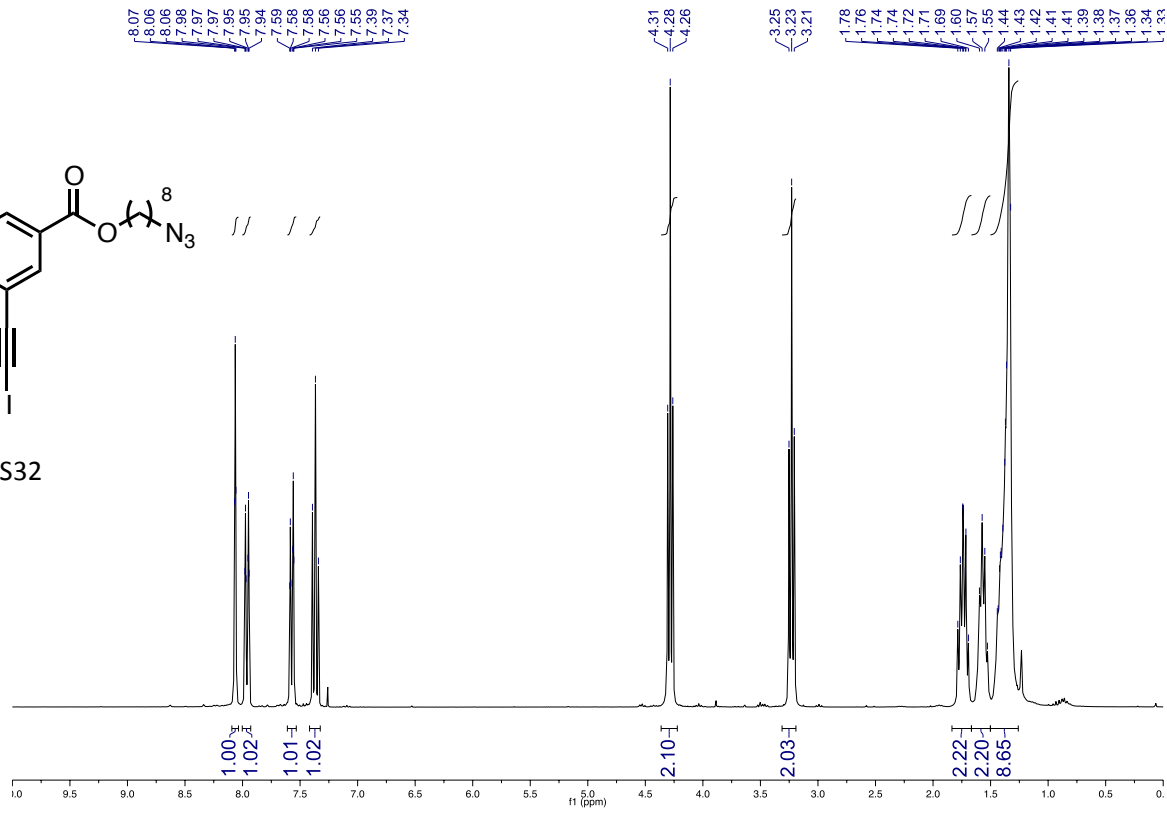




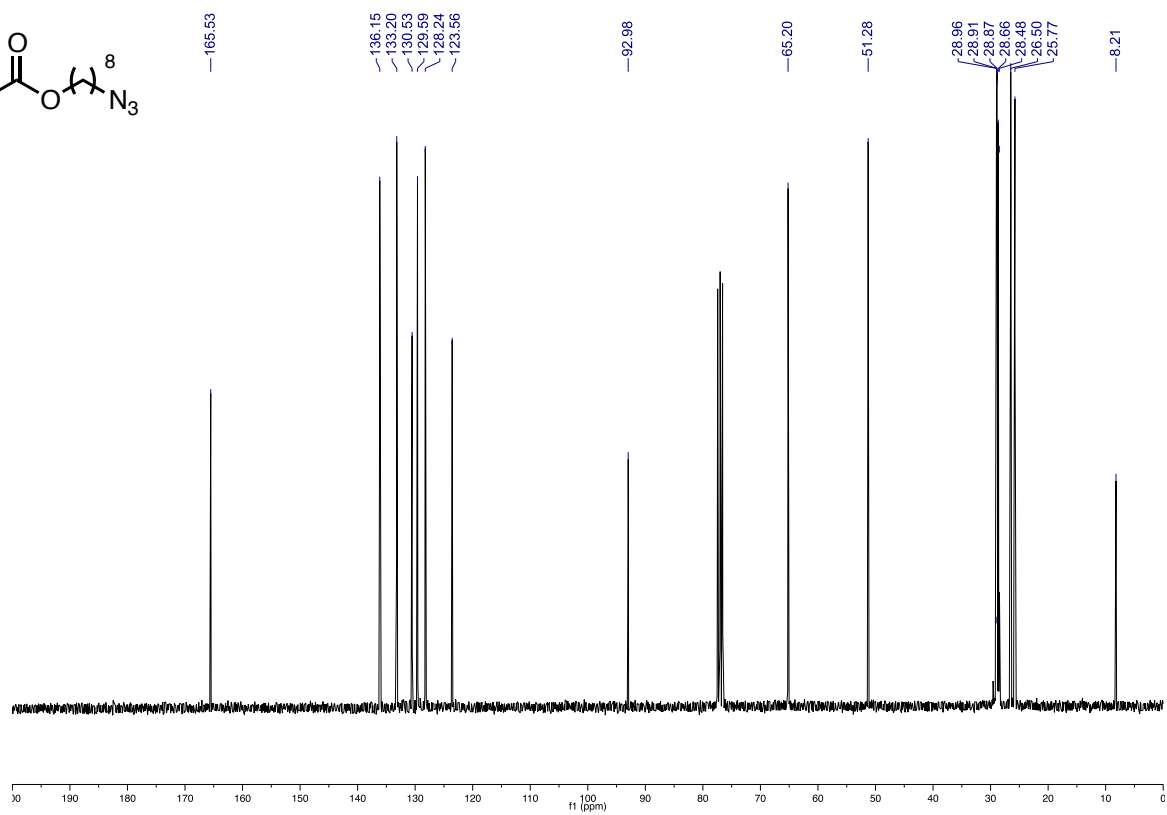
ပမ္းပမ္းပမ္း

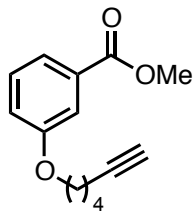


S32

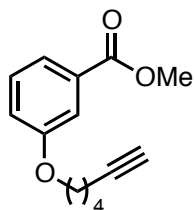
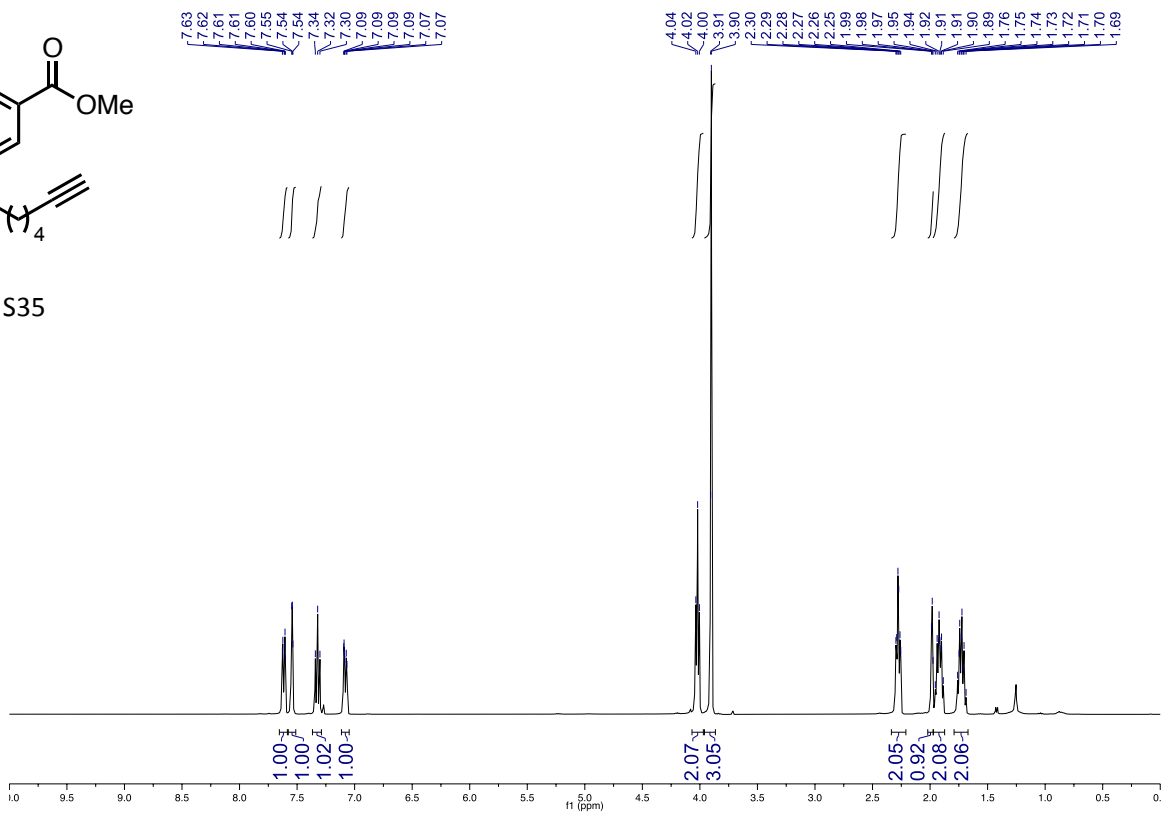


S32

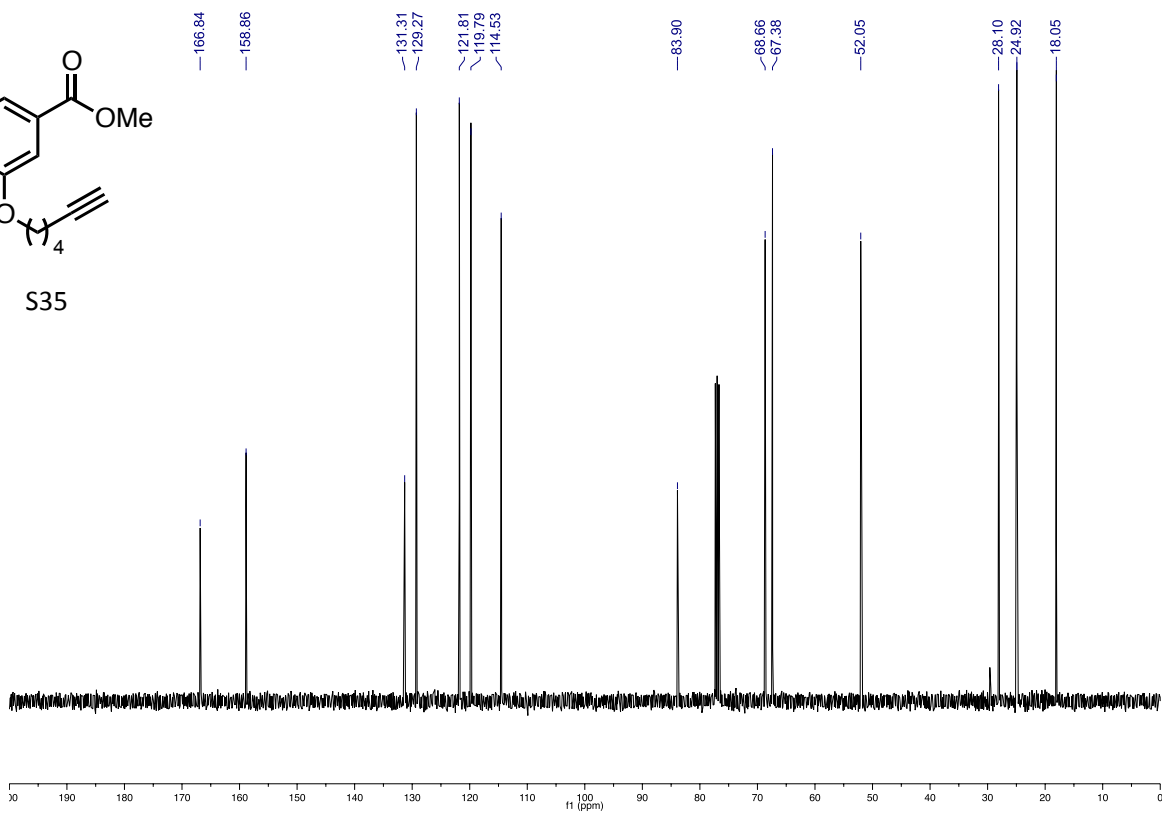


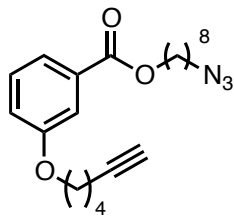


S35

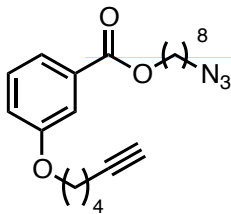
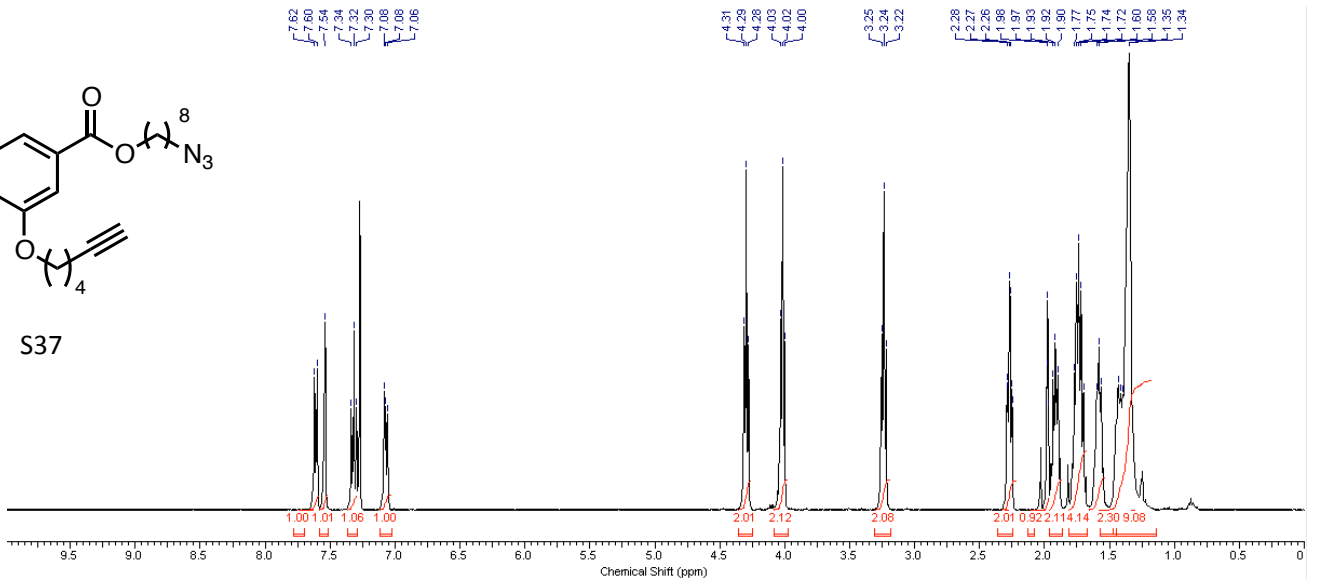


S35

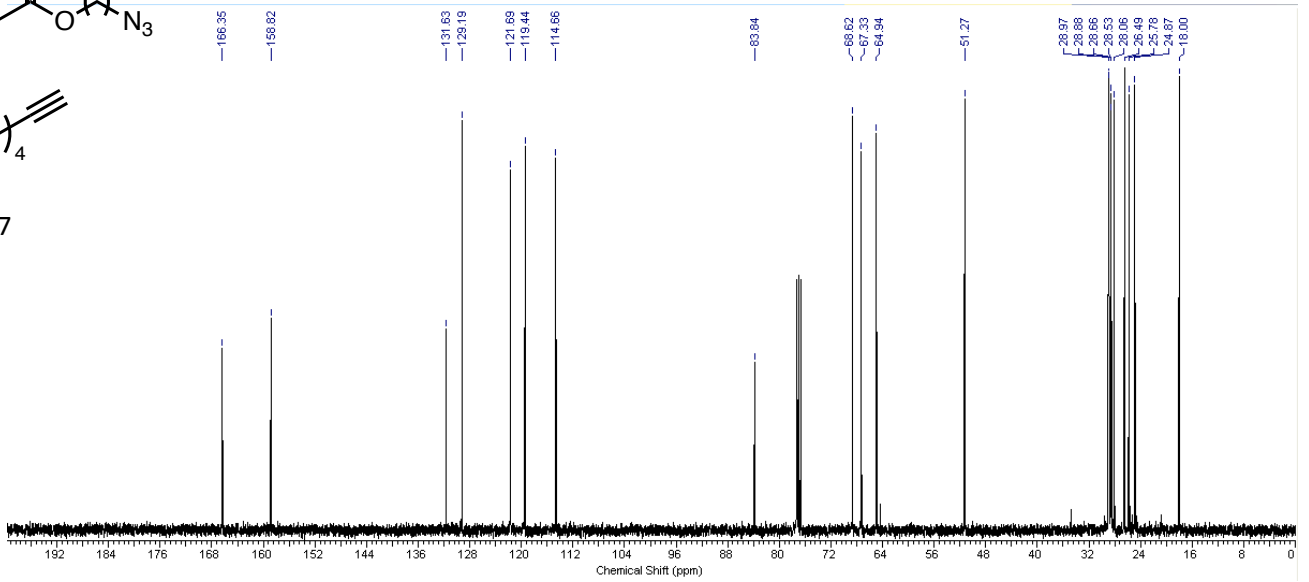




S37

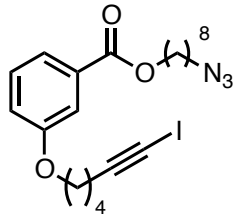


S37

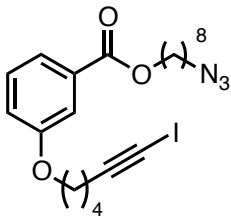
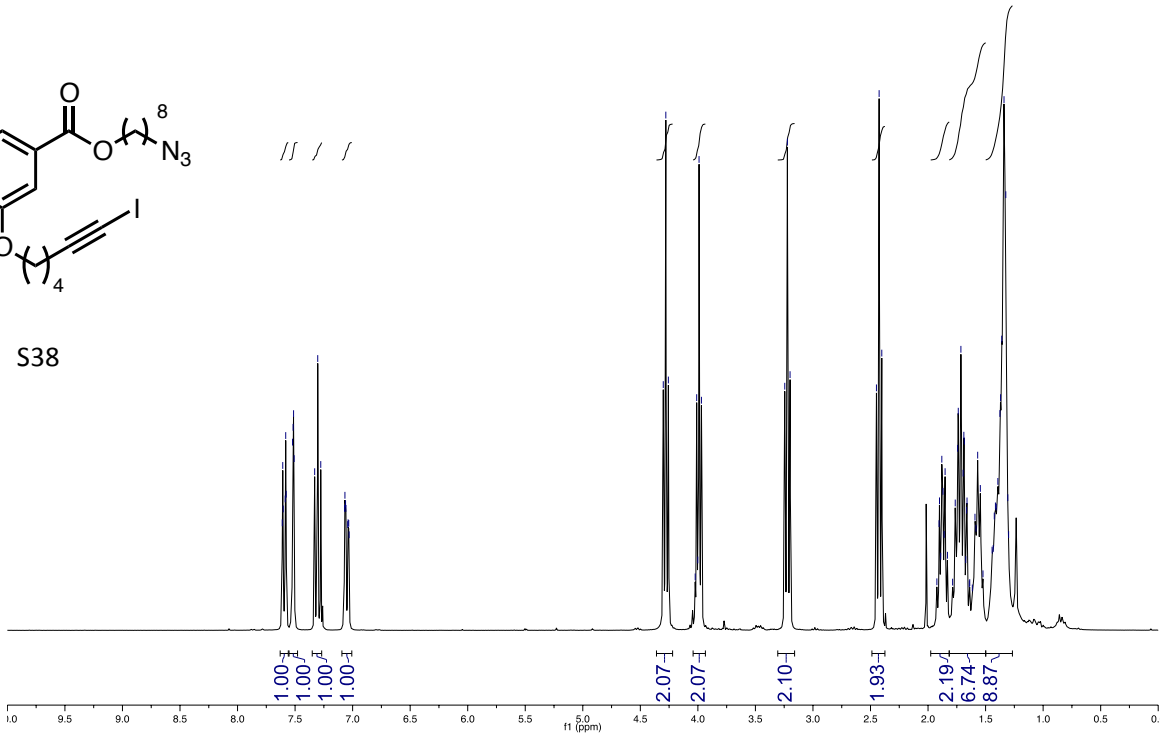


x6xxxxx

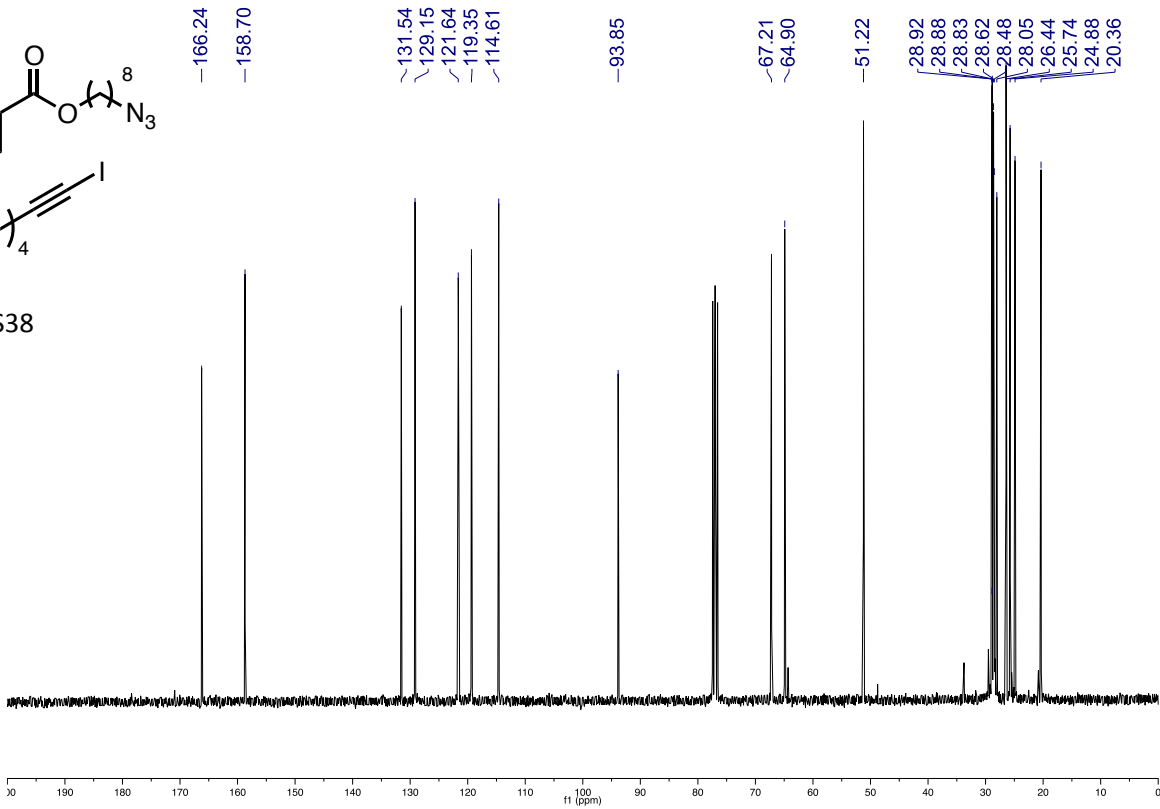
7.61
7.61
7.60
7.59
7.58
7.58
7.52
7.52
7.51
7.51
7.33
7.30
7.28
7.07
7.06
7.04
7.04
7.03
7.03
4.30
4.28
4.26
4.02
4.01
4.00
3.99
3.97
3.24
3.22
3.20
3.20
2.45
2.43
2.40
1.92
1.90
1.90
1.89
1.88
1.87
1.86
1.85
1.83
1.76
1.74
1.74
1.71
1.70
1.69
1.68
1.67
1.66
1.66
1.59
1.58
1.57
1.55
1.52
1.44
1.43
1.42
1.41
1.41
1.39
1.38
1.37
1.36
1.34
1.32
1.31
1.30



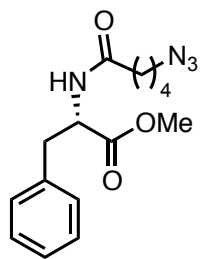
S38



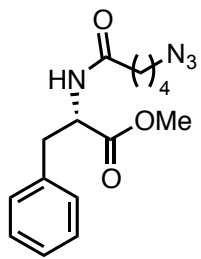
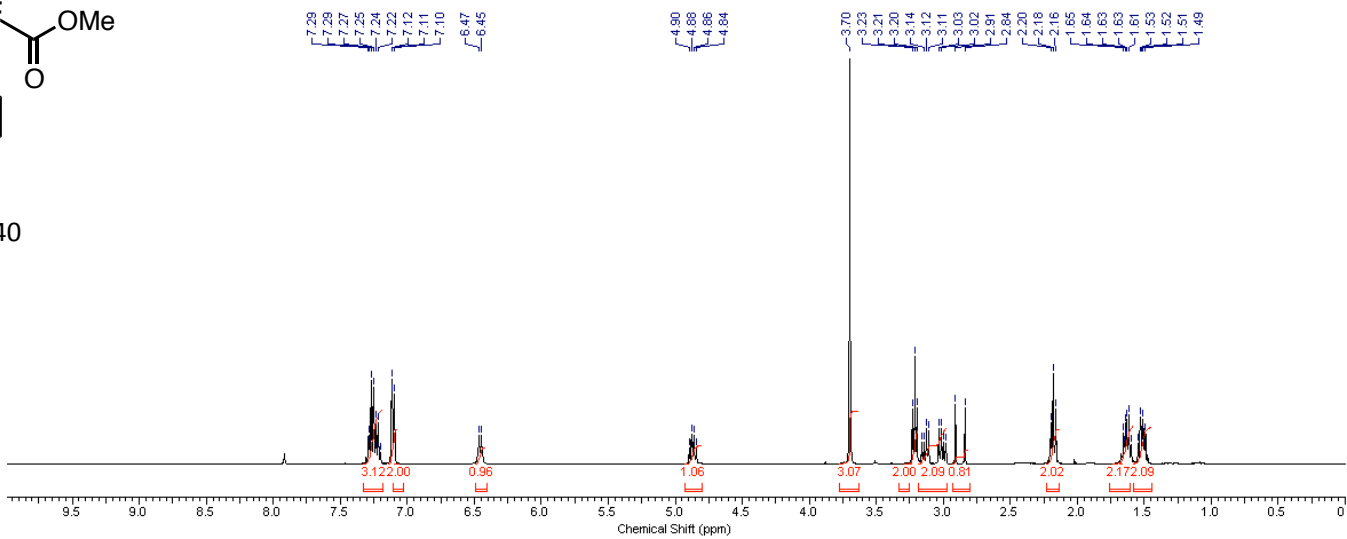
S38



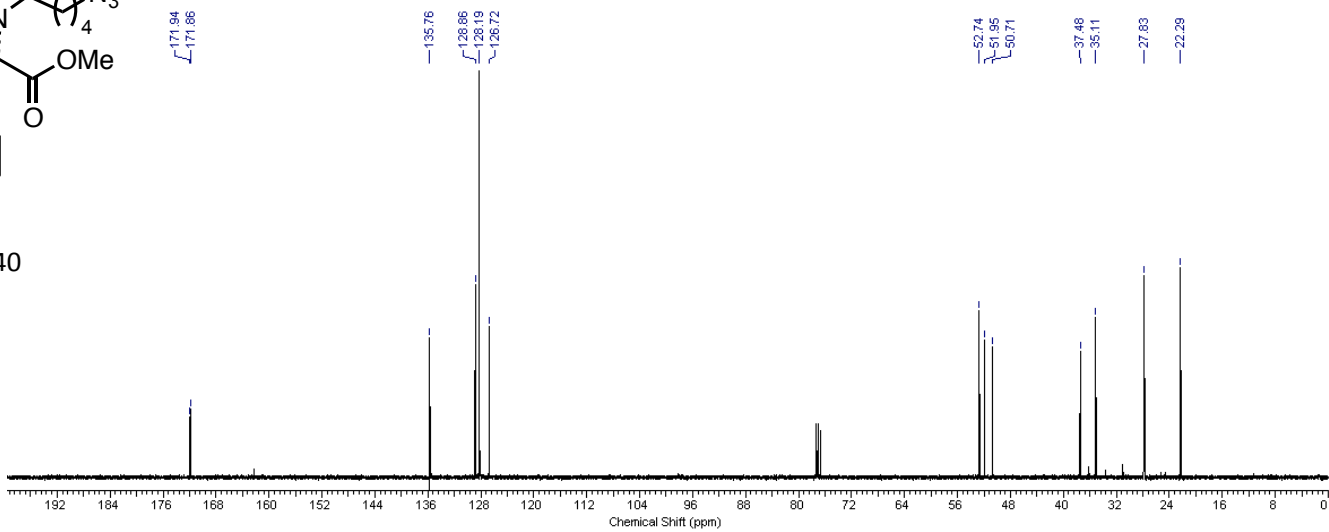
yyyyyy

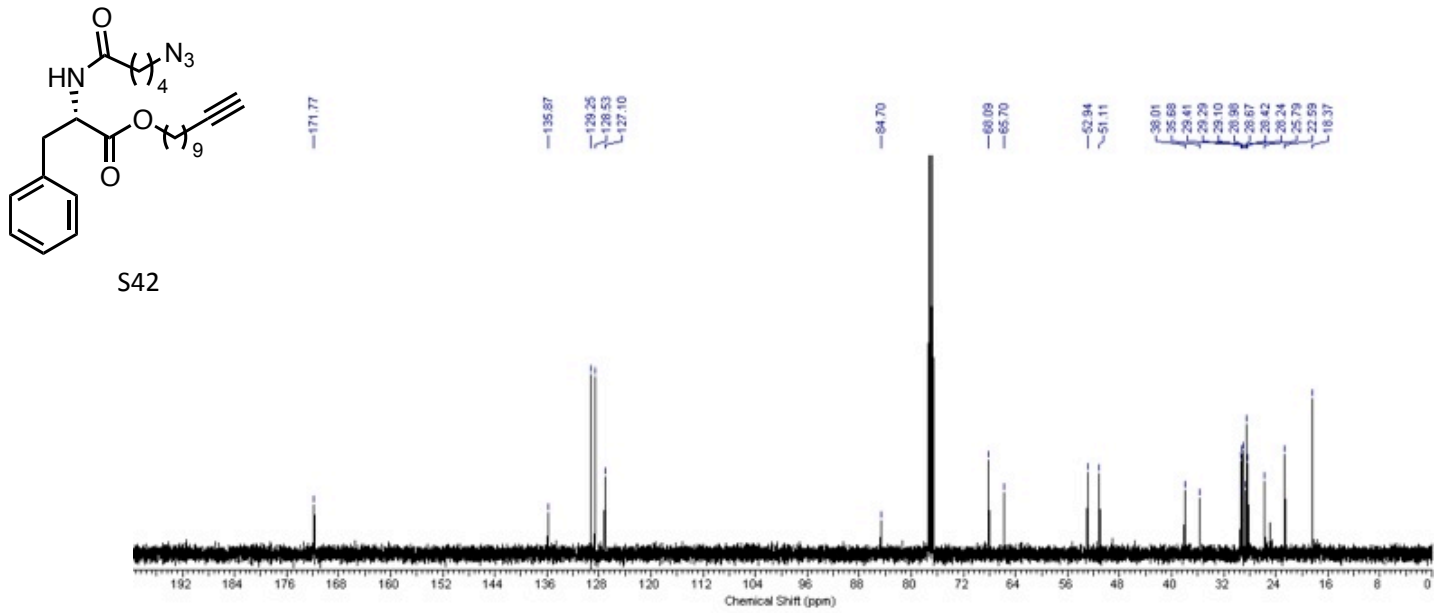
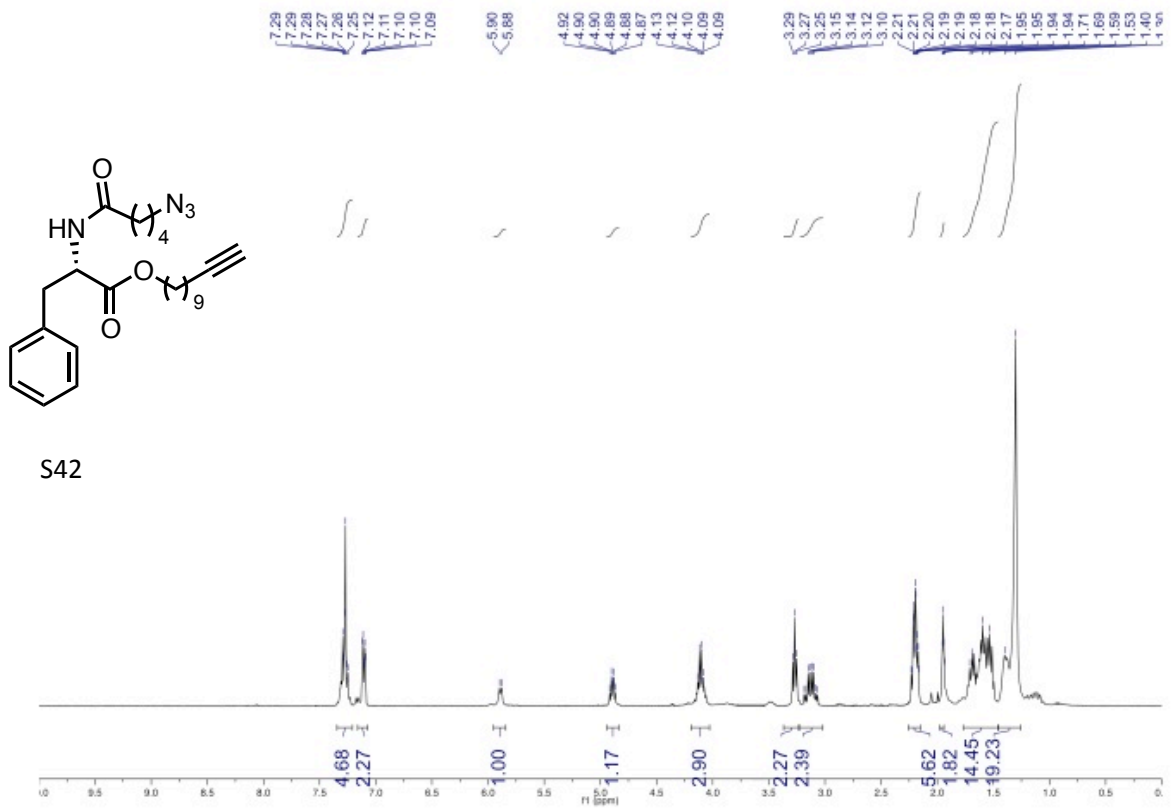


S40

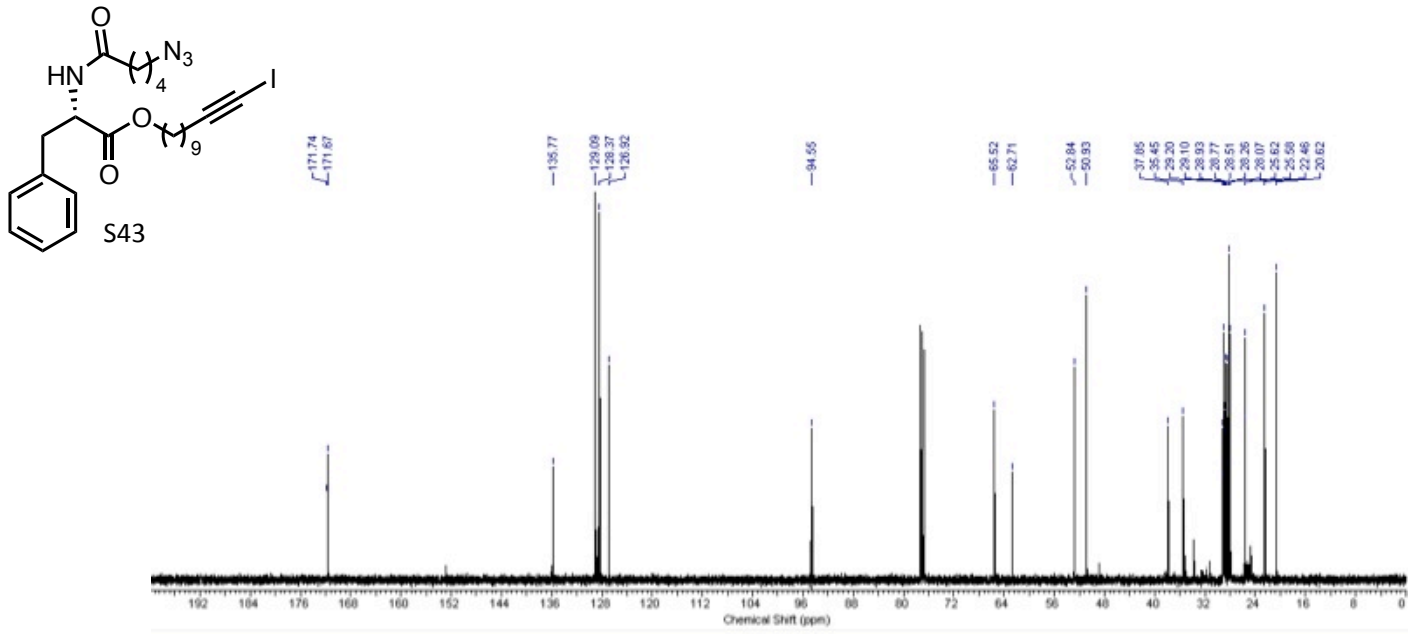
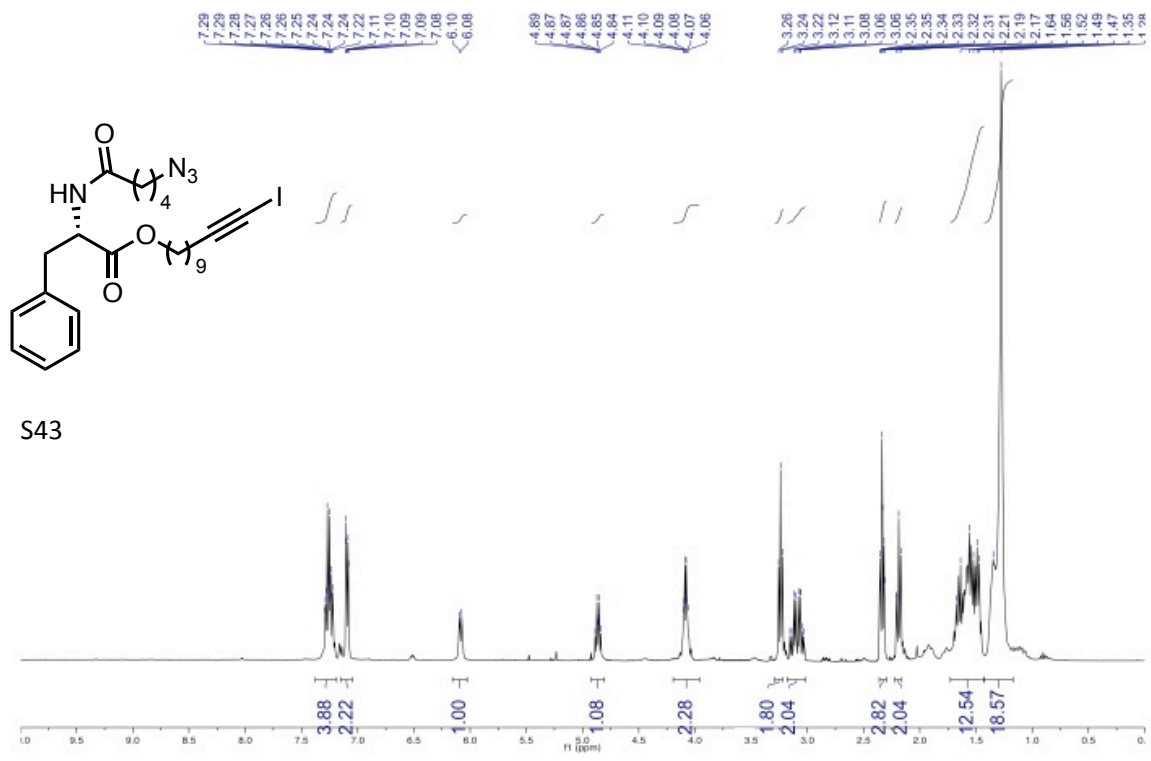


S40

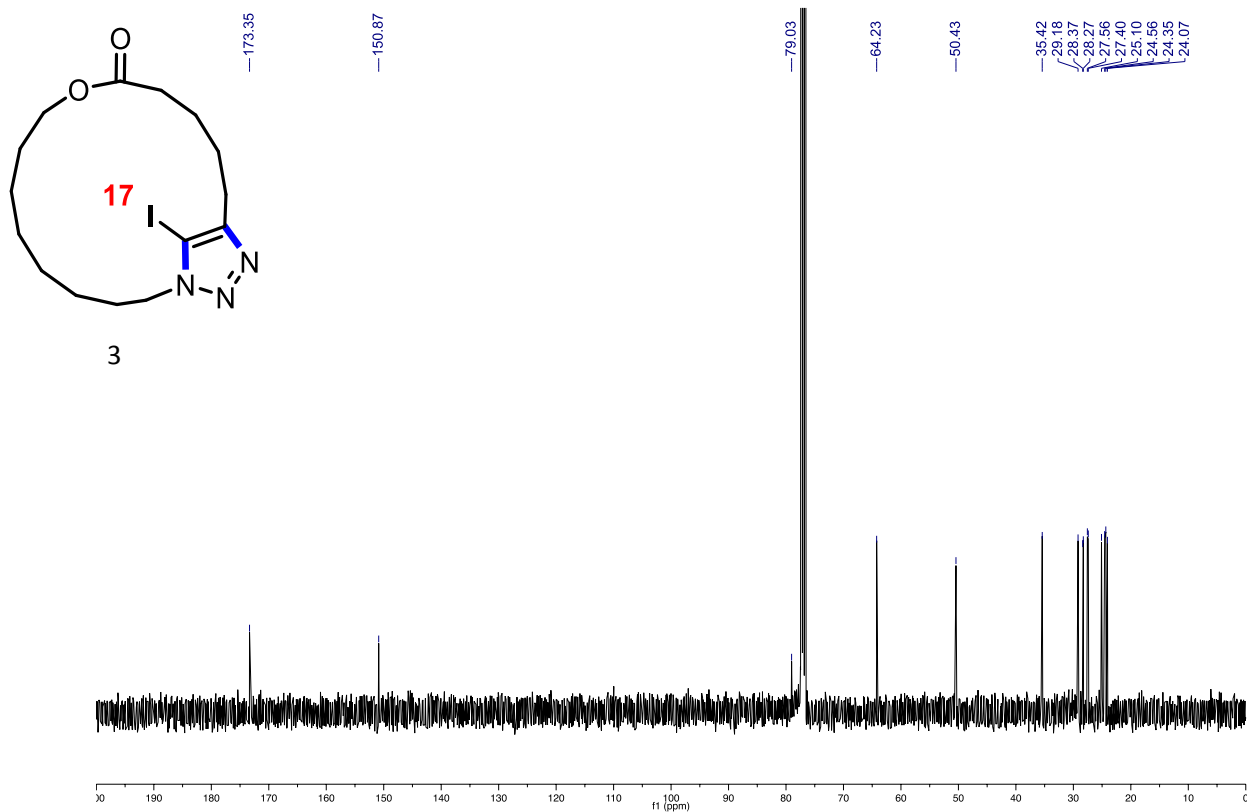
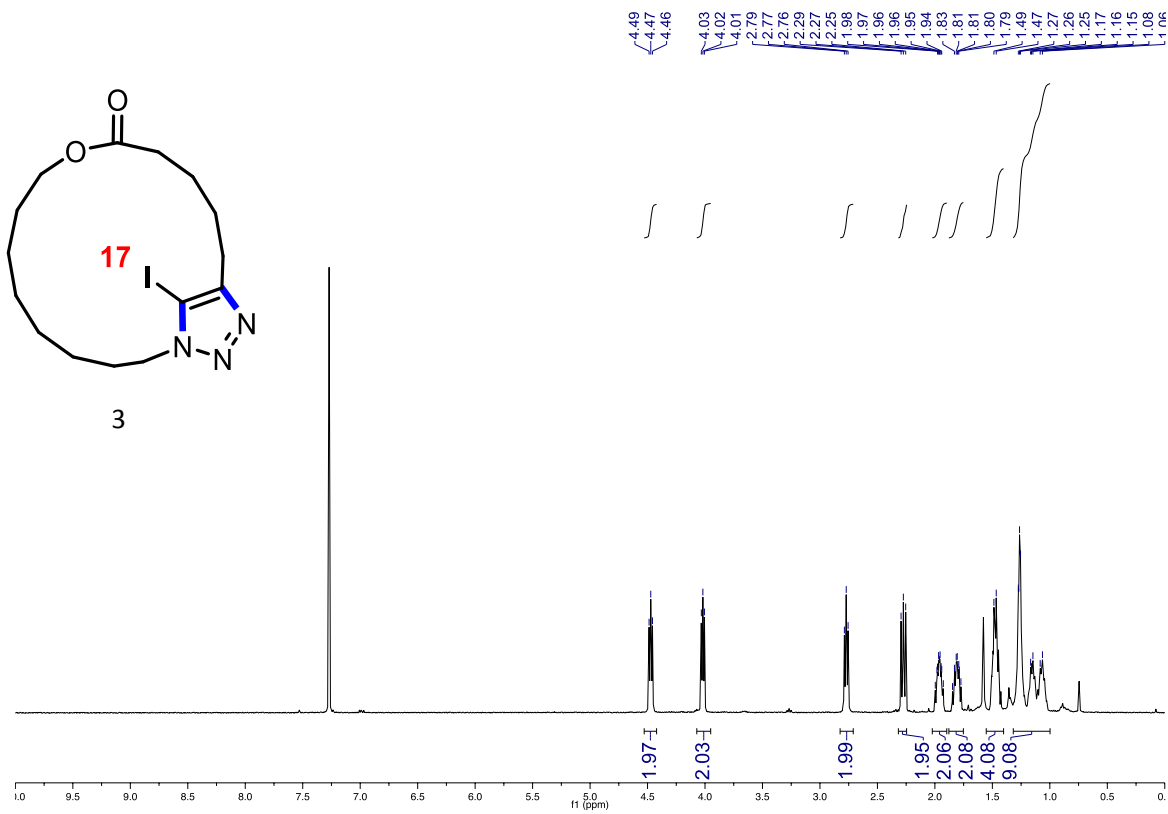


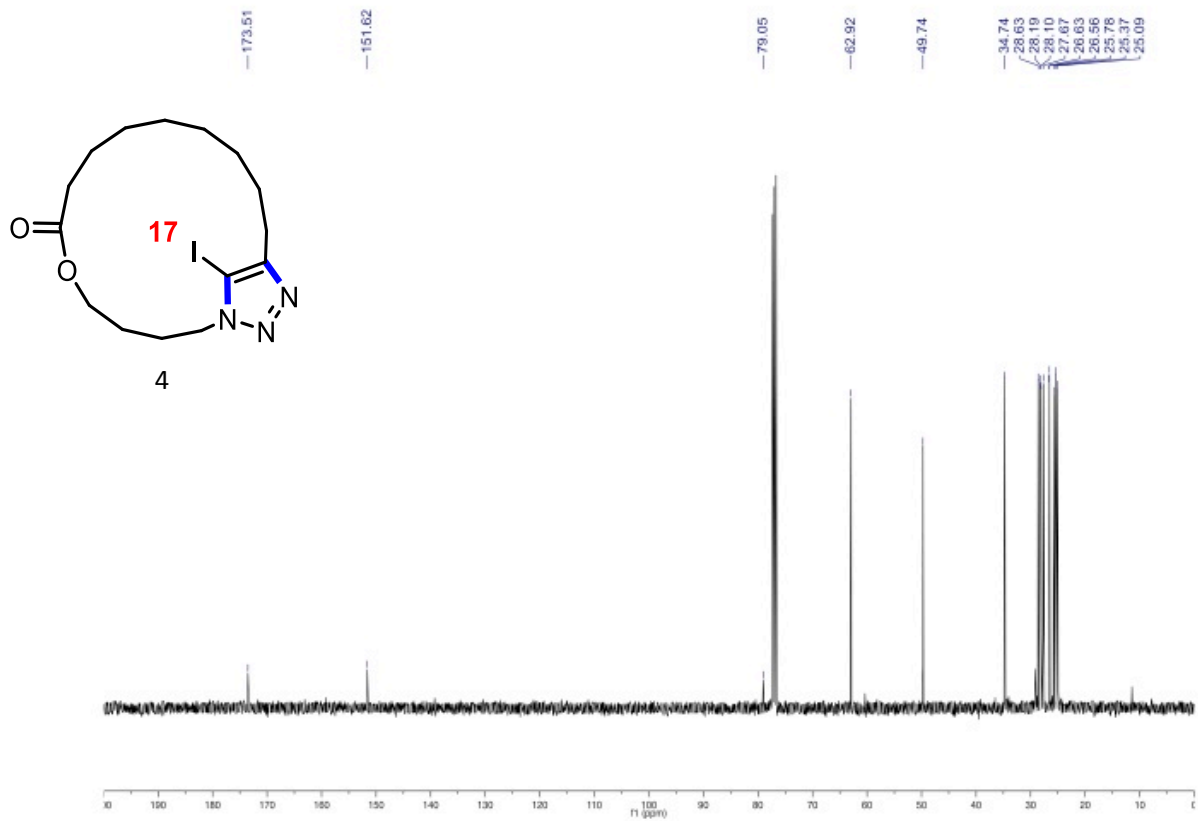
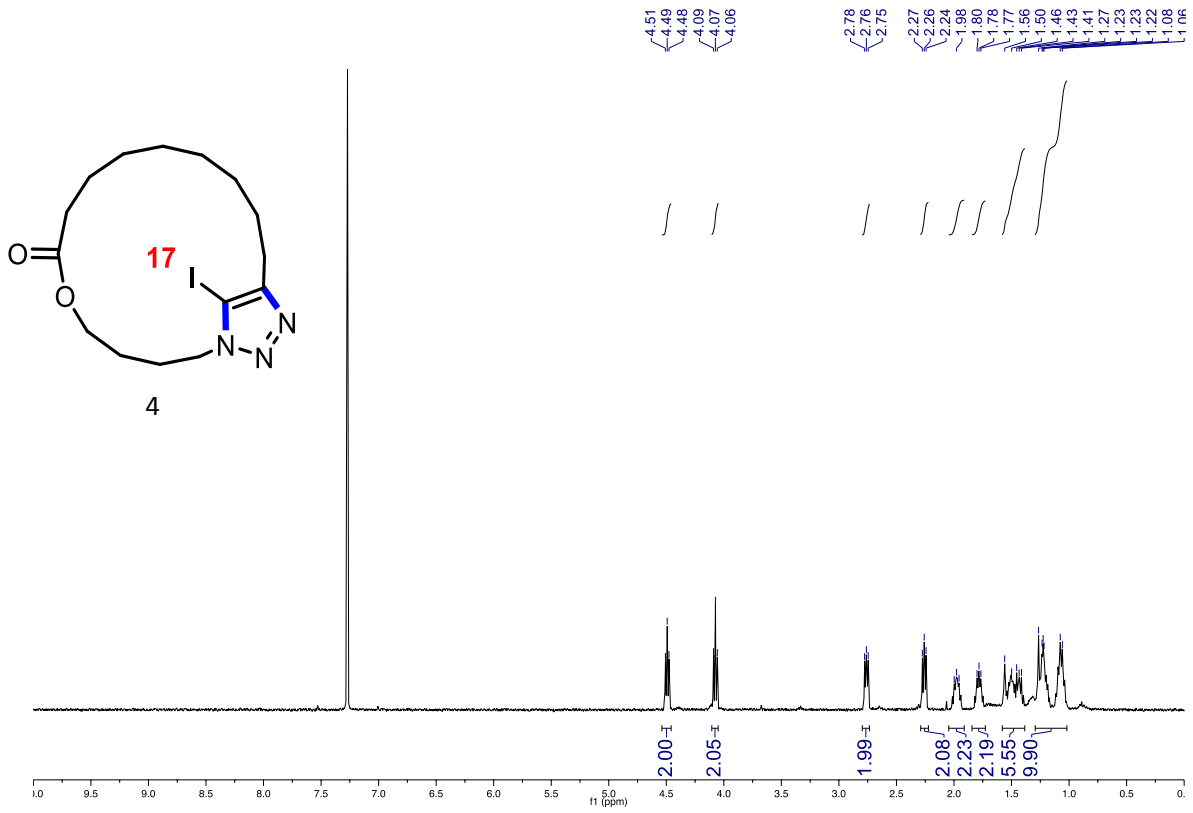


aaaaaaa

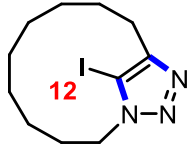


bbbbb

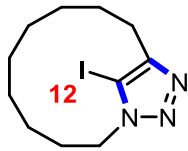
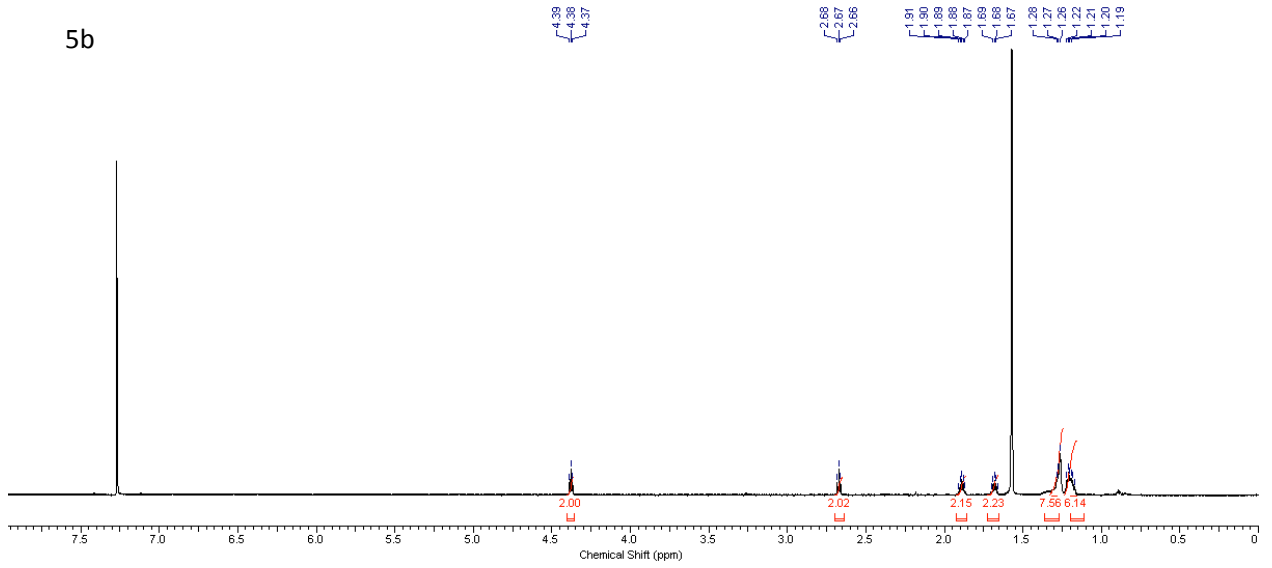




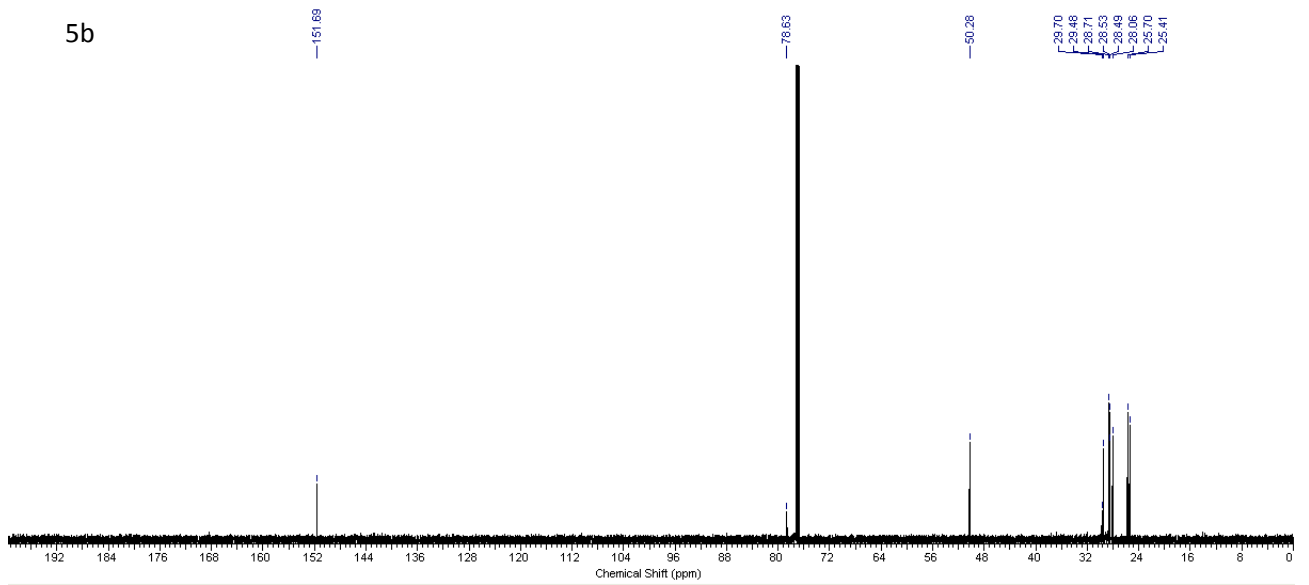
ddddd

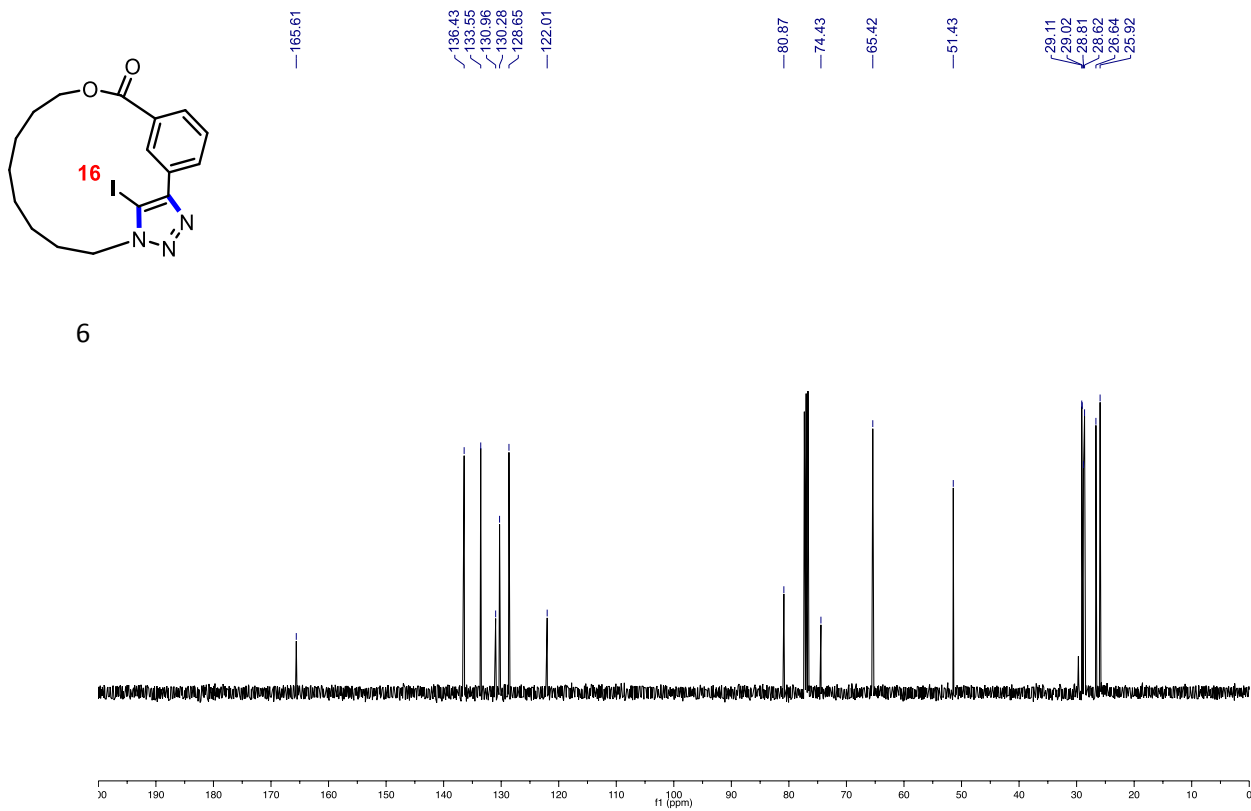
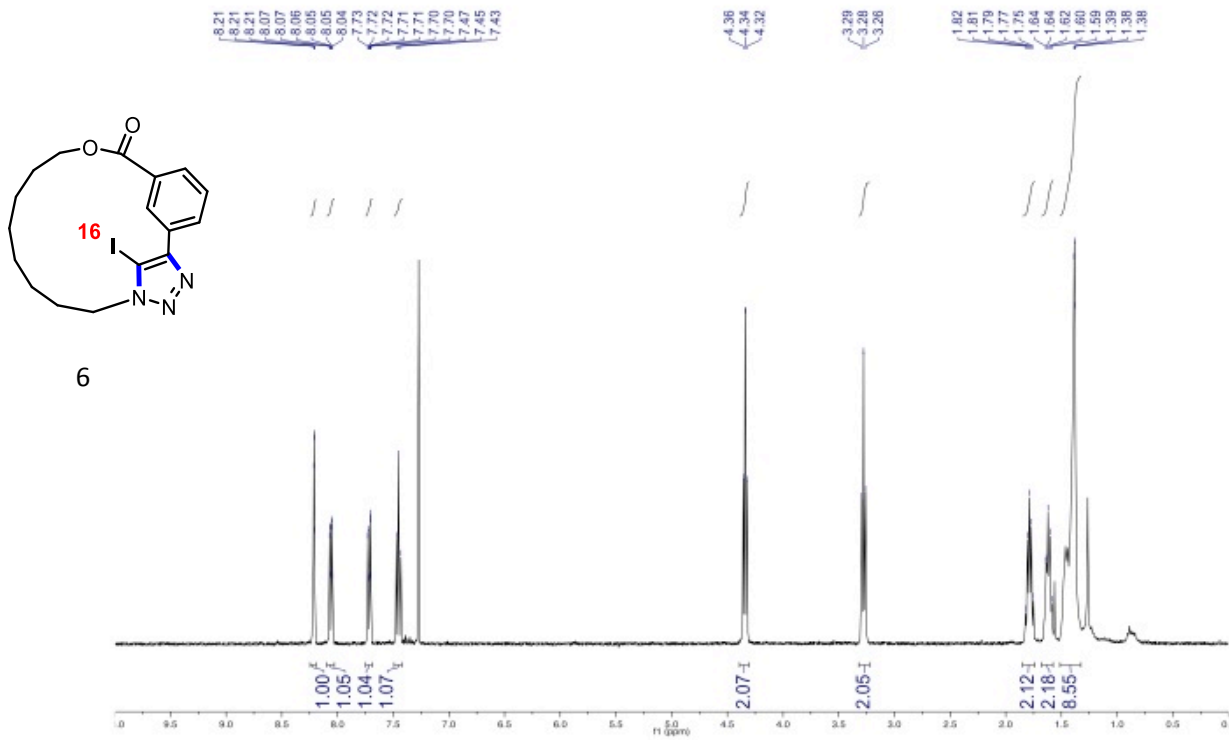


5b

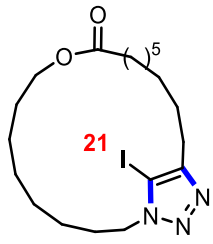


5b

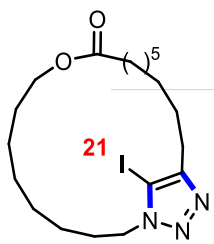
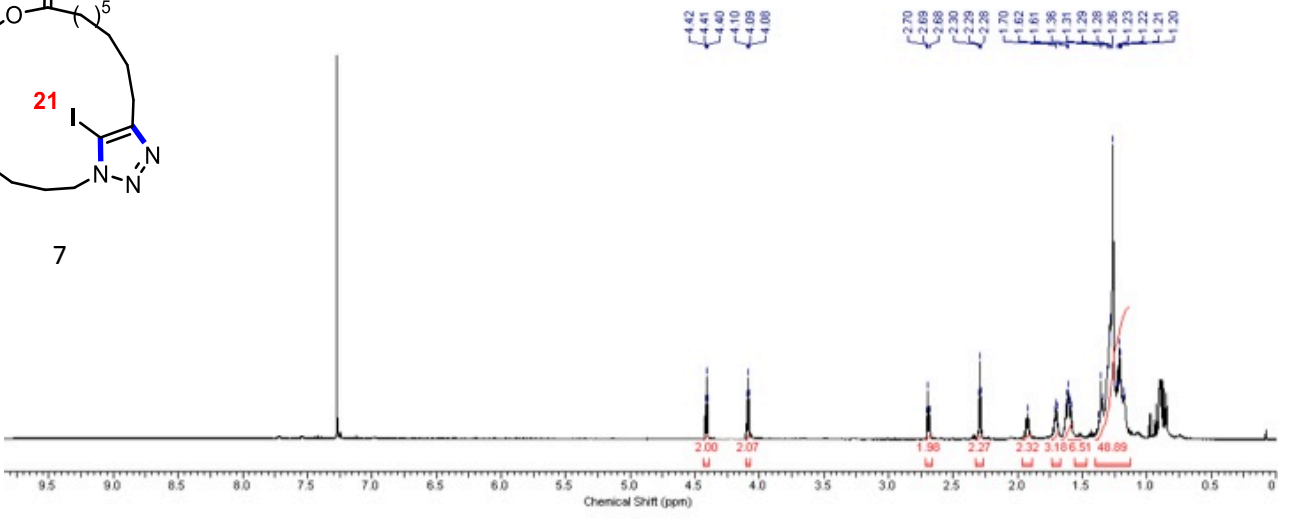




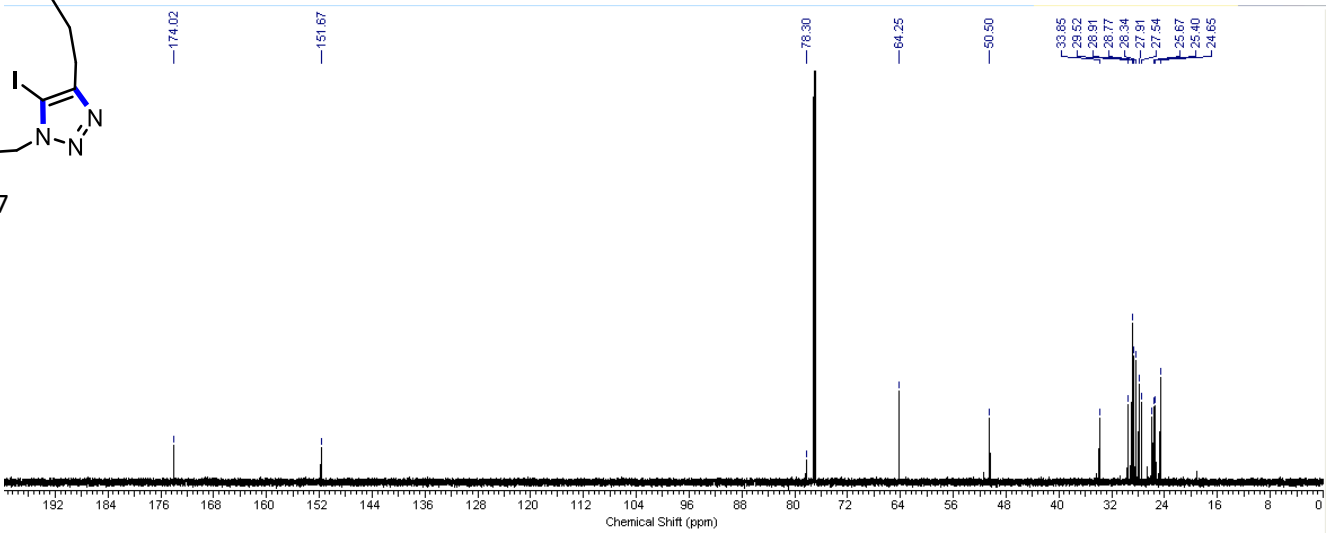
3fffff



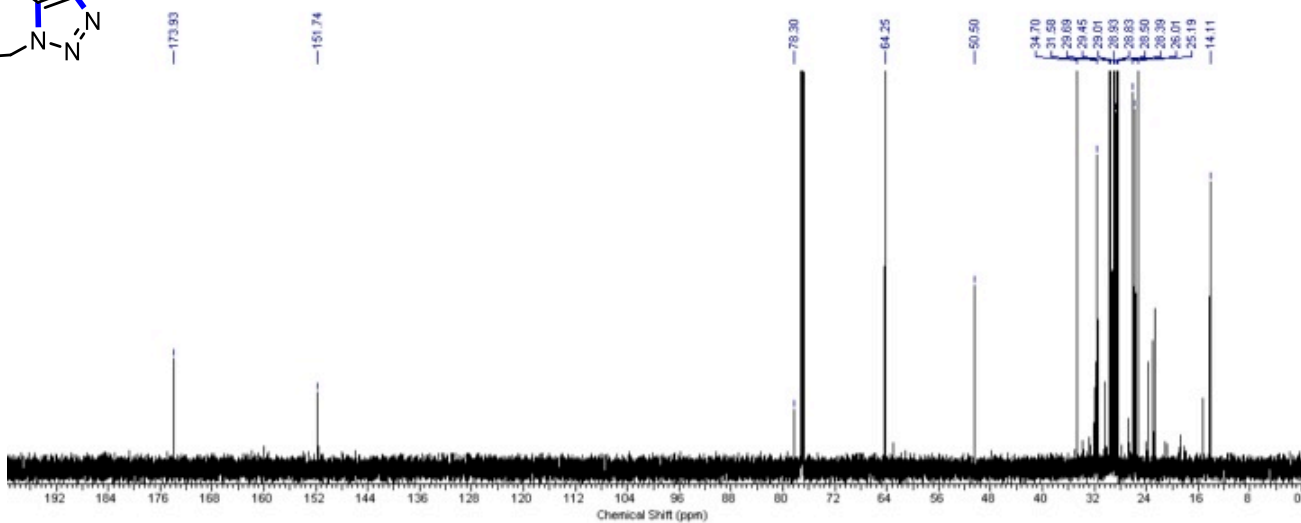
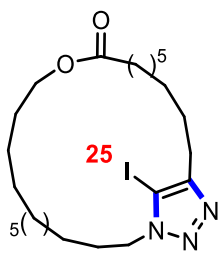
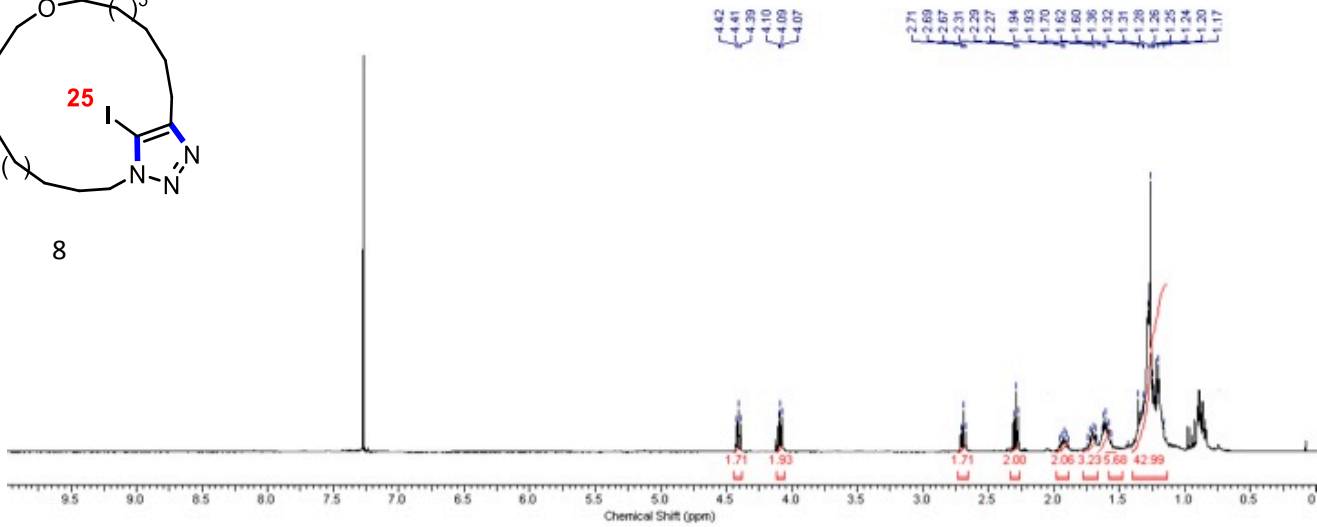
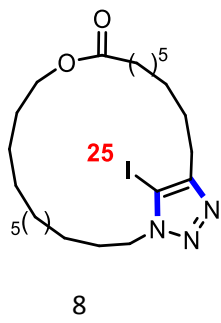
7



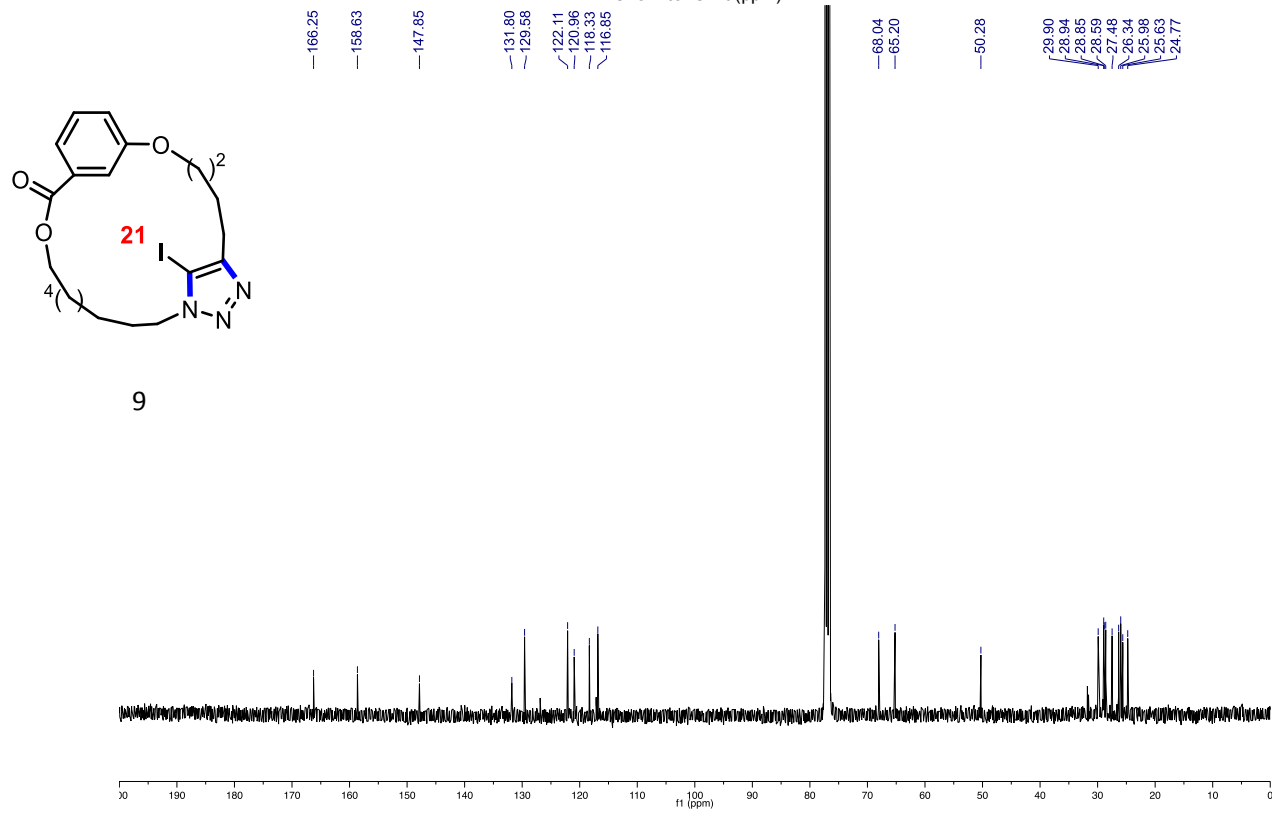
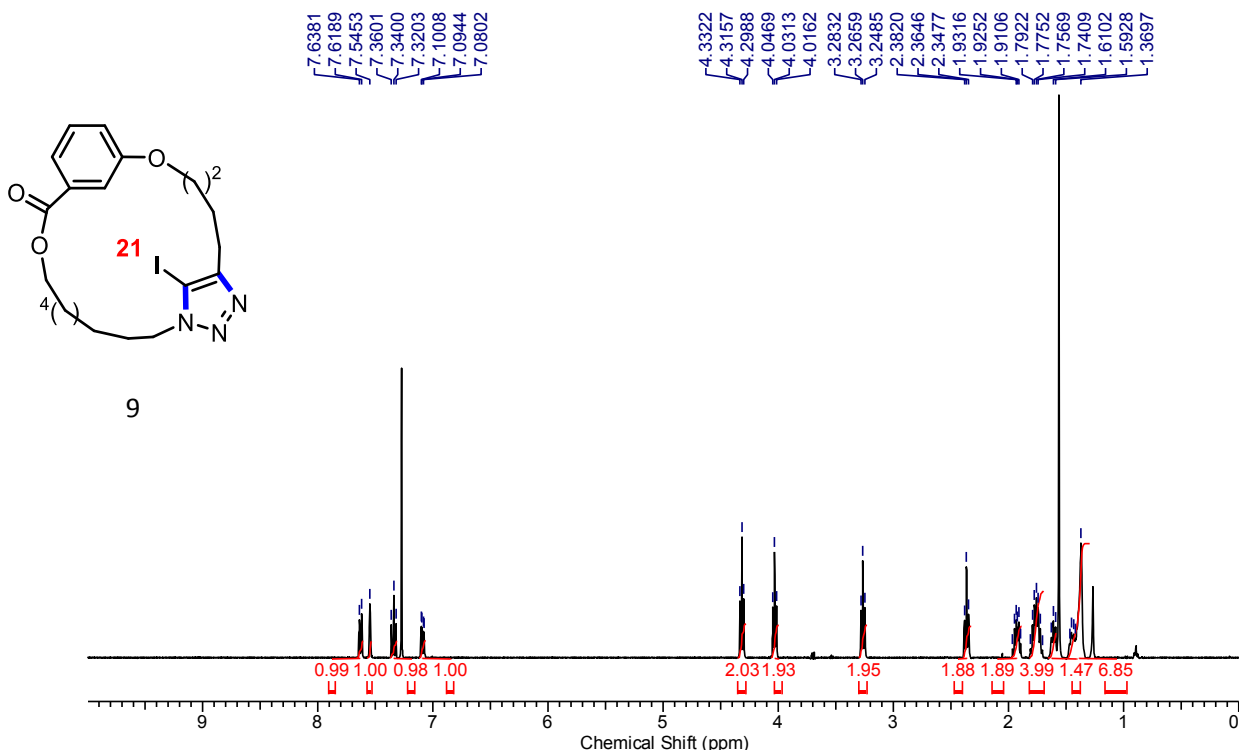
7



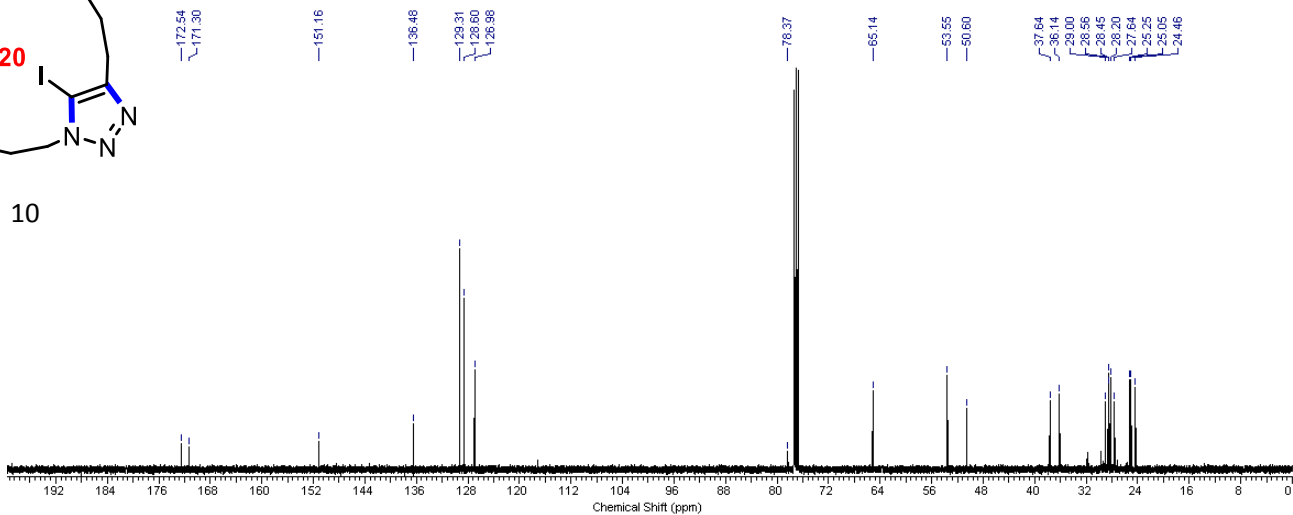
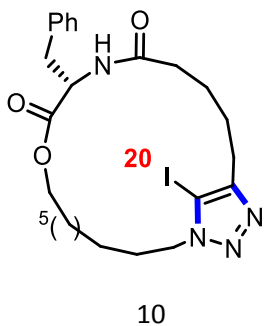
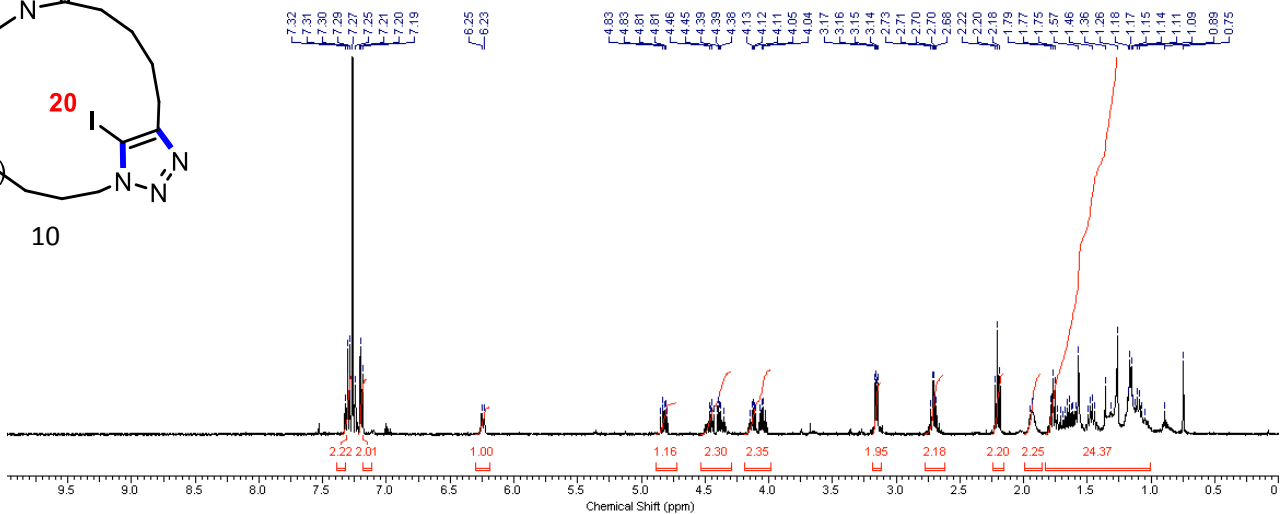
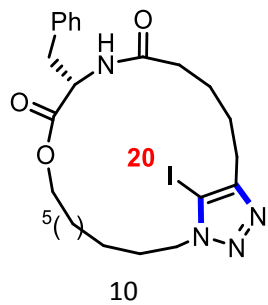
88888888

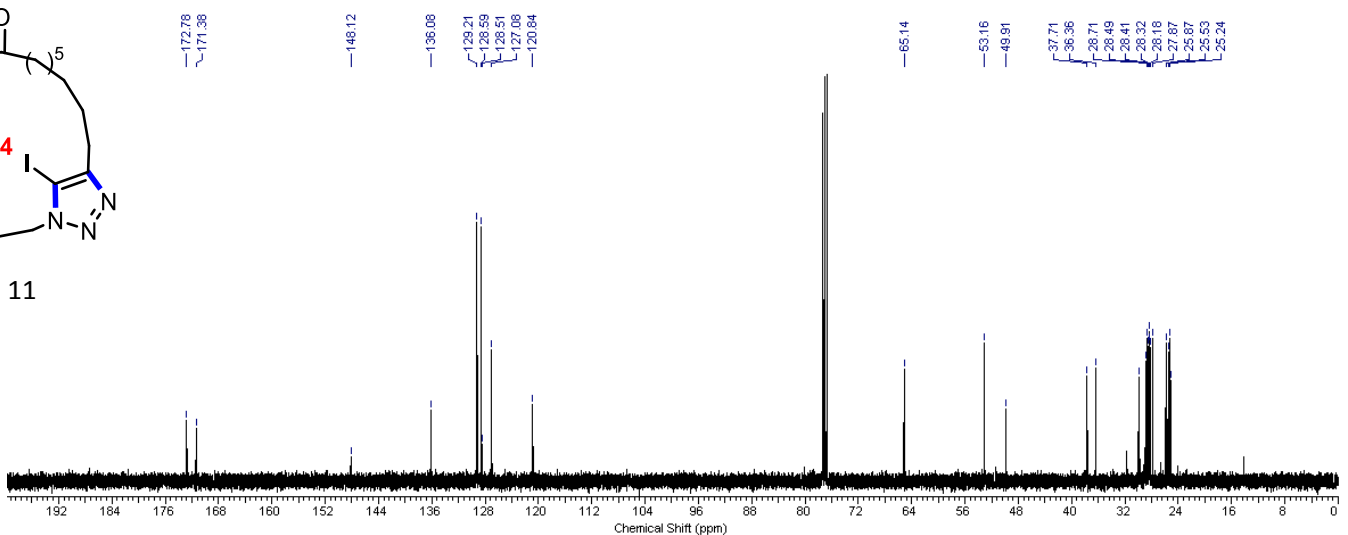
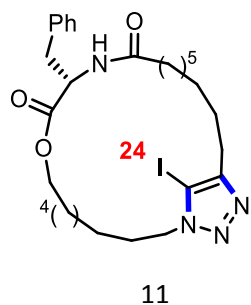
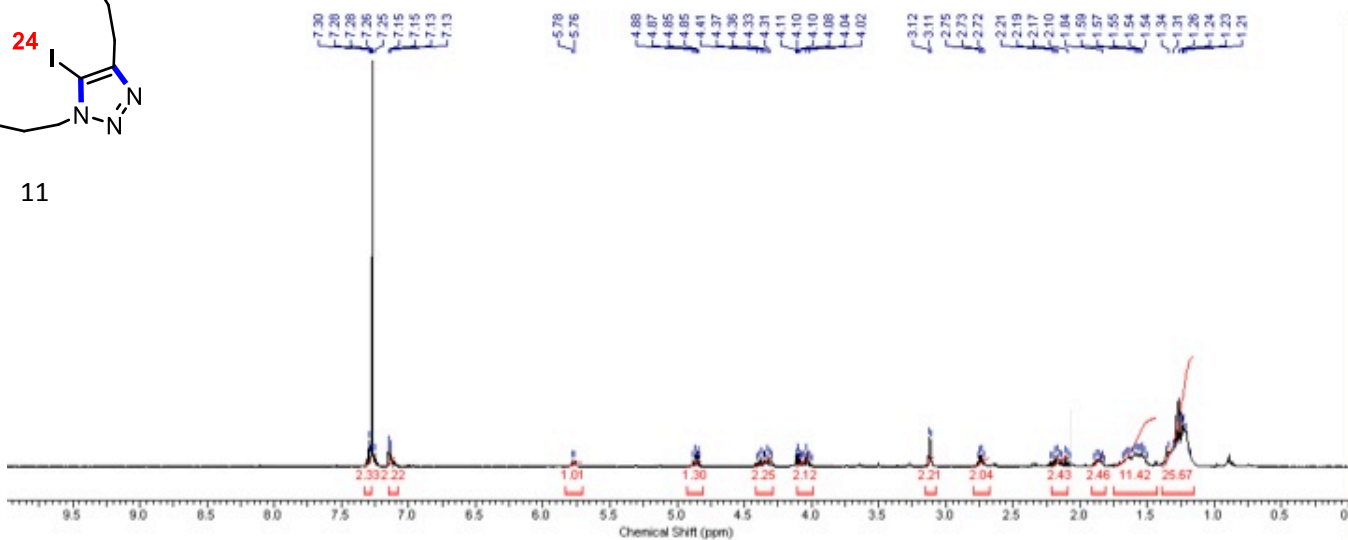
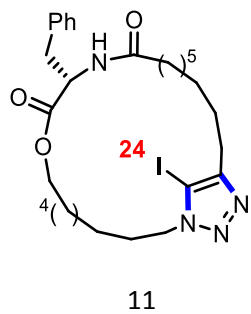


hhhhhhhh

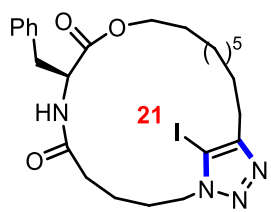


Siiiiiii

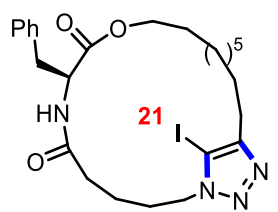
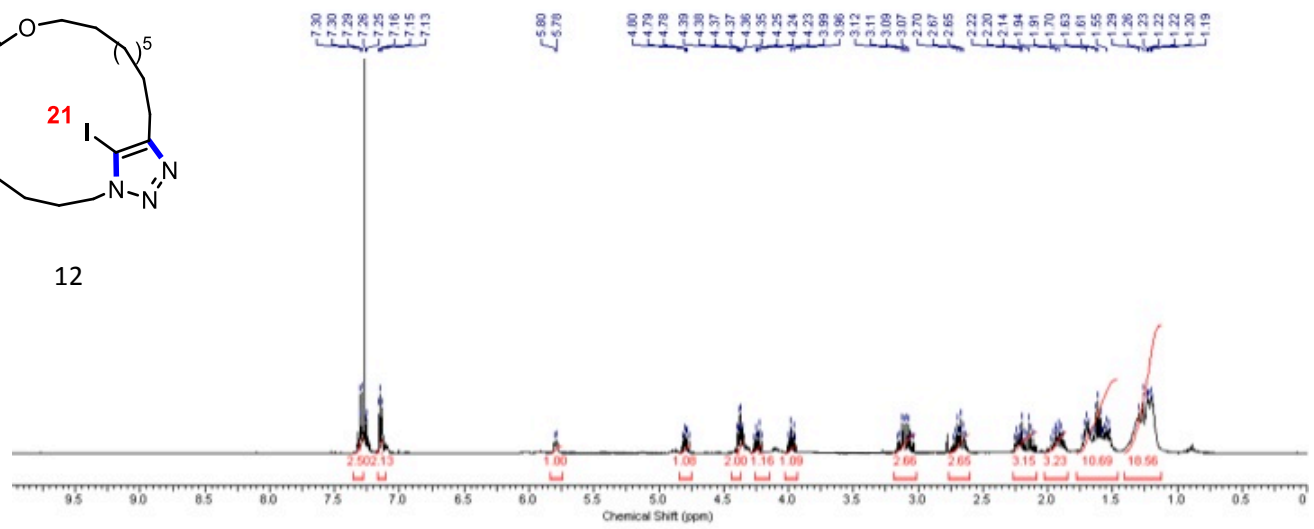




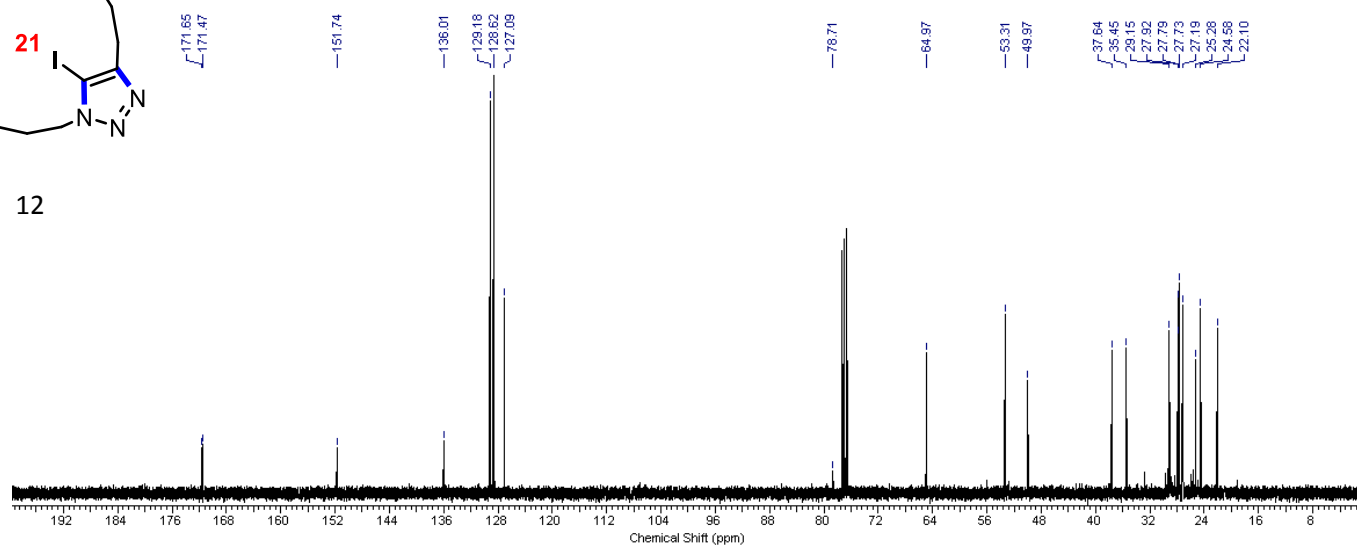
kk&kkkkk



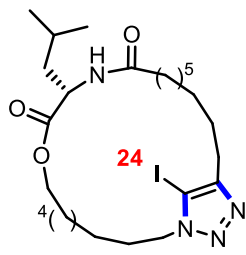
12



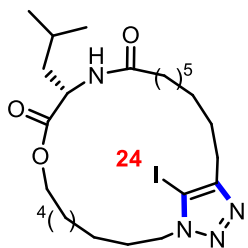
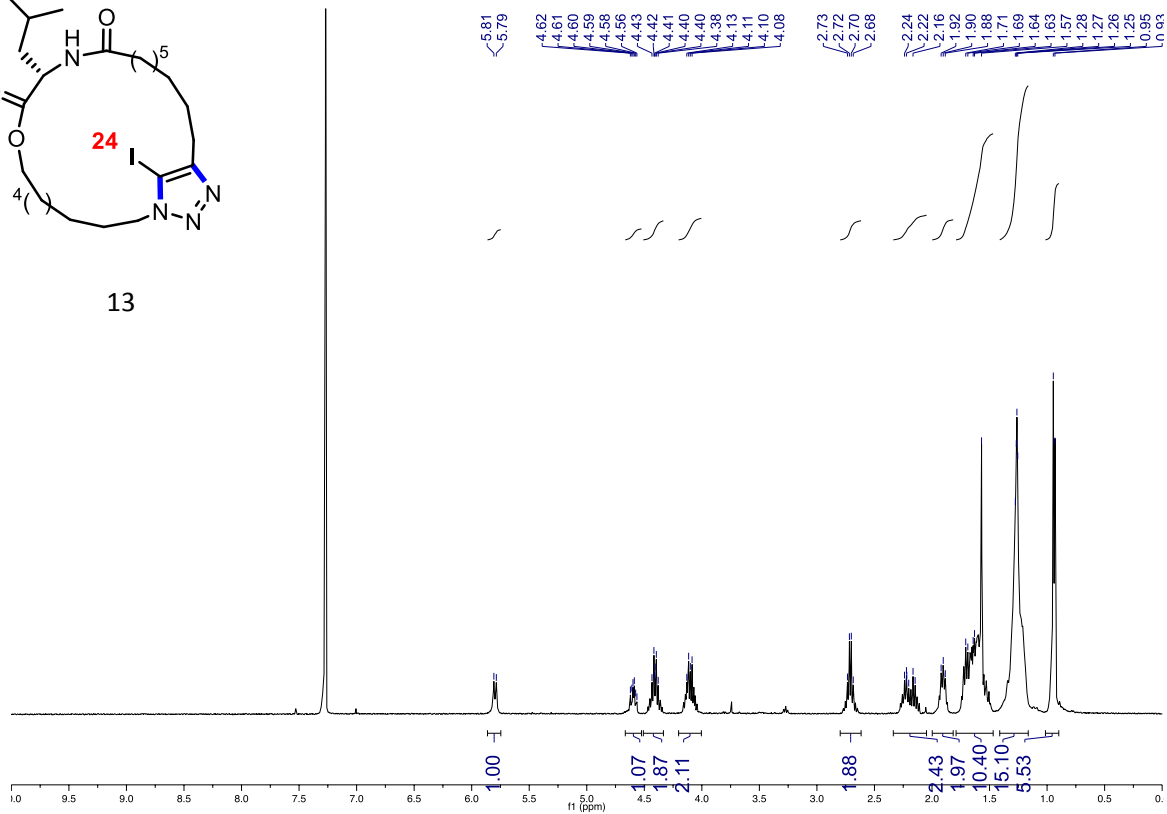
12



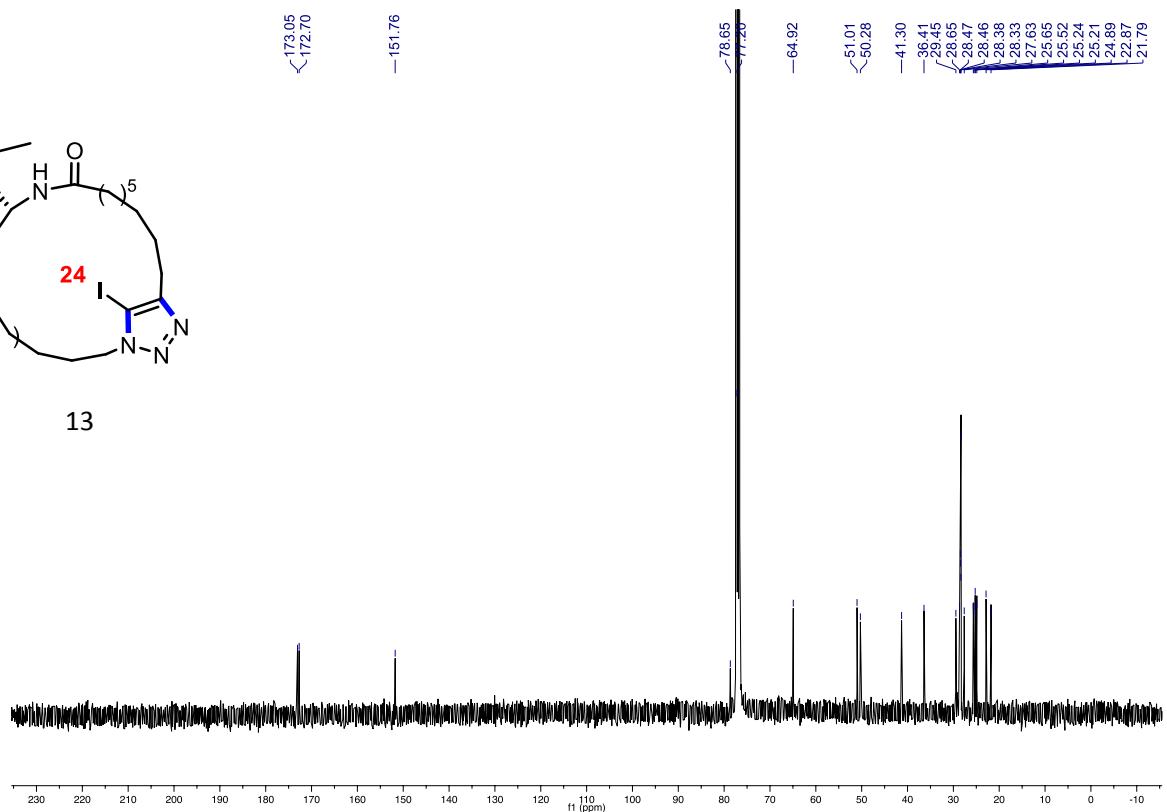
SI11111



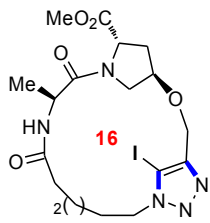
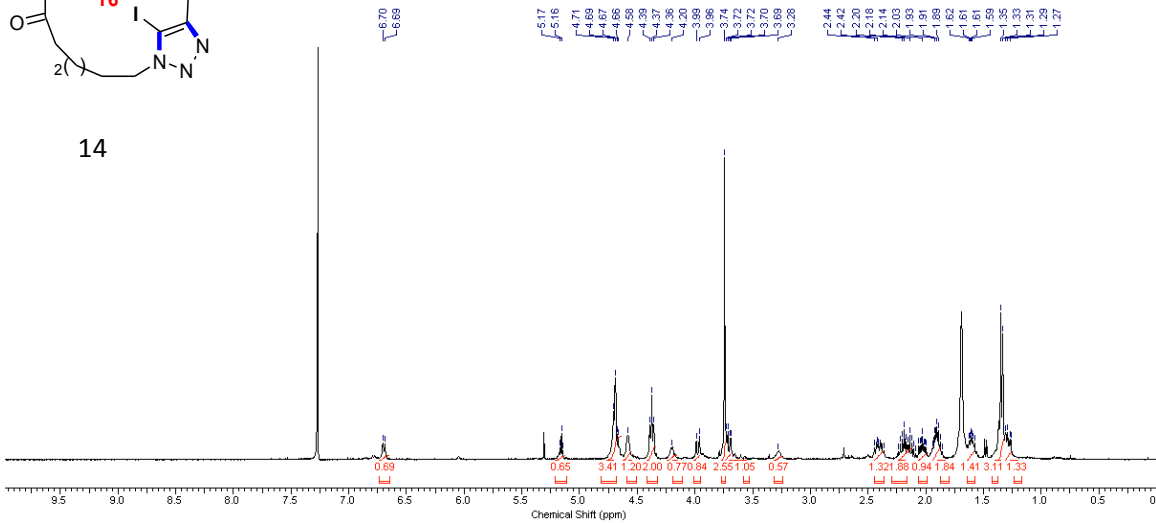
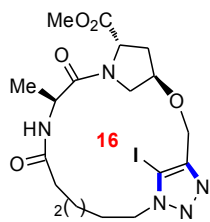
13



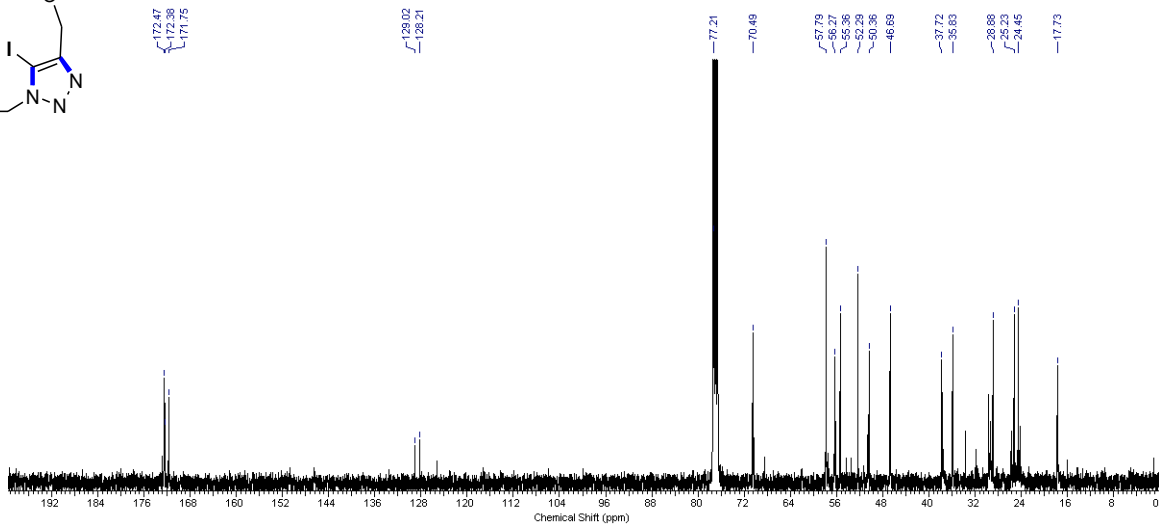
13



mmmmmmmm



14



ကကကကက

Chapter 19 : Supporting Information of Chapter 10: Efficient Continuous Flow Synthesis of Macrocyclic Triazoles

General:

All reactions that were carried out under anhydrous conditions were performed under an inert argon or nitrogen atmosphere in glassware that had previously been dried overnight at 120 °C or had been flame dried and cooled under a stream of argon or nitrogen.³⁵ All chemical products were obtained from Sigma-Aldrich Chemical Company or Strem Chemicals and were reagent quality. The following products were prepared according to their respective literature procedures: undec-10-yn-1-ol,³⁶ heneicos-20-yn-1-ol,³⁷ and 8-azido-octyl 3-ethynylbenzoate.³⁸ Technical solvents were obtained from VWR International Co. Anhydrous solvents (CH₂Cl₂, Et₂O, THF, DMF, Toluene, and hexanes) were dried and deoxygenated using a GlassContour system (Irvine, CA). Isolated yields reflect the mass obtained following flash column silica gel chromatography. Organic compounds were purified using the method reported by W. C. Still³⁹ and using silica gel obtained from Silicycle Chemical division (40-63 nm; 230-240 mesh). Analytical thin-layer chromatography (TLC) was performed on glass-

³⁵ Shriver, D. F.; Drezdon, M. A. in *The Manipulation of Air-Sensitive Compounds*; Wiley-VCH: New York, 1986.

³⁶ Bédard, A.-C.; Collins, S. K. *J. Am. Chem. Soc.* **2011**, *133*, 19976.

³⁷ Lumbroso, A.; Abermil, N.; Breit, B. *Chem. Sci.* **2012**, *3*, 789.

³⁸ Bédard, A.-C.; Collins, S. K. *Org. Lett.* **2014**, *16*, 5286.

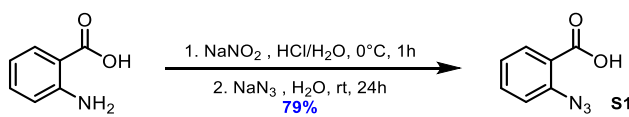
³⁹ Still, W. C.; Kahn, M.; Mitra, A. *J. Org. Chem.* **1978**, *43*, 2923.

backed silica gel 60 coated with a fluorescence indicator (Silicycle Chemical division, 0.25 mm, F₂₅₄). Visualization of TLC plate was performed by UV (254 nm), KMnO₄ or *p*-anisaldehyde stains. All mixed solvent eluents are reported as v/v solutions. Concentration refers to removal of volatiles at low pressure on a rotary evaporator. All reported compounds were homogeneous by thin layer chromatography (TLC) and by ¹H NMR. NMR spectra were taken in deuterated CDCl₃ using Bruker AV-300 and AV-400 instruments unless otherwise noted. Signals due to the solvent served as the internal standard (CHCl₃: δ 7.27 for ¹H, δ 77.0 for ¹³C). The ¹H NMR chemical shifts and coupling constants were determined assuming first-order behavior. Multiplicity is indicated by one or more of the following: s (singlet), d (doublet), t (triplet), q (quartet), m (multiplet), br (broad); the list of couplings constants (*J*) corresponds to the order of the multiplicity assignment. The ¹H NMR assignments were made based on chemical shift and multiplicity. The ¹³C NMR assignments were made on the basis of chemical shift. High resolution mass spectroscopy (HRMS) was done by the Centre régional de spectrométrie de masse at the Département de Chimie, Université de Montréal from an Agilent LC-MSD TOF system using ESI mode of ionization unless otherwise noted.

pppppppp

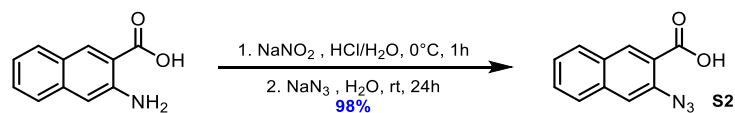
SYNTHESIS OF MACROCYCLIZATION PRECURSORS

General Procedure A for Azidation: To a stirred solution of concentrated hydrochloric acid in water (25 % v/v, 0.2 M) was added the aniline (1 equiv.) at 0 °C. An aqueous solution of sodium nitrite (1.2 equiv) was added dropwise to the reaction mixture once the starting material was completely dissolved. The reaction mixture was stirred at 0 °C for 1 hour. An aqueous solution of sodium azide (1.2 equiv.) was then added dropwise and the reaction mixture was stirred at room temperature for 24 hours to induce the precipitation of the aryl azide. The precipitate was isolated by filtration and was subsequently washed with water and ether. The desired product was finally dried under vacuum and was used without further purification.

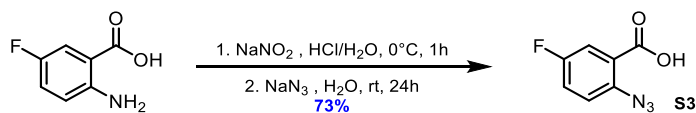


2-Azidobenzoic acid (S1): Following the General Procedure A, 2-aminobenzoic acid (0.586 g, 4.27 mmol, 1.0 equiv.) was dissolved in an aqueous solution of hydrochloric acid (20 mL) in a round bottom flask equipped with a stir bar. Aqueous solutions of sodium nitrite (0.345 g, 5.00 mmol, 1.2 equiv.) in 2 mL of water and of sodium azide (0.325 g, 5.00 mmol, 1.2 equiv.) in 2 mL of water were then added subsequently to the reaction mixture. Following filtration, the desired product was obtained as a beige solid (0.548 g, 79 % yield). NMR data was in accordance with what was previously reported.⁴⁰

⁴⁰ Barral, K.; Moorhouse, A. D.; Moses, J. E. *Org. Lett.* **2007**, *9*, 1809.

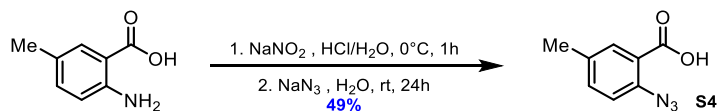


3-Azido-2-naphthoic acid (S2): Following the General Procedure A, 3-amino-2-naphthoic acid (1.00 g, 4.27 mmol, 1.0 equiv.) was dissolved in an aqueous solution of hydrochloric acid (20 mL) in a round bottom flask equipped with a stir bar. Aqueous solutions of sodium nitrite (0.345 g, 5.00 mmol, 1.2 equiv.) in 2 mL of water and of sodium azide (0.325 g, 5.00 mmol, 1.2 equiv.) in 2 mL of water were then added subsequently to the reaction mixture. Following filtration, the desired product was obtained as a red solid (0.892g, 98 % yield). ^1H NMR (400 MHz, DMSO- d_6) δ = 13.27 (br. s., 1H), 8.42 (s, 1H), 8.04 (d, J = 8.1 Hz, 1H), 7.97 (d, J = 8.1 Hz, 1H), 7.90 (s, 1H), 7.61 - 7.67 (m, 1H), 7.50 - 7.57 (m, 1H); ^{13}C NMR (100 MHz, DMSO- d_6) δ = 166.6, 135.3, 134.6, 132.0, 129.6, 128.8, 128.7, 126.6, 126.4, 123.6, 117.9; HRMS (ESI) m/z calculated for $\text{C}_{11}\text{H}_6\text{N}_3\text{O}_2$ $[\text{M}-\text{H}]^-$ 212.0466; found 212.0472.

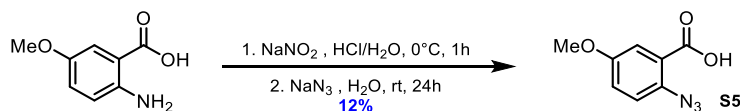


2-Azido-5-fluorobenzoic acid (S3): Following the General Procedure A, 2-amino-5-fluorobenzoic acid (0.662 g, 4.27 mmol, 1.0 equiv.) was dissolved in an aqueous solution of hydrochloric acid (20 mL) in a round bottom flask equipped with a stir bar. Aqueous solutions of sodium nitrite (0.345 g, 5.00 mmol, 1.2 equiv.) in 2 mL of water and of sodium azide (0.325 g, 5.00 mmol, 1.2 equiv.) in 2 mL of water were then added subsequently to the reaction mixture. Following filtration, the desired product was obtained as a white solid (0.57 g, 73 % yield). ^1H NMR (400 MHz, DMSO- d_6) δ = 13.47 (br. s., 1H), 7.56 (dd, J = 8.9, 3.0 Hz, 1H), 7.45 - 7.51 (m, 1H), 7.39 - 7.44 (m, 1H); ^{13}C NMR (100 MHz, DMSO- d_6) δ = 165.3 (d, J = 2.2 Hz), 158.5 (d, J = 243.4 Hz), 134.9 (d, J = 2.8 Hz), 125.6 (d, J = 7.2 Hz), 123.2 (d,

$J = 8.2$ Hz), 120.0 (d, $J = 23.3$ Hz), 117.3 (d, $J = 24.4$ Hz); ^{19}F NMR (375 MHz, DMSO- d_6) $\delta = 117.2$ (td, $J = 8.4, 4.8$ Hz); HRMS (ESI) m/z calculated for $\text{C}_7\text{H}_3\text{FN}_3\text{O}_2$ $[\text{M}-\text{H}]^-$ 180.0215; found 180.0221.



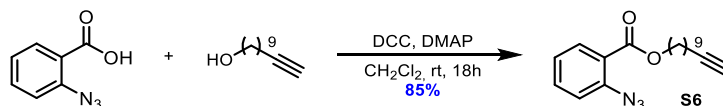
2-Azido-5-methylbenzoic acid (S4): Following the General Procedure A, 2-amino-5-methylbenzoic acid (0.646 g, 4.27 mmol, 1.0 equiv.) was dissolved in an aqueous solution of hydrochloric acid (20 mL) in a round bottom flask equipped with a stir bar. Aqueous solutions of sodium nitrite (0.345 g, 5.00 mmol, 1.2 equiv.) in 2 mL of water and of sodium azide (0.325 g, 5.00 mmol, 1.2 equiv.) in 2 mL of water were then added subsequently to the reaction mixture. Following filtration, the desired product was obtained as a beige solid (0.37 g, 49 % yield). ^1H NMR (400 MHz, DMSO- d_6) $\delta = 13.10$ (br. s., 1H), 7.59 (dd, $J = 1.6, 0.5$ Hz, 1H), 7.41 (ddd, $J = 8.2, 2.2, 0.7$ Hz, 1H), 7.24 (d, $J = 8.1$ Hz, 1H), 2.31 (s, 3H); ^{13}C NMR (100 MHz, DMSO- d_6) $\delta = 166.5, 136.0, 134.5, 133.6, 131.3, 123.7, 120.8, 20.1$; HRMS (ESI) m/z calculated for $\text{C}_8\text{H}_6\text{N}_3\text{O}_2$ $[\text{M}-\text{H}]^-$ 176.0466; found 176.0458.



2-Azido-5-methoxybenzoic acid (S5): Following the General Procedure A, 2-amino-5-methoxybenzoic acid (0.714 g, 4.27 mmol, 1.0 equiv.) was dissolved in an aqueous solution of hydrochloric acid (20 mL) in a round bottom flask equipped with a stir bar. Aqueous solutions of sodium nitrite (0.345 g, 5.00 mmol, 1.2 equiv.) in 2 mL of water and of sodium azide (0.325 g, 5.00 mmol, 1.2 equiv.) in 2 mL of water were then added subsequently to the reaction mixture. Following filtration, the desired product was obtained as a white solid (0.10

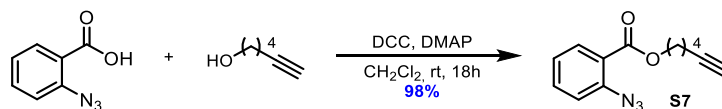
g, 12 % yield). ^1H NMR (400 MHz, DMSO- d_6) δ = 7.27 - 7.31 (m, 2H), 7.16 - 7.21 (m, 1H), 3.78 (s, 3H); ^{13}C NMR (100 MHz, DMSO- d_6) δ = 166.2, 156.2, 131.0, 125.0, 122.4, 119.0, 115.4, 55.6; HRMS (ESI) m/z calculated for $\text{C}_8\text{H}_6\text{N}_3\text{O}_3$ $[\text{M-H}]^-$ 192.0415; found 192.0407.

General Procedure B for Steglich Esterification: To a stirred solution of the alcohol (1 equiv.) and the carboxylic acid (1.5 equiv.) in dry dichloromethane (0.1 M) was added N,N' -dicyclohexylcarbodiimide (DCC, 2 equiv.) and 4-(dimethylamino)pyridine (DMAP, 3 equiv.) at room temperature. The reaction mixture was stirred at room temperature for 18 hours. Upon complete conversion of the starting material, the crude reaction mixture was placed in a freezer for 5 hours to induce the precipitation of the urea, which was subsequently removed by filtration. The filtrate was concentrated *in vacuo* to provide the crude reaction mixture which was purified by column chromatography on silica-gel to afford the desired product.

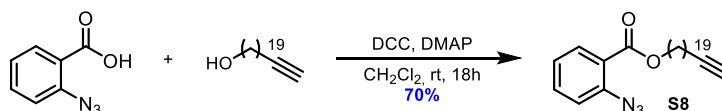


Undec-10-yn-1-yl 2-azidobenzoate (S6): Following the General Procedure B, undec-10-yn-1-ol (0.148 g, 0.879 mmol, 1.0 equiv.), 2-azidobenzoic acid (0.215 g, 1.32 mmol, 1.5 equiv.), DCC (0.363 g, 1.76 mmol, 2.0 equiv.) and DMAP (0.322 g, 2.64 mmol, 3.0 equiv.) were dissolved in anhydrous dichloromethane (10 mL) in a round bottom flask equipped with a stir bar. Following purification by column chromatography (100 % hexanes \rightarrow 10 % diethyl ether in hexanes), the desired product was obtained as a colorless oil (0.23 g, 85 % yield). ^1H NMR (400 MHz, CDCl_3) δ = 7.85 (ddd, J = 7.9, 1.7, 0.3 Hz, 1H), 7.50 - 7.56 (m, 1H), 7.25 (dd, J = 8.1, 0.8 Hz, 1H), 7.17 - 7.21 (m, 1H), 4.31 (t, J = 6.7 Hz, 2H), 2.19 (td, J = 7.1, 2.7 Hz, 2H), 1.94 (t, J = 2.6 Hz, 1H), 1.72 - 1.81 (m, 2H), 1.49 - 1.57 (m, 2H), 1.31 - 1.49 (m, 10H) ; ^{13}C

NMR (100 MHz, CDCl₃) δ = 165.4, 139.9, 133.0, 131.7, 124.4, 123.0, 119.9, 84.7, 68.1, 65.5, 29.3, 29.1, 29.0, 28.7, 28.6, 28.4, 26.0, 18.4; HRMS (ESI) m/z calculated for C₁₈H₂₄N₃O₂ [M+H]⁺ 314.1863; found 314.1863.

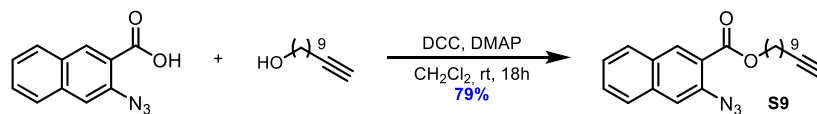


Hex-5-yn-1-yl 2-azidobenzoate (S7): Following the General Procedure B, hex-5-yn-1-ol (0.07 mL, 0.654 mmol, 1.0 equiv.), 2-azidobenzoic acid (0.160 g, 0.981 mmol, 1.5 equiv.), DCC (0.270 g, 1.31 mmol, 2.0 equiv.) and DMAP (0.240 g, 1.96 mmol, 3.0 equiv.) were dissolved in anhydrous dichloromethane (10 mL) in a round bottom flask equipped with a stir bar. Following purification by column chromatography (100 % hexanes \rightarrow 10 % diethyl ether in hexanes), the desired product was obtained as a colorless oil (0.16 g, 98 % yield). ¹H NMR (400 MHz, CDCl₃) δ = 7.86 (ddd, J = 7.8, 1.6, 0.4 Hz, 1H), 7.51 - 7.57 (m, 1H), 7.25 (ddd, J = 8.1, 1.0, 0.4 Hz, 1H), 7.17 - 7.22 (m, 1H), 4.35 (t, J = 6.4 Hz, 2H), 2.29 (td, J = 7.0, 2.7 Hz, 2H), 1.98 (t, J = 2.6 Hz, 1H), 1.87 - 1.95 (m, 2H), 1.67 - 1.76 (m, 2H); ¹³C NMR (100 MHz, CDCl₃) δ = 165.3, 140.0, 133.1, 131.7, 124.4, 122.8, 119.8, 83.8, 68.8, 64.8, 27.7, 25.0, 18.1; HRMS (ESI) m/z calculated for C₁₃H₁₄N₃O₂ [M+H]⁺ 244.1081; found 244.1077.

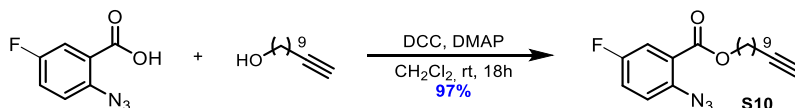


Henicos-20-yn-1-yl 2-azidobenzoate (S8): Following the General Procedure B, henicos-20-yn-1-ol (0.252 g, 0.817 mmol, 1.0 equiv.), 2-azidobenzoic acid (0.200 g, 1.23 mmol, 1.5 equiv.), DCC (0.337 g, 1.63 mmol, 2.0 equiv.) and DMAP (0.300 g, 2.45 mmol, 3.0 equiv.) were dissolved in anhydrous dichloromethane (10 mL) in a round bottom flask equipped with a stir bar. Following purification by column chromatography (100 % hexanes \rightarrow 10 % diethyl

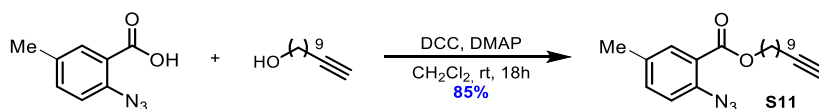
ether in hexanes), the desired product was obtained as a white solid (0.26 g, 70 % yield). ¹H NMR (400 MHz, CDCl₃) δ = 7.85 (ddd, *J* = 7.8, 1.6, 0.8 Hz, 1H), 7.50 - 7.56 (m, 1H), 7.25 (dd, *J* = 8.1, 0.7 Hz, 1H), 7.16 - 7.22 (m, 1H), 4.31 (t, *J* = 6.7 Hz, 2H), 2.19 (td, *J* = 7.11, 2.6 Hz, 2H), 1.94 (t, *J* = 2.7 Hz, 1H), 1.72 - 1.81 (m, 2H), 1.49 - 1.56 (m, 2H), 1.25 - 1.47 (m, 30H); ¹³C NMR (100 MHz, CDCl₃) δ = 165.4, 139.9, 133.0, 131.7, 124.4, 123.1, 119.9, 84.8, 68.0, 65.5, 29.7 (5C), 29.64 (2C), 29.60, 29.57, 29.52, 29.50, 29.2, 29.1, 28.8, 28.6, 28.5, 26.0, 18.4; HRMS (ESI) *m/z* calculated for C₂₈H₄₃N₃NaO₂ [M+Na]⁺ 476.3248; found 476.3247.



Undec-10-yn-1-yl 3-azido-2-naphthoate (S9): Following the General Procedure B, undec-10-yn-1-ol (0.211 g, 1.25 mmol, 1.0 equiv.), 3-azido-2-naphthoic acid (0.400 g, 1.88 mmol, 1.5 equiv.), DCC (0.516 g, 2.50 mmol, 2.0 equiv.) and DMAP (0.459 g, 3.75 mmol, 3.0 equiv.) were dissolved in anhydrous dichloromethane (15 mL) in a round bottom flask equipped with a stir bar. Following purification by column chromatography (100 % hexanes → 10 % diethyl ether in hexanes), the desired product was obtained as a colorless oil (0.36 g, 79 % yield). ¹H NMR (400 MHz, CDCl₃) δ = 8.38 (s, 1H), 7.88 (dd, *J* = 8.2, 0.7 Hz, 1H), 7.79 (dd, *J* = 8.3, 0.7 Hz, 1H), 7.62 (s, 1H), 7.57 - 7.61 (m, 1H), 7.46 - 7.52 (m, 1H), 4.38 (t, *J* = 6.7 Hz, 2H), 2.19 (td, *J* = 7.0, 2.7 Hz, 2H), 1.94 (t, *J* = 2.6 Hz, 1H), 1.77 - 1.86 (m, 2H), 1.51 - 1.58 (m, 2H), 1.29 - 1.51 (m, 10H); ¹³C NMR (100 MHz, CDCl₃) δ = 165.5, 136.3, 135.1, 133.0, 129.8, 129.0, 128.8, 126.4, 126.2, 122.6, 117.2, 84.7, 68.1, 65.7, 29.4, 29.2, 29.0, 28.7, 28.6, 28.4, 26.0, 18.4; HRMS (ESI) *m/z* calculated for C₂₂H₂₅N₃NaO₂ [M+Na]⁺ 386.1839; found 386.1839.

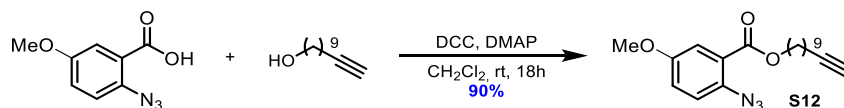


Undec-10-yn-1-yl 2-azido-5-fluorobenzoate (S10): Following the General Procedure B, undec-10-yn-1-ol (0.248 g, 1.47 mmol, 1.0 equiv.), 2-azido-5-fluorobenzoic acid (0.400 g, 2.21 mmol, 1.5 equiv.), DCC (0.608 g, 2.95 mmol, 2.0 equiv.) and DMAP (0.540 g, 4.42 mmol, 3.0 equiv.) were dissolved in anhydrous dichloromethane (15 mL) in a round bottom flask equipped with a stir bar. Following purification by column chromatography (100 % hexanes → 10 % diethyl ether in hexanes), the desired product was obtained as a colorless oil (0.47 g, 97 % yield). ^1H NMR (400 MHz, CDCl_3) δ = 7.56 (dd, J = 8.8, 2.9 Hz, 1H), 7.18 - 7.28 (m, 2H), 4.31 (t, J = 6.7 Hz, 2H), 2.19 (td, J = 7.1, 2.7 Hz, 2H), 1.94 (t, J = 2.6 Hz, 1H), 1.72 - 1.80 (m, 2H), 1.49 - 1.57 (m, 2H), 1.30 - 1.48 (m, 10H); ^{13}C NMR (100 MHz, CDCl_3) δ = 164.2 (d, J = 2.2 Hz), 158.9 (d, J = 246.2 Hz), 136.0 (d, J = 3.0 Hz), 124.2 (d, J = 7.2 Hz), 121.6 (d, J = 7.8 Hz), 120.3 (d, J = 23.3 Hz), 118.4 (d, J = 24.6 Hz), 84.7, 68.1, 65.8, 29.3, 29.1, 29.0, 28.7, 28.5, 28.4, 25.9, 18.4; ^{19}F NMR (375 MHz, CDCl_3) δ = 117.0 (ddd, J = 8.6, 7.3, 4.6 Hz); HRMS (ESI) m/z calculated for $\text{C}_{18}\text{H}_{23}\text{FN}_3\text{O}_2$ $[\text{M}+\text{H}]^+$ 332.1769; found 332.1768.



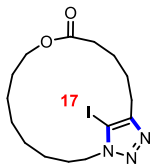
Undec-10-yn-1-yl 2-azido-5-methylbenzoate (S11): Following the General Procedure B, undec-10-yn-1-ol (0.222 g, 1.32 mmol, 1.0 equiv.), 2-azido-5-methylbenzoic acid (0.351 g, 1.98 mmol, 1.5 equiv.), DCC (0.545 g, 2.64 mmol, 2.0 equiv.) and DMAP (0.484 g, 3.96 mmol, 3.0 equiv.) were dissolved in anhydrous dichloromethane (15 mL) in a round bottom flask equipped with a stir bar. Following purification by column chromatography (100 %

hexanes → 10 % diethyl ether in hexanes), the desired product was obtained as a colorless oil (0.37 g, 85 % yield). ¹H NMR (400 MHz, CDCl₃) δ = 7.64 (dd, *J* = 1.6, 0.6 Hz, 1H), 7.33 (ddd, *J* = 8.2, 2.2, 0.7 Hz, 1H), 7.13 (d, *J* = 8.2 Hz, 1H), 4.30 (t, *J* = 6.7 Hz, 2H), 2.36 (s, 3H), 2.19 (td, *J* = 7.1, 2.7 Hz, 2H), 1.94 (t, *J* = 2.6 Hz, 1H), 1.72 - 1.81 (m, 2H), 1.49 - 1.57 (m, 2H), 1.30 - 1.48 (m, 10H); ¹³C NMR (100 MHz, CDCl₃) δ = 165.6, 137.1, 134.3, 133.7, 132.0, 122.8, 119.8, 84.7, 68.1, 65.4, 29.3, 29.2, 29.0, 28.7, 28.6, 28.4, 25.9, 20.7, 18.4; HRMS (ESI) *m/z* calculated for C₁₉H₂₆N₃O₂ [M+H]⁺ 328.2020; found 328.2019.



Undec-10-yn-1-yl 2-azido-5-methoxybenzoate (S12): Following the General Procedure B, undec-10-yn-1-ol (0.052 g, 0.311 mmol, 1.0 equiv.), 2-azido-5-methoxybenzoic acid (0.090 g, 0.466 mmol, 1.5 equiv.), DCC (0.128 g, 0.621 mmol, 2.0 equiv.) and DMAP (0.114 g, 0.932 mmol, 3.0 equiv.) were dissolved in anhydrous dichloromethane (5 mL) in a round bottom flask equipped with a stir bar. Following purification by column chromatography (100 % hexanes → 10 % diethyl ether in hexanes), the desired product was obtained as a colorless oil (0.10 g, 90 % yield). ¹H NMR (400 MHz, CDCl₃) δ = 7.37 (d, *J* = 2.9 Hz, 1H), 7.16 (d, *J* = 8.8 Hz, 1H), 7.08 (dd, *J* = 8.9, 3.1 Hz, 1H), 4.32 (t, *J* = 6.7 Hz, 2H), 3.83 (s, 3H), 2.19 (td, *J* = 7.0, 2.6 Hz, 2H), 1.94 (t, *J* = 2.7 Hz, 1H), 1.72 - 1.81 (m, 2H), 1.49 - 1.57 (m, 2H), 1.30 - 1.48 (m, 10H); ¹³C NMR (100 MHz, CDCl₃) δ = 165.3, 156.3, 132.4, 123.8, 121.3, 119.3, 116.0, 84.7, 68.1, 65.6, 55.7, 29.3, 29.1, 29.0, 28.7, 28.6, 28.4, 25.9, 18.4; HRMS (ESI) *m/z* calculated for C₁₉H₂₆N₃O₃ [M+H]⁺ 344.1969; found 344.1971.

SYNTHESIS OF MACROCYCLES



General procedure for the click macrocyclization using phase separation conditions in batch (C): Macrocycle (2): To an open sealed tube vessel equipped with a stirring bar was added the precursor (49 mg, 0.12 mmol, 1 equiv), polyethylene glycol 400 (3.33 mL) and methanol (1.67 mL). The mixture was stirred 30 seconds to mix the two solvents. Triethylamine (0.13 mL, 0.96 mmol, 8 equiv) and CuI (4.6 mg, 0.024 mmol, 20 mol%) were added to the mixture. The tube was sealed and heated at 60 °C for 17 h (no precaution was taken to remove air or moisture). The reaction was then cooled back to room temperature and the crude mixture was loaded directly on a silica column. Purification by chromatography (20→50 % ethyl acetate in hexane) afforded the product as a colorless semi-solid (47 mg, 95 %). ¹H NMR (400 MHz, CDCl₃) δ = 4.53-4.39 (m, 2H), 4.07-3.96 (m, 2H), 2.77 (t, *J* = 6.4 Hz, 2H), 2.32-2.20 (m, 2H), 2.00–1.93 (m, 2H), 1.85–1.77 (m, 2H), 1.51–1.43 (m, 4H), 1.28-1.03 (m, 8H); ¹³C NMR (100 MHz, CDCl₃) δ ppm = 173.4, 150.9, 79.0, 64.2, 50.4, 35.4, 29.2, 28.4, 28.3, 27.6, 27.4, 25.1, 24.6, 24.4, 24.1 ppm; HRMS (ESI) *m/z* calculated for C₁₅H₂₄N₃NaO₂ [M+Na]⁺, 428.0805; found: 428.0815.

General procedure for the click macrocyclization using phase separation conditions in continuous flow (D): Macrocycle (2): To a vial equipped with a stirring bar was added the precursor (49 mg, 0.12 mmol, 1 equiv), polyethylene glycol 400 (2.5 mL) and methanol (2.5 mL). The mixture was stirred 30 seconds to mix the two solvents. TMEDA (0.04 mL, 0.24

mmol, 2 equiv) and CuI (4.6 mg, 0.024 mmol, 20 mol%) were added to the mixture. The mixture was stirred at room temperature until everything was soluble then taken into a syringe. The reaction mixture was injected using a 5 mL injection loop into the flow reactor for a reaction time of 400 min (4 x 10 mL PFE reactors) at a flow rate of 0.1 mL/min. The flow reaction was conducted in a VapourTech R4 reactor and a R2+ pumping module. Upon completion, silica gel was added to the collection flask and the volatiles were removed under vacuum. The crude mixture was purified by chromatography (20→50 % ethyl acetate in hexane) and afforded the product as a colorless semi-solid (41 mg, 83 %).

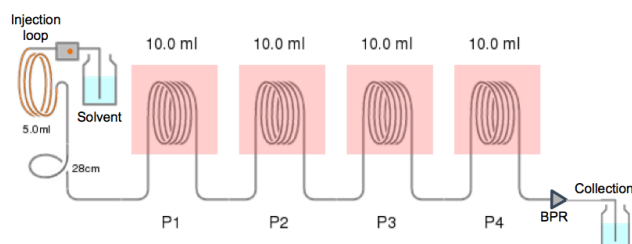
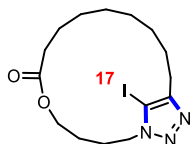
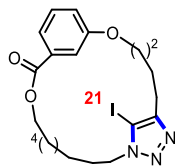


Figure S1. Continuous flow setup.

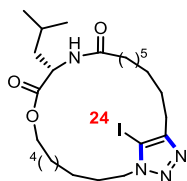


Macrocycle (3): Following the general procedure D described above, macrocycle **3** was isolated as a colorless semi-solid (45 mg, 90 %). NMR data was in accordance with what was previously reported.⁴¹

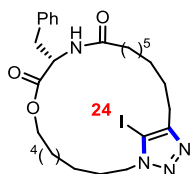
⁴¹ Bédard, A.-C.; Collins, S. K. *Org. Lett.* **2014**, *16*, 5286.



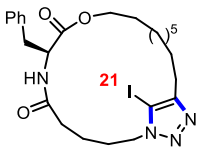
Macrocycle (4): Following the general procedure D described above, macrocycle **4** was isolated as a white solid (46 mg, 75 %). NMR data was in accordance with what was previously reported.⁷



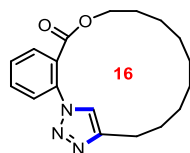
Macrocycle (5): Following the general procedure D described above, macrocycle **5** was isolated as a white solid (60 mg, 83 %). NMR data was in accordance with what was previously reported.⁷



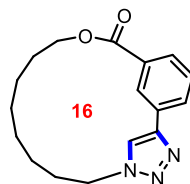
Macrocycle (6): Following the general procedure D described above, macrocycle **6** was isolated as a white solid (53 mg, 78 %). NMR data was in accordance with what was previously reported.⁷



Macrocycle (7): Following the general procedure D described above, macrocycle **7** was isolated as a white solid (55 mg, 86 %). NMR data was in accordance with what was previously reported.⁷



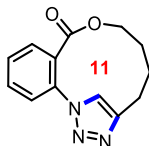
Macrocycle (8): Following the general procedure D described above, macrocycle **8** was isolated as a white solid. (38 mg, 87 %). ¹H NMR (400 MHz, CDCl₃) δ = 8.01 (dd, *J* = 6.0, 1.8 Hz, 1H), 7.69 - 7.57 (m, 2H), 7.53 (s, 1H), 7.46 (dd, *J* = 6.0, 1.8 Hz, 1H), 4.04 (t, *J* = 7.3 Hz, 2H), 2.85 - 2.77 (m, 2H), 1.82 - 1.69 (m, 2H), 1.50 - 1.41 (m, 2H), 1.40 - 1.20 (m, 10H); ¹³C NMR (100 MHz, CDCl₃) δ ppm = 166.0, 148.3, 136.1, 132.4, 131.5, 129.7, 128.3, 126.5, 122.2, 66.0, 29.9, 29.8, 29.70, 29.66, 29.6, 28.4, 25.8, 25.7 ppm; HRMS (ESI) *m/z* calculated for C₁₈H₂₄N₃O₂ [M+H]⁺, 314.1863; found: 314.1866.



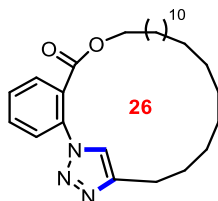
Macrocycle (9): Following the general procedure D described above, macrocycle **9** was isolated as a white solid. (31 mg, 85 %). ¹H NMR (400 MHz, CDCl₃) δ = 8.42 (s, 1H), 8.08 (d, *J* = 7.9 Hz, 1H), 8.00 (d, *J* = 7.9 Hz, 1H), 7.85 (s, 1H), 7.50 (t, *J* = 7.7 Hz, 1H), 4.41 (t, *J* = 7.1 Hz, 2H), 4.34 (t, *J* = 6.5 Hz, 2H), 1.95 (t, *J* = 6.7 Hz, 2H), 1.82 - 1.72 (m, 2H), 1.50 - 1.32 (m, 8H); ¹³C NMR (100 MHz, CDCl₃) δ ppm = 166.4, 146.8, 131.08, 131.05, 129.9, 129.1, 129.0,

bbbbbbbbb

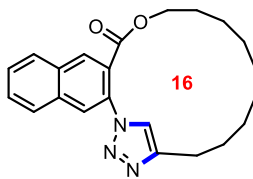
126.6, 119.9, 65.1, 50.4, 30.2, 28.8, 28.7, 28.6, 26.2, 25.8 ppm; HRMS (ESI) m/z calculated for $C_{17}H_{22}N_3O_2$ $[M+H]^+$, 300.1707; found: 300.1712



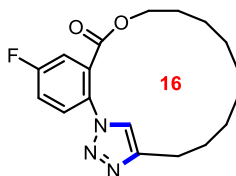
Macrocycle (10): Following the general procedure D described above, macrocycle **10** was isolated as a white solid. (19 mg, 66 %). 1H NMR (300 MHz, $CDCl_3$) δ = 8.04 (dd, J = 6.0, 1.8 Hz, 1H), 7.68 - 7.57 (m, 3H), 7.40 (dd, J = 6.0, 1.8 Hz, 1H), 4.22 (t, J = 5.6 Hz, 2H), 2.75 - 2.66 (m, 2H), 1.65 - 1.57 (m, 2H), 1.55 - 1.50 (m, 2H); ^{13}C NMR (75 MHz, $CDCl_3$) δ ppm = 166.2, 147.8, 135.9, 132.5, 131.7, 129.7, 128.1, 126.1, 121.9, 65.3, 28.3, 25.4, 25.3 ppm; HRMS (ESI) m/z calculated for $C_{13}H_{14}N_3O_2$ $[M+H]^+$, 244.1081; found: 244.1090.



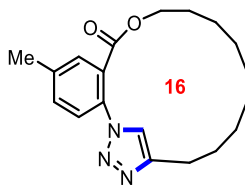
Macrocycle (11): Following the general procedure D described above, macrocycle **11** was isolated. (33 mg, 61 %). 1H NMR (400 MHz, $CDCl_3$) δ = 7.98 (d, J = 6.8 Hz, 1H), 7.64 (d, J = 7.5 Hz, 1H), 7.61 - 7.55 (m, 1H), 7.54 (s, 1H), 7.47 (d, J = 8.1 Hz, 1H), 4.09 (t, J = 7.3 Hz, 2H), 2.84 - 2.77 (m, 2H), 1.81 - 1.69 (m, 2H), 1.48 - 1.15 (m, 32H); ^{13}C NMR (175 MHz, $CDCl_3$) δ ppm = 165.8, 148.3, 136.2, 132.4, 131.2, 129.6, 128.1, 126.5, 122.3, 65.9, 29.7 (7 C), 29.63, 29.60, 29.50, 29.49, 29.44, 29.39, 29.3, 28.3, 25.74, 25.67, 25.6; HRMS (ESI) m/z calculated for $C_{28}H_{44}N_3O_2$ $[M+H]^+$, 454.3428; found: 454.3431



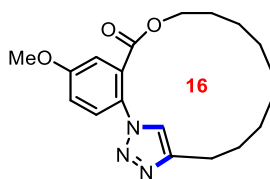
Macrocycle (12): Following the general procedure D described above, macrocycle **12** was isolated. (35 mg, 81 %). ^1H NMR (300 MHz, CDCl_3) δ = 8.51 (s, 1H), 8.04 - 7.99 (m, 1H), 7.94 - 7.88 (m, 2H), 7.71 (s, 1H), 7.69 - 7.64 (m, 2H), 4.32 - 4.22 (m, 2H), 2.97 - 2.87 (m, 2H), 1.90 - 1.76 (m, 2H), 1.56 - 1.48 (m, 2H), 1.43 - 1.19 (m, 10H); ^{13}C NMR (75 MHz, CDCl_3) δ ppm = 166.6, 147.7, 134.0, 132.9, 132.5, 132.2, 129.1, 128.8, 128.1, 128.0, 125.8, 124.8, 122.4, 65.4, 28.9, 27.2, 26.6, 26.5, 26.1, 25.1, 24.4, 24.3 ppm; HRMS (ESI) m/z calculated for $\text{C}_{22}\text{H}_{26}\text{N}_3\text{O}_2$ $[\text{M}+\text{H}]^+$, 364.2020; found: 364.2023.



Macrocycle (13): Following the general procedure D described above, macrocycle **13** was isolated as a white solid. (33 mg, 83 %). ^1H NMR (700 MHz, CDCl_3) δ = 7.72 (dd, J = 8.5, 2.8 Hz, 1H), 7.51 (s, 1 H), 7.45 (dd, J = 8.7, 4.7 Hz, 1H), 7.35 (dd, J = 14.0, 2.8 Hz, 1H), 4.05 (t, J = 7.2 Hz, 2H), 2.83 - 2.77 (m, 2H), 1.80 - 1.72 (m, 2H), 1.50 - 1.42 (m, 2H), 1.40 - 1.22 (m, 10H); ^{13}C NMR (175 MHz, CDCl_3) δ ppm = 164.7 (d, J = 2 Hz, 1C), 162.6 (d, J = 250.3 Hz, 1C), 148.3, 132.3 (d, J = 1.8 Hz, 1C), 130.4 (d, J = 8.8 Hz, 1C), 128.8 (d, J = 8.8 Hz, 1C), 122.5, 119.4 (d, J = 24.5 Hz, 1C), 118.5 (d, J = 24.5 Hz, 1C), 66.3, 29.9, 29.72, 29.67, 29.6 (2C), 28.3, 25.7, 25.6 ppm; HRMS (ESI) m/z calculated for $\text{C}_{18}\text{H}_{22}\text{FN}_3\text{O}_2$ $[\text{M}+\text{H}]^+$, 332.1769; found: 332.1784.

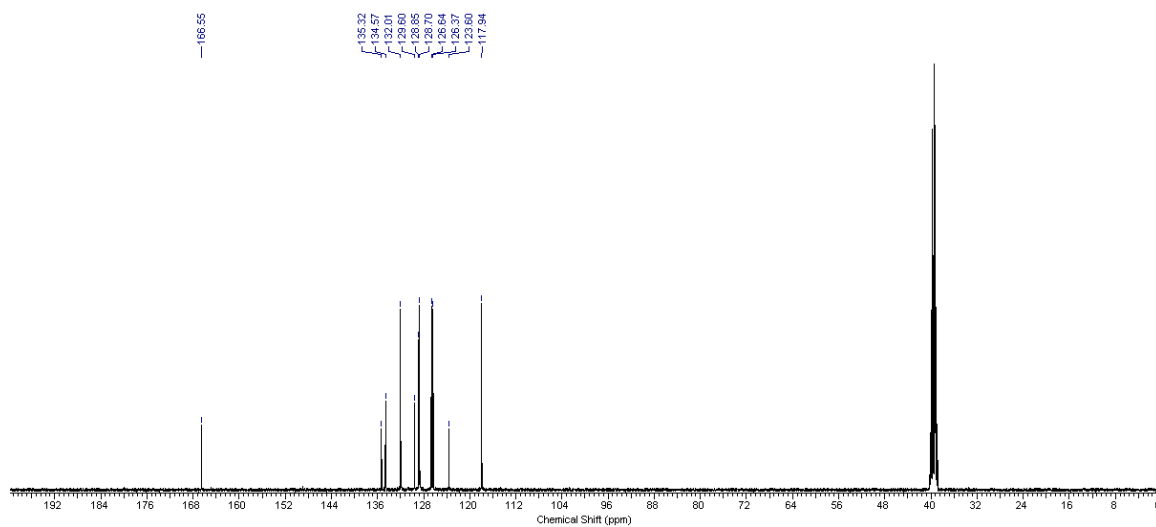
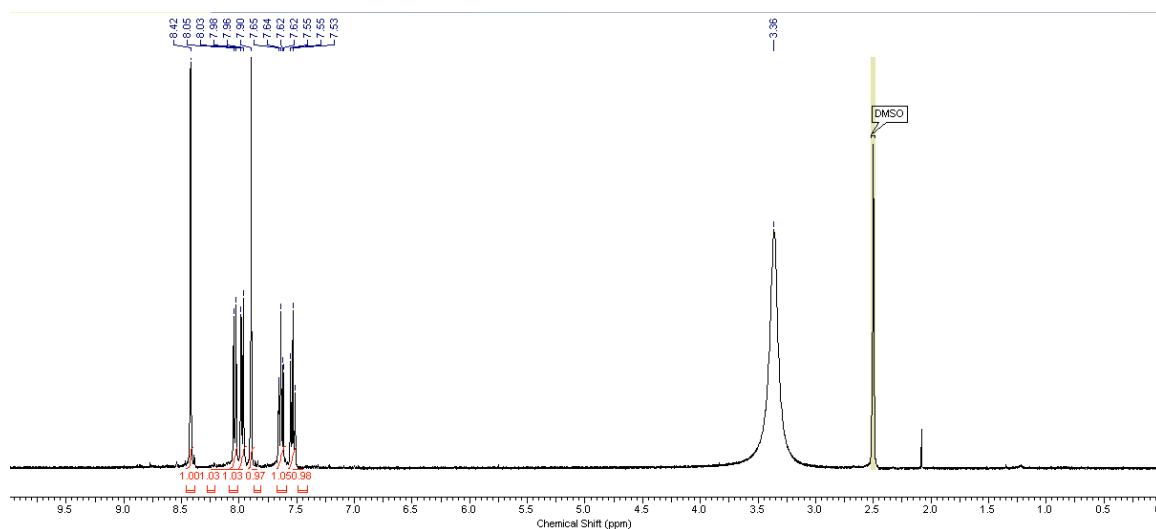
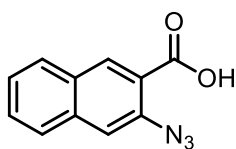


Macrocycle (14): Following the general procedure D described above, macrocycle **14** was isolated as a white solid. (29 mg, 76 %). ^1H NMR (500 MHz, CDCl_3) δ = 7.74 (d, J = 1.5 Hz, 1H), 7.58 (s, 1H), 7.41 (dd, J = 8.1, 2.0 Hz, 1H), 7.28 (d, J = 8.1 Hz, 1H), 4.23 - 4.16 (m, 2H), 2.91 - 2.84 (m, 2H), 2.47 (s, 3H), 1.85 - 1.76 (m, 2H), 1.53 - 1.45 (m, 2H), 1.41 - 1.18 (m, 10H); ^{13}C NMR (125 MHz, CDCl_3) δ ppm = 166.8, 147.7, 139.7, 133.3, 132.6, 131.7, 127.8, 125.5, 122.0, 65.4, 28.8, 27.2, 26.5, 26.0, 25.1, 24.3 (2C), 21.0 ppm; HRMS (ESI) m/z calculated for $\text{C}_{19}\text{H}_{25}\text{N}_3\text{O}_2$ $[\text{M}+\text{H}]^+$, 328.2020; found: 328.2025.

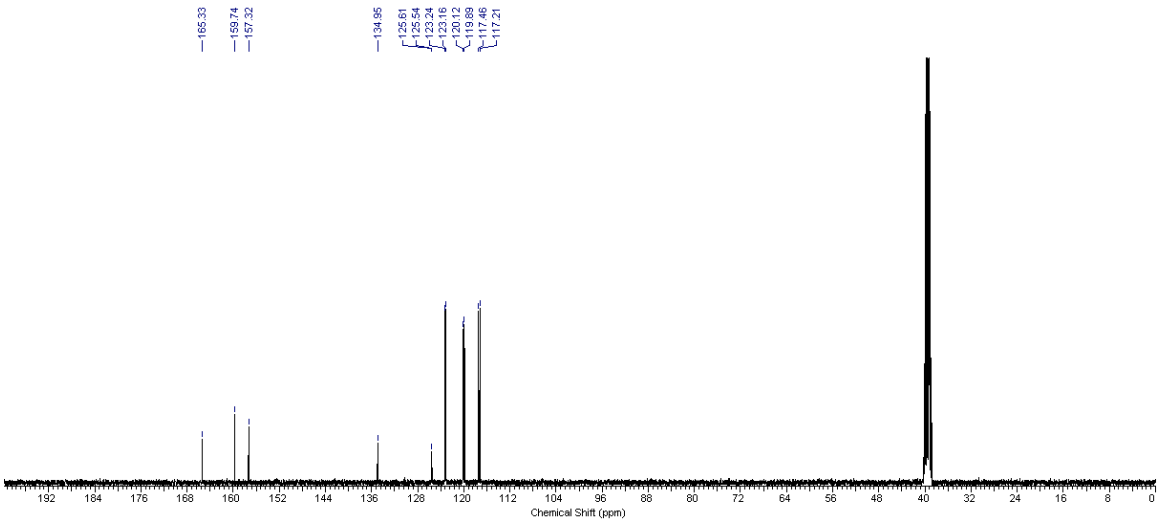
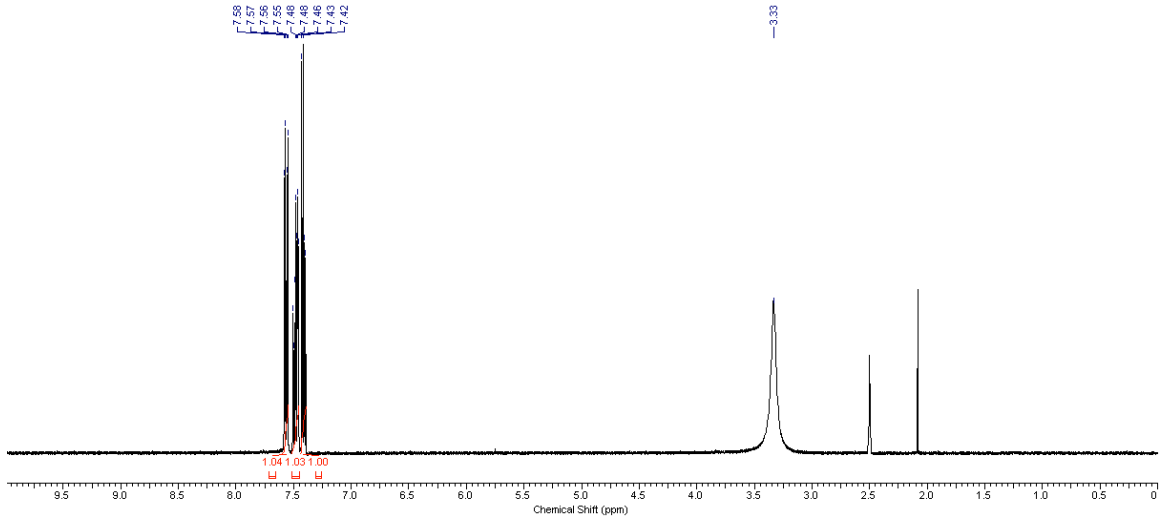
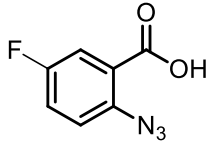


Macrocycle (15): Following the general procedure D described above, macrocycle **15** was isolated as a white solid (30 mg, 73 %). ^1H NMR (500 MHz, CDCl_3) δ = 7.54 (s, 1H), 7.43 (d, J = 2.9 Hz, 1H), 7.30 (d, J = 8.7 Hz, 1H), 7.11 (dd, J = 8.7, 2.9 Hz, 1H), 4.23 - 4.17 (m, 2H), 3.91 (s, 3H), 2.91 - 2.84 (m, 2H), 1.87 - 1.76 (m, 2H), 1.53 - 1.44 (m, 2H), 1.41 - 1.19 (m, 10H); ^{13}C NMR (125 MHz, CDCl_3) δ ppm = 166.4, 159.9, 147.6, 129.3, 128.8, 127.4, 122.3, 118.0, 115.6, 65.5, 55.9, 28.8, 27.2, 26.5, 26.4, 26.0, 25.1, 24.3, 24.2 ppm; HRMS (ESI) m/z calculated for $\text{C}_{19}\text{H}_{25}\text{N}_3\text{O}_3$ $[\text{M}+\text{H}]^+$, 344.1969; found: 344.1984.

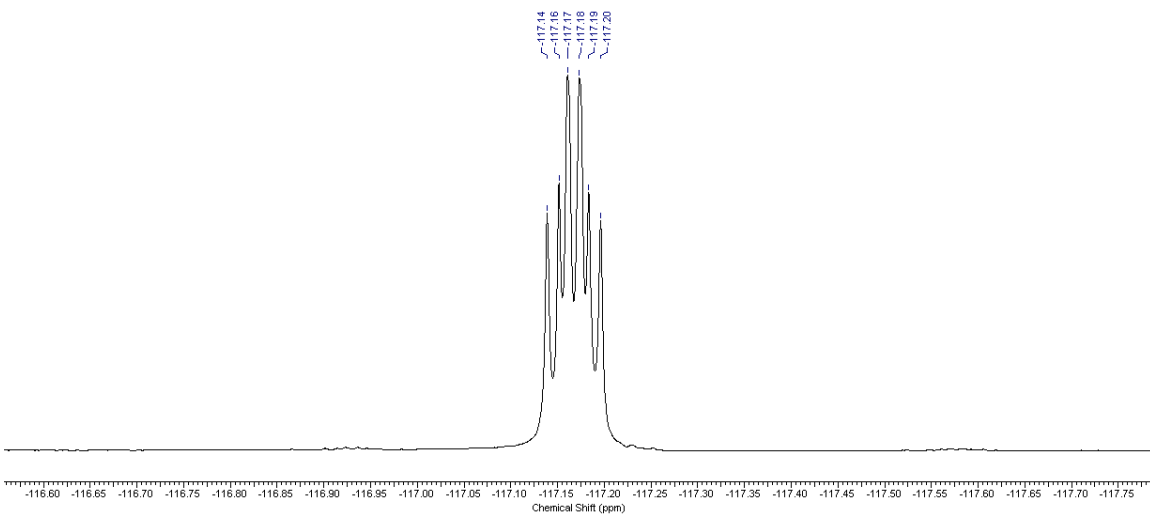
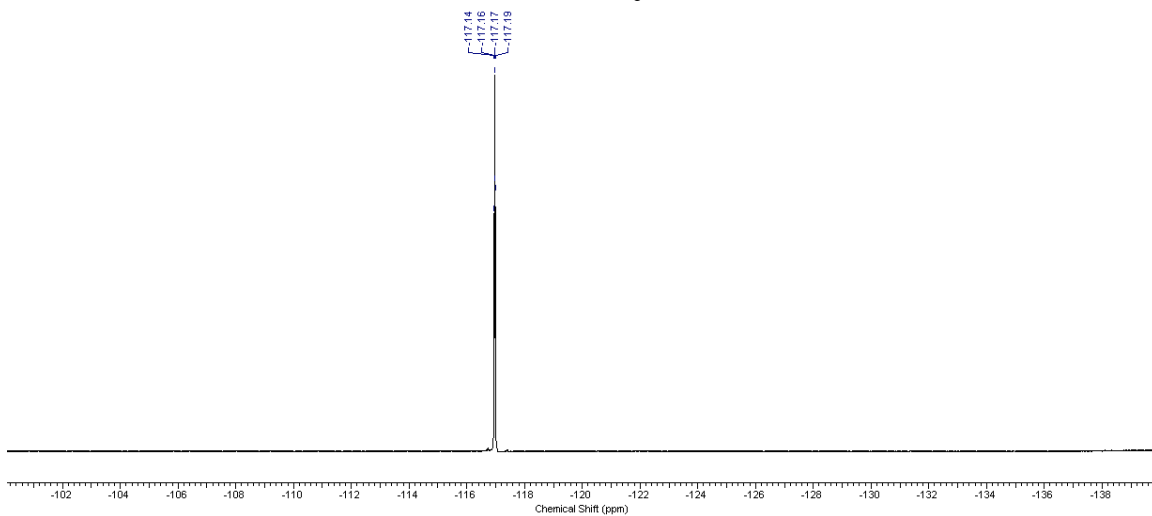
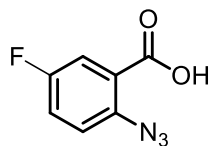
NMR DATA FOR ALL NEW COMPOUNDS



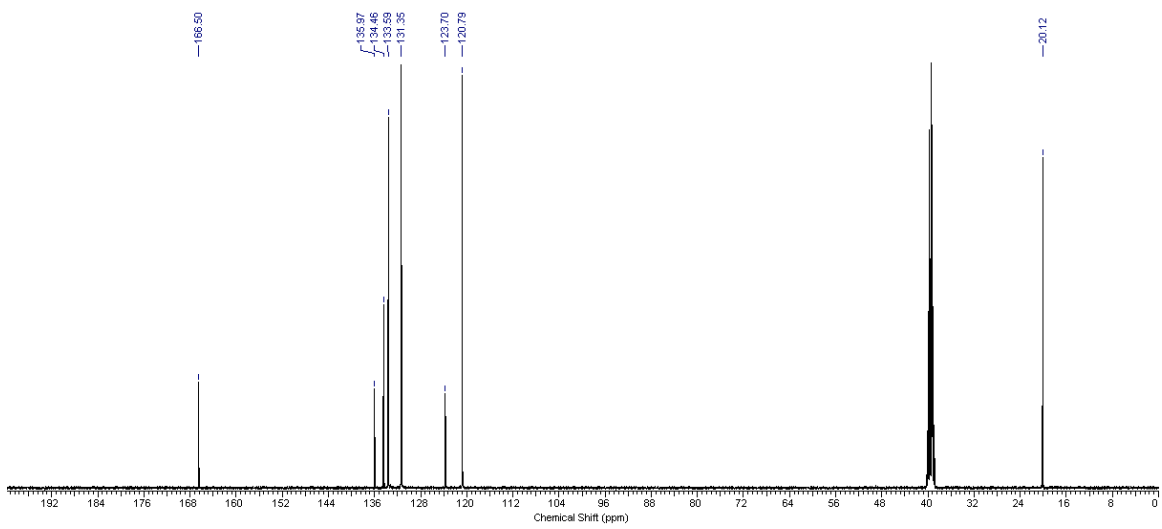
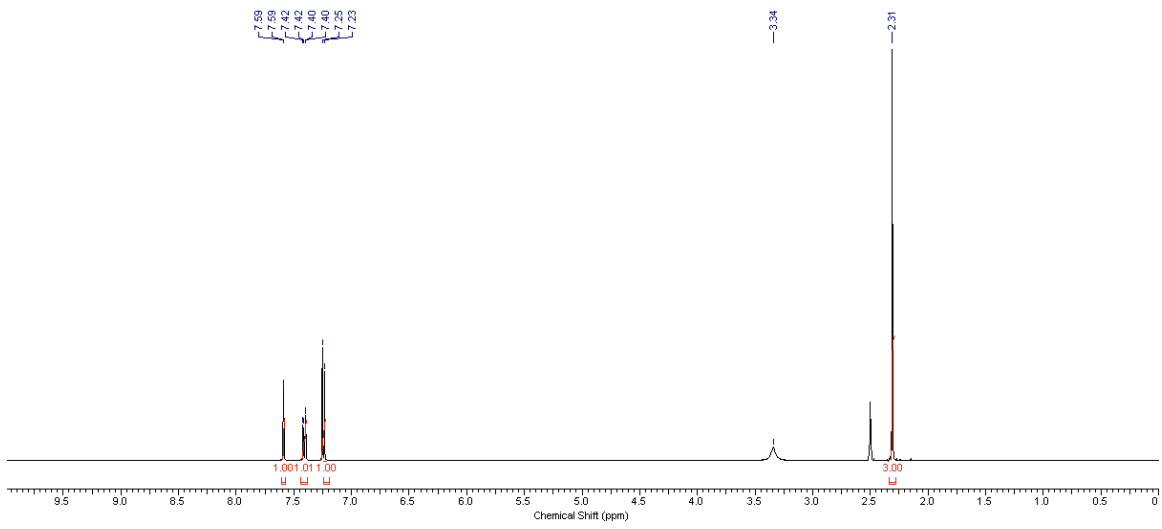
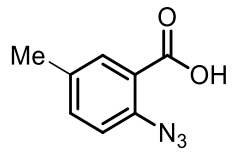
ffffff

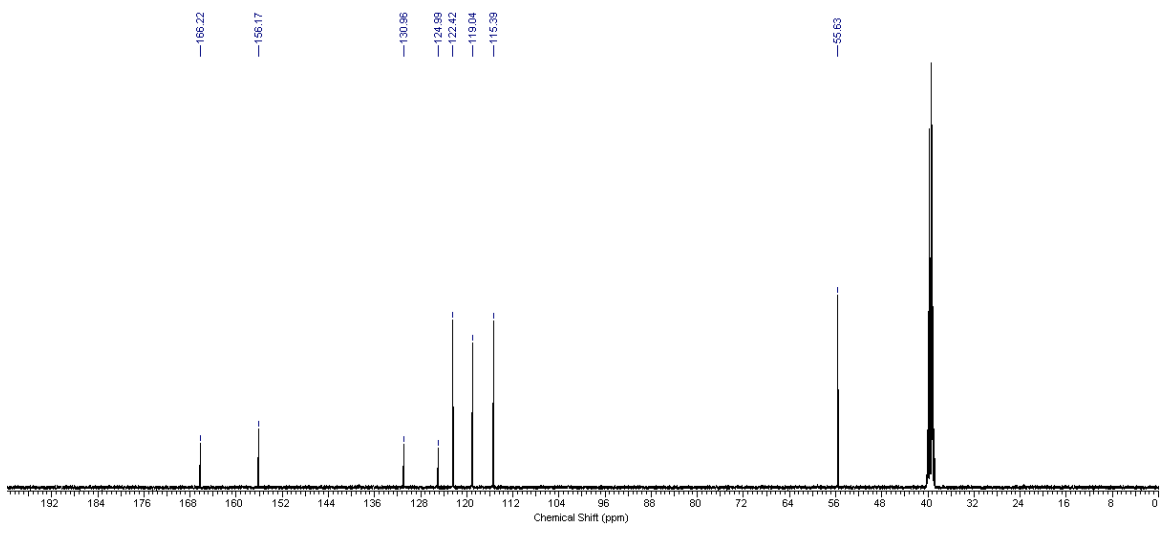
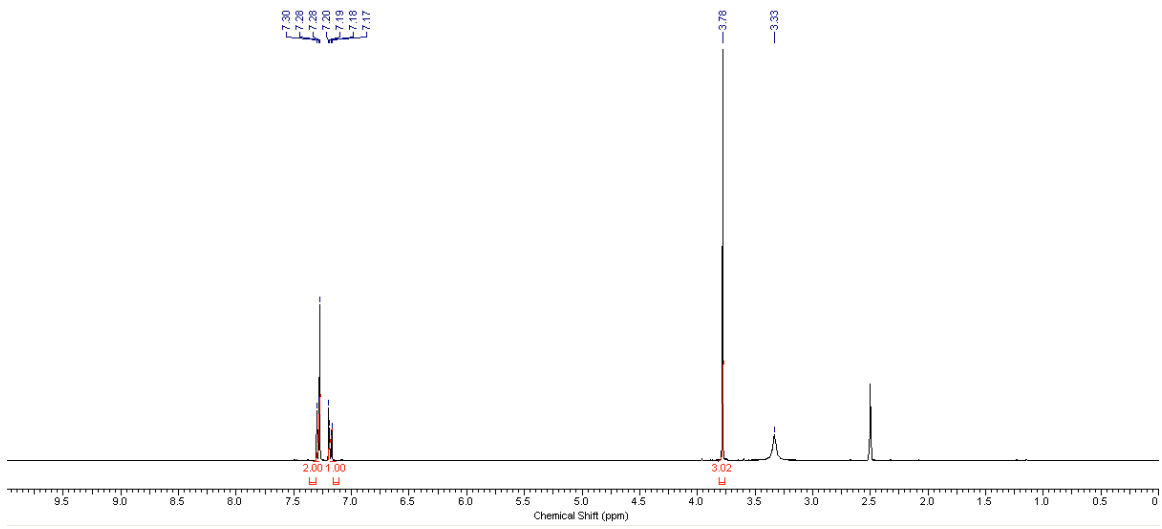
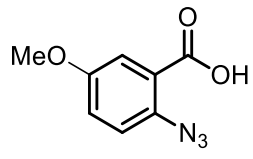


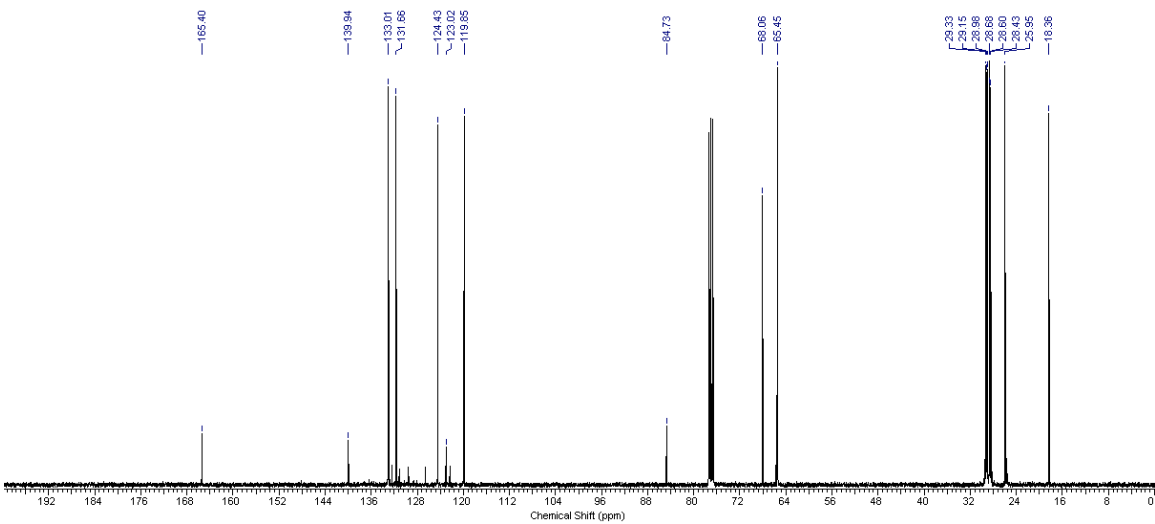
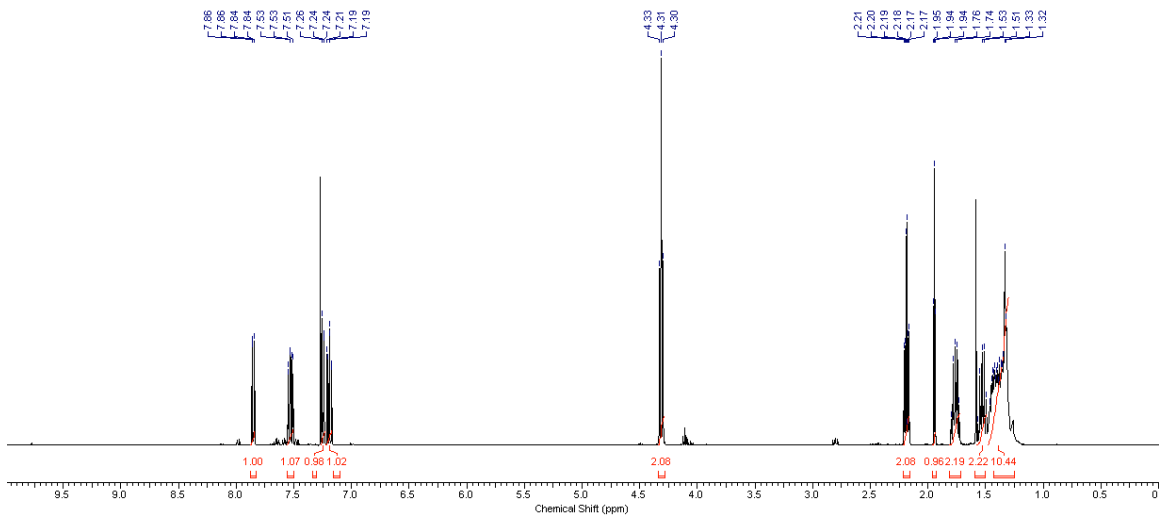
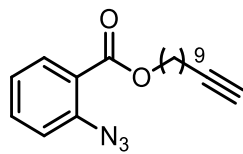
8888888888
8888888888



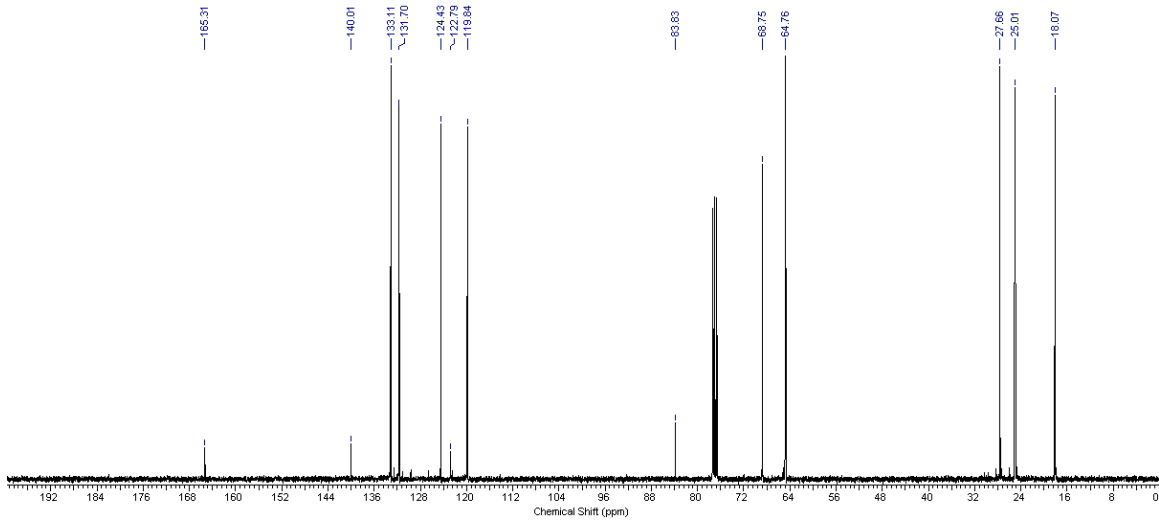
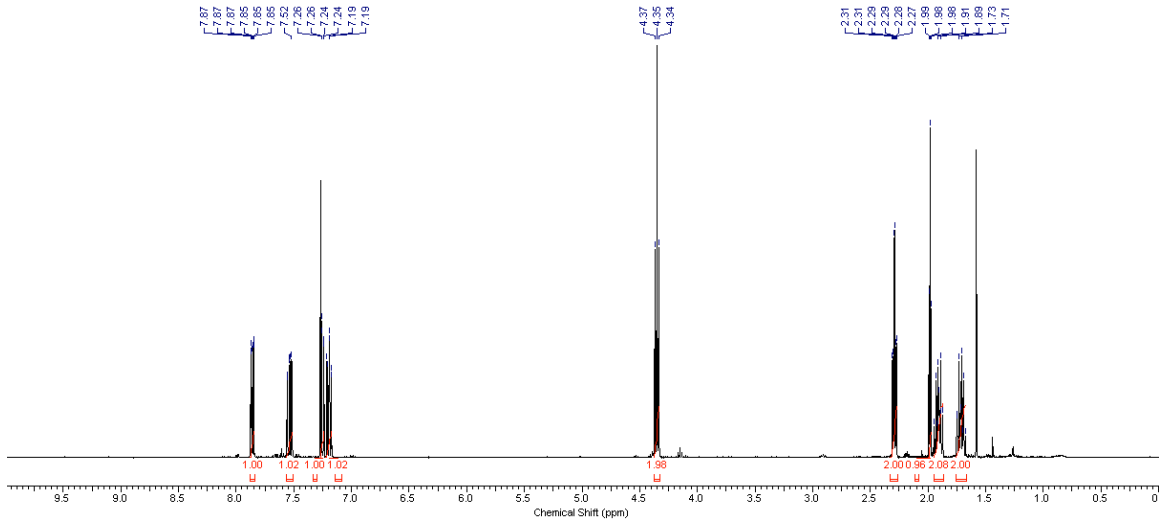
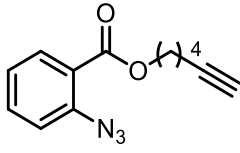
hhhhhhhh



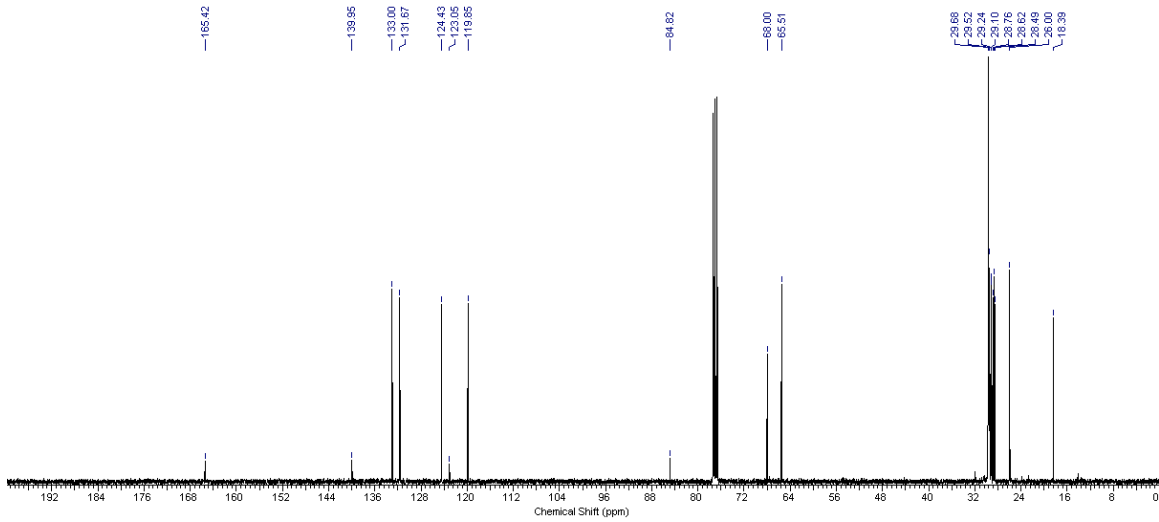
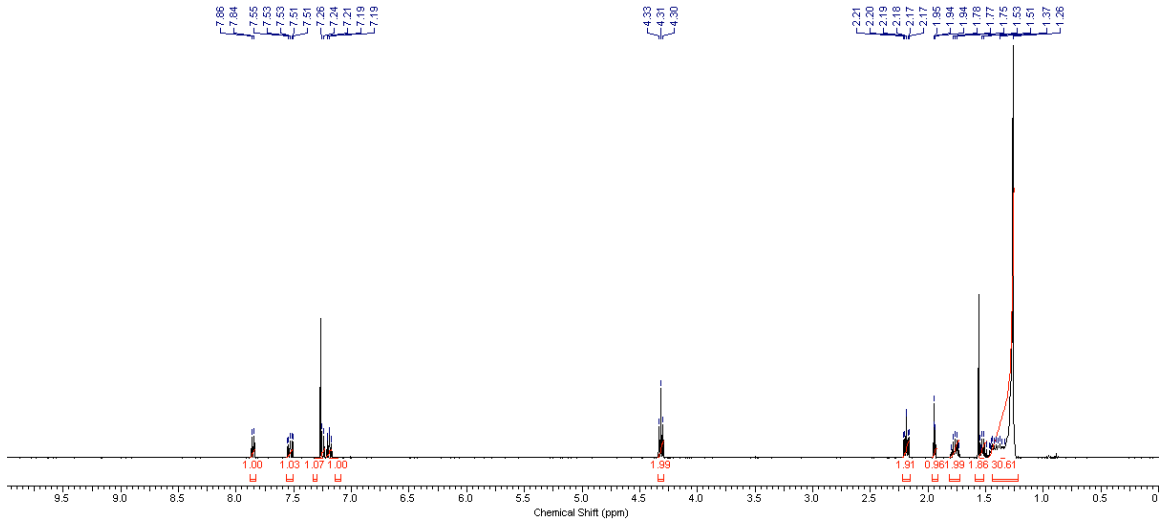
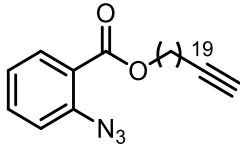




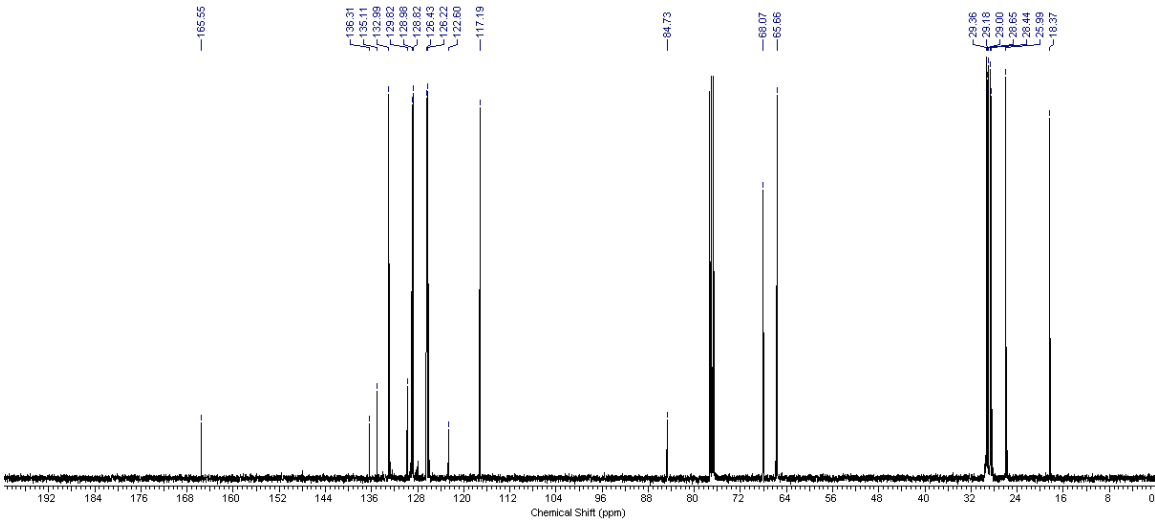
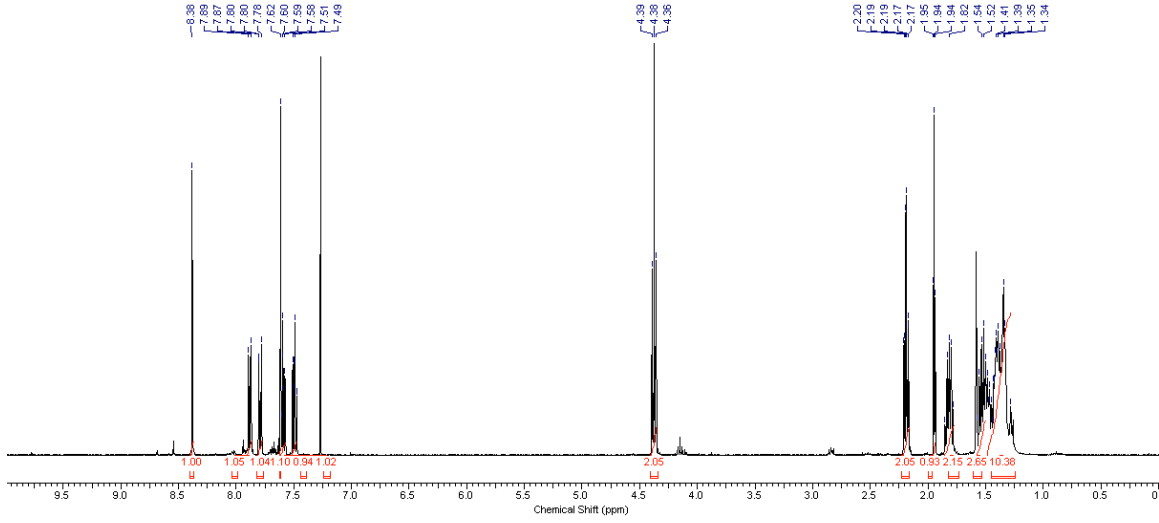
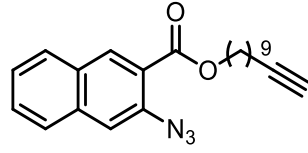
kkkkkkkkkk



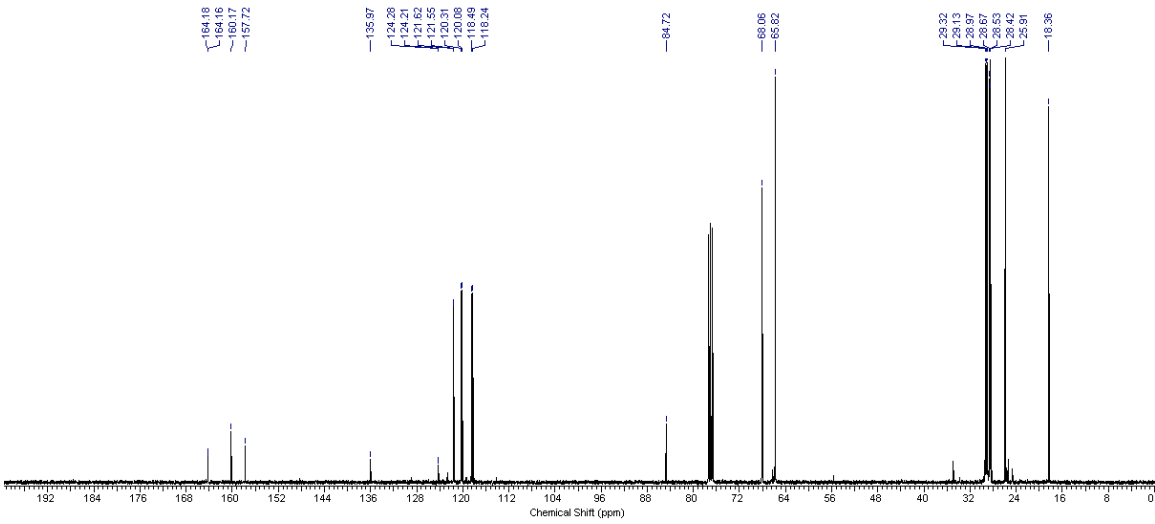
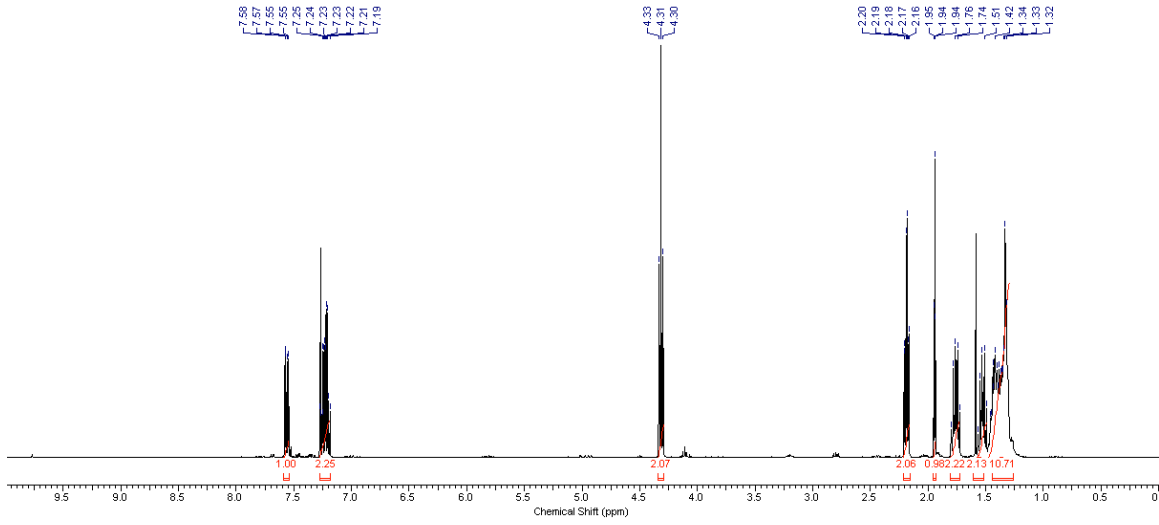
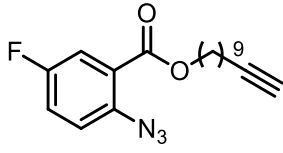
|||||||



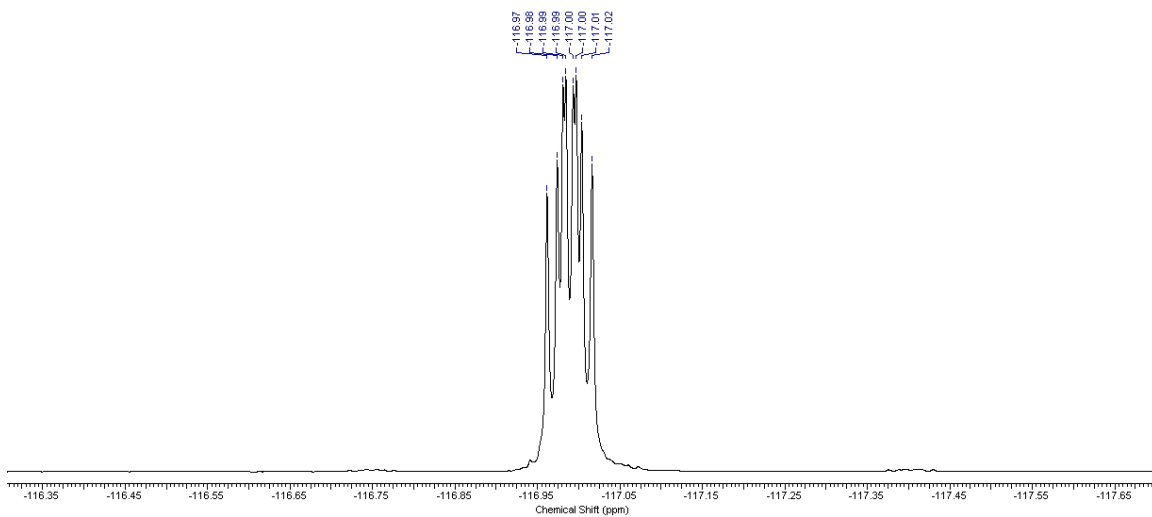
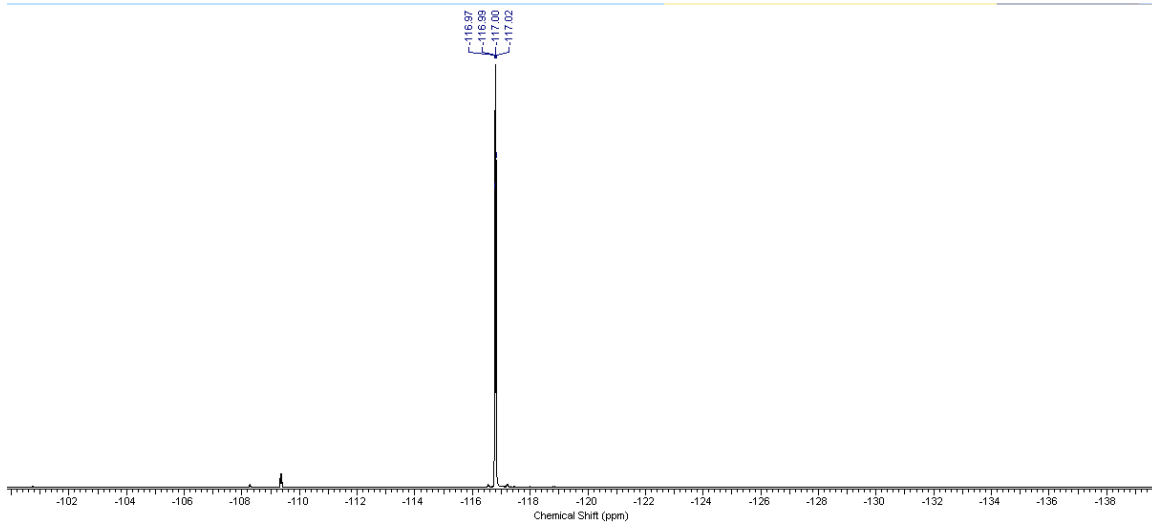
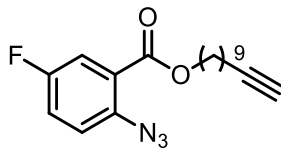
mmmmmmmmmm



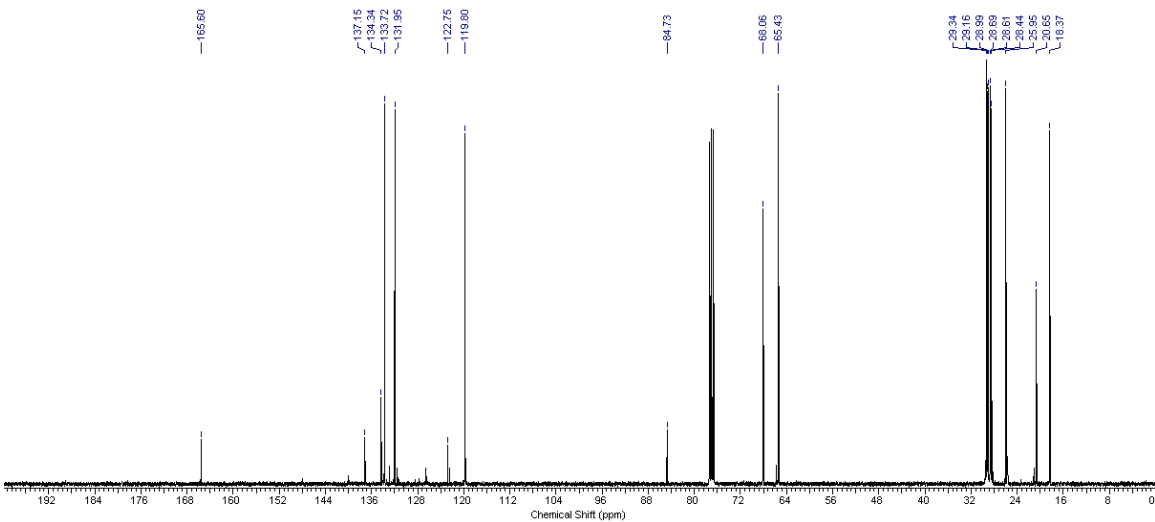
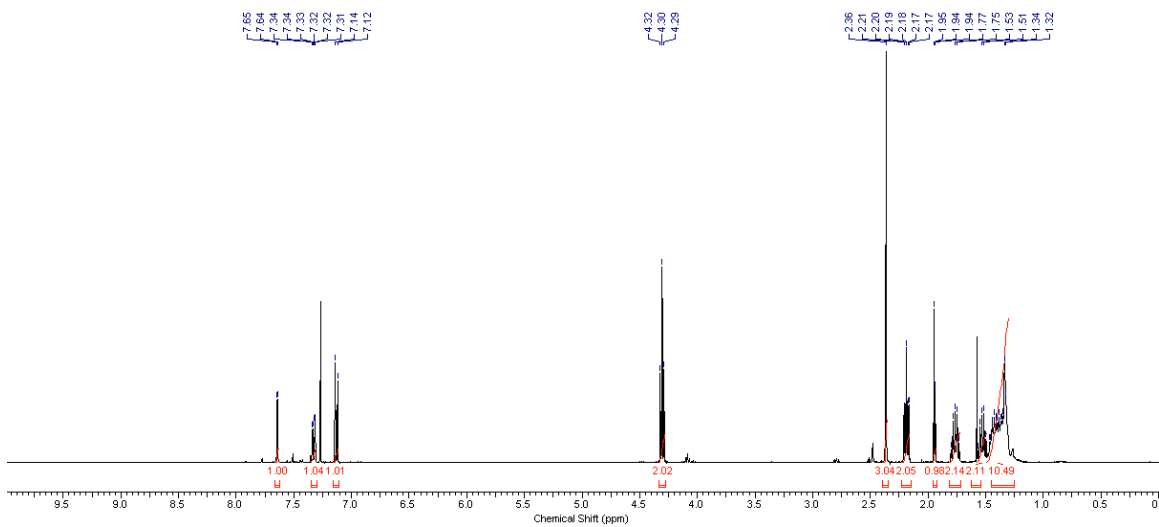
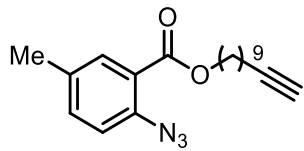
XXXXXXXXXX



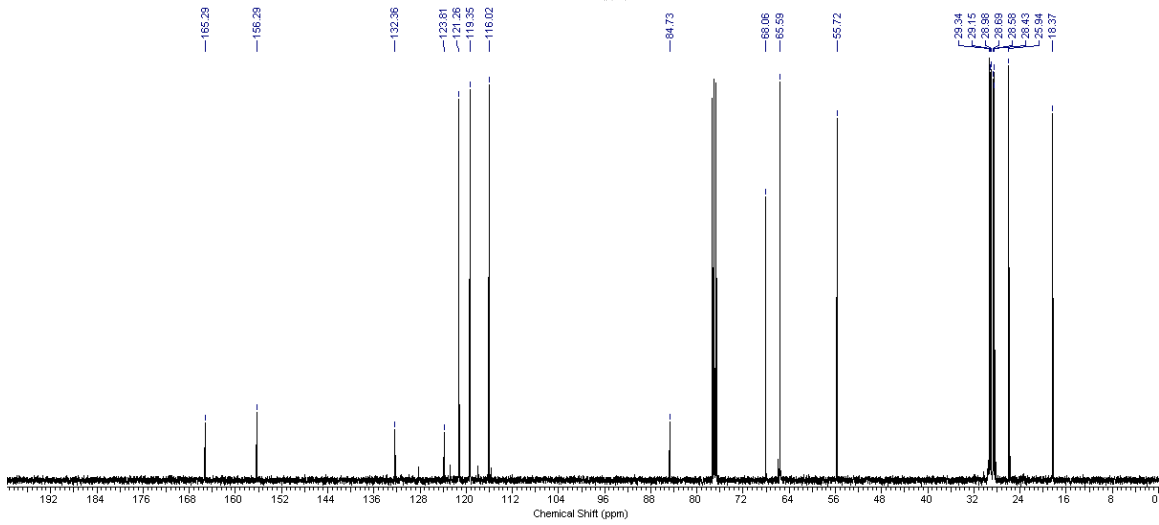
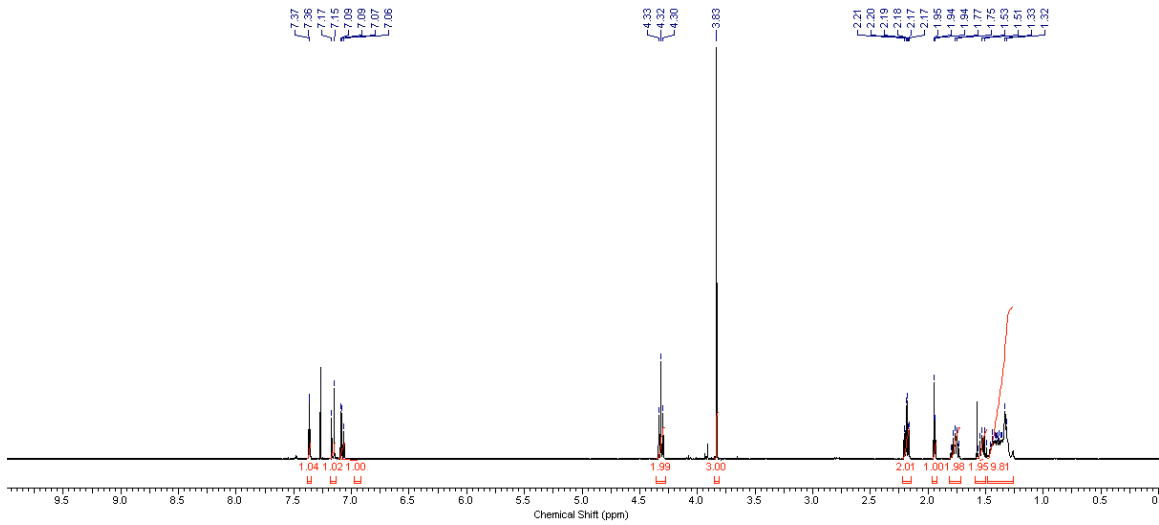
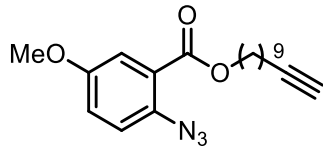
00000000

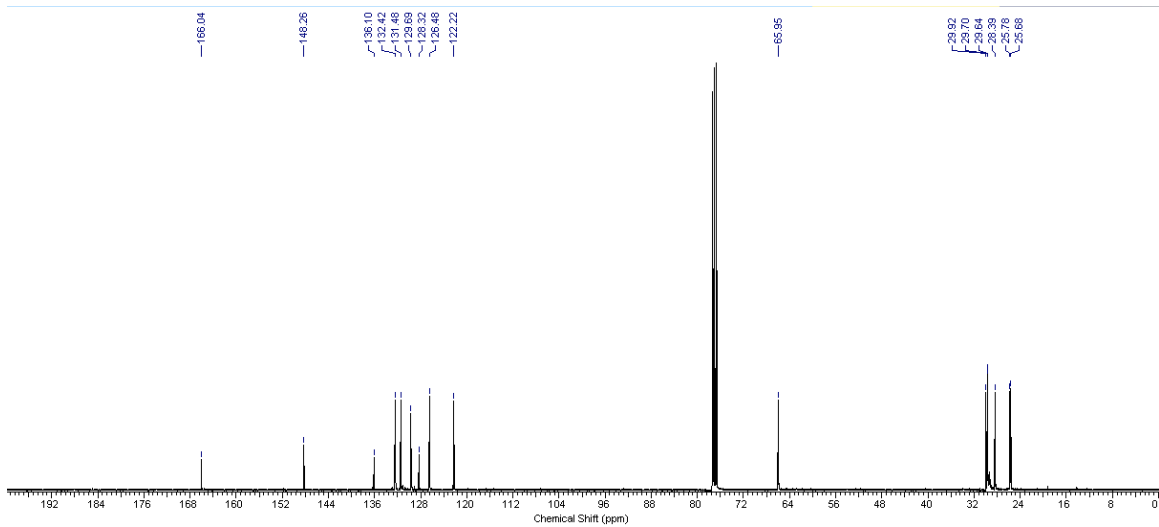
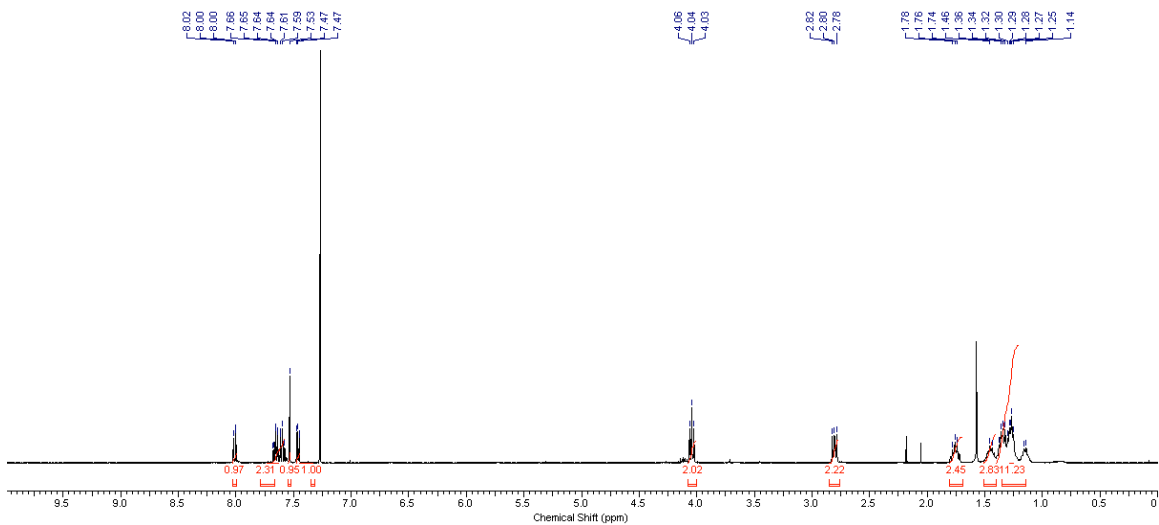
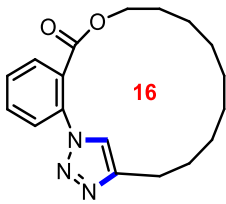


PPPPPPPPPP

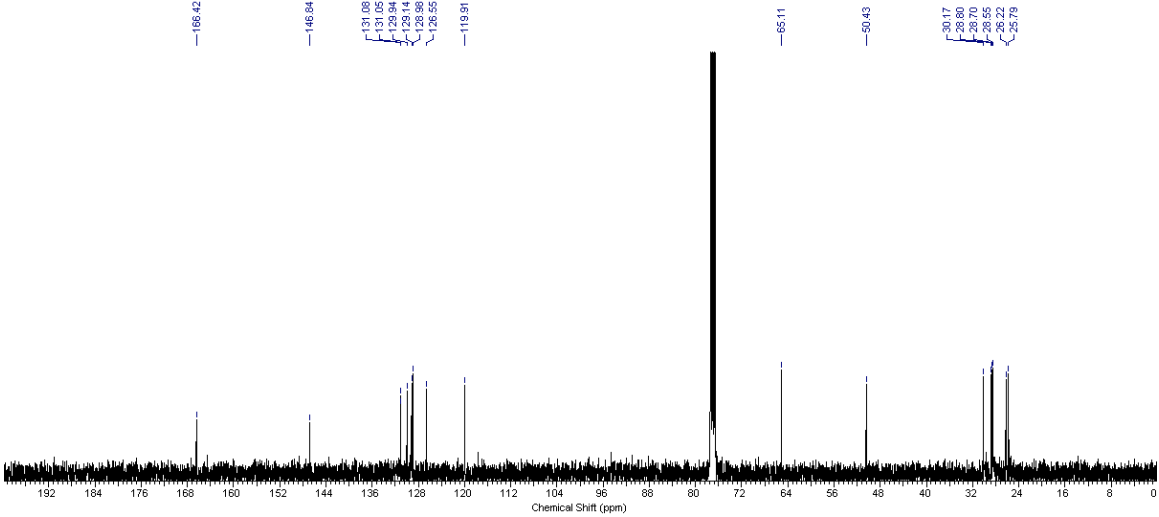
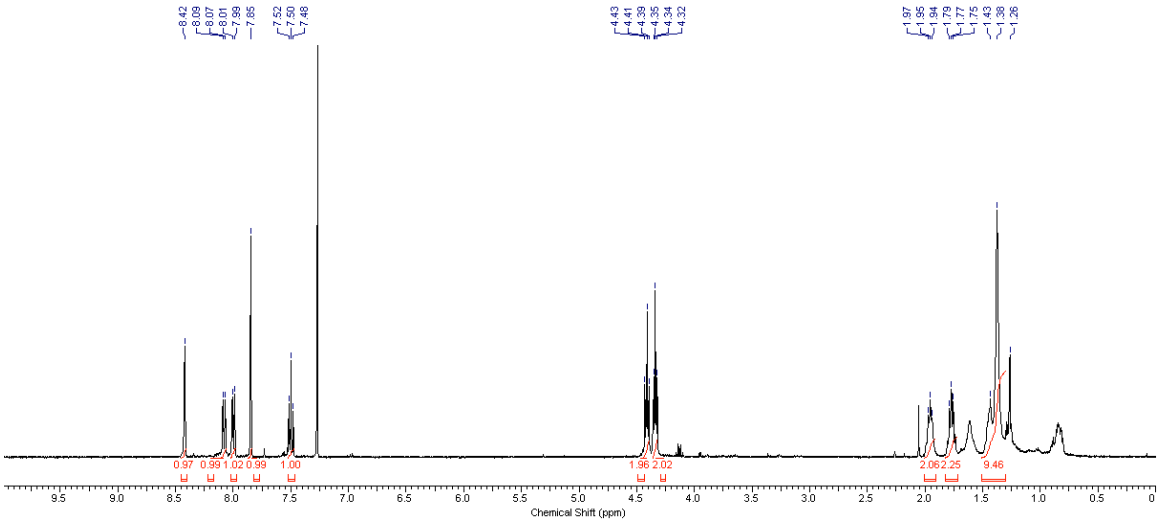
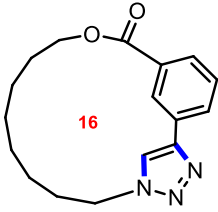


bbbbbbbbb

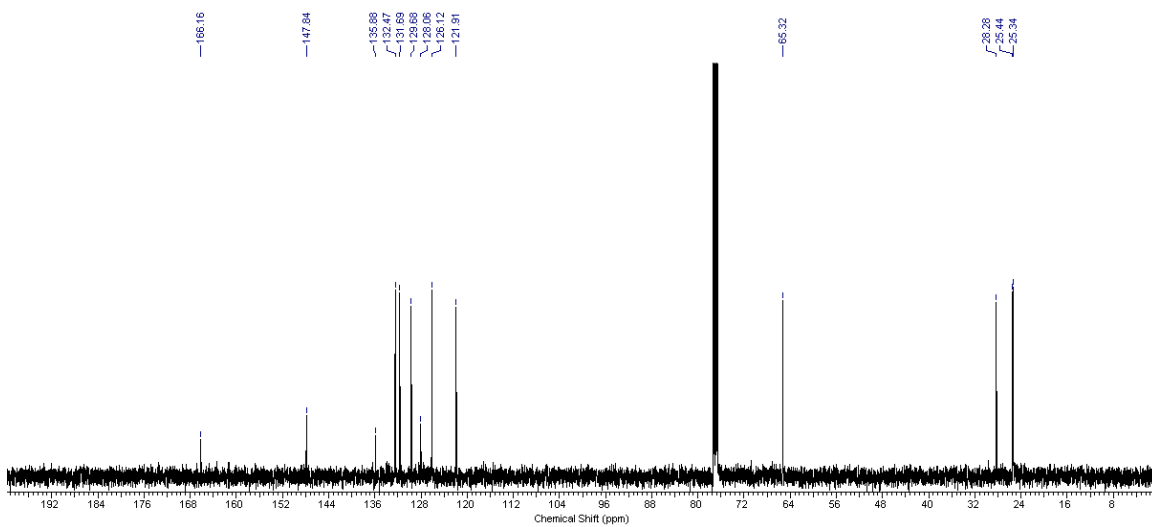
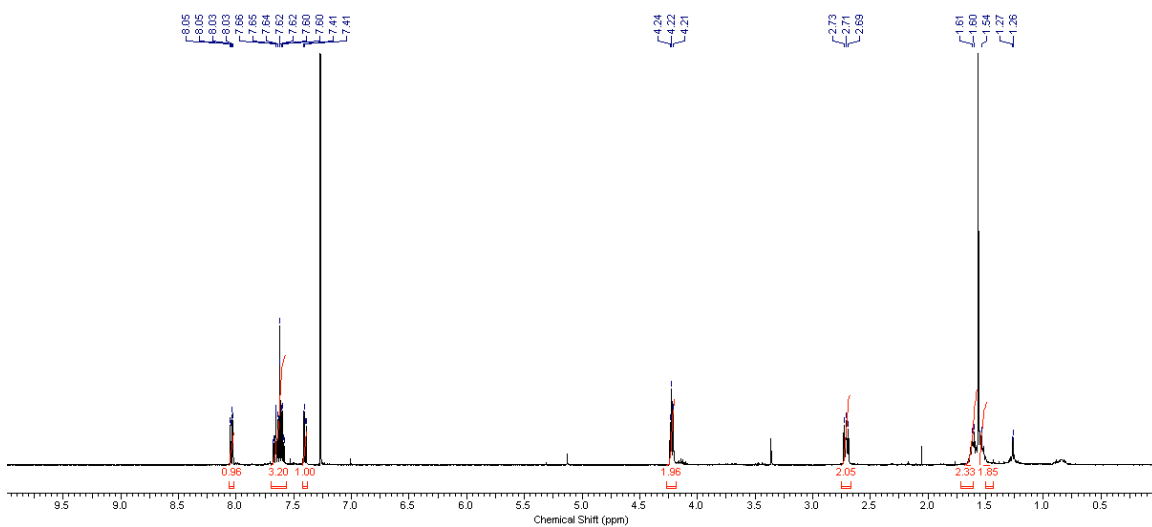
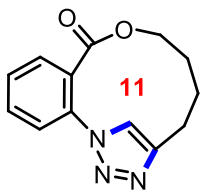




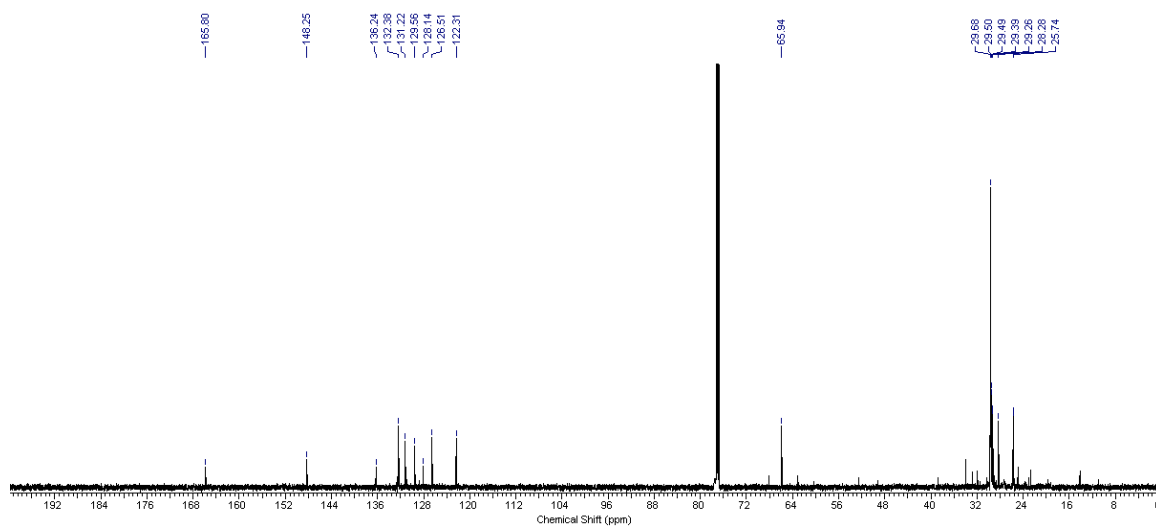
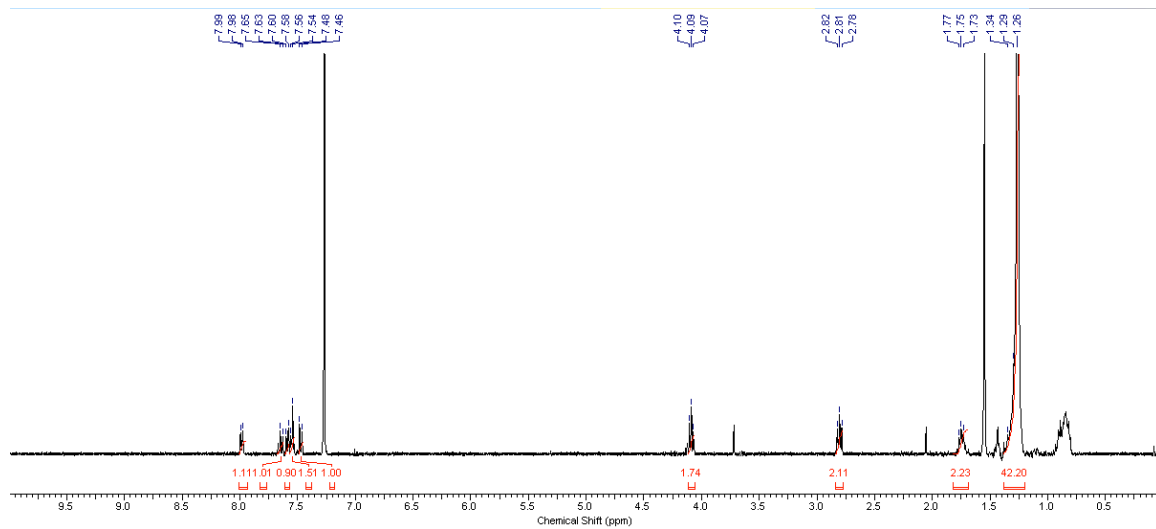
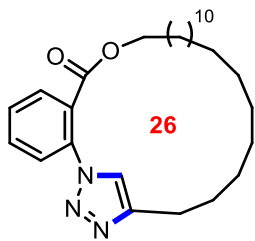
SSSSSSSS



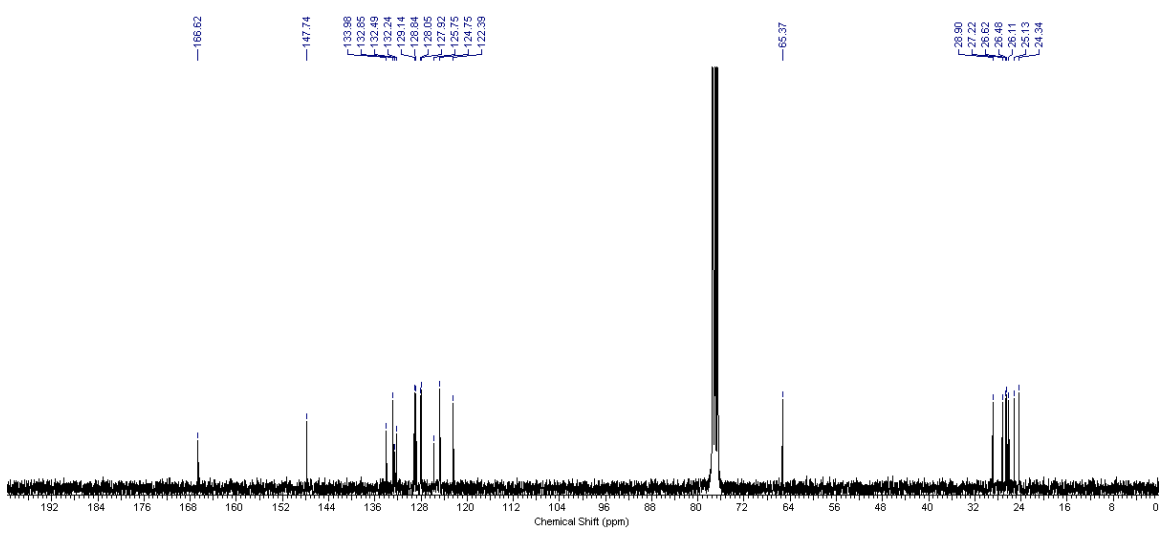
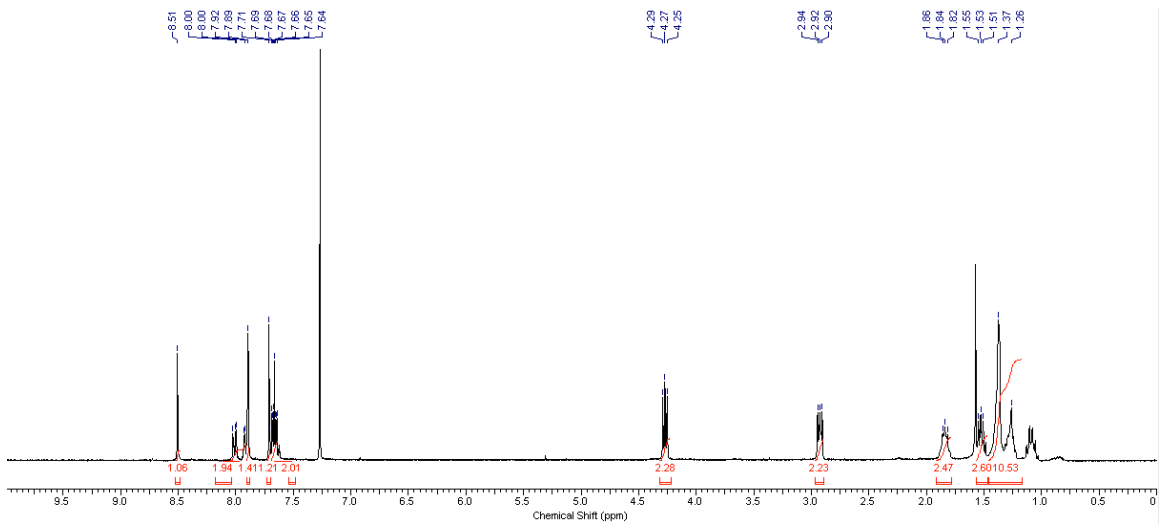
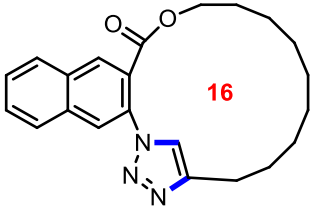
tttttttt

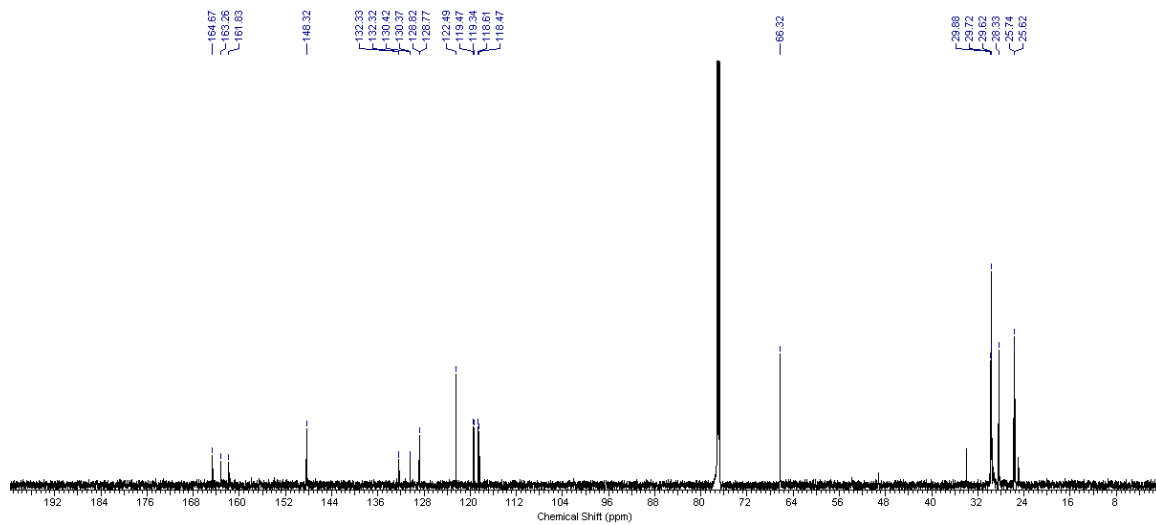
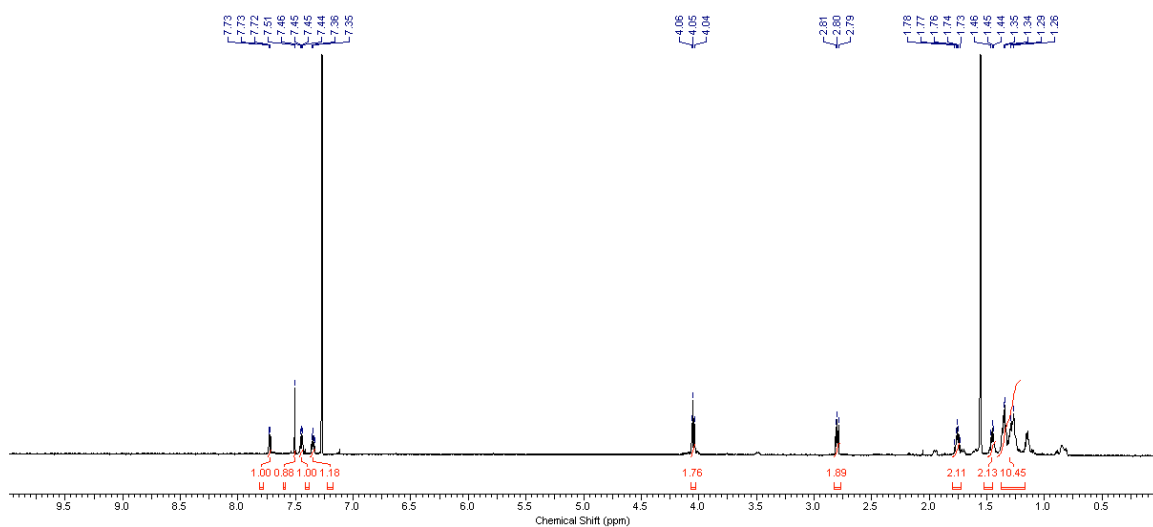
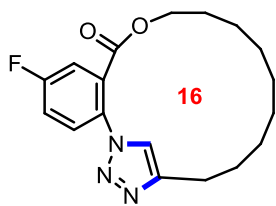


uuuuuuuuuu

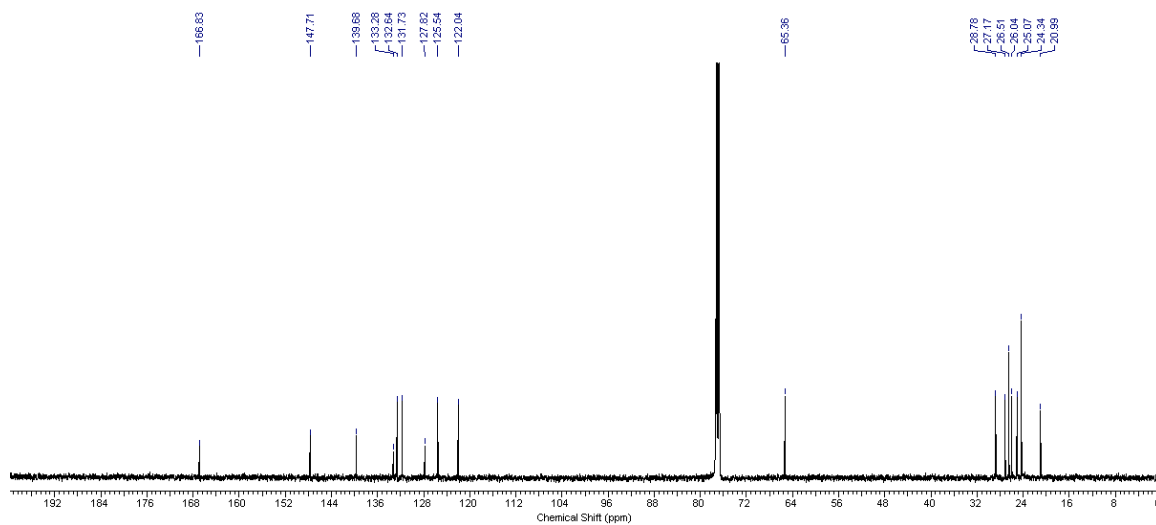
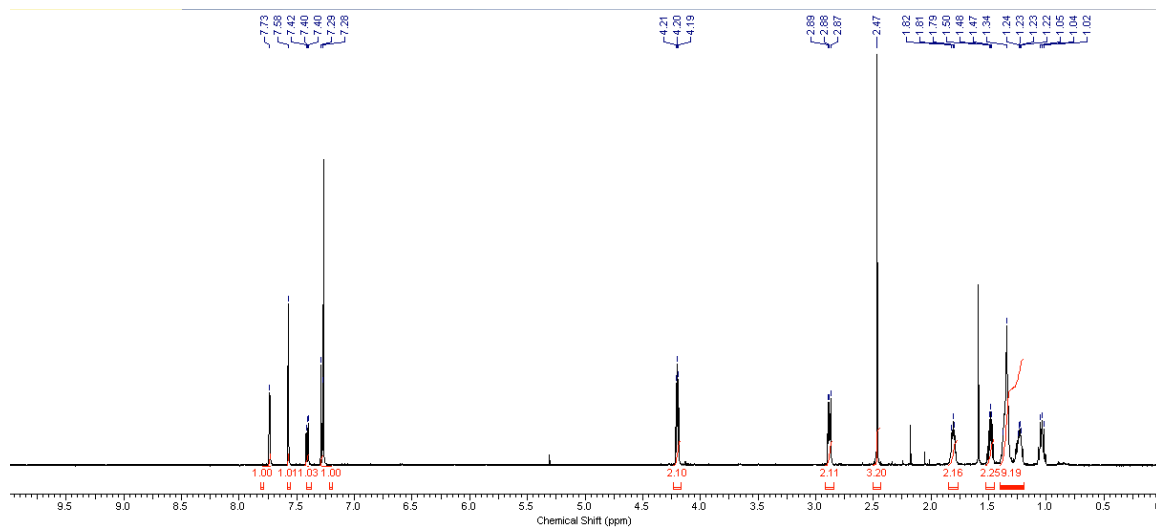
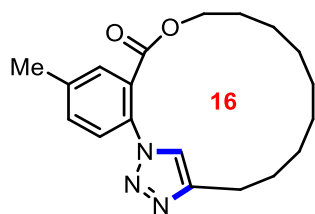


XXXXXXXXXX

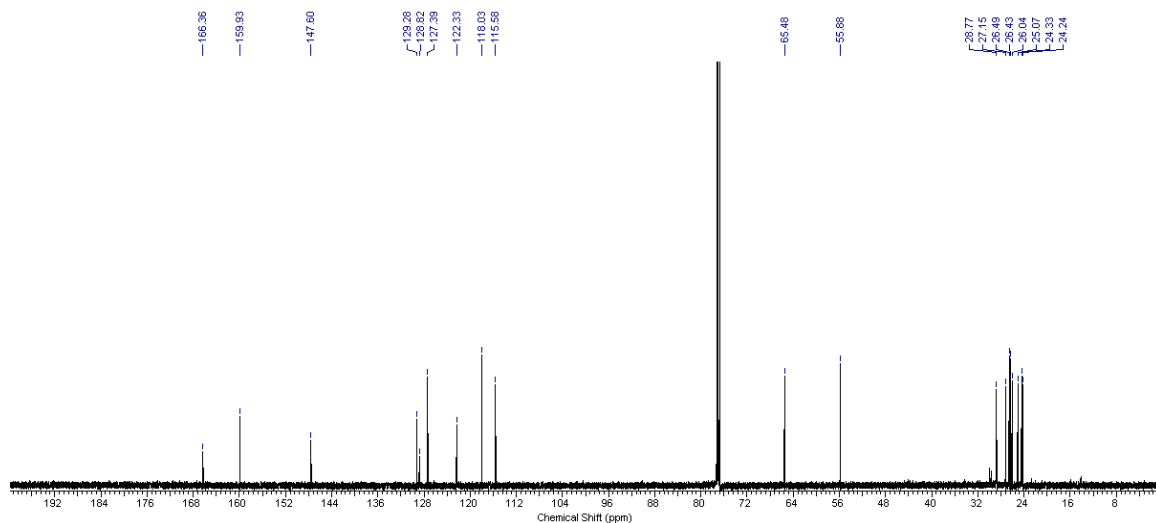
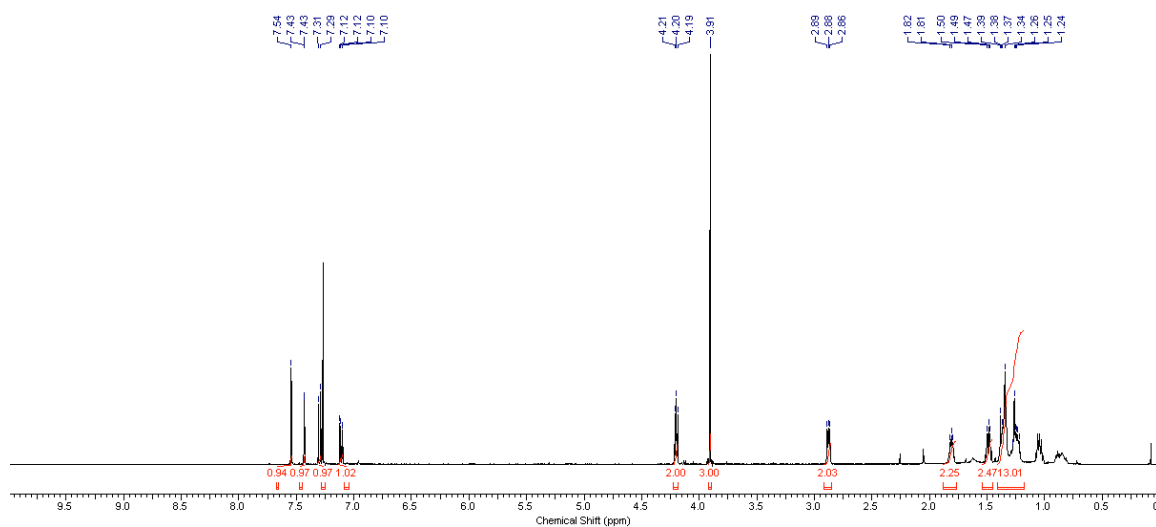
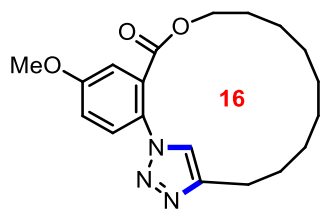




XXXXXXXXXX



yyyyyyyyyy



XXXXXXXXXX

aaaaaaaaa